

# Microwave Devices & Radar

## LECTURE NOTES VOLUME I

by Professor David Jenn

Contributors: Professors F. Levien, G. Gill, J. Knorr and J. Lebaric

---

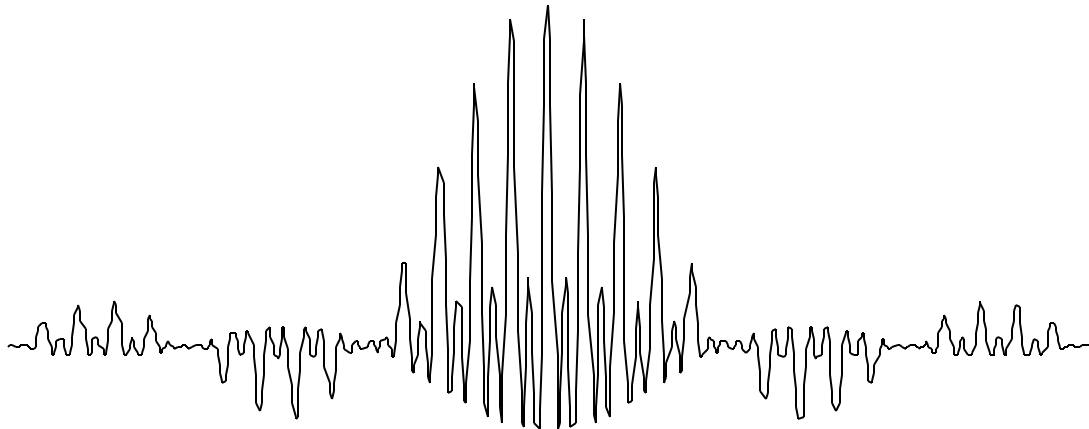


## Table of Contents

(ver4.7)

---

I-1	Table of Contents (1)	I-63	Jammer Burnthrough Range (1)
I-2	Table of Contents (2)	I-64	Jammer Burnthrough Range (2)
I-3	Table of Contents (3)	I-65	Noise Figure
I-4	Table of Contents (4)	I-66	Probability & Statistics Refresher (1)
I-5	Table of Contents (5)	I-67	Probability & Statistics Refresher (2)
I-6	Electromagnetic Fields and Waves (1)	I-68	Probability & Statistics Refresher (3)
I-7	Electromagnetic Fields and Waves (2)	I-69	Probability & Statistics Refresher (4)
I-8	Electromagnetic Fields and Waves (3)	I-70	Rayleigh Distribution (1)
I-9	Electromagnetic Fields and Waves (4)	I-71	Rayleigh Distribution (2)
I-10	Electromagnetic Fields and Waves (5)	I-72	Central Limit Theorem
I-11	Electromagnetic Fields and Waves (6)	I-73	Transformation of Variables
I-12	Electromagnetic Fields and Waves (7)	I-74	Fourier Transform Refresher (1)
I-13	Electromagnetic Fields and Waves (8)	I-75	Fourier Transform Refresher (2)
I-14	Electromagnetic Fields and Waves (9)	I-76	Fourier Transform Refresher (3)
I-15	Wave Reflection (1)	I-77	Fourier Transform Refresher (4)
I-16	Wave Reflection (2)	I-78	Fourier Transform Refresher (5)
I-17	Wave Reflection (3)	I-79	Modulation of a Carrier (1)
I-18	Wave Reflection (4)	I-80	Modulation of a Carrier (2)
I-19	Wave Reflection (5)	I-81	Modulation of a Carrier (3)
I-20	Wave Reflection (6)	I-82	Fourier Transform of a Pulse Train (1)
I-21	Antenna Patterns, Directivity and Gain	I-83	Fourier Transform of a Pulse Train (2)
I-22	Polarization of Radiation	I-84	Fourier Transform of a Pulse Train (3)
I-23	Wave Polarization	I-85	Response of Networks (1)
I-24	Electromagnetic Spectrum	I-86	Response of Networks (2)
I-25	Radar and ECM Frequency Bands	I-87	Response of Networks (3)
I-26	Radar Bands and Usage	I-88	Signals and Noise Through Networks (1)
I-27	Joint Electronics Type Designation	I-89	Signals and Noise Through Networks (2)
I-28	Examples of EW Systems	I-90	Signals and Noise Through Networks (3)
I-29	Radio Detection and Ranging (RADAR)	I-91	Rician Distribution
I-30	Time Delay Ranging	I-92	Probability of False Alarm (1)
I-31	Information Available From the Radar Echo	I-93	Probability of False Alarm (2)
I-32	Radar Classification by Function	I-94	Probability of False Alarm (3)
I-33	Radar Classification by Waveform	I-95	Probability of Detection (1)
I-34	Basic Form of the Radar Range Equation (1)	I-96	Probability of Detection (2)
I-35	Basic Form of the Radar Range Equation (2)	I-97	Probability of Detection (3)
I-36	Basic Form of the Radar Range Equation (3)	I-98	Probability of Detection
I-37	Characteristics of the Radar Range Equation	I-99	SNR Improvement Using Integration
I-38	Maximum Detection Range	I-100	SNR Improvement Using Integration
I-39	Generic Radar Block Diagram	I-101	Illustration of Coherent Integration
I-40	Brief Description of System Components	I-102	Approximate Antenna Model
I-41	Coordinate Systems	I-103	Number of Pulses Available
I-42	Radar Displays	I-104	Integration Improvement Factor
I-43	Pulsed Waveform	I-105	RRE for Pulse Integration
I-44	Range Ambiguities	I-106	RRE for Pulse Integration
I-45	Range Gates	I-107	RRE for Pulse Integration
I-46	Range Bins and Range Resolution	I-108	Radar Cross Section (1)
I-47	Radar Operational Environment	I-109	Radar Cross Section (2)
I-48	Ground Clutter From Sidelobes	I-110	Radar Cross Section of a Sphere
I-49	Survey of Propagation Mechanisms (1)	I-111	Radar Cross Section of a Cylinder
I-50	Survey of Propagation Mechanisms (2)	I-112	Target Scattering Matrix (1)
I-51	Survey of Propagation Mechanisms (3)	I-113	Target Scattering Matrix (2)
I-52	Radar System Design Tradeoffs	I-114	Example: Antenna as a Radar Target
I-53	Decibel Refresher	I-115	Scattering Mechanisms
I-54	Thermal Noise	I-116	Scattering Sources for a Complex Target
I-55	Noise in Radar Systems	I-117	Two Sphere RCS (1)
I-56	Noise in Radar Systems	I-118	Two Sphere RCS (2)
I-57	Ideal Filter	I-119	RCS of a Two Engine Bomber
I-58	Noise Bandwidth of an Arbitrary Filter	I-120	RCS of a Naval Auxiliary Ship
I-59	Signal-to-noise Ratio (S/N)	I-121	RCS of a Geometrical Components Jet
I-60	Example: Police Radar	I-122	Geometrical Components Jet
I-61	Attack Approach	I-123	Fluctuating Targets
I-62	Defeating Radar by Jamming	I-124	Swerling Types

I-125	Correction & Improvement Factors (1)	II-52	Surface Clutter (4)
I-126	Correction & Improvement Factors (2)	II-53	Backscatter From Extended Surfaces
I-127	Detection Range for Fluctuating Targets	II-54	Backscatter From Extended Surfaces
I-128	Example	II-55	Clutter Spectrum (1)
I-129	Defeating Radar by Low Observability	II-56	Clutter Spectrum (2)
I-130	Methods of RCS Reduction and Control	II-57	Clutter Spectrum (3)
I-131	Reduction by Shaping: Corner Reflector	II-58	Clutter Spectrum (4)
I-132	Application of Serrations to Reduce Edge Scattering	II-59	Clutter Spectrum (5)
I-133	Application of Serrations to Reduce Edge Scattering	II-60	Clutter Spectrum (6)
I-134	Traveling Waves	II-61	Clutter Spectrum (7)
I-135	Trailing Edge Resistive Strips	II-62	Sea States
I-136	Application of Reduction Methods	II-63	Sea Clutter
I-137	Low Observable Platforms: F-117	II-64	Example: AN/APS-200
I-138	Low Observable Platforms: B-2	II-65	Example: AN/APS-200
I-139	Low Observable Platforms: Sea Shadow	II-66	Example: AN/APS-200
II-1	Other Sources of Loss	II-67	Delay Line Canceler (1)
II-2	Atmospheric Attenuation	II-68	Delay Line Canceler (2)
II-3	Rain Attenuation	II-69	Delay Line Canceler (3)
II-4	Transmission Line Loss	II-70	Delay Line Canceler (4)
II-5	Antenna Beamshape Loss	II-71	Staggered and Multiple PRFs (1)
II-6	Collapsing Loss	II-72	Staggered and Multiple PRFs (2)
II-7	Noise Figure & Effective Temperature (1)	II-73	Staggered and Multiple PRFs (3)
II-8	Comments on Noise Figure & Temperature	II-74	Synchronous Detection (I and Q Channels)
II-9	Noise in Cascaded Networks (1)	II-75	Analog vs Digital Processing for MTI
II-10	Noise Figure & Effective Temperature (2)	II-76	Single Channel Receiver Block Diagram
II-11	Noise Figure From Loss	II-77	Synchronous Receiver Block Diagram
II-12	Examples (1)	II-78	SNR Advantage of Synchronous Detection (1)
II-13	Examples (2)	II-79	SNR Advantage of Synchronous Detection (2)
II-14	Examples (3)	II-80	Processing of a Coherent Pulse Train (1)
II-15	Examples (4)	II-81	Sampling Theorem (1)
II-16	Examples (5)	II-82	Sampling Theorem (2)
II-17	Examples (6)	II-83	Processing of a Coherent Pulse Train (2)
II-18	Examples (7)	II-84	Processing of a Coherent Pulse Train (3)
II-19	Doppler Frequency Shift (1)	II-85	Processing of a Coherent Pulse Train (4)
II-20	Doppler Frequency Shift (2)	II-86	Discrete Fourier Transform (DFT)
II-21	Doppler Frequency Shift (3)	II-87	Doppler Filtering Using the DFT (1)
II-22	Doppler Filter Banks	II-88	Doppler Filtering Using the DFT (2)
II-23	Example	II-89	Pulse Doppler Receiver
II-24	Example	II-90	Pulse Burst Mode
II-25	I and Q Representation	II-91	MTI Improvement Factors
II-26	Doppler Frequency Shift (4)	II-92	MTI Limitations (1)
II-27	CW Radar Problems (1)	II-93	MTI Limitations (2)
II-28	CW Radar Problems (2)	II-94	MTI Canceler Improvement Factors
II-29	CW Radar Problems (3)	II-95	MTI Canceler Improvement Factors
II-30	Frequency Modulated CW (FMCW)	II-96	Example
II-31	FMCW (2)	II-97	Coherent and Noncoherent Pulse Trains
II-32	FMCW (3)	II-98	Noncoherent Pulse Train Spectrum (1)
II-33	FMCW (4)	II-99	Noncoherent Pulse Train Spectrum (2)
II-34	FMCW Complications	II-100	Search Radar Equation (1)
II-35	FMCW Complications	II-101	Search Radar Equation (2)
II-36	MTI and Pulse Doppler Radar	II-102	Search Radar Equation (3)
II-37	MTI (1)	II-103	Search Radar Equation (4)
II-38	MTI (2)	II-104	Radar Tracking (1)
II-39	MTI (3)	II-105	Radar Tracking (2)
II-40	PD and MTI Problem: Eclipsing	II-106	Radar Tracking (3)
II-41	PD and MTI Problem: Range Ambiguities	II-107	Gain Control
II-42	Range Ambiguities (2)	II-108	Example
II-43	Range Ambiguities (3)	II-109	Example
II-44	Example	II-110	Monopulse Tracking (1)
II-45	PD and MTI Problem: Velocity Ambiguities	II-111	Monopulse Tracking (2)
II-46	Velocity Ambiguities (2)	II-112	Monopulse Tracking (3)
II-47	Airborne MTI and Pulse Doppler Operation	II-113	Monopulse Tracking (4)
II-48	Surface Clutter (1)	II-114	Monopulse Tracking (5)
II-49	Surface Clutter (2)	II-115	Monopulse Tracking (6)
II-50	Surface Clutter (3)	II-116	Monopulse Tracking (7)
II-51	Two-Way Pattern Beamwidth	II-117	Low Angle Tracking (1)

II-118	Low Angle Tracking (2)	III-58	Array Factor for 2D Arrays
II-119	Low Angle Tracking (3)	III-59	Gain of Phased Arrays
II-120	Low Angle Tracking (4)	III-60	Array Elements and Ground Planes
II-121	Tracking Error Due to Multipath	III-61	Array of Dipoles Above a Ground Plane
II-122	Low Angle Tracking (5)	III-62	Series Fed Waveguide Slot Array
II-123	Low Angle Tracking (6)	III-63	Low Probability of Intercept Radar (LPIR)
II-124	Atmospheric Refraction (1)	III-64	Low and Ultra Low Sidelobes
II-125	Atmospheric Refraction (2)	III-65	Antenna Pattern Control
II-126	Atmospheric Refraction (3)	III-66	Tapered Aperture Distributions
III-1	Receiver Types (1)	III-67	Calculation of Aperture Efficiency
III-2	Receiver Types (2)	III-68	Cosecant-Squared Antenna Pattern
III-3	Noise Power Spectral Density	III-69	Example
III-4	Matched Filters (1)	III-70	Array Example (1)
III-5	Matched Filters (2)	III-71	Array Example (2)
III-6	Matched Filters (3)	III-72	Array Example (3)
III-7	Matched Filters (4)	III-73	Array Example (4)
III-8	Matched Filters (5)	III-74	Calculation of Antenna Temperature
III-9	Matched Filters (6)	III-75	Multiple Beam Antennas (1)
III-10	Matched Filters (7)	III-76	Multiple Beam Antennas (2)
III-11	Complex Signals	III-77	Radiation Patterns of a Multiple Beam Array
III-12	Ambiguity Function (1)	III-78	Beam Coupling Losses for a 20 Element Array
III-13	Ambiguity Function (2)	III-79	Active vs Passive Antennas
III-14	Ambiguity Function (3)	III-80	SNR Calculation for a Lossless Feed Network
III-15	Ambiguity Function (4)	III-81	SNR Calculation for a Lossless Feed Network
III-16	Ambiguity Function (5)	III-82	Passive Two-Beam Array (1)
III-17	Range Accuracy (1)	III-83	Passive Two-Beam Array (2)
III-18	Range Accuracy (2)	III-84	Active Two-Beam Array (1)
III-19	Range Accuracy (3)	III-85	Active Two-Beam Array (2)
III-20	Range Accuracy (4)	III-86	Comparison of SNR: Active vs Passive
III-21	Velocity Accuracy	III-87	Example
III-22	Uncertainty Relation	III-88	Active Array Radar Transmit/Receive Module
III-23	Angular Accuracy	III-89	Digital Phase Shifters
III-24	Pulse Compression	III-90	Effect of Phase Shifter Roundoff Errors
III-25	Linear FM Pulse Compression (Chirp)	III-91	Digital Phase Shifters
III-26	Linear FM Pulse Compression (Chirp)	III-92	True Time Delay Scanning
III-27	Linear FM Pulse Compression (Chirp)	III-93	Time Delay vs Fixed Phase Scanning
III-28	Linear FM Pulse Compression (Chirp)	III-94	Beam Squint Due to Frequency Change
III-29	Chirp Filter Output Waveform	III-95	Time Delay Networks
III-30	Range Resolution (1)	III-96	Time Delay Using Fiber Optics
III-31	Range Resolution (2)	III-97	Digital Beamforming (1)
III-32	Pulse Compression Example	III-98	Digital Beamforming (2)
III-33	Chirp Complications	III-99	Monopulse Difference Beams
III-34	Digital Pulse Compression	III-100	Sum and Difference Beamforming
III-35	Barker Sequences	III-101	Waveguide Monopulse Beamforming Network
III-36	Pulse Compressor/Expander	III-102	Antenna Radomes
III-37	The Ideal Radar Antenna	III-103	Conformal Antennas & "Smart Skins"
III-38	Antenna Refresher (1)	III-104	Testing of Charred Space Shuttle Tile
III-39	Lens Antenna	III-105	Antenna Imperfections (Errors)
III-40	Solid Angles and Steradians	III-106	Smart Antennas (1)
III-41	Antenna Far Field	III-107	Smart Antennas (2)
III-42	Antenna Pattern Features	III-108	Microwave Devices
III-43	Antenna Refresher (2)	III-109	Transmission Line Refresher (1)
III-44	Antenna Refresher (3)	III-110	Transmission Line Refresher (2)
III-45	Directivity Example	III-111	Transmission Line Refresher (3)
III-46	Antenna Polarization Loss	III-112	Multiplexers
III-47	Parabolic Reflector Antenna	III-113	Rotary Joints
III-48	Parabolic Reflector Antenna Losses	III-114	Microwave Switches
III-49	Example	III-115	Circulators
III-50	Example	III-116	Waveguide Magic Tee
III-51	Radiation by a Line Source (1)	III-117	Filter Characteristics
III-52	Radiation by a Line Source (2)	III-118	Mixers (1)
III-53	Array Antennas (1)	III-119	Mixers (2)
III-54	Array Antennas (2)	III-120	Mixers (3)
III-55	Visible Region	III-121	Input-Output Transfer Characteristic
III-56	Array Antennas (3)	III-122	Intermodulation Products
III-57	Array Antennas (4)	III-123	Intermodulation Example

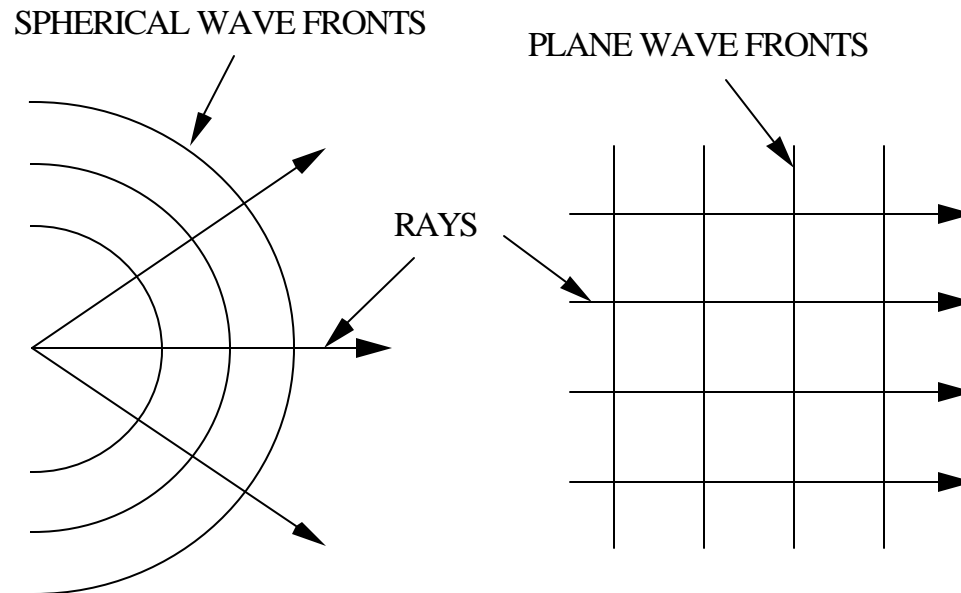
III-124	Amplifiers	IV-45	SAR Image
III-125	Low-Noise Amplifier	IV-46	SAR Range Equation
III-126	Intermodulation Products of Amplifiers	IV-47	SAR Problems (1)
III-127	Sample Microwave Amplifier Characteristic	IV-48	SAR Problems (2)
III-128	Power Capabilities of Sources	IV-49	Inverse Synthetic Aperture Radar (ISAR)
III-129	Development of Sources	IV-50	ISAR (2)
III-130	Transmitters (1)	IV-51	ISAR (3)
III-131	Transmitters (2)	IV-52	ISAR (4)
III-132	Klystrons	IV-53	HF Radars (1)
III-133	Klystron Operation	IV-54	HF Radars (2)
III-134	Cavity Magnetron	IV-55	HF Radars (3)
III-135	Magnetron Operation	IV-56	Typical HF OTH Radar Parameters
III-136	Eight Cavity Magnetron	IV-57	Typical HF Clutter and Target Spectrum
III-137	Magnetron Basics (1)	IV-58	Relocatable OTH Radar (ROTHR)
III-138	Magnetron Basics (2)	IV-59	HF Coastal Radar (CODAR)
III-139	Free-Electron Laser (FEL) Operation	IV-60	HF Radar Example (CONUS-B)
III-140	Free-Electron Lasers	IV-61	Stepped Frequency Radar (1)
III-141	Radar Waveform Parameter Measurements (1)	IV-62	Stepped Frequency Radar (2)
III-142	Radar Waveform Parameter Measurements (2)	IV-63	Stepped Frequency Radar (3)
III-143	Radar Waveform Parameter Measurements (3)	IV-64	Stepped Frequency Radar (4)
III-144	Radar Waveform Parameter Measurements (4)	IV-65	Stepped Frequency Radar (5)
III-145	Radar Waveform Parameter Measurements (5)	IV-66	Stepped Frequency Radar (6)
IV-1	Special Radar Systems and Applications	IV-67	Imaging of Moving Targets
IV-2	AN/TPQ-37 Firefinder Radar	IV-68	Stepped Frequency Imaging (1)
IV-3	Firefinder Radar Antenna (1)	IV-69	Stepped Frequency Imaging (2)
IV-4	Firefinder Radar Antenna (2)	IV-70	Stepped Frequency Imaging (3)
IV-5	AN/TPQ-37 Subarray	IV-71	Ultra-Wide Band Radar (1)
IV-6	Firefinder Radar Antenna (3)	IV-72	Ultra-Wide Band Radar (2)
IV-7	Patriot Air Defense Radar (1)	IV-73	Ultra-Wide Band Radar (3)
IV-8	Patriot Air Defense Radar (2)	IV-74	Ultra-Wide Band Radar (4)
IV-9	SCR-270 Air Search Radar	IV-75	Ultra-Wide Band Radar (5)
IV-10	SCR-270-D Radar	IV-76	Ultra-Wide Band Radar (6)
IV-11	SPY-1 Shipboard Radar	IV-77	Ultra-Wide Band Radar (7)
IV-12	X-Band Search Radar (AN/SPS-64)	IV-78	Ultra-Wide Band Radar (8)
IV-13	AN/SPS-64	IV-79	RCS Considerations
IV-14	C-Band Search Radar (AN/SPS-67)	IV-80	Time Domain Scattering
IV-15	AN/SPS-67	IV-81	F-111 Resonant Frequencies
IV-16	Combat Surveillance Radar (AN/PPS-6)	IV-82	Currents on a F-111 at its First Resonance
IV-17	AN/PPS-6	IV-83	Excitation of the First Resonance
IV-18	Early Air Surveillance Radar (AN/APS-31)	IV-84	Antenna Considerations
IV-19	AN/APS-31	IV-85	Brown Bat Ultrasonic Radar (1)
IV-20	AN/APS-40	IV-86	Brown Bat Ultrasonic Radar (2)
IV-21	AN/APS-40	IV-87	Doppler Weather Radar (1)
IV-22	Plan Position Indicator (PPI)	IV-88	Doppler Weather Radar (2)
IV-23	Radiometers (1)	IV-89	Doppler Weather Radar (3)
IV-24	Radiometers (2)	IV-90	Doppler Weather Radar (4)
IV-25	Radiometers (3)	IV-91	Doppler Weather Radar (5)
IV-26	Radiometers (4)	IV-92	Implementation and Interpretation of Data (1)
IV-27	Radiometers (5)	IV-93	Implementation and Interpretation of Data (2)
IV-28	Harmonic Radar (1)	IV-94	Implementation and Interpretation of Data (3)
IV-29	Harmonic Radar (2)	IV-95	Implementation and Interpretation of Data (4)
IV-30	Harmonic Radar Tracking of Bees	IV-96	Implementation and Interpretation of Data (5)
IV-31	Synthetic Aperture Radar (SAR)	IV-97	Clear Air Echoes and Bragg Scattering
IV-32	SAR (2)	IV-98	Weather Radar Example
IV-33	SAR (3)	IV-99	Monolithic Microwave Integrated Circuits
IV-34	Comparison of Array Factors	IV-100	Tile Concept
IV-35	Image Resolution	IV-101	Module Concept
IV-36	Unfocused SAR (1)	IV-102	MMIC Single Chip Radar (1)
IV-37	Unfocused SAR (2)	IV-103	MMIC Single Chip Radar (2)
IV-38	Focused SAR	IV-104	MMIC FMCW Single Chip Radar (1)
IV-39	Example	IV-105	MMIC FMCW Single Chip Radar (2)
IV-40	Cross Range Processing (1)	IV-106	Defeating Radar Using Chaff
IV-41	Cross Range Processing (2)	IV-107	Chaff (1)
IV-42	Cross Range Processing (3)	IV-108	Chaff (2)
IV-43	Motion Compensation	IV-109	Chaff (3)
IV-44	Radar Mapping	IV-110	Chaff and Flares

IV-111 Bistatic Radar (1)  
IV-112 Bistatic Radar (2)  
IV-113 Flight-Tracking Firm Takes Off  
IV-114 Bistatic Radar (3)  
IV-115 Bistatic Radar (4)  
IV-116 Bistatic Radar Example (1)  
IV-117 Bistatic Radar (5)  
IV-118 Bistatic Radar (6)  
IV-119 Bistatic Radar (7)  
IV-120 Bistatic Radar (8)  
IV-121 Bistatic Radar (9)  
IV-122 Bistatic Radar (10)  
IV-123 Bistatic Radar Example (2)  
IV-124 Line-of-Sight Constrained Coverage (1)  
IV-125 Line-of-Sight Constrained Coverage (2)  
IV-126 Bistatic Radar (11)  
IV-127 Bistatic Radar (12)  
IV-128 Bistatic Footprint and Clutter Area (1)  
IV-129 Bistatic Footprint and Clutter Area (2)  
IV-130 Bistatic Radar Cross Section (1)  
IV-131 Bistatic Radar Cross Section (2)  
IV-132 Bistatic Radar Example Revisited  
IV-133 Bistatic Radar Cross Section (3)  
IV-134 Cross Eye Jamming (1)  
IV-135 Cross Eye Jamming (2)  
IV-136 ECM for Conical Scanning  
IV-137 Ground Bounce ECM  
IV-138 Suppression of Sidelobe Jammers (1)  
IV-139 Suppression of Sidelobe Jammers (2)  
IV-140 CSLC Equations for an Array Antenna  
IV-141 CSLC Performance  
IV-142 Adaptive Antennas  
IV-143 Laser Radar (1)  
IV-144 Laser Radar (2)  
IV-145 Laser Radar (3)  
IV-146 Laser Radar (4)  
IV-147 Laser Radar (5)  
IV-148 Laser Radar (6)  
IV-149 Laser Radar (7)  
IV-150 Laser Radar (8)  
IV-151 Ground Penetrating Radar (1)  
IV-152 Ground Penetrating Radar (2)  
IV-153 Ground Penetrating Radar (3)  
IV-154 Ground Penetrating Radar (4)  
IV-155 Ground Penetrating Radar (5)  
IV-156 Ground Penetrating Radar (6)  
IV-157 Ground Penetrating Radar (7)  
IV-158 Ground Penetrating Radar (8)

# Electromagnetic Fields and Waves (1)

---

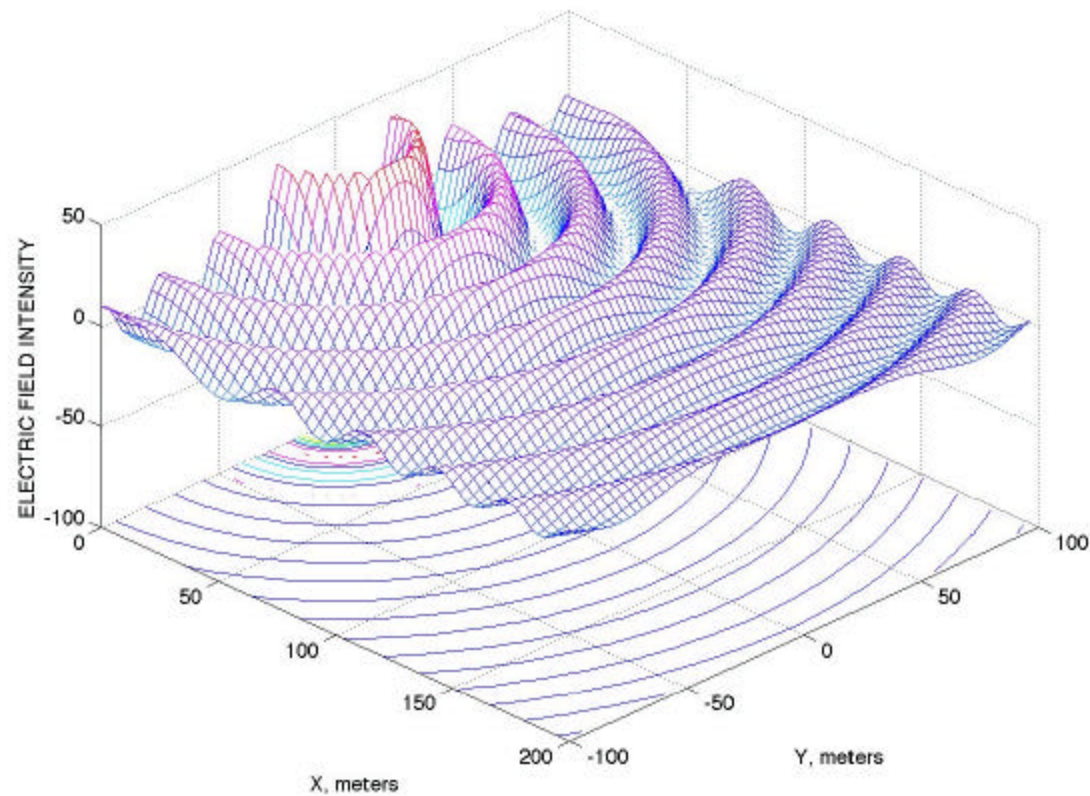
Radar is based on the sensing of electromagnetic waves reflected from objects. Energy is emitted from a source (antenna) and propagates outward. A point on the wave travels with a phase velocity  $u_p$ , which depends on the electronic properties of the medium in which the wave is propagating. From antenna theory: if the observer is sufficiently far from the source, then the surfaces of constant phase (wavefronts) are spherical. At even larger distances the wavefronts become approximately planar.



# Electromagnetic Fields and Waves (2)

---

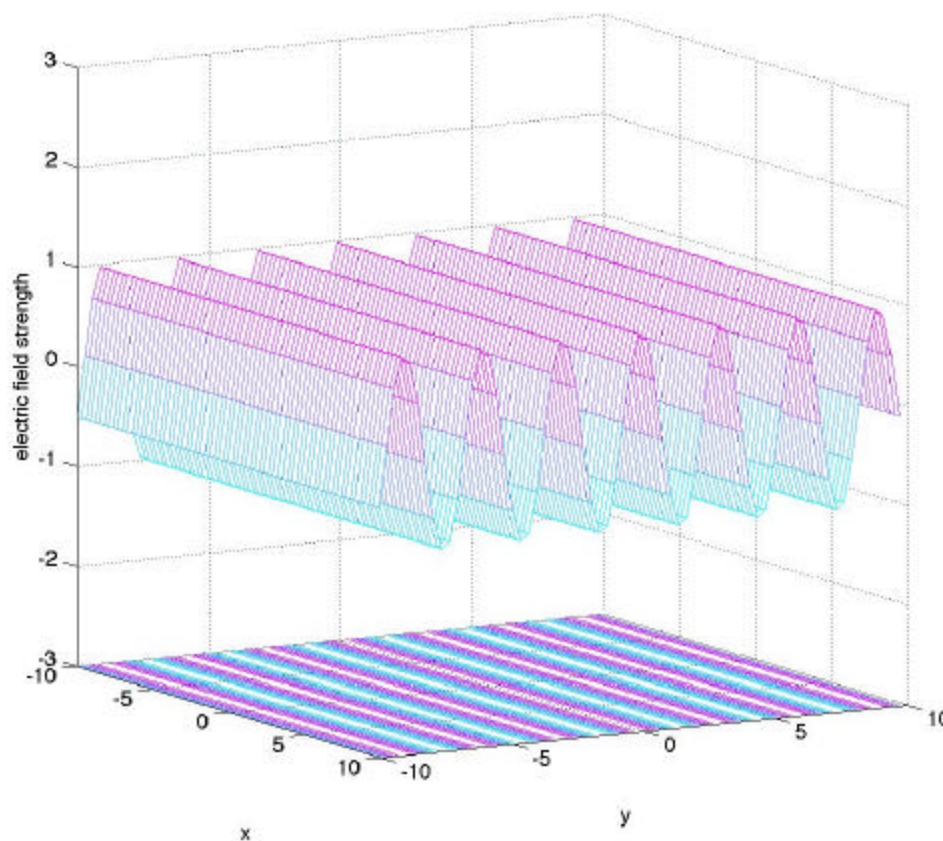
Snapshot of a spherical wave propagating outward from the origin. The amplitude of the wave  $\vec{E}(R, t) = \hat{\mathbf{q}} \frac{E_0}{R} \cos(\omega t - \mathbf{b}R)$  in the  $x$ - $y$  plane is plotted at time  $t = 0$





# Electromagnetic Fields and Waves (3)

Snapshot of a plane wave propagating in the +y direction  $\vec{E}(y,t) = \hat{z}E_0 \cos(\omega t - \beta y)$  at time  $t = 0$



# Electromagnetic Fields and Waves (4)

---

Electrical properties of a medium are specified by its constitutive parameters:

- permeability,  $\boldsymbol{\mu} = \boldsymbol{\mu}_0 \boldsymbol{\mu}_r$  (for free space,  $\boldsymbol{\mu} \equiv \boldsymbol{\mu}_0 = 4\pi \times 10^{-7}$  H/m)
- permittivity,  $\boldsymbol{\epsilon} = \boldsymbol{\epsilon}_0 \boldsymbol{\epsilon}_r$  (for free space,  $\boldsymbol{\epsilon} \equiv \boldsymbol{\epsilon}_0 = 8.85 \times 10^{-12}$  F/m)
- conductivity,  $\boldsymbol{\sigma}$  (for a metal,  $\boldsymbol{\sigma} \sim 10^7$  S/m)

Electric and magnetic field intensities:  $\vec{E}(x, y, z, t)$  V/m and  $\vec{H}(x, y, z, t)$  A/m

- vector functions of location in space and time, e.g., in cartesian coordinates

$$\vec{E}(x, y, z, t) = \hat{x}E_x(x, y, z, t) + \hat{y}E_y(x, y, z, t) + \hat{z}E_z(x, y, z, t)$$

- similar expressions for other coordinates systems
- the fields arise from current  $\vec{J}$  and charge  $\boldsymbol{r}_v$  on the source ( $\vec{J}$  is the volume current density in A/m<sup>2</sup> and  $\boldsymbol{r}_v$  is volume charge density in C/m<sup>3</sup>)

Electromagnetic fields are completely described by Maxwell's equations:

$$\begin{aligned} (1) \nabla \times \vec{E} &= -\boldsymbol{\mu} \frac{\partial \vec{H}}{\partial t} & (3) \nabla \cdot \vec{H} &= 0 \\ (2) \nabla \times \vec{H} &= \vec{J} + \boldsymbol{\epsilon} \frac{\partial \vec{E}}{\partial t} & (4) \nabla \cdot \vec{E} &= \boldsymbol{r}_v / \boldsymbol{\epsilon} \end{aligned}$$

# Electromagnetic Fields and Waves (5)

---

The wave equations are derived from Maxwell's equations:

$$\nabla^2 \vec{E} - \frac{1}{u_p^2} \frac{\partial^2 \vec{E}}{\partial t^2} = 0 \quad \nabla^2 \vec{H} - \frac{1}{u_p^2} \frac{\partial^2 \vec{H}}{\partial t^2} = 0$$

The phase velocity is  $u_p = \omega \sqrt{\mu \epsilon}$  (in free space  $u_p = c = 2.998 \times 10^8$  m/s)

The simplest solutions to the wave equations are plane waves. An example for a plane wave propagating in the  $z$  direction is:

$$\vec{E}(z, t) = \hat{x} E_0 e^{-\mathbf{a}z} \cos(\mathbf{w}t - \mathbf{b}z)$$

- $\mathbf{a}$  = attenuation constant (Np/m);  $\mathbf{b} = 2\mathbf{p}/\mathbf{l} =$  phase constant (rad/m)
- $\mathbf{l}$  = wavelength;  $\mathbf{w} = 2\mathbf{p}f$  (rad/sec);  $f$  = frequency (Hz);  $f = \frac{u_p}{\mathbf{l}}$

Features of this plane wave:

- propagating in the  $+z$  direction
- $x$  polarized (direction of electric field vector is  $\hat{x}$ )
- amplitude of the wave is  $E_0$

# Electromagnetic Fields and Waves (6)

---

Time-harmonic sources, currents, and fields: sinusoidal variation in time and space. Suppress the time dependence for convenience and work with time independent quantities called phasors. A time-harmonic plane wave is represented by the phasor  $\vec{E}(z)$

$$\vec{E}(z, t) = \text{Re} \left\{ \hat{x} E_0 e^{-(\mathbf{a} + j\mathbf{b})z} e^{j\omega t} \right\} = \text{Re} \left\{ \vec{E}(z) e^{j\omega t} \right\}$$

$\vec{E}(z)$  is the phasor representation;  $\vec{E}(z, t)$  is the instantaneous quantity

$\text{Re}\{\cdot\}$  is the real operator (i.e., “take the real part of”)

$$j = \sqrt{-1}$$

Since the time dependence varies as  $e^{j\omega t}$ , the time derivatives in Maxwell’s equations are replaced by  $\nabla / \partial t \equiv j\omega$ :

$$(1) \nabla \times \vec{E} = -j\omega \mu \vec{H} \quad (3) \nabla \cdot \vec{H} = 0$$

$$(2) \nabla \times \vec{H} = \vec{J} + j\omega \epsilon \vec{E} \quad (4) \nabla \cdot \vec{E} = \mathbf{r}_v / \epsilon$$

The wave equations are derived from Maxwell’s equations:

$$\nabla^2 \vec{E} - \mathbf{g}^2 \vec{E} = 0$$

$$\nabla^2 \vec{H} - \mathbf{g}^2 \vec{H} = 0$$

where  $\mathbf{g} = \mathbf{a} + j\mathbf{b}$  is the propagation constant.

# Electromagnetic Fields and Waves (7)

---

Plane and spherical waves belong to the to a class called transverse electromagnetic (TEM) waves. They have the following features:

1.  $\vec{E}$ ,  $\vec{H}$  and the direction of propagation  $\hat{k}$  are mutually orthogonal
2.  $\vec{E}$  and  $\vec{H}$  are related by the intrinsic impedance of the medium

$$\mathbf{h} = \sqrt{\frac{\mathbf{n}}{(\mathbf{e} - j\mathbf{s} / \mathbf{w})}} \Rightarrow \mathbf{h}_o = \sqrt{\frac{\mathbf{n}_o}{\mathbf{e}_o}} \approx 377 \Omega \text{ for free space}$$

The above relationships are expressed in the vector equation  $\vec{H} = \frac{\hat{k} \times \vec{E}}{\mathbf{h}}$

The time-averaged power propagating in the plane wave is given by the Poynting vector:

$$\vec{W} = \frac{1}{2} \text{Re} \{ \vec{E} \times \vec{H}^* \} \text{ W/m}^2$$

For a plane wave:  $\vec{W}(z) = \frac{1}{2} \frac{|E_o|^2}{\mathbf{h}} \hat{z}$

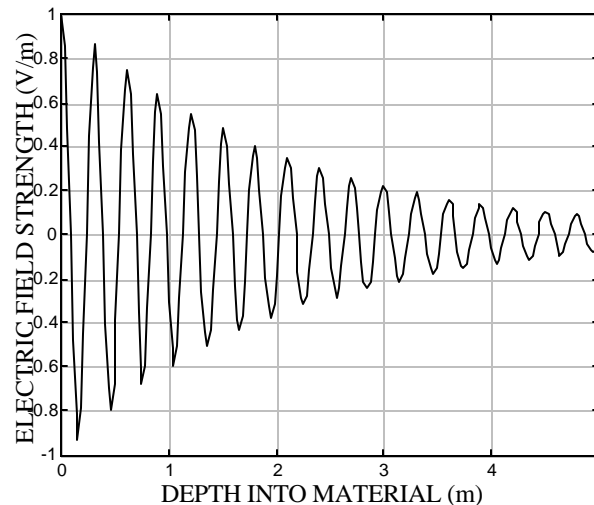
For a spherical wave:  $\vec{W}(R) = \frac{1}{2\mathbf{h}} \frac{|E_o|^2}{R^2} \hat{R}$  (inverse square law for power spreading)

# Electromagnetic Fields and Waves (8)

A material's conductivity causes attenuation of a wave as it propagates through the medium. Energy is extracted from the wave and dissipated as heat (ohmic loss). The attenuation constant determines the rate of decay of the wave. In general:

$$\mathbf{a} = \mathbf{w} \left\{ \frac{\mathbf{me}}{2} \left[ \sqrt{1 + \left( \frac{\mathbf{s}}{\mathbf{we}} \right)^2} - 1 \right] \right\}^{1/2} \quad \mathbf{b} = \mathbf{w} \left\{ \frac{\mathbf{me}}{2} \left[ \sqrt{1 + \left( \frac{\mathbf{s}}{\mathbf{we}} \right)^2} + 1 \right] \right\}^{1/2}$$

For lossless media  $\mathbf{s} = 0 \Rightarrow \mathbf{a} = 0$ . Traditionally, for lossless cases,  $k$  is used rather than  $\mathbf{b}$ . For good conductors ( $\mathbf{s} / \mathbf{we} \gg 1$ ),  $\mathbf{a} \approx \sqrt{\mathbf{pnfs}}$ , and the wave decays rapidly with distance into the material.

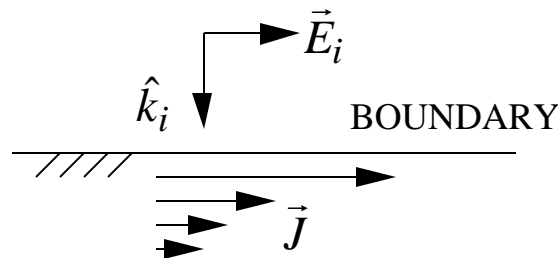


Sample plot of field vs. distance

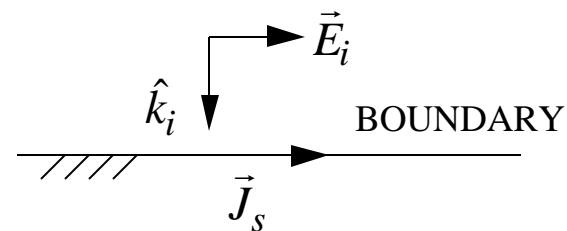
# Electromagnetic Fields and Waves (9)

For good conductors the current is concentrated near the surface. The current can be approximated by an infinitely thin current sheet, or surface current,  $\vec{J}_s$  A/m and surface charge,  $r_s$  C/m

Current in a good conductor

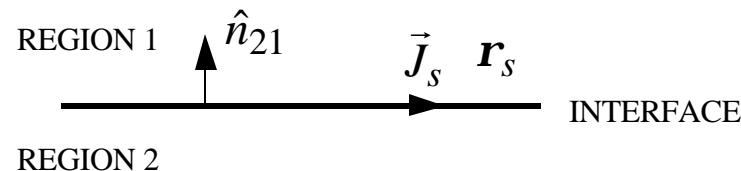


Surface current approximation



At an interface between two media the boundary conditions must be satisfied:

- (1)  $\hat{n}_{21} \times (\vec{E}_1 - \vec{E}_2) = 0$
- (2)  $\hat{n}_{21} \times (\vec{H}_1 - \vec{H}_2) = \vec{J}_s$
- (3)  $\hat{n}_{21} \cdot (\vec{E}_1 - \vec{E}_2) = r_s / \epsilon$
- (4)  $\hat{n}_{21} \cdot (\vec{H}_1 - \vec{H}_2) = 0$



# Wave Reflection (1)

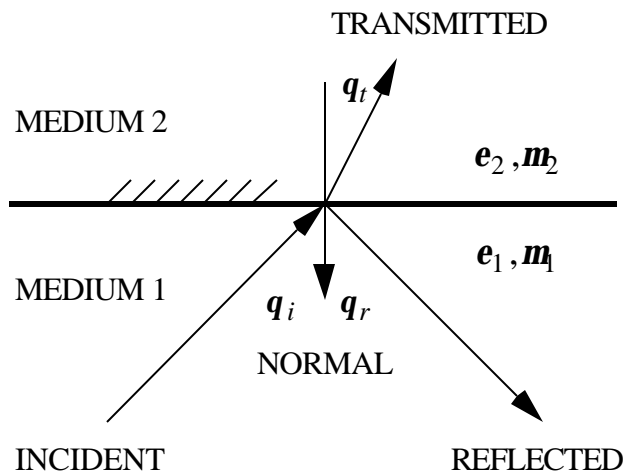
For the purposes of applying boundary conditions, the electric field vector is decomposed into parallel and perpendicular components  $\vec{E} = \vec{E}_\perp + \vec{E}_\parallel$

$\vec{E}_\perp$  is perpendicular to the plane of incidence

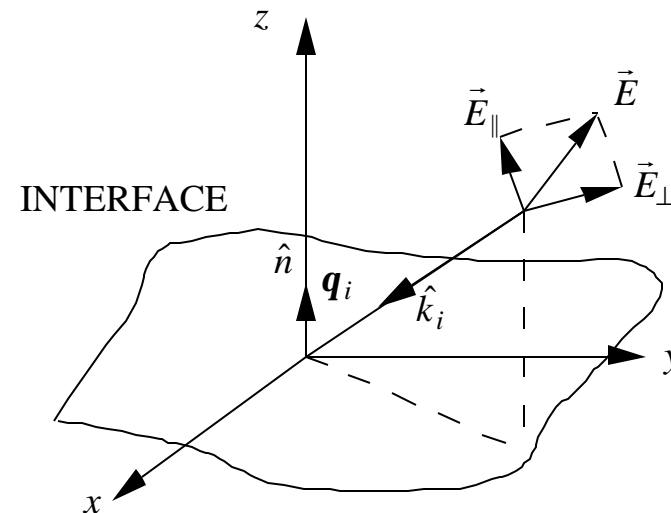
$\vec{E}_\parallel$  lies in the plane of incidence

The plane of incidence is defined by the vectors  $\hat{k}_i$  and  $\hat{n}$

PLANE WAVE INCIDENT ON AN INTERFACE BETWEEN TWO DIELECTRICS



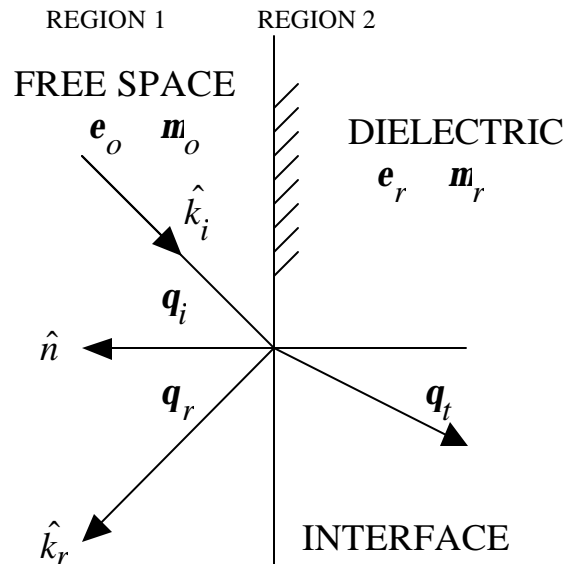
DECOMPOSITION OF AN ELECTRIC FIELD VECTOR INTO PARALLEL AND PERPENDICULAR COMPONENTS





# Wave Reflection (2)

Plane wave incident on an interface between free space and a dielectric



$$\sin q_i = \sin q_r = \sqrt{\epsilon_r \mu_r} \sin q_t$$

$$h_o = \sqrt{\frac{\mu_o}{\epsilon_o}} \text{ and } h = \sqrt{\frac{\mu_r \mu_o}{\epsilon_r \epsilon_o}} = h_o \sqrt{\frac{\mu_r}{\epsilon_r}}$$

Reflection and transmission coefficients:

Perpendicular polarization:

$$\Gamma_{\perp} = \frac{h \cos q_i - h_o \cos q_t}{h \cos q_i + h_o \cos q_t}$$

$$t_{\perp} = \frac{2h \cos q_i}{h \cos q_i + h_o \cos q_t}$$

$$E_{r\perp} = \Gamma_{\perp} E_{i\perp} \text{ and } E_{t\perp} = t_{\perp} E_{i\perp}$$

Parallel polarization:

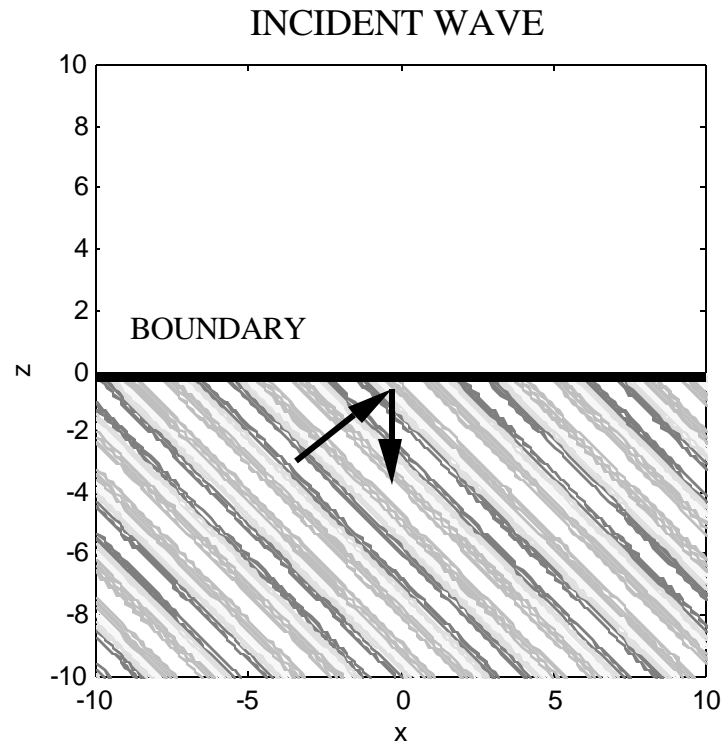
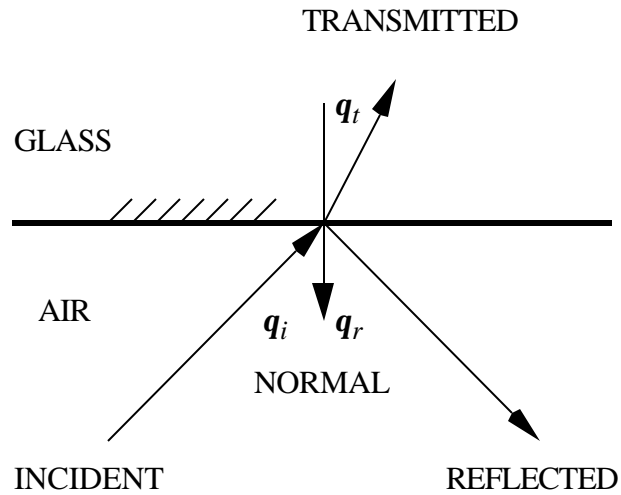
$$\Gamma_{\parallel} = \frac{h \cos q_t - h_o \cos q_i}{h \cos q_t + h_o \cos q_i}$$

$$t_{\parallel} = \frac{2h \cos q_i}{h \cos q_t + h_o \cos q_i}$$

$$E_{r\parallel} = \Gamma_{\parallel} E_{i\parallel} \text{ and } E_{t\parallel} = t_{\parallel} E_{i\parallel}$$

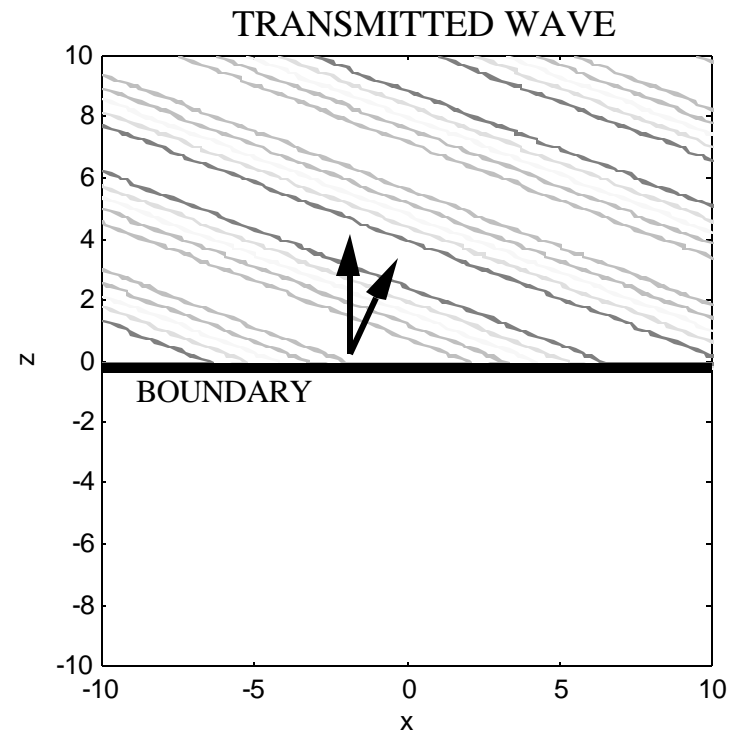
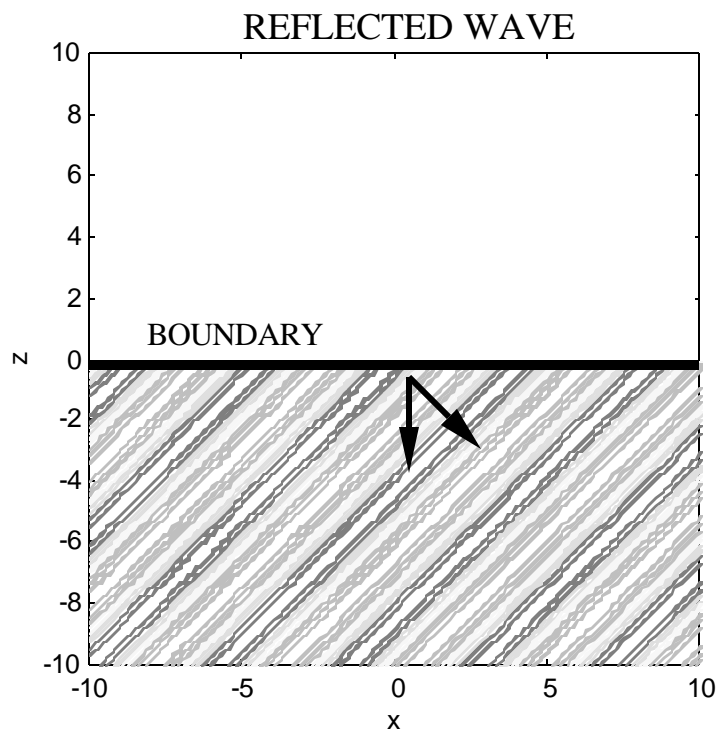
# Wave Reflection (3)

Example of a plane wave incident on a boundary between air and glass ( $\epsilon_r = 4, \mathbf{q}_i = 45^\circ$ )



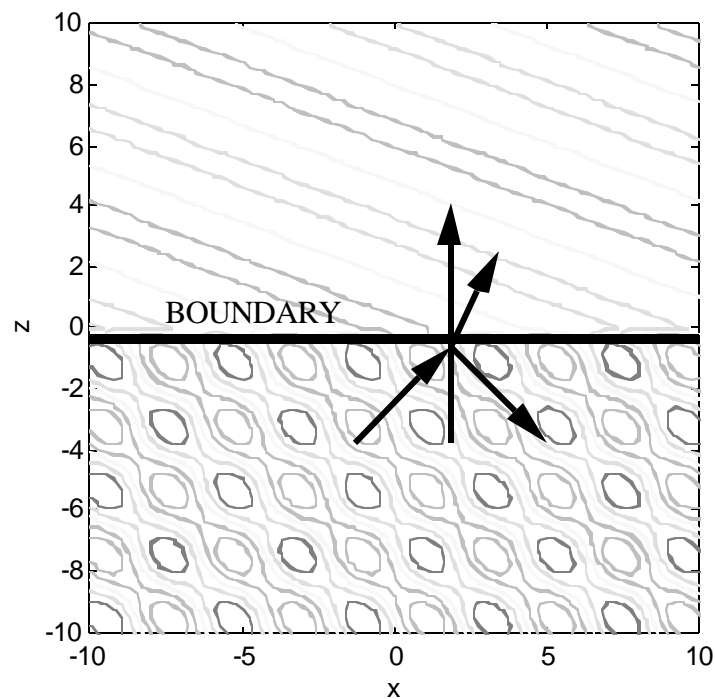
# Wave Reflection (4)

Example of a plane wave reflection: reflected and transmitted waves ( $\epsilon_r = 4, \theta_i = 45^\circ$ )



# Wave Reflection (5)

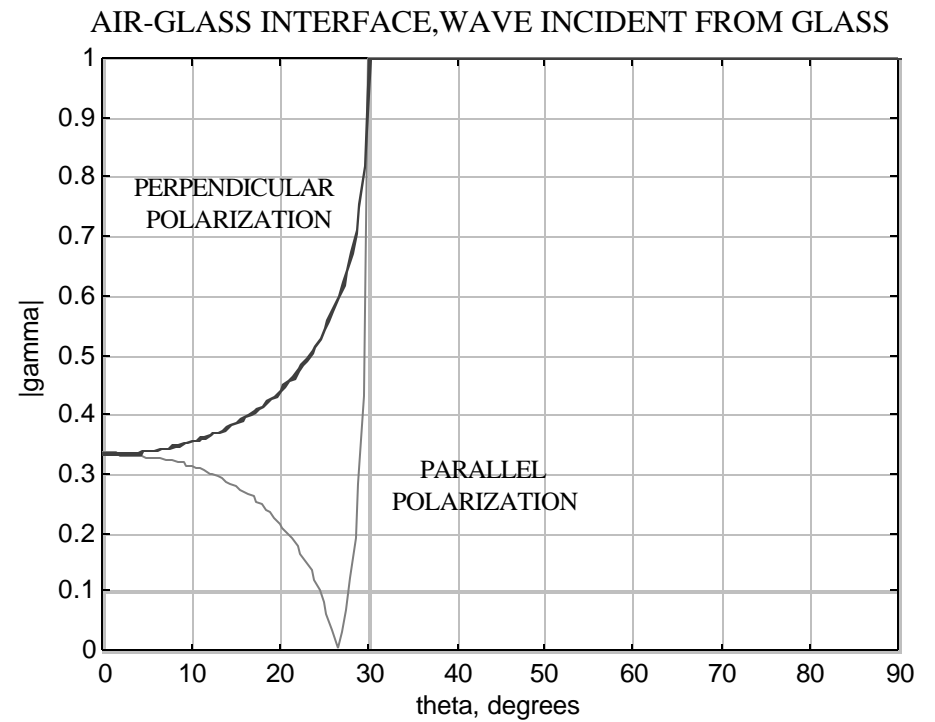
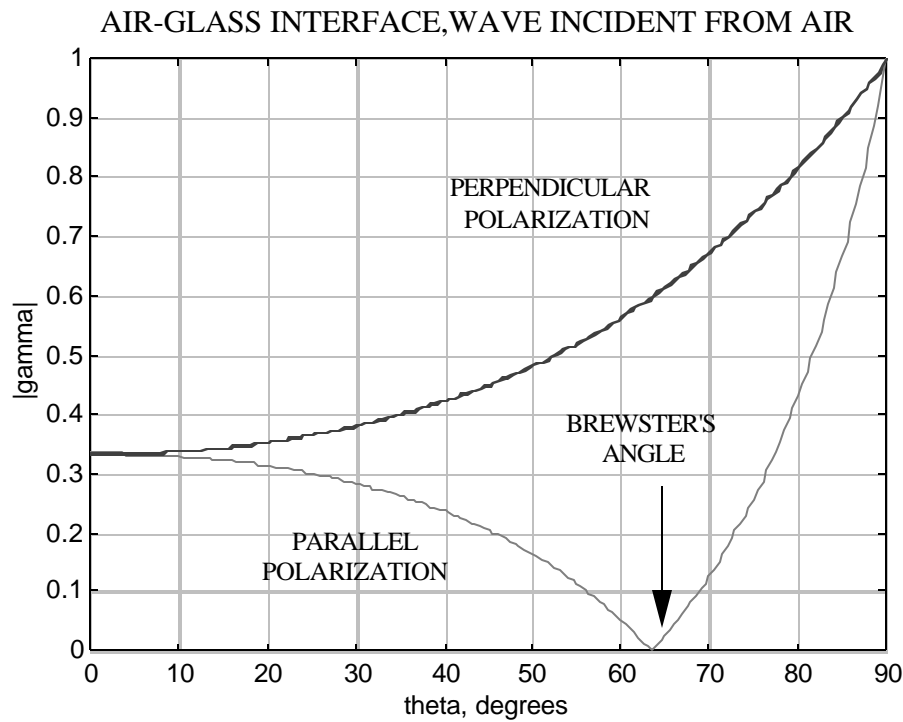
Example of a plane wave reflection: total field



- The total field in region 1 is the sum of the incident and reflected fields
- If region 2 is more dense than region 1 (i.e.,  $\epsilon_{r2} > \epsilon_{r1}$ ) the transmitted wave is refracted towards the normal
- If region 1 is more dense than region 2 (i.e.,  $\epsilon_{r1} > \epsilon_{r2}$ ) the transmitted wave is refracted away from the normal

# Wave Reflection (6)

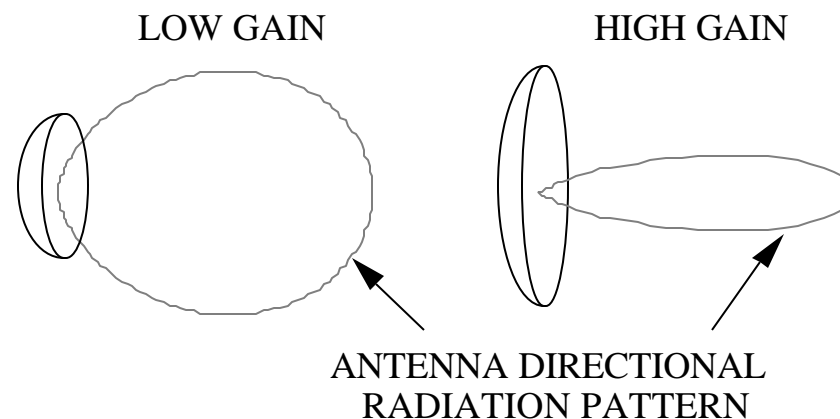
Boundary between air ( $\epsilon_r = 1$ ) and glass ( $\epsilon_r = 4$ )



# Antenna Patterns, Directivity and Gain

---

- The antenna pattern is a directional plot of the received or transmitted signal
- From a systems point of view, two important antenna parameters are gain and beamwidth
- Both gain and beamwidth are measures of the antenna's capability to focus radiation
- Gain includes loss that occurs within the antenna whereas directivity refers to a lossless antenna of the same type (i.e., it is an ideal reference)
- In general, an increase in gain is accompanied by a decrease in beamwidth, and is achieved by increasing the antenna size relative to the wavelength
- With regard to radar, high gain and narrow beams are desirable for long detection and tracking ranges and accurate direction measurement

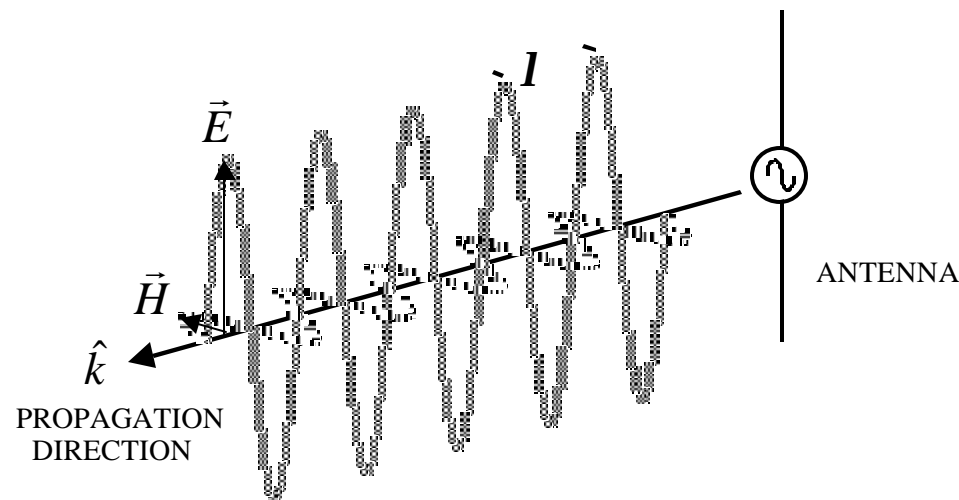


# Polarization of Radiation

---

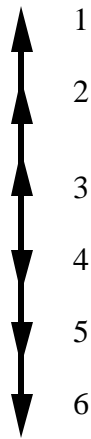
Example of a plane wave generated by a linearly polarized antenna:

1. Finite sources generate spherical waves, but they are locally planar over limited regions of space
2. Envelopes of the electric and magnetic field vectors are plotted
3.  $\vec{E}$  and  $\vec{H}$  are orthogonal to each other and the direction of propagation. Their magnitudes are related by the intrinsic impedance of the medium (i.e., TEM)
4. Polarization refers to the curve that the tip of  $\vec{E}$  traces out with time at a fixed point in space. It is determined by the antenna geometry and its orientation relative to the observer

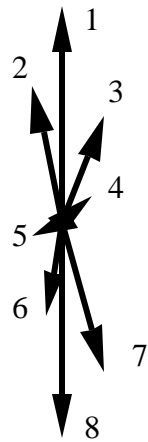


# Wave Polarization

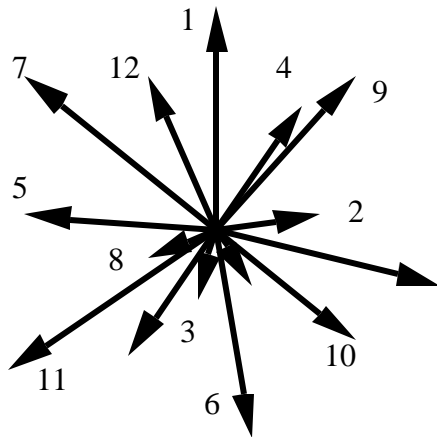
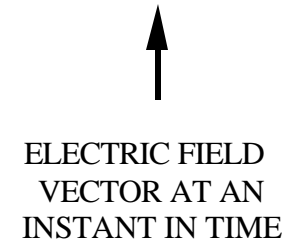
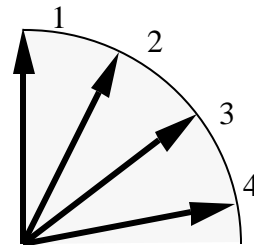
LINEAR  
POLARIZATION



PARTIALLY  
POLARIZED

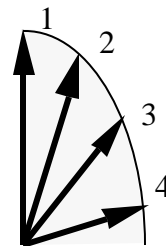


CIRCULAR  
POLARIZATION



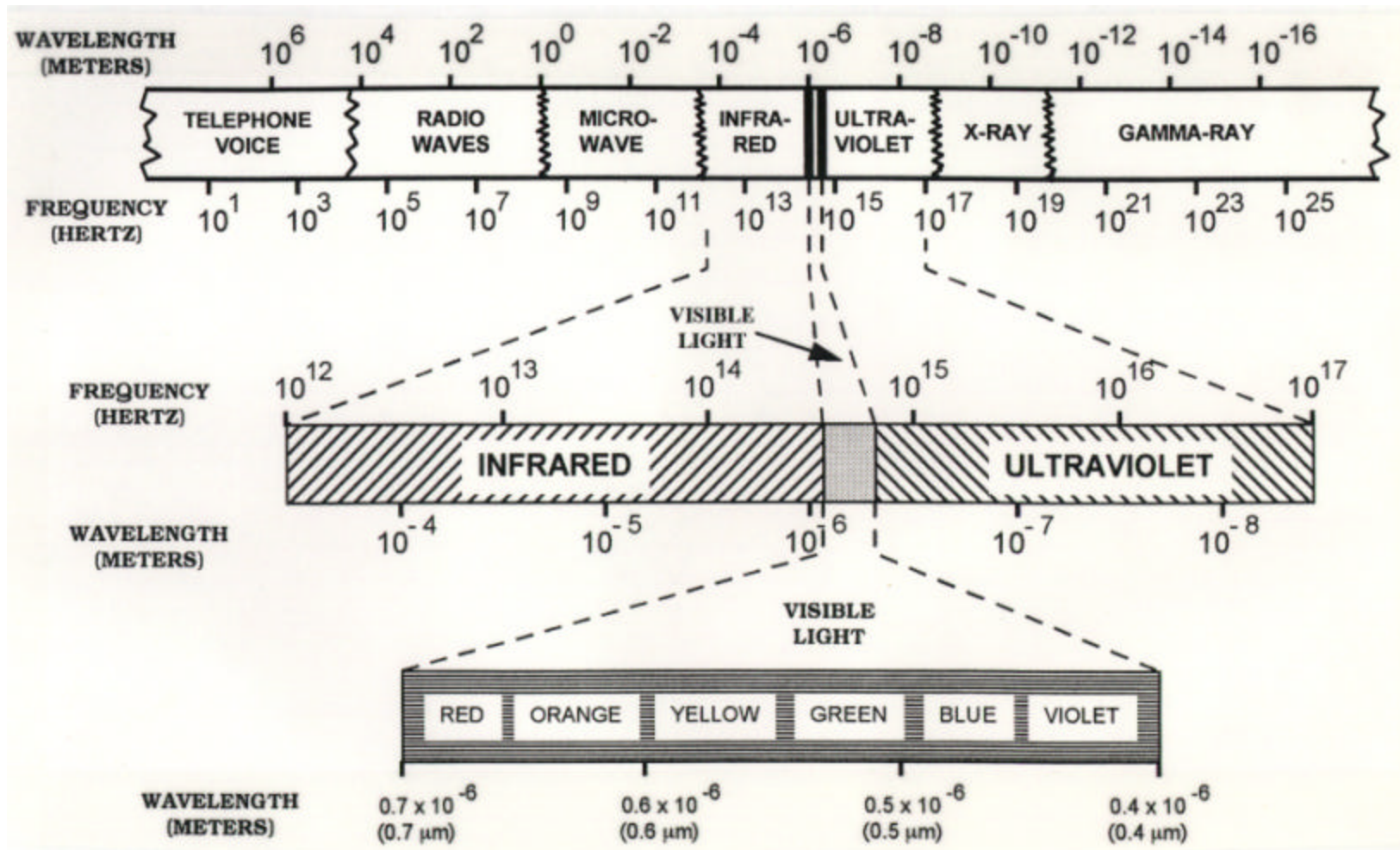
UNPOLARIZED  
(RANDOM  
POLARIZATION)

ELLIPTICAL  
POLARIZATION





# Electromagnetic Spectrum



# Radar and ECM Frequency Bands

Standard Radar Bands <sup>1</sup>		ECM Bands <sup>2</sup>	
Band Designation <sup>3</sup>	Frequency Range (MHz)	Band Designation	Frequency Range (MHz)
HF	3–30	Alpha	0–250
VHF <sup>4</sup>	30–300	Bravo	250–500
UHF <sup>4</sup>	300–1,000	Charlie	500–1,000
L	1,000–2,000	Delta	1,000–2,000
S	2,000–4,000	Echo	2,000–3,000
C	4,000–8,000	Foxtrot	3,000–4,000
X	8,000–12,000	Golf	4,000–6,000
K <sub>u</sub>	12,000–18,000	Hotel	6,000–8,000
K	18,000–27,000	India	8,000–10,000
K <sub>a</sub>	27,000–40,000	Juliett	10,000–20,000
millimeter <sup>5</sup>	40,000–300,000	Kilo	20,000–40,000
		Lima	40,000–60,000
		Mike	60,000–100,000

<sup>1</sup> From IEEE Standard 521-1976, November 30 1976.  
<sup>2</sup> From AFR 55-44 (AR105-96, OPNAVINST 3420.9B, MCO 3430.1), October 27, 1964.  
<sup>3</sup> British usage in the past has corresponded generally but not exactly to the letter-designated bands.  
<sup>4</sup> The following *approximate* lower frequency ranges are sometimes given letter designations: P-band (225–390 MHz), G-band (150–225 MHz), and I-band (100–150 MHz).  
<sup>5</sup> The following *approximate* higher frequency ranges are sometimes given letter designations: Q-band (36–46 GHz), V-band (46–56 GHz), and W-band (56–100 GHz).

# Radar Bands and Usage

<b>Band Designation</b>	<b>Frequency Range</b>	<b>Usage</b>
HF	3–30 MHz	OTH surveillance
VHF	30–300 MHz	Very-long-range surveillance
UHF	300–1,000 MHz	Very-long-range surveillance
L	1–2 GHz	Long-range surveillance En route traffic control
S	2–4 GHz	Moderate-range surveillance Terminal traffic control Long-range weather
C	4–8 GHz	Long-range tracking Airborne weather detection
X	8–12 GHz	Short-range tracking Missile guidance Mapping, marine radar Airborne intercept
K <sub>u</sub>	12–18 GHz	High-resolution mapping Satellite altimetry
K	18–27 GHz	Little use (water vapor)
K <sub>a</sub>	27–40 GHz	Very-high-resolution mapping Airport surveillance
millimeter	40–100+ GHz	Experimental

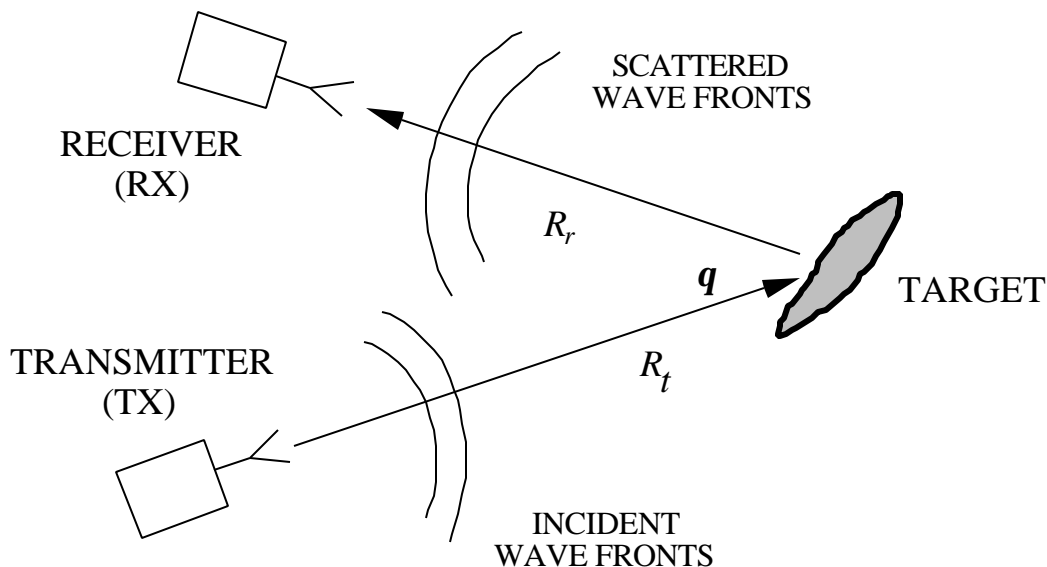
# Joint Electronics Type Designation

<u>First Letter</u>	<u>Second Letter</u>	<u>Third Letter</u>
A – Airborne (installed and operated in aircraft)	A – Infrared, heat radiation	A – Auxiliary assemblies (not complete operating sets used with or part of two or more sets or sets series)
B – Underwater mobile, submarine	B – Pigeon	B – Bombing
C – Air transportable (inactivated, do not use)	C – Carrier (wire)	C – Communications
D – Pilotless carrier	D – Radiac	D – Direction finder and/or reconnaissance
F – Fixed	E – Nupac	E – Ejection and/or release
G – Ground, general ground use (includes two or more ground-type installations)	F – Photographic	G – Fire control or search light directing
K – Amphibious	G – Telegraph or teletype	H – Recording and/or reproducing (graphic meteorological and sound)
M – Ground, mobile (installed as operating unit in a vehicle which has no function other than transporting the equipment)	I – Interphone and public address	L – Searchlight control (inactivated, use G)
P – Pack or portable (animal or man)	J – Electromechanical (not otherwise covered)	M – Maintenance and test assemblies (including tools)
S – Water surface craft	K – Telemetry	N – Navigational aids (including altimeters, beacons, compasses, racons, depth sounding, approach, and landing)
T – Ground, transportable	L – Countermeasures	P – Reproducing (inactivated, do not use)
U – General utility (includes two or more general installation classes, airborne, shipboard, and ground)	M – Meteorological	Q – Special, or combination of purposes
V – Ground, vehicular (installed in vehicle designed for functions other than carrying electronic equipment, etc., such as tanks)	N – Sound in air	R – Receiving, passive detecting
W – Water surface and underwater	P – Radar	S – Detecting and/or range and bearing
	Q – Sonar and underwater sound	T – Transmitting
	R – Radio	W – Control
	S – Special types, magnetics, etc., or combinations of types	X – Identification and recognition
	T – Telephone (wire)	
	V – Visual and visible light	
	W – Armament (peculiar to armament, not otherwise covered)	
	X – Facsimile or television	
	Y – Data processing	



# Radio Detection and Ranging (RADAR)

---



Bistatic: the transmit and receive antennas are at different locations as viewed from the target (e.g., ground transmitter and airborne receiver,  $q \neq 0$ )

Monostatic: the transmitter and receiver are colocated as viewed from the target (i.e., the same antenna is used to transmit and receiver,  $q = 0$ )

Quasi-monostatic: the transmit and receive antennas are slightly separated but still appear to be at the same location as viewed from the target (e.g., separate transmit and receive antennas on the same aircraft,  $q \approx 0$ )

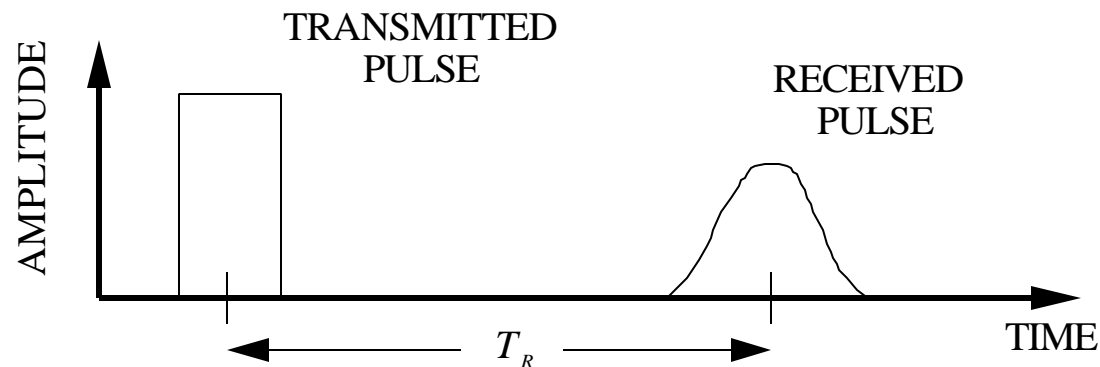
# Time Delay Ranging

---

Target range is the fundamental quantity measured by most radars. It is obtained by recording the round trip travel time of a pulse,  $T_R$ , and computing range from:

$$\begin{aligned} \text{bistatic:} \quad & R_t + R_r = cT_R \\ \text{monostatic:} \quad & R = \frac{cT_R}{2} \quad (R_r = R_t \equiv R) \end{aligned}$$

where  $c \approx 3 \times 10^8$  m/s is the velocity of light in free space.



# Information Available From the Radar Echo

---

"Normal" radar functions:

1. range (from pulse delay)
2. velocity (from doppler frequency shift)
3. angular direction (from antenna pointing)
4. target size (from magnitude of return)

Signature analysis and inverse scattering:

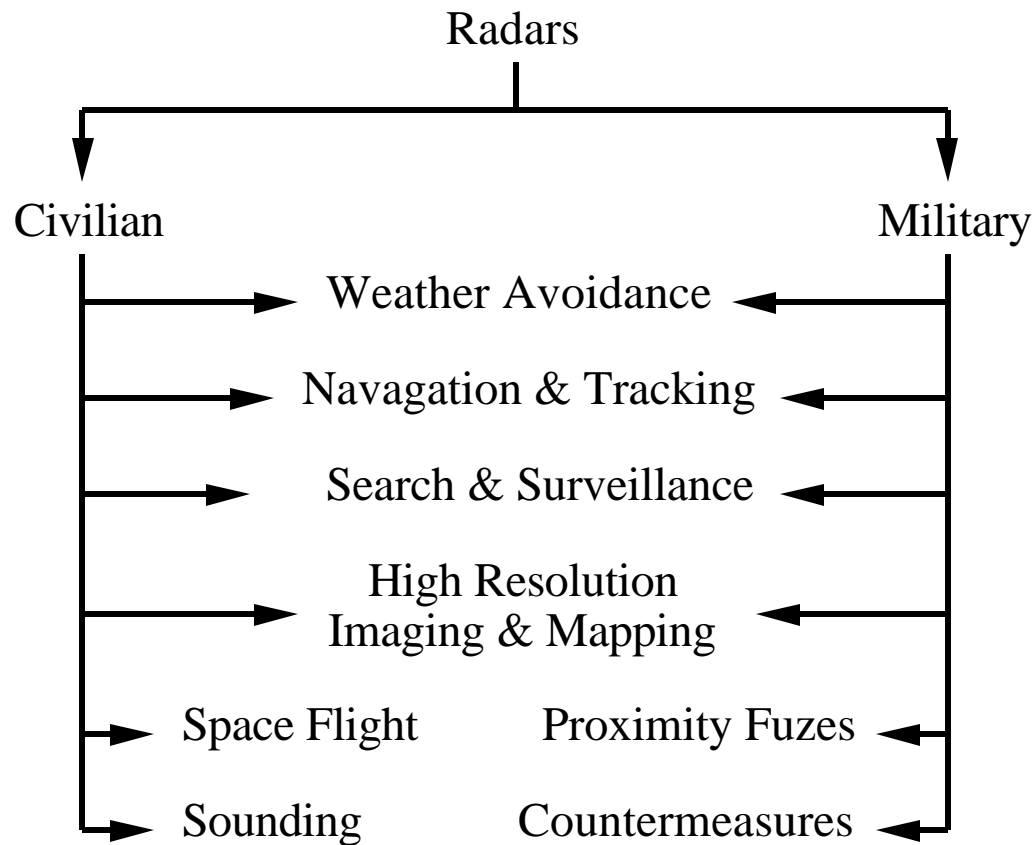
5. target shape and components (return as a function of direction)
6. moving parts (modulation of the return)
7. material composition

The complexity (cost & size) of the radar increases with the extent of the functions that the radar performs.



# Radar Classification by Function

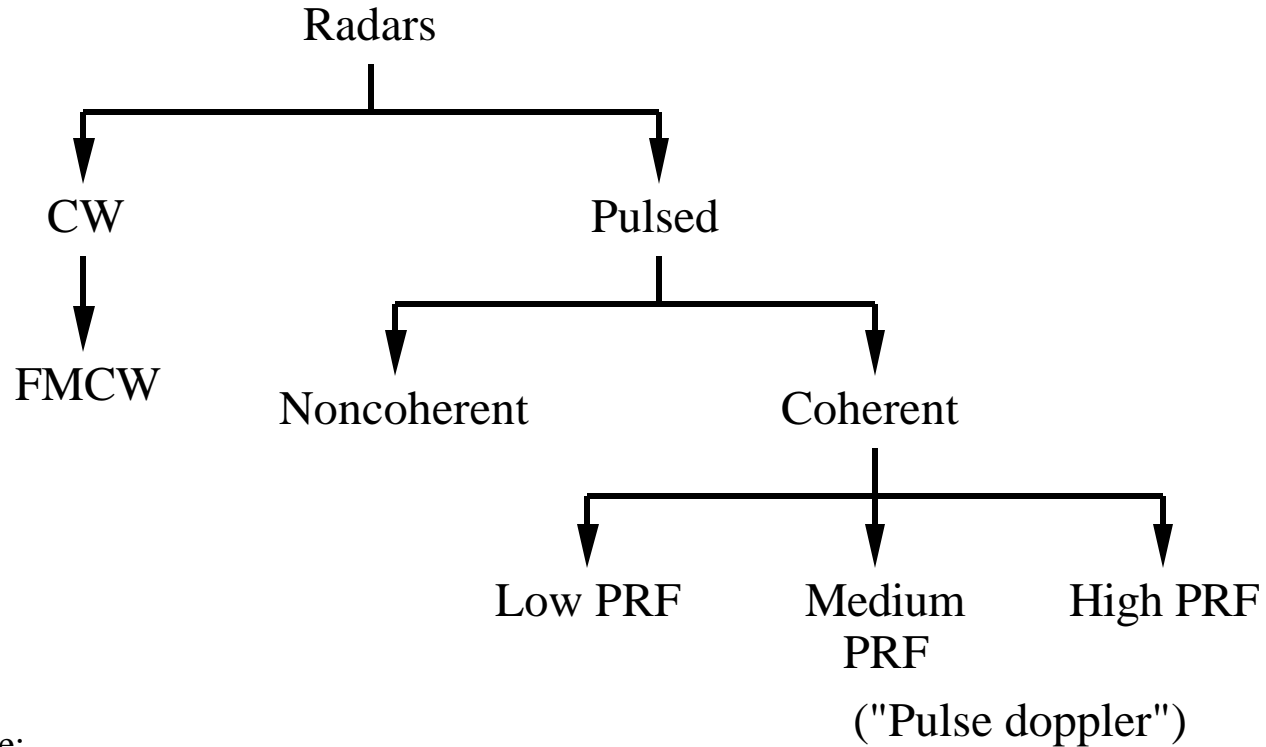
---



Many modern radars perform multiple functions ("multi-function radar")

# Radar Classification by Waveform

---



Note:

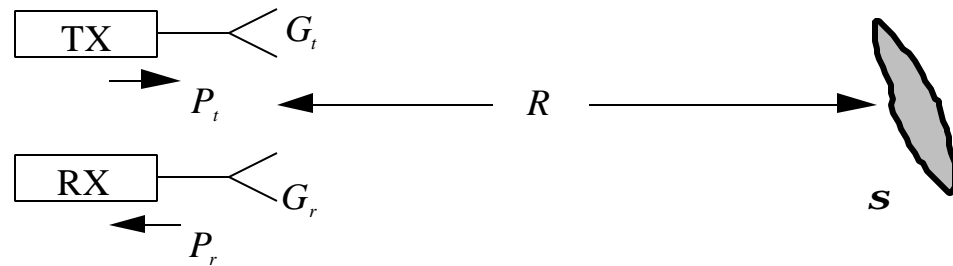
CW = continuous wave

FMCW = frequency modulated continuous wave

PRF = pulse repetition frequency

# Basic Form of the Radar Range Equation (1)

“Quasi-monostatic” geometry



$S$  = radar cross section (RCS) in square meters

$P_t$  = transmitter power, watts

$P_r$  = received power, watts

$G_t$  = transmit antenna gain in the direction of the target (assumed to be the maximum)

$G_r$  = receive antenna gain in the direction of the target (assumed to be the maximum)

$P_t G_t$  = effective radiated power (ERP)

From antenna theory:  $G_r = \frac{4\pi A_{er}}{\lambda^2}$

$A_{er} = A_p \boldsymbol{r}$  = effective area of the receive antenna

$A_p$  = physical aperture area of the antenna

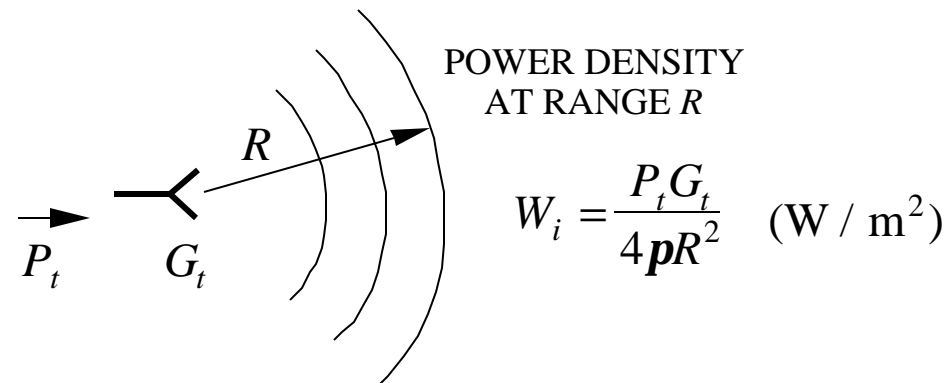
$\lambda$  = wavelength ( $= c / f$ )

$\boldsymbol{r}$  = antenna efficiency

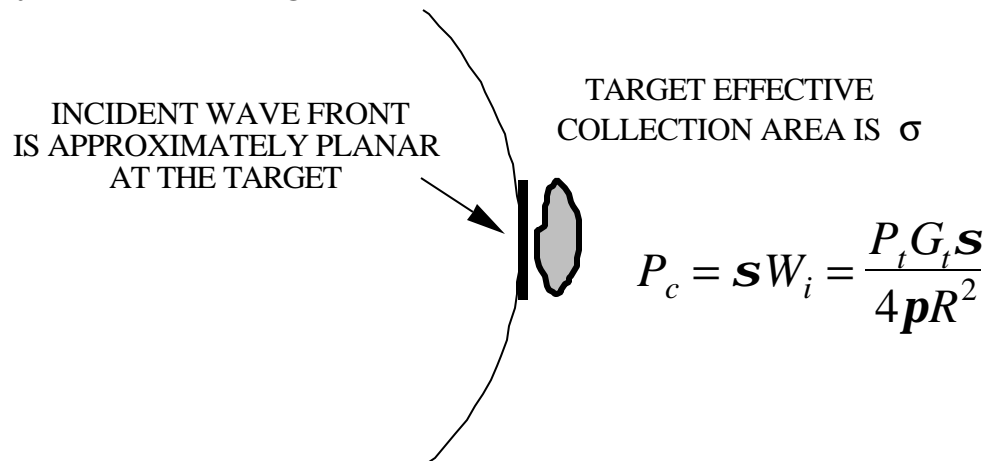
# Basic Form of the Radar Range Equation (2)

---

Power density incident on the target



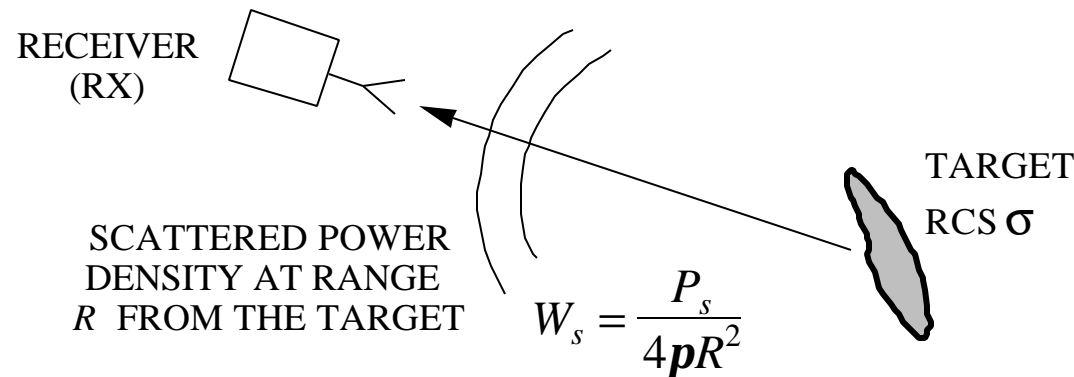
Power collected by the radar target



# Basic Form of the Radar Range Equation (3)

---

The RCS gives the fraction of incident power that is scattered back toward the radar. Therefore,  $P_s = P_c$  and the scattered power density at the radar is obtained by dividing by  $4\pi R^2$ .



The target scattered power collected by the receiving antenna is  $W_s A_{er}$ . Thus the maximum target scattered power that is available to the radar is

$$P_r = \frac{P_t G_t \sigma A_{er}}{(4\pi R^2)^2} = \frac{P_t G_t G_r \sigma l^2}{(4\pi)^3 R^4}$$

This is the classic form of the radar range equation (RRE).

# Characteristics of the Radar Range Equation

---

$$P_r = \frac{P_t G_t \sigma A_{er}}{(4\pi R^2)^2} = \frac{P_t G_t G_r \sigma l^2}{(4\pi)^3 R^4}$$

For monostatic systems a single antenna is generally used to transmit and receive so that  $G_t = G_r \equiv G$ .

This form of the RRE is too crude to use as a design tool. Factors have been neglected that have a significant impact on radar performance:

noise, system losses, propagation behavior, clutter, waveform limitations, etc.

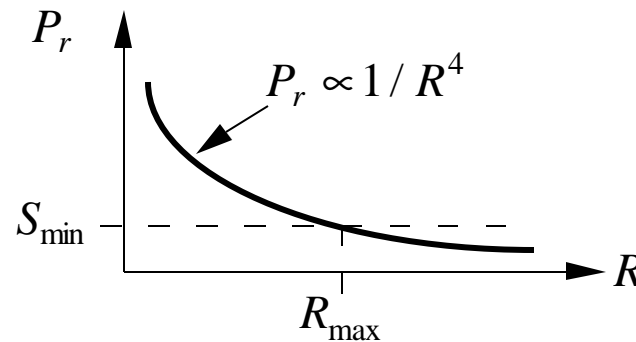
We will discuss most of these in depth later in the course.

This form of the RRE does give some insight into the tradeoffs involved in radar design. The dominant feature of the RRE is the  $1/R^4$  factor. Even for targets with relatively large RCS, high transmit powers must be used to overcome the  $1/R^4$  when the range becomes large.

# Maximum Detection Range

---

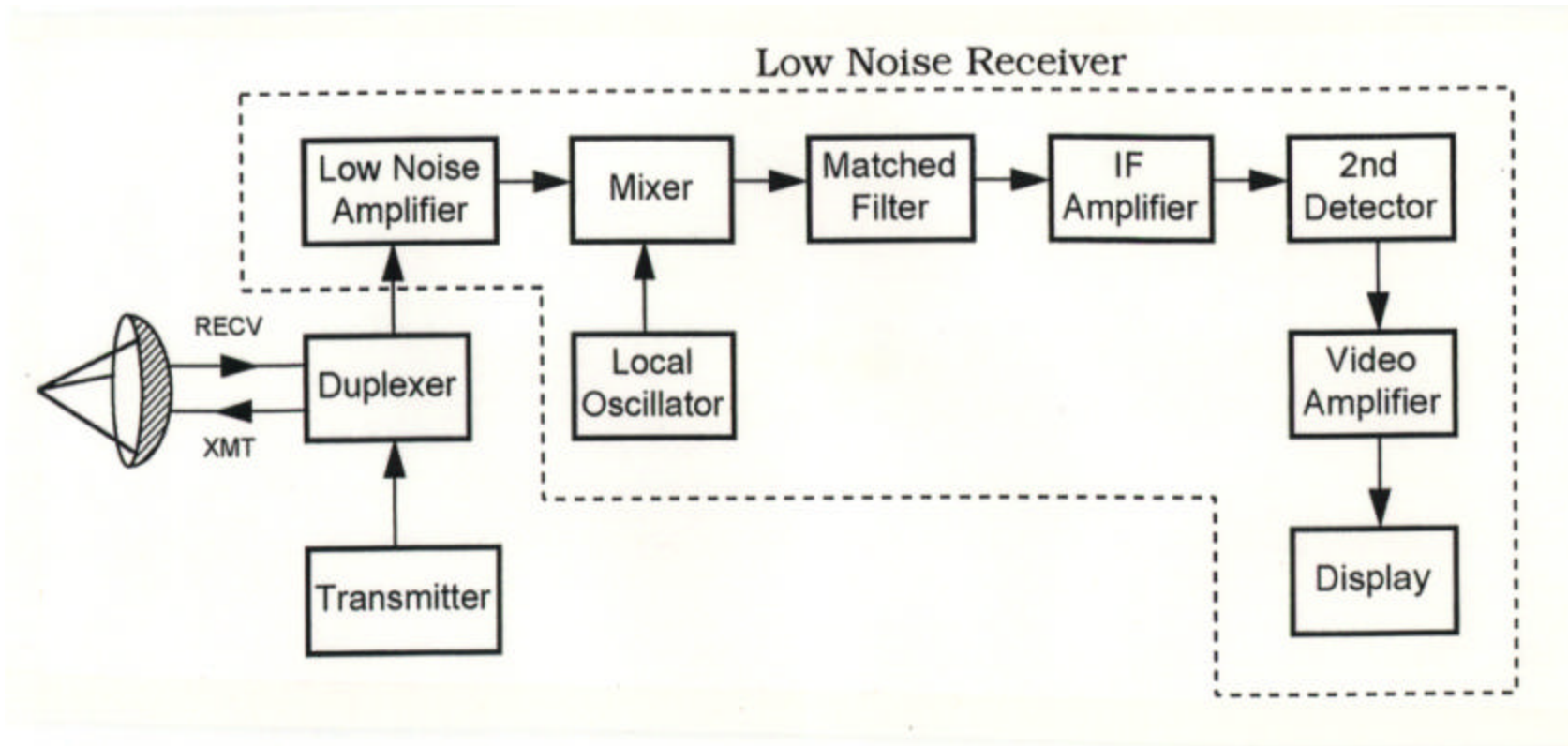
The minimum received power that the radar receiver can "sense" is referred to as the minimum detectable signal (MDS) and is denoted  $S_{\min}$ .



Given the MDS, the maximum detection range can be obtained:

$$P_r = S_{\min} = \frac{P_t G_t G_r s l^2}{(4p)^3 R^4} \Rightarrow R_{\max} = \left( \frac{P_t G_t G_r s l^2}{(4p)^3 S_{\min}} \right)^{1/4}$$

# Generic Radar Block Diagram



This receiver is a superheterodyne receiver because of the intermediate frequency (IF) amplifier.



# Brief Description of System Components

---

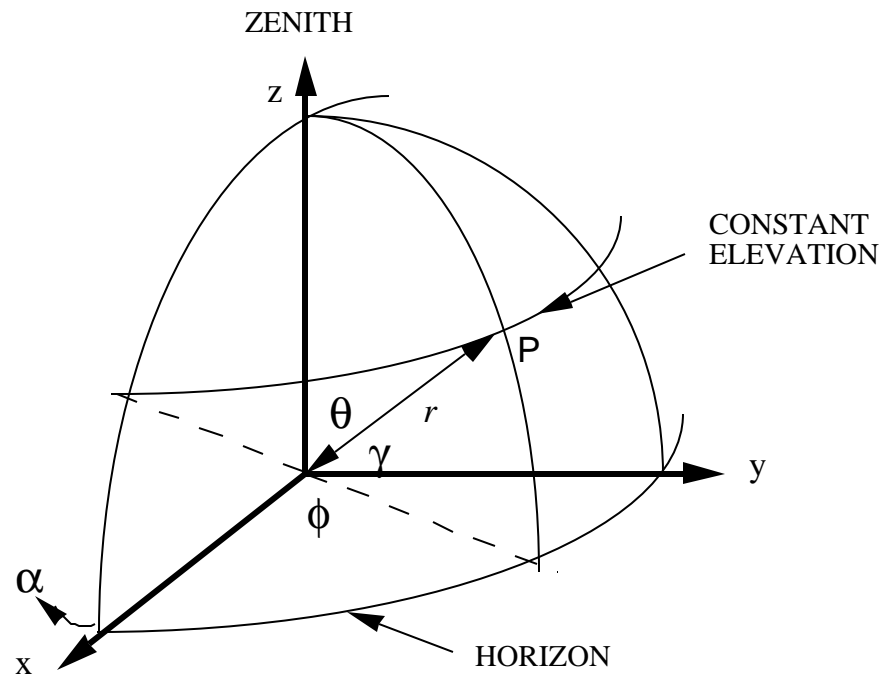
DUPLEXER	An antenna switch that allows the transmit and receive channels to share the antenna. Often it is a <u>circulator</u> . The duplexer must effectively isolate the transmit and receive channels.
TRANSMITTER	Generates and amplifies the microwave signal.
LOW NOISE AMPLIFIER (LNA)	Amplifies the weak received target echo without significantly increasing the noise level.
MIXER	Mixing (or heterodyning) is used to translate a signal to a higher frequency
MATCHED FILTER	Extracts the signal from the noise
IF AMPLIFIER	Further amplifies the intermediate frequency signal
DETECTOR	Translates the signal from IF to baseband (zero frequency)
VIDEO AMPLIFIER	Amplifies the baseband signal
DISPLAY	Visually presents the radar signal for interpretation by the operator

# Coordinate Systems

---

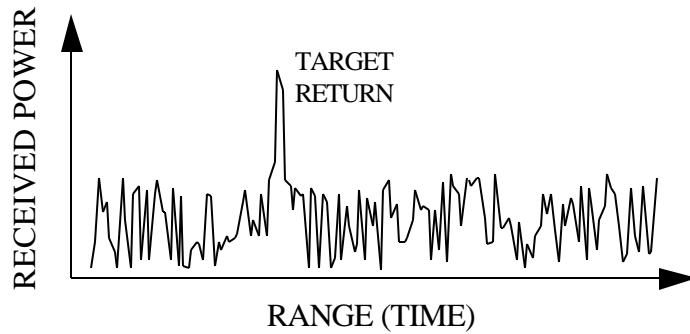
Radar coordinate systems: spherical polar:  $(r, \mathbf{q}, \mathbf{f})$   
azimuth/elevation:  $(\text{Az}, \text{El})$  or  $(\mathbf{a}, \mathbf{g})$

The radar is located at the origin of the coordinate system; the earth's surface lies in the  $x$ - $y$  plane. Azimuth is generally measured clockwise from a reference (like a compass) but the spherical system azimuthal angle  $\mathbf{f}$  is measured counterclockwise from the  $x$  axis. Therefore  $\mathbf{a} = 360 - \mathbf{f}$  and  $\mathbf{g} = 90 - \mathbf{q}$  degrees.

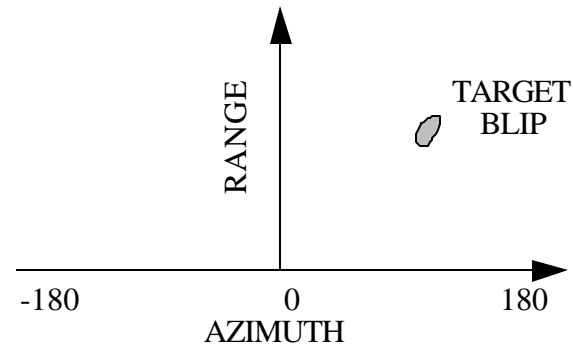


# Radar Displays

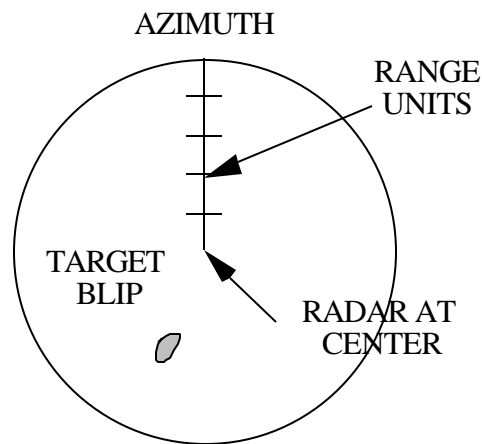
"A" DISPLAY



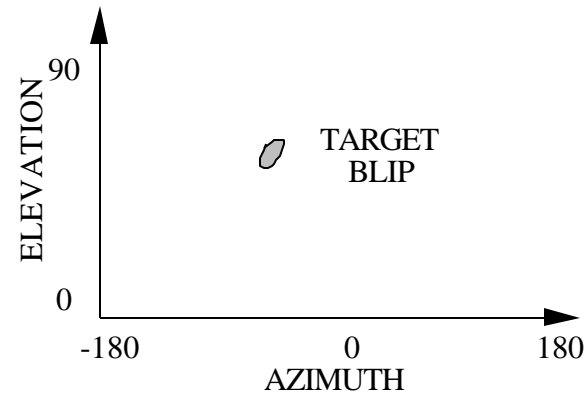
"B" DISPLAY



PLAN POSITION INDICATOR (PPI)



"C" DISPLAY

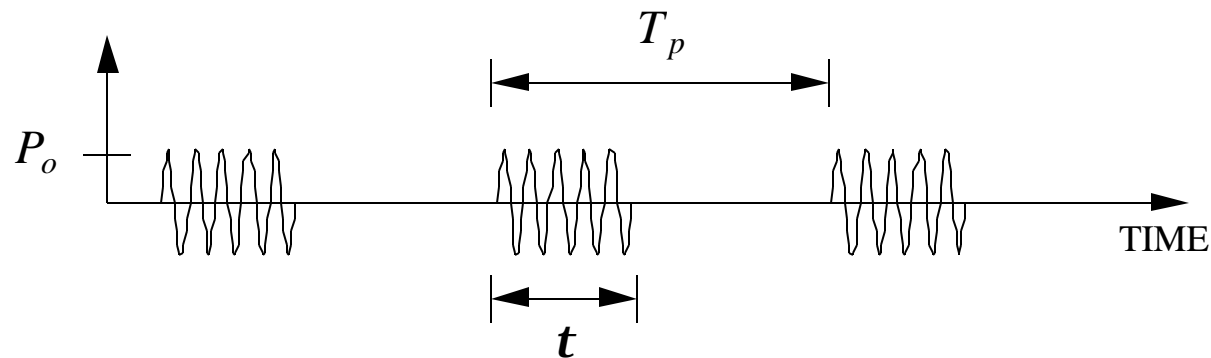


# Pulsed Waveform

In practice pulses are continuously transmitted to:

1. cover search patterns,
2. track moving targets,
3. integrate (sum) several target returns to improve detection.

The pulse train is a common waveform



where:

$N$  = number of pulses in the pulse train

$P_o$  = pulse amplitude (may be power or voltage)

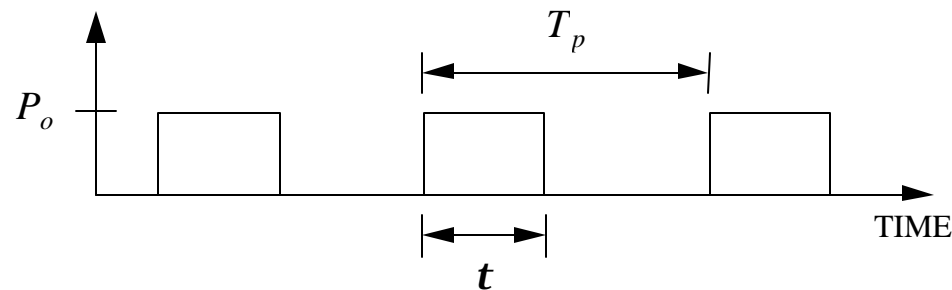
$t$  = pulse width (seconds)

$T_p$  = pulse period (seconds)

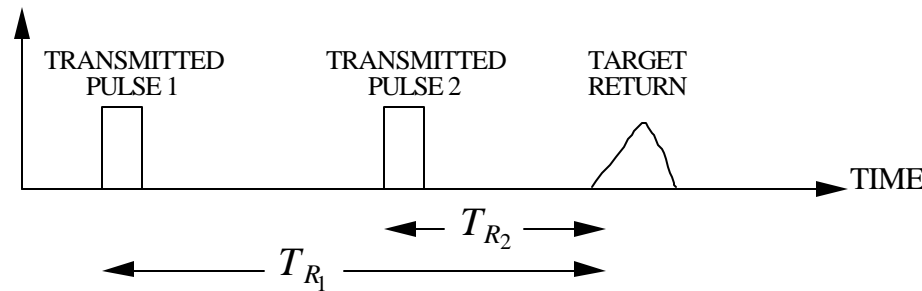
The pulse repetition frequency is defined as  $PRF = f_p = \frac{1}{T_p}$

# Range Ambiguities

For convenience we omit the sinusoidal carrier when drawing the pulse train



When multiple pulses are transmitted there is the possibility of a range ambiguity.

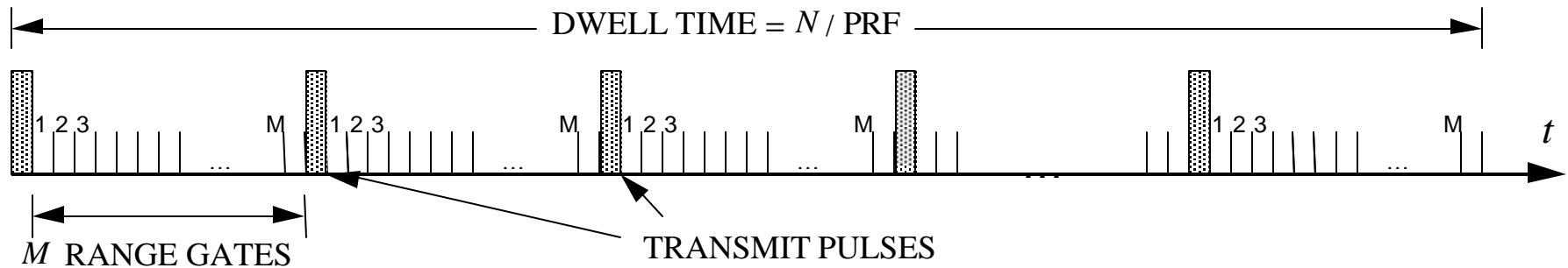


To determine the range unambiguously requires that  $T_p \geq \frac{2R}{c}$ . The unambiguous range is

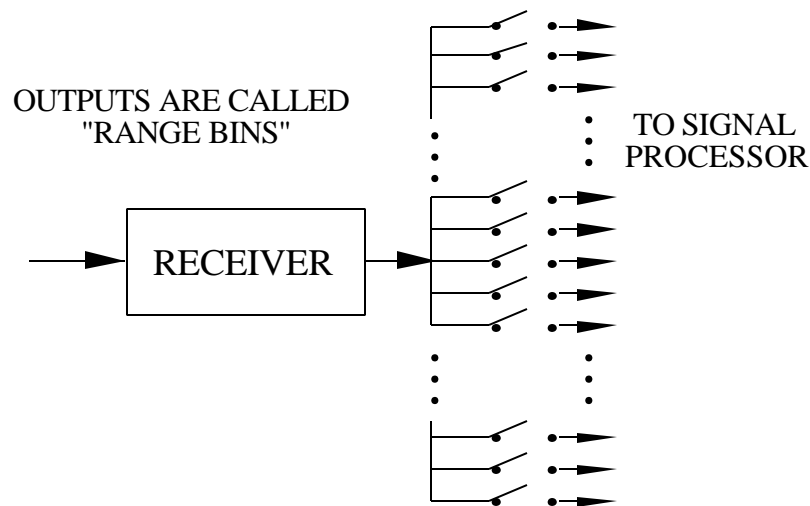
$$R_u = \frac{cT_p}{2} = \frac{c}{2f_p} \text{ where } f_p \text{ is the PRF.}$$

# Range Gates

Typical pulse train and range gates



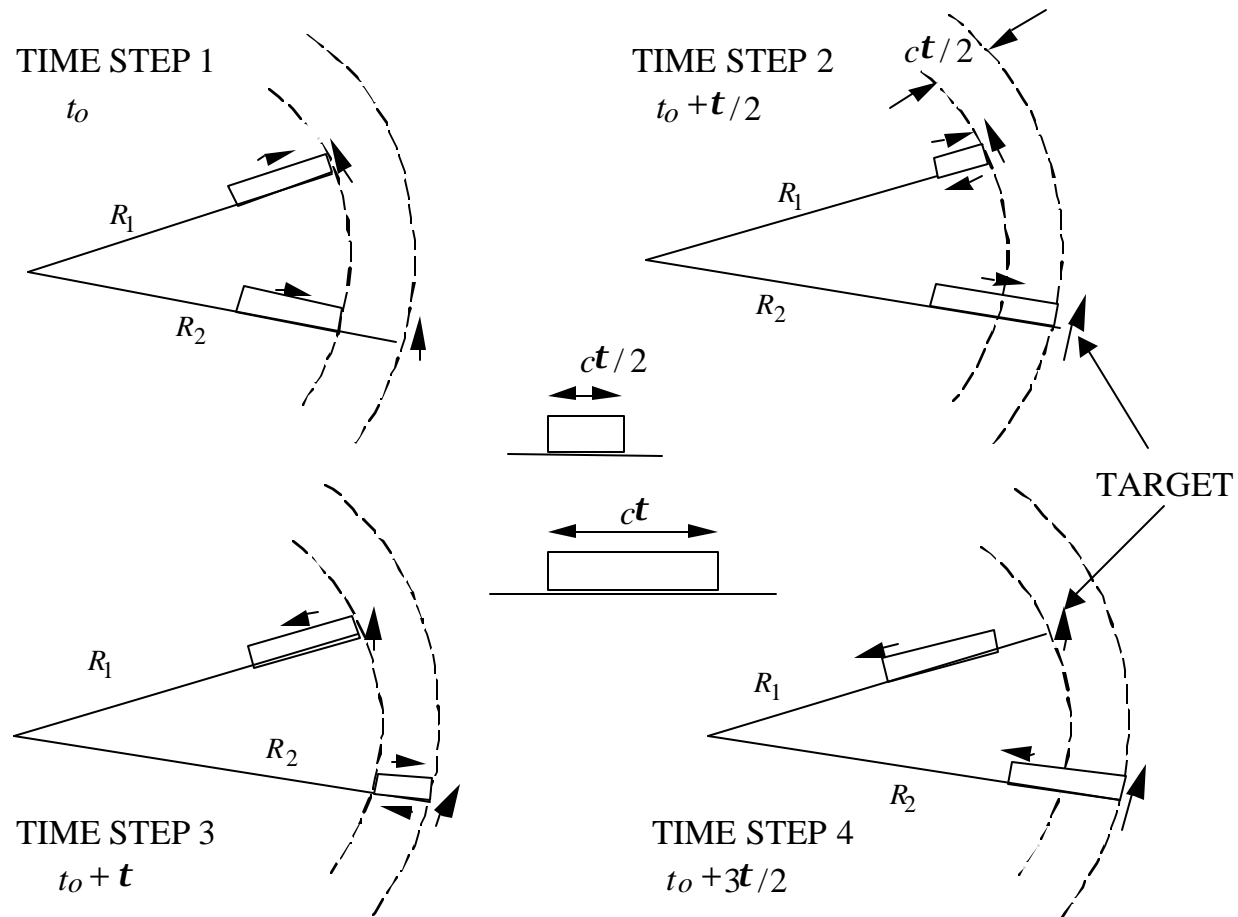
Analog implementation of range gates



- Gates are opened and closed sequentially
- The time each gate is closed corresponds to a range increment
- Gates must cover the entire interpulse period or the ranges of interest
- For tracking a target a single gate can remain closed until the target leaves the bin

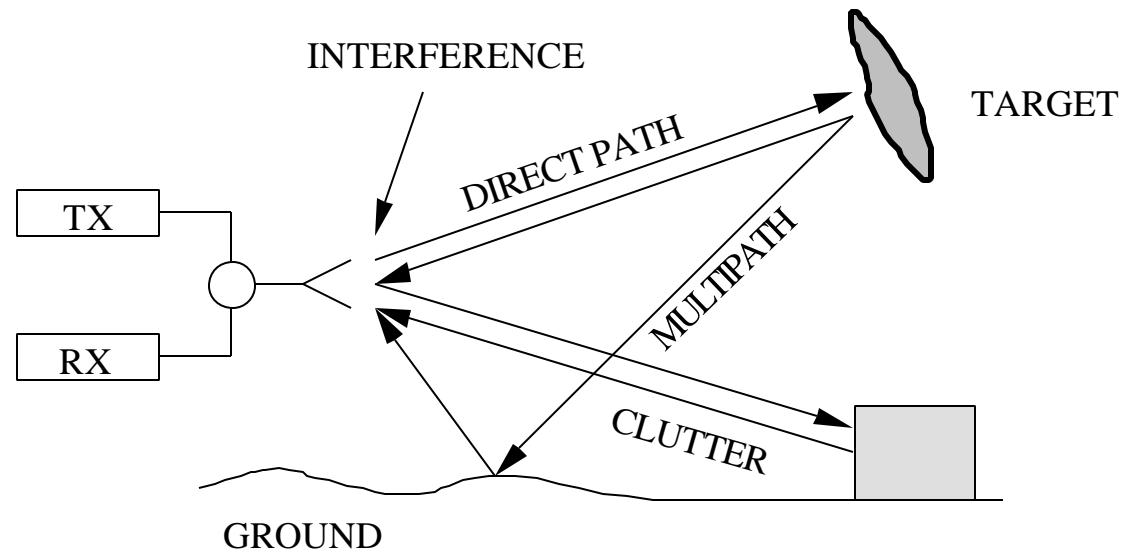
# Range Bins and Range Resolution

Two targets are resolved if their returns do not overlap. The range resolution corresponding to a pulse width  $t$  is  $\Delta R = R_2 - R_1 = ct/2$



# Radar Operational Environment

---



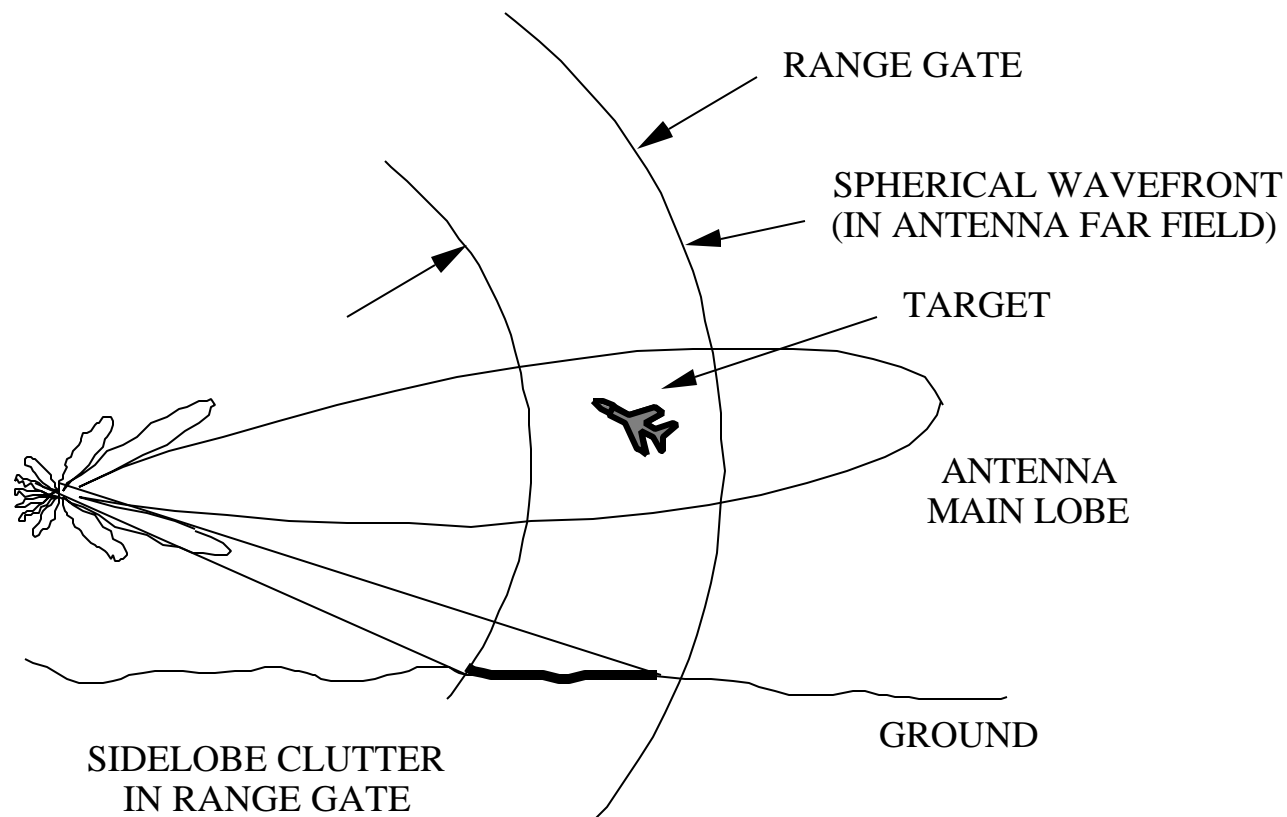
Radar return depends on:

1. target orientation (aspect angle) and distance (range)
2. target environment (other objects nearby; location relative to the earth's surface)
3. propagation characteristics of the path (rain, snow or foliage attenuation)
4. antenna characteristics (polarization, beamwidth, sidelobe level)
5. transmitter and receiver characteristics



# Ground Clutter From Sidelobes

Sidelobe clutter competes with the mainbeam target return

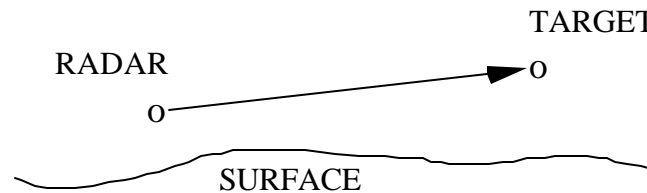


# Survey of Propagation Mechanisms (1)

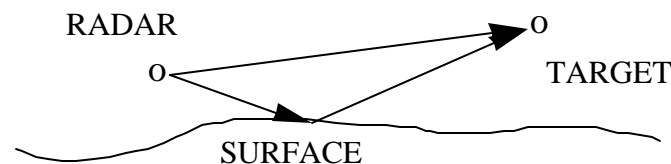
---

There are many propagation mechanisms by which signals can travel between the radar transmitter and receiver. Except for line-of-sight (LOS) paths, their effectiveness is generally a strong function of the frequency and radar/target geometry.

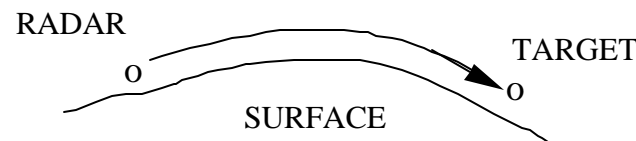
1. direct path or "line of sight" (most radars; SHF links from ground to satellites)



2. direct plus earth reflections or "multipath" (UHF broadcast; ground-to-air and air-to-air communications)



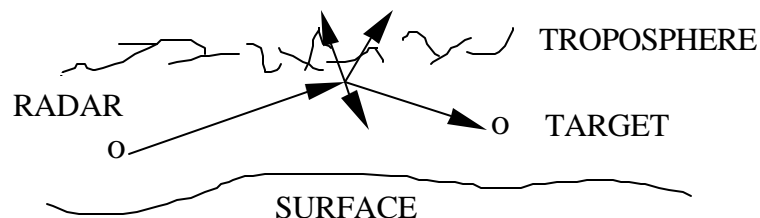
3. ground wave (AM broadcast; Loran C navigation at short ranges)



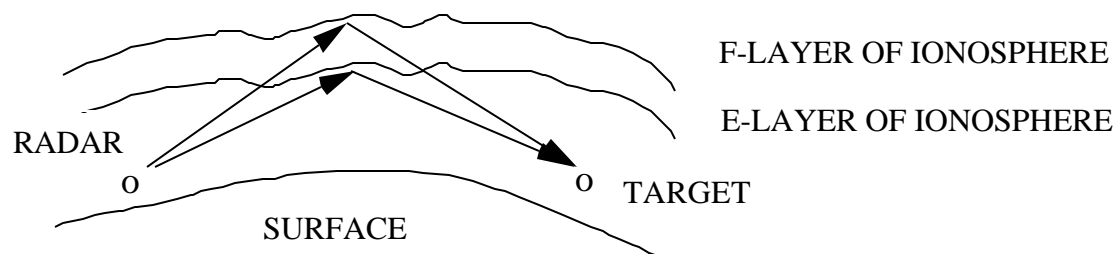
# Survey of Propagation Mechanisms (2)

---

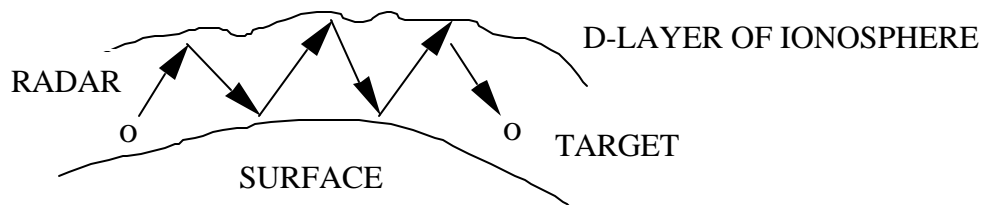
4. tropospheric paths or "troposcatter" (microwave links; over-the-hizon (OTH) radar and communications)



5. ionospheric hop (MF and HF broadcast and communications)



6. waveguide modes or "ionospheric ducting" (VLF and LF communications)

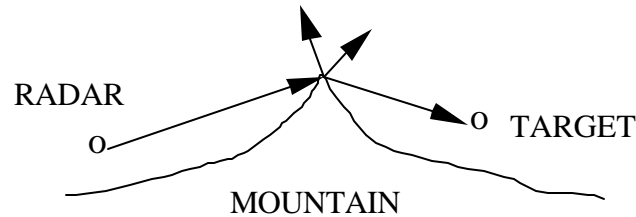


(Note: The distinction between waveguide modes and ionospheric hops is based more on the analysis approach used in the two frequency regimes rather than any physical difference.)

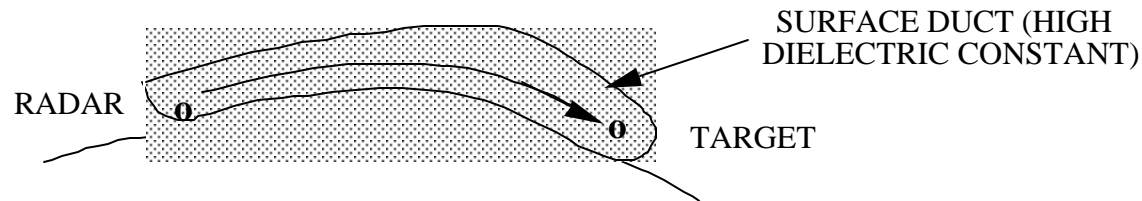
# Survey of Propagation Mechanisms (3)

---

## 7. terrain diffraction



## 8. low altitude and surface ducts (radar frequencies)



## 9. Other less significant mechanisms: meteor scatter, whistlers

# Radar System Design Tradeoffs

---

Choice of frequency affects:

size	high frequencies have smaller devices
transmit power	generally favors lower frequencies
antenna gain/HPWB	small high gain favors high frequencies
atmospheric attenuation	smaller loss a low frequencies
ambient noise	lowest in 1-10 GHz range
doppler shift	greater at high frequencies

Polarization affects:

- clutter and ground reflections
- RCS of the targets of interest
- antenna deployment limitations

Waveform selection affects:

- signal bandwidth (determined by pulse width)
- PRF (sets the unambiguous range)
- average transmitter power (determines maximum detection range)

# Decibel Refresher

---

In general, a dimensionless quantity  $Q$  in decibels (denoted  $Q_{\text{dB}}$ ) is defined by

$$Q_{\text{dB}} = 10 \log_{10}(Q)$$

$Q$  usually represents a ratio of powers, where the denominator is the reference, and  $\log_{10}$  is simply written as  $\log$ . Characters are added to the "dB" to denote the reference quantity, for example, dBm is decibels relative to a milliwatt. Therefore, if  $P$  is in watts:

$$P_{\text{dBW}} = 10 \log(P/1) \text{ or } P_{\text{dBm}} = 10 \log(P/0.001)$$

Antenna gain  $G$  (dimensionless) referenced to an isotropic source (an isotropic source radiates uniformly in all directions, and its gain is 1):  $G_{\text{dB}} = 10 \log(G)$

Note that:

1. Positive dB values  $> 1$ ; negative dB values  $< 1$
2. 10 dB represents an order of magnitude change in the quantity  $Q$
3. When quantities are multiplied their dB values add. For example, the effective radiated power (ERP) can be computed directly from the dB quantities:

$$\text{ERP}_{\text{dBW}} = (PG)_{\text{dBW}} = P_{\text{dBW}} + G_{\text{dB}}$$

---

Note: The ERP is also referred to as the effective isotropic radiated power, EIRP.

# Thermal Noise

---

Consider a receiver at the standard temperature,  $T_o = 290$  degrees Kelvin (K). Over a range of frequencies of bandwidth  $B_n$  (Hz) the available noise power is

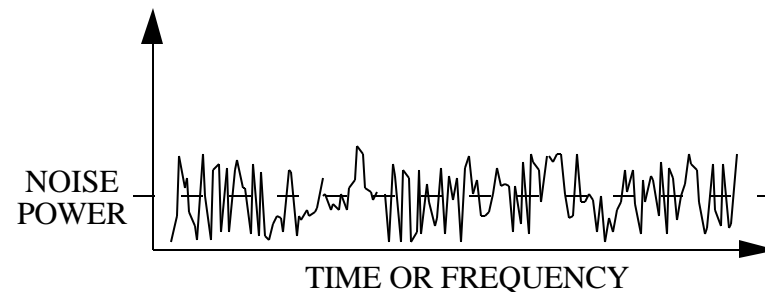
$$N_o = kT_o B_n$$

where  $k = 1.38 \times 10^{-23}$  (Joules/K) is Boltzman's constant.

Other radar components will also contribute noise (antenna, mixer, cables, etc.). We define a system noise temperature  $T_s$ , in which case the available noise power is

$$N_o = kT_s B_n.$$

(We will address the problem of computing  $T_s$  later.) The quantity  $kT_s$  is the noise spectral density (W/Hz)

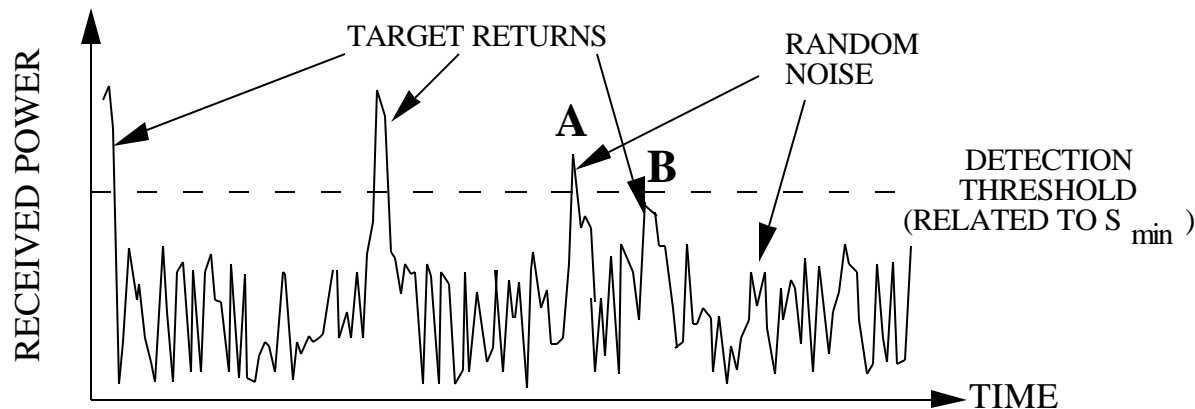


# Noise in Radar Systems

In practice the received signal is "corrupted" (distorted from the ideal shape and amplitude):

1. Noise is introduced in the radar system components (antenna, receiver, etc.) and by the environment (interference sources, propagation path, etc.).
2. Signal dispersion occurs. Frequency components of the waveform are treated differently by the radar components and the environment.
3. Clutter return exists.

Typical return trace appears as follows:



Threshold detection is commonly used. If the return is greater than the detection threshold a target is declared. **A** is a false alarm: the noise is greater than the threshold level but there is no target. **B** is a miss: a target is present but the return is not detected.



# Noise in Radar Systems

---

Conflicting requirements:

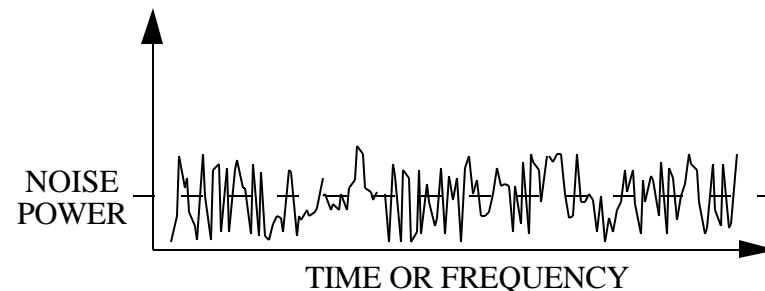
To avoid false alarms set the detection threshold higher

To avoid misses set the detection threshold lower

Noise is a random process and therefore we must use probability and statistics to assess its impact on detection and determine the "optimum" threshold level.

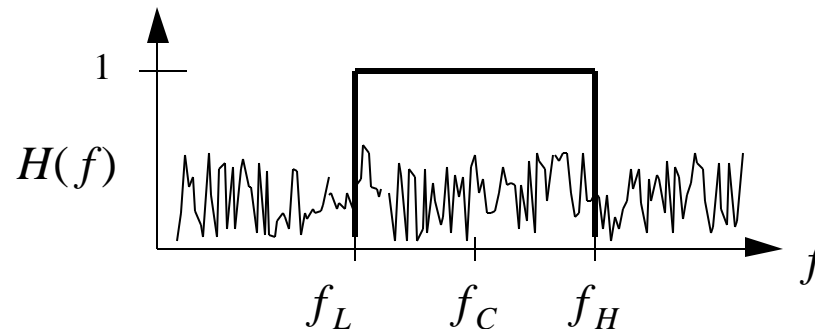
Thermal noise is generated by charged particles as they conduct. High temperatures result in greater thermal noise because of increased particle agitation.

Thermal noise exists at all frequencies. We will consider the noise to be constant with frequency ("white noise") and its statistics (average and variance) independent of time ("stationary").



# Ideal Filter

A filter is a device that passes signals with the desired frequencies and rejects all others. Below is shown the filter characteristic of an ideal bandpass filter. Filters are linear systems and the filter characteristic is the transfer function  $H(f)$  in the frequency domain. (Recall that  $H(f)$  is the Fourier transform of its impulse response,  $h(t)$ . For convenience  $H(f)$  is normalized.)

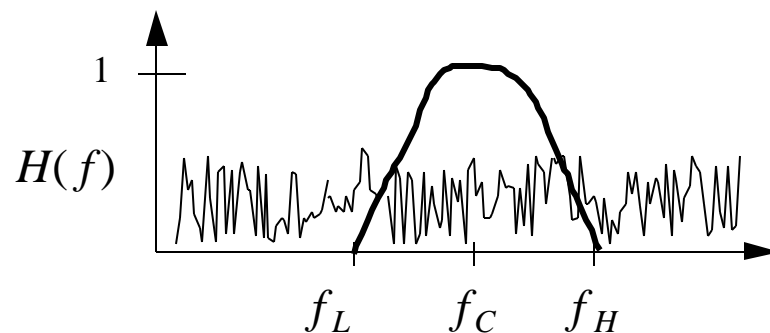


The bandwidth of this ideal filter is  $B = f_H - f_L$ . The center frequency is given by  $f_C = (f_H + f_L)/2$ . Signals and noise in the pass band emerge from the filter unaffected. Therefore the noise power passed by this filter is  $N_o = kT_s B$ . The noise bandwidth of an ideal filter is equal to the bandwidth of the filter:  $B_n = B$ .

# Noise Bandwidth of an Arbitrary Filter

---

In practice  $H(f)$  is not constant; in fact it may not even be symmetrical about the center frequency.



The noise bandwidth is defined as the bandwidth of an equivalent ideal filter with  $H(f)=1$ :

$$B_n = \frac{\int_{-\infty}^{\infty} |H(f)|^2 df}{|H(f_C)|^2}$$

Furthermore, real filters are not strictly bandlimited (i.e., the characteristic is not zero outside of the passband). In this case we usually use the actual filter characteristic inside the 3dB (or sometimes 10 dB) points and zero at frequencies outside of these points.

# Signal-to-Noise Ratio ( $S/N$ )

---

Considering the presence of noise, the important parameter for detection is the signal-to-noise ratio ( $S/N$ ). We already have an expression for the signal returned from a target ( $P_r$  from the radar equation), and therefore the signal-to-noise ratio is

$$\text{SNR} = \frac{P_r}{N_o} = \frac{P_t G_t G_r \sigma I^2}{(4\pi)^3 R^4 k T_s B_n}$$

At this point we will consider only two noise sources:

1. background noise collected by the antenna ( $T_A$ )
2. total effect of all other system components (system effective noise temperature,  $T_e$ )

so that

$$T_s = T_A + T_e$$

# Example: Police Radar

---

A police radar has the following parameters:

$$B_n = 1 \text{ kHz} \quad P_t = 100 \text{ mW} \quad D = 20 \text{ cm} \quad r = 0.6$$

$$f = 10.55 \text{ GHz} \quad T_s = 1000 \text{ K} \quad (S/N)_{\min} = 10 \text{ dB} \quad \mathbf{s} = 0.2 \text{ m}^2$$

$$A_{er} = A_p r = \mathbf{p}(D/2)^2 0.6 = 0.01884 \text{ m}^2, \quad \mathbf{l} = c/f = 3 \times 10^8 / 10.55 \times 10^9 = 0.028 \text{ m}$$

$$G = \frac{4\mathbf{p}A_{er}}{\mathbf{l}^2} = \frac{4\mathbf{p}(0.01884)}{0.028^2} = 292.6 = 24.66 \text{ dB}$$

$$N_o = kT_s B_n = (1.38 \times 10^{-23})(1000)(1000) = 1.38 \times 10^{-17}$$

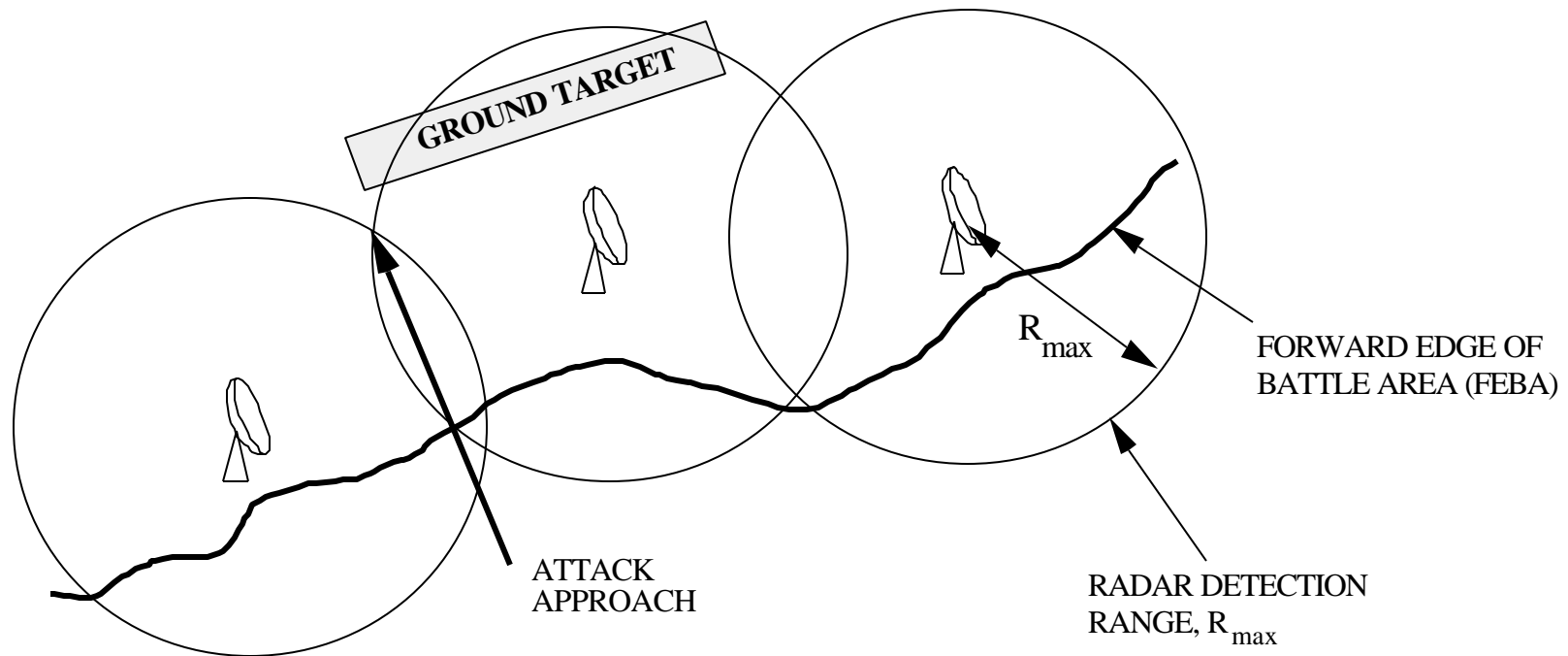
$$\text{SNR} = \frac{P_r}{N_o} = \frac{P_t G^2 \mathbf{s} \mathbf{l}^2}{(4\mathbf{p})^3 R^4 N_o} = 10 \text{ dB} = 10^{(10/10)} = 10$$

$$R^4 = \frac{P_t G^2 \mathbf{s} \mathbf{l}^2}{(4\mathbf{p})^3 10 N_o} = \frac{(0.1)(292.6)^2 (0.2)(0.028)^2}{(4\mathbf{p})^3 (1.38 \times 10^{-16})} = 4.9 \times 10^{12}$$

$$R = 1490 \text{ m} = 1.49 \text{ km} \approx 0.9 \text{ mi}$$

# Attack Approach

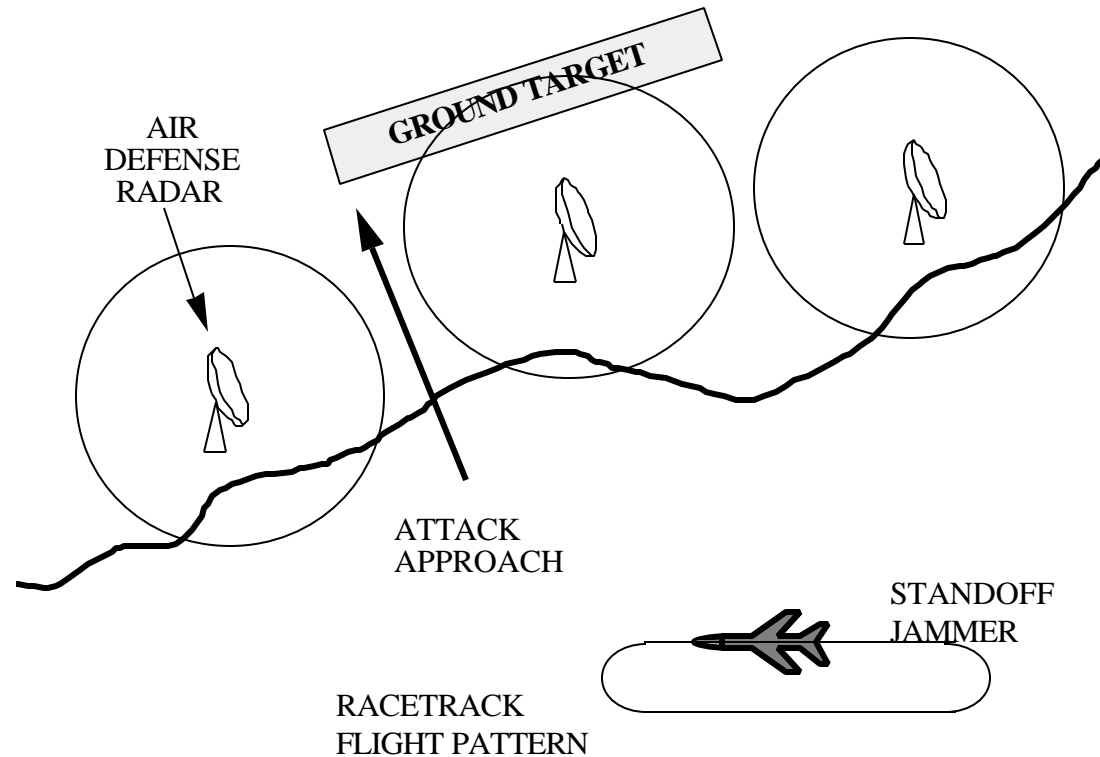
---



A network of radars are arranged to provide continuous coverage of a ground target.

Conventional aircraft cannot penetrate the radar network without being detected.

# Defeating Radar by Jamming

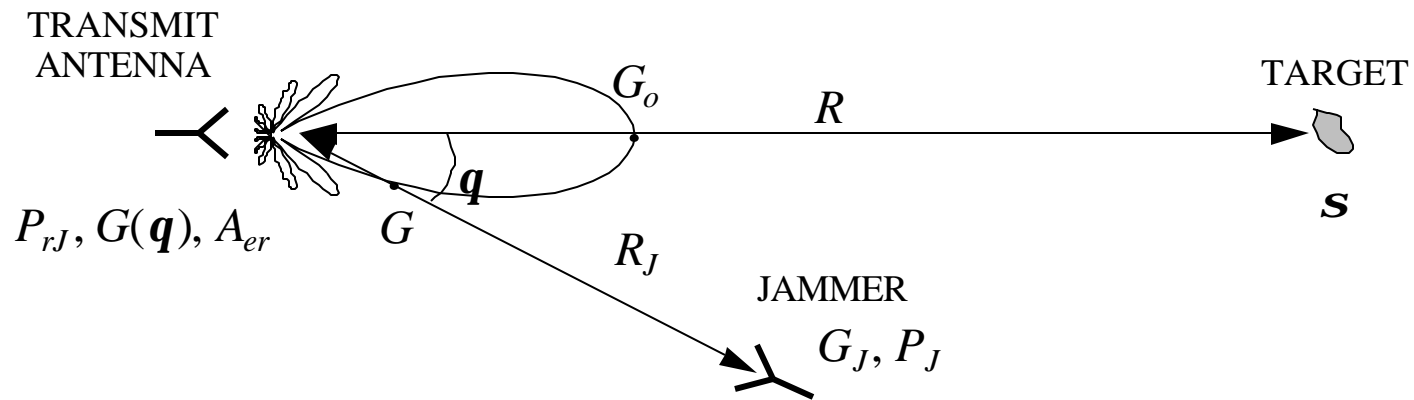


The barrage jammer floods the radar with noise and therefore decreases the SNR

The radar knows it's being jammed

# Jammer Burnthrough Range (1)

Consider a standoff jammer operating against a radar that is tracking a target



The jammer power received by the radar is

$$P_{rJ} = W_i A_{er} = \left( \frac{P_J G_J}{4\pi R_J^2} \right) \left( \frac{I^2 G(q)}{4\pi} \right) = \frac{P_J G_J I^2 G(q)}{(4\pi R_J)^2}$$

Defining  $G_o \equiv G(\mathbf{q} = 0)$ , the target return is

$$P_r = \frac{P_t G_o^2 I^2 S}{(4\pi)^3 R^4}$$



# Jammer Burnthrough Range (2)

---

The signal-to-jam ratio is

$$\text{SJR} = \frac{S}{J} = \frac{P_r}{P_{rJ}} = \left( \frac{P_t G_o}{P_J G_J} \right) \left( \frac{R_J^2}{R^4} \right) \left( \frac{\mathbf{s}}{4\mathbf{p}} \right) \left( \frac{G_o}{G(\mathbf{q})} \right)$$

The burnthrough range for the jammer is the range at which its signal is equal to the target return (SJR=1).

Important points:

1.  $R_J^2$  vs  $R^4$  is a big advantage for the jammer.
2.  $G$  vs  $G(\mathbf{q})$  is usually a big disadvantage for the jammer. Low sidelobe radar antennas reduce jammer effectiveness.
3. Given the geometry, the only parameter that the jammer has control of is the ERP ( $P_J G_J$ ).
4. The radar knows it is being jammed. The jammer can be countered using waveform selection and signal processing techniques.

# Noise Figure

---

Active devices such as amplifiers boost the signal but also add noise. For these devices the noise figure is used as a figure of merit:

$$F_n = \frac{(S/N)_{\text{in}}}{(S/N)_{\text{out}}} = \frac{S_{\text{in}} / N_{\text{in}}}{S_{\text{out}} / N_{\text{out}}}$$

For an ideal network that does not add noise  $F_n = 1$ .



Solve for the input signal:

$$S_{\text{in}} = \frac{S_{\text{out}}}{N_{\text{out}}} F_n N_{\text{in}} = \left( \frac{S}{N} \right)_{\text{out}} F_n (kT_o B_n)$$

Let  $S_{\text{in}} = S_{\text{min}}$  and find the maximum detection range

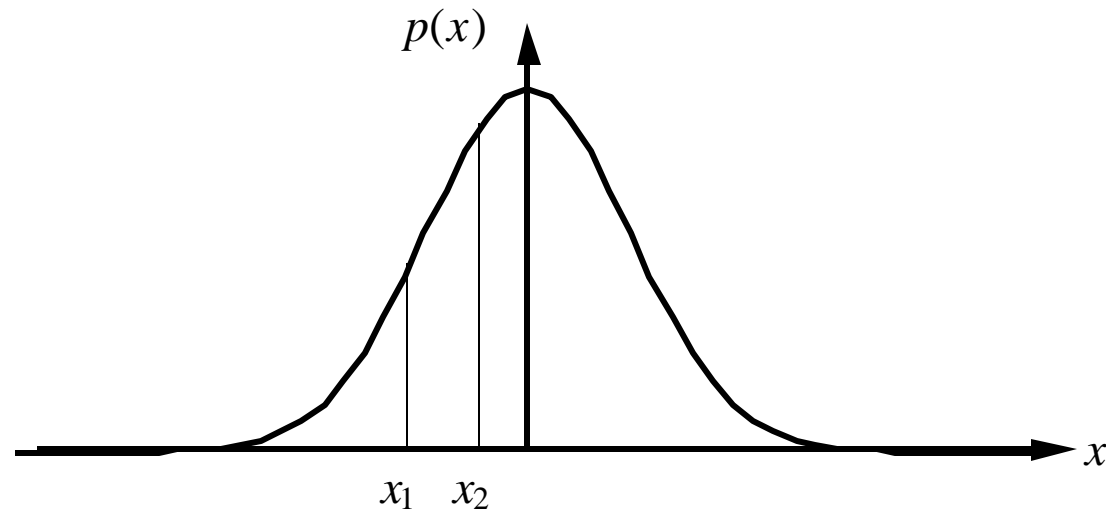
$$R_{\text{max}}^4 = \frac{P_t G_t A_{er} S}{(4p)^2 kT_o B_n F_n (S_{\text{out}} / N_{\text{out}})_{\text{min}}}$$

This equation assumes that the antenna temperature is  $T_o$ .

# Probability & Statistics Refresher (1)

---

Probability density function (PDF) of a random variable  $x$



Probability that  $x$  lies between  $x_1$  and  $x_2$ :

$$P(x_1 < x < x_2) = \int_{x_1}^{x_2} p(x) dx$$

Since  $p(x)$  includes all possible outcomes

$$\int_{-\infty}^{\infty} p(x) dx = 1$$

# Probability & Statistics Refresher (2)

---

The expected value (average, mean) is computed by

$$\langle x \rangle = \bar{x} = \int_{-\infty}^{\infty} x p(x) dx$$

In general, the expected value of any function of  $x$ ,  $g(x)$

$$\langle g(x) \rangle = \overline{g(x)} = \int_{-\infty}^{\infty} g(x) p(x) dx$$

Moments of the PDF:  $\langle x \rangle = \bar{x}$  is the first moment, ...,  $\langle x^m \rangle = \overline{x^m}$  is the  $m^{\text{th}}$  moment

Central moments of the PDF:  $\langle (x - \bar{x})^m \rangle$   $m^{\text{th}}$  central moment

The second central moment is the variance,  $\mathbf{s}^2 = \langle (x - \bar{x})^2 \rangle$

$$\overline{\mathbf{s}^2} = \int_{-\infty}^{\infty} (x - \bar{x})^2 p(x) dx = \int_{-\infty}^{\infty} (x^2 - 2x\bar{x} + \bar{x}^2) p(x) dx$$

$$\overline{\mathbf{s}^2} = \int_{-\infty}^{\infty} x^2 p(x) dx - 2\bar{x} \int_{-\infty}^{\infty} x p(x) dx + \bar{x}^2 \int_{-\infty}^{\infty} p(x) dx$$

with the final result:  $\mathbf{s}^2 = \langle (x - \bar{x})^2 \rangle = \overline{x^2} - \bar{x}^2$

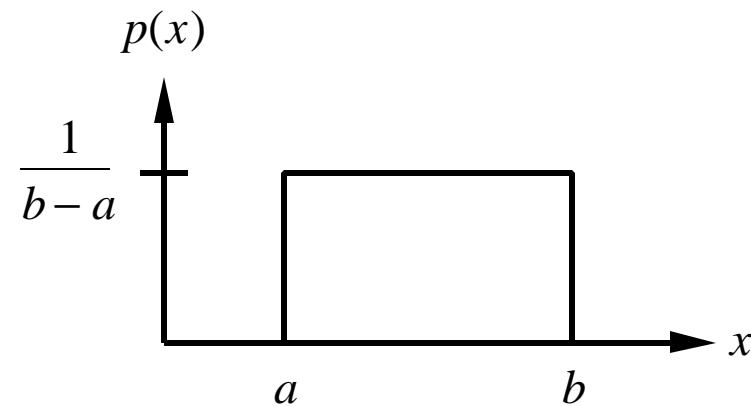
Physical significance:  $\bar{x}$  is the mean value (dc);  $\sqrt{\mathbf{s}^2}$  is the rms value

# Probability & Statistics Refresher (3)

---

Special probability distributions we will encounter:

## 1. Uniform PDF

$$p(x) = \begin{cases} \frac{1}{b-a}, & a < x < b \\ 0, & \text{else} \end{cases}$$


Expected value:

$$\langle x \rangle = \bar{x} = \int_{-\infty}^{\infty} x p(x) dx = \frac{1}{2} \frac{b^2 - a^2}{b - a} = \frac{b + a}{2}$$

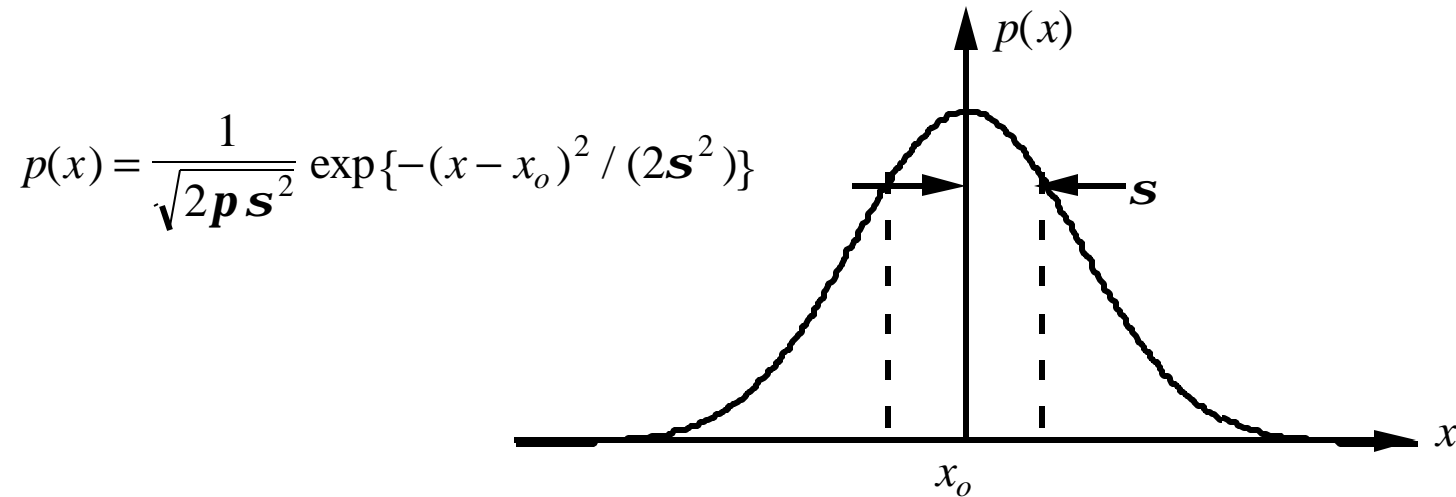
Variance:

$$\overline{s^2} = \langle (x - \bar{x})^2 \rangle = \int_a^b \left( \frac{(x - \bar{x})^2}{b - a} \right) dx = \frac{(b - a)^2}{12}$$

# Probability & Statistics Refresher (4)

---

## 2. Gaussian PDF



Expected value:  $\langle x \rangle = \bar{x} = \frac{1}{\sqrt{2\pi s^2}} \int_{-\infty}^{\infty} x \exp\left\{-\frac{(x - x_o)^2}{2s^2}\right\} dx = x_o$

Variance:  $\overline{x^2} = \frac{1}{\sqrt{2\pi s^2}} \int_{-\infty}^{\infty} x^2 \exp\left\{-\frac{(x - x_o)^2}{2s^2}\right\} dx = x_o^2 + s^2$

$$s^2 = \overline{x^2} - \bar{x}^2 = s^2$$

The standard normal distribution has  $\bar{x} = 0$  and  $s^2 = 1$ .

# Rayleigh Distribution (1)

---

Consider two independent gaussian distributed random variables  $x$  and  $y$

$$p_x(x) = \frac{1}{\sqrt{2ps^2}} \exp\left\{-x^2/(2s^2)\right\} \text{ and } p_y(y) = \frac{1}{\sqrt{2ps^2}} \exp\left\{-y^2/(2s^2)\right\}$$

The joint PDF of two independent variables is the product of the PDFs:

$$p_{xy}(x,y) = \frac{1}{2ps^2} \exp\left\{-(x^2 + y^2)/(2s^2)\right\}$$

If  $x$  and  $y$  represent noise on the real and imaginary parts of a complex signal, we are interested in the PDF of the magnitude,  $r^2 = x^2 + y^2$ . Transform to polar coordinates  $(r, \mathbf{f})$

$$\int_{-\infty}^{\infty} \int_{-\infty}^{\infty} p_{xy}(x,y) dx dy = \int_0^{\infty} \int_0^{2\pi} p_{r\mathbf{f}}(r,\mathbf{f}) r dr d\mathbf{f}$$

In polar form the PDF is independent of  $\mathbf{f}$

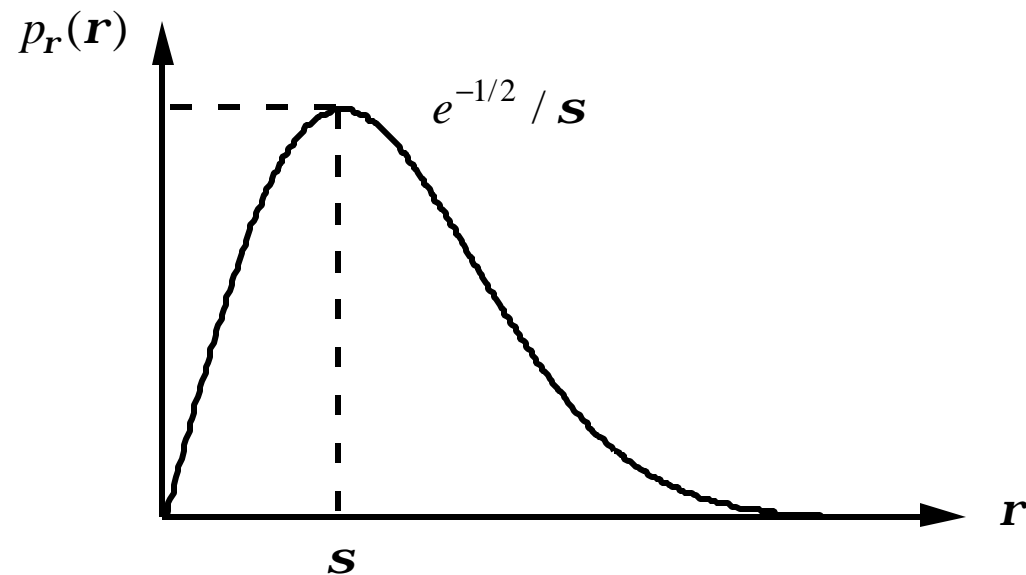
$$p_{r\mathbf{f}}(r,\mathbf{f}) = \frac{1}{2ps^2} \exp\left\{-r^2/2s^2\right\}$$

Therefore, the  $\mathbf{f}$  integration simply gives a factor of  $2\pi$ .

# Rayleigh Distribution (2)

The Rayleigh PDF is:

$$p_r(r) = \frac{r}{s^2} \exp\left\{-r^2 / (2s^2)\right\}$$



$s$  is the "mode" or most probable value

$\bar{r} = \sqrt{\frac{p}{2}} s$  is the expected value of  $r$

$\overline{r^2} = 2s^2$  (noise power) and the variance is  $\left(2 - \frac{p}{2}\right)s^2$



# Central Limit Theorem

---

The central limit theorem states that the probability density function of the sum of  $N$  independent identically distributed random variables is asymptotically normal. If  $x = x_1 + x_2 + \dots + x_N$ , where the  $x_i$  have mean  $\bar{x}$  and variance  $\mathbf{s}$  then

$$\lim_{N \rightarrow \infty} P\left(a \leq \frac{x - N\bar{x}}{\mathbf{s}\sqrt{N}} \leq b\right) = \frac{1}{\sqrt{2\mathbf{p}}} \int_a^b e^{-u^2/2} du$$

Samples from any distribution will appear normally distributed if we take "enough" samples. Usually 10 samples are sufficient.

For our purposes, the central limit theorem usually permits us to model most random processes as gaussian.

Example:  $N$  uniformly distributed random variables between the limits  $a$  and  $b$ .

The central limit theorem states that the joint PDF is gaussian with

$$\begin{aligned} \text{mean:} \quad & \bar{x} = N \frac{b+a}{2} \\ \text{variance:} \quad & \mathbf{s}^2 = \frac{N}{12} \left( \frac{b+a}{2} \right)^2 \end{aligned}$$

# Transformation of Variables

---

Given that a random variable has a PDF of  $p_x(x)$  we can find the PDF of any function of  $x$ , say  $g(x)$ . Let  $\mathbf{a} = g(x)$  and the inverse relationship denoted by  $x = \hat{g}(\mathbf{a})$ . Then

$$p_{\mathbf{a}}(\mathbf{a}) = p_x(x) \left| \frac{dx}{d\mathbf{a}} \right| = p_x(\hat{g}(\mathbf{a})) \left| \frac{d\hat{g}(\mathbf{a})}{d\mathbf{a}} \right|$$

Example: A random signal passed through a square law detector is squared (i.e., the output is proportional to  $x^2$ ). Thus let  $\mathbf{a} = x^2 \equiv g(x)$  or

$$x = \sqrt{\mathbf{a}} \equiv \hat{g}(\mathbf{a}) \text{ and } \frac{d\hat{g}(\mathbf{a})}{d\mathbf{a}} = \frac{d(\mathbf{a})^{1/2}}{d\mathbf{a}} = \frac{1}{2\sqrt{\mathbf{a}}}$$

Therefore,

$$p_{\mathbf{a}}(\mathbf{a}) = p_x(\sqrt{\mathbf{a}}) \frac{1}{2\sqrt{\mathbf{a}}}$$

Let

$$p_x(x) = \begin{cases} e^{-x}, & x > 0 \\ 0, & \text{else} \end{cases}$$

with the final result:

$$p_{\mathbf{a}}(\mathbf{a}) = \frac{1}{2\sqrt{\mathbf{a}}} e^{-\sqrt{\mathbf{a}}} \text{ for } \mathbf{a} > 0$$

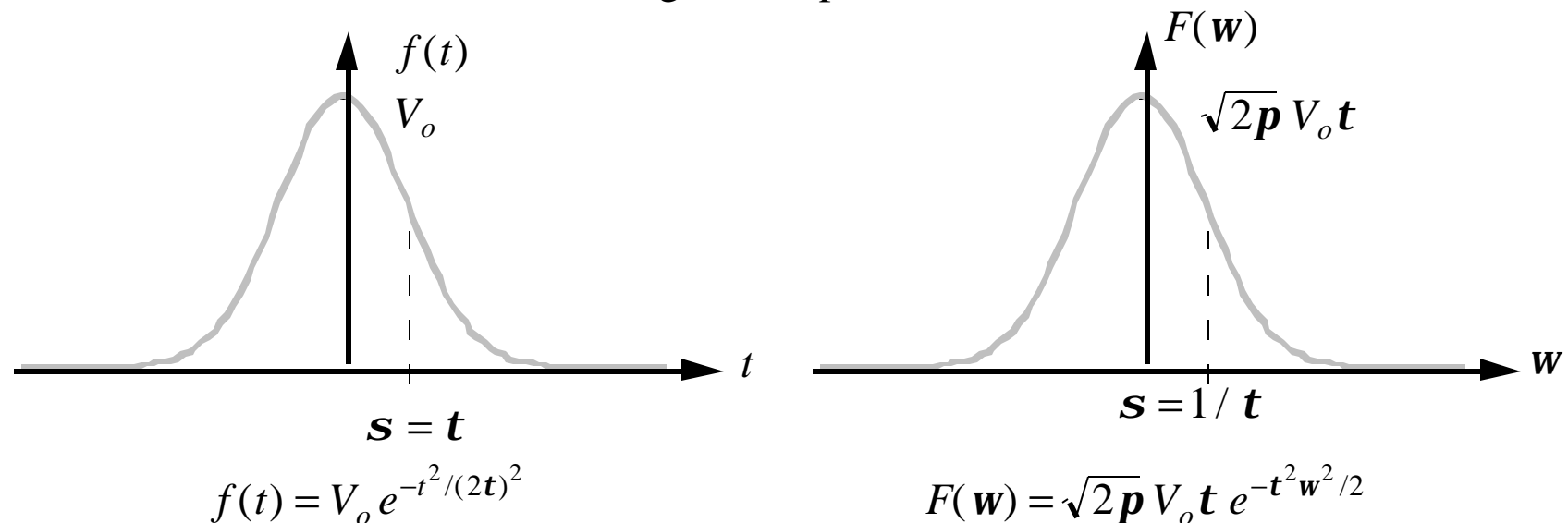
# Fourier Transform Refresher (1)

We will be using the Fourier transform and the inverse Fourier transform to move between time and frequency representations of a signal. A Fourier transform pair  $f(t)$  and  $F(\omega)$  (where  $\omega = 2\pi f$ ) are related by

$$f(t) = \frac{1}{2\pi} \int_{-\infty}^{\infty} F(\omega) e^{j\omega t} d\omega \leftrightarrow F(\omega) = \int_{-\infty}^{\infty} f(t) e^{-j\omega t} dt$$

Some transform pairs we will be using:

gaussian pulse

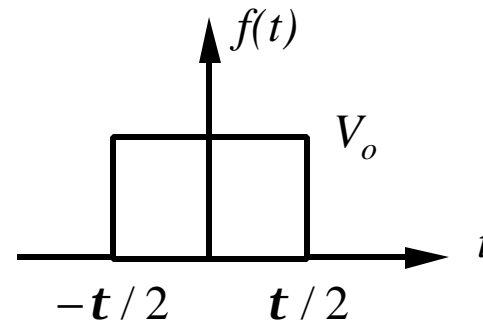


# Fourier Transform Refresher (2)

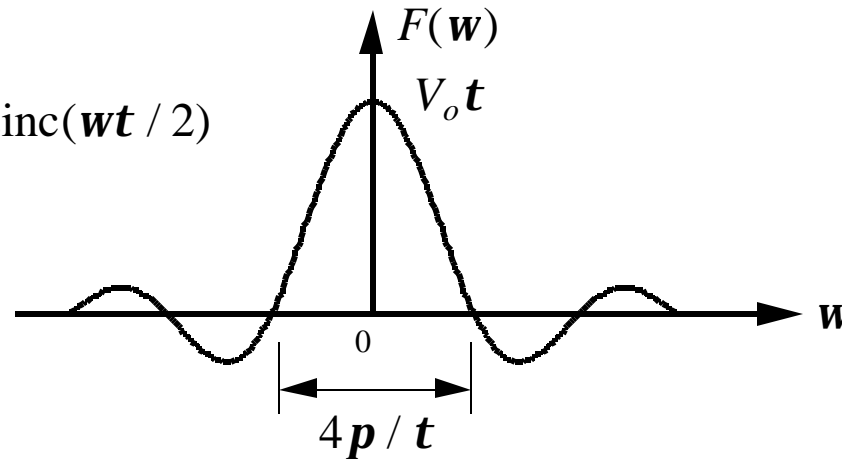
---

rectangular pulse

$$f(t) = \begin{cases} V_o, & |t| < t/2 \\ 0, & \text{else} \end{cases}$$



$$F(\omega) = V_o t \frac{\sin(\omega t / 2)}{\omega t / 2} \equiv V_o t \text{sinc}(\omega t / 2)$$



Bandwidth between first nulls for this signal:

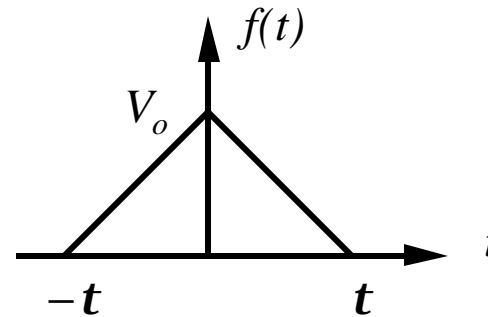
$$2(2\pi B_1) = 4\pi / t \Rightarrow B_1 = 1 / t$$

# Fourier Transform Refresher (3)

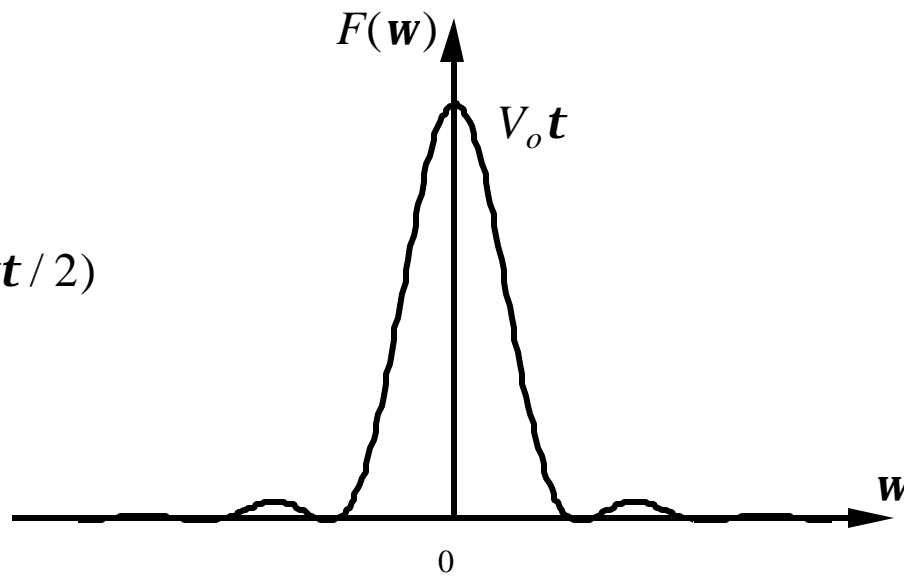
---

triangular pulse

$$f(t) = \begin{cases} V_o(1 - |t|/t), & |t| < t \\ 0, & \text{else} \end{cases}$$



$$F(\omega) = V_o t \operatorname{sinc}^2(\omega t / 2)$$



# Fourier Transform Refresher (4)

---

Important theorems and properties of the Fourier transform:

1. symmetry between the time and frequency domains

$$\text{if } f(t) \leftrightarrow F(\mathbf{w}), \text{ then } F(t) \leftrightarrow 2\mathbf{p} f(-\mathbf{w})$$

2. time scaling

$$f(at) \leftrightarrow 1/|a| F(\mathbf{w}/a)$$

3. time shifting

$$f(t-t_o) \leftrightarrow F(\mathbf{w}) e^{-j\mathbf{w}t_o}$$

4. frequency shifting

$$f(t) e^{j\mathbf{w}_o t} \leftrightarrow F(\mathbf{w} - \mathbf{w}_o)$$

5. time differentiation

$$\frac{d^n f(t)}{dt^n} \leftrightarrow (j\mathbf{w})^n F(\mathbf{w})$$

6. frequency differentiation

$$(-jt)^n f(t) \leftrightarrow \frac{d^n F(\mathbf{w})}{d\mathbf{w}^n}$$

# Fourier Transform Refresher (5)

---

7. conjugate functions

$$f^*(t) \leftrightarrow F^*(-\omega)$$

8. time convolution

$$f_1(t) \leftrightarrow F_1(\omega)$$

$$f_2(t) \leftrightarrow F_2(\omega)$$

$$f_1(t) * f_2(t) = \int_{-\infty}^{\infty} f_1(\mathbf{t}) f_2(t - \mathbf{t}) dt \leftrightarrow F_1(\omega) F_2(\omega)$$

9. frequency convolution

$$f_1(t) f_2(t) \leftrightarrow F_1(\omega) * F_2(\omega)$$

10. Parseval's formula

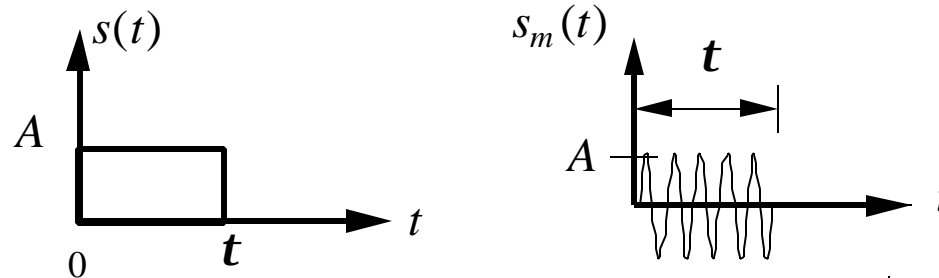
$$F(\omega) = A(\omega) e^{j\Phi(\omega)}, \quad |F(\omega)| = A(\omega)$$

$$\int_{-\infty}^{\infty} |f(t)|^2 dt = \frac{1}{2\pi} \int_{-\infty}^{\infty} A(\omega)^2 d\omega$$

# Modulation of a Carrier (1)

A carrier is modulated by a pulse to shift frequency components higher. (High frequency transmission lines and antennas are more compact and efficient than low frequency ones.) A sinusoidal carrier modulated by the waveform  $s(t)$  is given by

$$s_m(t) = s(t) \cos(\omega_c t) = \frac{s(t)}{2} [e^{j\omega_c t} + e^{-j\omega_c t}]$$



The Fourier transform of the modulated wave is easily determined using the shifting theorem

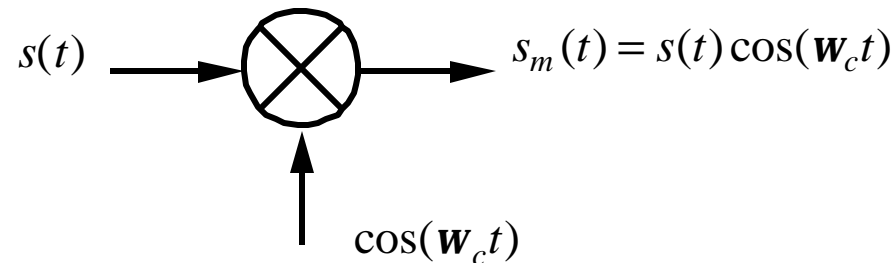
$$F_m(\omega) = \frac{1}{2} [F(\omega + \omega_c) + F(\omega - \omega_c)]$$

where  $s(t) \leftrightarrow F(\omega)$  and  $s_m(t) \leftrightarrow F_m(\omega)$ . Thus, in the case of a pulse,  $F(\omega)$  is a sinc function, and it has been shifted to the carrier frequency.



# Modulation of a Carrier (2)

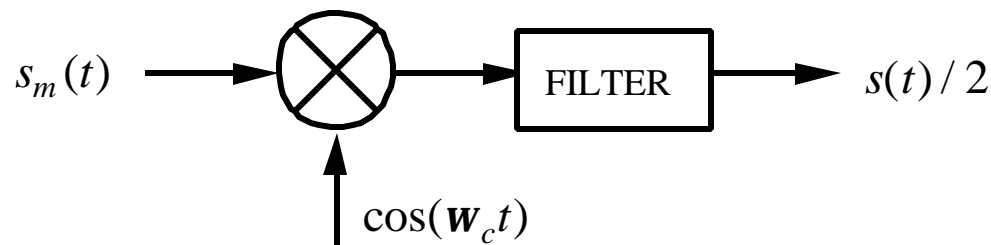
The frequency conversion, or shifting, is achieved using a modulator (mixer) which essentially multiplies two time functions



To recover  $s(t)$  from  $s_m(t)$  we demodulate. This can be done by multiplying again by  $\cos(\omega_c t)$

$$s_m(t) \cos(\omega_c t) = s(t) \cos^2(\omega_c t) = \frac{s(t)}{2} [1 + \cos(2\omega_c t)] = \frac{s(t)}{2} + \frac{s(t)}{4} [e^{j2\omega_c t} + e^{-j2\omega_c t}]$$

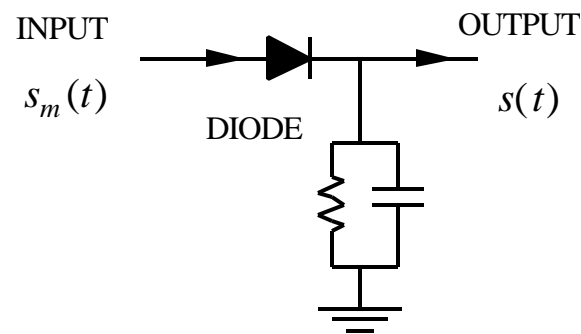
$s(t)/2$  is the desired baseband signal (centered at zero frequency). The other terms are rejected using filters.



# Modulation of a Carrier (3)

---

We can save work by realizing that  $s(t)$  is simply the envelope of  $s_m(t)$ . Therefore we only need an envelope detector:



In a real system both signal and noise will be present at the input of the detector

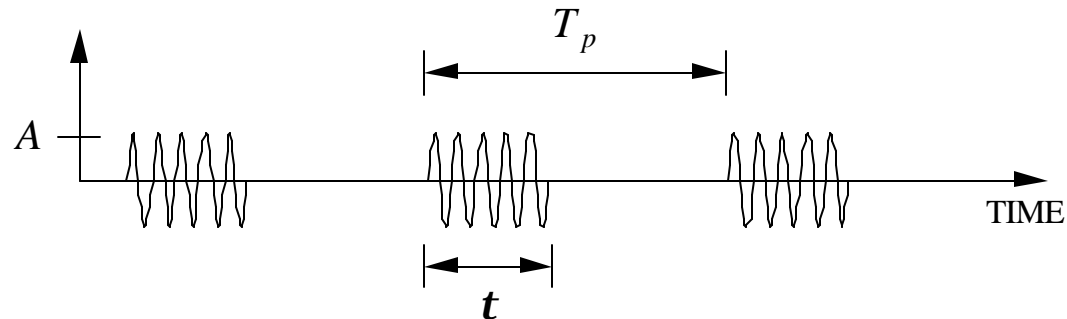
$$s_{\text{in}} = s_m(t) + n(t)$$

The noise is assumed to be gaussian white noise, that is, constant noise power as a function of frequency. Furthermore, the statistics of the noise (mean and variance) are independent of time. (This is a property of a stationary process.)

An important question that needs to be addressed is: how is noise affected by the demodulation and detection process? (Or, what is the PDF of the noise out of the detector?)

# Fourier Transform of a Pulse Train (1)

A coherent pulse train is shown below:



Coherent implies that the pulses are periodic sections of the same parent sinusoid. The finite length pulse train can be expressed as the product of three time functions:

1. infinite pulse train which can be expanded in a Fourier series

$$f_1(t) = a_0 + \sum_{n=1}^{\infty} a_n \cos(n\omega_o t)$$

where  $\omega_o = \frac{2\pi}{T_p} = 2\pi f_p$  and

$$a_0 = \frac{1}{T_p} \int_{-t/2}^{t/2} (1) dt = \frac{t}{T_p}$$

$$a_n = \frac{2}{T_p} \int_{-t/2}^{t/2} \cos(n\omega_o t) dt = \frac{2t}{T_p} \text{sinc}(n\omega_o T_p / 2)$$

# Fourier Transform of a Pulse Train (2)

---

2. rectangular window of length  $N_p T_p$  that turns on  $N_p$  pulses.

$$f_2(t) = \begin{cases} 1, & |t| \leq N_p T_p / 2 \\ 0, & \text{else} \end{cases}$$

3. infinite duration sinusoid  $f_3(t) = A \cos(\mathbf{w}_c t)$  where  $\mathbf{w}_c$  is the carrier frequency.

Thus the time waveform is:

$$f(t) = f_1(t) f_2(t) f_3(t) = \frac{A t}{T_p} \left\{ 1 + 2 \sum_{n=1}^{\infty} \cos(n \mathbf{w}_o t) \operatorname{sinc}(n \mathbf{w}_o t / 2) \right\} \cos(\mathbf{w}_c t)$$

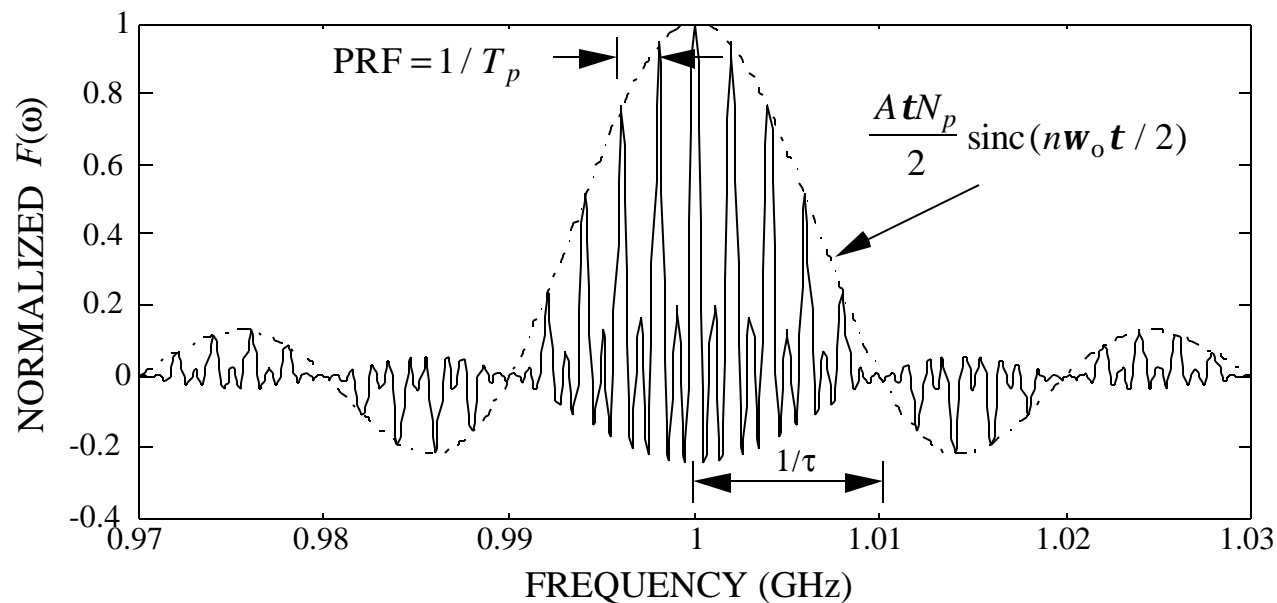
for  $|t| \leq N_p T_p / 2$ . Now we must take the Fourier transform of  $f(t)$ . The result is:

$$F(\mathbf{w}) = \frac{A t N_p}{T_p} \left\{ \operatorname{sinc} \left( (\mathbf{w} + \mathbf{w}_c) \frac{N_p T_p}{2} \right) + \sum_{n=1}^{\infty} \operatorname{sinc} \left( n \mathbf{w}_o \frac{t}{2} \right) \left[ \operatorname{sinc} \left( (\mathbf{w} + \mathbf{w}_c + n \mathbf{w}_o) \frac{N_p T_p}{2} \right) + \operatorname{sinc} \left( (\mathbf{w} + \mathbf{w}_c - n \mathbf{w}_o) \frac{N_p T_p}{2} \right) \right] \right. \\ \left. + \operatorname{sinc} \left( (\mathbf{w} - \mathbf{w}_c) \frac{N_p T_p}{2} \right) + \sum_{n=1}^{\infty} \operatorname{sinc} \left( n \mathbf{w}_o \frac{t}{2} \right) \left[ \operatorname{sinc} \left( (\mathbf{w} - \mathbf{w}_c + n \mathbf{w}_o) \frac{N_p T_p}{2} \right) + \operatorname{sinc} \left( (\mathbf{w} - \mathbf{w}_c - n \mathbf{w}_o) \frac{N_p T_p}{2} \right) \right] \right\}$$

# Fourier Transform of a Pulse Train (3)

A plot of the positive frequency portion of the spectrum for the following values:

$$N_p = 5, \quad f_c = 1 \text{ GHz}, \quad t = 0.1 \times 10^{-6} \text{ sec}, \quad T_p = 5t \text{ sec.}$$



- The envelope is determined by the pulse width; first nulls at  $\omega_c \pm 2\pi/t$ .
- The "spikes" are located at  $\omega_c \pm n\omega_o$ ; the width between the first nulls of each spike is  $4\pi/(N_p T_p)$ .
- The number of spikes is determined by the number of pulses.

# Response of Networks (1)

---

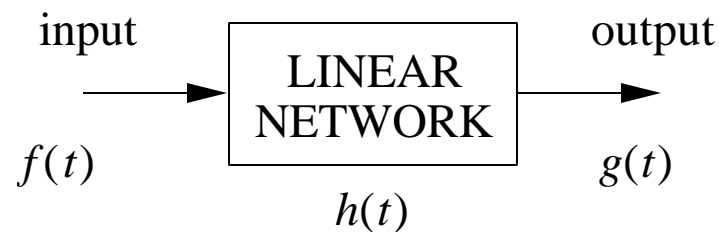
Consider a network that is:

linear, time invariant, stable (bounded output), causal

input:  $f(t) \leftrightarrow F(\mathbf{w})$ ;      output:  $g(t) \leftrightarrow G(\mathbf{w})$ ;      impulse response:  $h(t)$ ;

transfer function (frequency response):  $H(\mathbf{w}) = A(\mathbf{w})e^{j\Phi(\mathbf{w})}$

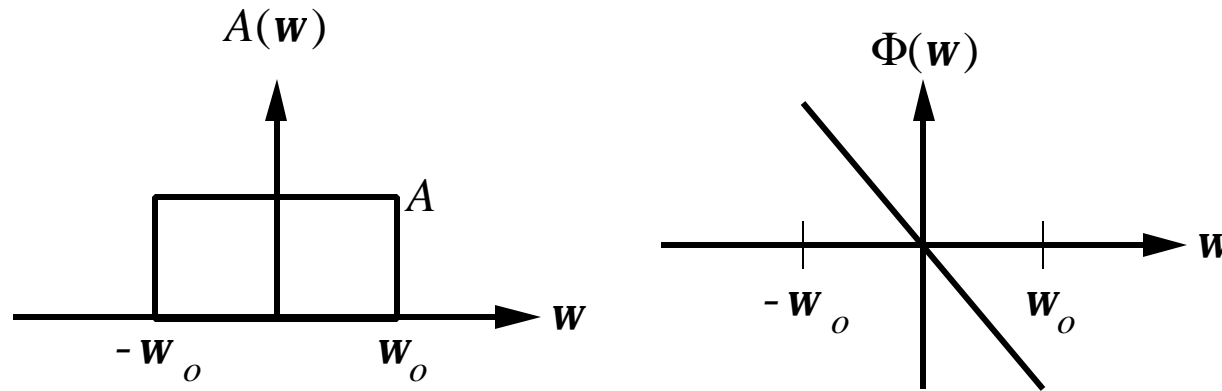
$$g(t) = \frac{1}{2\pi} \int_{-\infty}^{\infty} H(\mathbf{w})F(\mathbf{w})e^{j\mathbf{w}t} d\mathbf{w} \leftrightarrow G(\mathbf{w}) = H(\mathbf{w})F(\mathbf{w})$$



As an example, consider an ideal linear filter (constant amplitude and linear phase).

# Response of Networks (2)

Linear filter with cutoff frequency  $\omega_o = 2pB$ . What is the output if  $f(t)$  is a pulse?



Now  $F(\omega) = V_o t \text{sinc}(\omega t / 2)$  and  $G(\omega) = V_o t \text{sinc}(\omega t / 2) A e^{j\Phi(\omega)}$ . Let  $\Phi(\omega) = -t_o \omega$ :

$$g(t) = \frac{AV_o t}{2p} \int_{-\omega_o}^{\omega_o} \text{sinc}\left(\frac{\omega t}{2}\right) e^{j\omega(t-t_o)} d\omega$$

$$g(t) = \frac{AV_o t}{2p} 2 \int_0^{\omega_o} \text{sinc}\left(\frac{\omega t}{2}\right) \cos[\omega(t-t_o)] d\omega$$

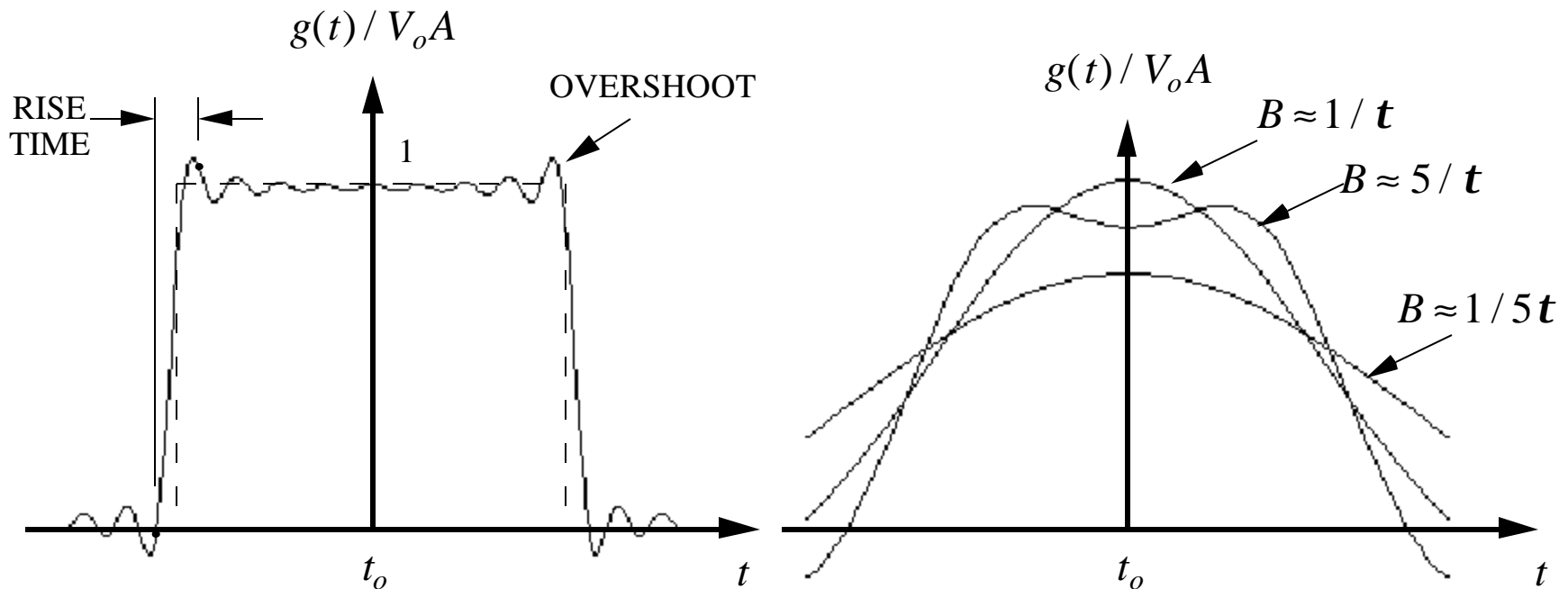
Use trig identity ( $\cos A \cos B = \dots$ ) and substitution of variables to reduce the integrals to "sine integral" form, which is tabulated.

# Response of Networks (3)

Final form of the output signal:

$$g(t) = \frac{AV_o}{p} \{ \text{Si} [w_o(t - t_o + t/2)] + \text{Si} [w_o(t - t_o - t/2)] \}$$

where  $\text{Si}(B) = \int_0^B \text{sinc}(a) da$ . Rule of thumb:  $B \approx 1/t$  for good pulse fidelity.

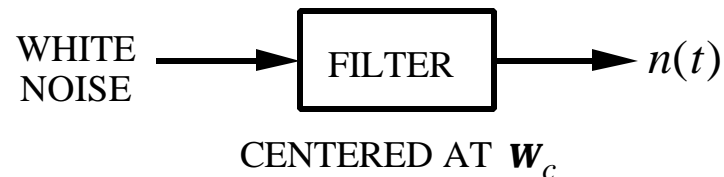




# Signals and Noise Through Networks (1)

---

Consider white noise through an envelope detector and filter

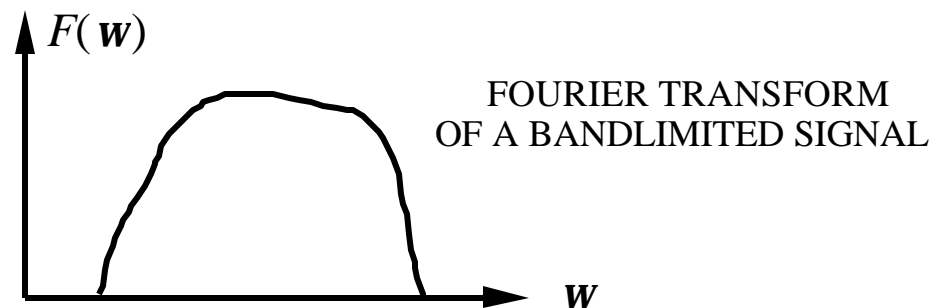


The noise at the output is a complex random variable

$$n(t) = r(t)e^{j(\omega_c t + \phi(t))} = x(t)\cos(\omega_c t) + y(t)\sin(\omega_c t)$$

The right-hand side is a rectangular form that holds for a narrowband process. The cosine term is the in-phase (I) term and the sine term the quadrature (Q) term.

Assume that the Fourier transform of  $s(t)$  is bandlimited, that is, its Fourier transform is zero except for a finite number of frequencies



# Signals and Noise Through Networks (2)

---

If the filter characteristic has the same bandwidth as  $s(t)$  and is shifted to the frequency  $\omega_c$  then the carrier modulated signal  $s_m(t)$  will pass unaffected. The signal plus noise at the output will be

$$s_{\text{out}}(t) = \underbrace{[s(t) + x(t)]}_{\equiv x', \text{ in-phase term}} \cos(\omega_c t) + \underbrace{y(t) \sin(\omega_c t)}_{\text{quadrature term}}$$

If  $x$  and  $y$  are normally distributed with zero mean and variance  $\mathbf{s}^2$ , their joint PDF is the product

$$p_{xy}(x, y) = \frac{e^{-(x^2 + y^2)/(2\mathbf{s})}}{2\mathbf{p}\mathbf{s}^2}$$

When the signal is added to the noise, the random variable  $x'$  is shifted

$$p_{x'y}(x', y) = \frac{e^{-[(\overset{x'}{\widetilde{x}} + s)^2 + y^2]/(2\mathbf{s})}}{2\mathbf{p}\mathbf{s}^2}$$

Now transform to polar coordinates:  $x' = r \cos \mathbf{q}$  and  $y = r \sin \mathbf{q}$  and use a theorem from probability theory

$$p_{r\mathbf{q}}(r, \mathbf{q}) dr d\mathbf{q} = p_{x'y}(x', y) dx' dy$$

# Signals and Noise Through Networks (3)

---

With some math we find that

$$p_{r\mathbf{q}}(r, \mathbf{q}) = \frac{1}{2p\mathbf{s}^2} e^{-s^2/(2\mathbf{s}^2)} \text{rexp}\left\{ \frac{(r^2 - 2rs\cos\mathbf{q})}{(2\mathbf{s}^2)} \right\}$$

At the output of the detector we are only dealing with  $p_r(r)$ , the phase gets integrated out. Thus we end up with the following expression for the PDF of the signal plus noise

$$p_r(r) = \frac{r}{2p\mathbf{s}^2} e^{-(s+r)^2/(2\mathbf{s}^2)} \underbrace{\int_0^{2p} e^{-rs\cos\mathbf{q}/\mathbf{s}^2} d\mathbf{q}}_{\equiv 2p I_0(rs/\mathbf{s}^2)}$$

where  $I_0(\cdot)$  is the modified Bessel function of the first kind (a tabulated function). Final form of the PDF is

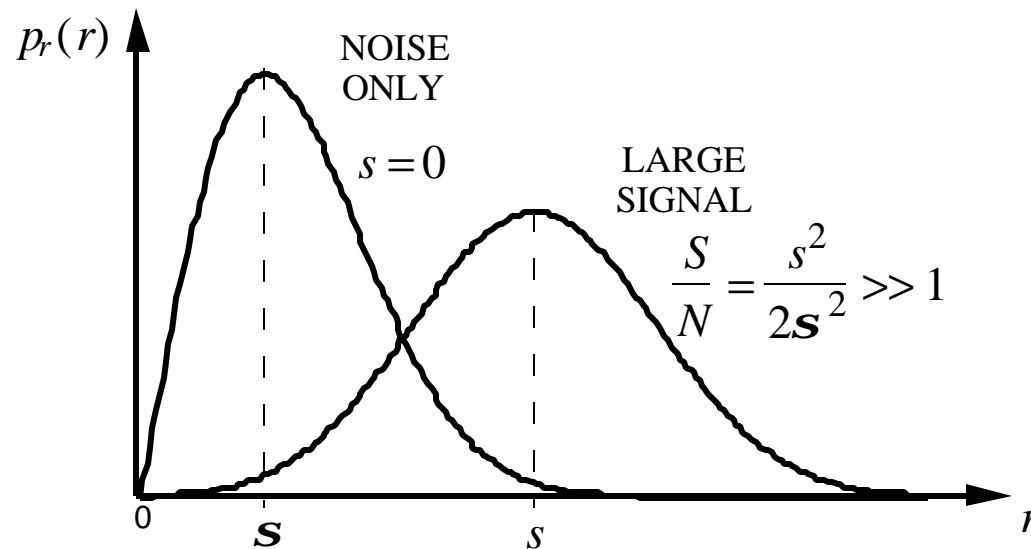
$$p_r(r) = \frac{r}{\mathbf{s}^2} e^{-(s+r)^2/(2\mathbf{s}^2)} I_0(rs/\mathbf{s}^2)$$

This is a Rician PDF. Note that for noise only present  $s = 0 \Rightarrow I_0(0) = 1$  and the Rician PDF reduces to a Rayleigh PDF.

(Note that Skolnik has different notation:  $s \rightarrow A$ ,  $r \rightarrow R$ ,  $\mathbf{s}^2 \rightarrow \mathbf{y}_o$ )

# Rician Distribution

Some examples of the Rician distribution:



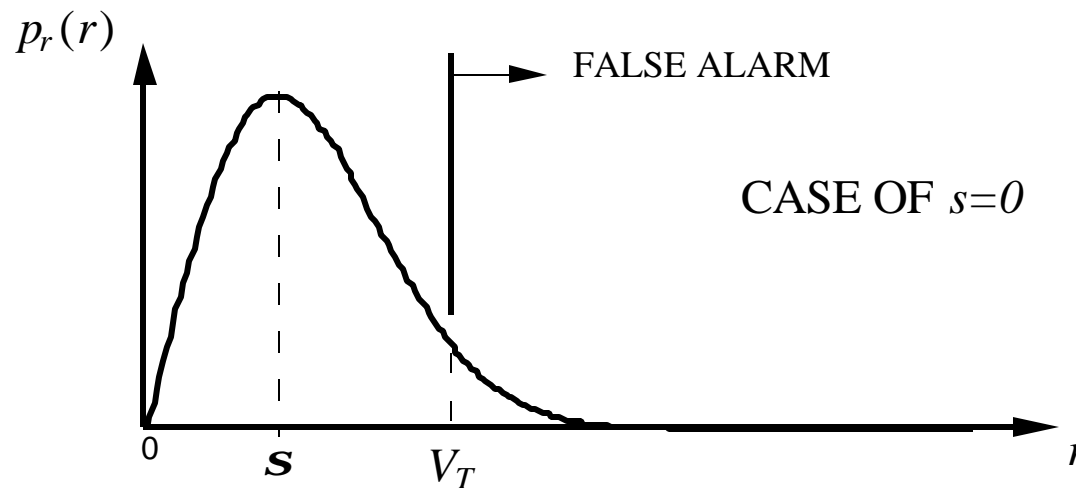
For  $s = 0$  the Rician distribution becomes a Rayleigh distribution.

For  $\frac{s^2}{2S^2} \gg 1$  the Rician distribution approaches a normal distribution.

# Probability of False Alarm (1)

For detection, a threshold is set. There are two cases to consider:  $s = 0$  and  $s \neq 0$ .

1.  $s = 0$ : If the signal exceeds the threshold a target is declared even though there is none present

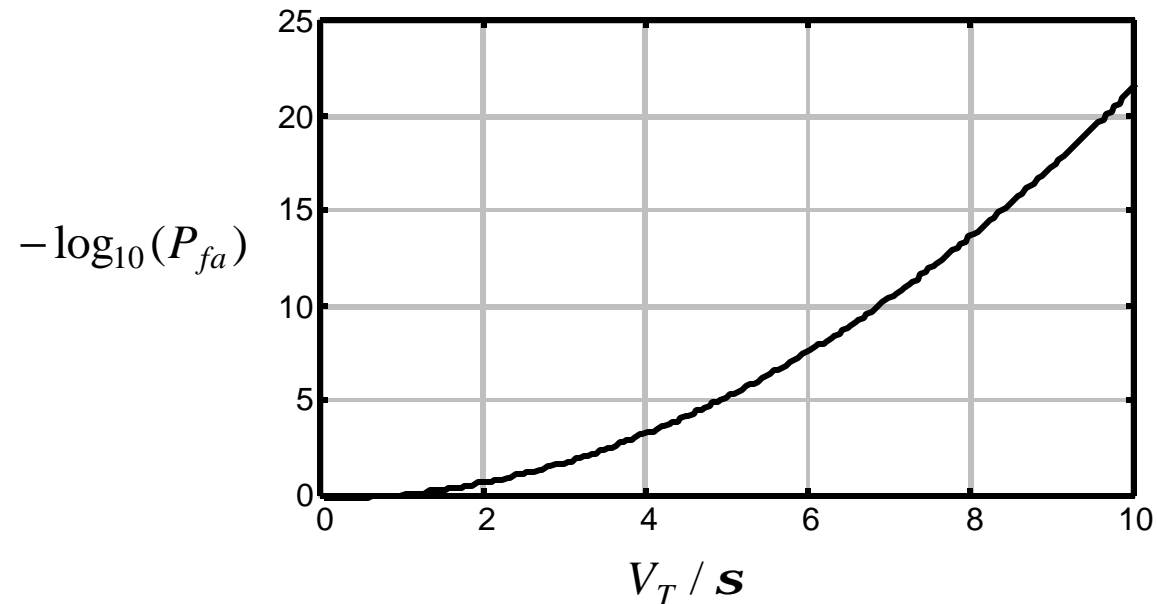


The probability of a false alarm is the area under the PDF to the right of  $V_T$

$$P_{fa} = \int_{V_T}^{\infty} p_r(r) dr = \int_{V_T}^{\infty} \frac{r}{\mathbf{s}^2} e^{-r^2 / (2\mathbf{s}^2)} dr = e^{-V_T^2 / (2\mathbf{s}^2)}$$

# Probability of False Alarm (2)

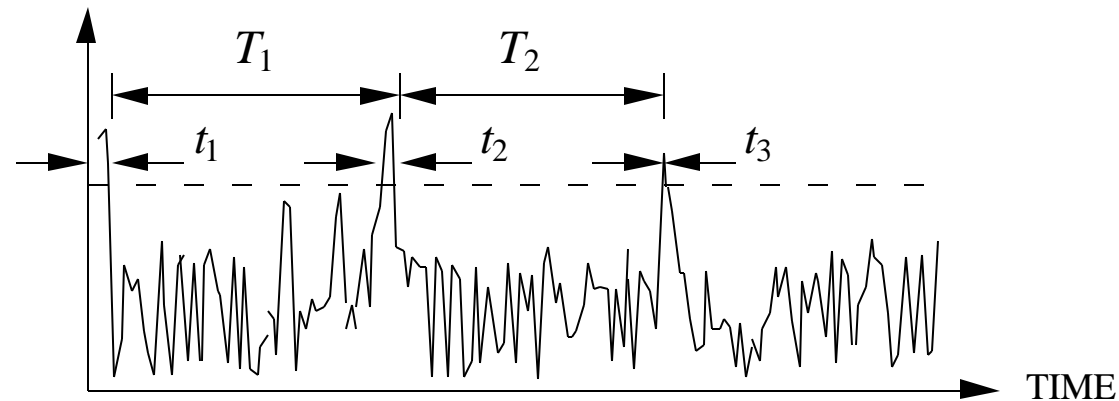
Probability of a false alarm vs. threshold level (this is essentially Figure 2.5 in Skolnik)



Probability of a false alarm can also be expressed as the fraction of time that the threshold is crossed divided by the total observation time:

$$P_{fa} = \frac{\text{time that the threshold has been crossed}}{\text{time that the threshold could have been crossed}}$$

# Probability of False Alarm (3)



or, referring to the figure (see Figure 2.4)

$$P_{fa} = \frac{\sum_n t_n}{\sum_n T_n} = \frac{\langle t_n \rangle}{\langle T_n \rangle} \approx \frac{1/B_n}{T_{fa}}$$

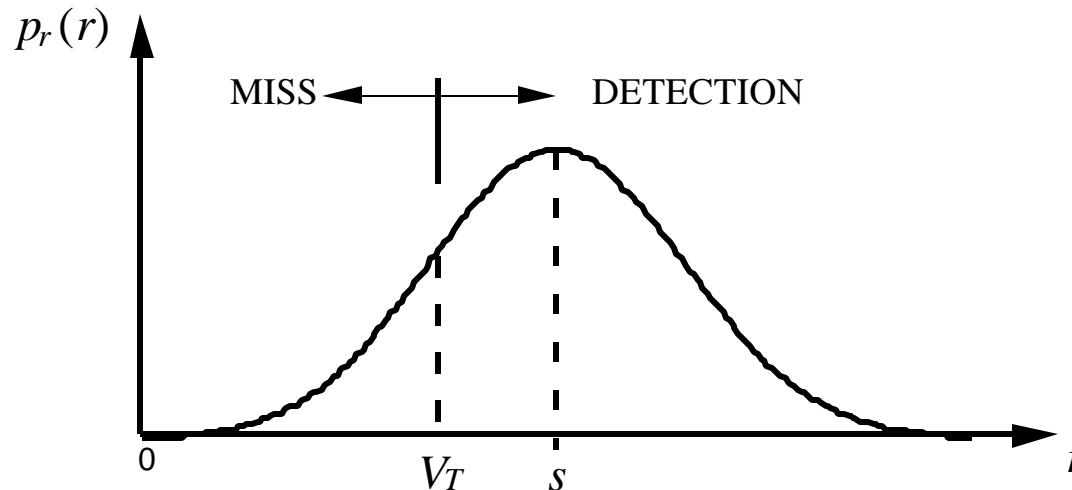
where  $T_{fa}$  is the false alarm time, a quantity of more practical interest than  $P_{fa}$ .

Finally,

$$P_{fa} = \frac{1}{T_{fa} B_n} = e^{-V_T^2 / (2s^2)}$$

# Probability of Detection (1)

2.  $s \neq 0$ : There is a target present. The probability of detecting the target is given by the area under the PDF to the right of  $V_T$



$$P_d = \int_{V_T}^{\infty} p_r(r) dr = \int_{V_T}^{\infty} \frac{r}{\mathbf{s}^2} e^{-(s^2-r^2)/(2\mathbf{s}^2)} I_0(rs/\mathbf{s}^2) dr$$

The probability of a miss is given by the area under the PDF to the left of  $V_T$ , or since the total area under the curve is 1,

$$P_m = 1 - P_d$$



## Probability of Detection (2)

---

For a large SNR =  $\frac{s^2}{2\mathbf{s}^2} \gg 1$  and a large argument approximation for the modified Bessel function can be used in the expression for the PDF:  $I_0(x) \approx e^x / (2px)$ . The Rician PDF is approximately gaussian

$$p_r(r) = \frac{1}{2\mathbf{p}\mathbf{s}^2} e^{-(s-r)^2 / (2\mathbf{s}^2)}$$

Use the standard error function notation

$$\text{erf}(x) = \frac{1}{\sqrt{\mathbf{p}}} \int_0^x e^{-u^2} du$$

which is tabulated in handbooks. The probability of detection becomes

$$P_d = \frac{1}{2} \left\{ 1 - \text{erf} \left( \frac{V_T}{\sqrt{2\mathbf{s}^2}} - \sqrt{\text{SNR}} \right) \right\}, \quad \text{SNR} \gg 1$$

Recall that

$$P_{fa} = e^{-V_T^2 / (2\mathbf{s}^2)}$$

# Probability of Detection (3)

---

Eliminate  $V_T$  and solve for the SNR

$$\text{SNR} \approx A + 0.12AB + 1.7B$$

where  $A = \ln(0.62 / P_{fa})$  and  $B = \ln[P_d / (1 - P_d)]$ . This is referred to as Albertsheim's approximation, and is good for the range  $10^{-7} \leq P_{fa} \leq 10^{-3}$  and  $0.1 \leq P_d \leq 0.9$

Note: The SNR is not in dB. This equation gives the same results as Figure 2.6

- Design Process:
1. choose an acceptable  $P_{fa}$  ( $10^{-3}$  to  $10^{-12}$ )
  2. find  $V_T$  for the chosen  $P_{fa}$
  3. choose an acceptable  $P_d$  (0.5 to 0.99)
  4. for the chosen  $P_d$  and  $V_T$  find the SNR

# Probability of Detection (4)

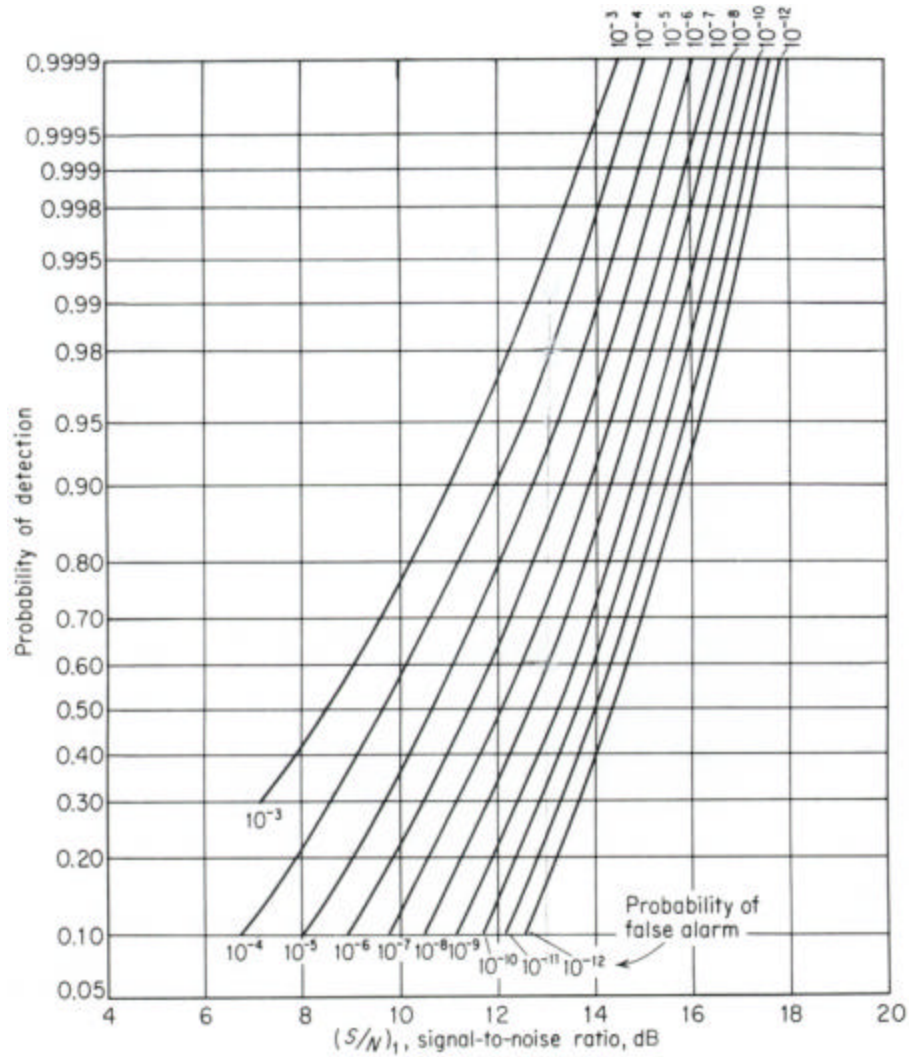
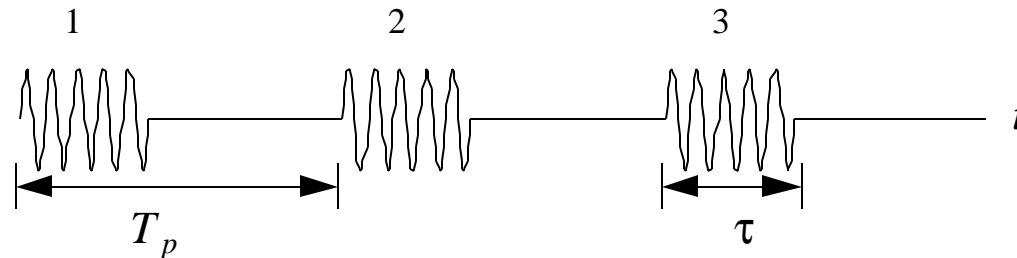


Figure 2.6 in Skolnik

# SNR Improvement Using Integration

The SNR can be increased by integrating (summing) the returns from several pulses. Integration can be coherent or noncoherent.

1. Coherent integration (predetection integration): performed before the envelope detector (phase information must be available). Coherent pulses must be transmitted.



Returns from pulses 1 and 2 are delayed in the receiver so that they are contiguous (i.e., they touch) and then summed coherently. The result is essentially a pulse length  $n$  times greater than that of a single pulse when  $n$  pulses are used. The noise bandwidth is  $B_n \approx 1/(nt)$  compared to  $B_n \approx 1/t$  for a single pulse. Therefore the noise has been reduced by a factor  $n$  and

$$\text{SNR} \propto \frac{n(P_r)_1}{B_n}$$

where  $(P_r)_1$  is the received power for a single pulse. The improvement in SNR by coherently integrating  $n$  pulses is  $n$ . This is also referred to as a perfect integrator.

# SNR Improvement Using Integration

---

2. Noncoherent integration (postdetection integration): performed after the envelope detector. The magnitudes of the returns from all pulses are added.

Procedure:

- $N$  samples (pulses) out of the detector are summed
- the PDF of each sample is Ricean
- the joint PDF of the  $N$  samples is obtained from a convolution of Ricean PDFs
- once the joint PDF is known, set  $V_T$  and integrate to find expressions for  $P_{fa}$  and  $P_d$

Characteristics:

- noise never sums to zero as it can in the coherent case
- does not improve signal-to-clutter ratio
- only used in non-coherent radars (most modern radars are coherent)

Improvement:

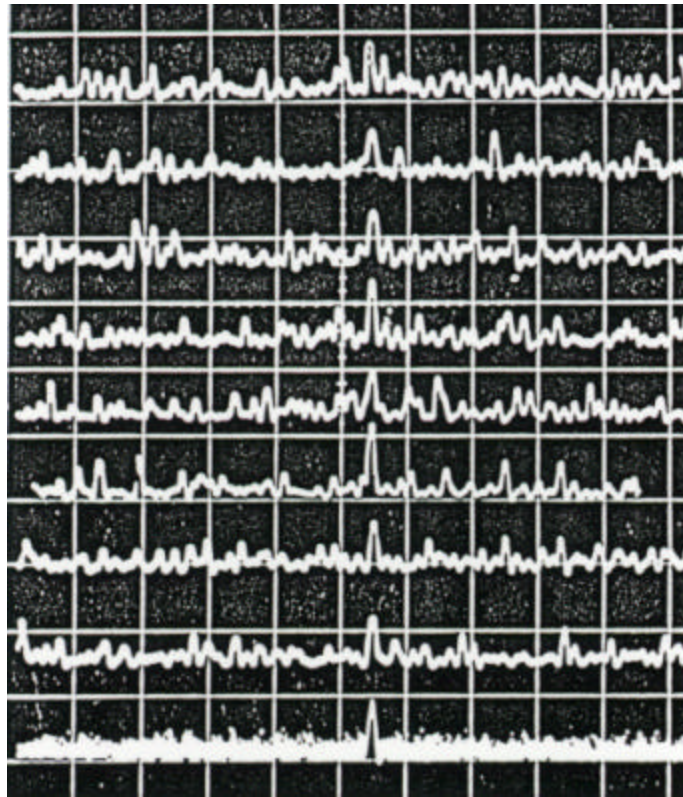
$$\text{SNR} \propto \frac{n_{\text{eff}}(P_r)_1}{B_n}$$

where the effective number of pulses is  $n_{\text{eff}} \approx n$  for small  $n$  and  $n_{\text{eff}} \approx \sqrt{n}$  for large  $n$

# Illustration of Noncoherent Integration

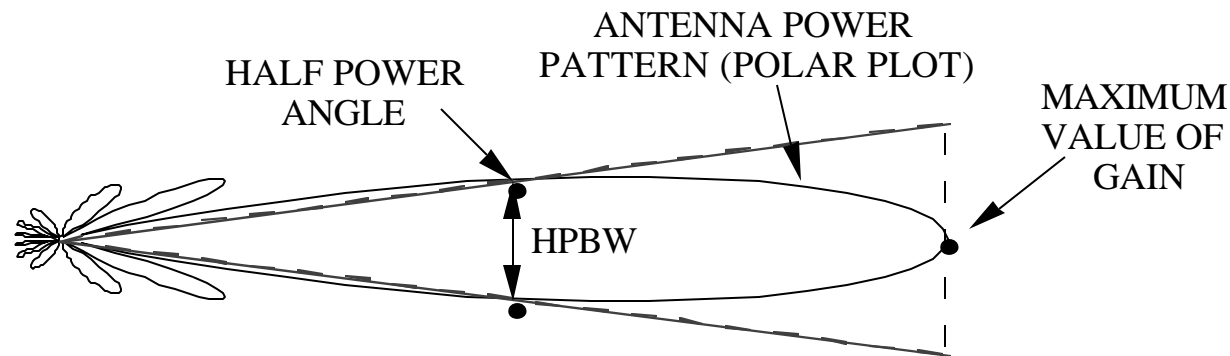
---

The last trace shows the integrated signal.



From Byron Edde, *Radar: Principles, Technology, Applications*, Prentice-Hall

# Approximate Antenna Model



For systems analysis an approximation of the actual antenna pattern is sufficient. We ignore the beam shape and represent the antenna pattern by

$$G = \begin{cases} G_o, & \text{within HPBW } (= \mathbf{q}_B) \\ 0, & \text{outside of HPBW} \end{cases}$$

where  $G_o$  is the maximum antenna gain. Thus the sidelobes are neglected and the gain inside of the half power beamwidths is constant and equal to the maximum value.

# Number of Pulses Available

---

The antenna beam moves through space and only illuminates the target for short periods of time. Use the approximate antenna model

$$G(\mathbf{q}) = \begin{cases} G_o, & |\mathbf{q}| < \mathbf{q}_H (= \mathbf{q}_B / 2) \\ 0, & \text{else} \end{cases}$$

where  $G_o$  is the maximum gain and  $\mathbf{q}_H$  the half power angle and  $\mathbf{q}_B$  the half power beamwidth (HPBW). If the aperture has a diameter  $D$  and uniform illumination, then

$\mathbf{q}_B \approx \lambda / D$ . The beam scan rate is  $\mathbf{w}_s$  in revolutions per minute or  $\frac{d\mathbf{q}_s}{dt} = \dot{\mathbf{q}}_s$  in degrees per second. (The conversion is  $\frac{d\mathbf{q}_s}{dt} = 6\mathbf{w}_s$ .) The time that the target is in the beam (dwell time<sup>1</sup> or look) is

$$t_{\text{ot}} = \mathbf{q}_B / \dot{\mathbf{q}}_s$$

and the number of pulses that will hit the target in this time is

$$n_B = t_{\text{ot}} f_p$$

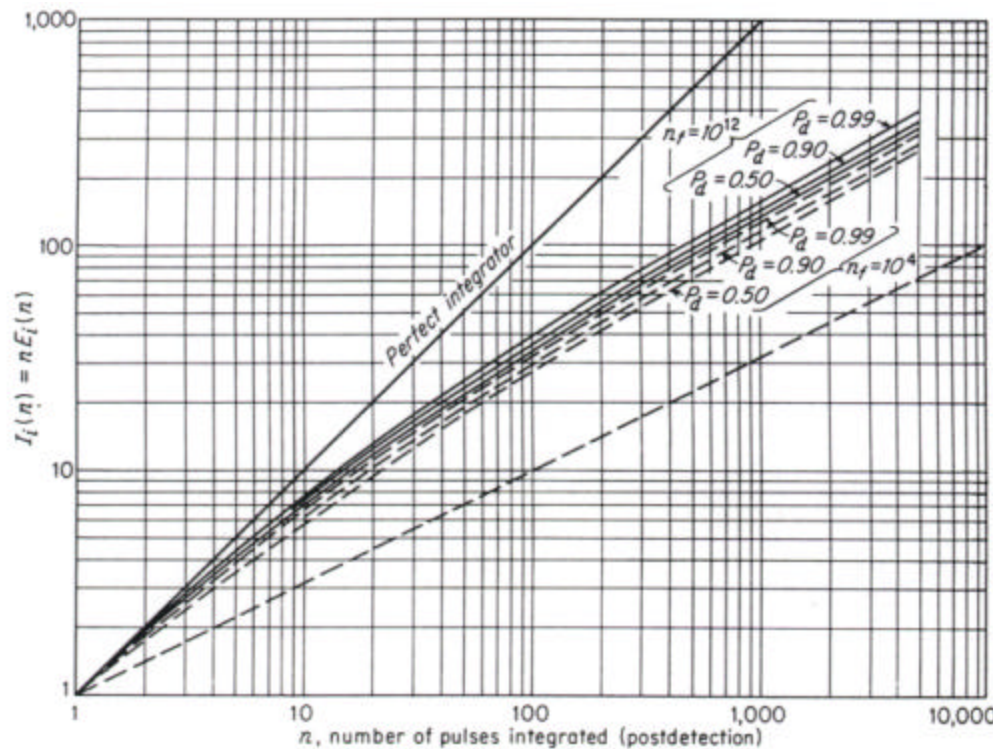
---

<sup>1</sup> The term dwell time does not have a standardized definition. It can also mean the time that a pulse train is hitting the target, or data collection time. By this definition, if multiple PRFs are used while the target is in the beam, then there can be multiple dwells per look.



# Integration Improvement Factor

The integration efficiency is defined as  $E_i(n) = \frac{\text{SNR}_1}{n (\text{SNR}_n)}$  where  $\text{SNR}_1$  is the signal-to-noise ratio for one pulse and  $\text{SNR}_n$  is that to obtain the same  $P_d$  as  $\text{SNR}_1$  when integrating  $n$  pulses. The improvement in signal-to-noise ratio when  $n$  pulses are integrated is the integration improvement factor:  $I_i(n) = n E_i(n)$



Skolnik Figure 2.7 (a)

- for a square law detector
- false alarm number

$$n_{fa} = 1 / P_{fa} = T_{fa} B_n$$

# RRE for Pulse Integration

---

To summarize:

Coherent (predetection) integration:  $E_i(n) = 1$  and  $I_i(n) = n$

$$\text{SNR}_n = \frac{1}{n} \text{SNR}_1$$

Noncoherent (postdetection) integration:  $I_i(n) < n$

In the development of the RRE we used the single pulse SNR; that is

$$(\text{SNR}_{\text{out}})_{\text{min}} = \text{SNR}_1$$

For  $n$  pulses integrated

$$(\text{SNR}_{\text{out}})_{\text{min}} = \text{SNR}_n = \frac{\text{SNR}_1}{nE_i(n)}$$

This quantity should be used in the RRE.

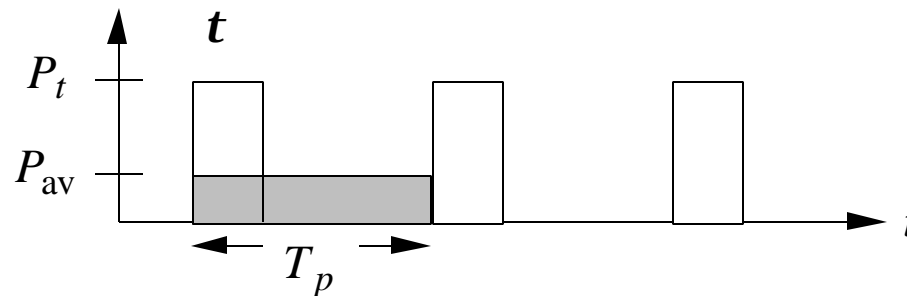
# RRE for Pulse Integration

Integrating pulses increases the detection range of a radar by increasing the signal-to-noise ratio

$$R_{\max}^4 = \frac{P_t G_t A_{er} S n E_i(n)}{(4p)^2 k T_s B_n (\text{SNR})_1}$$

where  $(\text{SNR})_1$  is the signal-to-noise ratio for single pulse detection.

In the RRE,  $P_t$  is the peak pulse envelope power. The duty cycle is the fraction of the interpulse period that the pulse is on ( $= t / T_p$ )



$P_{\text{av}}$  is the average power: computed as if the energy in the pulse ( $= P_t t$ ) were spread over the entire interpulse period  $T_p$ :  $P_{\text{av}} = P_t t / T_p$ . Using the average power gives a form of the RRE that is waveform independent.

# RRE for Pulse Integration

---

Note that ordinarily  $P_t$  is the time-averaged power (one half the maximum instantaneous) when working with a pulse train waveform

$$R_{\max}^4 = \frac{P_t G_t A_{er} S n E_i(n)}{(4p)^2 k T_s B_n \text{SNR}_1}$$

Design process using Figures 2.6 and 2.7:

1. choose an acceptable  $P_{fa}$  from  $P_{fa} = 1/(T_{fa} B_n)$
2. choose an acceptable  $P_d$  (0.5 to 0.99) and with  $P_{fa}$  find  $\text{SNR}_1$  from Figure 2.6
3. for the chosen  $P_d$ , and false alarm number  $n_{fa} = 1/P_{fa} = T_{fa} B_n$  find the integration improvement factor,  $I_i(n)$ , from Figure 2.7(a)

Design process using Albersheim's approximation:

The SNR per pulse when  $n$  pulses are integrated noncoherently is approximately

$$\text{SNR}_n, \text{dB} \approx -5 \log n + \left(6.2 + 4.54 / \sqrt{n + 0.44}\right) \log(A + 0.12AB + 1.7B)$$

where  $A = \ln(0.62 / P_{fa})$  and  $B = \ln[P_d / (1 - P_d)]$ ,  $10^{-7} \leq P_{fa} \leq 10^{-3}$ , and  $0.1 \leq P_d \leq 0.9$

# Radar Cross Section (1)

Definition of radar cross section (RCS)

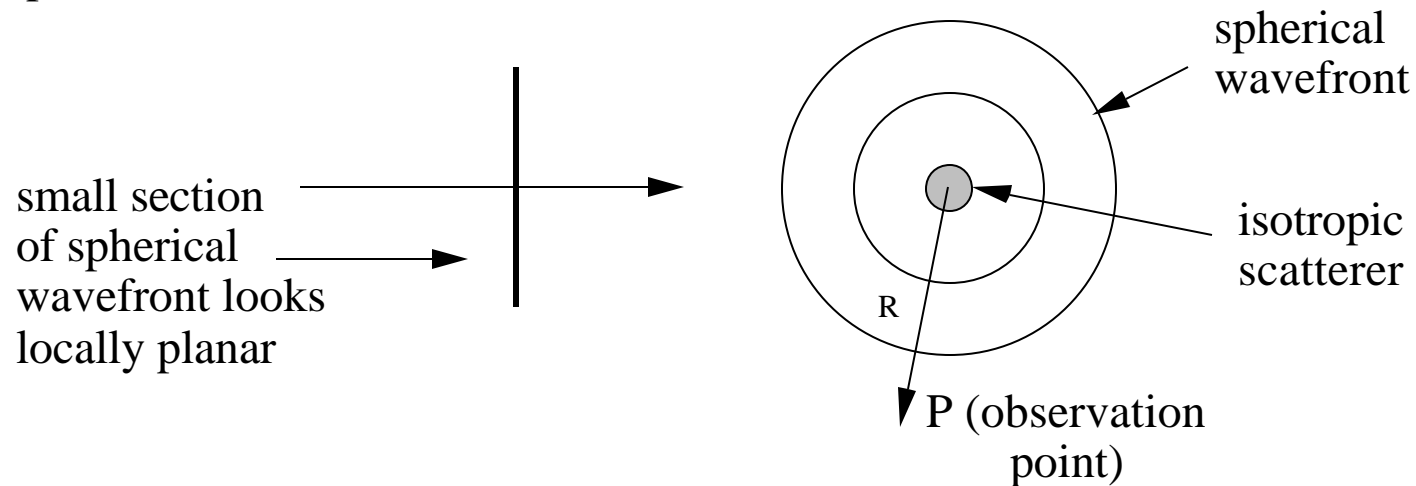
$$\mathbf{s} = \frac{\text{power reflected toward source per unit solid angle}}{\text{incident power density}/4\mathbf{p}} = \lim_{R \rightarrow \infty} 4\mathbf{p} R^2 \frac{|\vec{W}_s|}{|\vec{W}_i|}$$

$\vec{W}_i$  = power density incident on the target (Poynting vector)

$\vec{W}_s$  = scattered power density from target returned to the radar

Expressed in decibels relative to a square meter (dBsm):  $\mathbf{s}_{\text{dBsm}} = 10\log_{10}(\mathbf{s})$ .

RCS is used to describe a target's scattering properties just as gain (or directivity) is used for an antenna. An isotropic scatterer will scatter equally in all directions (i.e., a spherical wave)

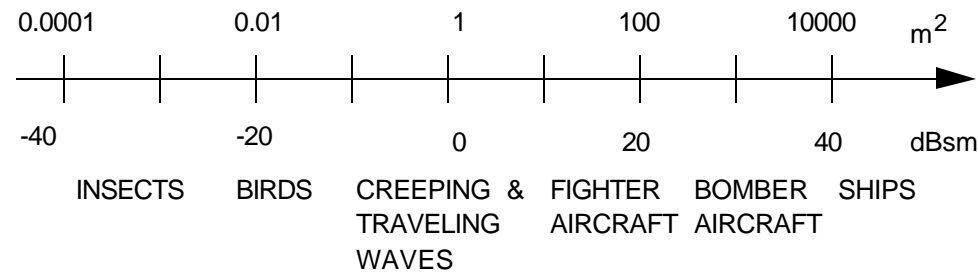


# Radar Cross Section (2)

RCS is a function of:

1. wave properties (polarization and frequency)
2. aspect angle (viewing angle)

Typical values of RCS:

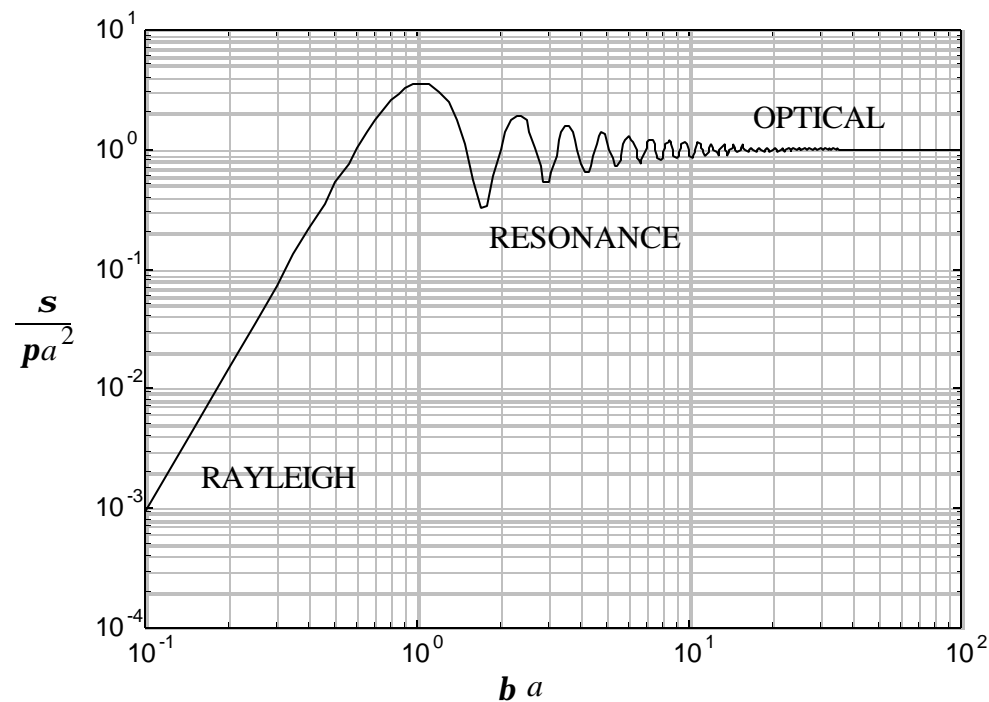


Consider an arbitrary target with a "characteristic dimension,"  $L$ . The RCS has three distinct frequency regions as illustrated by the RCS of a sphere:

1. low frequencies (Rayleigh region):  $kL \ll 1$   
 $\sigma \propto 1/L^4$ ,  $\sigma$  vs  $kL$  is smooth,  $\sigma \propto (\text{volume})^2$
2. resonance region (Mie region):  $kL \approx 1$ ,  $\sigma$  vs  $kL$  oscillates
3. high frequencies (optical region):  $kL \gg 1$ ,  $\sigma$  vs  $kL$  is smooth and may be independent of  $L$

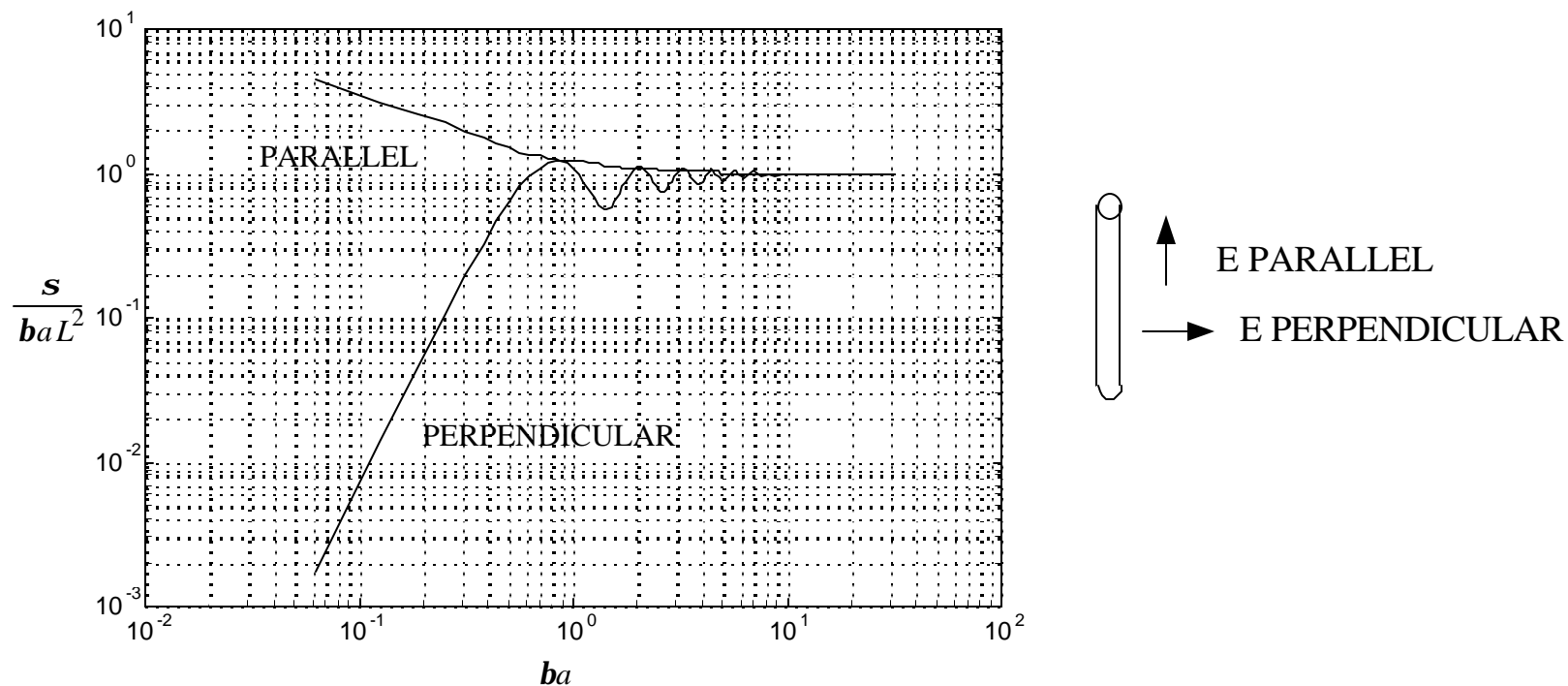
# Radar Cross Section of a Sphere

Monostatic RCS of a sphere,  $b = 2p / l$  ( $= k$ ),  $a =$  radius, illustrates the three frequency regions: (1) Rayleigh, (2) Mie, and (3) optical



# Radar Cross Section of a Cylinder

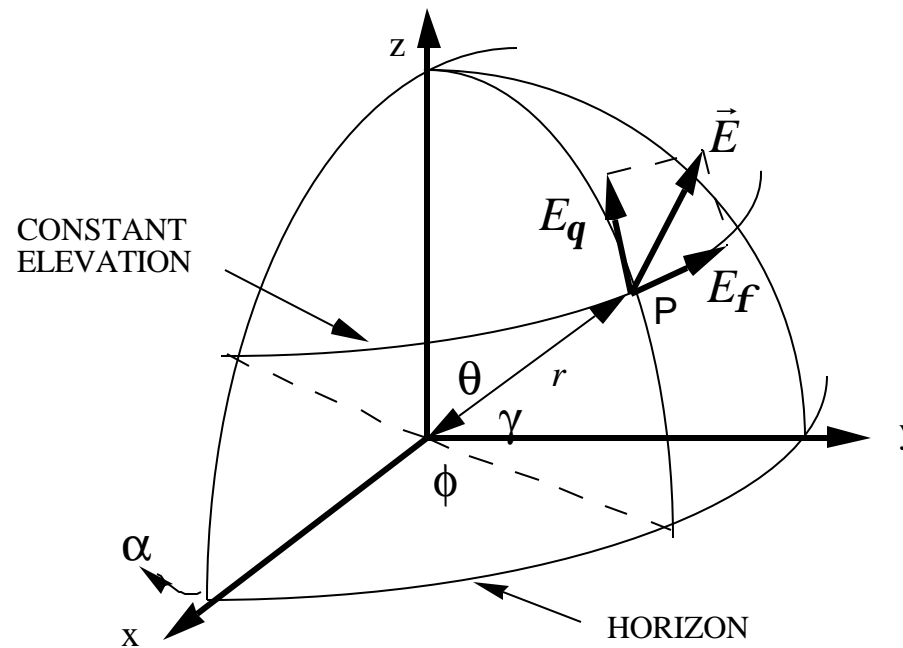
Monostatic RCS of a cylinder,  $b = 2p / l$  ( $= k$ ),  $a =$  radius, illustrates dependence on polarization.  $L$  is the length.





# Target Scattering Matrix (1)

---



Arbitrary wave polarization can be decomposed into spherical components.

$$\vec{E}_i = E_{iq}\hat{q} + E_{if}\hat{f}$$

Similarly for the scattered field

$$\vec{E}_s = E_{sq}\hat{q} + E_{sf}\hat{f}$$

# Target Scattering Matrix (2)

---

Define the RCS for combinations of incident and scattered wave polarizations

$$s_{pq} = \lim_{R \rightarrow \infty} 4pR^2 \frac{|\vec{E}_{sp}|^2}{|\vec{E}_{iq}|^2}$$

where  $p, q = \mathbf{q}$  or  $\mathbf{f}$ . The index  $p$  denotes the polarization of the scattered wave and  $q$  the polarization of the incident wave. In general, a scattering matrix can be defined that relates the incident and scattered fields

$$\begin{bmatrix} E_{sq} \\ E_{sf} \end{bmatrix} = \frac{1}{\sqrt{4pR^2}} \begin{bmatrix} s_{qq} & s_{qf} \\ s_{fq} & s_{ff} \end{bmatrix} \begin{bmatrix} E_{iq} \\ E_{if} \end{bmatrix}$$

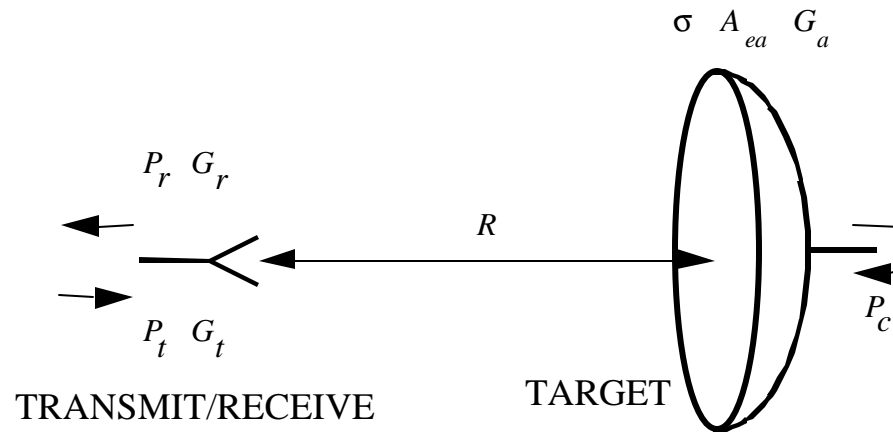
where

$$s_{pq} = \sqrt{s_{pq}} e^{j\mathbf{y}_{pq}}, \quad \mathbf{y}_{pq} = \tan^{-1} \left\{ \frac{\text{Im}(E_{sp} / E_{iq})}{\text{Re}(E_{sp} / E_{iq})} \right\}$$

Copolarized RCS:  $p = q$  cross polarized:  $p \neq q$

# Example: Antenna as a Radar Target

Antenna at range  $R$



Received power is

$$P_r = \underbrace{\left( \frac{P_t G_t}{4pR^2} \right) (A_{ea})}_{P_s} \left( \frac{4pA_{ea}}{I^2} \right) \left( \frac{1}{4pR^2} \right) (A_{er})$$

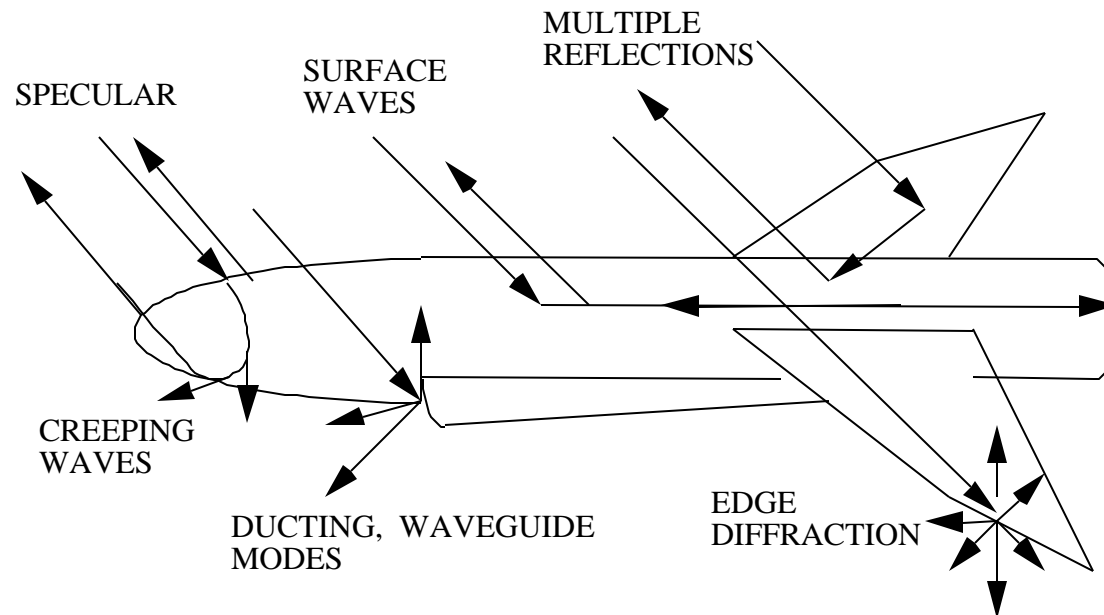
Compare this result with the original form of the radar equation and find that

$$A_{ea}^2 = \frac{I^2 S}{4p} \Rightarrow S = \frac{4pA_{ea}^2}{I^2} \approx \frac{4pA_p^2}{I^2}$$

Important result -- applies to any large relatively flat scattering area.

# Scattering Mechanisms

---



Scattering mechanisms are used to describe wave behavior. Especially important for standard radar targets (planes, ships, etc.) at radar frequencies:

specular = "mirror like" reflections that satisfy Snell's law

surface waves = the body acts like a transmission line guiding waves along its surface

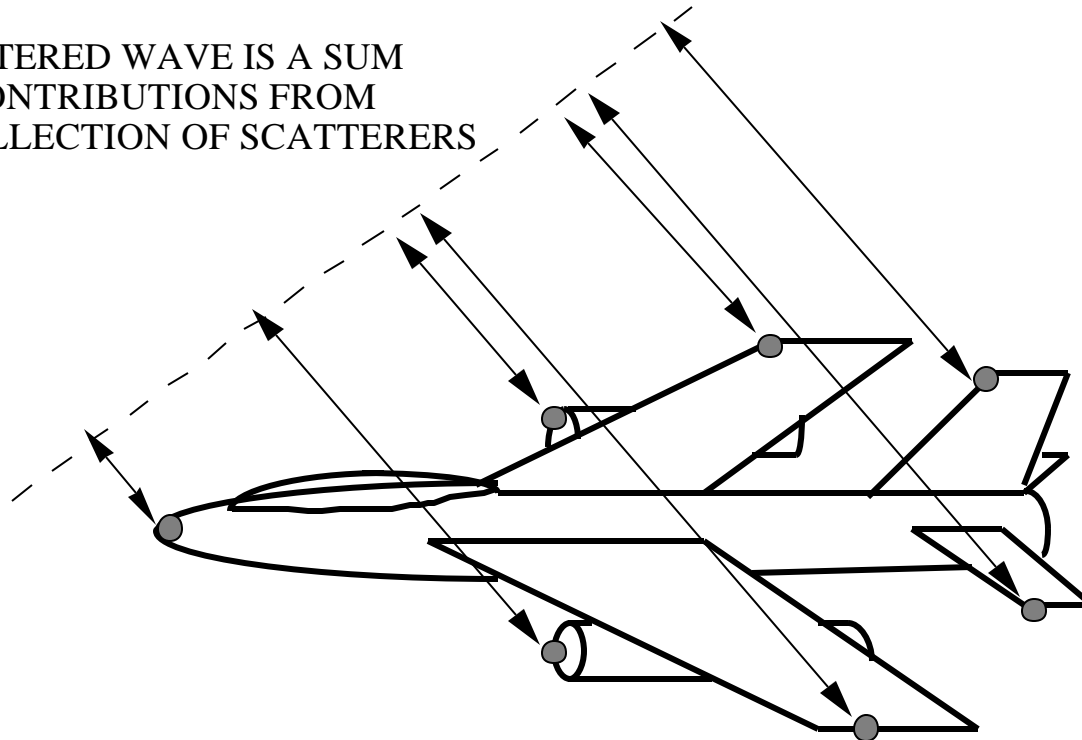
diffraction = scattered waves that originate at abrupt discontinuities (e.g., edges)

# Scattering Sources for a Complex Target

---

Typical for a target in the optical region (i.e., target large compared to wavelength)

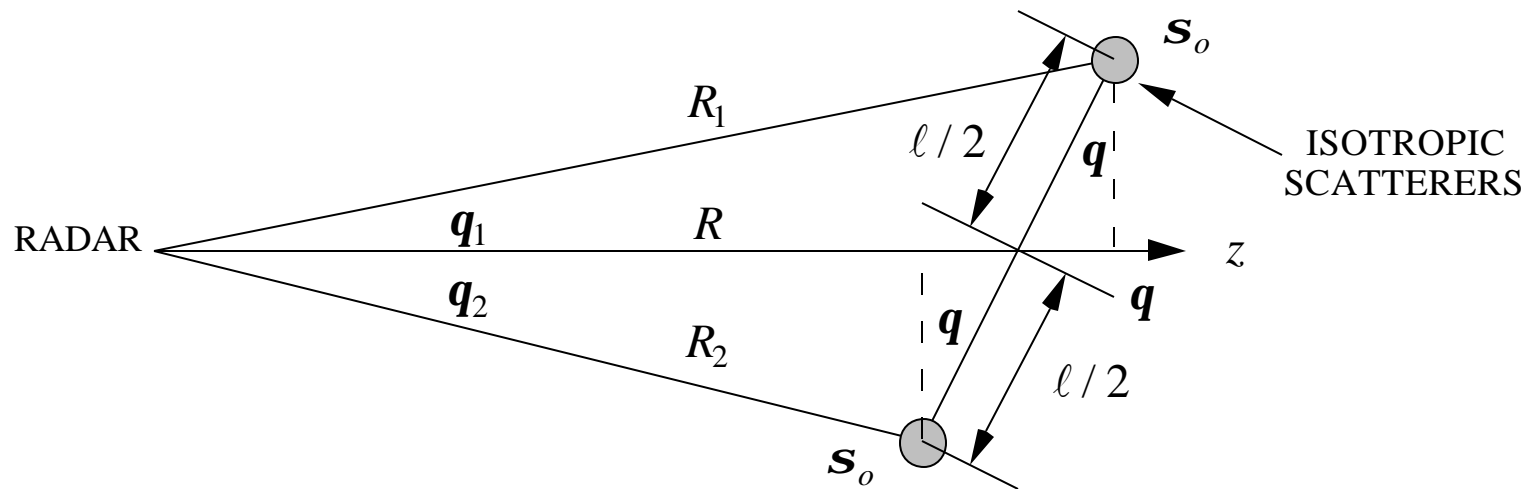
SCATTERED WAVE IS A SUM  
OF CONTRIBUTIONS FROM  
A COLLECTION OF SCATTERERS



In some directions all scattering sources may add in phase and result in a large RCS.  
In other directions some sources may cancel other sources resulting in a very low RCS.

# Two Sphere RCS (1)

Consider the RCS obtained from two isotropic scatterers (approximated by spheres).



Law of cosines:

$$R_1 = \sqrt{R^2 + (\ell/2)^2 - 2R(\ell/2)\cos(\mathbf{q} + \mathbf{p}/2)} = R\sqrt{1 + (\ell/2R)^2 + 2(\ell/2R)\sin \mathbf{q}}$$

$$R_2 = \sqrt{R^2 + (\ell/2)^2 - 2R(\ell/2)\cos(\mathbf{q} - \mathbf{p}/2)} = R\sqrt{1 + (\ell/2R)^2 - 2(\ell/2R)\sin \mathbf{q}}$$

Let  $\mathbf{a} = \ell \sin \mathbf{q} / R$  and note that

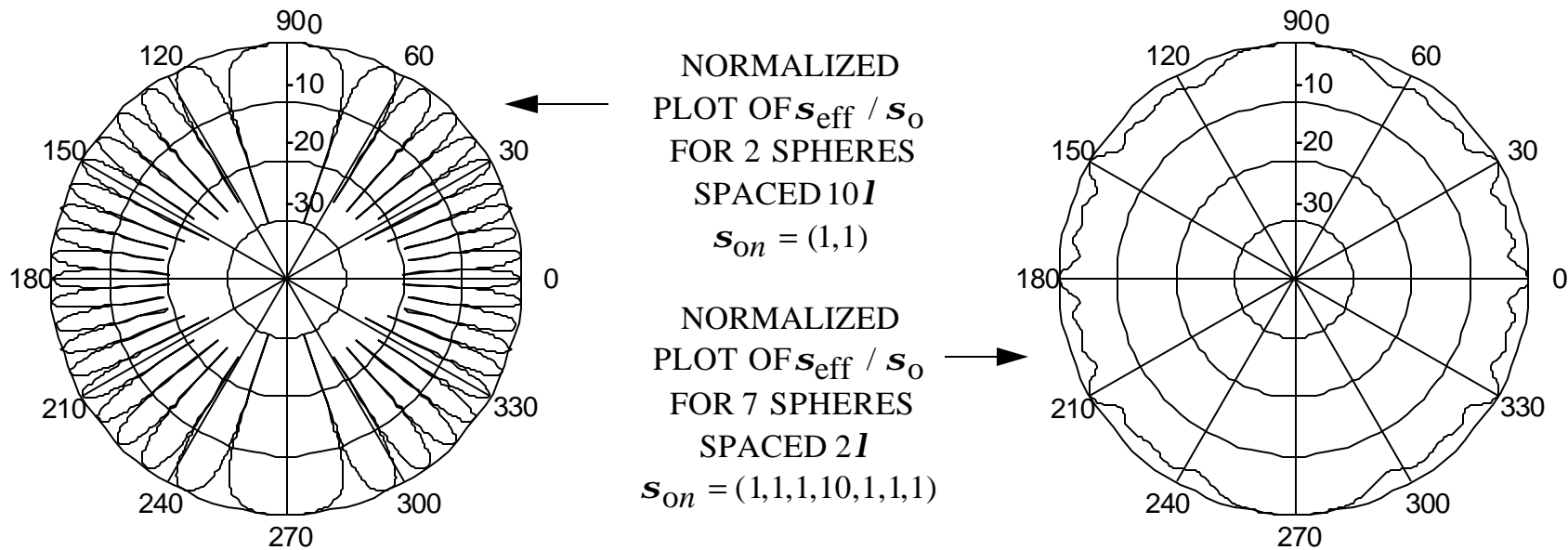
$$(1 \pm \mathbf{a})^{1/2} = 1 \pm \frac{1}{2} \mathbf{a} \mp \underbrace{\frac{3}{8} \mathbf{a}^2 \pm \dots}_{\text{NEGLECT SINCE } \mathbf{a} \ll 1}$$

# Two Sphere RCS (2)

Keeping the first two terms in each case leads to the approximate expressions  $R_1 \approx R + (\ell/2) \sin \mathbf{q}$  and  $R_2 \approx R - (\ell/2) \sin \mathbf{q}$ . Total received field for two spheres is:

$$P_{\text{tot}} \propto \left( \frac{\sqrt{s_o}}{R_1^2} e^{-j2kR_1} + \frac{\sqrt{s_o}}{R_2^2} e^{-j2kR_2} \right)^2 = \frac{s_o}{R^4} \underbrace{\left( e^{-jkl \sin \mathbf{q}} + e^{+jkl \sin \mathbf{q}} \right)^2}_{=4 \cos^2(kl \sin \mathbf{q})}$$

where  $k = 2\mathbf{p} / \mathbf{l}$ . The "effective RCS" of the two spheres is  $s_{\text{eff}} = 4s_o \cos^2(kl \sin \mathbf{q})$ . This can easily be extended to  $N$  spheres.

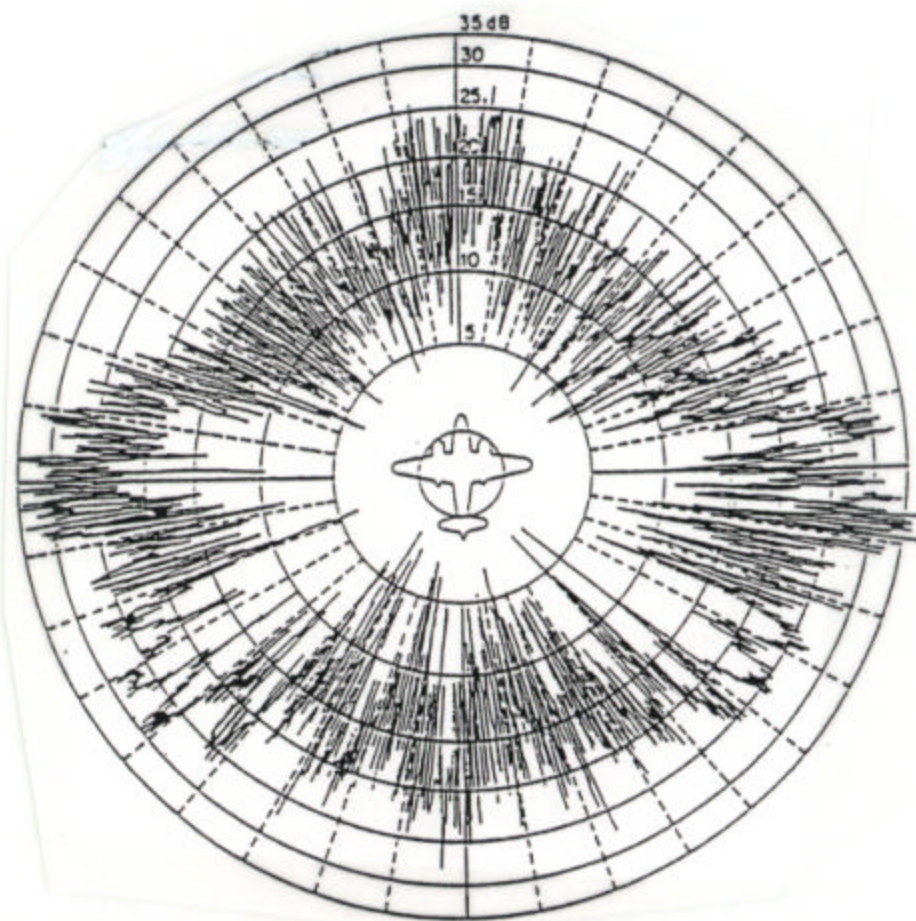


# RCS of a Two Engine Bomber

S-Band (3000 MHz)

Horizontal Polarization

Maximum RCS = 40 dBsm



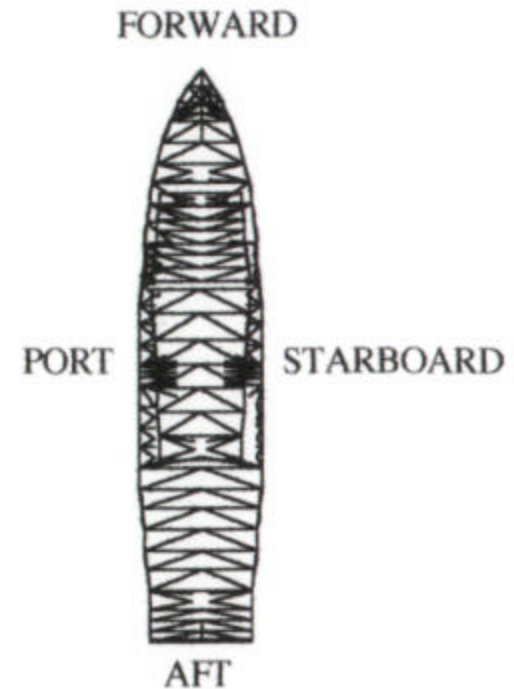
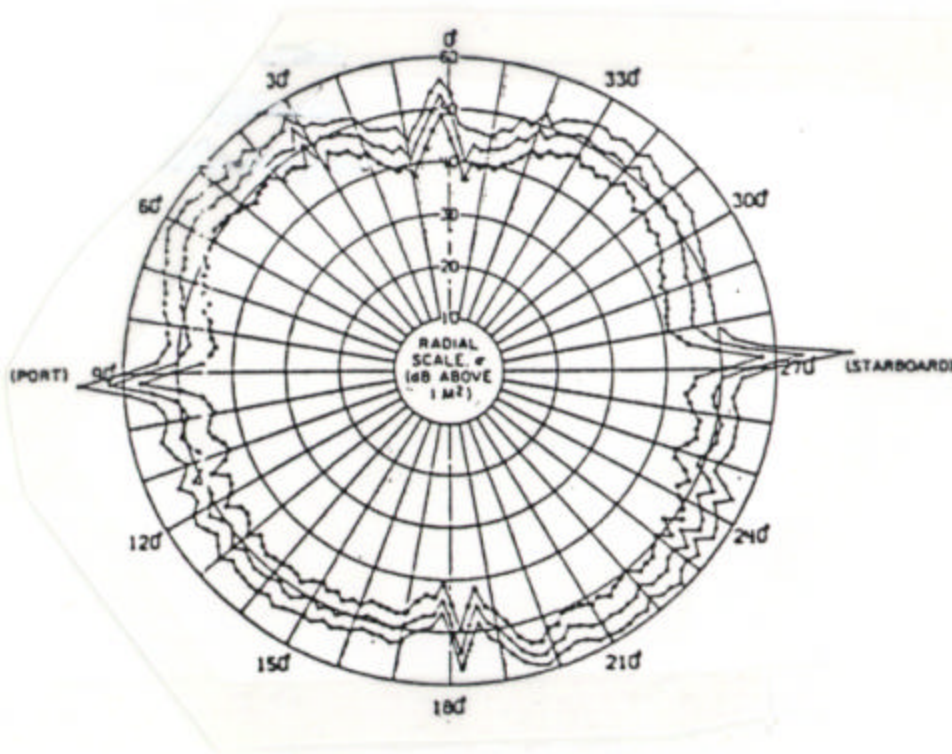


# RCS of a Naval Auxiliary Ship

S-Band (2800 MHz)

Horizontal Polarization

Maximum RCS = 70 dBsm



(Curves correspond to 20<sup>th</sup>, 50<sup>th</sup> and 80<sup>th</sup> percentiles)

# RCS of a Geometrical Components Jet

---

Frequency = 1 GHz

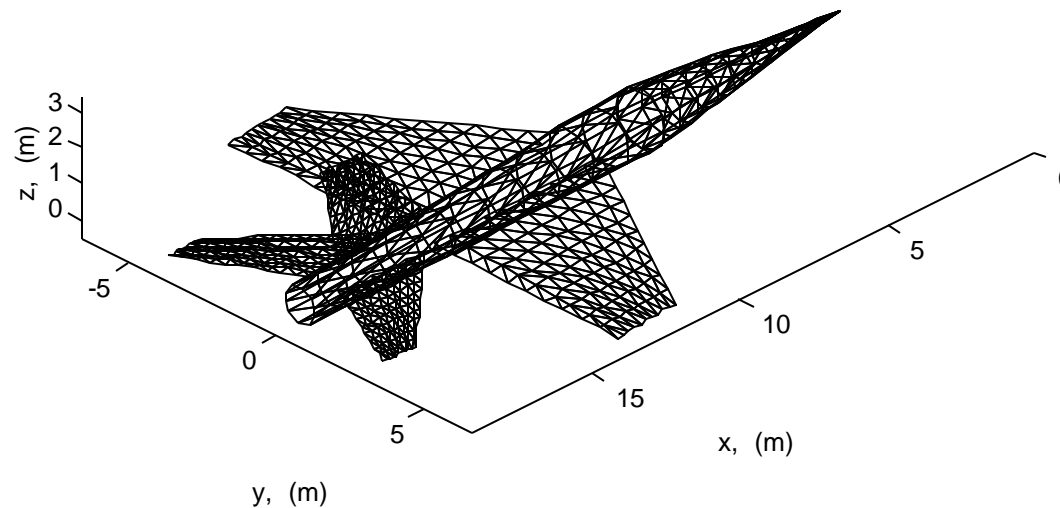
Bistatic and monostatic azimuth patterns

Bistatic advantages:

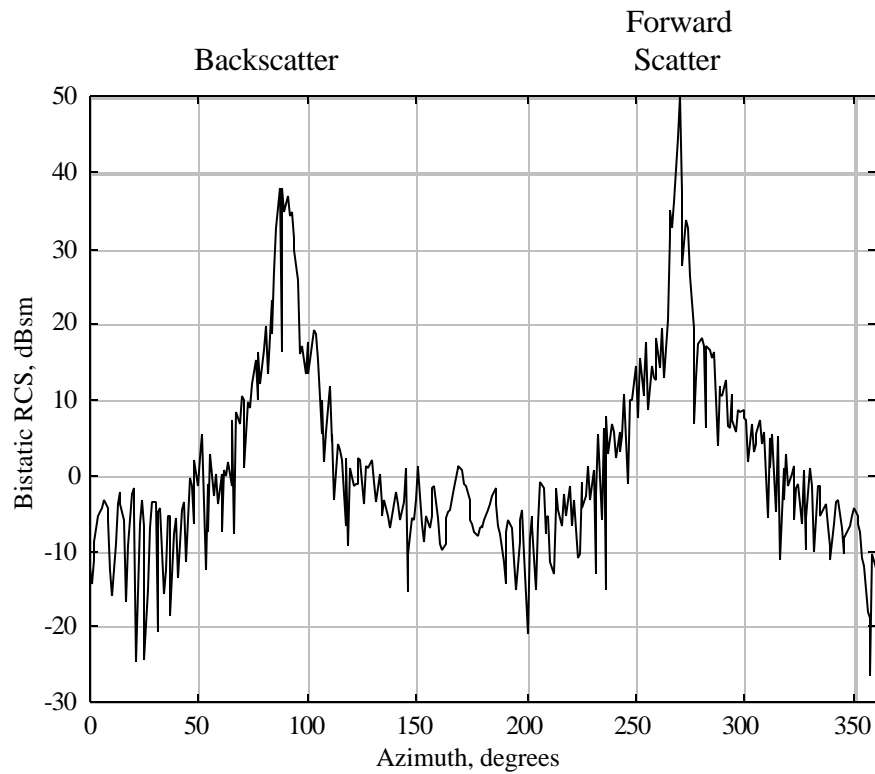
- always a large RCS in the forward direction ( $\mathbf{f} = \mathbf{f}_i + 180^\circ$ )
- forward scatter can be larger than backscatter
- lobes are wider (in angular extent)

Bistatic disadvantage:

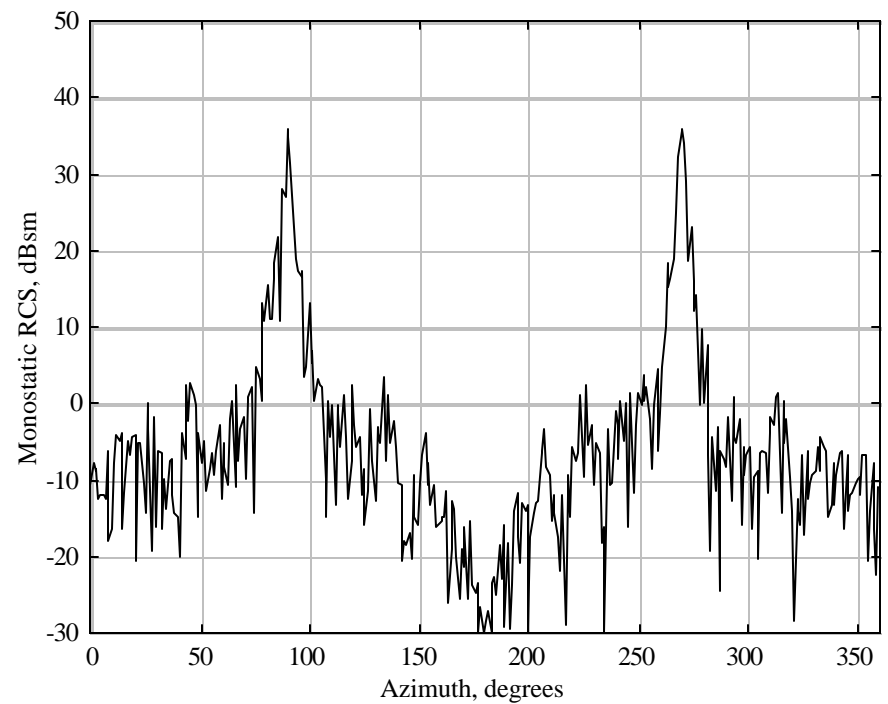
- restricted radar transmit/receive geometry



# Geometrical Components Jet



Bistatic,  $f_i = 90^\circ$



Monostatic

# Fluctuating Targets

---

The target return appears to vary with time due to sources other than a change in range:

1. meteorological conditions and path variations
2. radar system instabilities (platform motion and equipment instabilities)
3. target aspect changes

For systems analysis purposes we only need to know the "gross" behavior of a target, not the detailed physics behind the scattering. Let the  $\mathbf{s}$  be a random variable with a probability density function (PDF) that depends on the factors above. Two PDFs are commonly used:

1.  $p(\mathbf{s}) = \frac{1}{\bar{\mathbf{s}}} e^{-\mathbf{s} / \bar{\mathbf{s}}}$  (this is a negative exponential PDF)

These are Rayleigh targets which consist of many independent scattering elements of which no single one (or few) predominate.

2.  $p(\mathbf{s}) = \frac{4\mathbf{s}}{\bar{\mathbf{s}}^2} e^{-2\mathbf{s} / \bar{\mathbf{s}}}$

These targets have one main scattering element that dominates, together with smaller independent scattering sources.

# Swerling Types

---

Using PDFs #1 and #2 we define four Swerling target types:

Type I: PDF #1 with slow fluctuations (scan-to-scan)

Type II: PDF #1 with rapid fluctuations (pulse-to-pulse)

Type III: PDF #2 with slow fluctuations (scan-to-scan)

Type IV: PDF #2 with rapid fluctuations (pulse-to-pulse)

When the target scattering characteristics are unknown, Type I is usually assumed.

Now we modify our design procedure (same as in Skolnik's 2<sup>nd</sup> edition)

1. Find the SNR for a given  $P_{fa}$  and  $P_d$  as before
2. Get a correction factor from Figure 2.23 in Skolnik (reproduced on the next page)
3. Get  $I_i(n)$  from Figure 2.24 (2<sup>nd</sup> edition in Skolnik if more than one pulse is used)
4. Use  $\bar{S}$  in the radar equation for RCS

Note: There are many charts available to estimate the SNR from integrating  $n$  pulses for fluctuating targets (e.g., charts by Swerling, Blake, Kantor and Marcum). Although the details of the processes are different, they all involve modifying the SNR for a single pulse by the appropriate fluctuation loss and estimating the integration improvement factor.

# Correction & Improvement Factors (1)

---

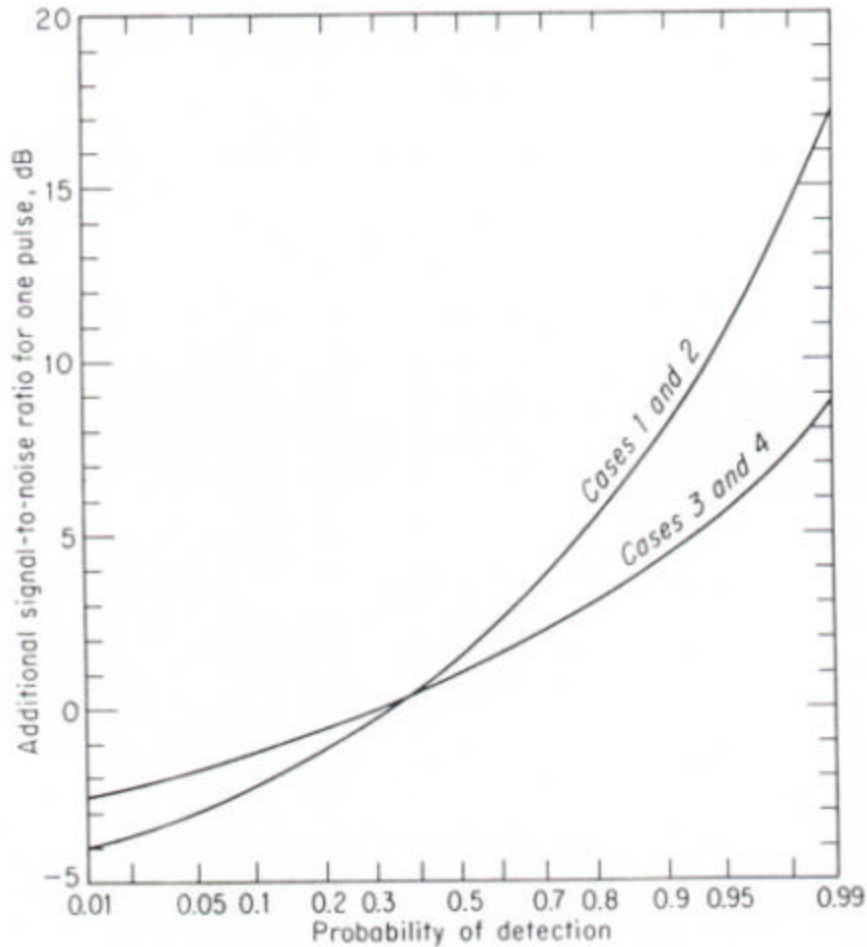


Figure 2.23 in Skolnik

# Correction & Improvement Factors (2)

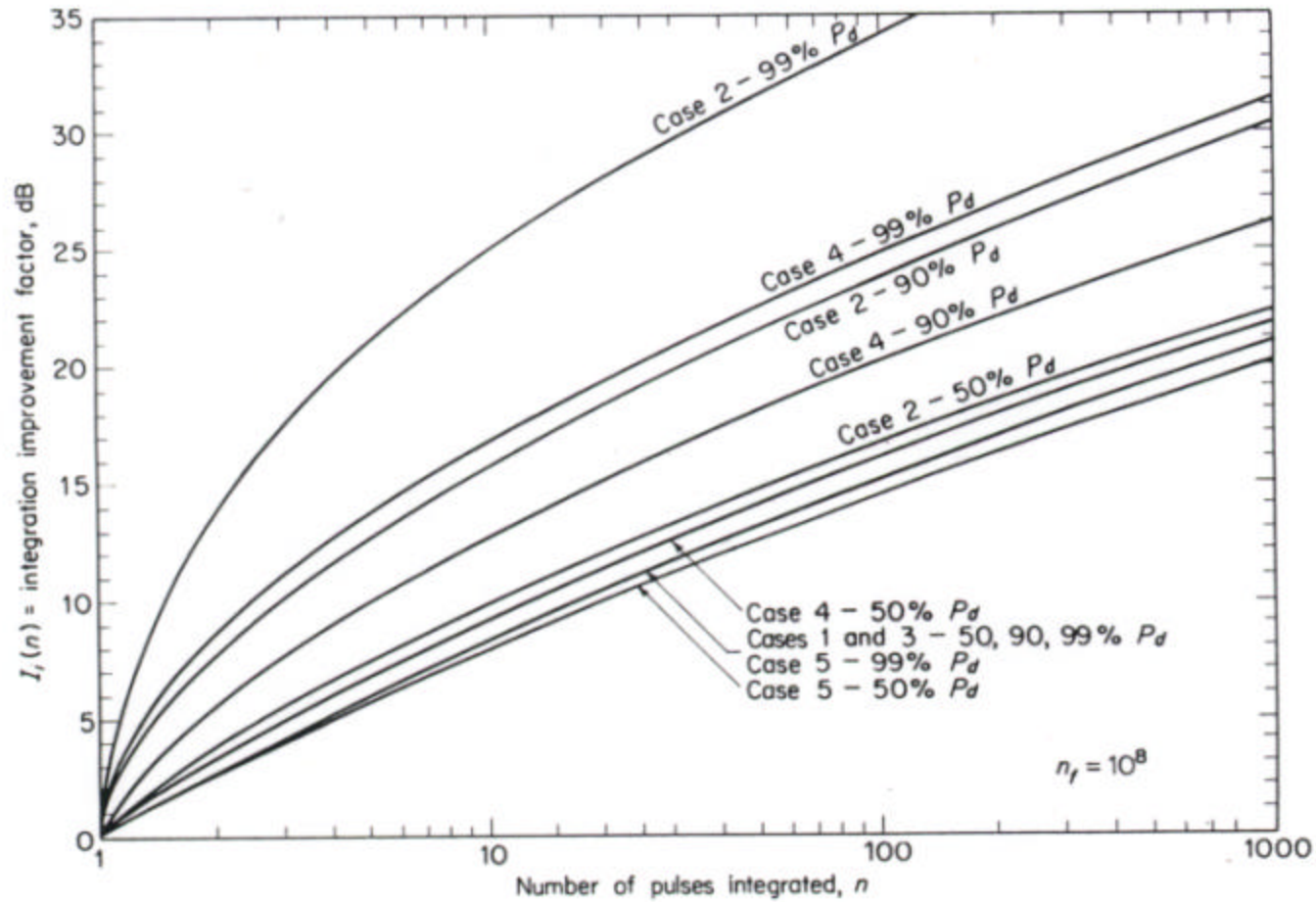


Figure 2.24 in Skolnik (2<sup>nd</sup> edition)

# Detection Range for Fluctuating Targets

---

The maximum detection range for a fluctuating target is given by

$$R_{\max}^4 = \frac{P_{\text{av}} G_t A_{er} \bar{S} n E_i(n)}{(4p)^2 k T_s B_n t f_p \text{SNR}_1}$$

where  $I_i(n) = n E_i(n)$  and

$$\text{SNR}_1 = (\text{SNR}_1 \text{ for } P_d \text{ and } P_{fa} \text{ from Figure 2.6}) \times$$

(correction factor from Figure 2.23)

(Note: if the quantities are in dB then they are added not multiplied.)

In general, the effect of fluctuations is to require higher SNRs for high probability of detection and lower values for low probability of detection, than those with non-fluctuating targets.



# Example

---

A target's RCS is described by a single predominant scatterer whose echo fluctuates from pulse-to-pulse (Type IV). Find the SNR required if  $P_{fa} = 10^{-10}$ ,  $n = 15$  and  $P_d = 0.95$ .

Method 1: (as described in Skolnik 2<sup>nd</sup> edition)

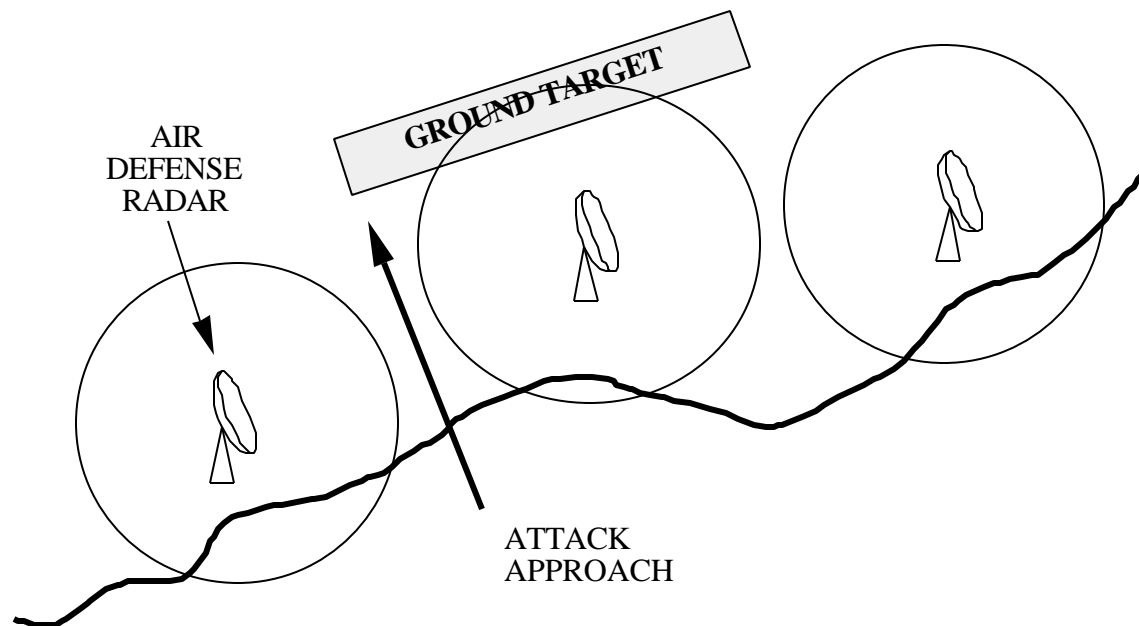
1. From Figure 2.6:  $\text{SNR}_1 = 15.5 \text{ dB} = 35.5$
2. From Figure 2.23, the correction factor (fluctuation loss,  $L_f$ ) for the Type IV target and  $P_d = 0.95$  is about 5.5 dB. Thus, for one pulse,  $\text{SNR}_1 = 15.5 \text{ dB} + 5.5 \text{ dB} = 21 \text{ dB}$
3. From Figure 2.24  $I_i(n) \approx 15 \text{ dB}$ . For  $n$  pulses  $\text{SNR}_n = \text{SNR}_1 / I_i(n)$ , or in dB  $\text{SNR}_n = \text{SNR}_1 - I_i(n) = 21 \text{ dB} - 15 \text{ dB} = 6 \text{ dB}$

Method 2: (as described in Skolnik 3<sup>rd</sup> edition, generally less accurate than Method 1)

1. Follow steps 1 and 2 from above
2. Adjust the fluctuation loss according to  $L_f(n_e) = (L_f)^{1/n_e}$  where  $n_e$  is defined on page 69. (For Swerling Types I and III  $n_e = 1$ ; for Types II and IV  $n_e = n$ .) Working in dB  $L_f(15) = 5.5/15 = 0.37 \text{ dB}$
3. Use Figure 2.7 to get the integration improvement factor,  $I_i \approx 10 \text{ dB}$
4.  $\text{SNR}_n = \text{SNR}_1 + L_f(n_e) - I_i(n) = 15.5 \text{ dB} + 0.37 \text{ dB} - 10 \text{ dB} = 5.87 \text{ dB}$

# Defeating Radar by Low Observability

---



Detection range depends on RCS,  $R_{\max} \propto \sqrt[4]{S}$ , and therefore RCS reduction can be used to open holes in a radar network.

Want to reduce RCS with a particular threat in mind:  
clutter environment, frequency band, polarization, aspect, radar waveform, etc.

There are cost and performance limitations to RCS reduction

# Method of RCS Reduction and Control

---

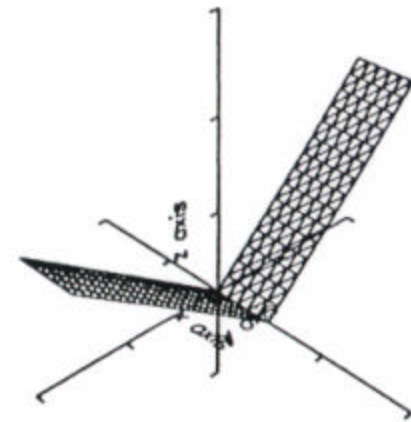
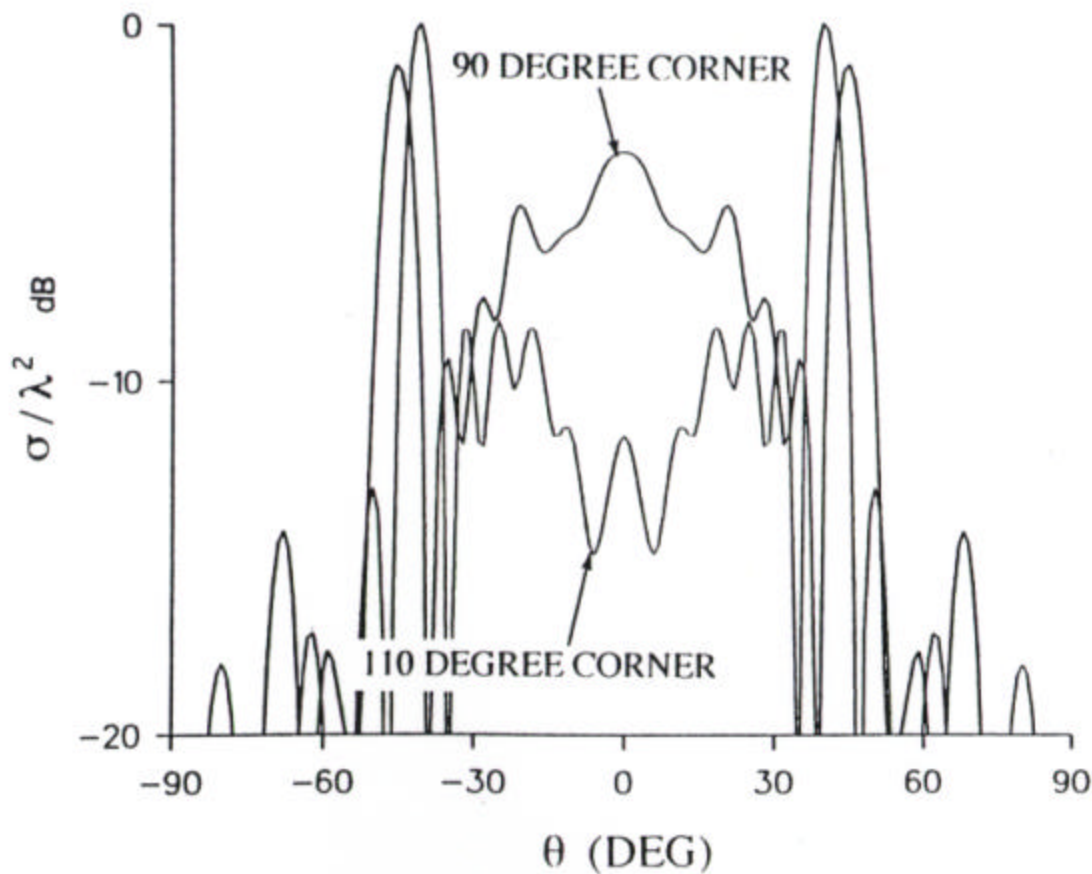
Four approaches:

1. geometrical shaping - Direct the specular or traveling waves to low-priority directions. This is a high-frequency technique.
2. radar absorbing material (RAM) - Direct waves into absorbing material where it is attenuated. Absorbers tend to be heavy and thick.
3. passive cancellation - A second scattering source is introduced to cancel with scattering sources on the "bare" target. Effective at low frequencies for small targets.
4. active cancellation - Devices on the target either modify the radar wave and retransmits it (semi-active) or, generates and transmits its own signal. In either case the signal radiated from the target is adjusted to cancel the target's skin return. Requires expensive hardware and computational resources on the target.

Except for shaping, these methods are narrowband reduction techniques. Wideband radar is an effective way to defeat narrowband reduction methods.

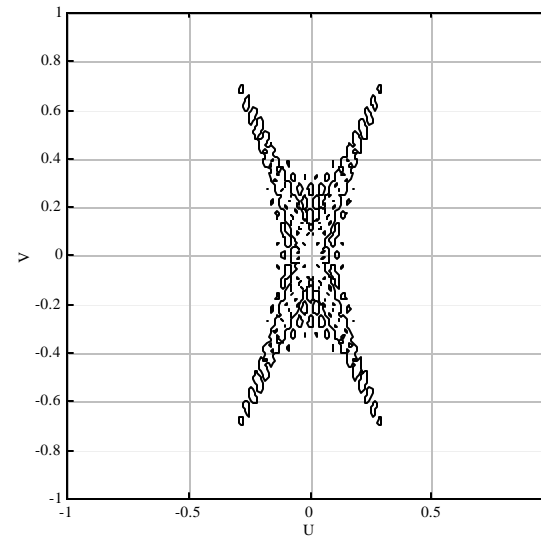
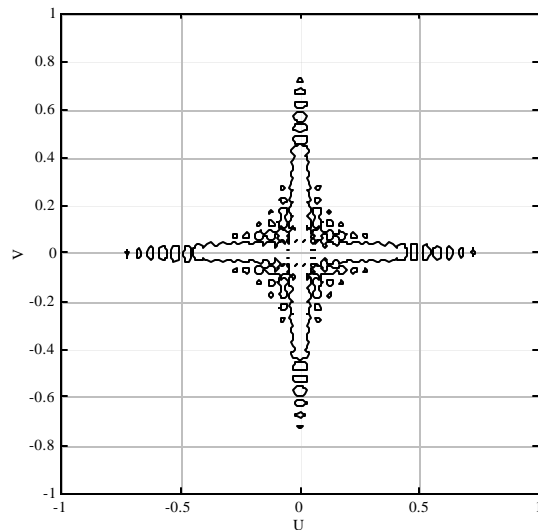
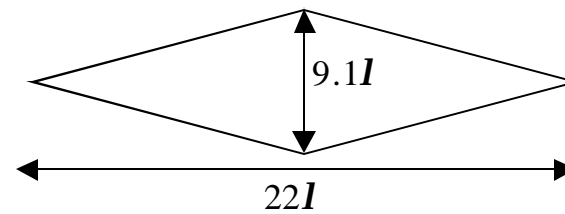
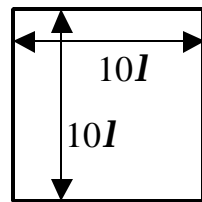
# Corner Reflector Reduction by Shaping

A 90 degree corner reflector has high RCS in the angular sector between the plates due to multiple reflections. Dihedrals are avoided in low observable designs (e.g., aircraft tail surfaces are canted).



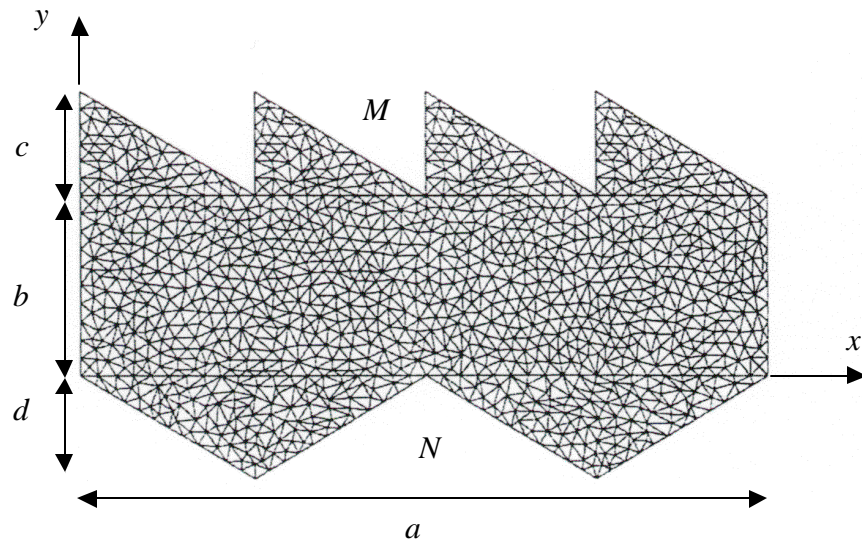
# RCS of Shaped Plates

RCS contours of square and diamond shaped plates. Both have an area of  $100 \text{ m}^2$ .  
 Contours enclose areas where  $\sigma / l^2 > 20 \text{ dB}$



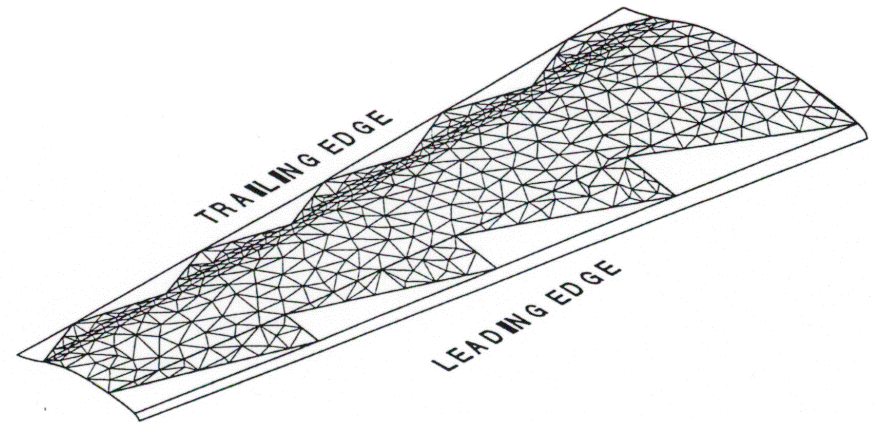
# Application of Serrations to Reduce Edge Scattering

---

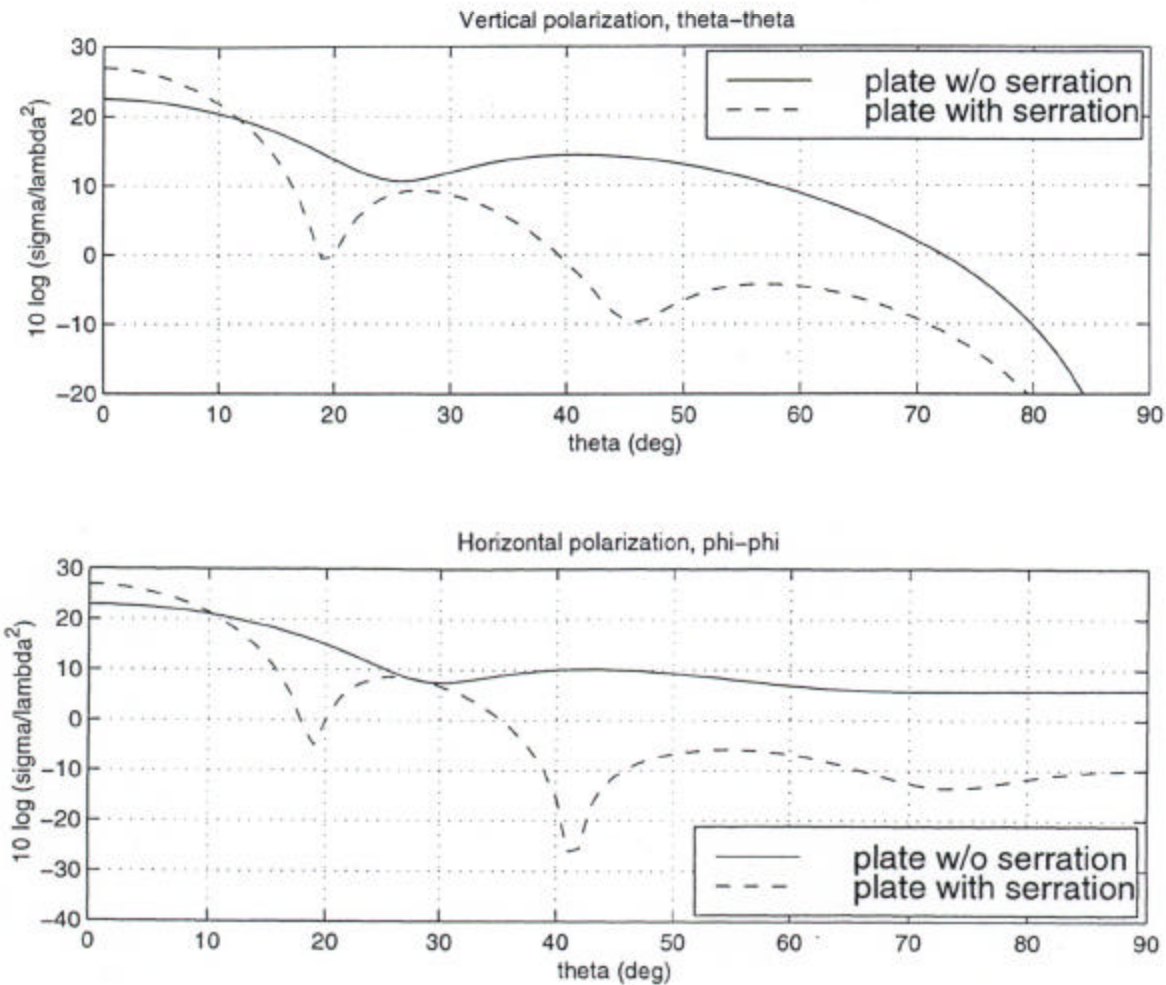


GENERAL PLATE APPLICATION

AIRFOIL APPLICATION



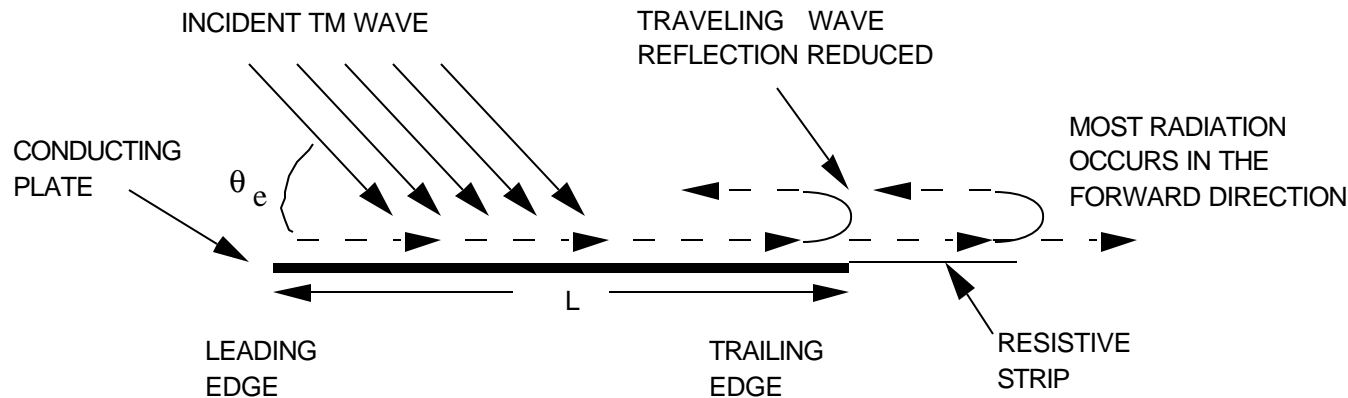
# Application of Serrations to Reduce Edge Scattering



(RESULTS FOR  $a = 4l$ ,  $b = l$ ,  $c = 0.577l$ ,  $M = 4$ ,  $N = 2$ )

# Traveling Waves

A traveling wave is a very loosely bound surface wave that occurs for gently curved or flat conducting surfaces. The surface acts as a transmission line; it "captures" the incident wave and guides it until a discontinuity is reached. The surface wave is then reflected, and radiation occurs as the wave returns to the leading edge of the surface.



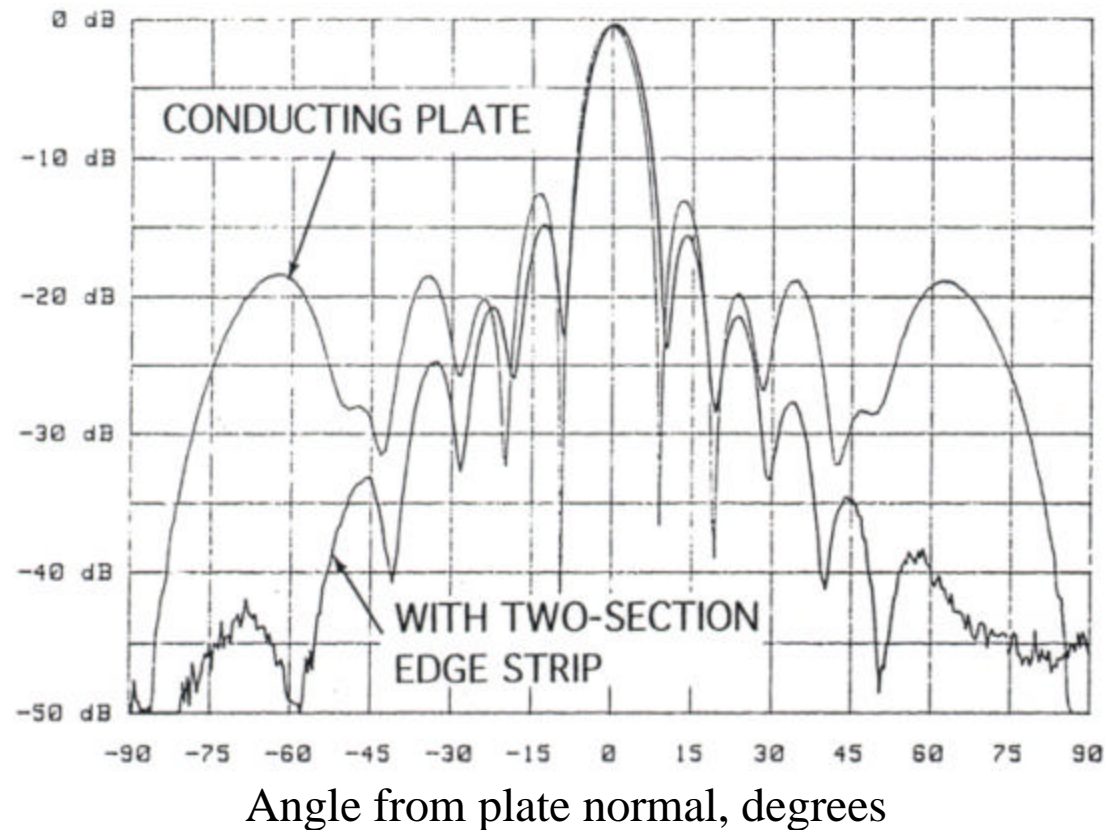
For a conducting surface the electric field must have a component perpendicular to the leading and trailing edges for a traveling wave to be excited. This is referred to as transverse magnetic (TM) polarization because the magnetic field is transverse to the plane of incidence. (Recal that the plane of incidence is defined by the wave propagation vector and the surface normal. Therefore, TM is the same as parallel polarization.) Transverse electric (TE) polarization has the electric field transverse to the plane of incidence. (TE is the same as perpendicular polarization.)



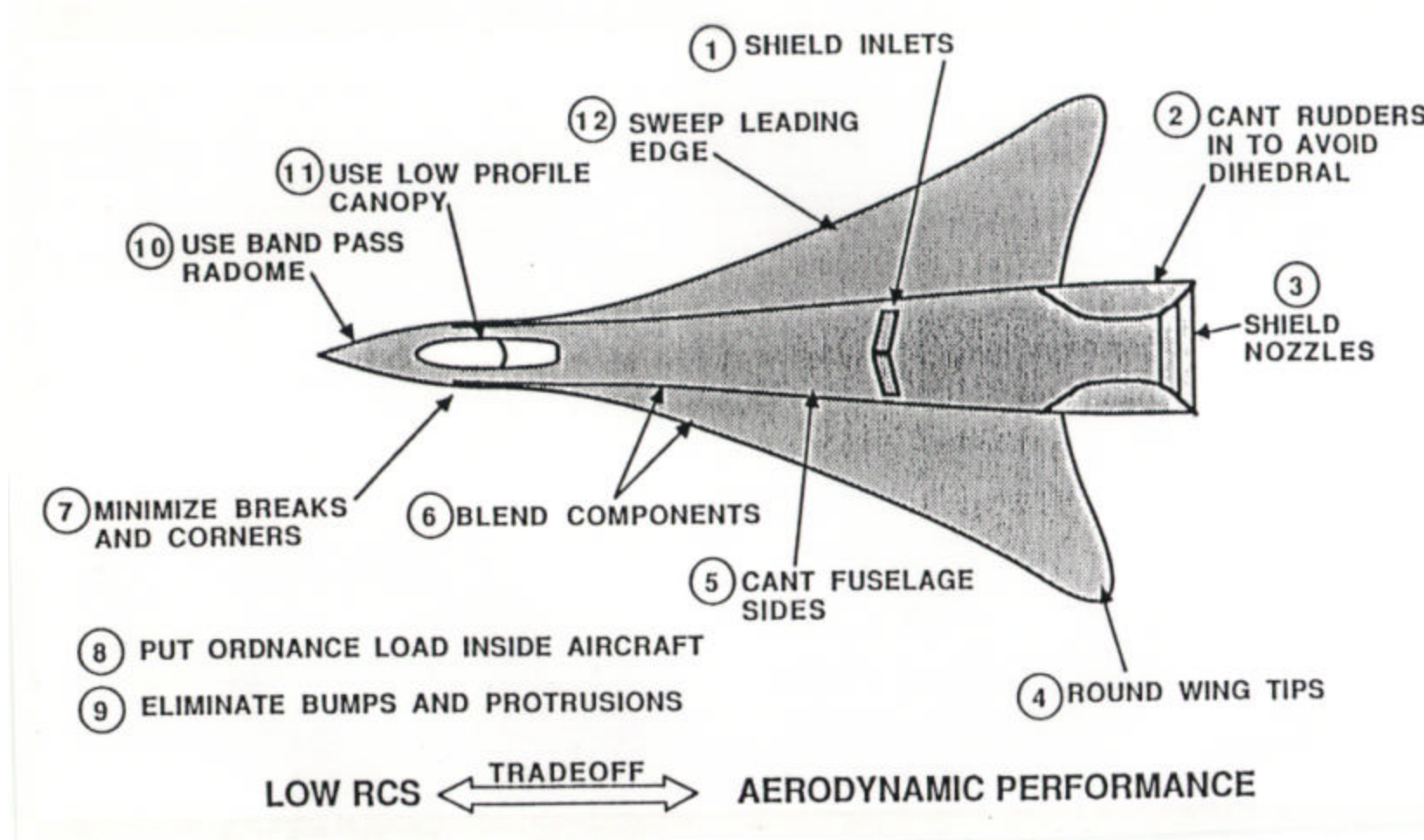
# Trailing Edge Resistive Strips

Quarter wave resistive strips can be used to eliminate traveling wave reflections at trailing edges

Normalized RCS of a plate with and without edge strips



# Application of Reduction Methods



From Prof. A. E. Fuhs

# Low Observable Platforms: F-117

---



*(USAF Photo)*

# Low Observable Platforms: B-2

---



*(USAF Photo)*

# Low Observable Platforms: Sea Shadow

---



*(USN Photo)*

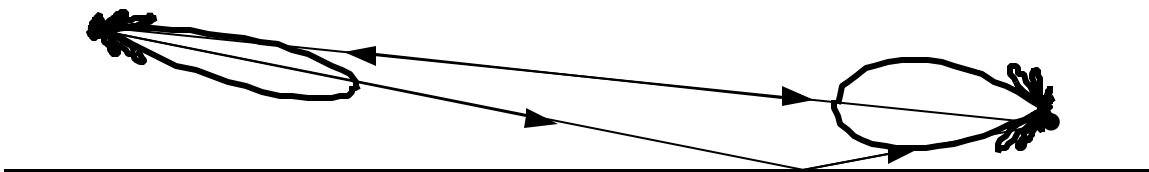
# Microwave Devices & Radar

## LECTURE NOTES VOLUME III

by Professor David Jenn

Contributors: Professors F. Levien, G. Gill, J. Knorr and J. Lebaric

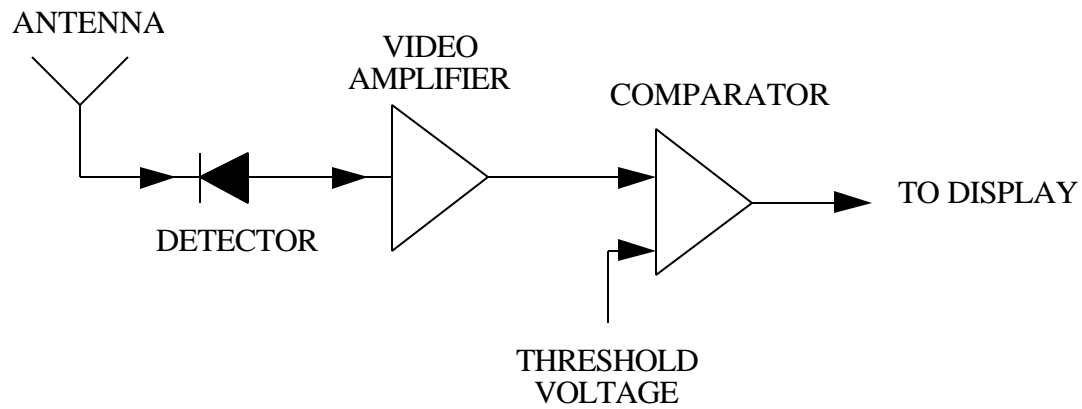
---



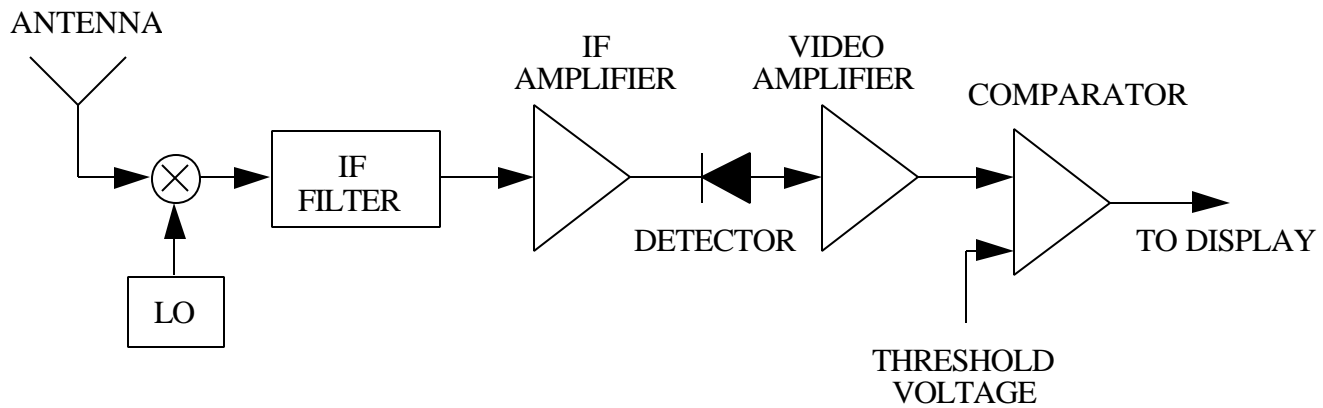
# Receiver Types (1)

---

Basic crystal video receiver:

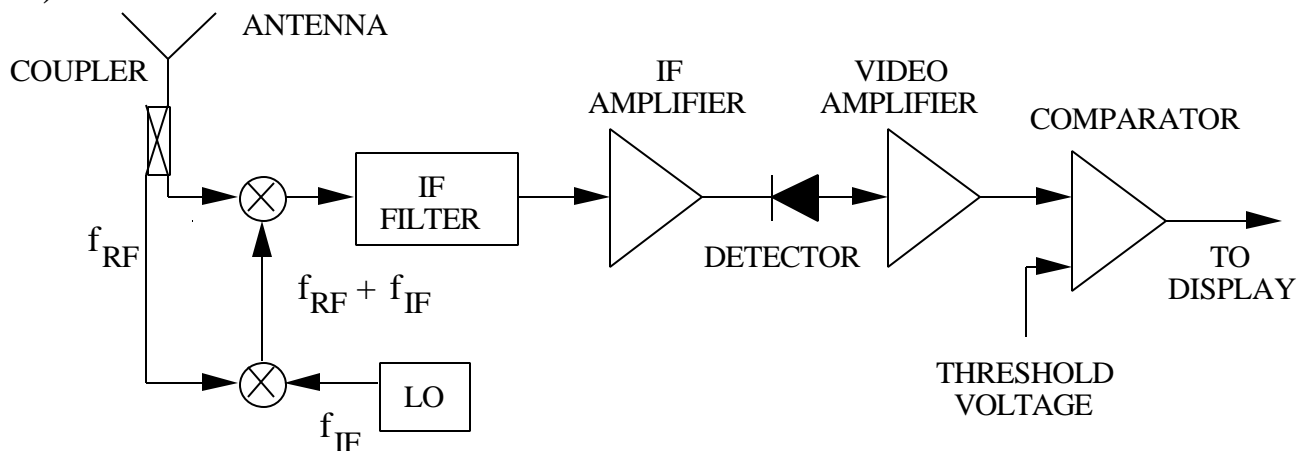


Superheterodyne receiver:

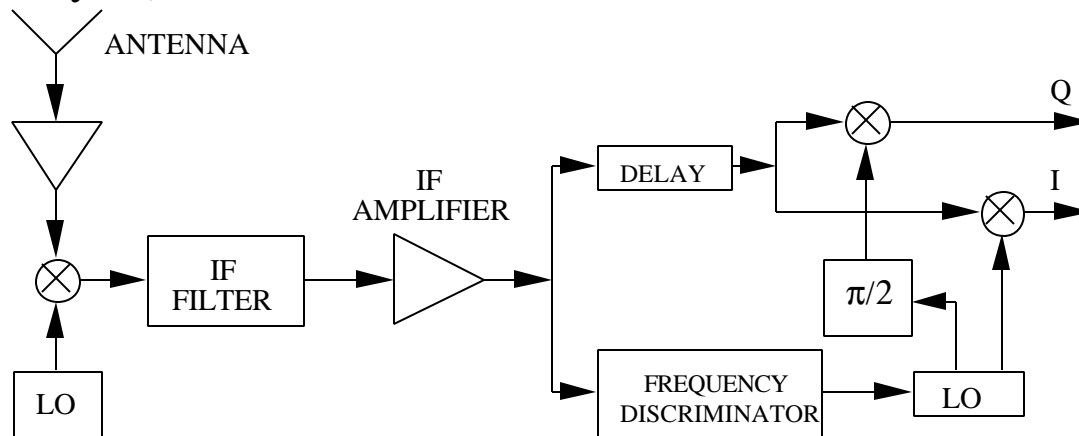


# Receiver Types (2)

Homodyne receiver: (In general, any receiver that derives the LO signal from the received RF signal.)



I/Q (zero frequency IF) receiver:





# Noise Power Spectral Density

---

A "noise signal" in the time domain is denoted as  $n(t)$  and its power spectral density (or simply power spectrum) is  $S_N(f)$  (i.e., therefore  $n(t) \leftrightarrow S_N(f)$ ). White noise is zero mean and has a constant power spectrum

$$S_N(f) \equiv n_o / 2 = kT$$

The factor of 1/2 is typically added because the noise power is defined only for positive frequencies, but the power spectral density frequently occurs in integrals with  $-\infty < f < \infty$  or  $-B < f < B$ . The noise power in a band of frequencies between  $f_1$  and  $f_2$  ( $\Delta f = f_2 - f_1$ ) is the integral of the power spectral density:

$$N_o = \int_{f_1}^{f_2} (n_o / 2) df = \frac{n_o \Delta f}{2}$$

( $N_o$  is usually used to denote the noise power of thermal noise. In general  $N$  is used.)

The total noise power is infinite since

$$N_o = \int_{-\infty}^{\infty} (n_o / 2) df = \infty$$

and thus true white noise does not exist. It is a useful model for situations where the noise bandwidth is so large that it is out of the range of the frequencies of interest.

# Matched Filters (1)

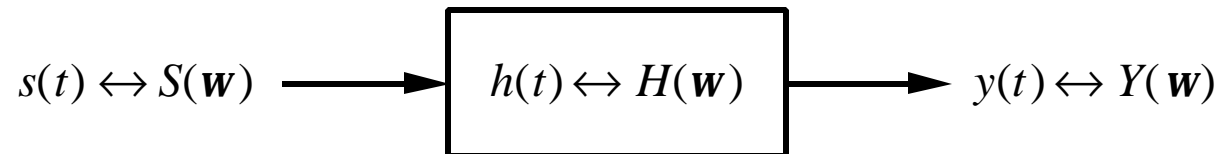
---

Bandwidth tradeoff for filters:

large bandwidth  $\rightarrow$  signal fidelity, large noise

small bandwidth  $\rightarrow$  signal distorted; low noise

The optimum filter characteristic depends on the waveform. It is referred to as the matched filter. It maximizes the peak signal to mean noise power ratio.



$$y(t) = s(t) * h(t) = \int_0^t s(\mathbf{t}) \underbrace{h(t - \mathbf{t})}_{\substack{\text{IMPULSE} \\ \text{RESPONSE}}} dt$$

or

$$Y(\omega) = H(\omega)S(\omega)$$

What  $H(\omega)$  (also expressed as  $H(f)$ ) will maximize the output SNR?

## Matched Filters (2)

---

Assume a time limited signal that has a maximum output at time  $t = t_1$ . The maximum at the output is

$$\begin{aligned} y(t_1) &= \frac{1}{2\pi} \int_{-\infty}^{\infty} S(\omega) H(\omega) e^{j\omega t_1} d\omega \\ &= \int_0^{t_1} s(\tau) h(t_1 - \tau) d\tau = \int_0^{t_1} s(t_1 - \tau) h(\tau) d\tau \end{aligned}$$

For a  $1 \Omega$  load the instantaneous output power is  $S = y^2(t)$ . Consider a differential band of frequencies between  $f$  and  $f + df$ . The noise signal spectra at the input and output are  $S_N(f)$  and  $Y_N(f)$ , respectively. Therefore

$$Y_N(f) = S_N(f) H(f)$$

Mean-squared noise power at the output:

$$N = \overline{\mathbf{s}_N^2} = \left\langle \int_{-\infty}^{\infty} |Y_N(f)|^2 df \right\rangle = \left\langle \int_{-\infty}^{\infty} |S_N(f) H(f)|^2 df \right\rangle$$

## Matched Filters (3)

---

The noise power spectral density for white (gaussian) noise is

$$n_o(f) = 2\langle |S_N(f)| \rangle = k T_o \equiv n_o$$

The noise power at the output is

$$\overline{s_N^2} = \frac{1}{2} \int_{-\infty}^{\infty} |H(f)|^2 n_o(f) df = \int_0^{\infty} |H(f)|^2 n_o df$$

From Parseval's theorem:

$$\overline{s_N^2} = \frac{n_o}{2} \int_{-\infty}^{\infty} h^2(t) dt$$

so that

$$\text{SNR} = \frac{y^2(t_1)}{\overline{s_N^2}} = \frac{\left| \int_0^{t_1} s(t_1 - t) h(t) dt \right|^2}{\frac{n_o}{2} \int_{-\infty}^{\infty} h^2(t) dt} = \frac{\left| \int_{-\infty}^{\infty} S(\omega) e^{j\omega t_1} H(\omega) d\omega \right|^2}{\mathbf{p} n_o \int_{-\infty}^{\infty} |H(\omega)|^2 d\omega}$$

Schwartz inequality

$$\left| \int s(x) h(x) dx \right|^2 \leq \left| \int s(x) dx \right|^2 \left| \int h(x) dx \right|^2$$

# Matched Filters (4)

---

Note that  $s(t)$  and  $h(t)$  are real

$$\text{SNR} \leq \frac{\int_0^{t_1} s^2(t_1 - t) dt \int_{-\infty}^{\infty} h^2(t) dt}{\frac{n_o}{2} \int_{-\infty}^{\infty} h^2(t) dt} = \frac{\int_{-\infty}^{\infty} |S(\omega)e^{j\omega t_1}|^2 d\omega \int_{-\infty}^{\infty} |H(\omega)|^2 d\omega}{p n_o \int_{-\infty}^{\infty} |H(\omega)|^2 d\omega}$$

The maximum will occur when the equality holds

$$h(t) = \begin{cases} \mathbf{a} s(t_1 - t), & t < t_1 \\ 0, & t > t_1 \end{cases} \quad \text{or} \quad H(\omega) = \mathbf{a} [S(\omega)e^{j\omega t_1}]^* = \mathbf{a} S^*(\omega)e^{-j\omega t_1}$$

where  $\mathbf{a}$  is a constant. This is the matched filter impulse response. The maximum SNR is

$$\text{SNR} \leq \frac{\int_0^{t_1} s^2(t) dt}{n_o / 2} = \frac{2E}{n_o}$$

The signal energy is  $E \equiv \int_0^{t_1} s^2(t) dt$  (Note: in general  $E \equiv \int_{-\infty}^{\infty} s^2(t) dt$ .)

# Matched Filters (5)

---

In the frequency domain:

$$H(\omega) = \mathbf{a} \left[ S(\omega) e^{j\omega t_1} \right]^* = \mathbf{a} S^*(\omega) e^{-j\omega t_1}$$

(This is equation 5.15 in Skolnik when  $\mathbf{a}$  is replaced with  $G_a$ .) Some important points:

1. The matched filter characteristics depend on the waveform.
2. It doesn't matter what the waveform is, if a matched filter is used in the receiver the  $SNR=2E/n_o$
3.  $t_1$  may be very large, which implies long delays and consequently a physically large filter.
4. The output of the matched filter is the autocorrelation function of the input signal

$$y(t) \equiv R(t - t_1) = \int_{-\infty}^{\infty} s(\mathbf{t}) s(t_1 - t + \mathbf{t}) dt$$

Example: Find the matched filter characteristic for a pulse of width  $\mathbf{t}$  and amplitude 1

$$p_{\mathbf{t}}(t) \leftrightarrow S(\omega) = \mathbf{t} \operatorname{sinc}(\omega \mathbf{t} / 2)$$

# Matched Filters (6)

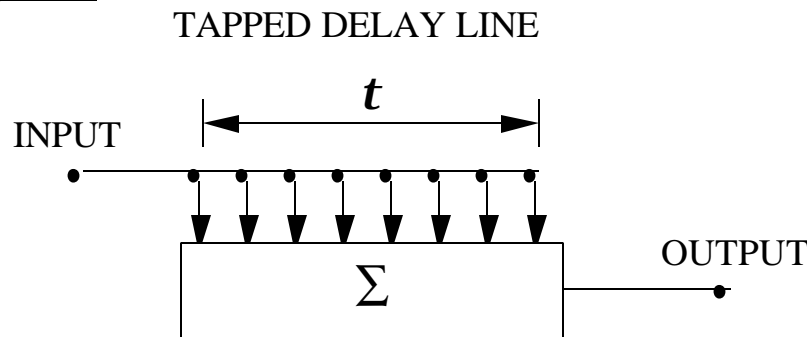
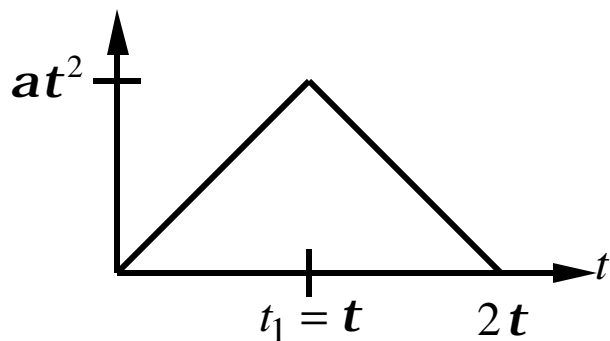
The matched filter characteristic for this waveform is

$$H(\omega) = a S^*(\omega) e^{-j\omega t_1} = a t \operatorname{sinc}(\omega t / 2) e^{-j\omega t}$$

The choice of  $t_1 = t$  is somewhat arbitrary. The output signal spectrum is

$$Y(\omega) = S(\omega) H(\omega) = a t^2 \operatorname{sinc}^2(\omega t / 2) e^{-j\omega t}$$

The output waveform is the inverse Fourier transform: a time delayed triangle. The matched filter is realized using a tapped delay line



The output signal builds as the input signal arrives at more taps. After time  $t$  (end of the pulse) some taps are no longer excited and the output signal level decays. After  $2t$  none of the taps are excited.

# Matched Filters (7)

---

The signal energy is

$$E = \int_0^t p_t^2(t) dt = t$$

and the impulse response of the filter is

$$h(t) = a p_t(t)$$

The signal to noise ratio is

$$\text{SNR} = \frac{\left| \int_0^t p_t(t_1 - t) h(t) dt \right|^2}{\frac{n_o}{2} \int_0^t h^2(t) dt} = \frac{a^2 t^2}{\frac{n_o}{2} a^2 t} = \frac{2E}{n_o}$$

as expected for a matched filter.



# Complex Signals

---

A narrowband signal can be cast in the following form:

$$s(t) = g(t)\cos(\omega_c t + \Phi(t))$$

or, in terms of in-phase (I) and quadrature (Q) components

$$s(t) = g_I(t)\cos(\omega_c t) - g_Q(t)\sin(\omega_c t)$$

where

$$g_I(t) = g(t)\cos(\Phi(t))$$

$$g_Q(t) = g(t)\sin(\Phi(t))$$

Define the complex envelope of the signal as

$$u(t) = g_I(t) + j g_Q(t)$$

Thus the narrowband signal can be expressed as a complex signal (also called an analytic signal)

$$s(t) = \text{Re} \left\{ u(t)e^{j\omega_c t} \right\}$$

It is sufficient to deal with the complex envelope of a signal (to within a phase shift and constant factor).

# Ambiguity Function (1)

---

Matched filter output signal,  $y(t)$ , in terms of the complex envelope,  $u(t)$

$$y(t) = \frac{\mathbf{a}}{2} e^{-j\omega_c t_1} \int_{-\infty}^{\infty} u(\mathbf{t}) u(\mathbf{t} - t + t_1) dt$$

If there is a doppler frequency shift

$$s(t) = \text{Re} \left\{ \underbrace{u(t)e^{j\omega_d t}}_{\text{NEW ENVELOPE}} e^{j\omega_c t} \right\}$$

Neglect constant amplitude and phase factors

$$y(t) = \int_{-\infty}^{\infty} u(\mathbf{t}) e^{j\omega_d \mathbf{t}} u^*(\mathbf{t} - t) dt = \int_{-\infty}^{\infty} \underbrace{u(t)e^{j\omega_d t}}_{\text{SIGNAL TERM}} \underbrace{u^*(t - \mathbf{t})}_{\text{FILTER TERM}} dt$$

This is the ambiguity function

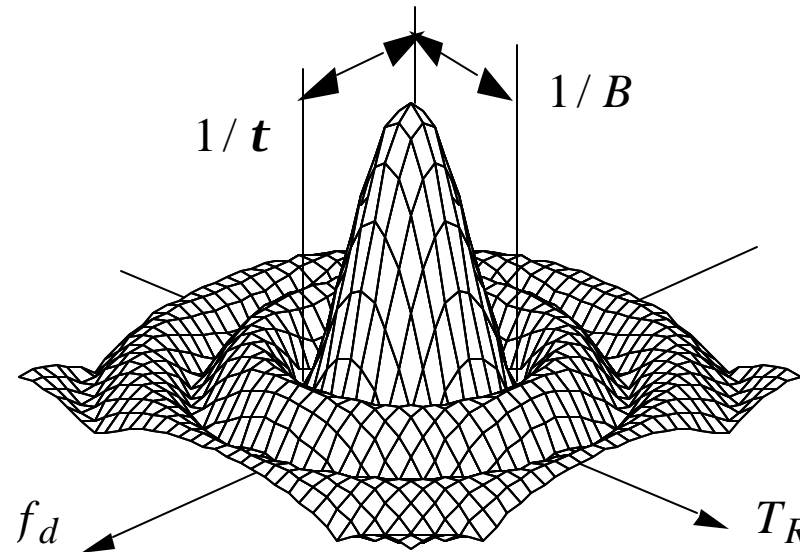
$$\mathbf{c}(\mathbf{t}, \omega_d) = \int_{-\infty}^{\infty} u(t) e^{j\omega_d t} u^*(t - \mathbf{t}) dt$$

# Ambiguity Function (2)

Since  $\mathbf{t}$  is a time delay, let it be the round trip transit time for range  $R$ ,  $T_R$ . Also, express the doppler frequency in Hertz:

$$|\mathbf{c}(T_R, f_d)|^2 = \left| \int_{-\infty}^{\infty} u(t) e^{j2\mathbf{p} f_d t} u^*(t - T_R) dt \right|^2$$

A plot of  $|\mathbf{c}|^2$  is called an ambiguity diagram. Typical plot:



# Ambiguity Function (3)

---

Properties of the ambiguity function:

1. Peak value is at  $T_R = f_d = 0$  and is equal to  $2E$ .
2. The function has even symmetry in both  $T_R$  and  $f_d$ .
3. Peaks in the diagram other than at  $T_R = f_d = 0$  represent ambiguities. Therefore only a single narrow peak is desired (central "spike").
4. Region under the curve is equivalent to energy, and is constant

$$\iint |\mathbf{c}|^2 dT_R df_d = (2E)^2$$

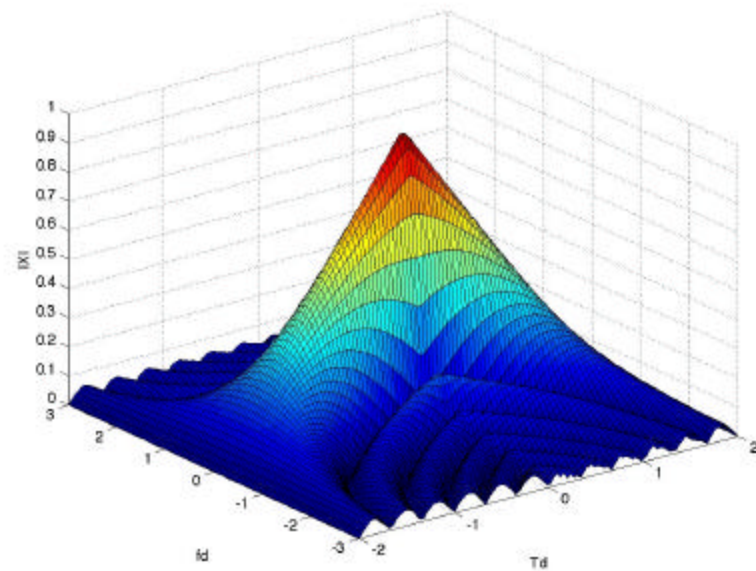
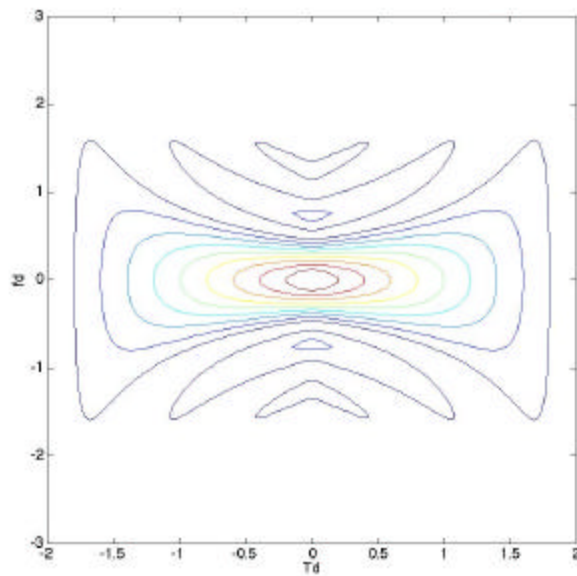
Information available from the ambiguity function:

1. accuracy: indicated by the width of the central spike
2. resolution: width of the central spike and its closeness to other spikes
3. ambiguities: spikes along  $T_R$  are range ambiguities; spikes along  $f_d$  are velocity ambiguities
4. clutter suppression: good clutter rejection where the function has low values

# Ambiguity Function (4)

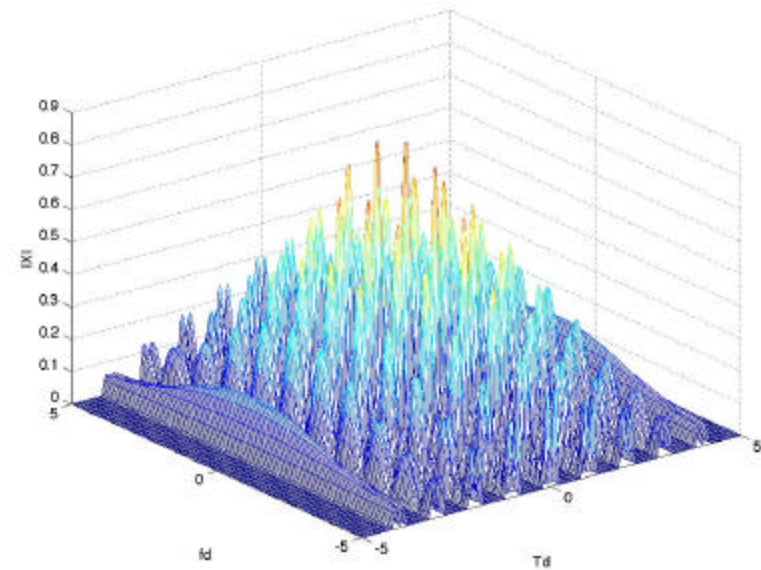
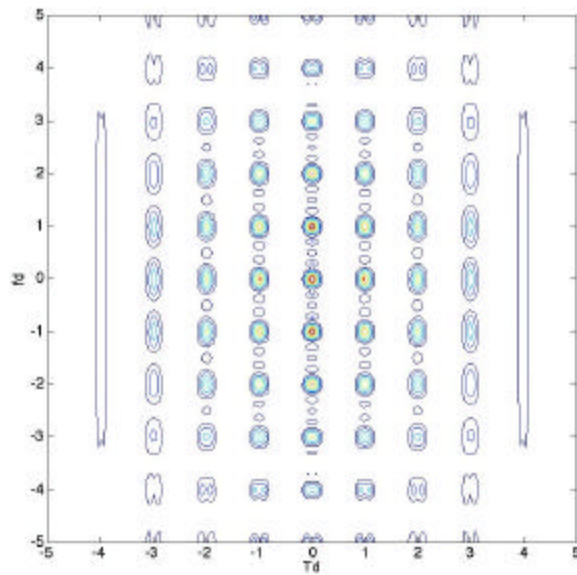
---

Example (after Levanon): single pulse,  $t = 2$



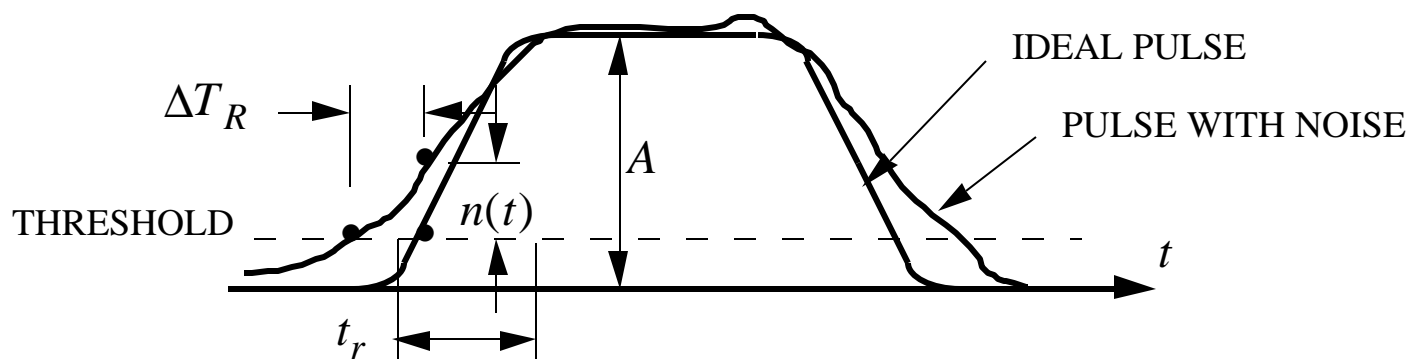
# Ambiguity Function (5)

Example (after Levanon): pulse train,  $t = 0.2$  and  $T_p = 1$



# Range Accuracy (1)

The range accuracy depends on the pulse leading edge threshold; that is the time at which we consider the pulse to have arrived.



The measured pulse (i.e., pulse with noise) crosses the threshold too soon by an amount  $\Delta T_R$ . This is equivalent to a range error. The slope of the measured pulse in the vicinity of the threshold is

$$\text{slope} \approx \frac{n(t)}{\Delta T_R}$$

The slope of the uncorrupted pulse is

$$\text{slope} \approx \frac{A}{t_r}$$

## Range Accuracy (2)

---

Assume that the slopes are approximately equal

$$\frac{A}{t_r} \approx \frac{n(t)}{\Delta T_R} \Rightarrow \Delta T_R \approx \frac{n(t) t_r}{A}$$

Take expectation of each side

$$\begin{aligned} \langle (\Delta T_R)^2 \rangle &\approx \left( \frac{t_r}{A} \right)^2 \langle n^2(t) \rangle \\ \overline{(\Delta T_R)^2} &\approx \left( \frac{t_r}{A} \right)^2 \overline{n^2(t)} \end{aligned}$$

$t_r$  is limited by the IF amplifier bandwidth  $t_r \approx 1/B$ , or

$$\overline{n(t)^2} = n_o B$$

Therefore the rms range delay error is

$$\sqrt{\overline{(\Delta T_R)^2}} \equiv \mathbf{dT}_R = \sqrt{\frac{n_o B}{A^2 B^2}} = \sqrt{\frac{n_o}{A^2 B}}$$



## Range Accuracy (3)

---

Use pulse energy rather than amplitude:  $E = \frac{A^2 t}{2}$

$$dT_R = \sqrt{\frac{t}{(2E/n_o)B}}$$

Average the leading and trailing edge measurements

$$dT_R \approx \sqrt{\left(\Delta T_R^2\right)_1 + \left(\Delta T_R^2\right)_2} = \sqrt{2} \sqrt{\Delta T_R^2}$$

Final result, based on a rectangular pulse,

$$dT_R = \sqrt{\frac{t}{(2E/n_o)2B}}$$

Skolnik has results for several different pulse shapes in terms of the effective bandwidth of the pulse.

# Range Accuracy (4)

---

General equation for an arbitrary pulse shape:

$$dT_R = \frac{1}{B_e \sqrt{2E/n_o}}$$

where the effective bandwidth of the pulse is defined by (Skolnik uses  $\mathbf{b}$ ).

$$B_e^2 = \frac{\int_{-\infty}^{\infty} (2\mathbf{p}f)^2 |S(f)|^2 df}{\int_{-\infty}^{\infty} |S(f)|^2 df} = \frac{1}{E} \int_{-\infty}^{\infty} (2\mathbf{p}f)^2 |S(f)|^2 df$$

For a rectangular pulse  $S(f) \propto \text{sinc}(\mathbf{p}ft)$  and with some math (see Skolnik for details)

$$B_e^2 \approx 2B/t$$

Therefore,  $dT_R = \sqrt{\frac{t}{4BE/n_o}}$  which corresponds to a range error of  $dR = \frac{c}{2} dT_R$

# Velocity Accuracy

---

Method of "inverse probability" gives an expression for the rms frequency error:

$$df = \frac{1}{t_e \sqrt{2E/n_o}}$$

$t_e$  is the effective time duration of the pulse defined as

$$t_e^2 = \frac{\int_{-\infty}^{\infty} (2pt)^2 s^2(t) dt}{\int_{-\infty}^{\infty} s^2(t) dt}$$

(Skolnik uses  $\mathbf{a}$ .) For a rectangular pulse  $t_e^2 = (pt)^2 / 3$  which gives

$$df = \frac{\sqrt{3}}{pt \sqrt{2E/n_o}}$$

# Uncertainty Relation

---

There is a tradeoff between range and velocity accuracies: a narrow spectrum and short time waveform cannot be achieved simultaneously. This is expressed in the uncertainty relation:

$$B_e t_e \geq \mathbf{p}$$

The effective time-bandwidth product must be greater than  $\mathbf{p}$ . The "poorest" waveform in this sense is the gaussian pulse for which  $B_e t_e = \mathbf{p}$ . To improve both  $dT_R$  and  $df$  requires

1. increase  $E/n_o$
2. select a waveform with

large  $\mathbf{a}$   $\rightarrow$  long time duration

large  $\mathbf{b}$   $\rightarrow$  wide bandwidth

# Angular Accuracy

---

Recall that there is a Fourier transform relationship between an antenna's aperture distribution and the far-field pattern. Therefore the pulse/bandwidth formulas for velocity accuracy can be extended to antenna pointing

$$dq = \frac{I}{w_e \sqrt{2E/n_o}}$$

$w_e$  is the effective aperture width of the antenna

$$w_e^2 = \frac{\int_{-\infty}^{\infty} (2px')^2 |A(x')|^2 dx'}{\int_{-\infty}^{\infty} |A(x')|^2 dx'}$$

(Skolnik uses  $g$  and has moved  $I$  from the top formula to the numerator of  $w_e$ .) For a uniform amplitude distribution over an aperture of width  $D$ ,  $w_e^2 = (pD)^2 / 3$  which gives

$$dq = \frac{\sqrt{3}}{p(D/I)\sqrt{2E/n_o}} = \frac{0.628q_B}{\sqrt{2E/n_o}}$$

where  $q_B = 0.88I / D$  has been used.

# Pulse Compression

---

Short pulses are good for small range resolution, but there are problems in practice:

1. difficult to get high energy on the target unless the short pulses are very high peak power
2. short pulses require very wide bandwidth hardware

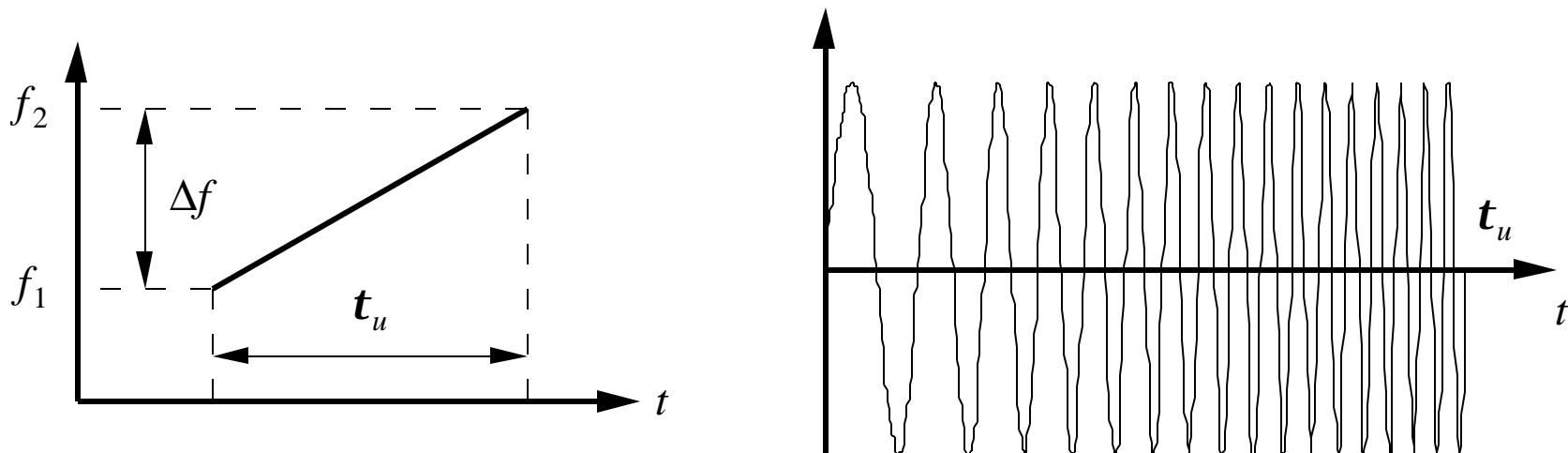
Pulse compression refers to several methods that allow "long time" waveforms to be used, yet get some of the advantages of a "short time" waveform. Three methods are:

1. Chirp: most common  
simple analog implementation  
doppler tolerant  
capable of high pulse compression ratio (PCR)
2. Binary phase codes:  
second most common  
easy digital implementation (apply separately to I and Q channels)  
doppler sensitive  
best for low PCRs
3. Low sidelobe codes:  
more difficult to implement; increased complexity  
doppler sensitive

# Linear FM Pulse Compression (Chirp)

---

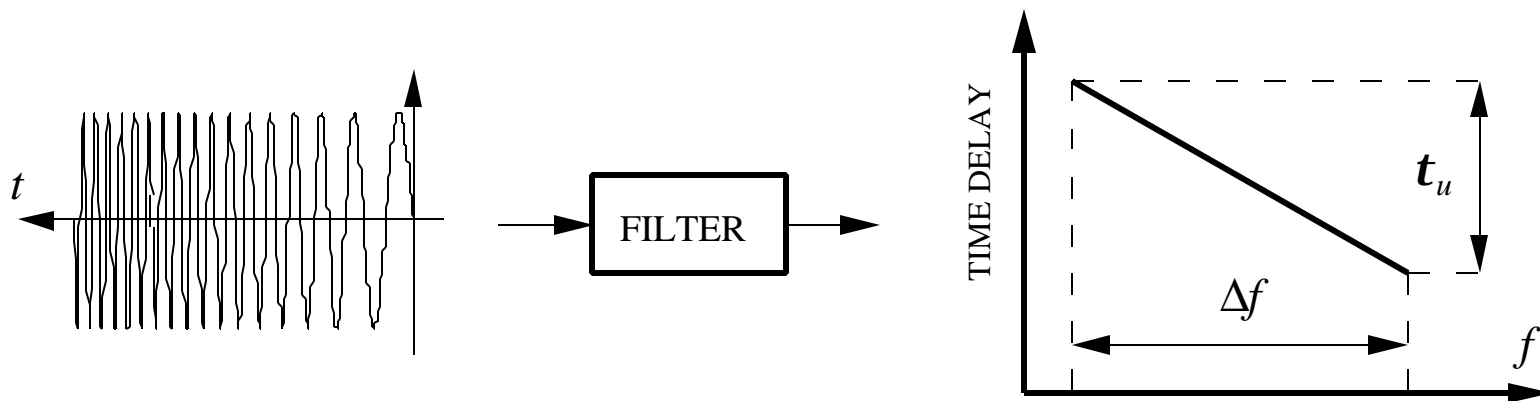
The carrier frequency of each pulse is increased at a constant rate throughout its duration.



$\Delta f$  is the frequency deviation and  $t_u$  is the uncompressed pulse width. Low frequencies are transmitted first so they arrive at the receiver first. A filter is used in the receiver that introduces a frequency dependent time lag that decreases at the exact rate at which the frequency of the received echo increases. The front of the pulse is slowed relative to the trailing edge. As a result of the time delay, the pulse "bunches up" and emerges from the filter with a much larger amplitude and shorter width.

# Linear FM Pulse Compression (Chirp)

Illustration of the dispersive (frequency dependent) filter:



To see how the original waveform appears to be compressed, we look at its spectrum at the output of the filter. Let:

$s(t)$  = signal into filter (received chirp waveform)

$h(t)$  = matched filter impulse response

$g(t)$  = output signal (compressed pulse)



# Linear FM Pulse Compression (Chirp)

---

Using complex signal notation, the output is:

$$g(t) = \int_{-\infty}^{\infty} s(\mathbf{a}) h^*(t - \mathbf{a}) d\mathbf{a}$$

The input (chirp) signal is:

$$s(t) = p_{t_u}(t) \exp\left[j(\omega_c t + \mathbf{m}^2 / 2)\right]$$

where

$$p_{t_u}(t) = \text{pulse of width } t_u$$

$$\mathbf{m} = \text{FM slope constant} = 2p \underbrace{B}_{\Delta f} / t_u$$

The impulse response of the matched filter is:

$$h(t) = p_{t_u}(-t) \exp\left[j(-\omega_c t + \mathbf{m}^2 / 2)\right]$$

The received chirp signal after mixing (i.e., at IF)

$$s_{IF}(t) = p_{t_u}(t) \exp\left[j\{(\omega_{IF} - \omega_d)t + \mathbf{m}^2 / 2\}\right]$$

# Linear FM Pulse Compression (Chirp)

Now perform the convolution

$$g(t) = \int_{-t_u}^{t_u} \exp\left[j((\omega_{IF} - \omega_d)a + \frac{m a^2}{2})\right] \exp\left[j(\omega_{IF}(t - a) + \frac{m(t - a)^2}{2})\right] da$$

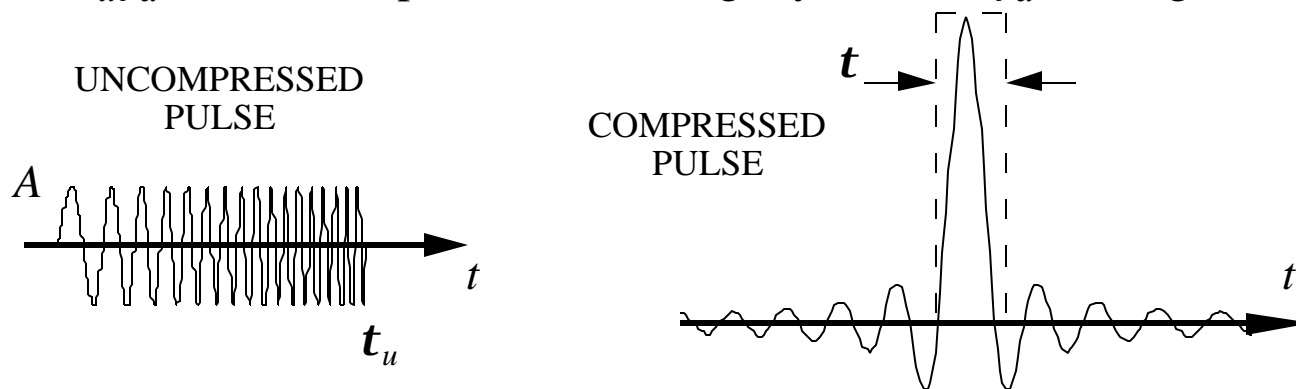
for  $t > 0$ . Evaluate the integral to get

$$g(t) = (t_u - t) e^{j(\omega_{IF} - \omega_d + \frac{m}{2})t} \text{sinc}(p(t_u - t)(f_d + Bt/t_u))$$

where  $2pB = m t_u$  has been used. The pulse compression ratio (PCR) is

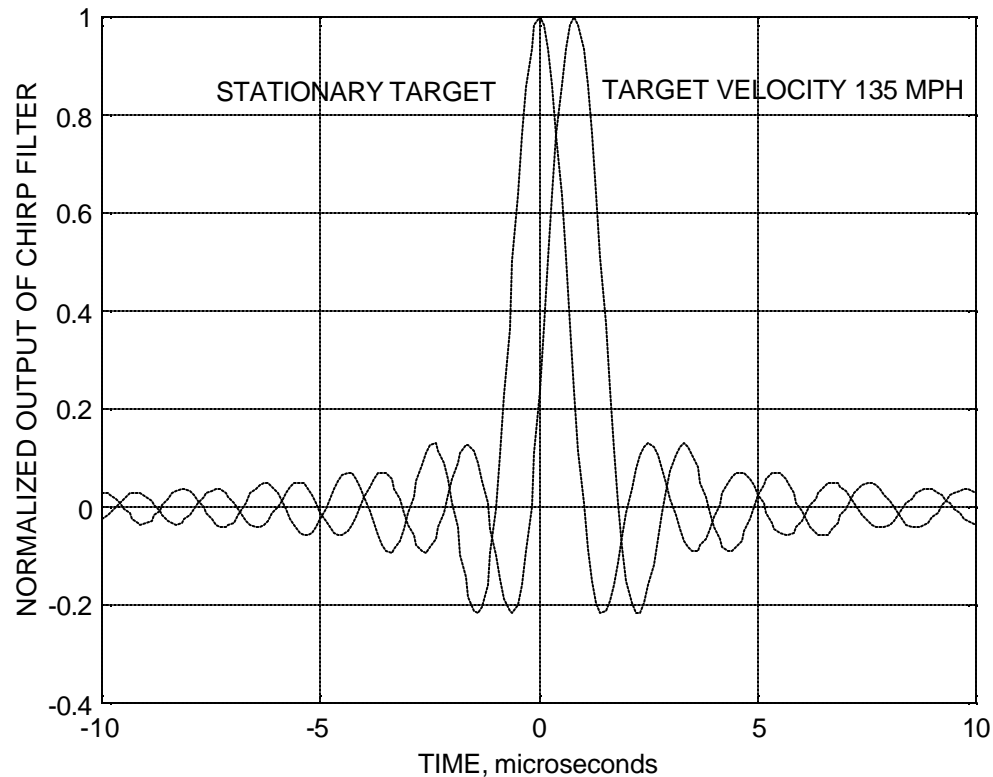
$$\text{PCR} = t_u \Delta f \equiv t_u / t$$

Typical values: 100 to 300 (upper limit is about  $10^5$ ). The peak value of  $g(t)$  occurs at time  $t = -t_u f_d / B$ . This represents an ambiguity because  $f_d$  is not generally known.



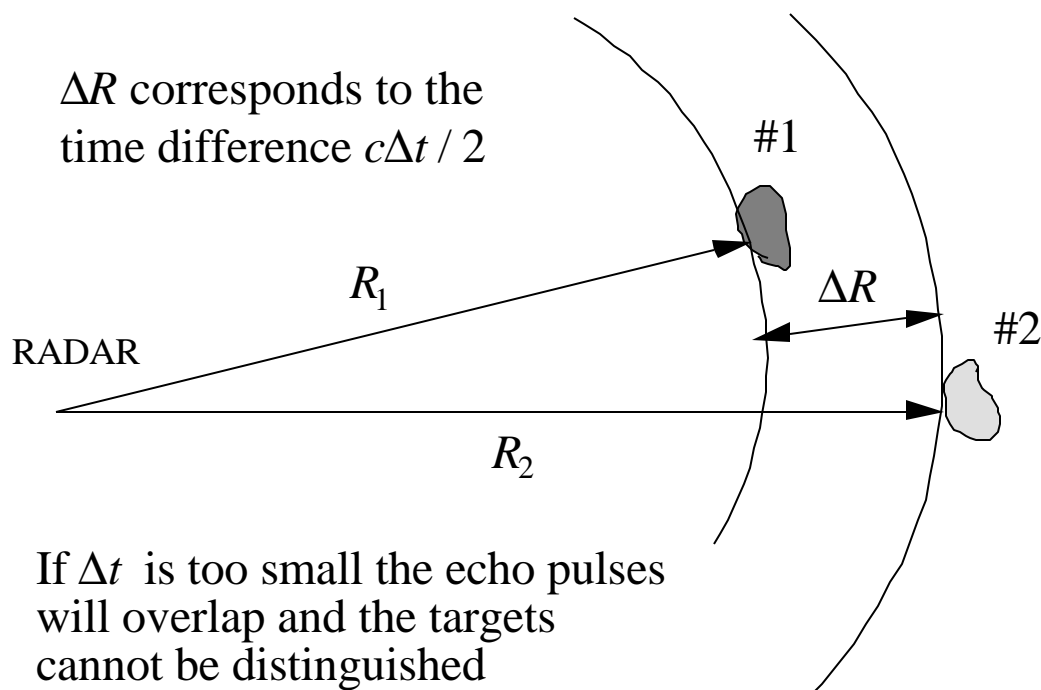
# Chirp Filter Output Waveform

The doppler shift from a moving target causes a time shift in the maximum output of the matched filter. Example:  $\Delta f = 1$  MHz, PCR=200,  $f_c = 10$  GHz



# Range Resolution (1)

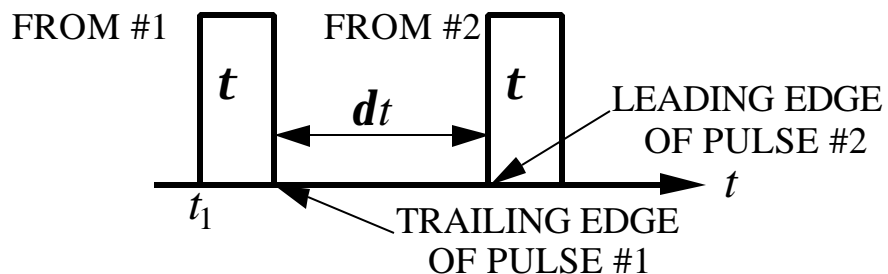
Resolution refers to the ability of the radar to distinguish two closely spaced targets. The echo returns must be sufficiently separated. Small  $\Delta R \Rightarrow$  small pulsewidth  $t$ .



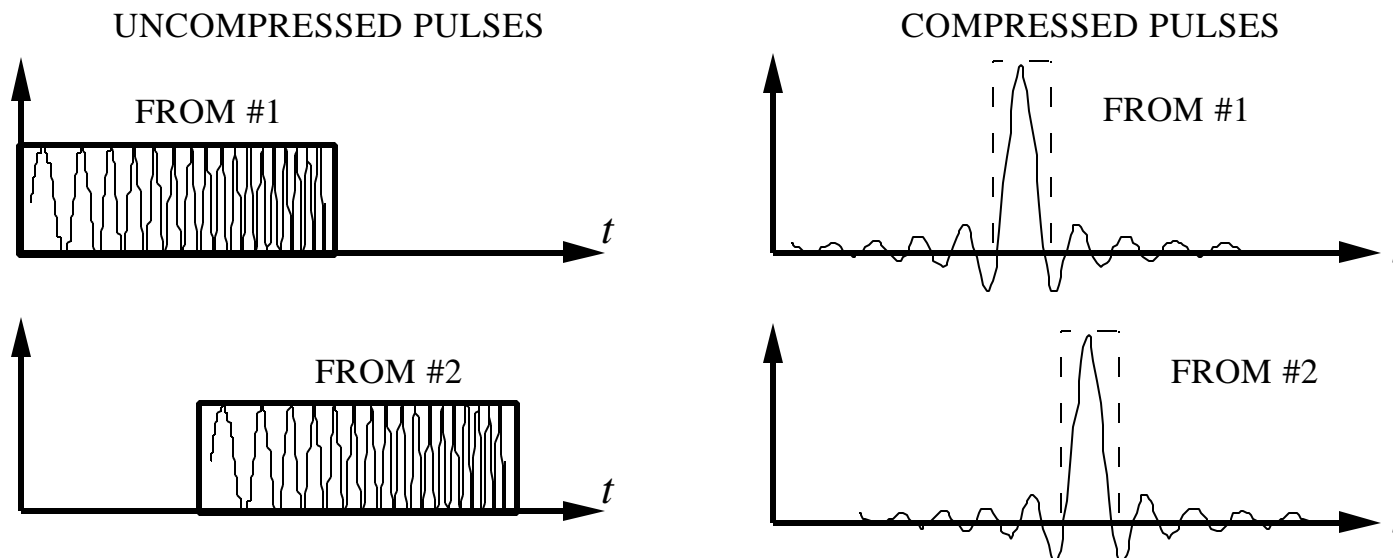
# Range Resolution (2)

To distinguish the two pulses  
 $dt \geq 0$  which implies

$$t \leq 2\Delta R / c$$



Pulse compression can improve a radar's resolution



# Pulse Compression Example

---

FM chirp waveform transmits for  $t_u = 10 \text{ ns}$ . What frequency deviation is required to increase the peak SNR by 10 dB at the output of an ideal pulse compression filter?

Definition of PCR:  $\text{PCR} = t_u \Delta f = 10 \times 10^{-6} \Delta f$

The PCR is also the increase in peak SNR. Therefore

$$(10 \times 10^{-6}) \Delta f = 10 \text{ dB} = 10 \Rightarrow \Delta f = 1 \times 10^6 = 1 \text{ MHz}$$

Range resolution of the uncompressed pulse is

$$\Delta R = \frac{ct_u}{2} = \frac{3 \times 10^8 (10^{-5})}{2} = 1500 \text{ m}$$

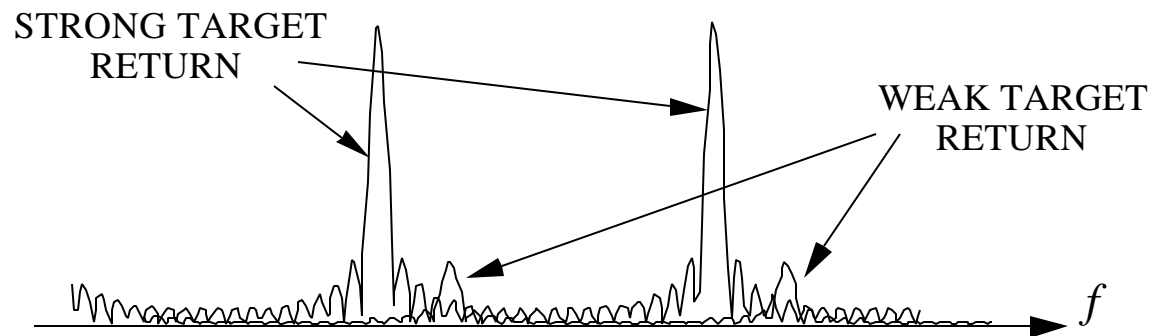
The compressed pulse width is  $t = \frac{t_u}{\text{PCR}}$  and the resolution is

$$\Delta R = \frac{ct}{2} = \frac{3 \times 10^8 (10^{-6})}{2} = 150 \text{ m}$$

# Chirp Complications

---

1. Chirp introduces a slight doppler frequency ambiguity. The radar cannot distinguish between an intended frequency shift and an induced doppler shift.
2. The chirp filter output for each pulse is a sinc function. For a train of pulses the sinc functions overlap and sidelobes from a strong target can mask a weak target.

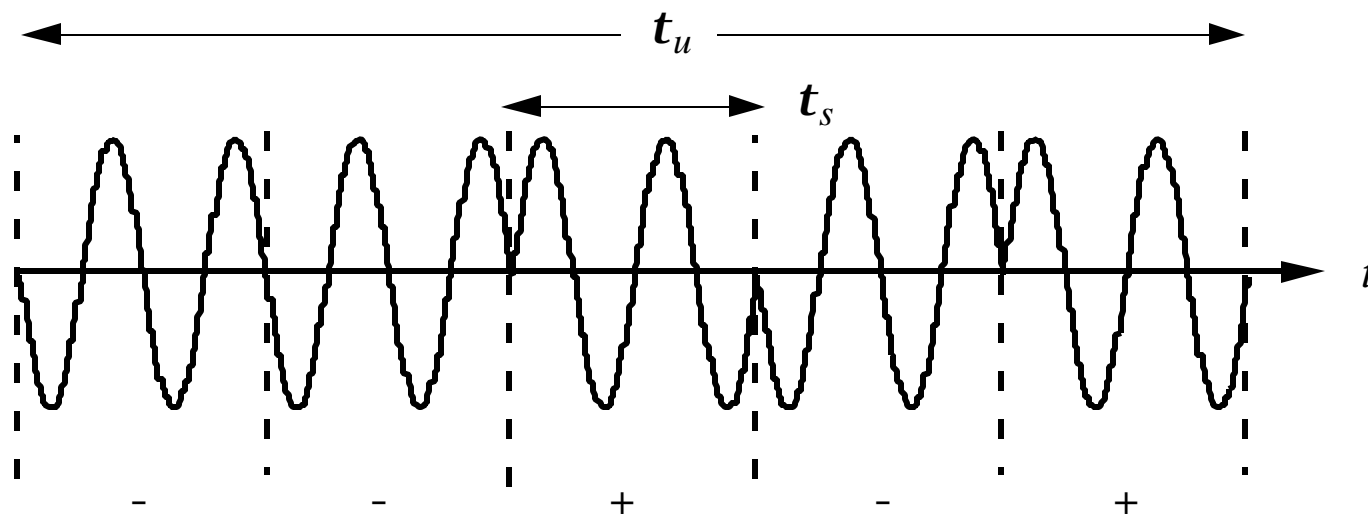


The solution is to use phase weighting (i.e., nonlinear FM).

# Digital Pulse Compression

Digital pulse compression utilizes phase-coded waveforms. Usually these are bi-phase modulated waveforms; they yield the widest bandwidth for a given sequence length.

Example of a bi-phase modulated waveform of length five.  $t_u$  is the illumination length of the pulse (uncompressed pulse length);  $t_s$  is the subpulse length.



Types of codes:

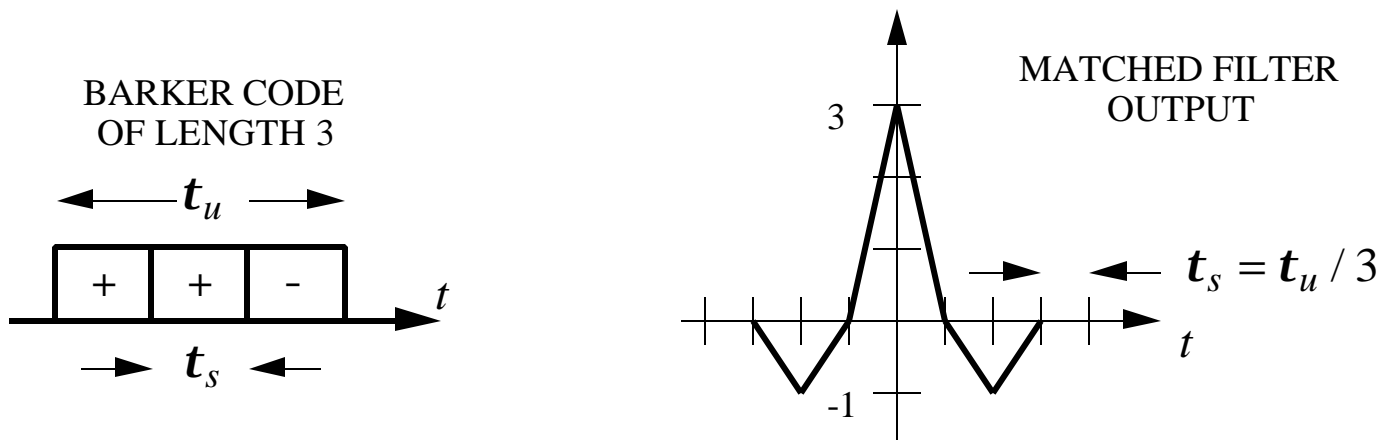
1. Barker sequences
2. Pseudorandom sequences
3. Frank codes



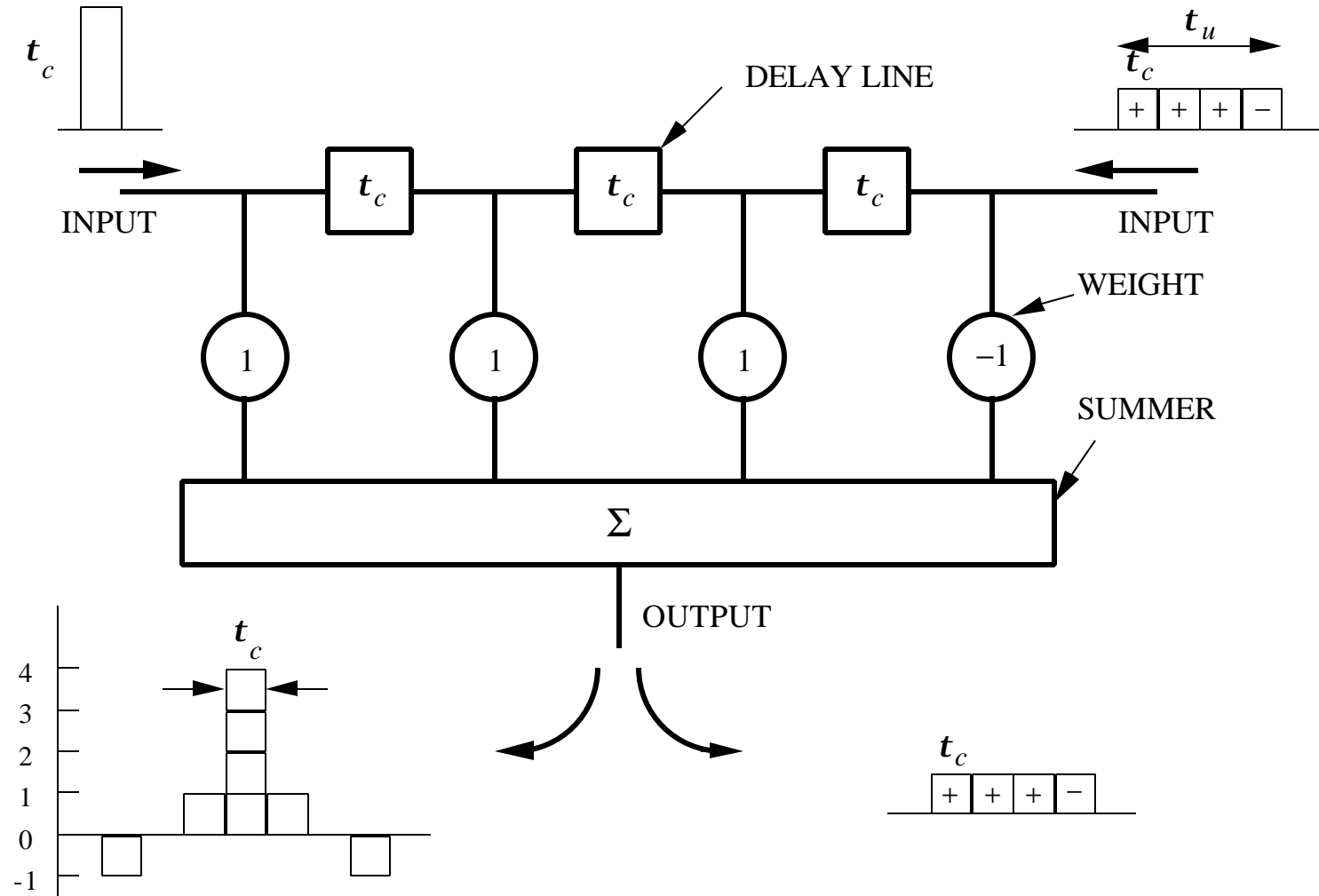
# Barker Sequences

## Characteristics:

- $N$  is the number of bits in the sequence
- Its matched filter output (the autocorrelation function of the sequence) contains only three absolute values: 0, 1, and  $N$
- There are only seven known sequences of lengths 2, 3, 4, 5, 7, 11, and 13
- The longest sequence is only 13 bits (security problems)
- All sidelobes are the same level. Levels range from 6 dB to 22.3 dB



# Pulse Compressor/Expander



# The Ideal Radar Antenna

---

- Search: Low sidelobes  
High gain on transmit  
Fast sector coverage  
Wide bandwidth  
High power on transmit  
High signal-to-noise ratio on receive
- Tracking: Low sidelobes  
Narrow beam  
Accurate beam pointing  
Wide bandwidth  
High signal-to-noise ratio on receive
- In general: Physical limitations (size, weight, volume, etc.)  
Low cost  
Maintainability  
Robust with regard to failures; built in test (BIT)  
Ability to upgrade  
Resistant to countermeasures

# Antenna Refresher (1)

---

Classification of antennas by size (relative to wavelength).

Let  $\ell$  be the antenna dimension:

1. electrically small,  $\ell \ll \lambda$ : primarily used at low frequencies where the wavelength is long
2. resonant antennas,  $\ell \approx \lambda / 2$ : most efficient; examples are slots, dipoles, patches
3. electrically large,  $\ell \gg \lambda$ : can be composed of many individual resonant antennas; good for radar applications (high gain, narrow beam, low sidelobes)

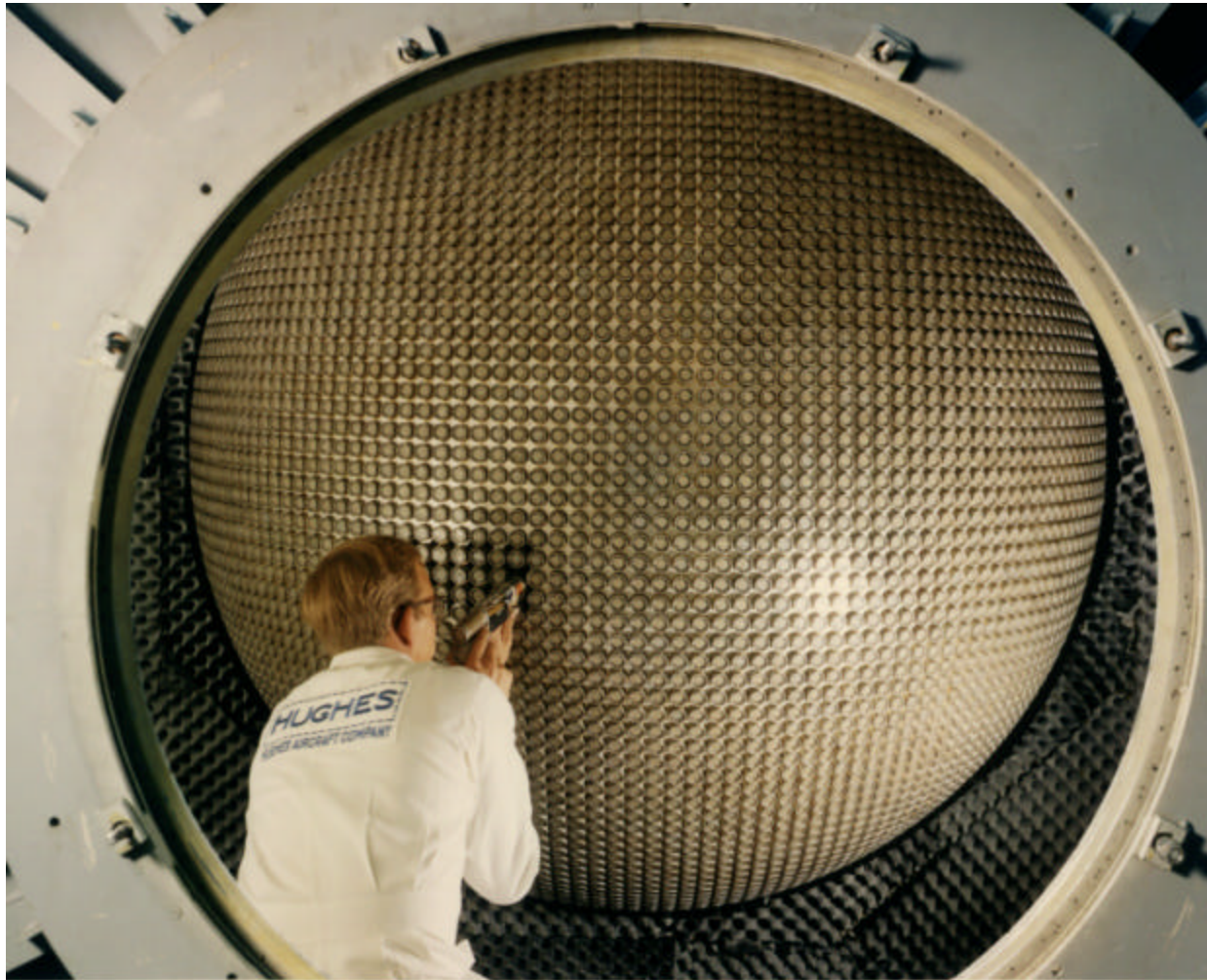
Classification of antennas by type:

1. reflectors
2. lenses
3. arrays

Other designations: wire antennas, aperture antennas, broadband antennas

# Lens Antenna

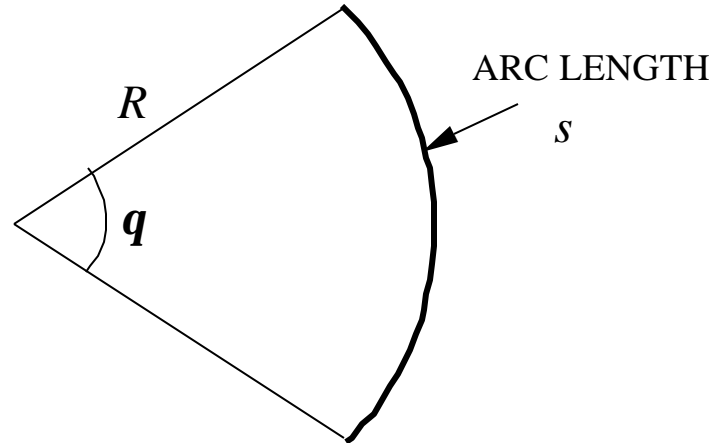
---



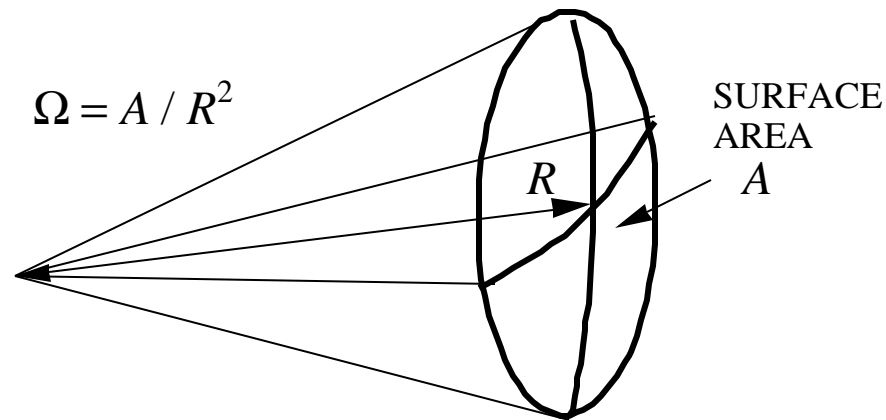
# Solid Angles and Steradians

---

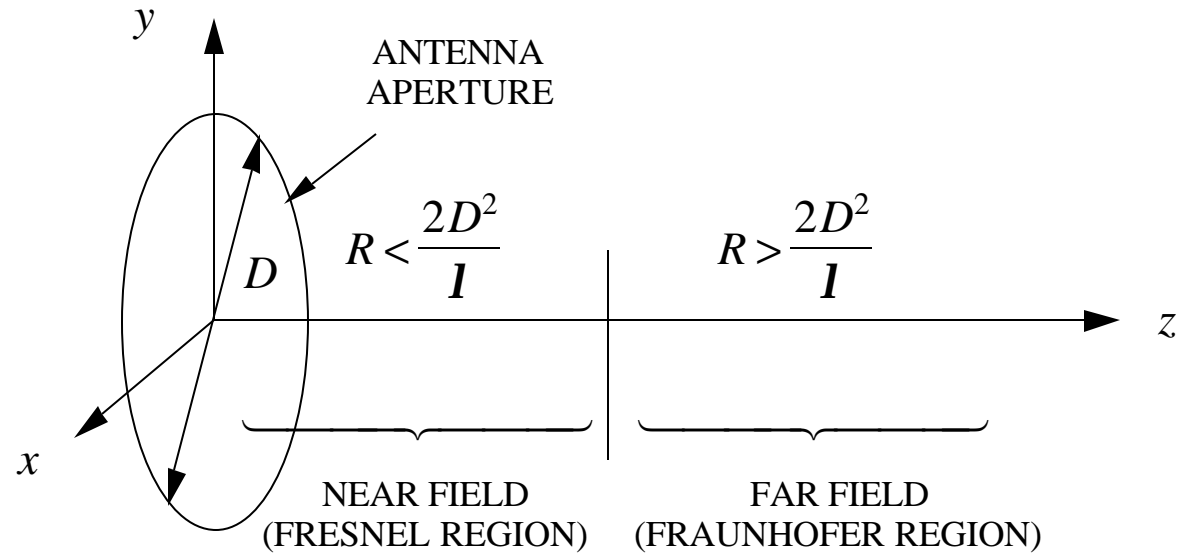
Plane angles:  $s = Rq$ , if  $s = R$  then  $q = 1$  radian



Solid angles:  $\Omega = A / R^2$ , if  $A = R^2$ , then  $\Omega = 1$  steradian



# Antenna Far Field

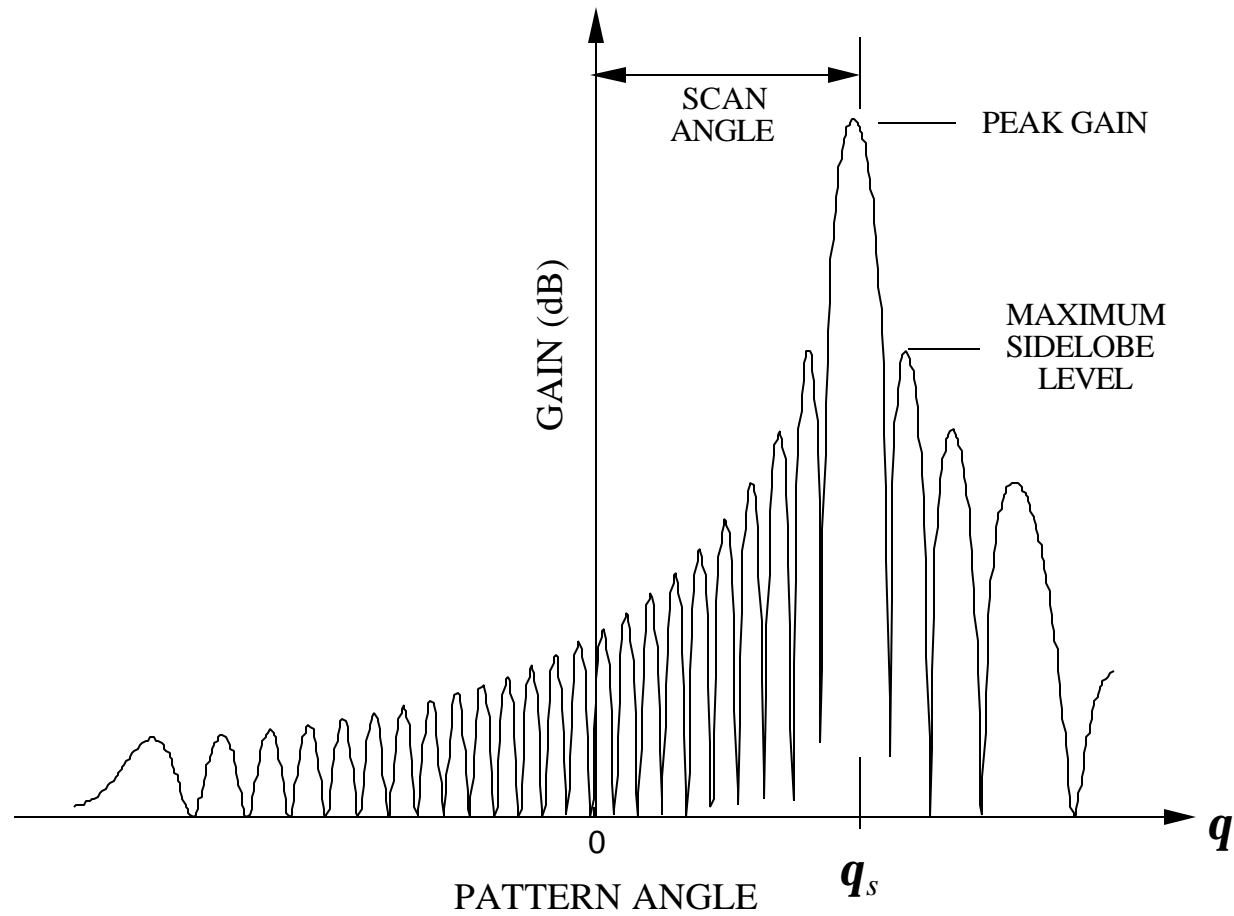


Far field conditions:  $R > 2D^2 / l$ ,  $D \gg l$ , and  $R \gg l$

In the antenna far field:

1.  $E_R = 0$
2.  $E_q, E_f \propto 1/R$
3. wave fronts are spherical

# Antenna Pattern Features





## Antenna Refresher (2)

---

Directive gain is a measure of the antenna's ability to focus energy

$$G_D(\mathbf{q}, \mathbf{f}) = \frac{\text{radiation intensity in the direction } (\mathbf{q}, \mathbf{f})}{\text{radiated power}/4\pi}$$

Radiation intensity in the direction  $(\mathbf{q}, \mathbf{f})$  in units of W/sr (sr = steradian):

$$U(\mathbf{q}, \mathbf{f}) = R^2 |\vec{W}(\mathbf{q}, \mathbf{f})| = \frac{R^2}{Z_o} \vec{E}(\mathbf{q}, \mathbf{f}) \cdot \vec{E}(\mathbf{q}, \mathbf{f})^* = \frac{R^2}{Z_o} |\vec{E}(\mathbf{q}, \mathbf{f})|^2$$

Maximum radiation intensity is  $U_{\max} = U(\mathbf{q}_{\max}, \mathbf{f}_{\max}) = \frac{R^2}{Z_o} |\vec{E}_{\max}|^2$

Average radiation intensity:

$$U_{\text{ave}} = \frac{1}{4\pi} \int_0^{2\pi} \int_0^{\pi} U(\mathbf{q}, \mathbf{f}) \sin \theta \, d\theta \, d\phi = \frac{1}{4\pi Z_o} \int_0^{2\pi} \int_0^{\pi} |\vec{E}(\mathbf{q}, \mathbf{f})|^2 R^2 \sin \theta \, d\theta \, d\phi$$

In the far-field of an antenna  $E_R = 0$  and  $E_q, E_f \propto 1/R$ . The beam solid angle is

$$\Omega_A = \frac{1}{|\vec{E}_{\max}|^2} \int_0^{2\pi} \int_0^{\pi} |\vec{E}(\mathbf{q}, \mathbf{f})|^2 \sin \theta \, d\theta \, d\phi = \int_0^{2\pi} \int_0^{\pi} |\vec{E}_{\text{norm}}(\mathbf{q}, \mathbf{f})|^2 \sin \theta \, d\theta \, d\phi$$

(Skolnik uses  $B$ )

## Antenna Refresher (3)

---

The directive gain can be written as

$$G_D(\mathbf{q}, \mathbf{f}) = \frac{4p}{\Omega_A} |\vec{E}_{\text{norm}}(\mathbf{q}, \mathbf{f})|^2$$

The maximum value of the directive gain occurs in the direction of the main beam peak for a focused antenna. The maximum value of the directive gain is called the directivity. Since the maximum value of  $|\vec{E}_{\text{norm}}(\mathbf{q}, \mathbf{f})|^2$  is one,

$$G_D = G_D(\mathbf{q}, \mathbf{f})|_{\text{max}} = \frac{4p}{\Omega_A}$$

Directive gain only depends on the antenna pattern. It does not include any losses incurred in forming the pattern.

Gain includes the effect of loss

$$G(\mathbf{q}, \mathbf{f}) = G_D(\mathbf{q}, \mathbf{f})\mathbf{r}$$

where  $\mathbf{r}$  is the antenna efficiency. Sources of loss depend on the particular type of antenna. Most electrically large antennas have losses due to nonuniform aperture illumination,  $\mathbf{r}_a$ , and mismatch loss (reflection of energy at the input terminals),  $\mathbf{r}_m$ . Therefore  $\mathbf{r} = \mathbf{r}_a \mathbf{r}_m$ .

# Directivity Example

---

An antenna has a far-field pattern of the form

$$\vec{E}(\mathbf{q}, \mathbf{f}) = \begin{cases} \hat{\mathbf{q}} E_0 \cos^n \mathbf{q} \frac{e^{-jkR}}{R}, & \mathbf{q} < \mathbf{p}/2 \\ 0, & \mathbf{q} > \mathbf{p}/2 \end{cases}$$

where  $n$  is an integer. The normalized electric field is

$$|\vec{E}_{\text{norm}}| = \left| \frac{E_0 \cos^n \mathbf{q} e^{-jkR} / R}{E_0 e^{-jkR} / R} \right| = |\cos^n \mathbf{q}|, \quad \mathbf{q} < \mathbf{p}/2$$

The resulting beam solid angle is

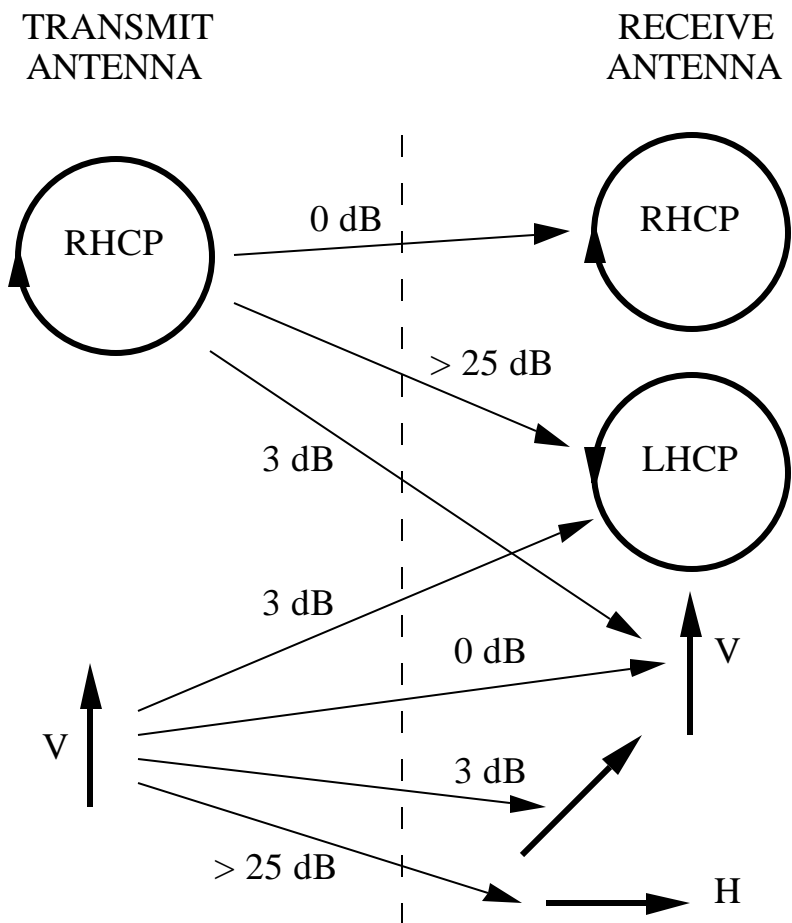
$$\Omega_A = \int_0^{\mathbf{p}/2} \int_0^{2\mathbf{p}} |\cos^n \mathbf{q}|^2 \sin \mathbf{q} d\mathbf{q} d\mathbf{f} = 2\mathbf{p} \left[ -\frac{\cos^{2n+1} \mathbf{q}}{2n+1} \right]_0^{\mathbf{p}/2} = \frac{2\mathbf{p}}{2n+1}$$

and directivity

$$G_D = \frac{4\mathbf{p}}{\Omega_A} = \frac{4\mathbf{p}}{2\mathbf{p}/(2n+1)} = 2(2n+1)$$

# Antenna Polarization Loss

Summary of polarization losses for polarization mismatched antennas

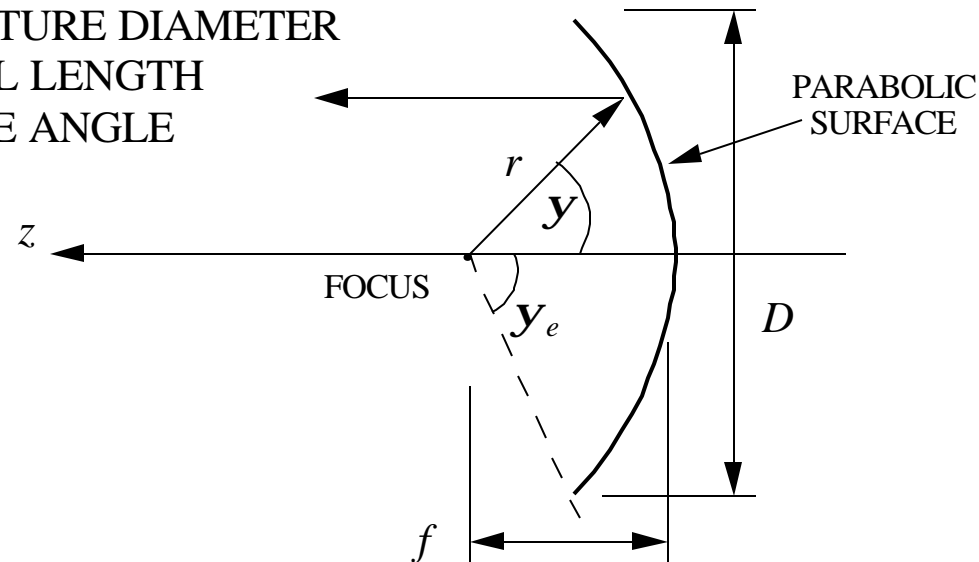


# Parabolic Reflector Antenna

$D$  = APERTURE DIAMETER

$f$  = FOCAL LENGTH

$y_e$  = EDGE ANGLE



Spherical waves emanating from the focal point are converted to plane waves after reflection from the parabolic surface. The ratio  $f / D$  is a design parameter. Some important relationships:

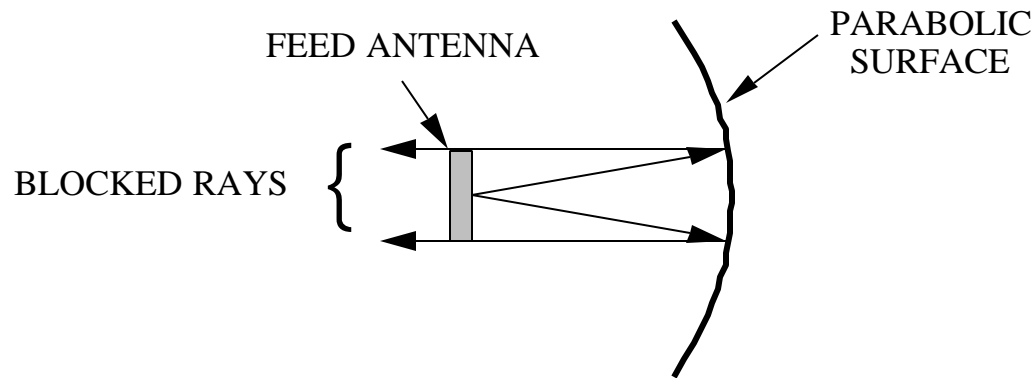
$$r = \frac{2f}{1 + \cos y}$$

$$y_e = 2 \tan^{-1} \left( \frac{1}{4f/D} \right)$$

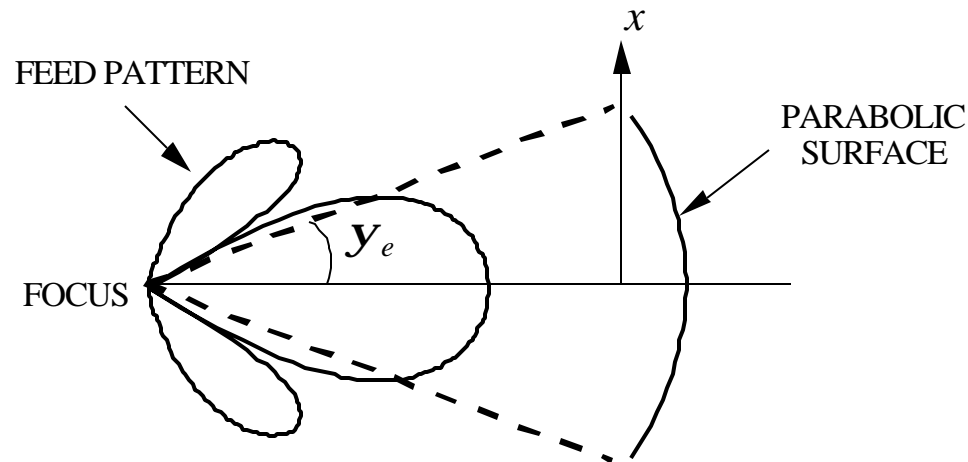
# Parabolic Reflector Antenna Losses

---

1. Feed blockage reduces gain and increases sidelobe levels



2. Spillover reduces gain



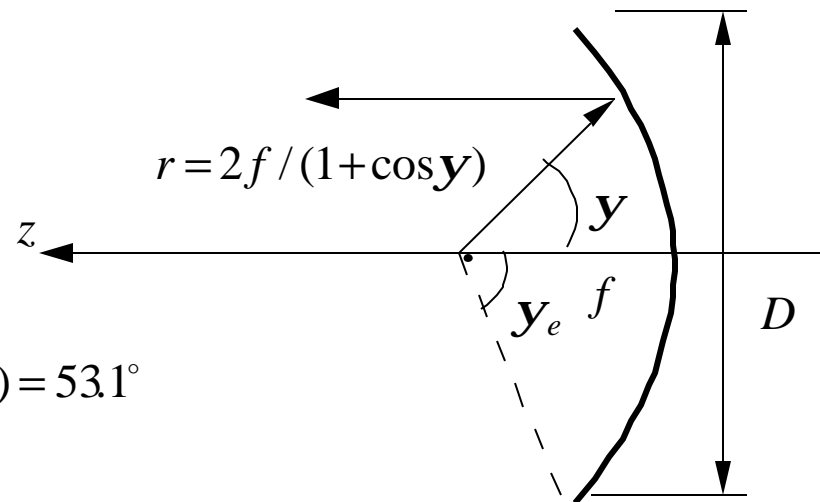
# Example

A circular parabolic reflector with  $f / D = 0.5$  has a feed with a pattern  $E(\mathbf{y}) = \cos \mathbf{y}$  for  $\mathbf{y} \leq \mathbf{p} / 2$ . The aperture illumination is

$$A(\mathbf{y}) = \frac{e^{-jkr}}{r} |E(\mathbf{y})| = \frac{e^{-jkr}}{r} \cos \mathbf{y}$$

$$|A(\mathbf{y})| = \cos \mathbf{y} (1 + \cos \mathbf{y}) / (2f)$$

$$\mathbf{y}_e = 2 \tan^{-1} \left( \frac{1}{4f/D} \right) = (2)(26.56) = 53.1^\circ$$



The edge taper is  $\frac{|A(\mathbf{y}_e)|}{|A(0)|} = \frac{\cos \mathbf{y}_e (1 + \cos \mathbf{y}_e) / (2f)}{2 / (2f)} = 0.4805 = -6.37 \text{ dB}$

The feed pattern required for uniform illumination is

$$\frac{|A(\mathbf{y}_e)|}{|A(0)|} = \frac{|E(\mathbf{y})| (1 + \cos \mathbf{y}) / 2f}{|E(0)| / f} = \frac{|E(\mathbf{y})| (1 + \cos \mathbf{y})}{2} \equiv 1 \Rightarrow |E(\mathbf{y})| = \frac{2}{1 + \cos \mathbf{y}} = \sec^2 \left( \frac{\mathbf{y}}{2} \right)$$

# Example

---

The spillover loss is obtained from fraction of feed radiated power that falls outside of the reflector edge angles. The power intercepted by the reflector is

$$\begin{aligned}
 P_{\text{int}} &= \int_0^{2p} \int_0^{y_e} \cos^2 \mathbf{y} \sin \mathbf{y} \, d\mathbf{f} d\mathbf{y} = 2\mathbf{p} \int_0^{y_e} \cos^2 \mathbf{y} \sin \mathbf{y} \, d\mathbf{y} \\
 &= -2\mathbf{p} \left[ \frac{\cos^3 \mathbf{y}}{3} \right]_0^{y_e} = 0.522\mathbf{p}
 \end{aligned}$$

The total power radiated by the feed is

$$\begin{aligned}
 P_{\text{rad}} &= \int_0^{2p} \int_0^{p/2} \cos^2 \mathbf{y} \sin \mathbf{y} \, d\mathbf{f} d\mathbf{y} = 2\mathbf{p} \int_0^{p/2} \cos^2 \mathbf{y} \sin \mathbf{y} \, d\mathbf{y} \\
 &= -2\mathbf{p} \left[ \frac{\cos^3 \mathbf{y}}{3} \right]_0^{p/2} = 0.667\mathbf{p}
 \end{aligned}$$

Thus the fraction of power collected by the reflector is

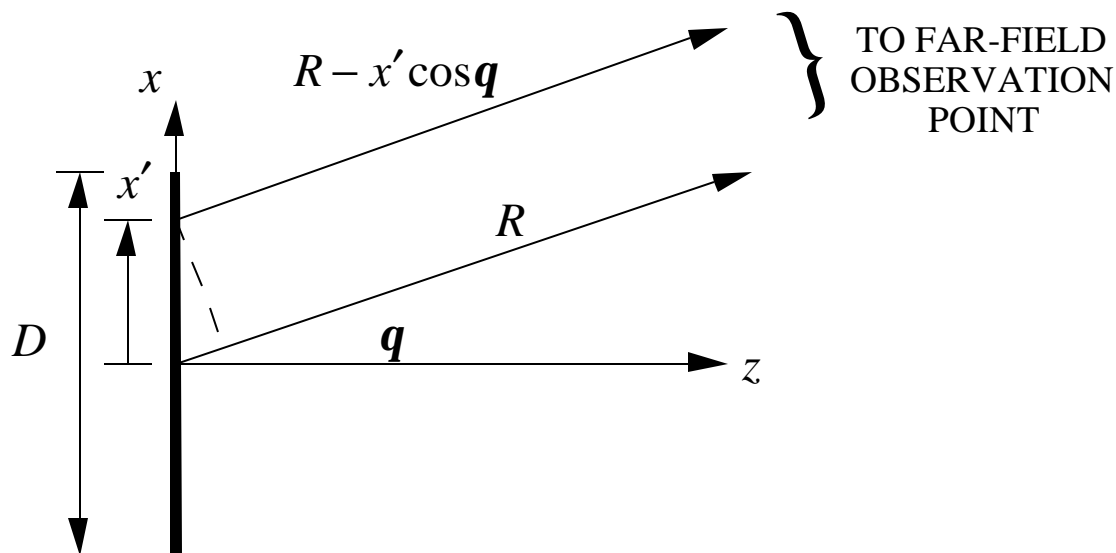
$$P_{\text{int}} / P_{\text{rad}} = 0.522 / 0.667 = 0.78$$

This is the spillover efficiency, which in dB is  $10 \log(0.78) = -1.08$  dB.



# Radiation by a Line Source (1)

---



Differential radiated field at the observation point from a differential length of source located at  $x'$  (unit amplitude):

$$dE_x = \frac{jkZ_o e^{-jk(R-x'\sin q)}}{4p |R - x'\sin q|} dx' \approx \frac{jkZ_o e^{-jkR}}{4p R} e^{jkx'\sin q} dx'$$

## Radiation by a Line Source (2)

---

Assume that the amplitude and phase along the source vary as  $A(x')$  and  $\Psi(x')$ . The total radiated field from the line source is:

$$E_x = \int dE_x = \frac{jkZ_o e^{-jkR}}{4\mathbf{p}R} \int_{-D/2}^{D/2} A(x') e^{jk\Psi(x')} e^{jkx' \sin \mathbf{q}} dx'$$

Note that this is in the form of a Fourier transform between the domains  $x'$  and  $k \sin \mathbf{q}$ .

Example:  $A(x') = 1$  and  $\Psi(x') = 0$  (uniform illumination)

$$E_x = \int dE_x = \frac{jkZ_o e^{-jkR}}{4\mathbf{p}R} \underbrace{\int_{-D/2}^{D/2} e^{jkx' \sin \mathbf{q}} dx'}_{=D \operatorname{sinc}\left(\frac{kD}{2} \sin \mathbf{q}\right)}$$

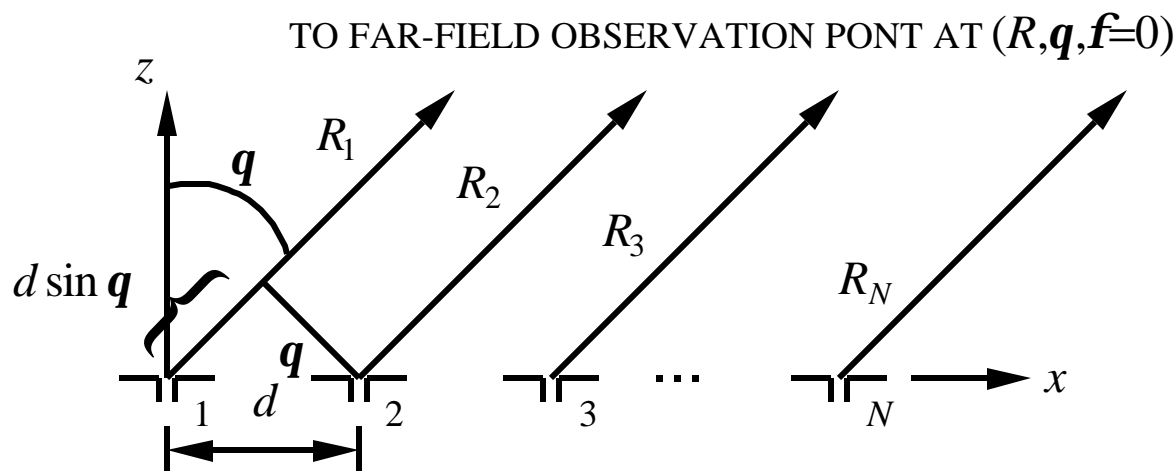
In the far-field only the  $\mathbf{q}$  and  $\mathbf{f}$  components exist

$$E_{\mathbf{q}} = E_x \cos \mathbf{q} = \frac{jkDZ_o e^{-jkR}}{4\mathbf{p}R} \cos \mathbf{q} \operatorname{sinc}\left(\frac{kD}{2} \sin \mathbf{q}\right)$$

Note that  $E_{\mathbf{f}} = E_x \sin \mathbf{f} = 0$  since  $\mathbf{f} = 0$ . A uniform aperture function is a "spatial pulse" and its Fourier transform is a sinc function in the spatial frequency domain ( $k \sin \mathbf{q}$ ).

# Array Antennas (1)

Arrays are collections of antennas that are geometrically arranged and excited to achieve a desired radiation pattern. Example: a linear array of dipoles



Assume:

1. equally spaced elements
2. uniformly excited (equal power to all elements)
3. identical elements
4. neglect "edge effects" (mutual coupling changes near edges)

In the far field vectors from the elements to the observation point are approximately parallel so that  $R_n = R_1 - (n - 1)d \sin \mathbf{q}$

# Array Antennas (2)

---

The element pattern for the array is the radiation pattern ( $E_q$ ) of a short dipole of length  $\Delta$  ( $\Delta \ll \lambda$ )

$$g_n(\mathbf{q}) = \frac{jI_o \Delta}{4\pi R_n} e^{-jkR_n} Z_o k \cos \mathbf{q} = \frac{jI_o \Delta}{4\pi R_1} e^{-j(kR_1 - (n-1)y)} Z_o k \cos \mathbf{q} = g_1(\mathbf{q}) e^{j(n-1)y}$$

where  $y = kd \sin \mathbf{q}$ . Since  $R_n \gg nd \sin \mathbf{q}$  we have replaced  $R_n$  in the denominator with  $R_1$  which is approximately  $R_n$ . The total far field of the array is given by

$$\begin{aligned} E(\mathbf{q}) &= \sum_{n=1}^N g_n(\mathbf{q}) = g_1(\mathbf{q}) \sum_{n=1}^N e^{jkd(n-1)\sin \mathbf{q}} = g_1(\mathbf{q}) \sum_{n=0}^{N-1} (e^{jy})^n \\ &= g_1(\mathbf{q}) \frac{1 - e^{jNy}}{1 - e^{jy}} = g_1(\mathbf{q}) \frac{\sin(Ny/2)}{\sin(y/2)} e^{j(N-1)y/2} \end{aligned}$$

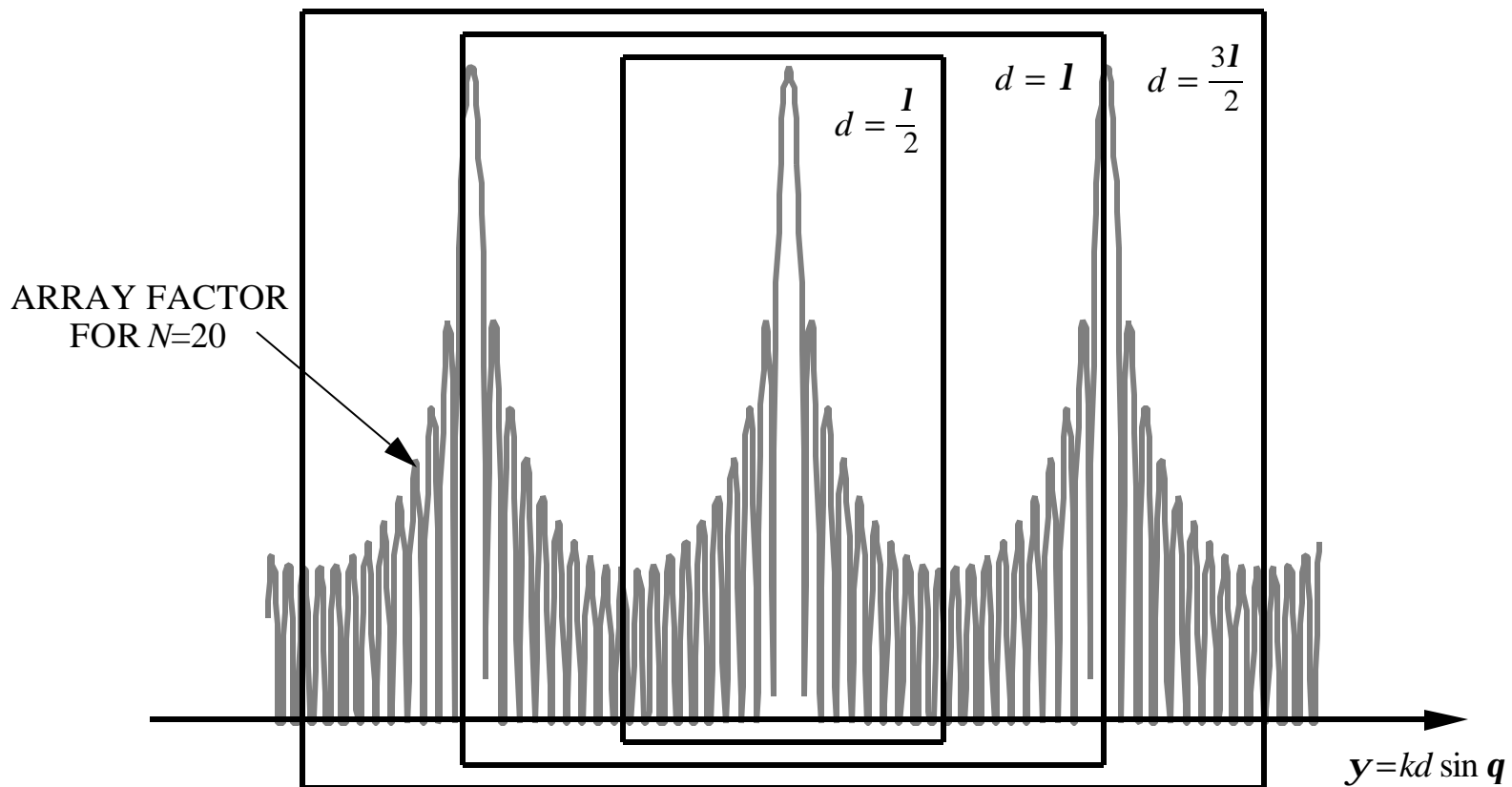
The magnitude gives the radiation pattern magnitude

$$|E(\mathbf{q})| = |g_1(\mathbf{q})| \left| \frac{\sin(Ny/2)}{\sin(y/2)} \right| = \left| \begin{array}{c} \text{ELEMENT} \\ \text{FACTOR (EF)} \end{array} \right| \cdot \left| \begin{array}{c} \text{ARRAY} \\ \text{FACTOR (AF)} \end{array} \right|$$

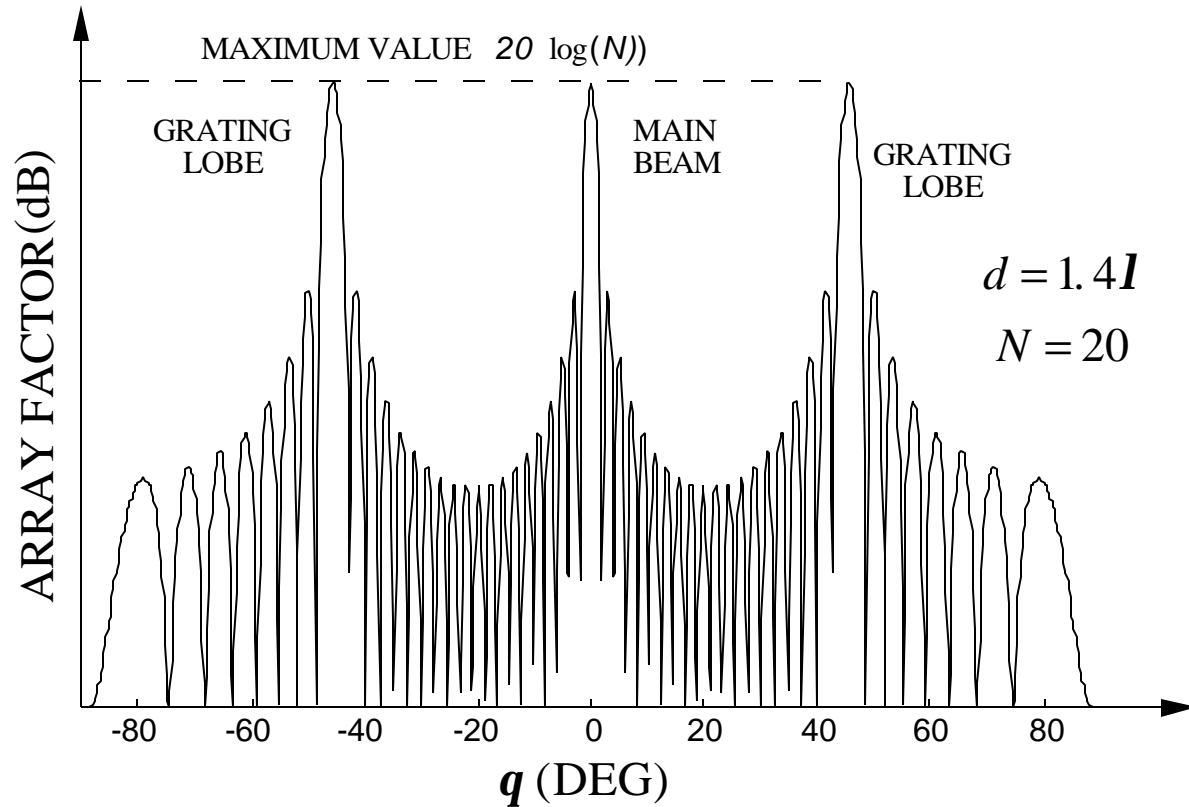
This result holds in general for an array of identical elements and is referred to as the principle of pattern multiplication. The array factor is only a function of the array geometry and excitation; the element factor only depends on the element characteristics.

# Visible Region

The region of the array factor that corresponds to  $-90^\circ \leq \mathbf{q} \leq 90^\circ$  is referred to as the visible region.



# Array Antennas (3)



Grating lobes occur when the denominator of the array factor is zero, or

$$y_m / 2 = pm \Rightarrow \sin q_m = ml / d \Rightarrow q_m = \sin^{-1}(ml / d)$$

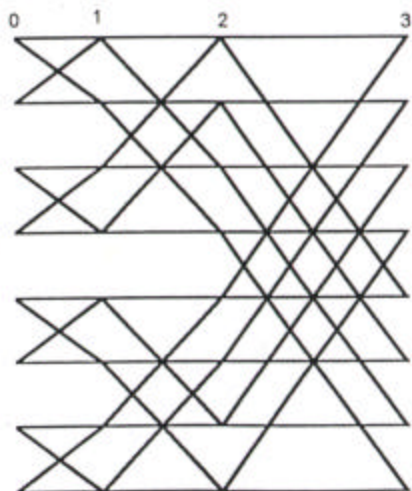
for  $m = \pm 1, \pm 2, \dots$

# Array Antennas (4)

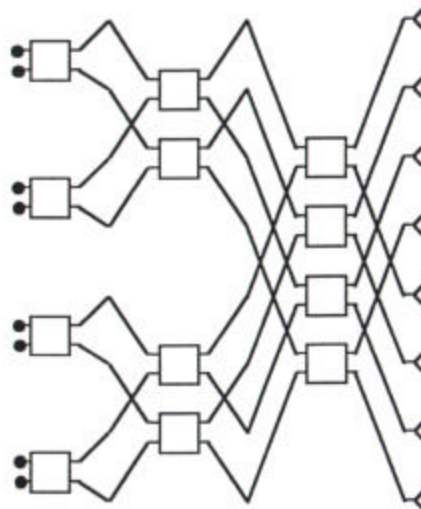
---

Recall that there is a Fourier transform relationship between a continuous aperture distribution  $A(x')$  and the radiation pattern  $E(k \sin \mathbf{q})$ . An array can be viewed as a sampled version of a continuous aperture, and therefore the array excitation function and far-field pattern are related by the discrete Fourier transform. The discrete Fourier transform is usually implemented using the fast Fourier transform (FFT) algorithm. Note the similarity between the FFT and Butler matrix. Grating lobes are a form of aliasing, which occurs because the Nyquist sampling theorem has been violated.

Cooley-Tukey FFT (1965)



Butler matrix feed (1960)



# Array Factor for 2D Arrays

---

Previous results for one dimension can be extended to two dimensions. Let the array lie in the  $x - y$  plane with element spacings  $d_x$  and  $d_y$ . The number of elements are  $N_x$  and  $N_y$ . For large arrays with no grating lobes the gain can be expressed as

$$G(\mathbf{q}, \mathbf{f}) = \frac{4pA_p r}{I^2} \underbrace{\left| \frac{g_1(\mathbf{q}, \mathbf{f})}{g_{1\max}} \right|^2}_{\text{NORMALIZED ELEMENT FACTOR}} \underbrace{\left| \frac{\sin(N_x(\mathbf{y}_x - \mathbf{y}_{sx})/2)}{N_x \sin((\mathbf{y}_x - \mathbf{y}_{sx})/2)} \right|^2 \left| \frac{\sin(N_y(\mathbf{y}_y - \mathbf{y}_{sy})/2)}{N_y \sin((\mathbf{y}_y - \mathbf{y}_{sy})/2)} \right|^2}_{\text{NORMALIZED ARRAY FACTOR}}$$

where

$$\begin{aligned} \mathbf{y}_x &= kd_x \sin \mathbf{q} \cos \mathbf{f}, & \mathbf{y}_{sx} &= kd_x \sin \mathbf{q}_s \cos \mathbf{f}_s \\ \mathbf{y}_y &= kd_y \sin \mathbf{q} \sin \mathbf{f}, & \mathbf{y}_{sy} &= kd_y \sin \mathbf{q}_s \sin \mathbf{f}_s \end{aligned}$$

The physical area of the array is approximately  $A_p = d_x d_y N_x N_y$ . The main beam direction is given by  $(\mathbf{q}_s, \mathbf{f}_s)$ .



# Gain of Phased Arrays

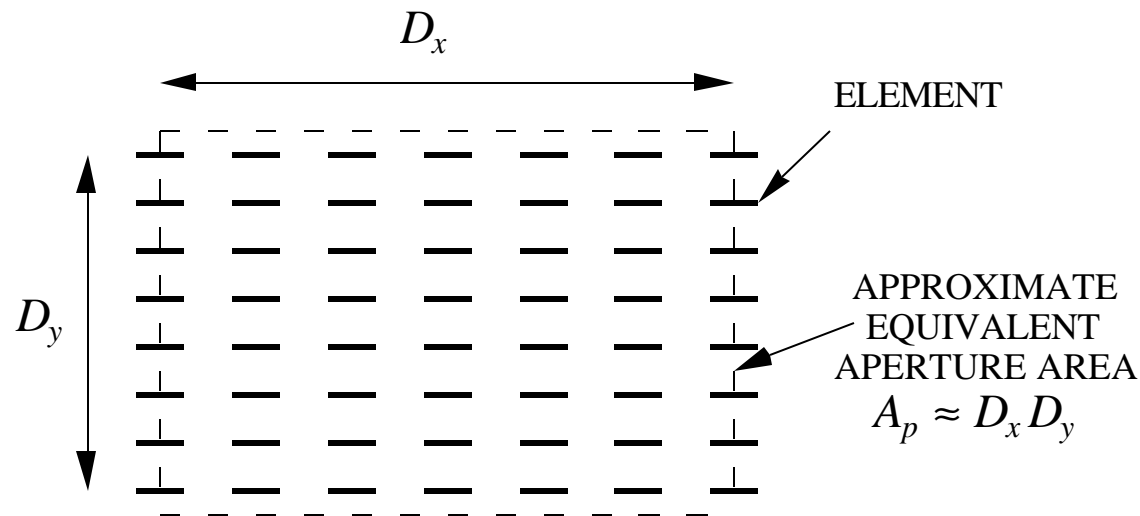
From the definition of directive gain:

$$G_D = \frac{4p}{\Omega_A} |\vec{E}_{\text{norm}}|^2$$

This cannot be reduced to a closed form expression in general. However, assuming that the principle of pattern multiplication holds and that the array is large

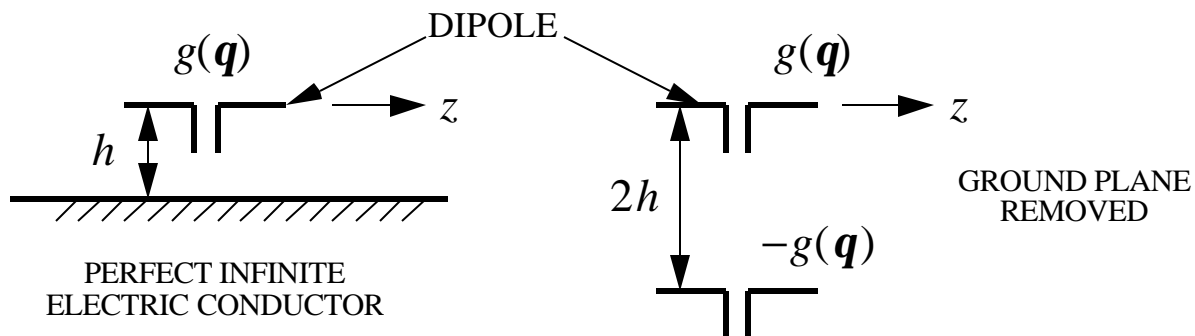
$$G_D = \frac{4pA_e}{I^2} |AF_{\text{norm}}(\mathbf{q}, \mathbf{f})|^2 |g_{\text{norm}}(\mathbf{q}, \mathbf{f})|^2$$

where the subscript "norm" denotes normalized (i.e., divided by the maximum value). As usual,  $A_e = \eta A_p$  (efficiency times physical aperture area)

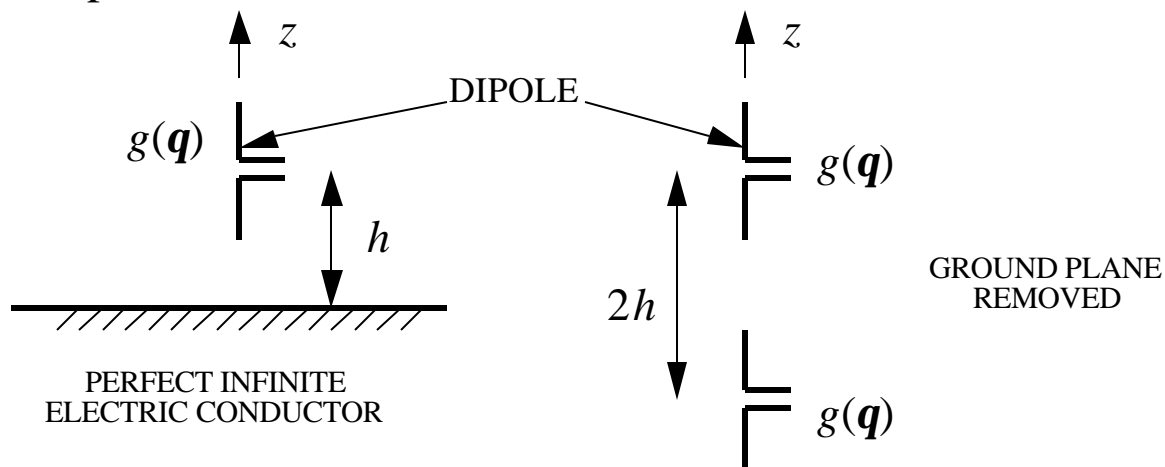


# Array Elements and Ground Planes

Ground planes are used to increase directivity. If the ground plane is a perfect conductor and infinite, the method of images can be used. For a horizontal dipole:

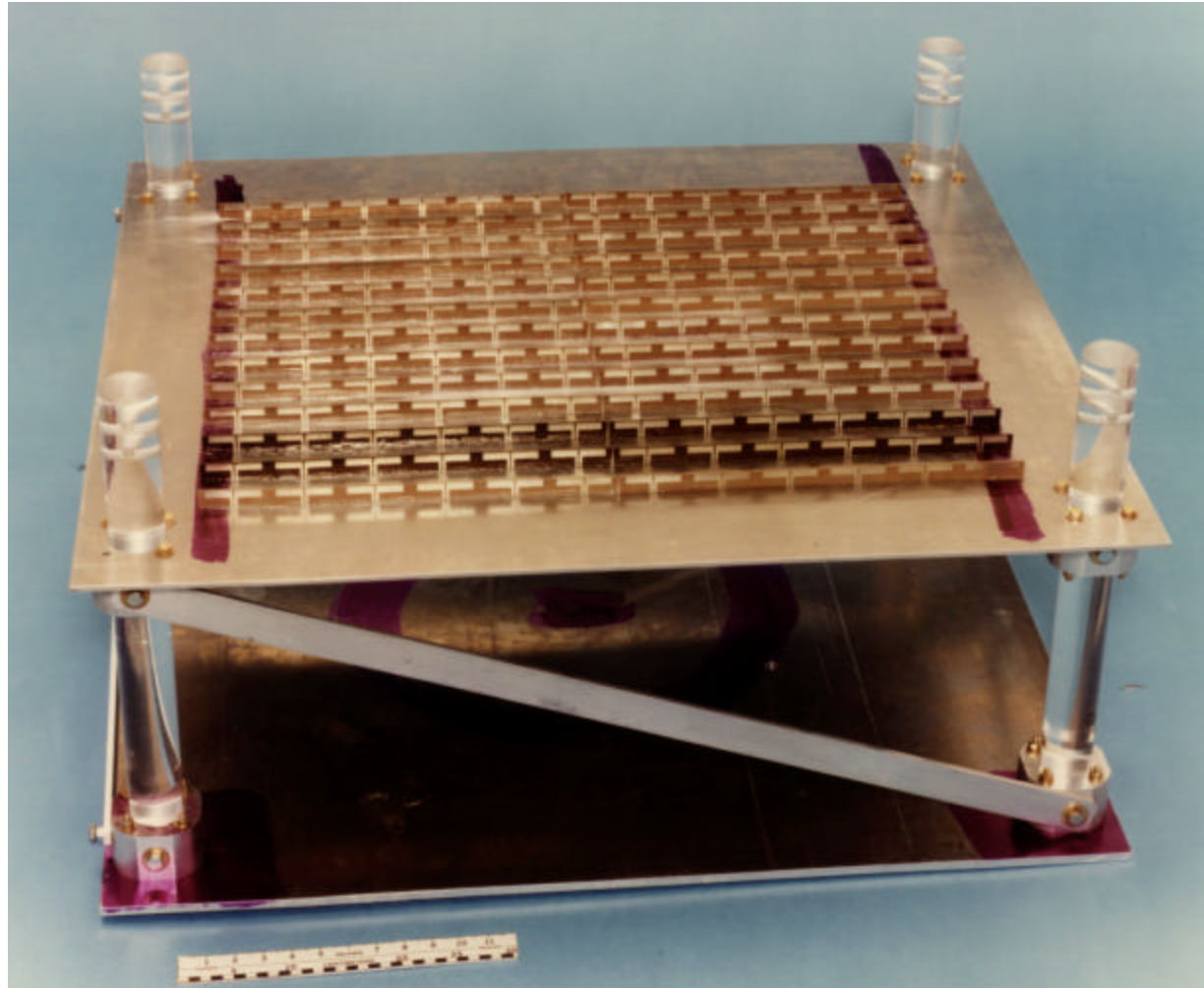


For a vertical dipole:



# Array of Dipoles Above a Ground Plane

---



# Series Fed Waveguide Slot Arrays

---



# Low Probability of Intercept Radar (LPIR)

---

Low probability of intercept (LPI) strategy employs:

1. Wideband "noise-like" waveforms
2. Limit radiated power to the absolute minimum required for tracking or detection (power management). Low  $P_t$  also reduces clutter illumination. Sensitivity time control (STC) can be used in conjunction with power management to reduce clutter return by reducing the receiver gain for near-in targets. Reducing  $G$  as a function of  $R$  is equivalent to reducing  $G$  as a function of  $t$ .
3. Control spatial radiation characteristics:
  - low sidelobe levels
  - narrow beams
  - rapid scanning (short target dwells)

# Low and Ultra Low Sidelobes

---

Definitions (not standardized):

<u>Classification</u>	<u>Maximum Sidelobe Level Relative to Peak</u>
Low sidelobes	-20 to -40 dB
Ultra-low sidelobes	less than -40 dB

Typical “state-of-the-art” for a large array is -40 dB

Motivation includes:      Low observability and low probability of intercept  
                                    Anti-jam  
                                    Reduced clutter illumination

Common low sidelobe distributions:

                                    Taylor, modified Taylor (sum beams)  
                                    Bayliss (difference beams)

Practical limitations:      Manufacturing and assembly errors

# Antenna Pattern Control

---

Common aperture distribution functions:

1. Chebyshev: yields the minimum beamwidth for a specified sidelobe level; all sidelobes are equal; only practical for a small number of elements.
2. Binomial: has no sidelobes; only practical for a small number of elements.
3. Taylor: specify the maximum sidelobe level and rate of falloff of sidelobe level.
4. Cosine-on-a-pedestal: (cosine raised to a power plus a constant) wide range of sidelobe levels and falloff rates; Hamming window is one of these.
5. Bayliss: for low sidelobe difference beams.

Pattern synthesis: given a specified pattern, find the required aperture distribution

1. Fourier-integral method: take the inverse Fourier transform of the far-field pattern to obtain the aperture distribution.
2. Woodward's method: use the  $\text{sinc}(\cdot)$  as a sampling function and find the required weights to match the desired pattern.

For a focused beam the amplitude distribution is always symmetric about the center of the array. To scan a focused beam a linear phase is introduced across the antenna aperture.

# Tapered Aperture Distributions

The shape of the aperture distribution can be used to reduce the sidelobes of the radiation pattern.

<u>Advantages</u>	<u>Disadvantages</u>
reduced clutter return	more complicated feed
low probability of intercept	reduced gain
less susceptible to jamming	increased beamwidth

Performance can be computed from Table 9.1 in Skolnik

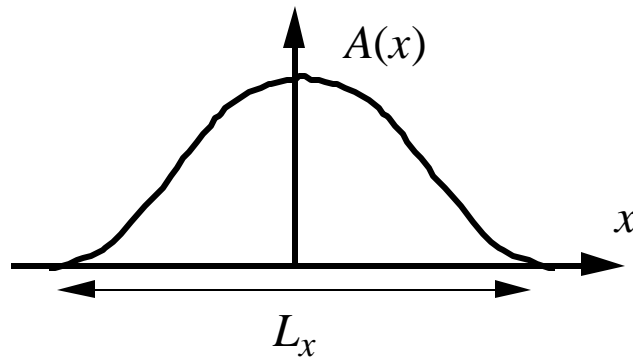
$\lambda = \text{wavelength}; a = \text{aperture width}$			
Type of distribution, $ z  < 1$	Relative gain	Half-power beamwidth, deg	Intensity of first sidelobe, dB below maximum intensity
Uniform; $A(z) = 1$	1	$51\lambda/a$	13.2
Cosine; $A(z) = \cos^n(\pi z/2)$ :			
$n = 0$	1	$51\lambda/a$	13.2
$n = 1$	0.810	$69\lambda/a$	23
$n = 2$	0.667	$83\lambda/a$	32
$n = 3$	0.575	$95\lambda/a$	40
$n = 4$	0.515	$111\lambda/a$	48
Parabolic; $A(z) = 1 - (1 - \Delta)z^2$ :			
$\Delta = 1.0$	1	$51\lambda/a$	13.2
$\Delta = 0.8$	0.994	$53\lambda/a$	15.8
$\Delta = 0.5$	0.970	$56\lambda/a$	17.1
$\Delta = 0$	0.833	$66\lambda/a$	20.6
Triangular; $A(z) = 1 -  z $	0.75	$73\lambda/a$	26.4
Circular; $A(z) = \sqrt{1 - z^2}$	0.865	$58.5\lambda/a$	17.6
Cosine-squared plus pedestal;			
$0.33 + 0.66 \cos^2(\pi z/2)$	0.88	$63\lambda/a$	25.7
$0.08 + 0.92 \cos^2(\pi z/2)$ , Hamming	0.74	$76.5\lambda/a$	42.8



# Calculation of Aperture Efficiency

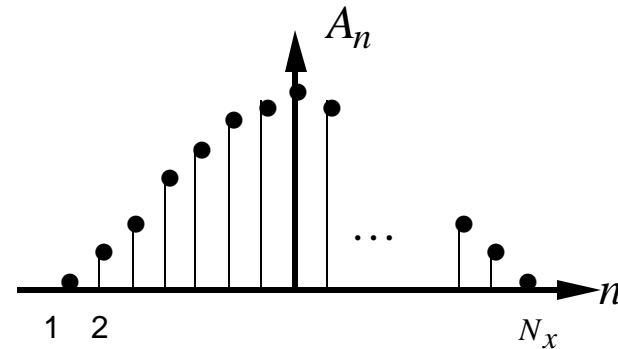
## Continuous aperture

$$\mathbf{r}_a = \frac{\left| \int_{-L_x/2}^{L_x/2} \int_{-L_y/2}^{L_y/2} A(x,y) dx dy \right|^2}{A_p \int_{-L_x/2}^{L_x/2} \int_{-L_y/2}^{L_y/2} |A(x,y)|^2 dx dy}$$



## Discrete Array

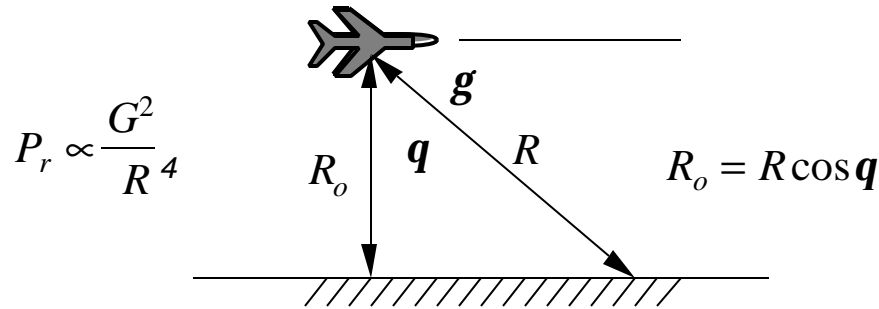
$$\mathbf{r}_a = \frac{\left| \sum_{n=1}^{N_x} \sum_{m=1}^{N_y} A_{mn} \right|^2}{N_x N_y \sum_{n=1}^{N_x} \sum_{m=1}^{N_y} |A_{mn}|^2}$$



Example: Cosine distribution:  $A(x) = \cos\{px / L_x\}$ ,  $-L_x/2 \leq x \leq L_x/2$

$$\mathbf{r}_a = \frac{\left| \int_{-L_x/2}^{L_x/2} \cos\{px / L_x\} dx \right|^2}{L_x \int_{-L_x/2}^{L_x/2} |\cos\{px / L_x\}|^2 dx} = \frac{\left\{ 2 \int_0^{L_x/2} \cos\{px / L_x\} dx \right\}^2}{2 L_x \int_0^{L_x/2} \cos^2\{px / L_x\} dx} = \frac{4(L_x/p)^2}{2L_x(L_x/4)} = \frac{8}{p^2} \approx -0.91 \text{ dB}$$

# Cosecant-Squared Antenna Pattern



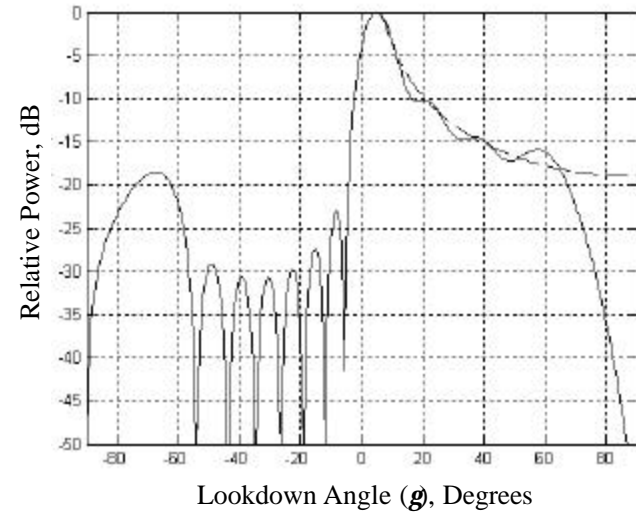
For uniform ground illumination:

$$\frac{G(0)^2}{R_0^4} = \frac{G(q)^2}{R^4}$$

or

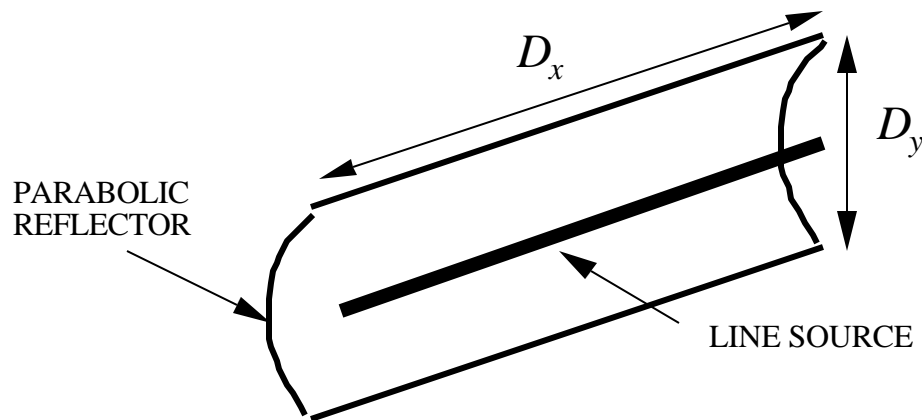
$$G(q) = G(0) \frac{R^2}{R_0^2} = G(0) \csc^2 q$$

Typical cosecant-squared pattern



# Example

Fan beam generated by a cylindrical paraboloid with a line source that provides uniform illumination in azimuth but  $\cos(py' / D_y)$  in elevation



Sidelobe levels from Table 9.1

- uniform distribution in azimuth ( $x$ ):  
SLL = 13.2 dB
- cosine in elevation ( $y$ ):  
SLL = 23 dB

Find  $D_x$  and  $D_y$  for azimuth and elevation beamwidths of 2 and 12 degrees

$$q_{el} = 69l / D_y = 12^\circ \Rightarrow D_y = 5.75l$$

$$q_{az} = 51l / D_x = 2^\circ \Rightarrow D_x = 25.5l$$

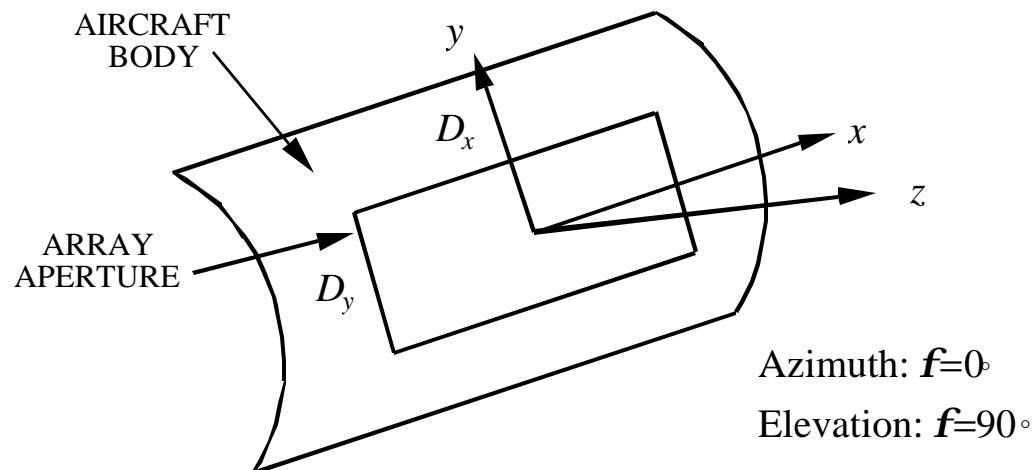
The aperture efficiency is  $r_a = (1)(0.81)$  and the gain is

$$G = \frac{4pA_p}{l^2} r = \frac{4p(5.75l)(25.5l)}{l^2} (1)(0.81) = 1491.7 = 31.7 \text{ dB}$$

# Array Example (1)

Design an array to meet the following specifications:

1. Azimuth sidelobe level 30 dB
2.  $\pm 45$  degree scan in azimuth; no elevation scan; no grating lobes
3. Elevation HPBW of 5 degrees
4. Gain of at least 30 dB over the scan range



Restrictions:

1. Elements are vertical ( $\hat{y}$ ) dipoles over a ground plane
2. Feed network estimated to have 3 dB of loss
3. Dipole spacings are:  $0.4l \leq d_x \leq 0.8l$  and  $0.45l \leq d_y \leq 0.6l$

## Array Example (2)

---

Restrictions (continued):

4. errors and imperfections will increase the SLL about 2 dB so start with a -32 dB sidelobe distribution ( $r_a = 0.81$ ):  $A(x') = 0.2 + 0.8 \cos^2(\mathbf{p}x' / 2)$
5. minimize the number of phase shifters used in the design

Step 1: start with the gain to find the required physical area of the aperture

$$G = G_D \mathbf{r} = \frac{4\mathbf{p}A_p}{I^2} \mathbf{r} \cos \mathbf{q} \geq 30 \text{ dB}$$

$\cos \mathbf{q}$  is the projected area factor, which is a minimum at 45 degrees. The efficiency includes tapering efficiency (0.81) and feed loss (0.5). Therefore

$$G = \frac{4\mathbf{p}A_p}{I^2} (0.707)(0.81)(0.5) = 10^3$$

or,  $A_p / I^2 = (D_x / I)(D_y / I) \approx (N_x d_x / I)(N_y d_y / I) = 278.1$ .

Step 2: uniform illumination in elevation; must have a HPBW of 5 degrees

$$\left| \frac{\sin(N_y k d_y \sin \mathbf{q} / 2)}{N_y \sin(k d_y \sin \mathbf{q} / 2)} \right|_{\mathbf{q}=2.5^\circ} = 0.707 \Rightarrow D_y = N_y d_y = 10I$$

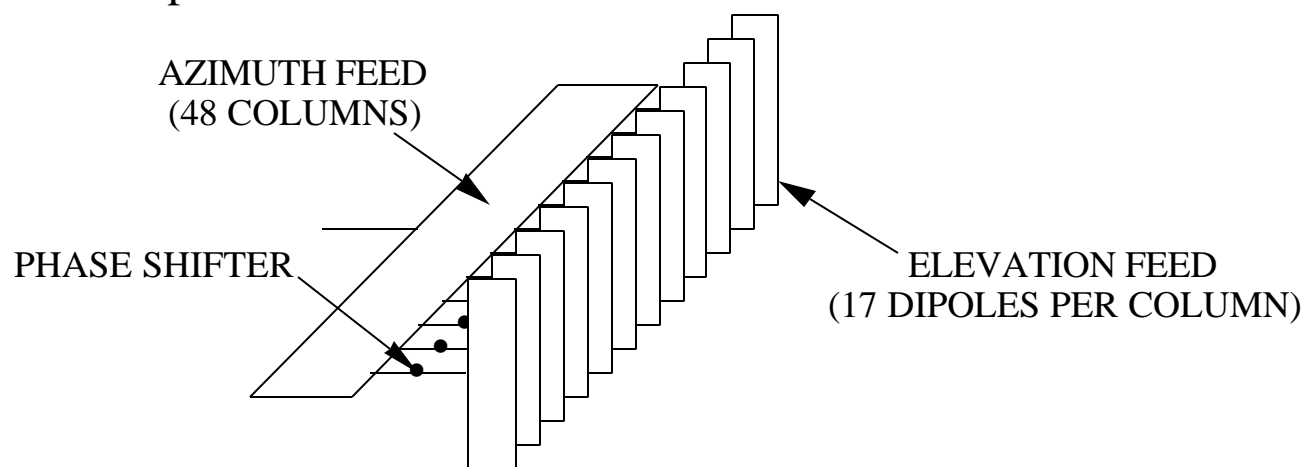
## Array Example (3)

This leads to  $D_x = A_p / D_y = 28l$ . To minimize the number of elements choose the largest allowable spacing:  $d_y = 0.6l \Rightarrow N_y = D_y / d_y = 17$

Step 3: azimuth spacing must avoid grating lobes which occur when

$$\begin{aligned} \sin \mathbf{q}_n - \sin \mathbf{q}_s &= n\mathbf{l} / d_x & (\mathbf{q}_n \leq -90^\circ, n = -1, \mathbf{q}_s = 45^\circ) \\ -1 - 0.707 &= -\mathbf{l} / d_x & \Rightarrow d_x \leq 0.585l \end{aligned}$$

Again, to minimize the number of elements, use the maximum allowable spacing ( $0.585l$ ) which gives  $N_x = D_x / d_x = 48$ . Because the beam only scans in azimuth, one phase shifter per column is sufficient.



## Array Example (4)

---

Step 4: Find the azimuth beamwidth at scan angles of 0 and 45 degrees. Letting  $\mathbf{q}_H = \mathbf{q}_B / 2$

$$\left| \frac{\sin(N_x kd_x (\pm \sin \mathbf{q}_H - \sin \mathbf{q}_s) / 2)}{N_x \sin(kd_x (\pm \sin \mathbf{q}_H - \sin \mathbf{q}_s) / 2)} \right| = 0.707$$

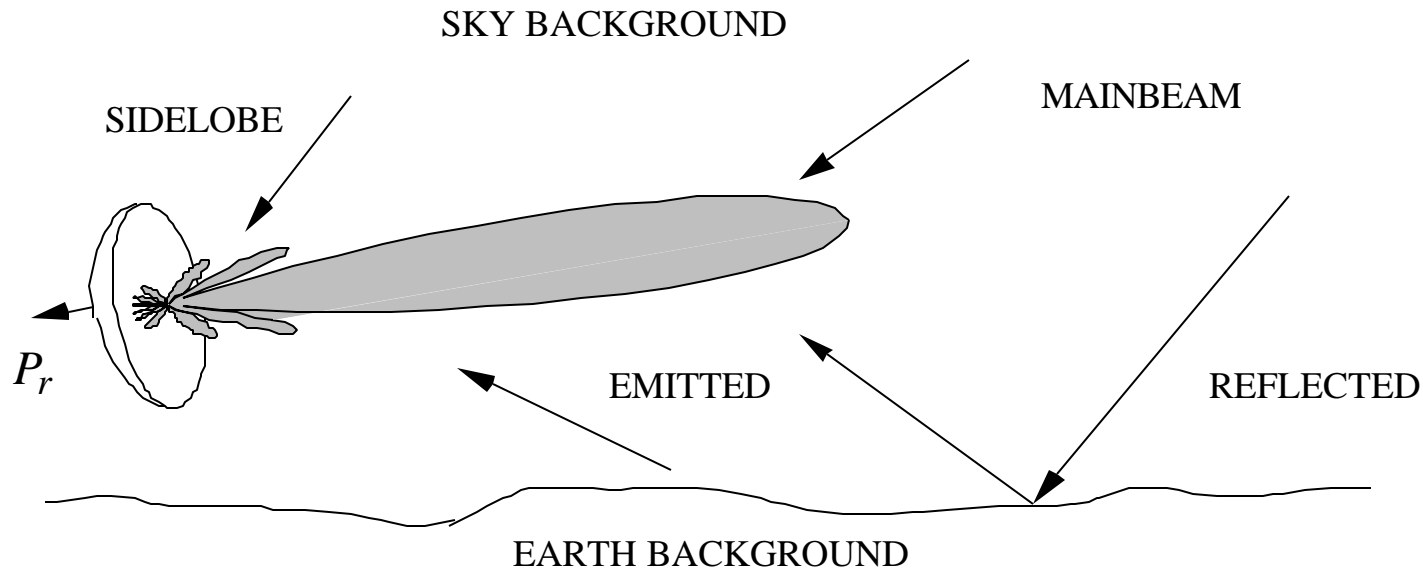
Solve this numerically for  $\mathbf{q}_s = 0$  and 45 degrees. Note that the beam is not symmetrical when it is scanned to 45 degrees. Therefore the half power angles are different on the left and right sides of the maximum

$$\mathbf{q}_s = 0^\circ : \quad \mathbf{q}_{H^+} = -\mathbf{q}_{H^-} = 0.91^\circ \quad \Rightarrow \quad \text{HPBW, } \mathbf{q}_B = \mathbf{q}_{H^+} - \mathbf{q}_{H^-} = 2(0.91) = 1.82^\circ$$

$$\mathbf{q}_s = 45^\circ : \quad \mathbf{q}_{H^+} = 46.3^\circ, \mathbf{q}_{H^-} = 43.75^\circ \quad \Rightarrow \quad \text{HPBW, } \mathbf{q}_B = 46.3^\circ - 43.75^\circ = 2.55^\circ$$

We have not included the element factor, which will affect the HPBW at 45 degrees.

# Calculation of Antenna Temperature



The antenna collects noise power from background sources. The noise level can be characterized by the antenna temperature

$$T_A = \frac{\int_0^P \int_0^{2P} T_B(\mathbf{q}, f) G(\mathbf{q}, f) \sin \mathbf{q} d\mathbf{q} df}{\int_0^P \int_0^{2P} G(\mathbf{q}, f) \sin \mathbf{q} d\mathbf{q} df}$$

$T_B$  is the background brightness temperature and  $G$  the antenna gain.

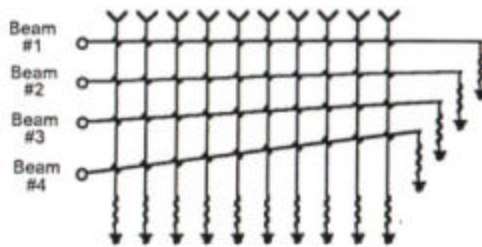


# Multiple Beam Antennas (1)

---

Several beams share a common aperture (i.e., use the same radiating elements)

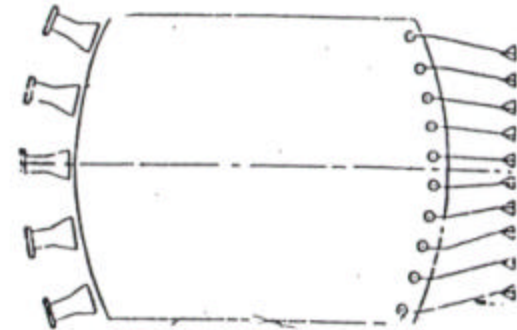
Arrays



Reflectors



Lenses



- Advantages:
- Cover large search volumes quickly
  - Track multiple targets simultaneously
  - Form "synthetic" beams
- Disadvantages:
- Beam coupling loss
  - Increased complexity in the feed network

Sources of beam coupling loss: (1) leakage and coupling of signals in the feed network, and (2) non-orthogonality of the beam patterns

## Multiple Beam Antennas (2)

---

Multiple beams are a means of increasing the rate of searching radar resolution cells (i.e., the radar system bandwidth). The overall system bandwidth depends on the number of range cells ( $N_{\text{range}}$ ), doppler cells ( $N_{\text{dop}}$ ), and angle cells ( $N_{\text{ang}}$ ):

$$N_{\text{sys}} = N_{\text{range}} \times N_{\text{dop}} \times N_{\text{ang}}$$

$$N_{\text{sys}} = \left( \frac{1}{f_p t} \right) \times (f_p t_{ot}) \times \underbrace{\left( \frac{\Omega_s}{q_e q_a} \right)}_{t_f / t_{ot}} = \frac{t_f}{t}$$

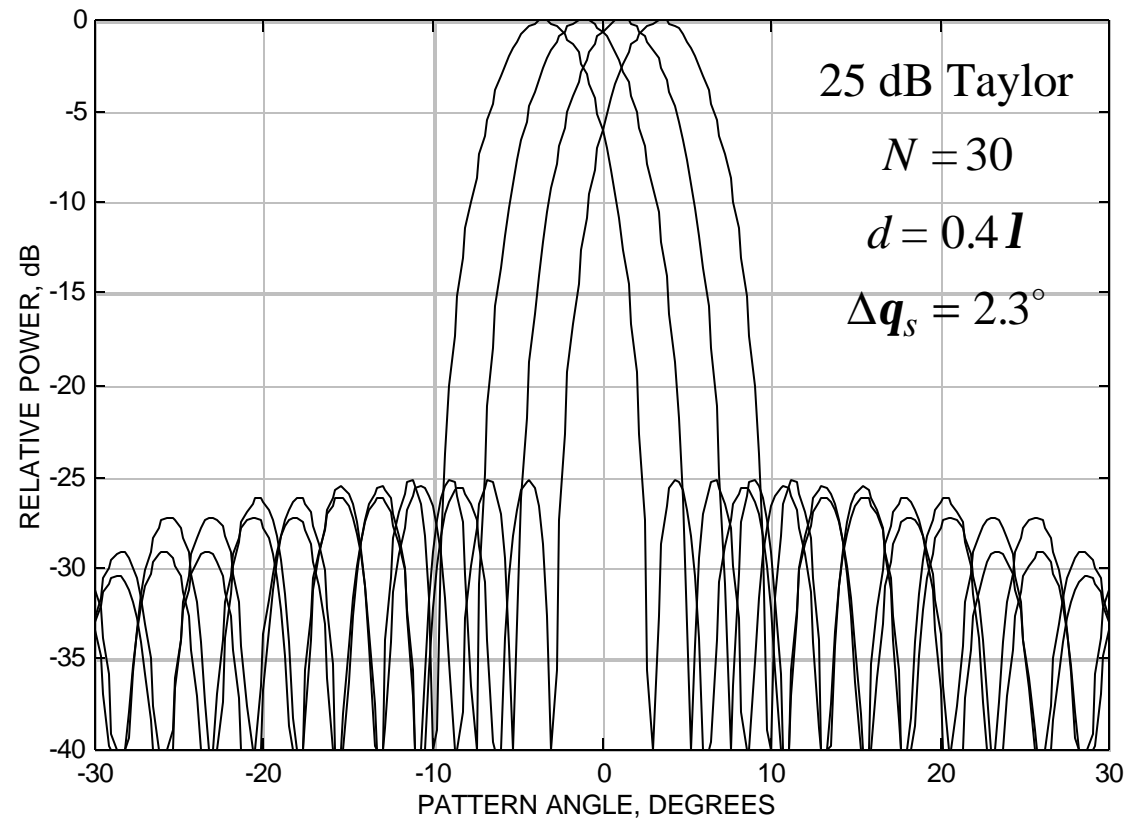
The bandwidth of the system can be increased by adding more beams and receivers. If the instantaneous bandwidth of a receiver is  $B \approx 1/t$  and  $m$  channels are used then

$$N_{\text{sys}} = t_f B_{\text{eff}} \quad \Rightarrow \quad B_{\text{eff}} = mB$$

Example: A radar with 8 beams, a pulse width of 0.25  $\mu\text{s}$ , and a rotation rate of 10 rpm ( $t_f = 6$  sec) has  $N_{\text{sys}} = \frac{(6)(8)}{0.25 \times 10^{-6}} = 2 \times 10^8$  resolution cells and an effective system bandwidth of 32 MHz.

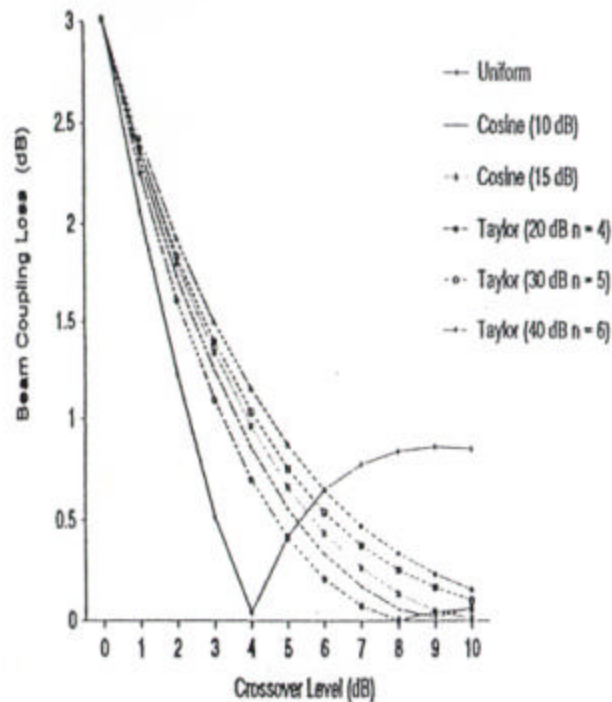
# Radiation Patterns of a Multiple Beam Array

---

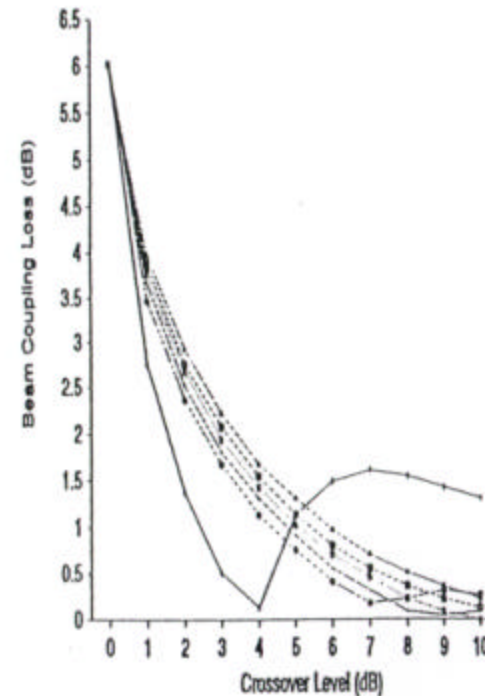


# Beam Coupling Losses for a 20 Element Array

2 Beams



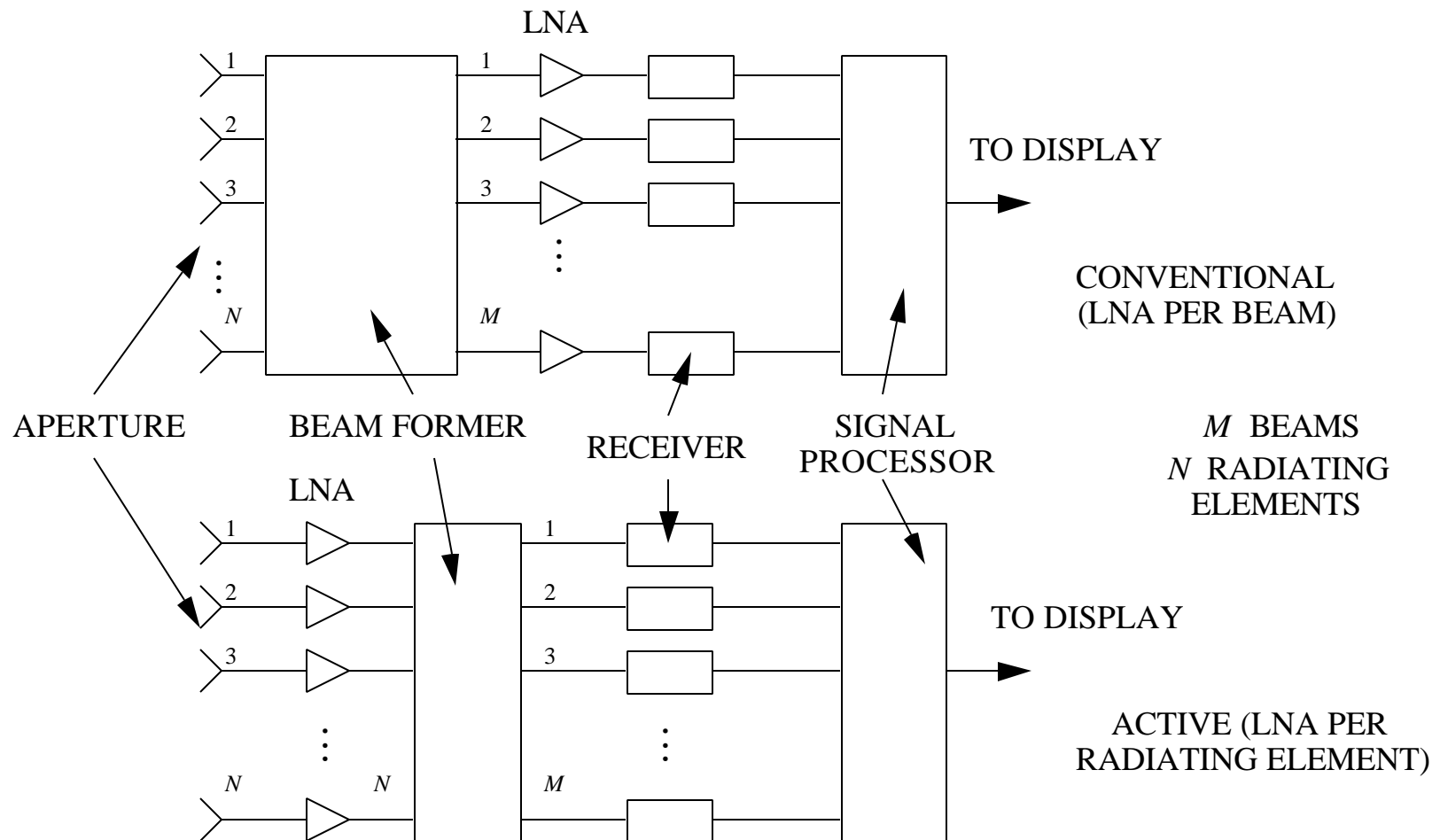
4 Beams



For  $m$  and  $n$  to be orthogonal beams : 
$$\frac{1}{Z_o} \int_0^{2\pi} \int_0^{\pi} \vec{E}_m(\mathbf{q}, \mathbf{f}) \cdot \vec{E}_n^*(\mathbf{q}, \mathbf{f}) R^2 \sin \mathbf{q} d\mathbf{q} d\mathbf{f} = 0$$

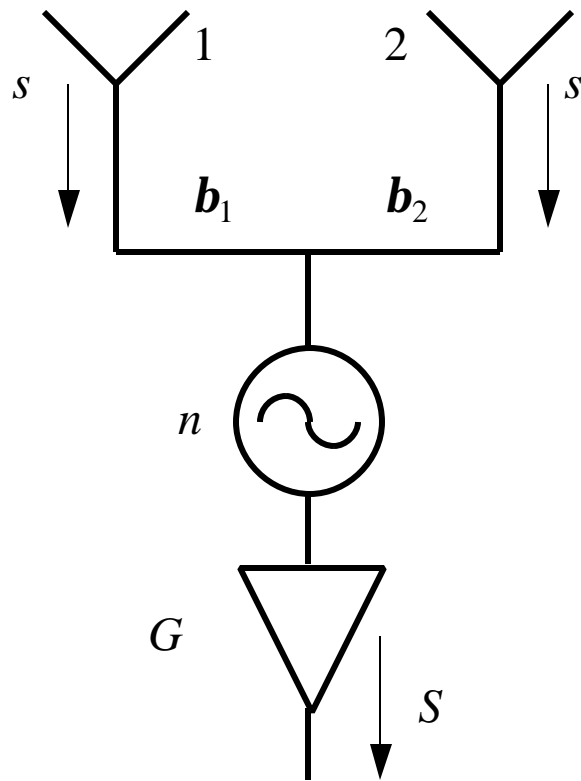
Example: If the beams are from a uniformly illuminated line source then  $\vec{E}_n(\mathbf{q}, \mathbf{f})$ ,  $\vec{E}_m(\mathbf{q}, \mathbf{f}) \propto \text{sinc}(\cdot)$  and adjacent beams are orthogonal if the crossover level is 4 dB.

# Active vs. Passive Antennas

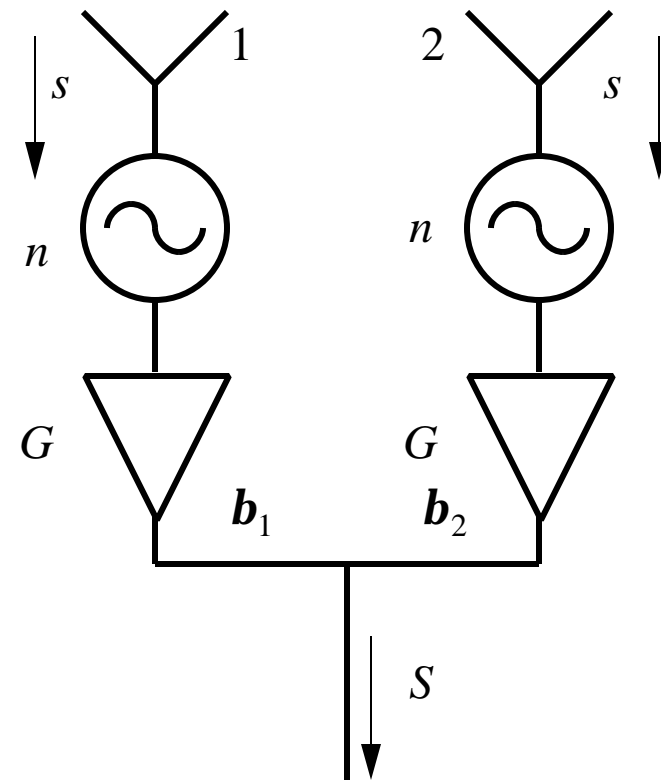


# SNR Calculation for a Lossless Feed Network

Amplification after beamforming



Amplification before beamforming



The power coupling coefficients are  $b_1$  and  $b_2$ . For a lossless coupler  $b_1 + b_2 = 1$ .

# SNR Calculation for a Lossless Feed Network

---

Amplification after beamforming:

$$N = nG$$

$$S = \left( \sqrt{s} \sqrt{\mathbf{b}_1} \sqrt{G} + \sqrt{s} \sqrt{\mathbf{b}_2} \sqrt{G} \right)^2 = sG \left( \sqrt{\mathbf{b}_1} + \sqrt{\mathbf{b}_2} \right)^2$$

$$\frac{S}{N} = \frac{sG \left( \sqrt{\mathbf{b}_1} + \sqrt{\mathbf{b}_2} \right)^2}{nG(\mathbf{b}_1 + \mathbf{b}_2)} = 2r_a \frac{s}{n}$$

where  $r_a = \frac{\left( \sqrt{\mathbf{b}_1} + \sqrt{\mathbf{b}_2} \right)^2}{2(\mathbf{b}_1 + \mathbf{b}_2)}$  is the aperture efficiency. Since  $\frac{s}{n}$  is the SNR for a single element, if  $r_a = 1$  then the gain is 2.

Amplification before beamforming:

$$N = nG\mathbf{b}_1 + nG\mathbf{b}_2 = nG$$

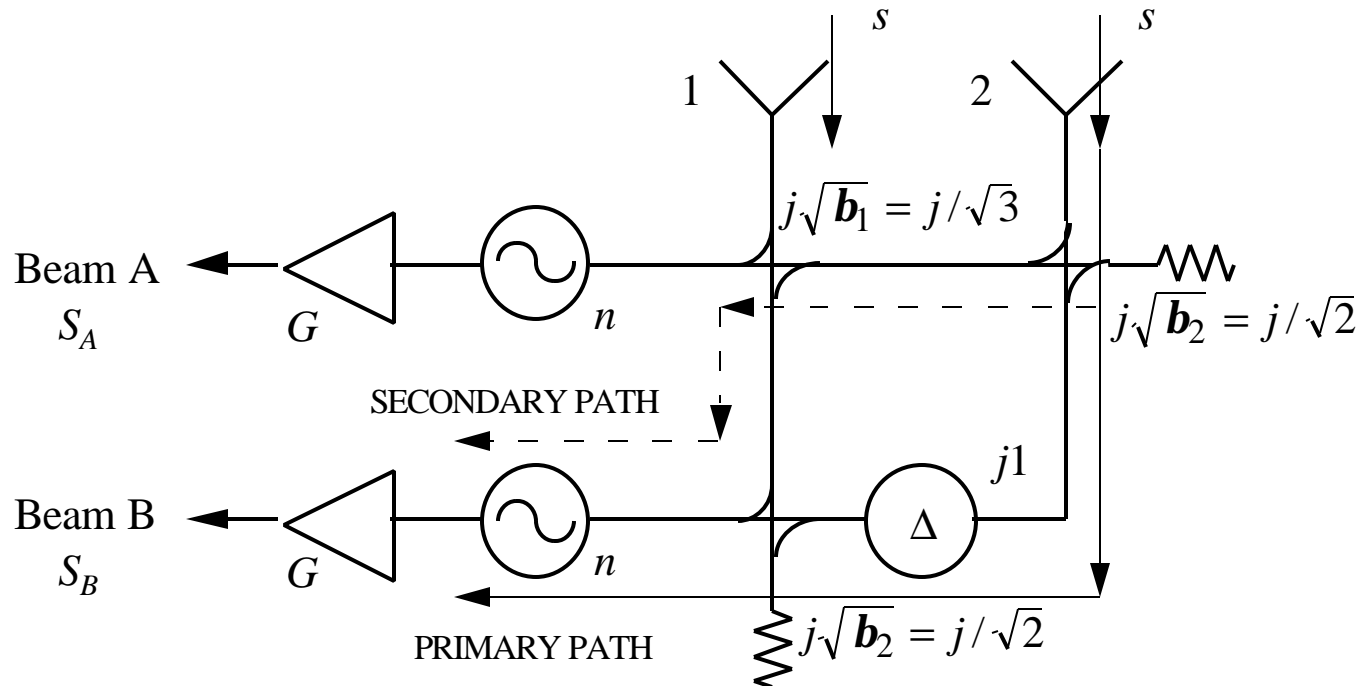
$$S = sG \left( \sqrt{\mathbf{b}_1} + \sqrt{\mathbf{b}_2} \right)^2$$

$$\frac{S}{N} = \frac{sG \left( \sqrt{\mathbf{b}_1} + \sqrt{\mathbf{b}_2} \right)^2}{nG(\mathbf{b}_1 + \mathbf{b}_2)} = 2r_a \frac{s}{n}$$

Note that the location of the amplifiers does not affect the gain of a lossless antenna.

# Passive Two-Beam Array (1)

Amplification after beamforming



Coupling coefficients:  $j\sqrt{b_1}$  and  $j\sqrt{b_2}$   
 For uniform illumination:

Transmission coefficients:  $t_1$  and  $t_2$   
 Lossless couplers:  $t_i + b_i = 1, i = 1, 2$

$$b_1 = 1/3, b_2 = 1/2, \Delta = \frac{e^{jP}}{\sqrt{3}}$$



## Passive Two-Beam Array (2)

---

Amplification after beamforming:

For beam A:  $S = sG(\sqrt{\mathbf{b}_1} + \sqrt{\mathbf{b}_2}\sqrt{\mathbf{t}_1})^2$  and  $N = nG$ . Using the coupling values on the last chart

$$\left(\frac{S}{N}\right)_A = 2\frac{s}{n}\mathbf{r}_a(\mathbf{b}_1 + \mathbf{b}_2\mathbf{t}_1) = \frac{4}{3}\mathbf{r}_a\frac{s}{n}$$

where the aperture efficiency for beam A is  $\mathbf{r}_a = \frac{(\sqrt{\mathbf{b}_1} + \sqrt{\mathbf{b}_2}\sqrt{\mathbf{t}_1})^2}{2(\mathbf{b}_1 + \mathbf{b}_2\mathbf{t}_1)} = \frac{(2A)^2}{2(2A)} = 1$ .

$A$  is the excitation amplitude (which is just a constant scale factor). For beam B the analysis is more complicated because there are two signal paths. The SNR is

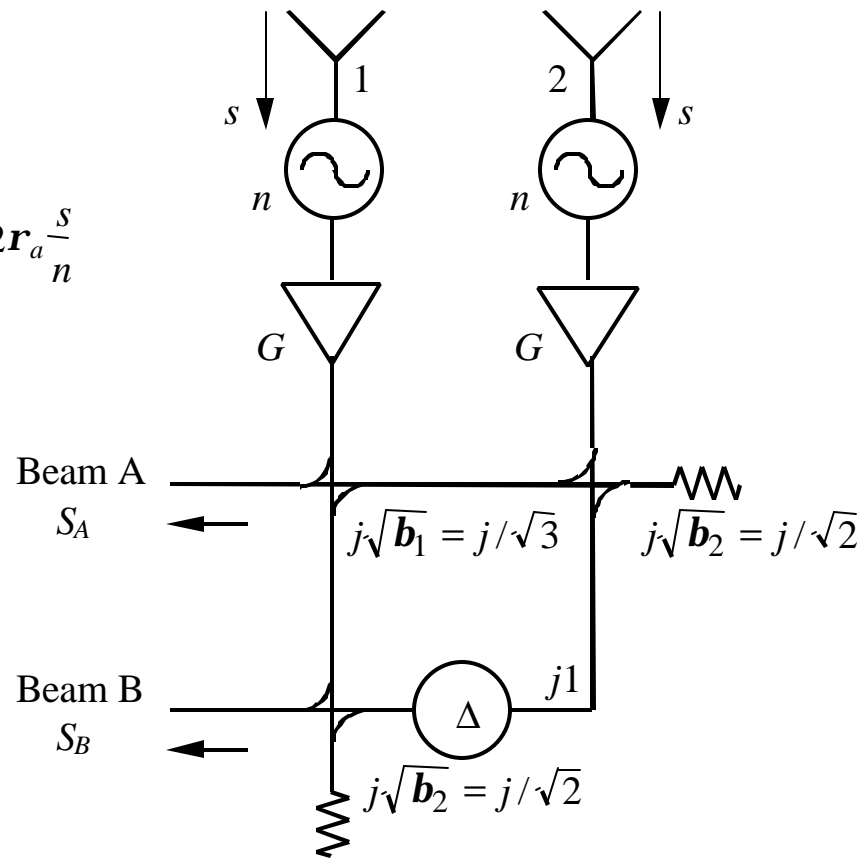
$$\left(\frac{S}{N}\right)_B = \frac{s}{n}2\mathbf{r}_a\left(\mathbf{b}_2\mathbf{t}_1 + |t_2\Delta - \mathbf{b}_2\sqrt{\mathbf{b}_1}|^2\right) = \frac{4}{3}\mathbf{r}_a\frac{s}{n}$$

where the aperture efficiency for beam B is  $\mathbf{r}_a = \frac{(\sqrt{\mathbf{t}_2} + \sqrt{\mathbf{b}_2}\sqrt{\mathbf{t}_1})^2}{2(\mathbf{b}_2\mathbf{t}_1 + |t_2\Delta - \mathbf{b}_2\sqrt{\mathbf{b}_1}|^2)} = 1$ . Note

the factor of 4/3 in both cases. (The gain of a lossless antenna would have the factor 2.)

# Active Two-Beam Array (1)

$$\left(\frac{S}{N}\right)_A = \left(\frac{S}{N}\right)_B = 2r_a \frac{s}{n}$$



## Active Two-Beam Array (2)

---

Amplification before beamforming:

For beam A:  $S = sG(\sqrt{\mathbf{b}_1} + \sqrt{\mathbf{b}_2}\sqrt{\mathbf{t}_1})^2$  and  $N = nG(\mathbf{b}_1 + \mathbf{b}_2\mathbf{t}_1)$  which gives

$$\left(\frac{S}{N}\right)_A = 2\mathbf{r}_a \frac{s}{n}$$

where, as before, the aperture efficiency for beam A is  $\mathbf{r}_a = 1$ .

For beam B:  $N = nG(\mathbf{b}_2\mathbf{t}_1 + \mathbf{b}_1\mathbf{b}_2^2 + \mathbf{t}_2^2) = 2nG/3$  and with some work it is found that  $S = sG4\mathbf{b}_2\mathbf{t}_1$ . The corresponding SNR is

$$\left(\frac{S}{N}\right)_B = 2\mathbf{r}_a \frac{s}{n}$$

where the aperture efficiency for beam B is also  $\mathbf{r}_a = 1$ . Note that the factor of 2 is the same as for a lossless antenna. The signal levels are the same for amplification before and after beamforming. It is only the noise level that has changed.

# Comparison of SNR: Active vs. Passive

---

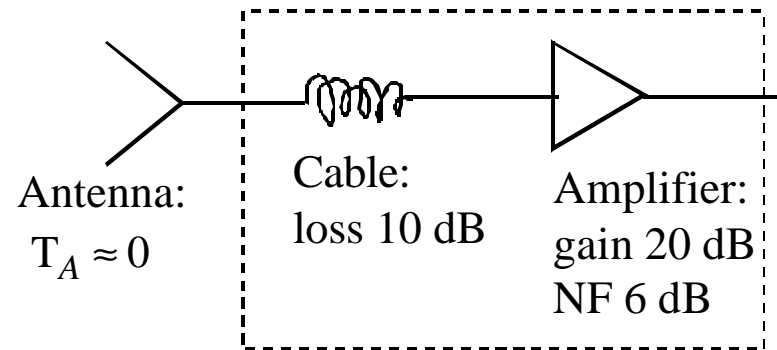
**PASSIVE** (Amplification after beamforming): The antenna gain is the SNR improvement (neglecting noise introduced by the antenna).

**ACTIVE** (Amplification before beamforming):

1. The SNR performance can be significantly better than the gain indicates.
2. Beam coupling losses can be recovered.
3. SNR degradation is only determined by the aperture efficiency. All other losses are recovered.
4. The coupler match looking into the sidearms does not affect the SNR.

# Example

Consider the receiver channel shown below:



The effective noise temperature of the dashed box is

$$F_e = F_1 + \frac{F_2 - 1}{A_1} = L_x + \frac{NF - 1}{1/L_x} = 10 + \frac{4 - 1}{0.1} = 40 \rightarrow 16 \text{ dB}$$

A low noise amplifier has a noise figure near one. If we use a LNA that has a NF of 1.5 dB

$$F_e = 10 + \frac{1.4 - 1}{0.1} = 14 \rightarrow 11.5 \text{ dB}$$

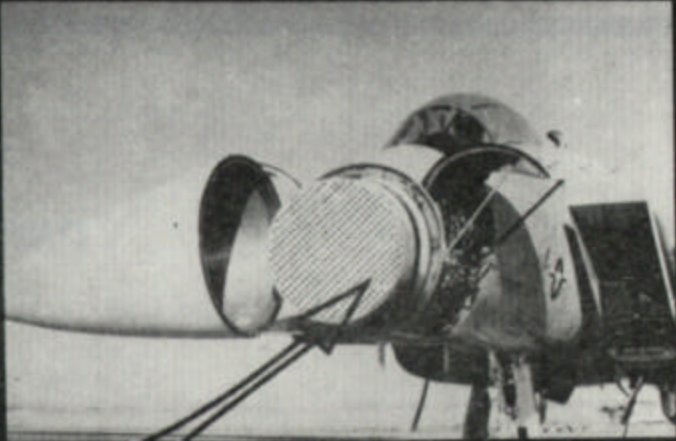
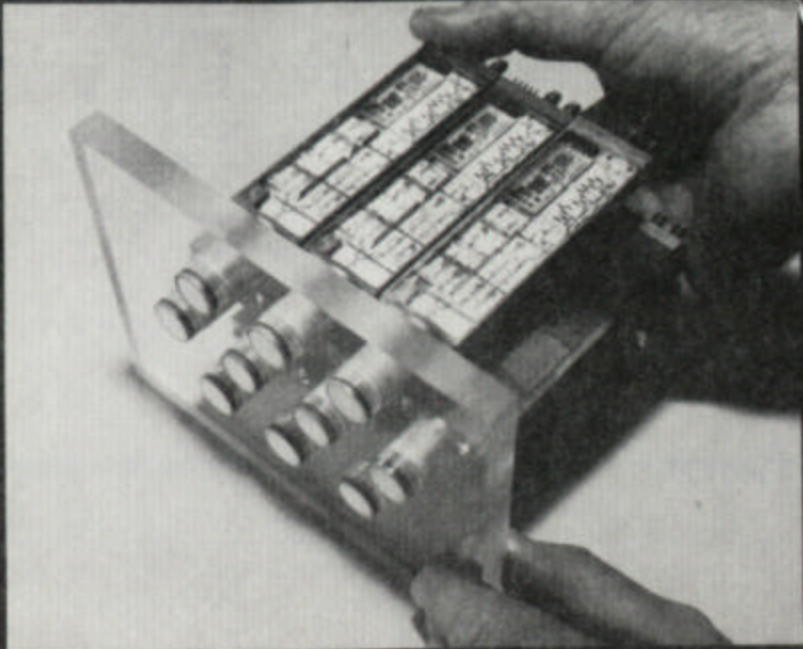
However, if we use a LNA before the cable

$$F_e = 1.4 + \frac{10 - 1}{100} = 1.49 \rightarrow 1.73 \text{ dB}$$

Losses “behind” the amplifier can be recovered. Use a LNA and place it as close to the antenna as possible. Antennas that incorporate amplifiers are called active antennas.

# Active Array Radar Transmit/Receive Module

- 10 PROTOTYPE MODULES COMPLETE
- 2 WATTS RF OUTPUT
- 1 GHz BANDWIDTH
- 2.7 dB RECEIVER NOISE FIGURE
- 5-BIT PIN-DIODE PHASE SHIFTER



ACTIVE ARRAYS PROVIDE:

- IMPROVED PERFORMANCE
- ENHANCED RELIABILITY
- SMALLER VOLUME
- AGILE BEAM

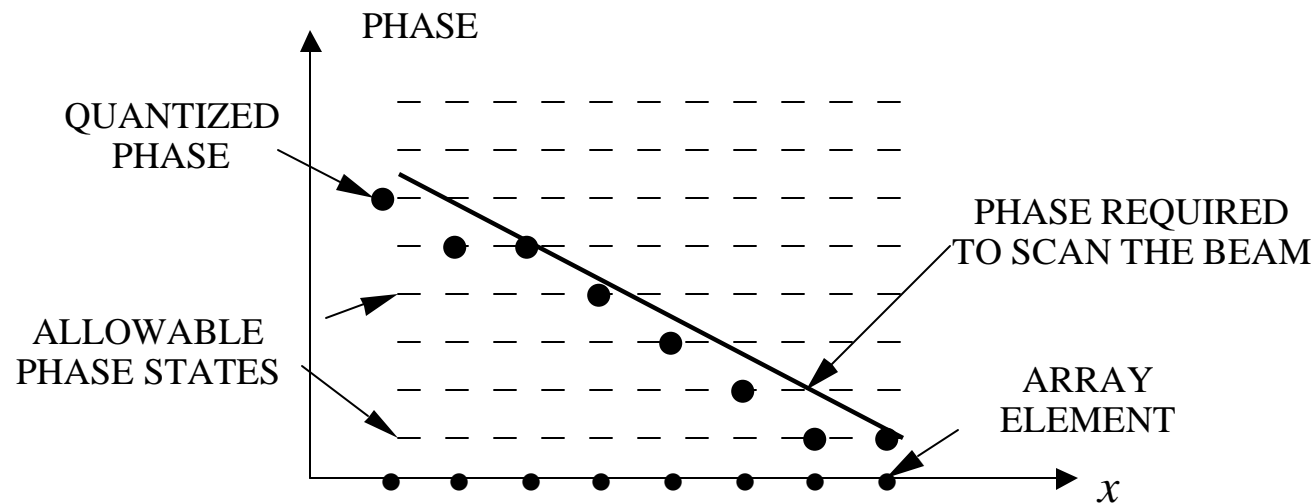
APRIL 1981

# Digital Phase Shifters

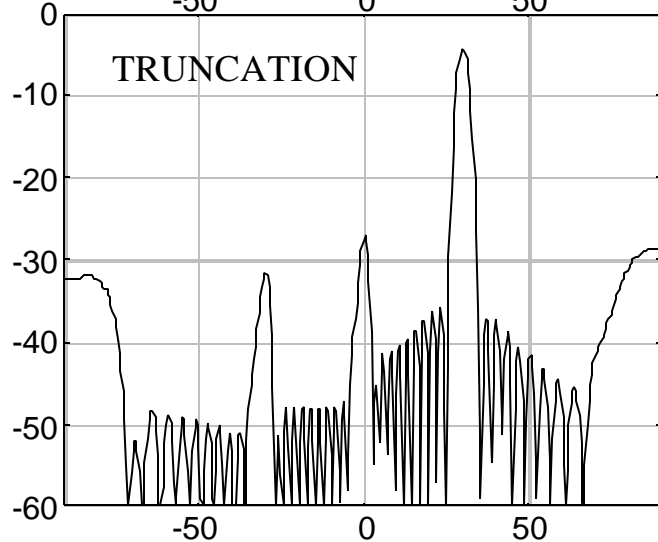
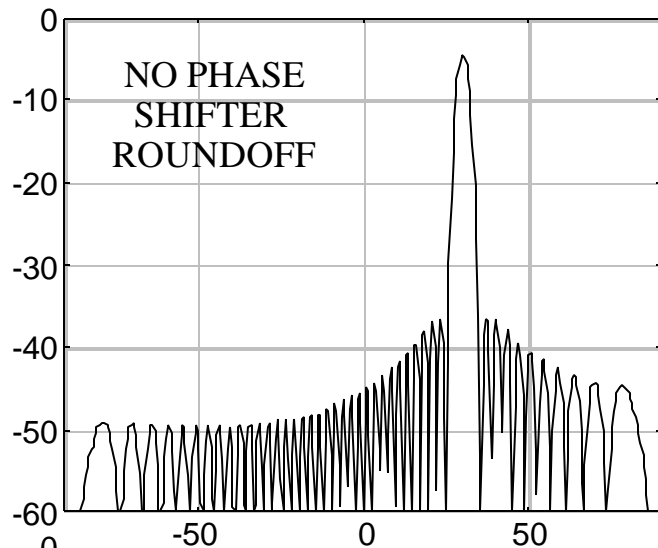
Phase shifters are used to "tilt" the phase across the array aperture for scanning. Diode phase shifters are only capable of providing discrete phase intervals. A  $n$  bit phase shifter has  $2^n$  phase states. The quantization levels are separated by  $\Delta f = 360^\circ / 2^n$ . The fact that the exact phase cannot always be obtained results in:

1. gain loss
2. increase in sidelobe level
3. beam pointing error

Example of phase truncation:

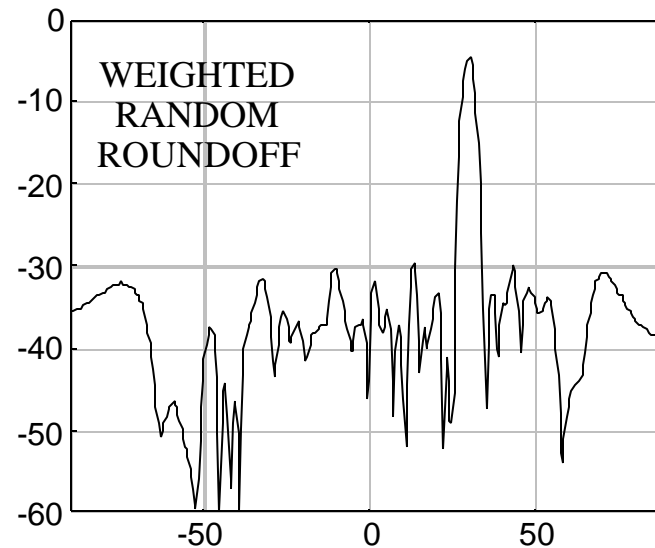


# Effect of Phase Shifter Roundoff Errors



Truncation causes beam pointing errors. Random roundoff methods destroy the periodicity of the quantization errors. The resultant rms error is smaller than the maximum error using truncation.

Linear array, 60 elements,  $d = 0.4\lambda$   
4 bit phase shifters

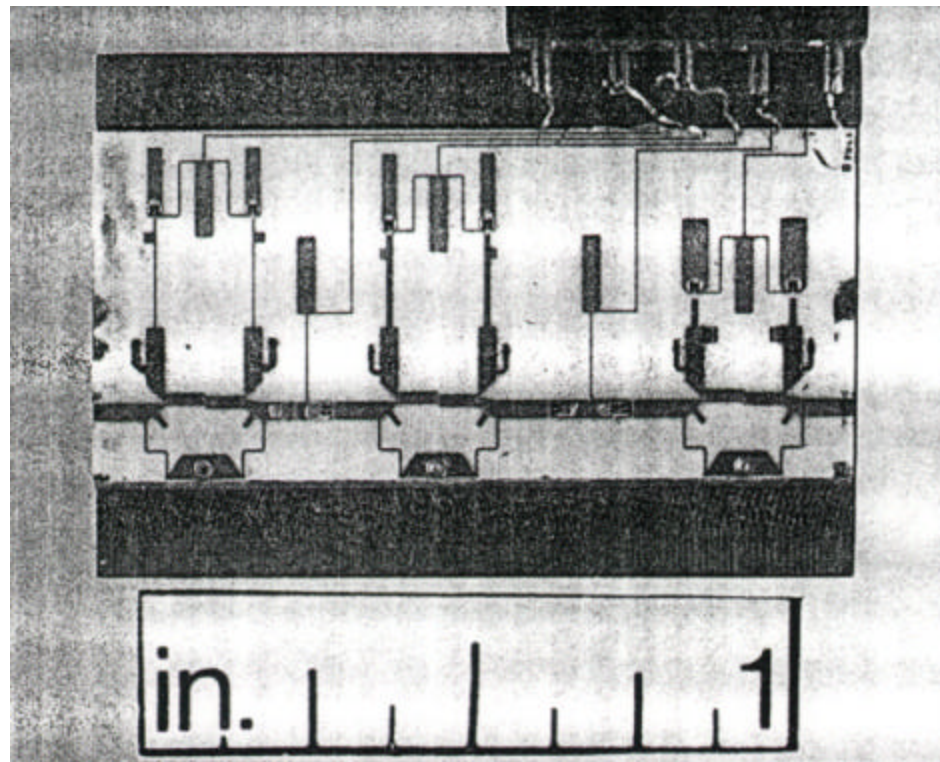




# Digital Phase Shifter

---

- X-band 5-bit PIN diode phase shifter



From Hughes Aircraft Co.

# True Time Delay Scanning

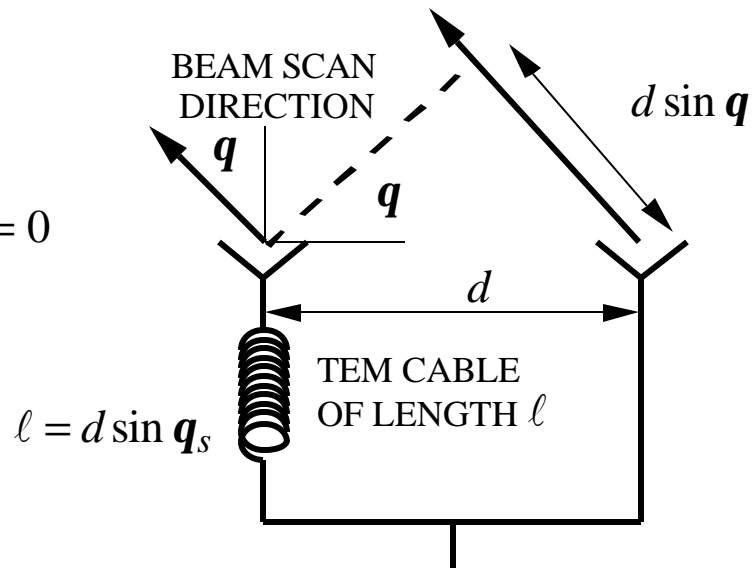
Array factor for an array with the beam scanned to angle  $\mathbf{q}_s$ :

$$AF(\mathbf{q}) = \sum_{n=1}^N A_n e^{j(n-1)kd(\sin \mathbf{q} - \sin \mathbf{q}_s)} = \sum_{n=1}^N A_n e^{j(n-1)(\mathbf{y} - \mathbf{y}_s)}$$

where  $\mathbf{y}_s = kd \sin \mathbf{q}_s$ . For a uniformly excited array ( $A_n = 1$ )

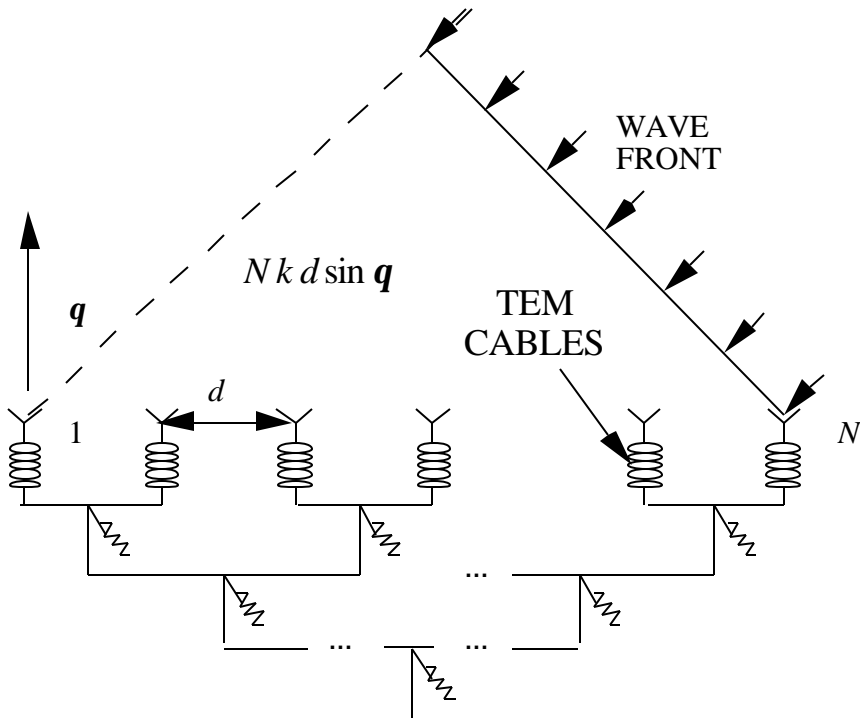
$$|AF(\mathbf{q})| = \left| \frac{\sin\left(\frac{Nkd}{2}(\sin \mathbf{q} - \sin \mathbf{q}_s)\right)}{\sin\left(\frac{kd}{2}(\sin \mathbf{q} - \sin \mathbf{q}_s)\right)} \right| = \left| \frac{\sin(N(\mathbf{y} - \mathbf{y}_s)/2)}{\sin((\mathbf{y} - \mathbf{y}_s)/2)} \right|$$

$$\begin{aligned} \mathbf{y}|_{\mathbf{q}=\mathbf{q}_s} - \mathbf{y}_s &= 0 \\ \frac{2pd}{l} \sin \mathbf{q}_s - \mathbf{y}_s &= 0 \\ \mathbf{y}_s &= \frac{2pd}{l} \sin \mathbf{q}_s \end{aligned}$$

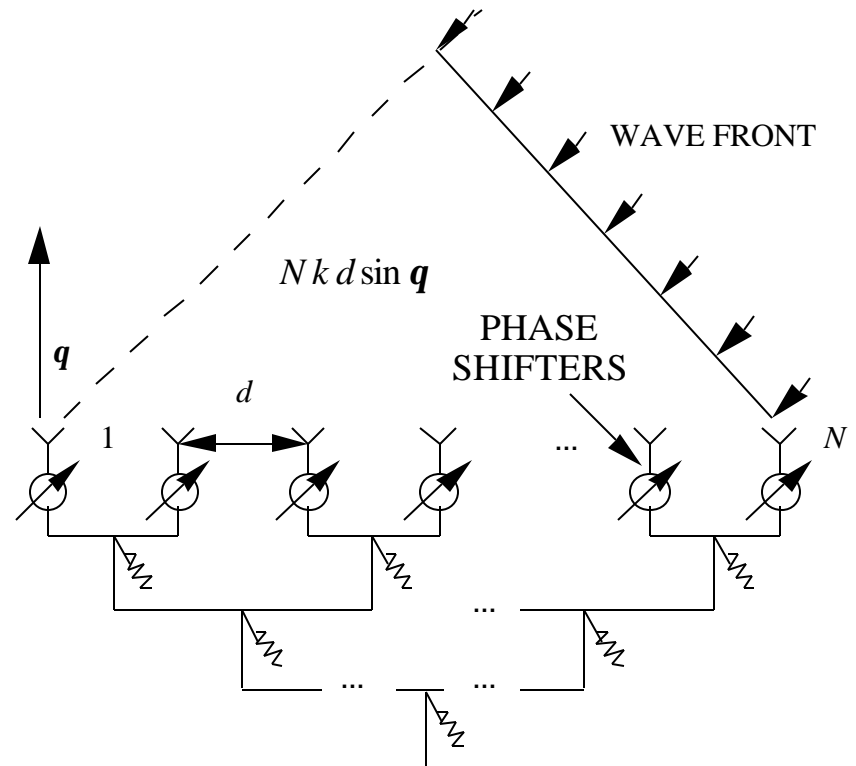


# Time Delay vs. Fixed Phase Scanning

BEAM SCANNING USING CABLES TO PROVIDE "TRUE TIME DELAY"

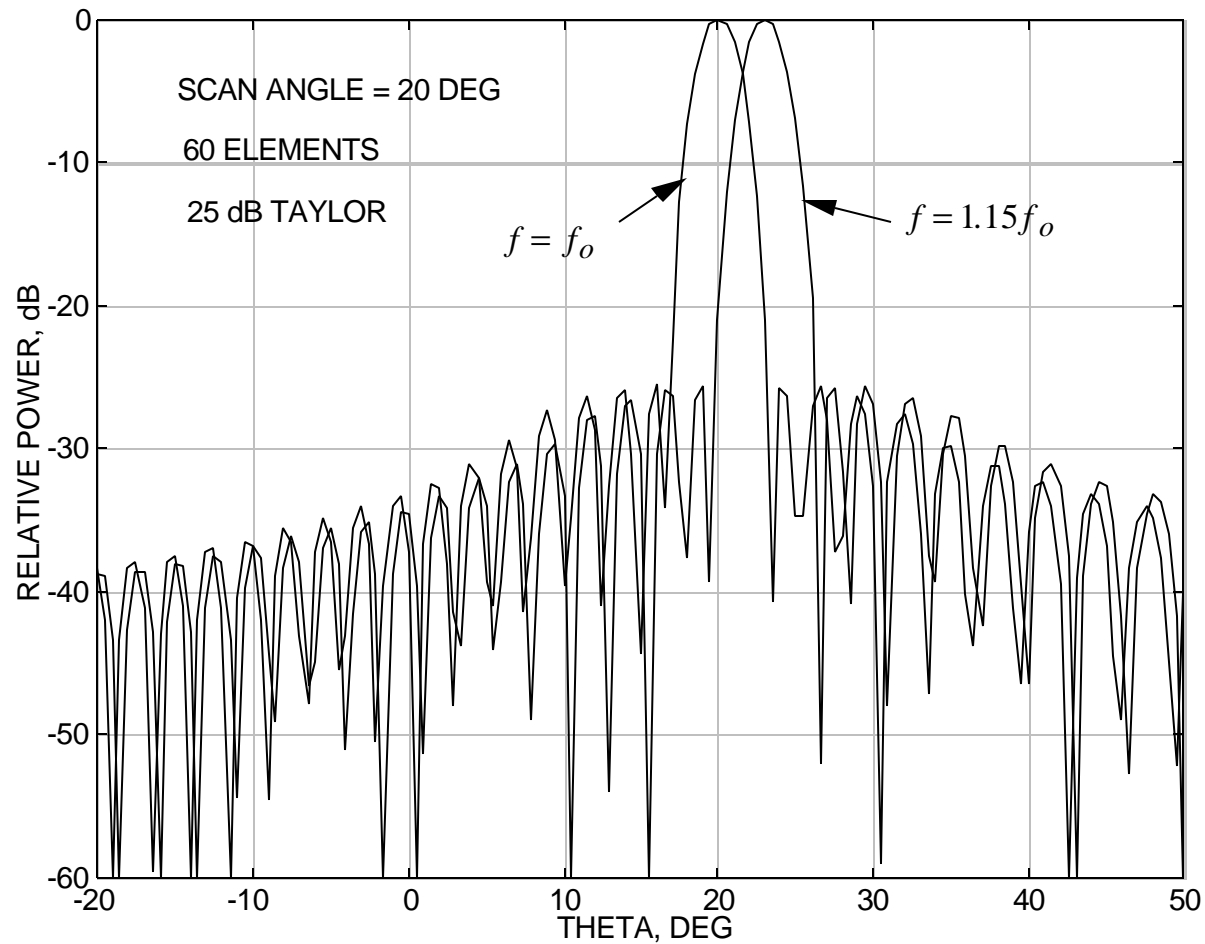


BEAM SCANNING WITH PHASE SHIFTERS GIVES A PHASE THAT IS CONSTANT WITH FREQUENCY

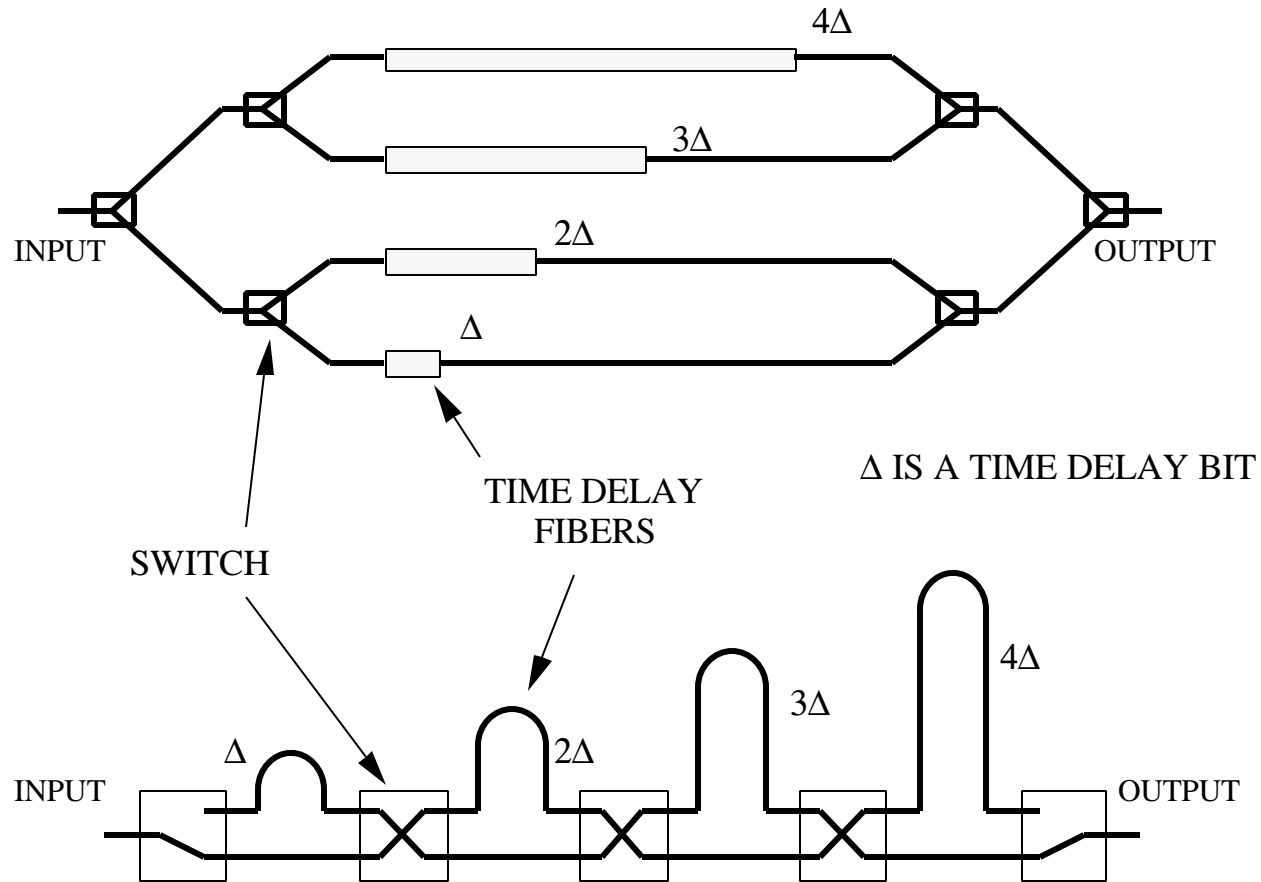


# Beam Squint Due to Frequency Change

Phase shifters provide a phase that is approximately constant with frequency

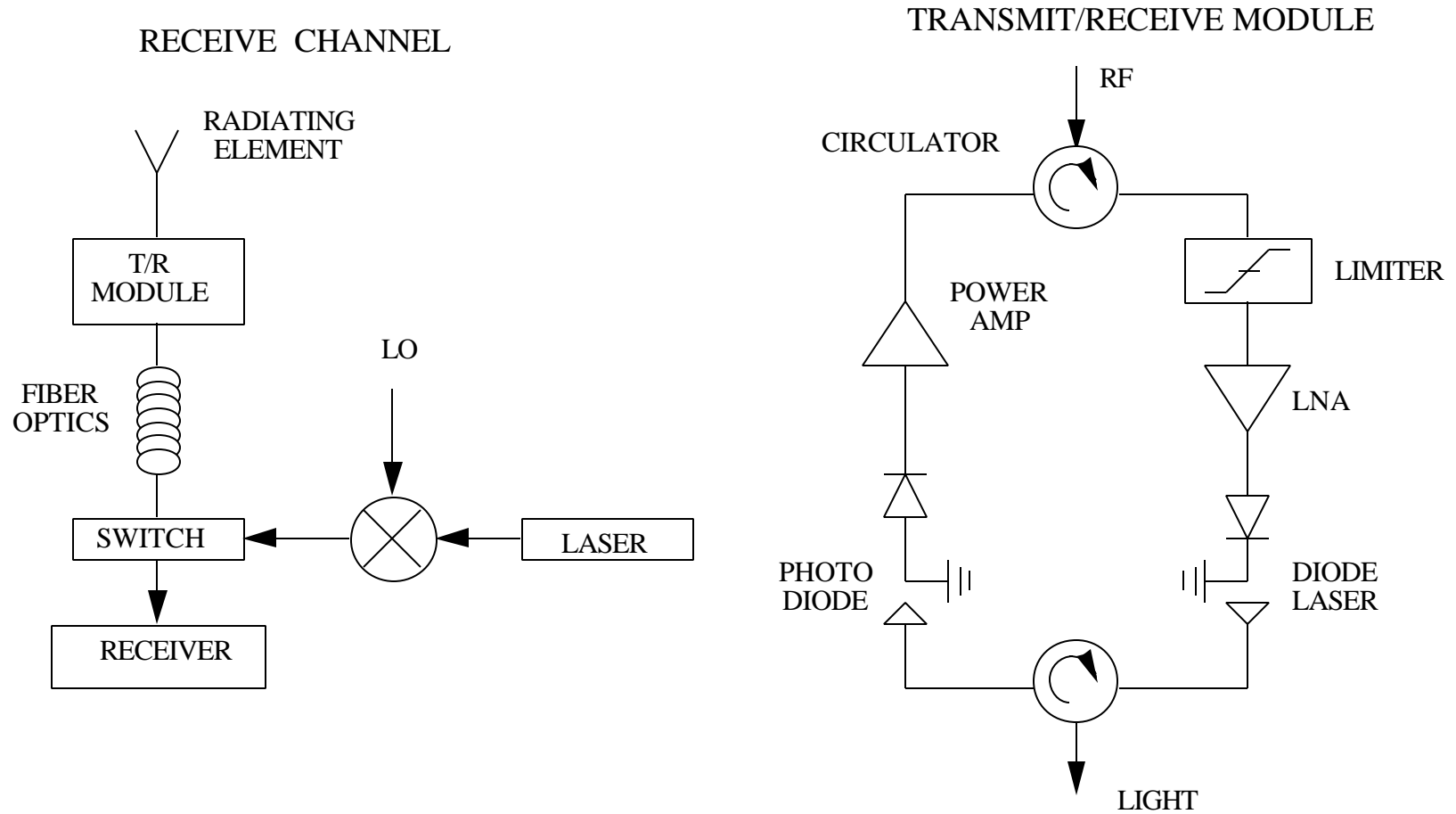


# Time Delay Networks

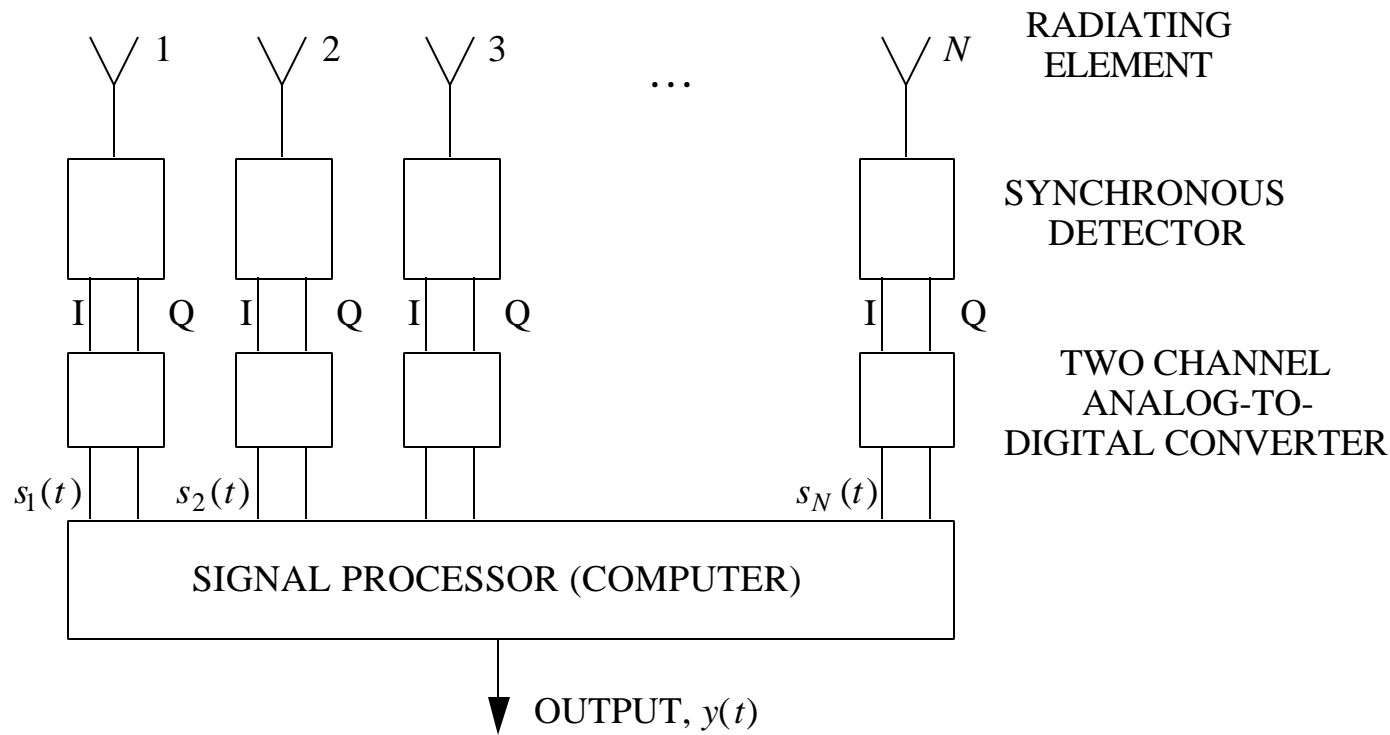


# Time Delay Using Fiber Optics

Large phase shifts (electrical lengths) can be obtained with fibers



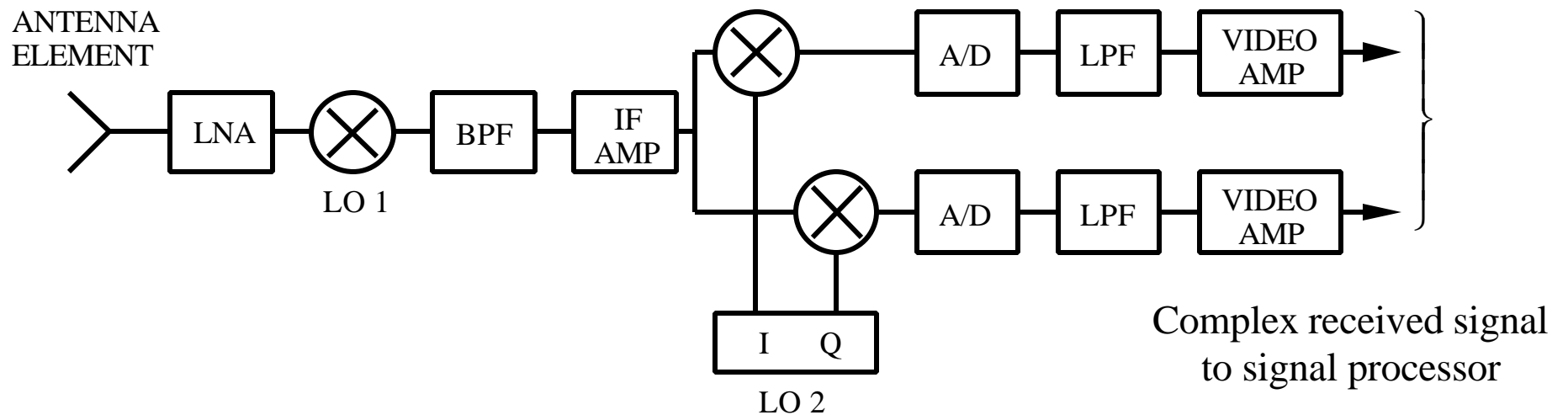
# Digital Beamforming (1)



Assuming a narrowband signal,  $y(t) = \sum_{n=1}^N w_n s_n(t)$ . The complex signal (I and Q, or equivalently, amplitude and phase) are measured and fed to the computer. Element responses become array storage locations in the computer. The weights are added and the sums computed to find the array response. In principle any desired beam characteristic can be achieved, including multiple beams.

# Digital Beamforming (2)

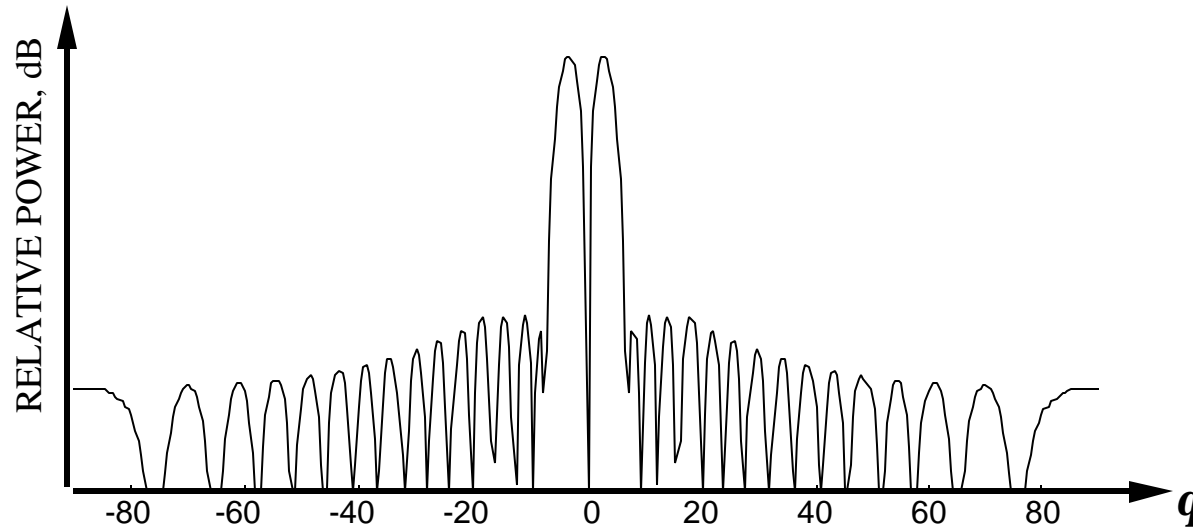
Implementation of digital beamforming using I and Q channels:



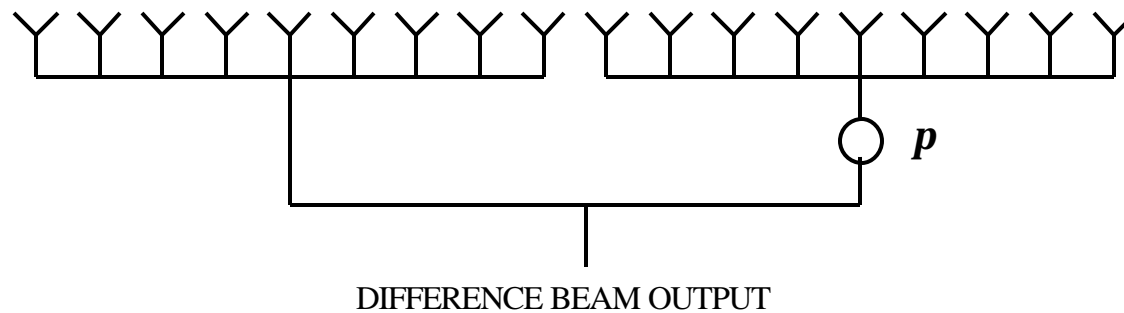


# Monopulse Difference Beams

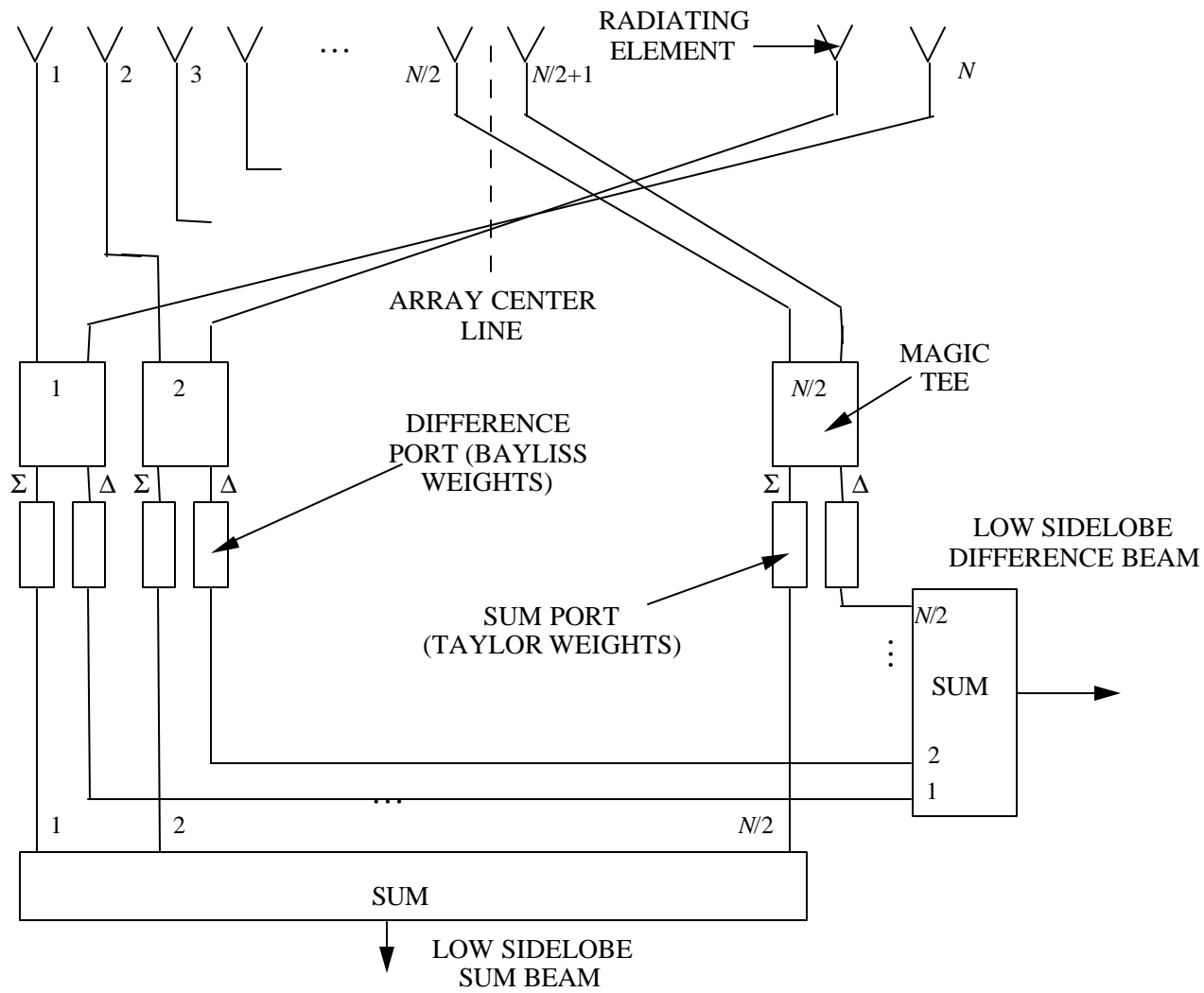
Example of a low sidelobe difference beam obtained using a Bayliss amplitude distribution



Formation of difference beams by subtraction of two subarrays

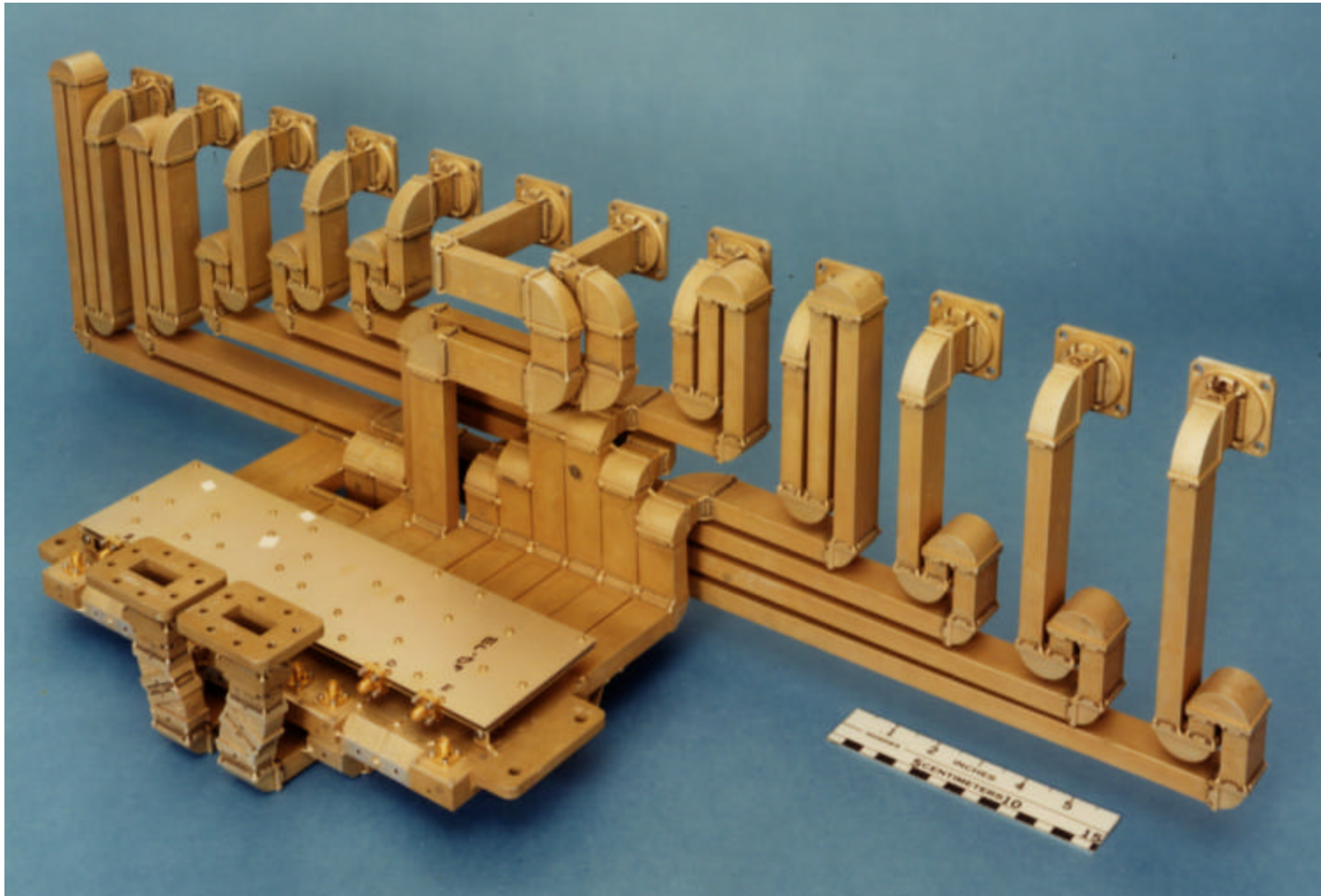


# Sum and Difference Beamforming



# Waveguide Monopulse Beamforming Network

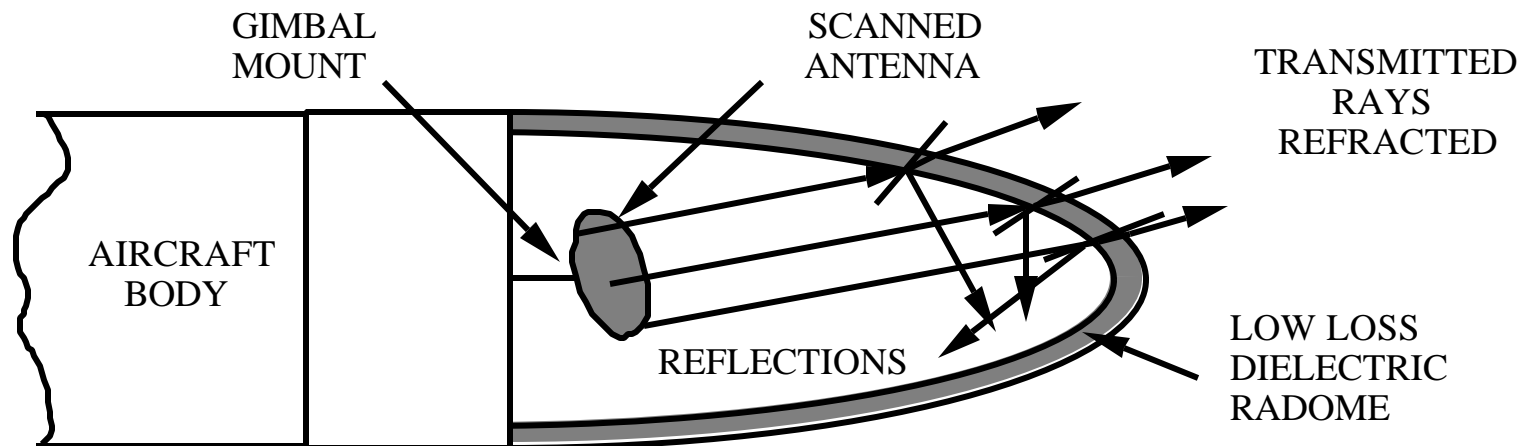
---



# Antenna Radomes

The purpose of a radome (from radar dome) is to protect the antenna from the harsh operational environment (aerodynamic and thermal stresses, weather, etc.). At the same time it must be electromagnetically transparent at the operating frequency of the radar. The antenna pattern with a radome will always be different than that without a radome. Undesirable effects include:

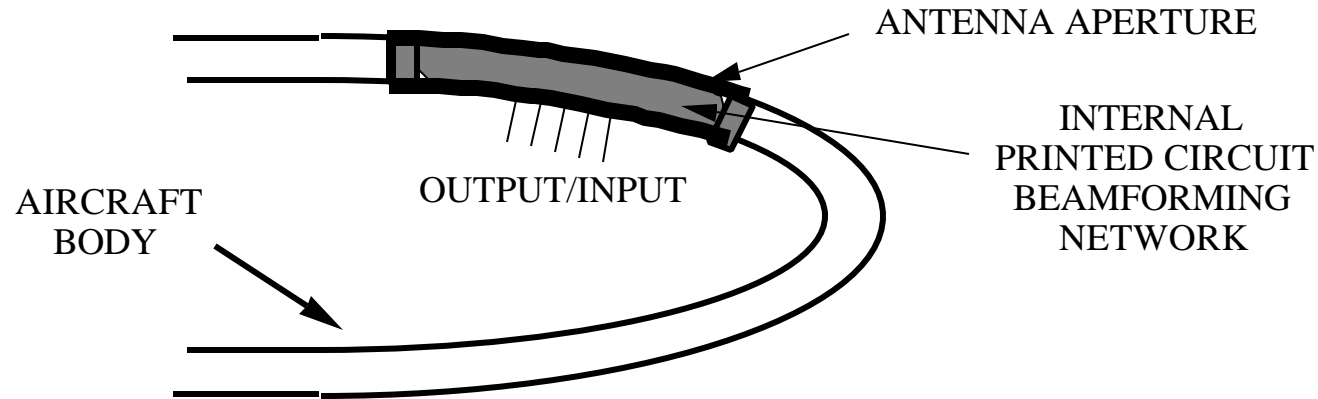
1. gain loss due to lossy radome material and multiple reflections
2. beam pointing error from refraction by the radome wall
3. increased sidelobe level from multiple reflections



These effects range from small for flat non-scanning antennas with flat radomes to severe for scanning antennas behind doubly curved radomes.

# Conformal Antennas & "Smart Skins"

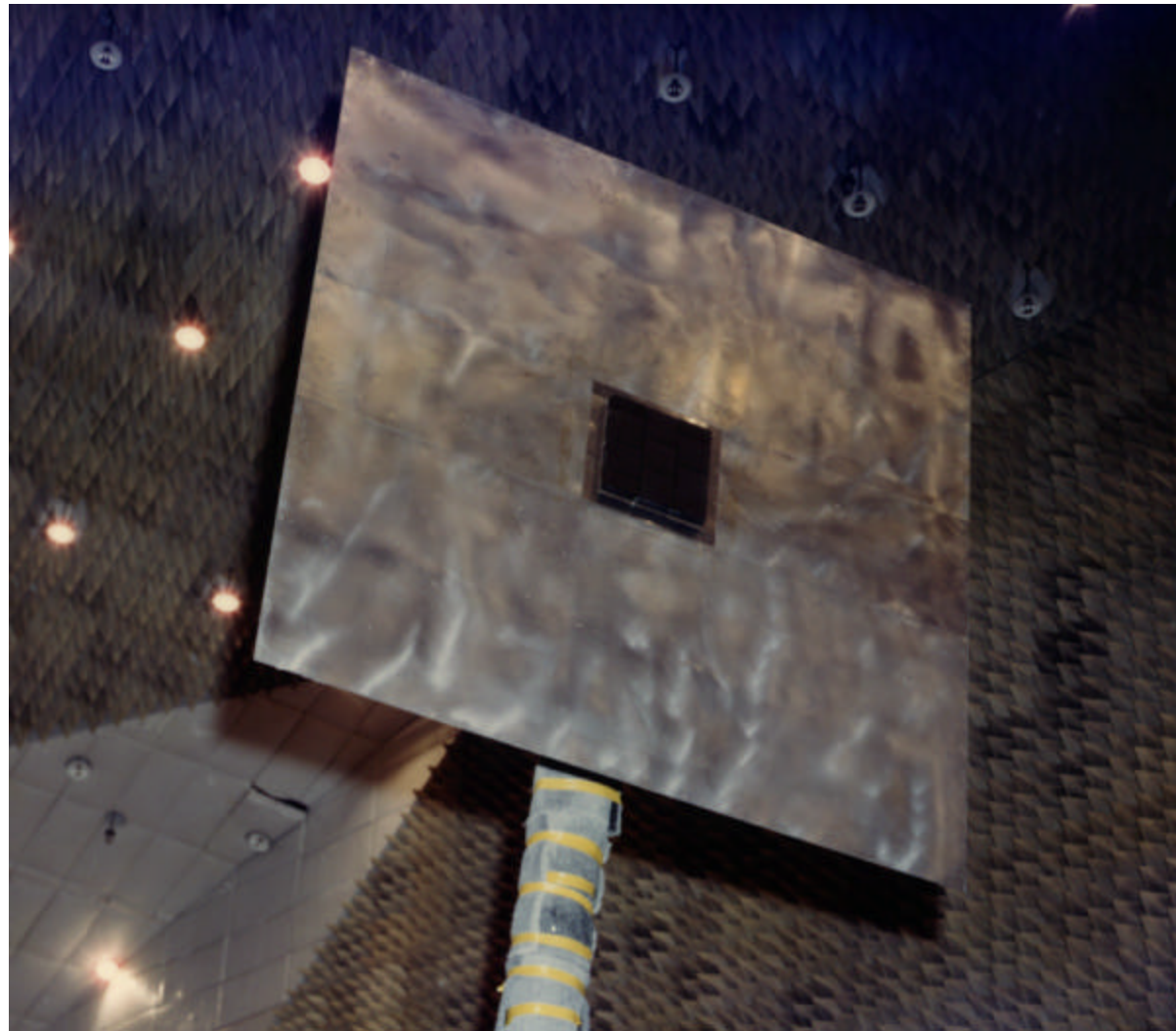
---



1. Conformal antenna apertures conform to the shape of the platform.
2. Typically applied to composite surfaces; the antenna beamforming network and circuitry are interlaced with the platform structure and skin
3. Can be active antennas with processing embedded (i.e., adaptive)
4. Self-calibrating and fault isolation (i.e., identification of failures can be incorporated (this function is referred to as build in test equipment, BITE)
5. Can be reconfigurable (portion of the aperture that is active can be changed)
6. Infrared (IR) and other sensors can be integrated into the antenna

# Testing of Charred Space Shuttle Tile

---



# Antenna Imperfections (Errors)

---

- Causes:
1. Manufacturing and assembly tolerances
    - a) machining of parts
    - b) alignment and assembly
    - c) material electrical properties
    - d) thermal expansion and contraction
    - e) gravitational deformation
  2. Failures

- Effects:
1. Reduced gain
  2. Increased sidelobe level
  3. Reduced power handling capability

For an array of  $N$  elements:

$$G \approx \frac{4p A_e}{l^2} \left( P_{\text{norm}} (1 - \overline{\Delta^2} - \overline{\mathbf{d}^2}) + \frac{\overline{\Delta^2} + \overline{\mathbf{d}^2}}{N r_a} \right)$$

where  $P_{\text{norm}} = |\vec{E}|^2 / |\vec{E}_{\text{max}}|^2 =$  normalized error free power pattern,  $r_a =$  aperture efficiency, and  $\overline{\Delta^2}, \overline{\mathbf{d}^2} =$  variance of amplitude and phase errors, respectively (assumed to be small)

# Smart Antennas (1)

---

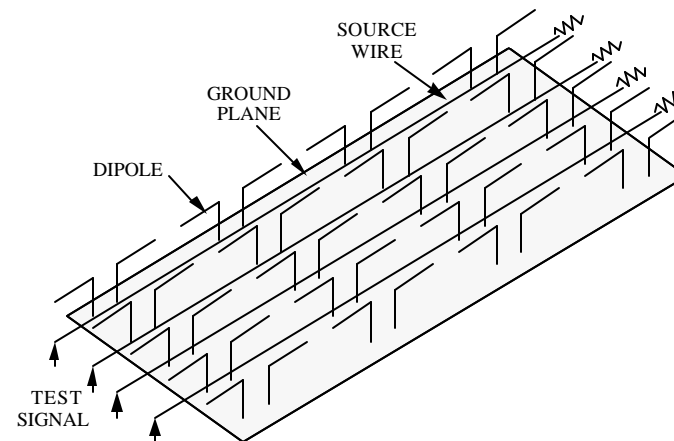
Antennas with built-in multi-function capabilities are often called smart antennas. If they are conformal as well, they are known as smart skins. Functions include:

- Self calibrating: adjust for changes in the physical environment (i.e., temperature).
- Self-diagnostic (built-in test, BIT): sense when and where faults or failures have occurred.

Tests can be run continuously (time scheduled with other radar functions) or run periodically. If problems are diagnosed, actions include:

- Limit operation or shutdown the system
- Adapt to new conditions/reconfigurable

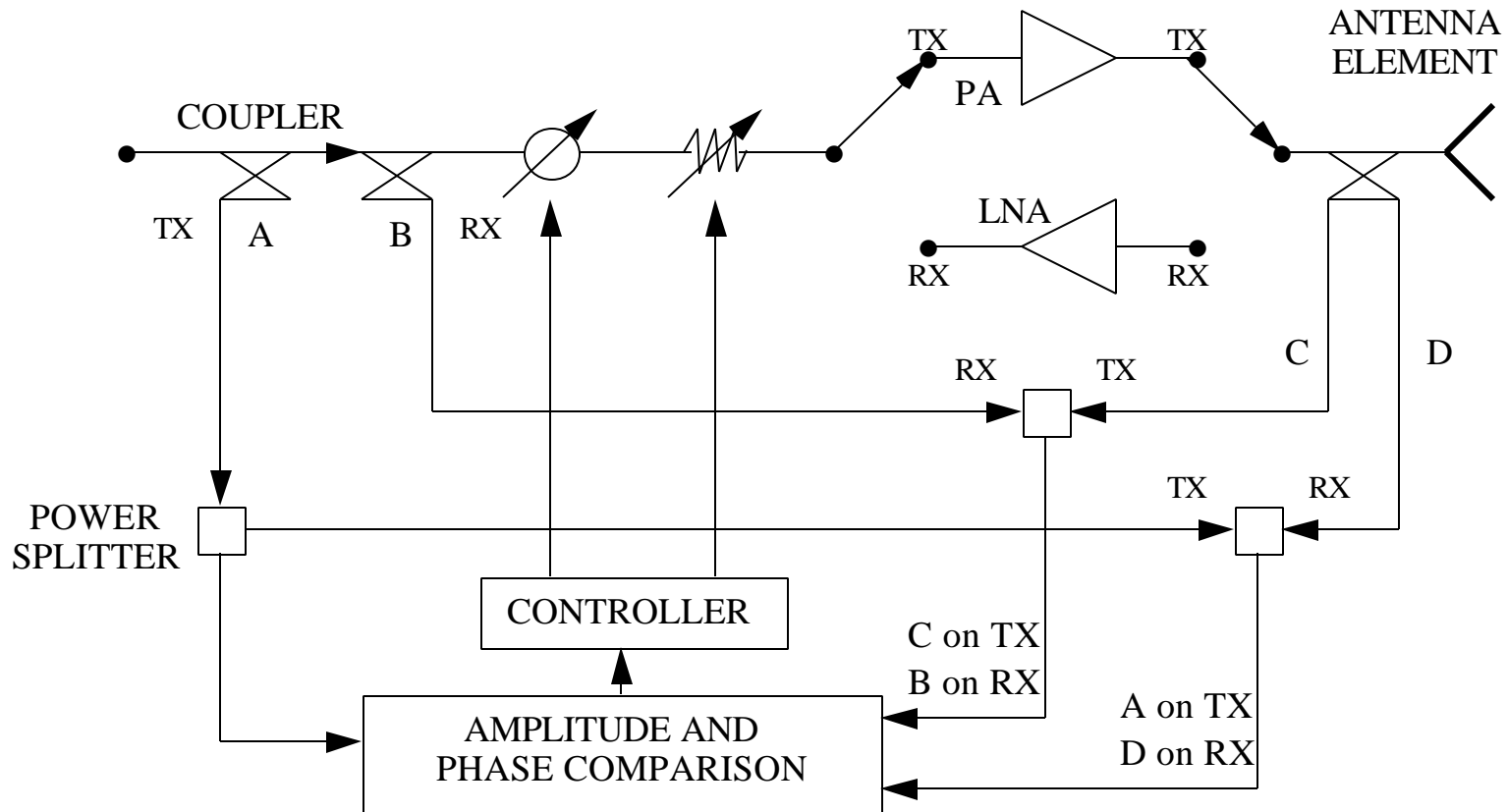
Example: a test signal is used to isolate faulty dipoles and transmission lines





# Smart Antennas (2)

Example of a self-calibrating, self-diagnostic transmit/receive module



# Microwave Devices

---

## Passive:

- Transmission lines
- Switches
- Magic tees
- Rotary joints
- Circulators
- Filters

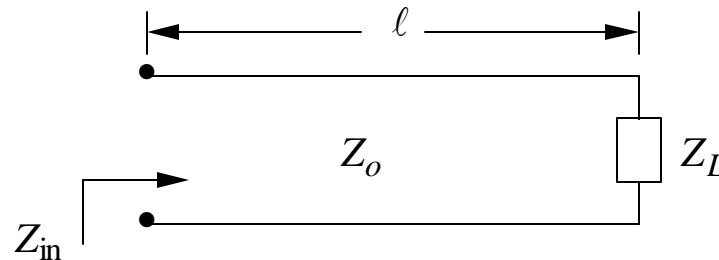
## Active:

- Tubes
- Solid state amplifiers
- Mixers

# Transmission Line Refresher (1)

---

Finite length loaded transmission line:



$Z_o$  = characteristic impedance; depends on line geometry and material and wavelength  $\mathbf{n}$ ,  $\mathbf{e}$ ,  $\mathbf{l}$ , and  $\mathbf{s}$ ; real for lossless lines; approximately real for low-loss lines

$Z_L$  = load impedance; generally complex

$Z_{in}$  = input impedance

$$Z_{in} = Z_o \frac{Z_L + Z_o \tanh(\mathbf{g}\ell)}{Z_o + Z_L \tanh(\mathbf{g}\ell)}$$

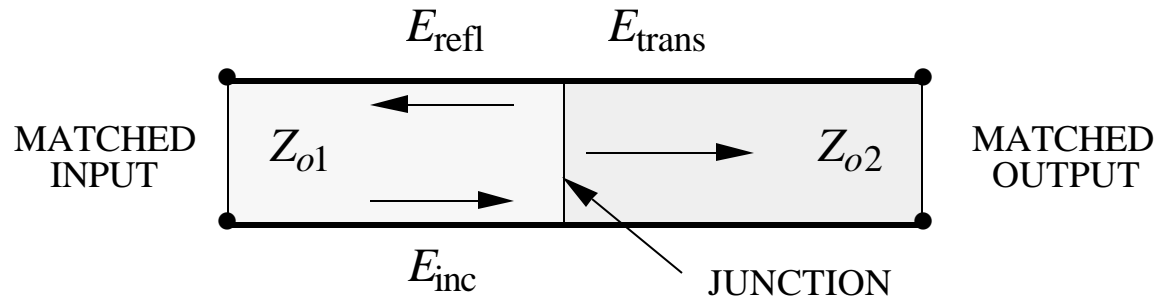
$\mathbf{g} = \mathbf{a} + j\mathbf{b}$  = propagation constant (depends on line geometry and material and frequency)

For a lossless line  $\mathbf{a} = 0$  (and low loss line  $\mathbf{a} \approx 0$ ):

$$Z_{in} \approx Z_o \frac{Z_L + jZ_o \tan(\mathbf{b}\ell)}{Z_o + jZ_L \tan(\mathbf{b}\ell)}$$

# Transmission Line Refresher (2)

Reflection coefficient of a load or junction:



$Z_{o1}$  = characteristic impedance of transmission line 1

$Z_{o2}$  = characteristic impedance of transmission line 2

$E_{inc}$  = incident electric field;  $E_{refl}$  = reflected electric field;  $E_{trans}$  = transmitted electric field

Reflection coefficient of the junction: 
$$\Gamma = \frac{|E_{refl}|}{|E_{inc}|} = \frac{Z_{o2} - Z_{o1}}{Z_{o2} + Z_{o1}}$$

Voltage standing wave ratio (VSWR): 
$$s = \frac{|E_{max}|}{|E_{min}|} = \frac{1 + |\Gamma|}{1 - |\Gamma|} \quad (1 \leq s < \infty)$$

Return loss: 
$$RL = -20 \log(|\Gamma|) \text{ dB}$$

# Transmission Line Refresher (3)

---

Matching and tuning transmission line circuits:

Mismatches cause reflections, but multiple mismatches can be "tuned" by forcing the reflections to cancel (add destructively). This approach is generally narrow-band because most load impedances are a strong function of frequency.

"Off-the-shelf" hardware is usually designed to have a characteristic impedance of  $50 \Omega$  ( $Z_o = 50 + j0 \Omega$ ). Therefore, when devices are combined, reflections will be small and the input impedance of a chain of devices independent of line lengths. For example, if  $Z_L = Z_o$ :

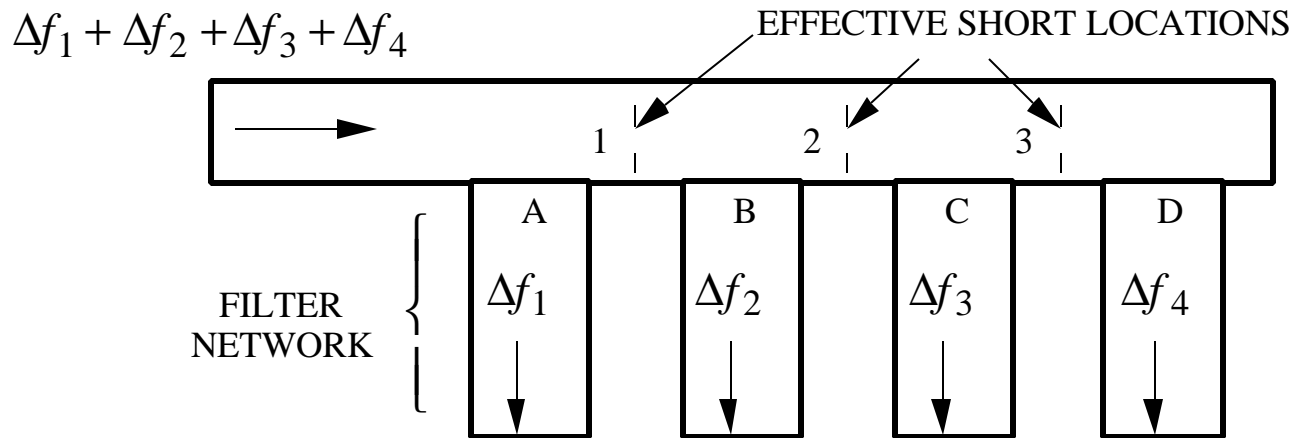
$$Z_{\text{in}} = Z_o \frac{Z_o + jZ_o \tan(\mathbf{b}\ell)}{Z_o + jZ_o \tan(\mathbf{b}\ell)} \rightarrow Z_o$$

Devices such as antennas and amplifiers have matching networks added to the input and output ports to provide a  $50 \Omega$  impedance.

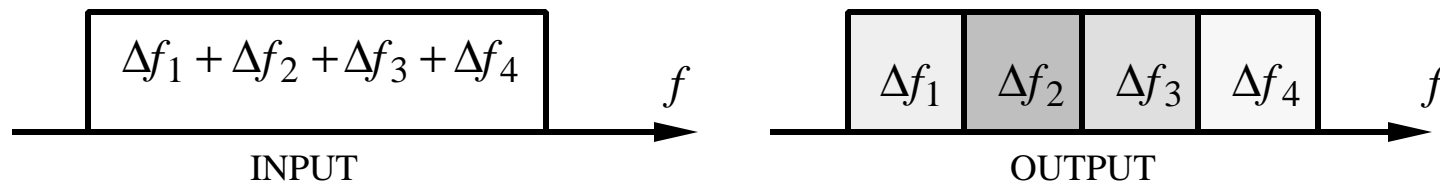
Matching elements include:    quarter-wave steps  
   transmission line stubs  
   lumped elements (resistors, capacitors and inductors)

# Multiplexers

Multiplexers are frequency selective circuits used to separate signals by frequency spectrum. They are comprised of filter networks. An example is a waveguide manifold multiplexer:

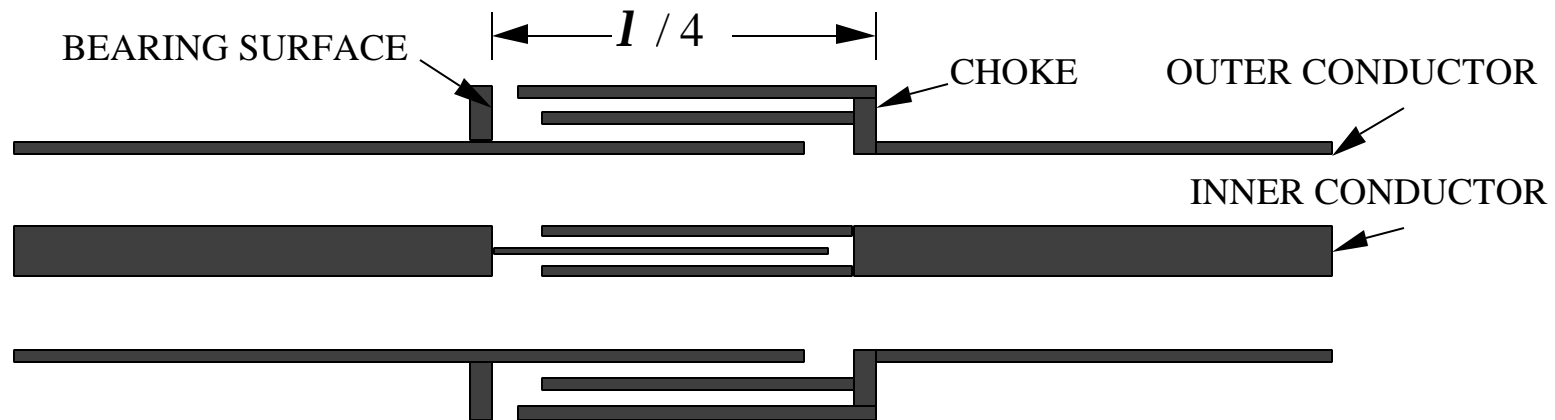


The plane at 1 appears as a short in the band  $\Delta f_1$ , but matched at other frequencies. The waveguide junction at A appears matched at  $\Delta f_1$ , but shorted at other frequencies. Similarly for planes 2, 3, 4 and junctions B, C, D. Frequency characteristic:



# Rotary Joints

Microwave rotary joints allow the antenna to rotate without twisting the transmission line that feeds the antenna. Example of a coaxial rotary joint:

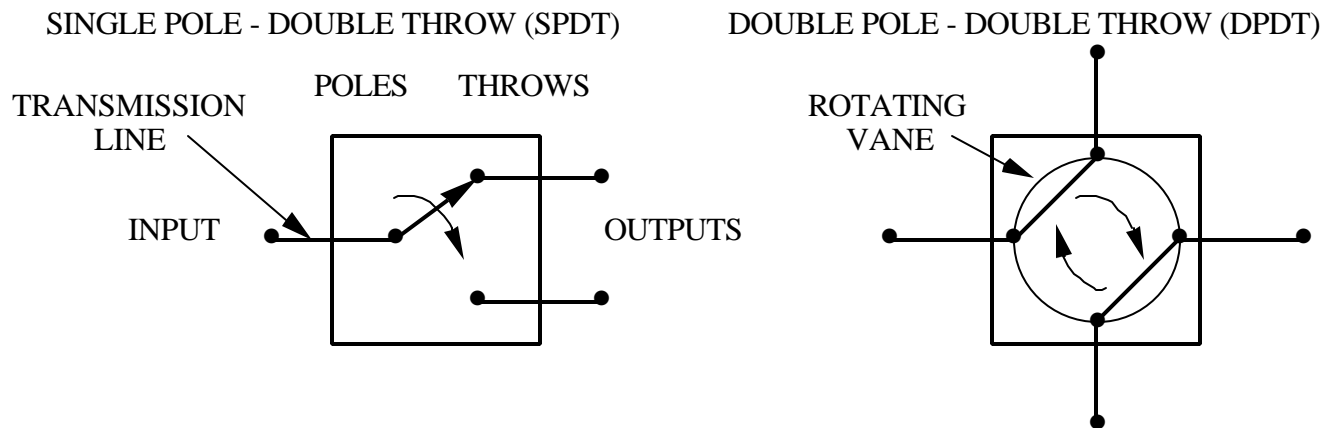


There is no efficient, reliable rotary joint in rectangular waveguide. Therefore, most rotary joints are made with circular waveguide because of the simple construction. Thus transitions from rectangular to circular cross sections are required.

Multichannel rotary joints are also possible for monopulse sum and difference channels.

# Microwave Switches

Microwave switches are used to control signal transmission between circuit devices. A general representation of a switch is given in terms of "poles" and "throws"



Switches can be constructed in any type of transmission line or waveguide. Common types:

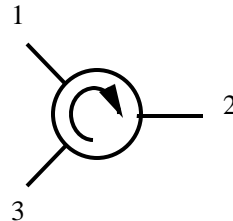
Type	Principle	Applied to:
Mechanical	Rotating or moving parts	All types
Diode	Forward/backward bias yields low/high impedance	Stripline, microstrip, waveguide
Gas discharge	Confined gas is ionized	Waveguide
Circulator	Magnetized ferrite switches circulation direction	Stripline, microstrip, waveguide



# Circulators

---

Circulators "circulate" the signal from port to port in the direction indicated by the arrow



Ideally:

- Signal into port 1 emerges out port 2; signal out port 3 is zero.
- Signal into port 2 emerges out port 3; signal out port 1 is zero.
- Signal into port 3 emerges out port 1; signal out port 2 is zero.

In practice:

1. There is some insertion loss in the forward (arrow) direction. Values depend on the type of circulator. They range from 0.5 dB to several dB.
2. There is leakage in the reverse (opposite arrow) direction. Typical values of isolation are 20 to 60 dB. That is, the leakage signal is 20 to 60 dB below the signal in the forward direction.
3. Increasing the isolation comes at the expense of size and weight

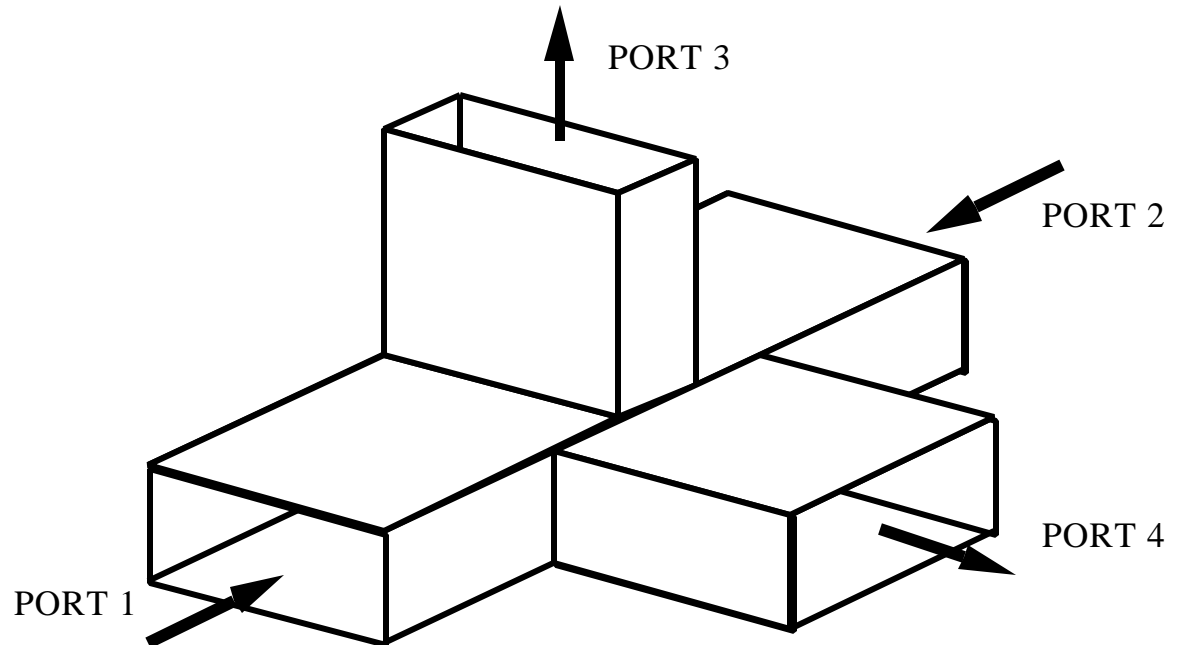
- Uses:
1. Allow a transmitter and receiver to share a common antenna without switching
  2. Attenuate reflected signals (load the third port)

# Waveguide Magic Tee

Ports 1 and 2 are the "sidearms." Port 4 is the "sum" port and 3 the "difference" port.

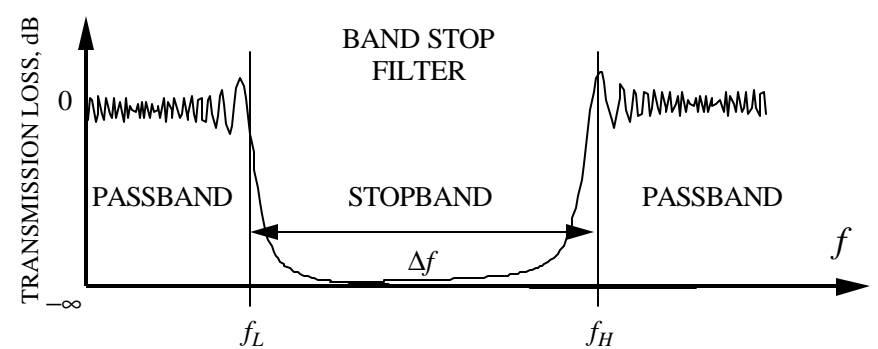
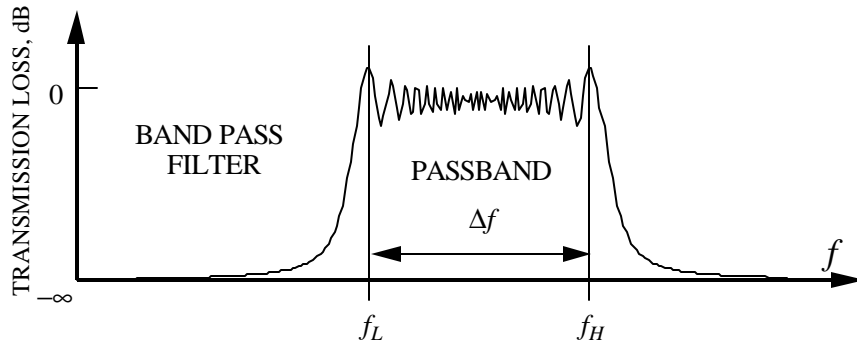
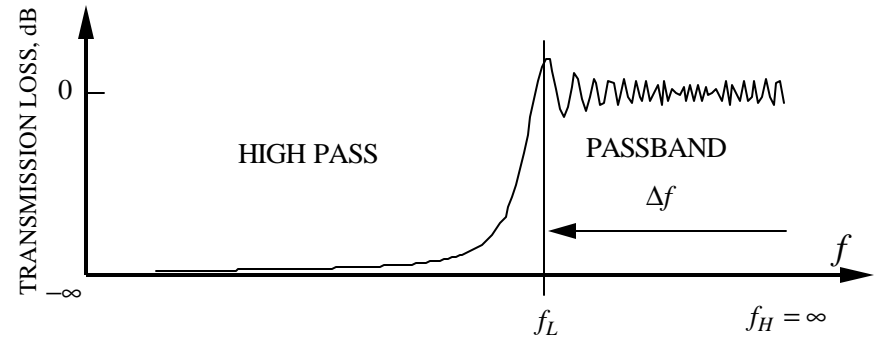
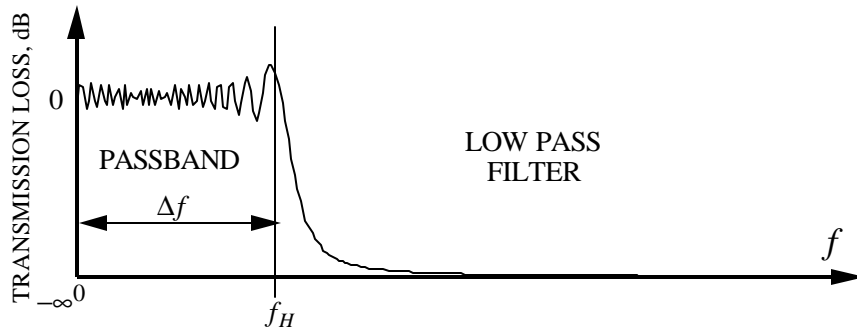
<u>Sidearm excitation</u>	<u>Port 3</u>	<u>Port 4</u>
$A_1 = ae^{jf}, A_2 = ae^{jf}$	$A_3 = 0$	$A_4 = 2a$
$A_1 = ae^{jf}, A_2 = ae^{jf+p}$	$A_3 = 2a$	$A_4 = 0$

"Magic" originates from the fact that it is the only 4-port device that can be simultaneously matched at all ports.



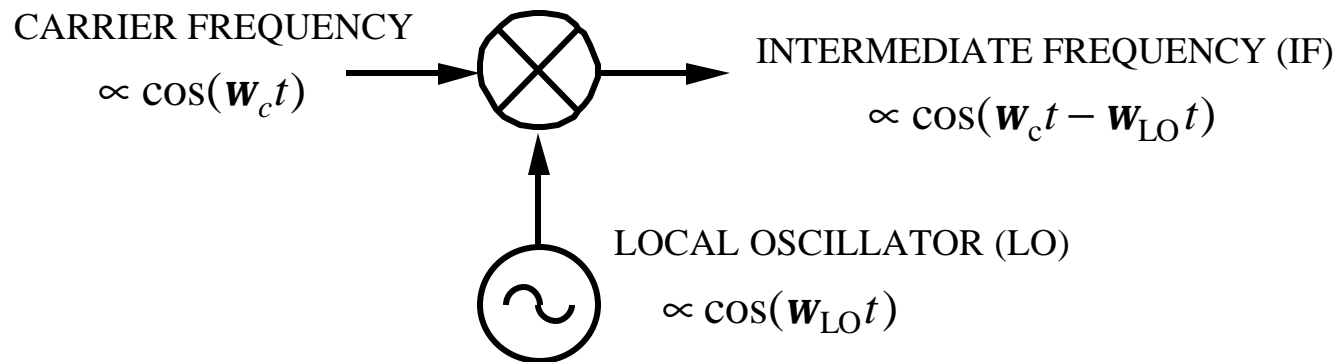
# Filter Characteristics

Filters are characterized by their transfer functions  $|H(f)| = |t| = \sqrt{1 - |\Gamma|^2}$ , where  $\Gamma$  is reflection coefficient. It is usually plotted as return loss in dB ( $20 \log_{10}(|\Gamma|)$ ) or transmission loss in dB ( $20 \log_{10}(|t|)$ ). Note that in many cases the phase of the transfer function is also important.



# Mixers (1)

Mixers are multipliers; they multiply two CW signals (sinusoids). The signal from the antenna is at the carrier frequency. The second signal generated by the local oscillator is usually lower than the carrier frequency.



The output signal contains all of the cross products obtained by multiplying the two sinusoids. By trig identity:

$$\cos(\omega_c t) \cos(\omega_{LO} t) \propto \cos(\omega_c t - \omega_{LO} t) + \cos(\omega_c t + \omega_{LO} t)$$

The  $f_c + f_{LO}$  (i.e.,  $\omega_c + \omega_{LO}$ ) is discarded by filtering and receiver processing is performed on the  $f_c - f_{LO}$  term. The difference frequency  $f_c - f_{LO}$  is called the intermediate frequency (IF).

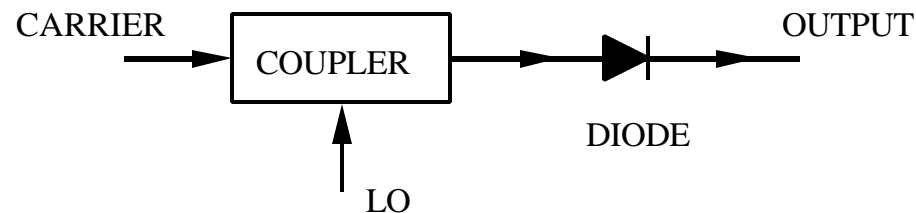
# Mixers (2)

Mixers are a means of frequency conversion. Converting to a frequency lower than the carrier is done primarily for convenience. If

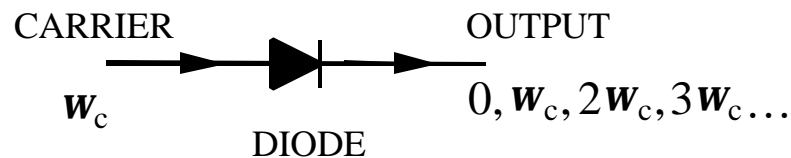
$f_{LO} < f_c$  this process is referred to as heterodyning

$f_{LO} = f_c$  this process is referred to as homodyning

We have defined a mixer as a multiplier of two sinusoids. In most cases nonlinear devices are used to perform frequency conversion. A simple example is a single-ended diode mixer:

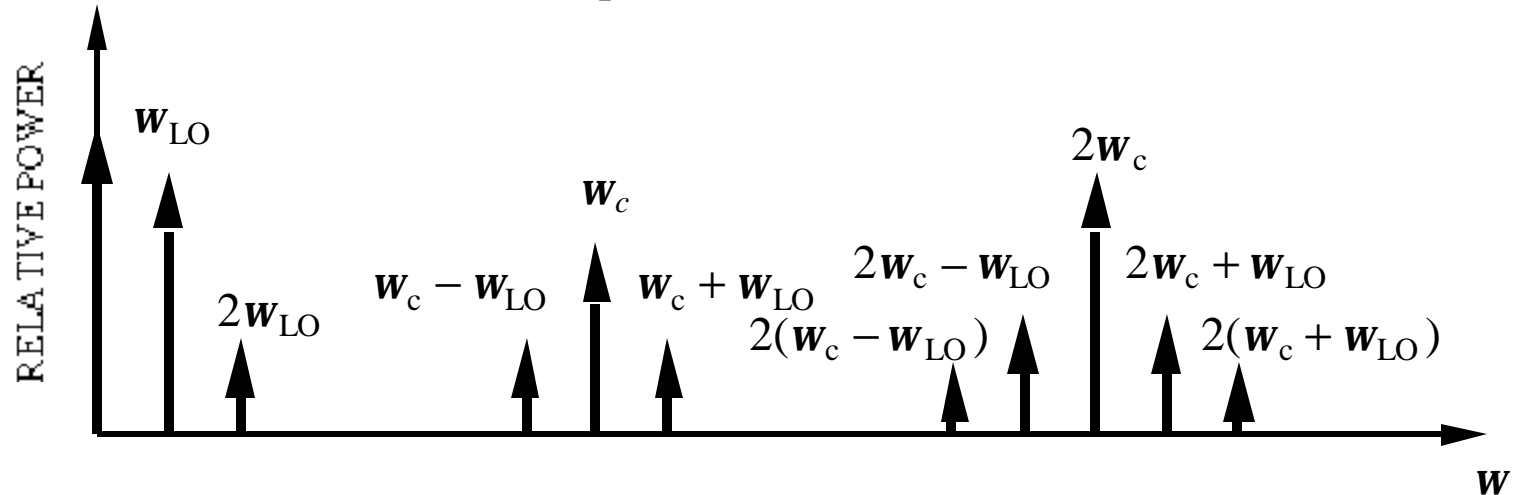


The diode is nonlinear; that is, the output for a single frequency input not only contains an input frequency term, but all of the harmonic terms as well



# Mixers (3)

When two sinusoids are combined in a diode mixer, the harmonics of both frequencies are present as well as all of the cross products. A few of them are shown below:



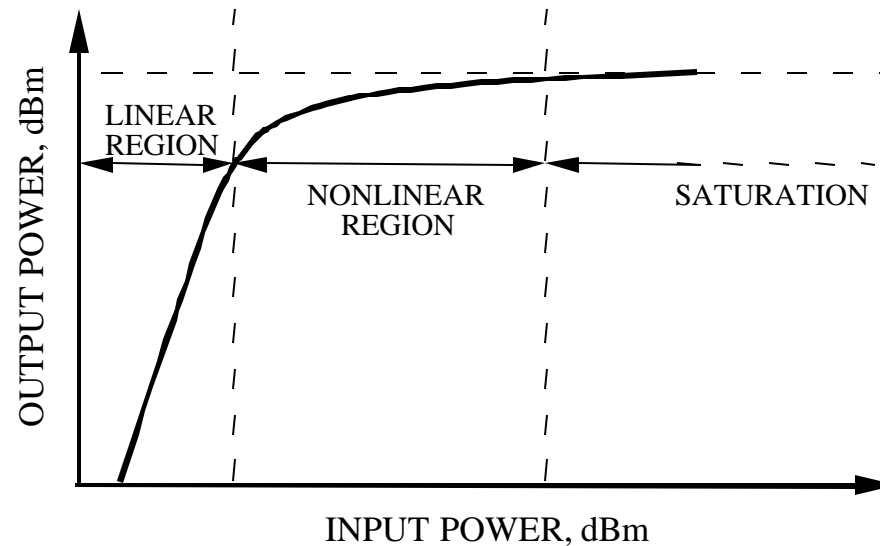
These are intermodulation products and must be controlled by proper mixer design to achieve high conversion efficiency and good noise performance.

The above results are based on a "small signal analysis" which assumes that the carrier signal level is much smaller than the LO voltage.

Even if the noise at both inputs is uncorrelated, the noise at the output is partially correlated. The noise figure depends on the impedances presented to all significant harmonics, not just the carrier and LO frequencies.

# Input-Output Transfer Characteristic

Applies to transmitters (power amplifiers) and receivers (low noise amplifiers, mixers).



- Region characteristics:
1. linear,  $P_{\text{out}} \propto P_{\text{in}}$
  2. saturation,  $P_{\text{out}} \approx \text{constant}$
  3. nonlinear,

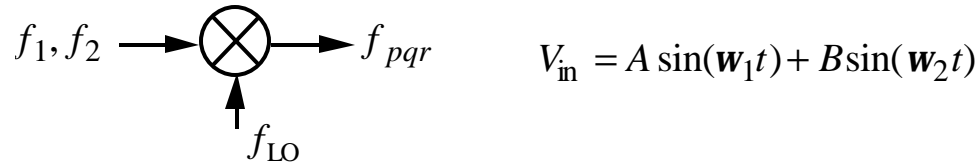
For a single input frequency  $\Rightarrow$

$$V_{\text{out}} \propto \underbrace{a_1 V_{\text{in}}}_{\substack{\text{FUNDAMENTAL} \\ \omega_c}} + \underbrace{a_2 V_{\text{in}}^2}_{\substack{\text{SECOND} \\ \text{HARMONIC,} \\ 2\omega_c}} + \underbrace{a_3 V_{\text{in}}^3}_{\substack{\text{THIRD} \\ \text{HARMONIC,} \\ 3\omega_c}} + \dots$$

# Intermodulation Products

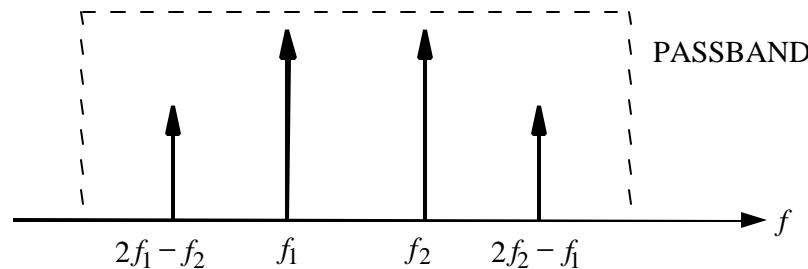
In the nonlinear region  $V_{out} \propto a_1 V_{in} + a_2 V_{in}^2 + a_3 V_{in}^3 + \dots$ . If the input signal  $V_{in}$  contains more than one frequency, say  $f_1$  and  $f_2$ , then all combinations of the two frequencies and their harmonics will be present in the output

$$f_{pqr} = \pm p f_1 \pm q f_2 \pm r f_{LO} \quad p, q, r = 0, 1, 2, \dots$$



These are intermodulation products (IM):  
 $p$  or  $q = 0$ , single tone IM  
 $p, q, r = 1, 2, \dots$  multi-tone IM

Example: Both stationary target return ( $f_1 = f_c$ ) and moving target return ( $f_2 = f_c + f_d$ ) are passed through an amplifier. The third order IM (from the  $V_{in}^3$  term) can lie in the passband. IM can cause signal distortion and potentially misinterpretation as a target.





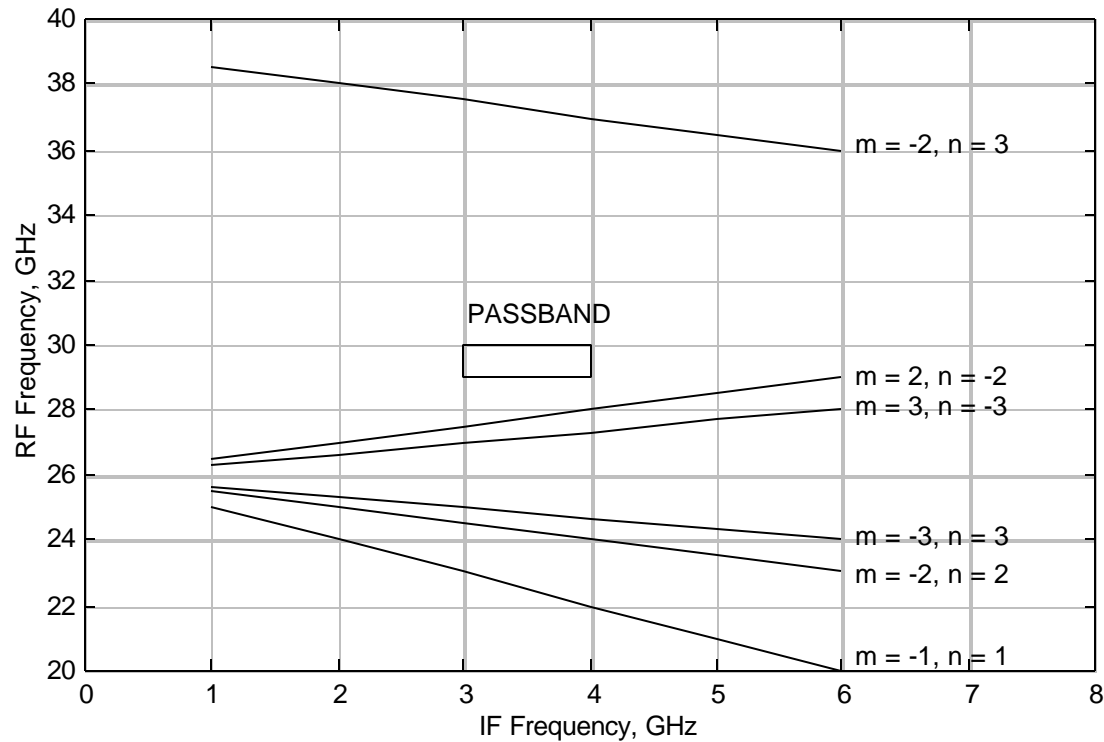
# Intermodulation Example

Mixer RF passband:  $29 \leq f_{RF} \leq 30$  GHz

LO frequency:  $f_{LO} = 26$  GHz

IF passband:  $f_{IF} = f_{RF} - f_{LO} = \begin{Bmatrix} 30 \\ 29 \end{Bmatrix} - 26 = \begin{Bmatrix} 3 \\ 4 \end{Bmatrix}$  GHz

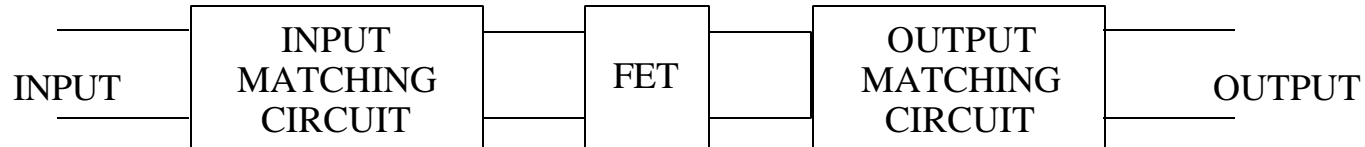
Other intermodulation products:  $f_{IF} = m f_{RF} - n f_{LO} \Rightarrow f_{RF} = \frac{1}{m}(f_{IF} - n f_{LO})$



# Amplifiers

Most receive amplifiers use gallium arsenide field effect transistors (GaAs FETs). Bipolar transistors are used at low microwave frequencies and performance is improving at higher microwave frequencies.

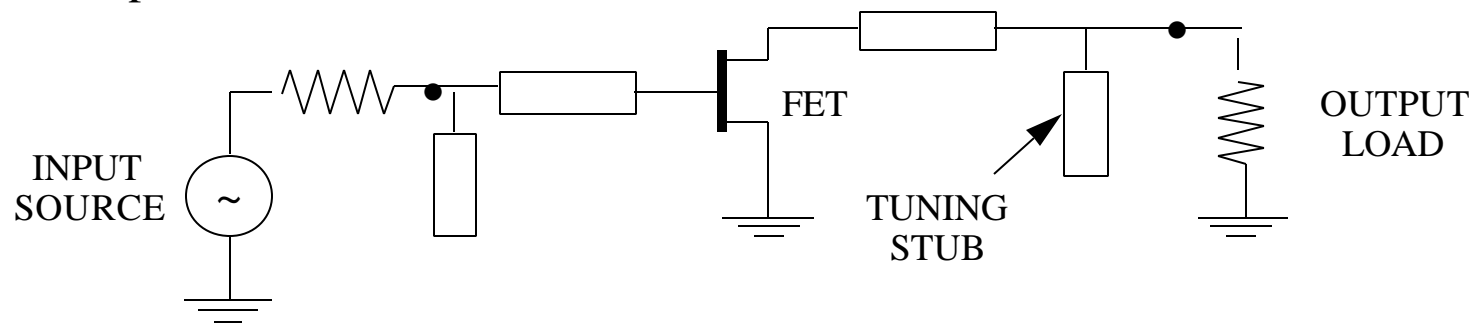
General circuit:



Design parameters:

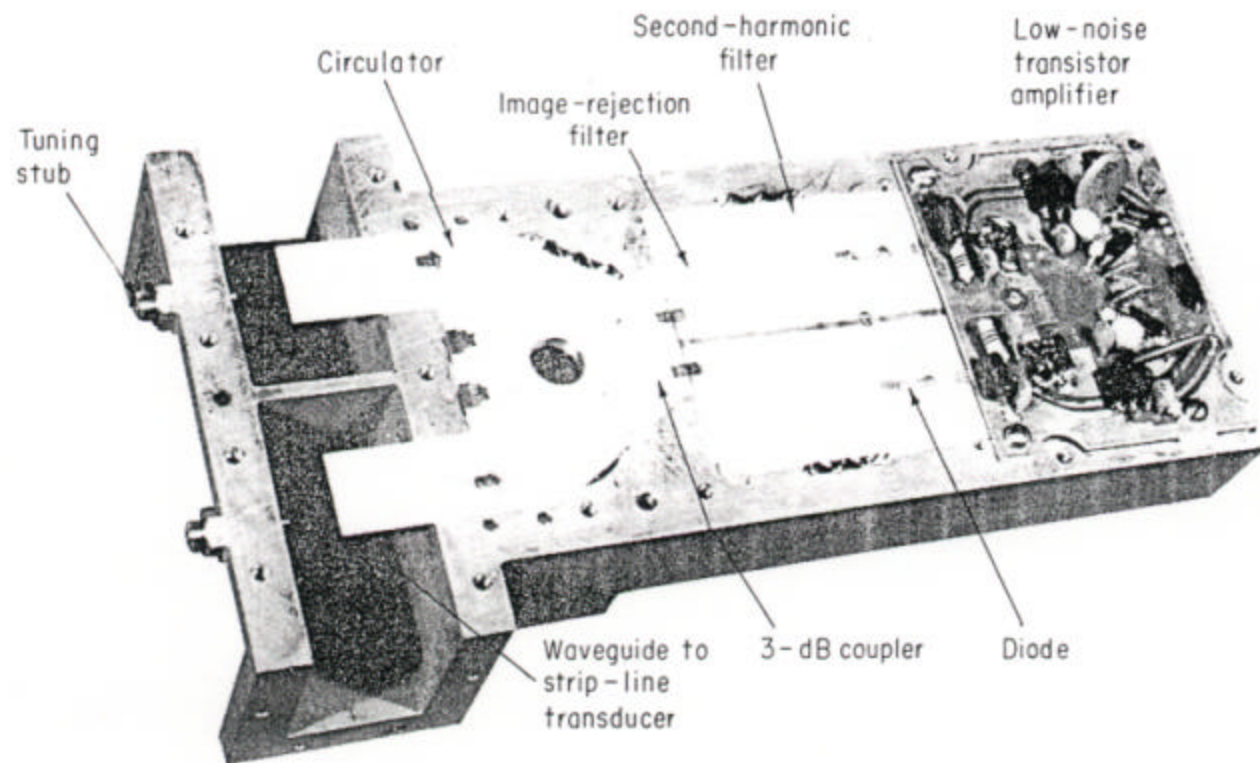
1. transducer gain (ratio of the power delivered to the load to the power available from the source)
2. stability
3. noise figure

Typical amplifier circuit:



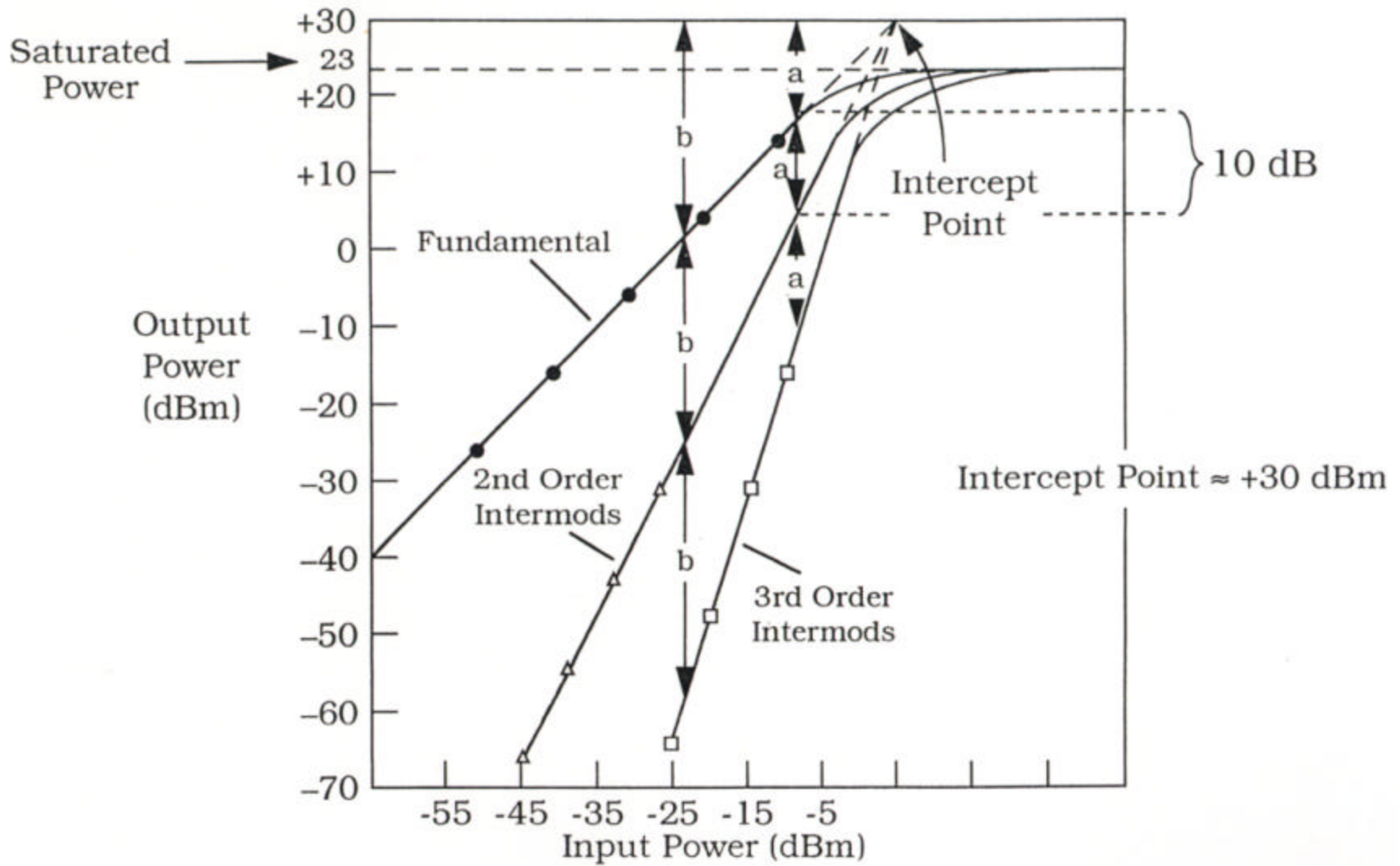
# Low-Noise Amplifier

This is an example of older technology that uses discrete elements. Current designs use integrated circuits.



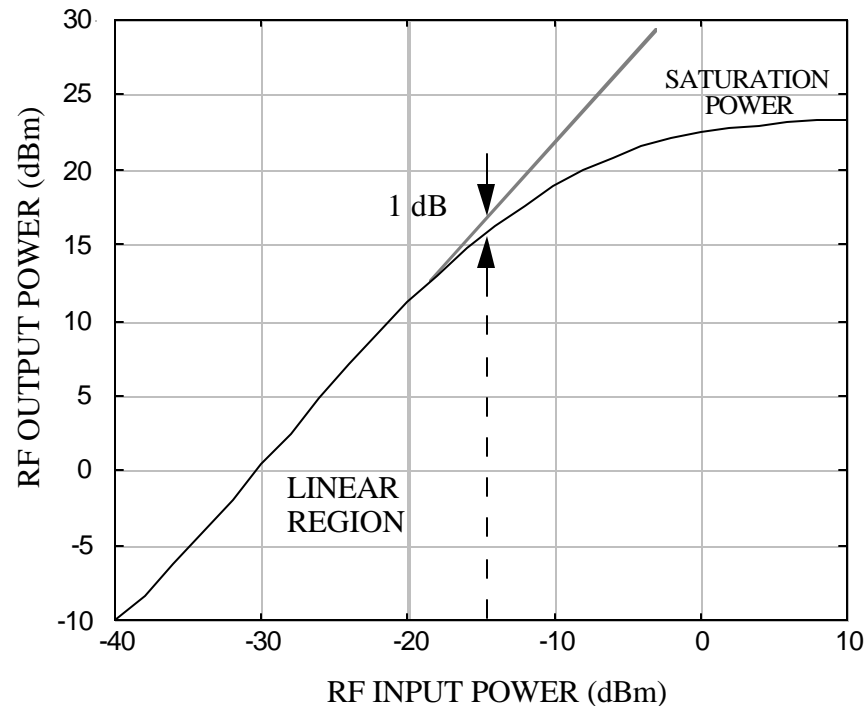
From *Microwave Semiconductor Devices and Their Circuit Applications* by Watson

# Intermodulation Products of Amplifiers



# Sample Microwave Amplifier Characteristic

Example: Amplifier transfer function



$$\text{Gain, } G = \frac{\text{Power Out}}{\text{Power In}}$$

Linear gain: 30 dB

Saturation power: 23 dBm

Saturation efficiency: 10%

Saturation gain: 20 dB

Power at 1 dB compression: 16 dBm

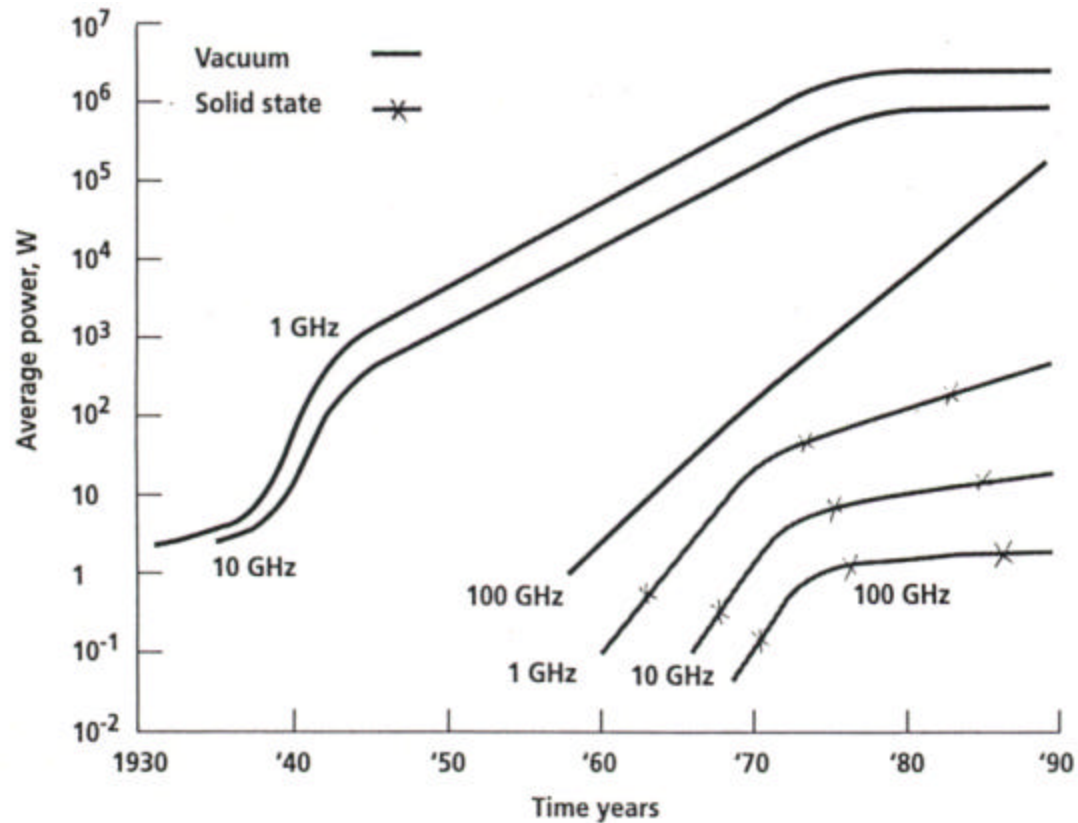
Efficiency at 1 dB compression: 3%

Gain at 1 dB compression: 29 dB

Voltage: 25 V

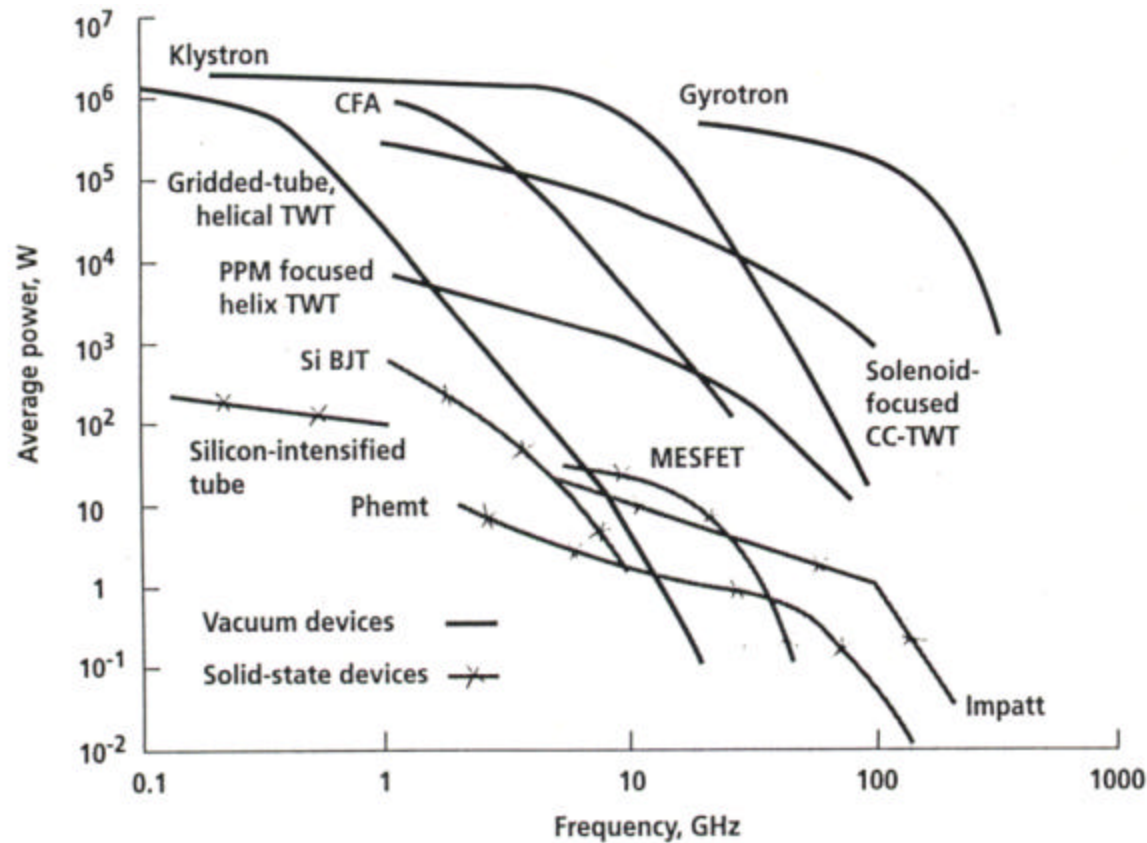
Current: 40 mA

# Development of Sources



From Symons – “Tubes: Still Vital After All These Years,” IEEE Spectrum, April 1998

# Power Capabilities of Sources



BJT = bipolar junction transistor  
 CC-TWT = constant-current traveling-wave tube  
 CFA = crossed-field amplifier

Impatt = impact avalanche and transit time diode  
 Phemt = pseudomorphic high-electron-mobility transistor  
 PPM = periodic permanent-magnet

From Symons – “Tubes: Still Vital After All These Years,” IEEE Spectrum, April 1998

# Transmitters (1)

Transmitter types: klystrons  
 traveling wave tubes (TWTs)  
 crossed field amplifiers (CFAs)  
 solid state amplifiers  
 magnetrons

## SUMMARY OF TRANSMITTER CHARACTERISTICS

Parameter	Klystron	TWT	Linear CFA	Reentrant CFA	Solid State	Magnetron
Gain	High	High	Low	Low	Moderate	N/A
Bandwidth	Narrow	Wide	Wide	Wide	Wide	N/A
Noise	Low	Low	Moderate	Moderate	Low	Moderate
DC voltage	High	High	Moderate	Moderate	Low	Moderate
X-rays	High	High	Low	Low	None	Low
Size	Large	Medium	Medium	Small	Medium (Arrayed)	Small
Weight	Heavy	Medium	Medium	Light	Medium	Light
Efficiency	Low	Low	Moderate	Moderate	Moderate	High

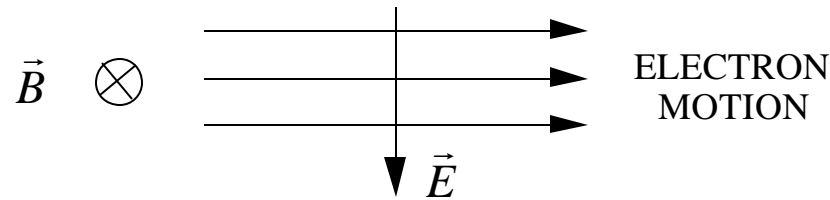


# Transmitters (2)

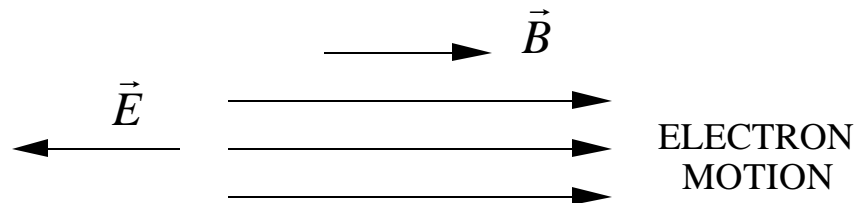
---

Microwave tube classification:

Crossed field: The dc electric field is perpendicular to the magnetic field. The general motion of the electrons is perpendicular to both fields. These are also known as "M-type" tubes. Examples are magnetrons and crossed field amplifiers.

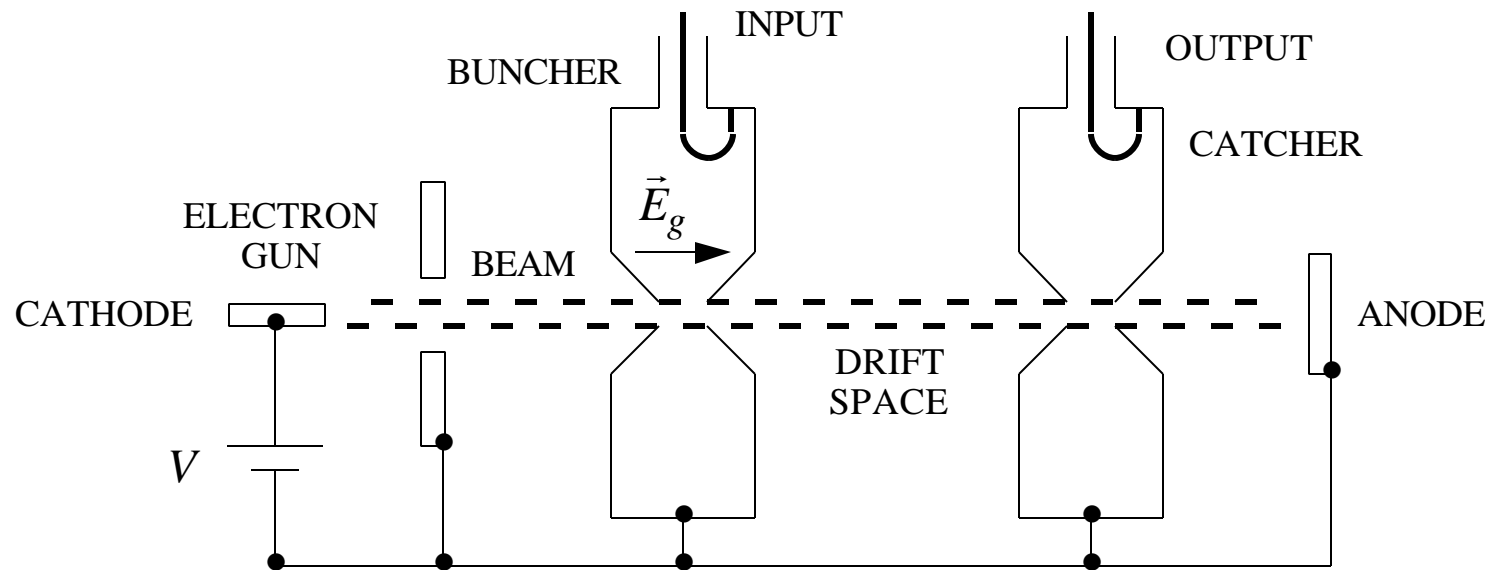


Linear beam: The general direction of the electron beam is parallel or antiparallel with the field vectors. Examples are klystrons and traveling wave tubes.



# Klystrons

The oscillating electric field in the gap ( $\vec{E}_g$ ) accelerates or decelerates electrons from the cathode. This causes "bunching" of the electrons into packets. They transfer their energy to the catcher cavity.



# Klystron Operation

---

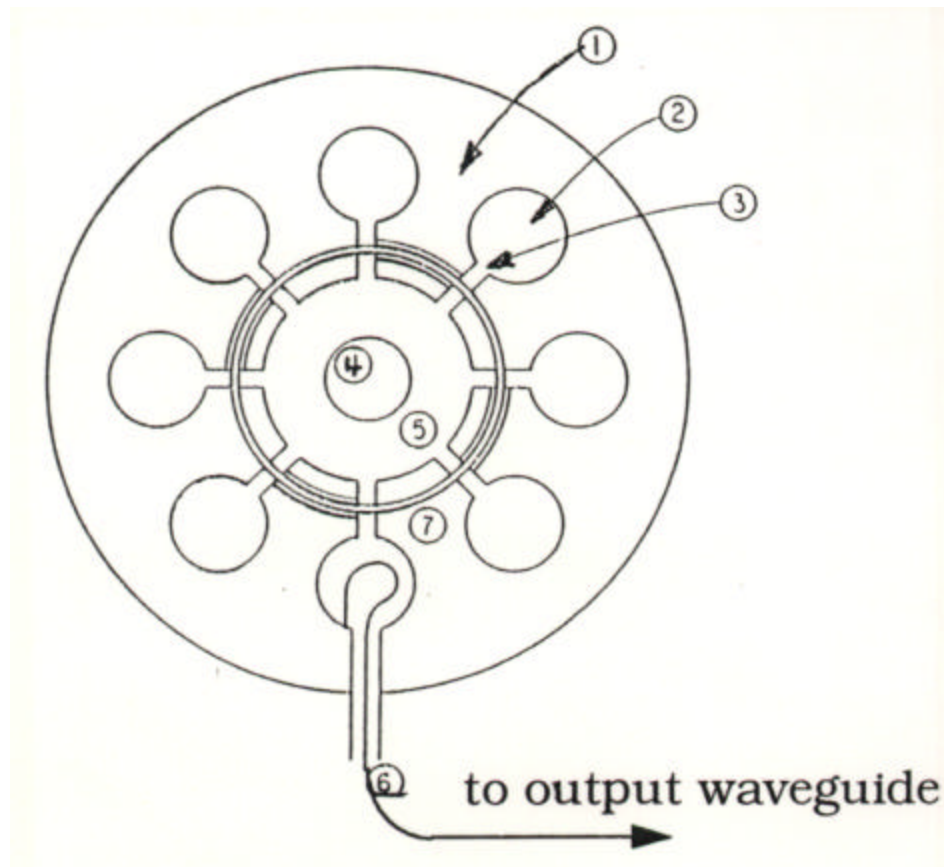
A klystron consists of a cathode and anode separated by an interaction space. In a two cavity klystron, the first cavity acts as a “buncher” and velocity modulates the electron beam. The second cavity is separated from the buncher by a drift space, which is chosen so that the AC current at the second cavity (the “catcher”) is a maximum. The second cavity is excited by the AC signal impressed on the beam in the form of a velocity modulation with a resultant production of an AC current. The AC current on the beam is such that the level of excitation of the second cavity is much greater than that in the buncher cavity, and hence amplification takes place. If desired, a portion of the amplified output can be fed back to the buncher cavity in a regenerative manner to obtain self-sustained oscillations.

The catcher cavity can be replaced by a reflector, in which case it is referred to as a reflex klystron. The reflector forces the beam to pass through the buncher cavity again, but in the opposite direction. By the proper choice of the reflector voltage the beam can be made to pass through in phase with the initial modulating field. The feedback is then positive, and the oscillations will build up in amplitude until the system losses and nonlinear effects prevent further buildup.

(From: *Foundations of Microwave Engineering*, by R. E. Collin)

# Cavity Magnetron

Cross section of a typical cavity magnetron



- 1. anode
- 2. cavity
- 3. coupling slot
- 4. cathode
- 5. interaction space
- 6. coupling loop
- 7. strapping

# Magnetron Operation

---

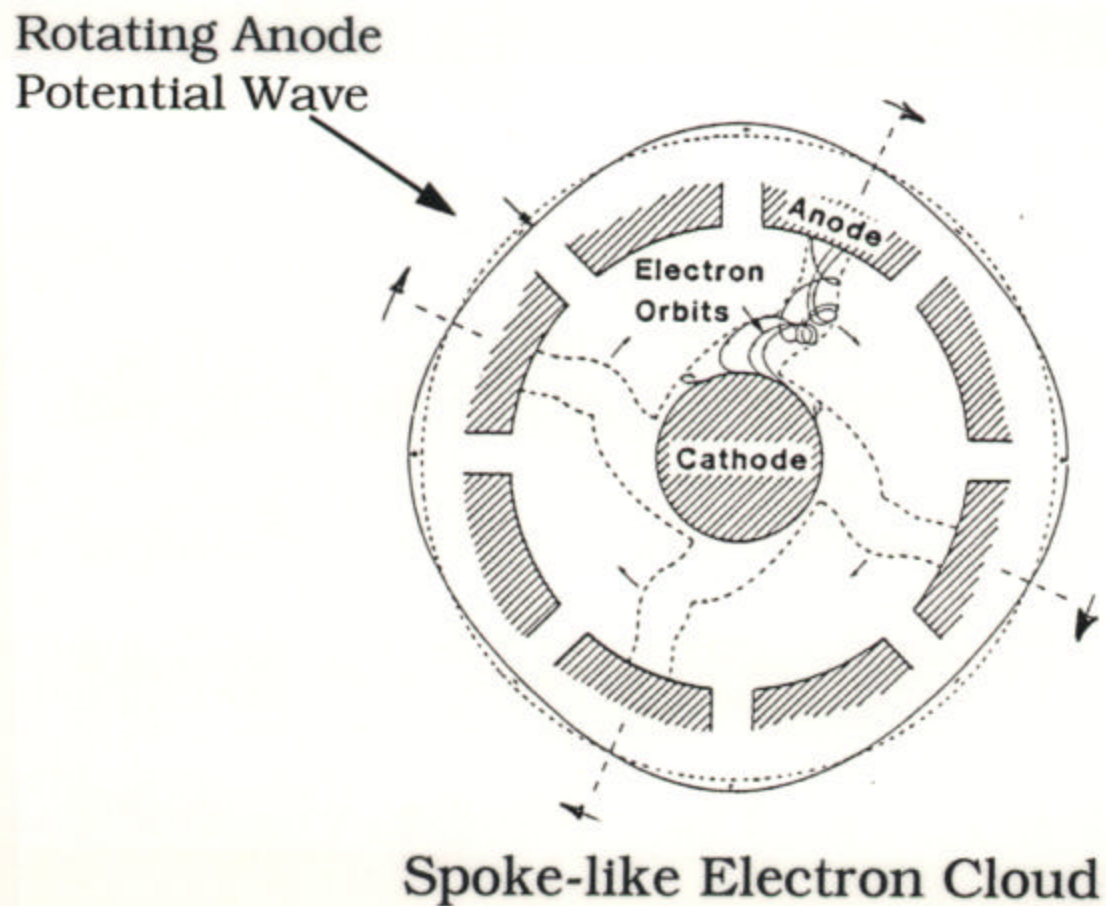
A magnetron consists of a number of identical resonators arranged in a cylindrical pattern around a cylindrical cathode. A permanent magnet is used to produce a strong magnetic field  $B_o$  normal to the cross section. The anode is kept at a high voltage relative to the cathode. Electrons emitted from the cathode are accelerated toward the anode block, but the presence of the magnetic field produces a force ( $-ev_r B_o$ ) in the azimuthal direction which causes the electron trajectory to be deflected in the same direction.

If there is present an AC electromagnetic field in the interaction space that propagates in the azimuthal direction with a phase velocity  $wr$ , strong interaction between the field and the circulating electron cloud can take place. The usual mode of operation is the  $p$  mode where the phase change between adjacent cavities is  $p$  radians. Each cavity with its input gap acts as a short-circuited transmission line a quarter of a wavelength long, and hence has a maximum electric field across the gap. A synchronism between the AC field and the electron cloud implies that those electrons located in the part of the field that acts to slow the electrons give up energy (and vice versa). Electrons that slow down move radially outward and are intercepted by the anode. Electrons that are accelerated by the AC field move radially inward until they are in phase with the field, and thus give up energy to the field. When the latter happens, they slow down and move to the anode. Therefore the only electrons lost from the interaction space are those that have given up a net amount of energy.

(From: *Foundations of Microwave Engineering*, by R. E. Collin)

# Eight Cavity Magnetron

Electron cloud in the interaction space of an eight cavity magnetron



# Magnetron Basics (1)

---

Three fields present:  $\vec{E}$  due to voltage applied between anode and cathode  
 $\vec{B}$  due to magnet  
 $\vec{E}_{RF}$  in the interaction space

If  $\vec{B}$  is strong enough electrons will be prevented from reaching the anode (this is magnetic insulation). The critical value of the magnetic field density is

$$\vec{B}_c = \frac{m_o c}{e d_e} \sqrt{g^2 - 1}$$

where:  $d_e = \text{effective gap} = \frac{r_a^2 - r_c^2}{2r_a}$  ( $r_a = \text{anode radius}$ ;  $r_c = \text{cathode radius}$ )

$$g = \text{relativistic factor} = \frac{1}{\sqrt{1 - (v/c)^2}} = 1 + \frac{eV_o}{m_o c^2}$$

$e = \text{electronic charge}$ ;  $m_o = \text{mass}$ ;  $V_o = \text{beam voltage}$

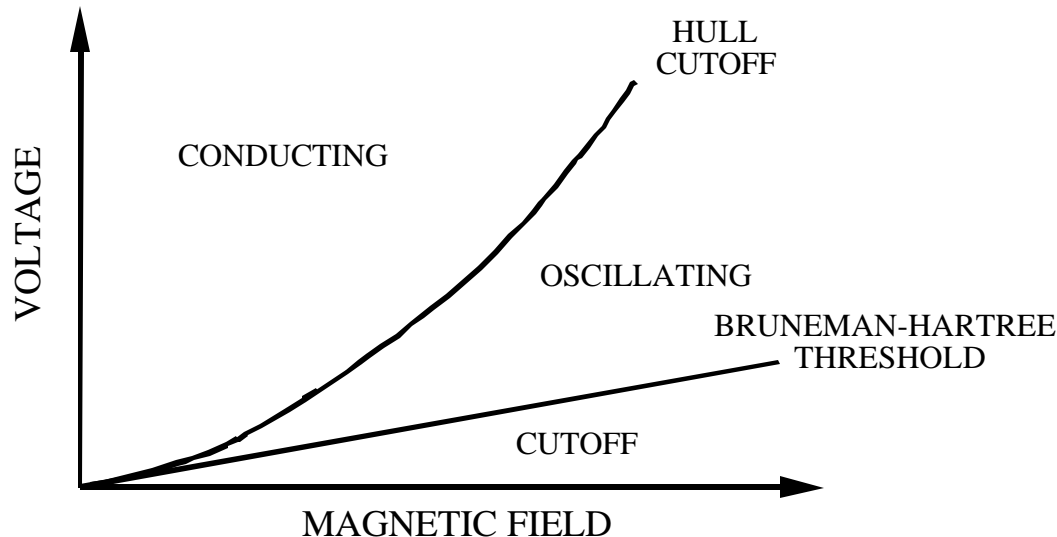
The cathode orbit drift velocity is

$$\vec{v}_d = \frac{\vec{E} \times \vec{B}}{|\vec{B}|^2}$$

# Magnetron Basics (2)

The Bruneman-Hartree resonance condition for mode  $n$ :

$$B_{BH} = \frac{2m^2}{e^2} eV_o \frac{r_a^2}{r_a^2 - r_c^2} \frac{n}{\omega_n}$$



Usually the cavities are spaced half a wavelength at the RF. The drift velocity must equal the phase velocity. At alternating cavities the electrons reach the anode. Therefore “spokes” arise which rotate around the interaction space. RF energy grows at the expense of the kinetic and potential energy of the electrons.



# Free-Electron Laser (FEL) Operation

---

A free electron laser consists of an electron beam, a periodic pump field and the radiation field. The electron beam passes through the pump field and begins to oscillate. (The pump field is usually a static periodic magnetic field called a “wiggler,” but in principle it can be any field capable of producing a transverse electron oscillation.) The oscillating electrons radiate, and the combination of the radiation field and wiggler field produces a beat wave which tends to bunch electrons in the axial direction. The bunching force provided by the beating of the radiation and wiggler fields is due to a so-called pondermotive wave, which is characterized by a periodic axial force. The bunched electrons radiate more coherently, thereby strengthening the radiation, which causes more bunching, then produces stronger and more coherent radiation, and so forth. The electrons in the beam are not bound to any nucleus, hence the term “free electron.”

Like all lasers, a FEL can operate as either an amplifier or oscillator. Amplifiers require high growth rates so that large gains in the radiation field can occur in a reasonable distance. This requirement generally restricts the use of FELs to millimeter wavelengths or shorter. The most important FEL attributes are broad frequency-tuning ability, high efficiency (> 40%), wide bandwidth, and high power (> 10 MW at millimeter wave frequencies).

*(From: High-Power Microwave Sources, Chapter 6, by J. A. Pasour)*

# Free-Electron Lasers

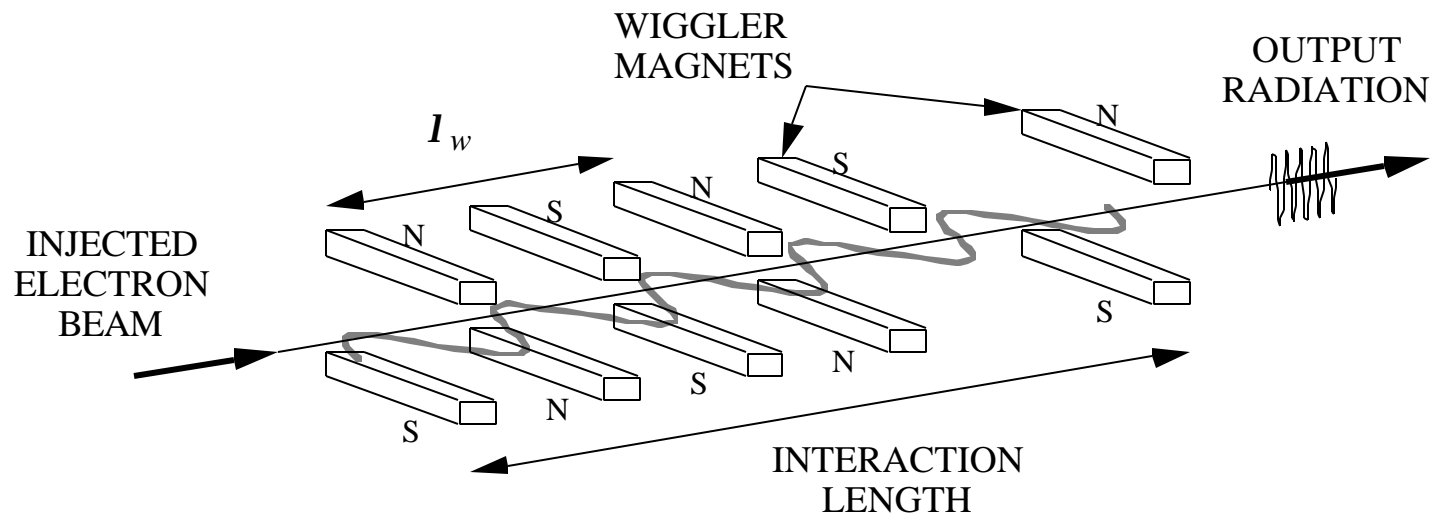
Example of a basic free electron laser

$\lambda = \lambda_w / (2g_o^2)(1 + K_w^2/2) =$  radiation wavelength

$K_w = eB_w / mck_w =$  wiggler strength parameter

$\lambda_w = 2p / k_w$  wiggler period;  $B_w =$  wiggler magnetic field;

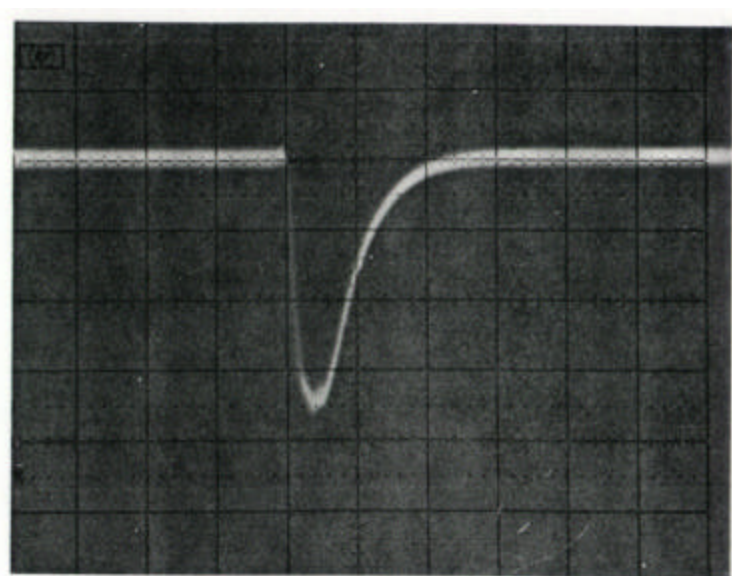
$e =$  electron charge;  $m =$  electron rest mass;  $c =$  speed of light



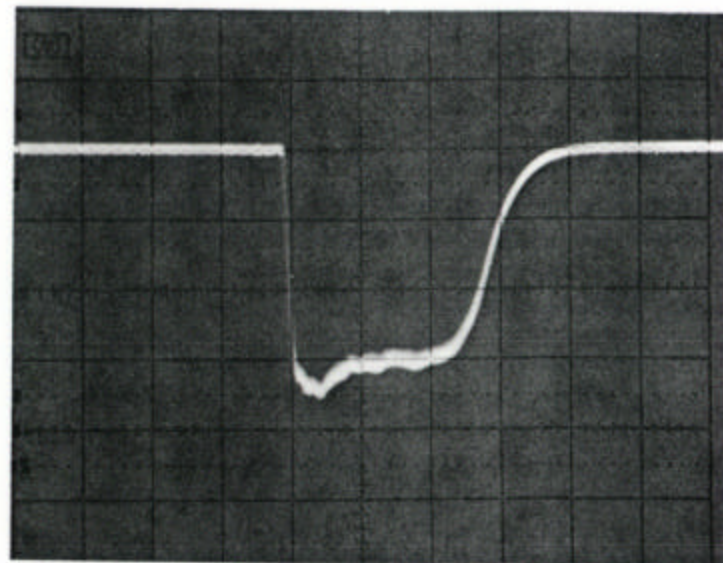
# Radar Waveform Parameter Measurements (1)

---

AN/APS-10 short pulse width



AN/APS-10 long pulse width

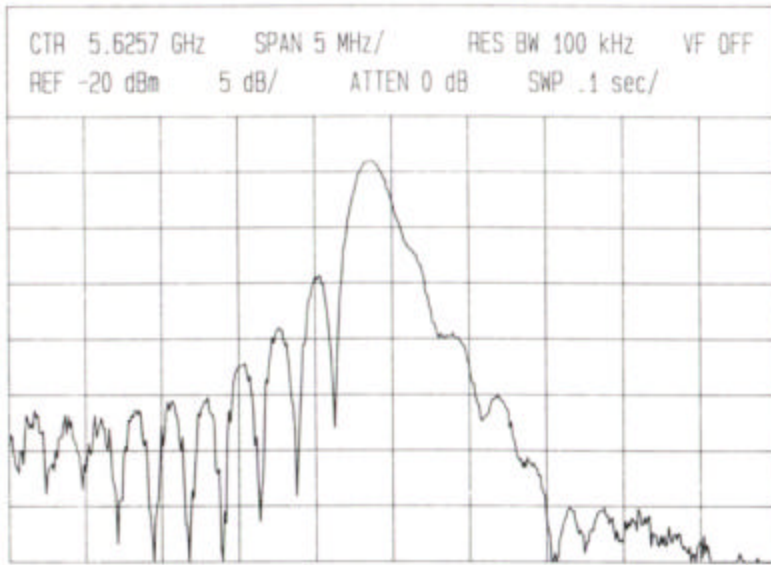


(Figures from HP Application Note 174-14)

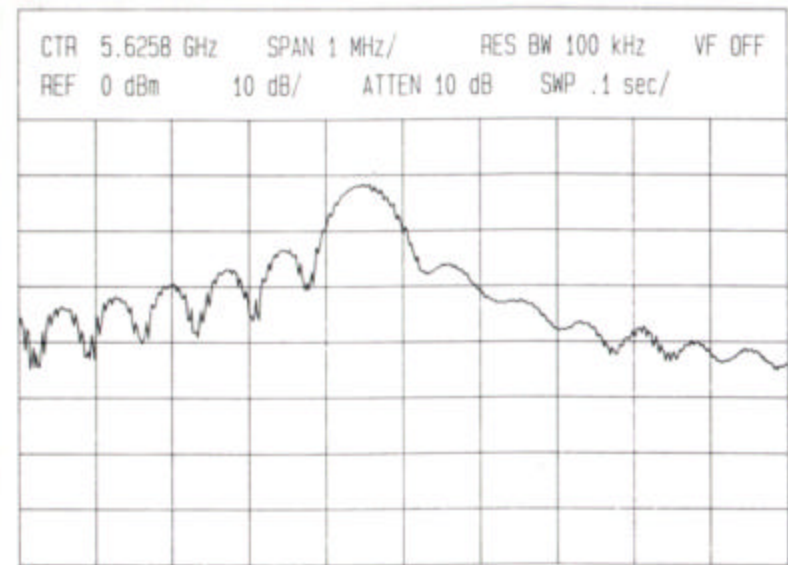
# Radar Waveform Parameter Measurements (2)

---

AN/APS-10 short pulse spectrum



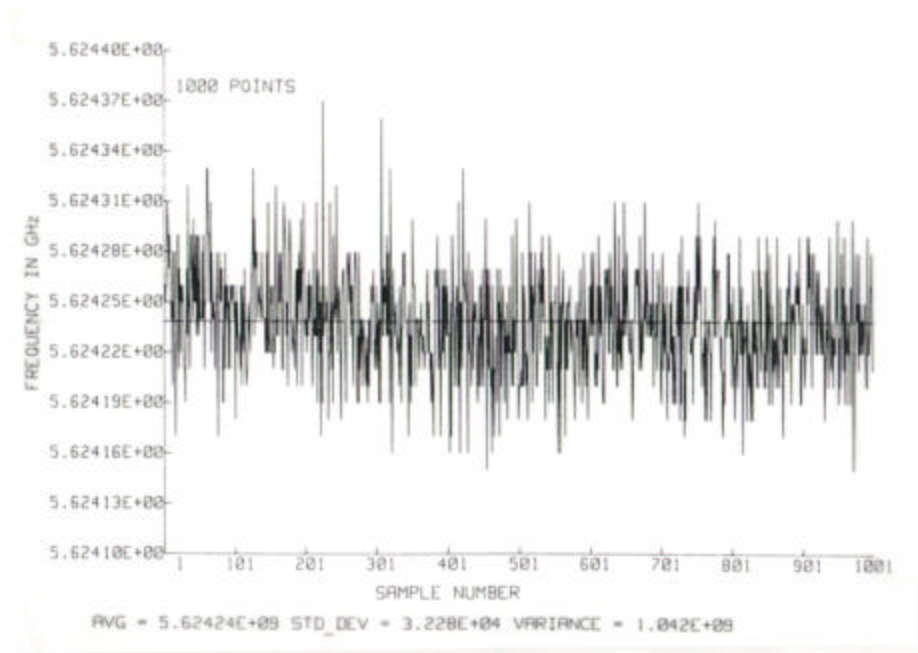
AN/APS-10 long pulse spectrum



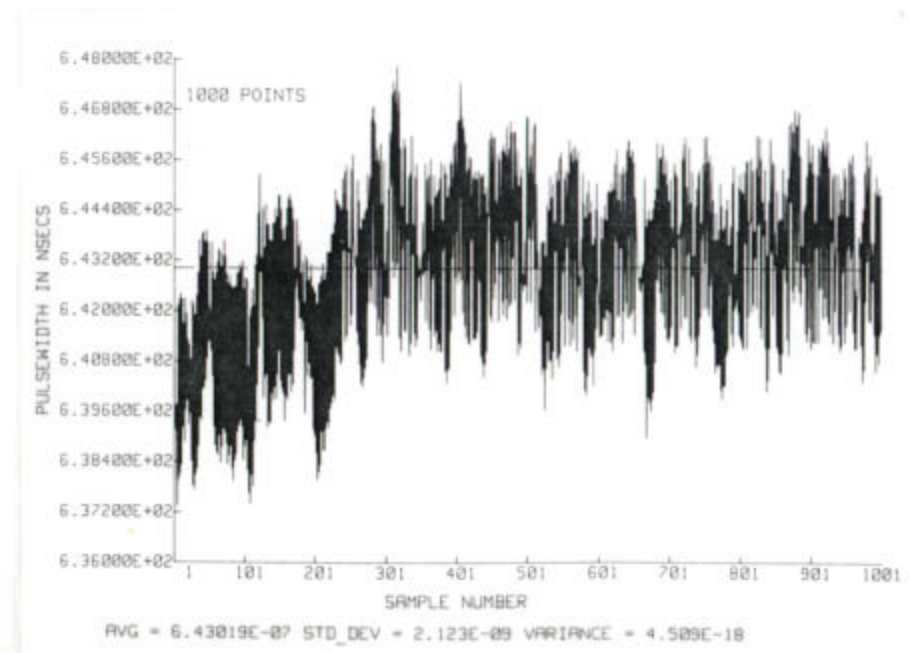
(Figures from HP Application Note 174-14)

# Radar Waveform Parameter Measurements (3)

AN/APS-10 frequency point plot  
(1000 points over 10 minutes)



AN/APS-10 pulse width point plot  
(short pulse width)

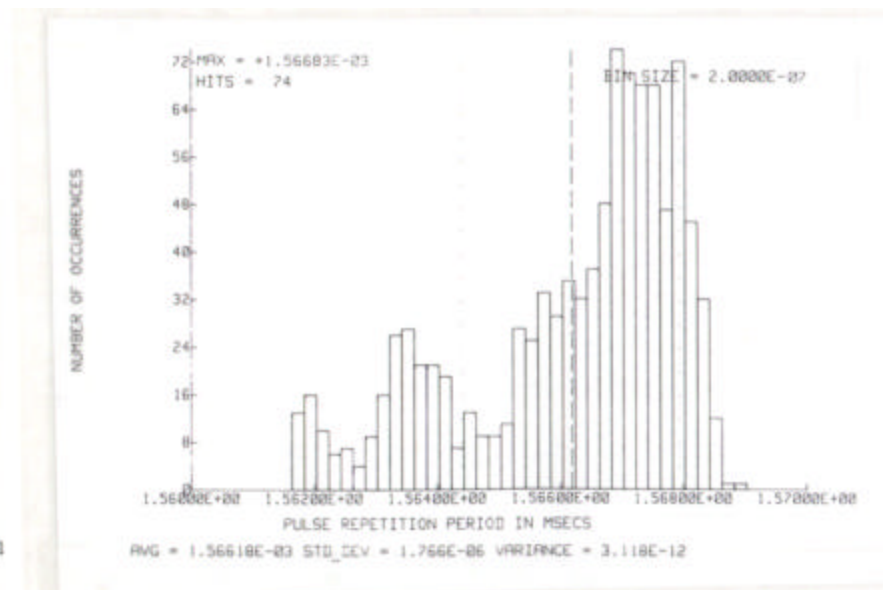
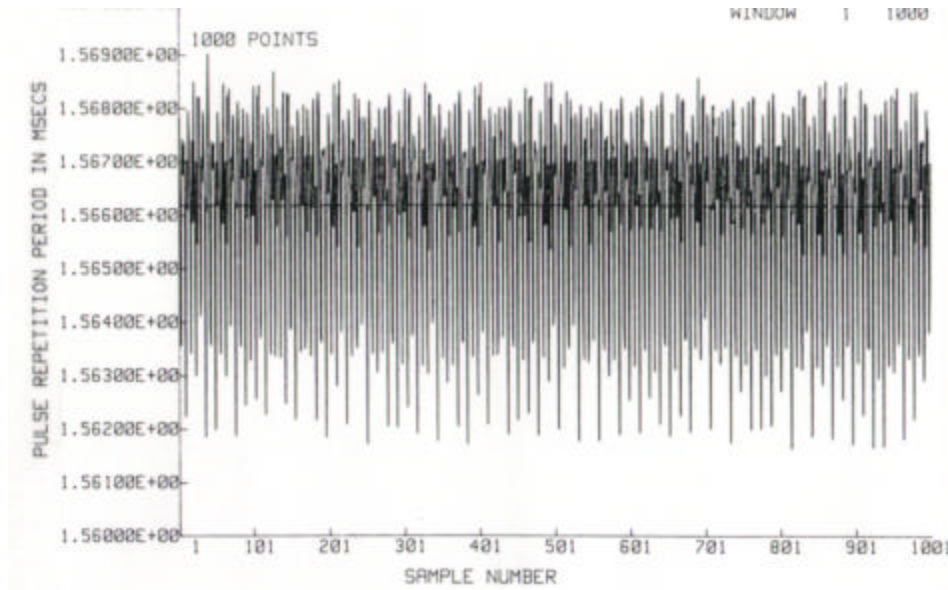


(Figures from HP Application Note 174-14)

# Radar Waveform Parameter Measurements (4)

AN/APS-10 pulse repetition period  
(1000 points over 10 minutes)

AN/APS-10 pulse repetition period  
histogram (PDF)



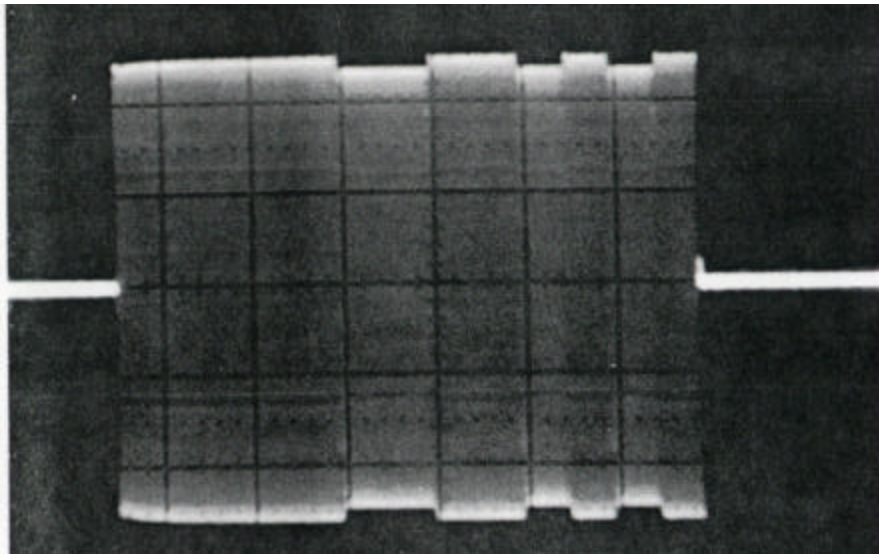
(Figures from HP Application Note 174-14)

# Radar Waveform Parameter Measurements (5)

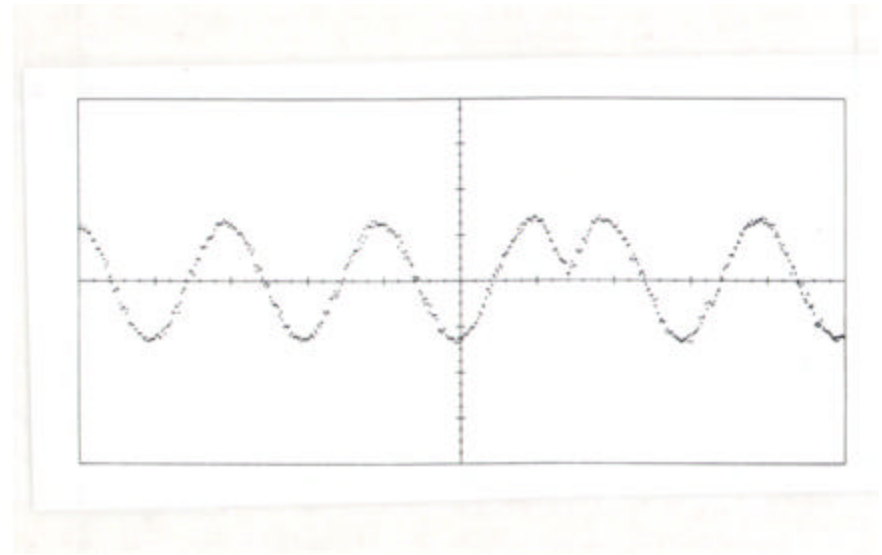
---

## Barker Coded Waveform

60 MHz IF signal



Phase shift in 60 MHz IF signal



(Figures from HP Application Note 174-14)

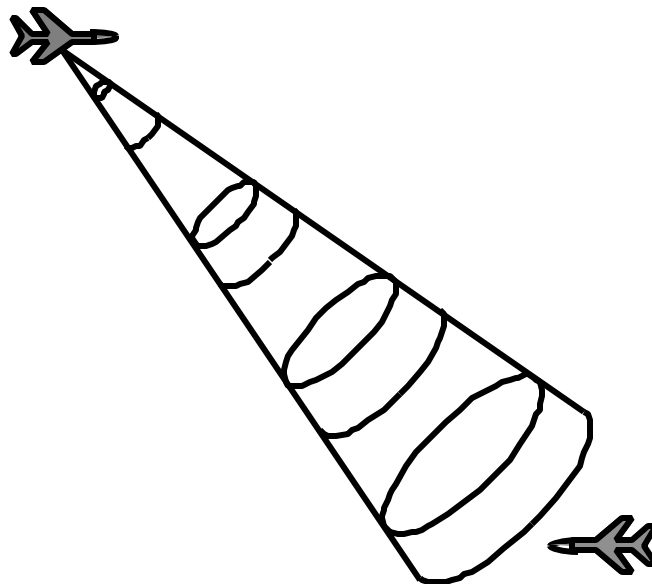
# Microwave Devices & Radar

## LECTURE NOTES VOLUME II

by Professor David Jenn

Contributors: Professors F. Levien, G. Gill, J. Knorr, and J. Lebaric

---





# Other Sources of Loss

---

There are many sources of loss that are not accounted for in the basic form of the radar range equation. Similarly, there are several signal processing methods available to increase the effective signal level. Thus general loss and gain factors are added to the RRE:

$$\text{SNR} = \frac{P_r}{N_o} = \frac{P_t G_t G_r s l^2 G_p}{(4\pi)^3 R^4 k T_s B_n L}$$

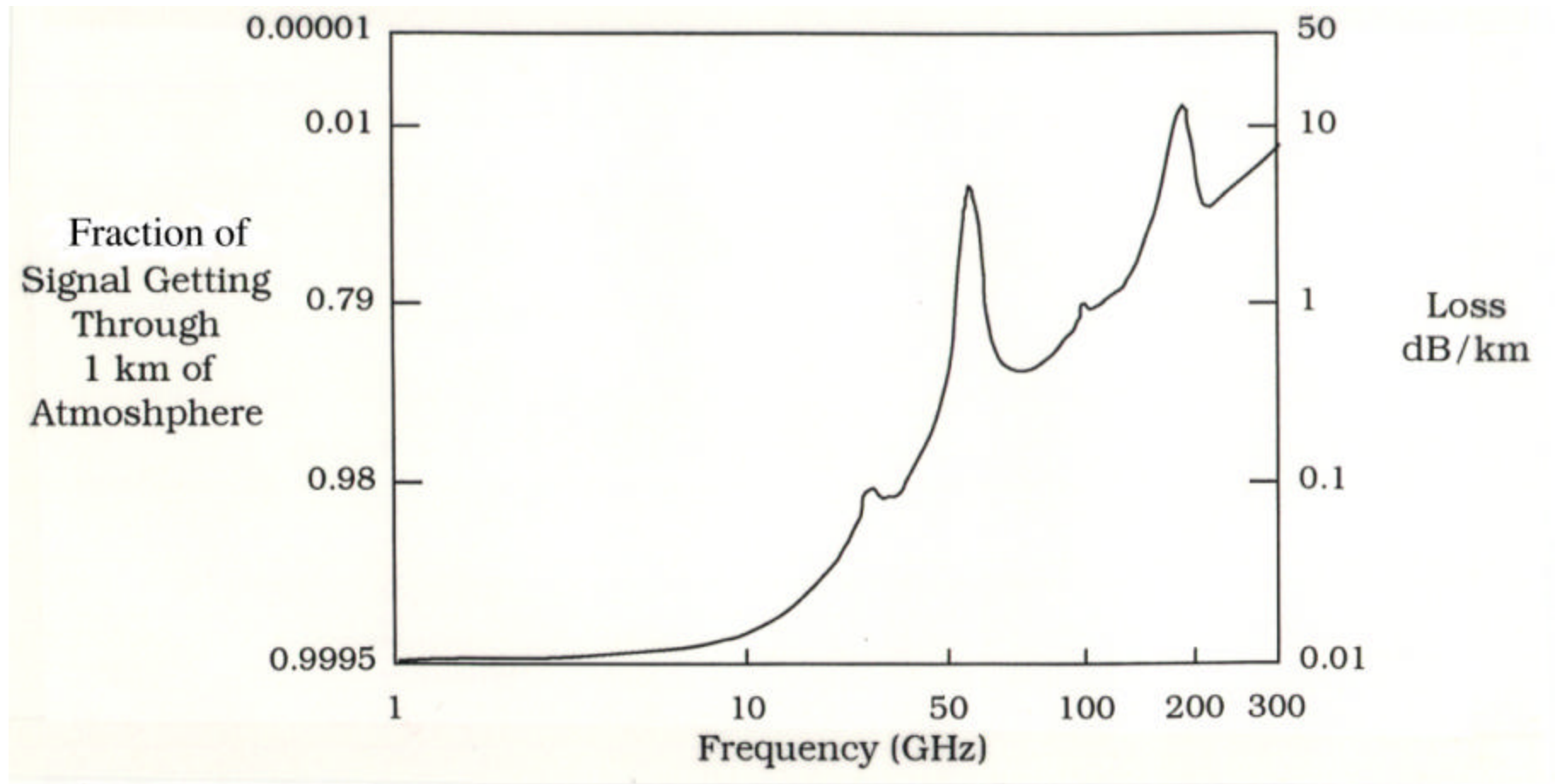
$L$  is a "catch all" loss factor ( $>1$ ). A fraction of the loss can be attributed to each source if its contribution is known. For instance,  $L = L_b L_B L_x L_a L_c$  where the loss sources are:

1. transmission line loss,  $L_x$
2. atmospheric attenuation and rain loss,  $L_a$  ( $1/L_a = e^{-2aR}$ ,  $a$  = one-way power attenuation coefficient)
3. secondary background noise and interference sources,  $L_b$
4. antenna beamshape loss,  $L_B$
5. collapsing loss,  $L_c$

$G_p$  is the processing gain which can be achieved by integration and various correlation methods.

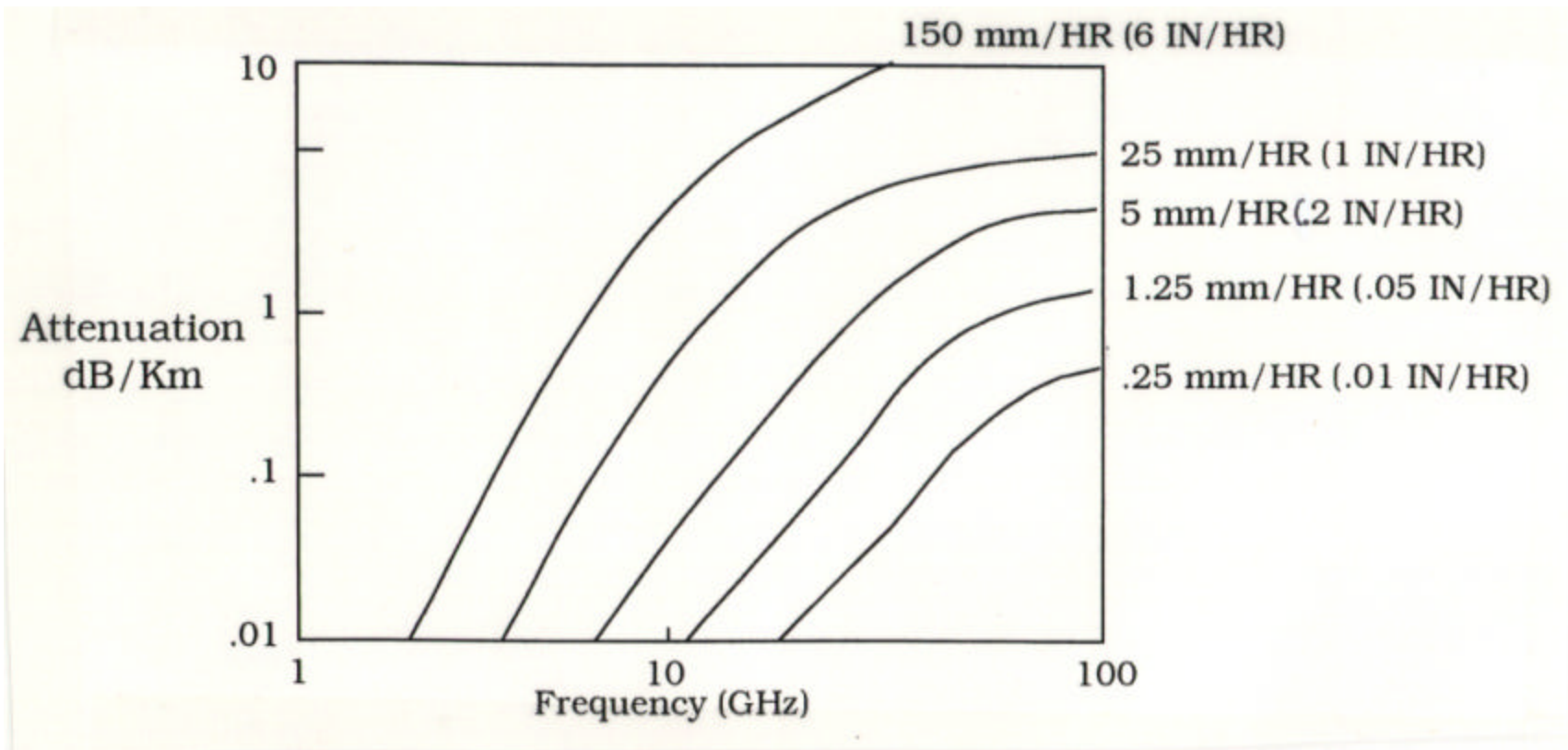
# Atmospheric Attenuation

---



# Rain Attenuation

---

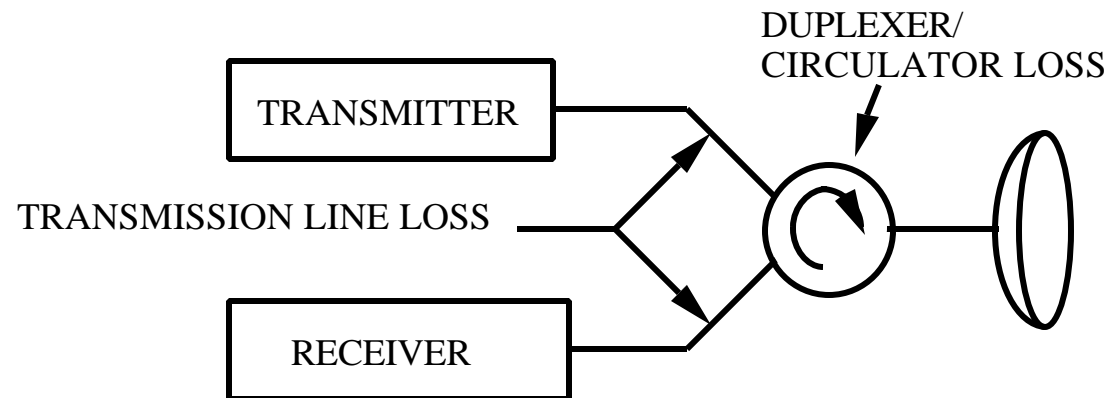


# Transmission Line Loss

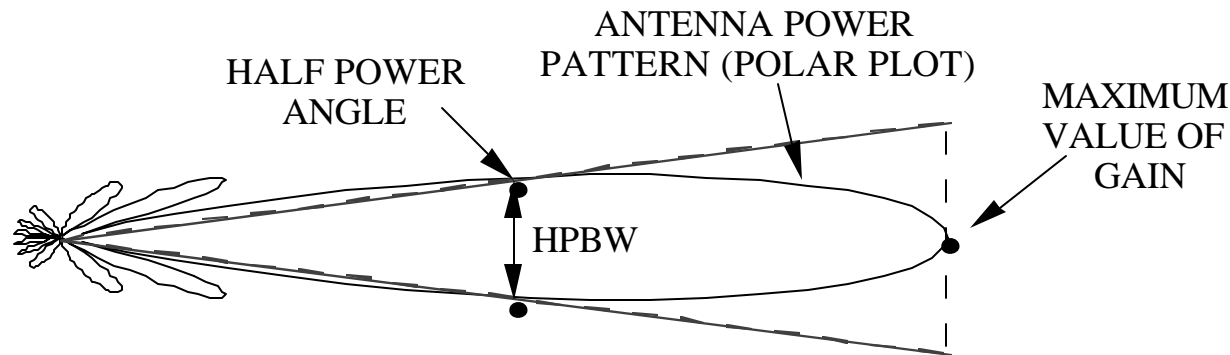
---

Transmission lines between the antenna and receiver and transmitter can have significant losses. Traditionally these have been called plumbing loss because the primary contributor was long sections of waveguide. Sources of loss include:

1. cables and waveguide runs (0.25 to 1 dB per meter)
2. devices have insertion loss  
duplexer, rotary joints, filters, switches, etc.
3. devices and connectors have mismatch loss ( $VSWR \neq 1$ )



# Antenna Beamshape Loss

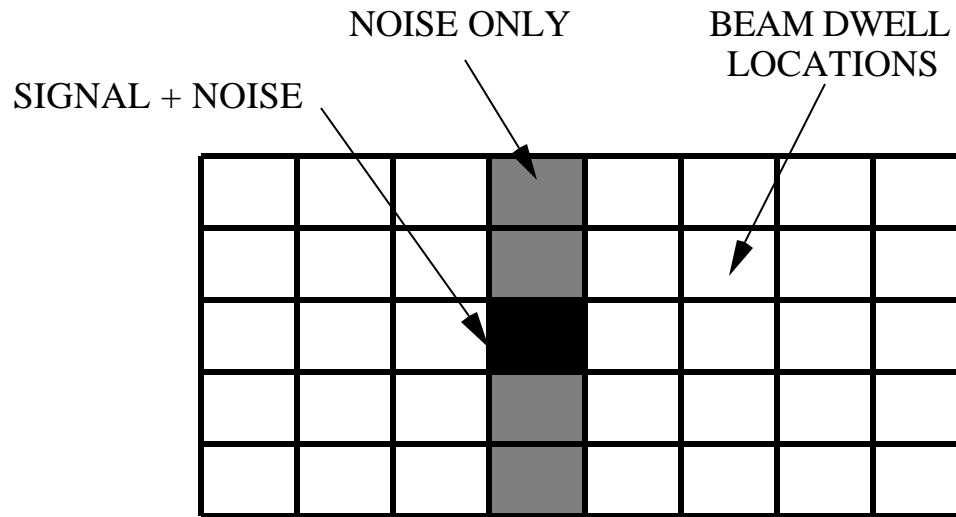


In the form of the RRE with pulse integration, constant gain has been assumed for all pulses (the duration of  $t_{ot}$ ). The gain is actually changing with scan across the target. The result is lower SNR than with the approximate antenna model. The beamshape loss for a Gaussian beam,  $G(\mathbf{q}) = G_o \exp[-2.773(\mathbf{q} / \mathbf{q}_B)^2]$ , when integrating  $n$  (odd) pulses is

$$L_B \approx \frac{n}{1 + 2 \sum_{m=1}^{(n-1)/2} e^{-5.55m^2 / (n_B - 1)^2}}$$

per dimension of beamshape. (For example, a "fan beam" is one dimensional). The loss tends to 1.6 dB for a large number of pulses.

# Collapsing Loss



Collapsing loss can arise from several sources:

- the outputs from several receivers are added when only one contains the signal
- the outputs from several antenna beams are combined when only one contains signal

The effect is the same as adding extra noise pulses, say  $m$ , in which case the collapsing loss can be defined as

$$\frac{1}{L_c} = \frac{(n \text{ signal plus noise channels} + m \text{ noise only channels})}{(n \text{ signal plus noise channels})} = \frac{(\text{SNR})_{m+n}}{(\text{SNR})_n}$$

# Noise Figure & Effective Temperature (1)

---

Definition of noise figure:

$$F_n = \frac{(S/N)_{\text{in}}}{(S/N)_{\text{out}}} = \frac{S_{\text{in}} / N_{\text{in}}}{S_{\text{out}} / N_{\text{out}}} = \frac{N_{\text{out}}}{k T_o B_n G}$$

where  $G = \frac{S_{\text{out}}}{S_{\text{in}}}$ . By convention, noise figure is defined at the standard temperature of  $T_o = 290$  K. The noise out is the amplified noise in plus the noise added by the device

$$F_n = \frac{GN_{\text{in}} + \Delta N}{k T_o B_n G} = 1 + \frac{\Delta N}{k T_o B_n G}$$

$\Delta N$  can be viewed as originating from an increase in temperature. The effective temperature is

$$F_n = 1 + \frac{k T_e B_n G}{k T_o B_n G} = 1 + \frac{T_e}{T_o}$$

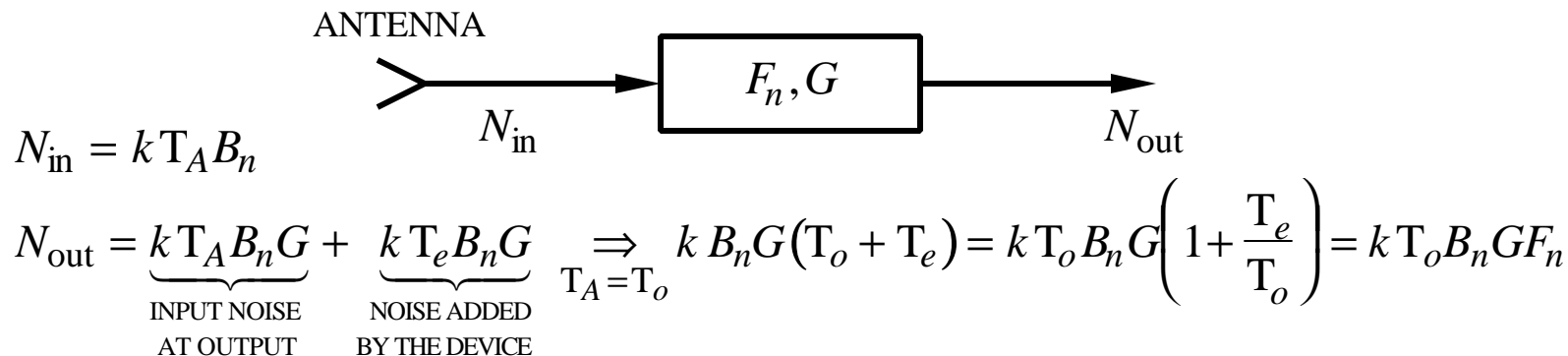
Solve for effective temperature in terms of noise figure

$$T_e = (F_n - 1)T_o$$

# Comments on Noise Figure & Temperature

---

- Originally the term noise figure referred to the dB value and noise factor to the numeric value. Today both terms are synonymous.
- Noise figure is only unique when the input noise level is defined. It must always be reduced to a number that is proportional to noise temperature to be used in calculations.
- If the antenna temperature is unknown it is usually assumed that  $T_A = T_o$

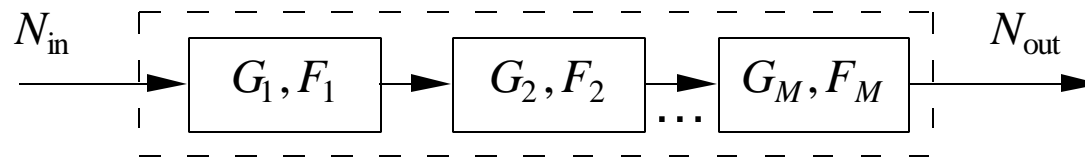


Thus, if  $T_A = T_o$  then  $k T_o B_n F_n$  can be substituted for  $k T_s B_n$  in the RRE.



# Noise in Cascaded Networks (1)

Examine how the noise figure is affected when  $M$  devices are cascaded



- Note:
1. same  $B_n$  for each stage
  2. total gain is  $G = G_1 G_2 \cdots G_M$
  3. denote the overall noise figure as  $F_o$
  4. devices are impedance matched

Noise from the first amplifier:  $[(F_1 - 1)kT_o B_n] G_1 G_2 \cdots G_M$

Noise from the second amplifier:  $[(F_2 - 1)kT_o B_n] G_2 G_3 \cdots G_M$

Extending to  $M$  stages:

$$N_{out} = kT_o B_n \left\{ \prod_{m=1}^M G_m + (F_1 - 1)G_1 \prod_{m=2}^M G_m + \cdots + (F_M - 1)G_M \right\}$$

But  $N_{out}$  has the form  $kT_o B_n F_o G$ . Comparing with the above,

$$F_o = F_1 + \frac{F_2 - 1}{G_1} + \frac{F_3 - 1}{G_1 G_2} + \cdots + \frac{F_M - 1}{G_1 G_2 \cdots G_{M-1}}$$

# Noise Figure & Effective Temperature (2)

---

Summary of noise figure and effective temperature for cascaded networks:

The overall noise figure for  $M$  cascaded devices with noise figures  $F_1, F_2, \dots, F_M$  and gains  $G_1, G_2, \dots, G_M$  is

$$F_o = F_1 + \frac{F_2 - 1}{G_1} + \frac{F_3 - 1}{G_1 G_2} + \dots + \frac{F_M - 1}{G_1 G_2 \dots G_{M-1}}$$

The overall effective temperature for  $M$  cascaded devices with temperatures  $T_1, T_2, \dots, T_M$  and gains  $G_1, G_2, \dots, G_M$  is

$$T_e = T_1 + \frac{T_2}{G_1} + \frac{T_3}{G_1 G_2} + \dots + \frac{T_M}{G_1 G_2 \dots G_{M-1}}$$

# Noise Figure From Loss

---

1. Transmission line: The fraction of electric field incident on a transmission line of length  $d$  that is transmitted is given by

$$G_x = \frac{1}{L_x} = e^{-2\mathbf{a}d} \leq 1$$

where  $\mathbf{a}$  is the attenuation constant. (The factor of two in the exponent is due to the fact that  $\mathbf{a}$  is a voltage attenuation constant.) Therefore,  $F_n = L_x = e^{2\mathbf{a}d} \geq 1$ .

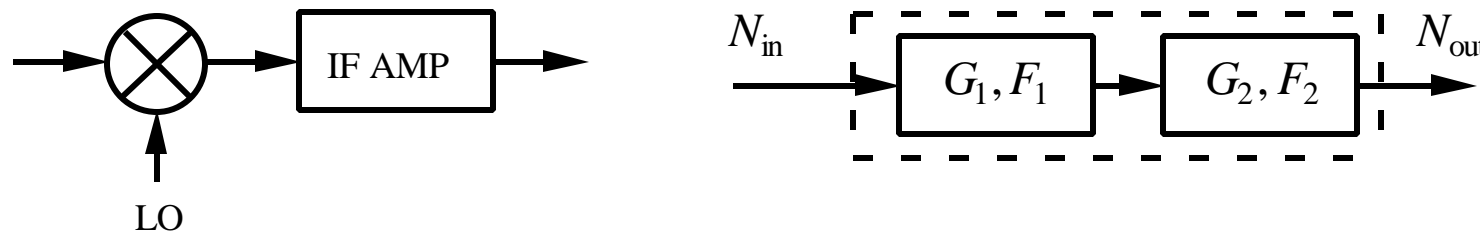
2. Mixer: Conversion loss for a mixer is

$$L_c = \frac{\text{RF power in}}{\text{IF power out}} \geq 1$$

Typical values are 4 to 6 dB. If a mixer is considered as a simple lossy two-port network (input at the carrier frequency; output at the IF frequency), then a commonly used approximation is  $G_c = 1/L_c$  and  $F_n = L_c$ .

# Examples (1)

1. A radar with the following parameters requires SNR = 10 dB for a target RCS of 5 m<sup>2</sup>: antenna gain = 30 dB, P<sub>t</sub> = 200 kW, f = 10 GHz, t = 1 ns, T<sub>A</sub> = 200 K  
 receiver mixer: 10 dB conversion loss and 3 dB noise figure  
 IF amplifier: 6 dB noise figure



$$F_o = F_1 + \frac{F_2 - 1}{G_1} = 2 + \frac{4 - 1}{0.1} = 32$$

We need the system noise temperature T<sub>s</sub> = T<sub>e</sub> + T<sub>A</sub> = 31T<sub>o</sub> + T<sub>A</sub> = 9190 K. Thus kT<sub>s</sub>B<sub>n</sub> = 1.3 × 10<sup>-13</sup> W. It has been assumed that B<sub>n</sub> ≈ 1/t. Now N<sub>out</sub> = kT<sub>s</sub>B<sub>n</sub>G<sub>1</sub>G<sub>2</sub> so that

$$SNR = 10 = \frac{P_t G^2 s I^2 G_1 G_2}{(4p)^3 R^4 N_{out} L} = \frac{P_t G^2 s I^2}{(4p)^3 R^4 k T_s B_n L}$$

(L is for system losses such as beamshape loss, collapsing loss, etc., of which we have no information.)

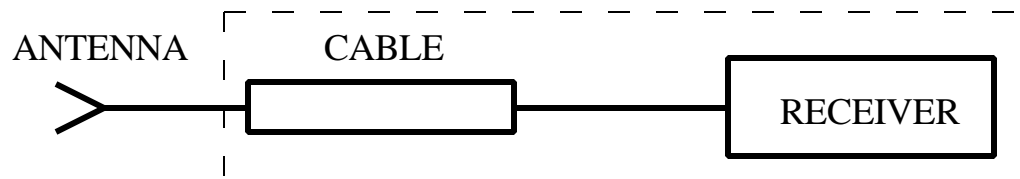
## Examples (2)

---

$$R^4 = \frac{(2 \times 10^5)(10^3)^2(5)(0.03)^2}{(4p)^3(10)(1.3 \times 10^{-13})} = 3.48 \times 10^{17}$$

or  $R = 24303 \text{ m} \approx 15 \text{ miles}$ . The range can be increased by using a low-noise amplifier (LNA) before the mixer.

2. Consider the radar receiver shown below:



antenna temperature,  $T_A = 150 \text{ K}$

receiver effective temperature,  $T_{eR} = 400 \text{ K}$

cable loss: 6 dB at 290 K

noise figure of the receiver:  $F_{nR} = 1 + \frac{T_{eR}}{T_o} = 2.38$

noise figure of the cable:  $F_{nL} = \frac{1}{G_L} = L = 4$

## Examples (3)

---

noise figure of the dashed box:  $F_n = F_{nL} + \frac{F_{nR} - 1}{G_L} = 4 + \frac{1.38}{0.25} = 9.52$

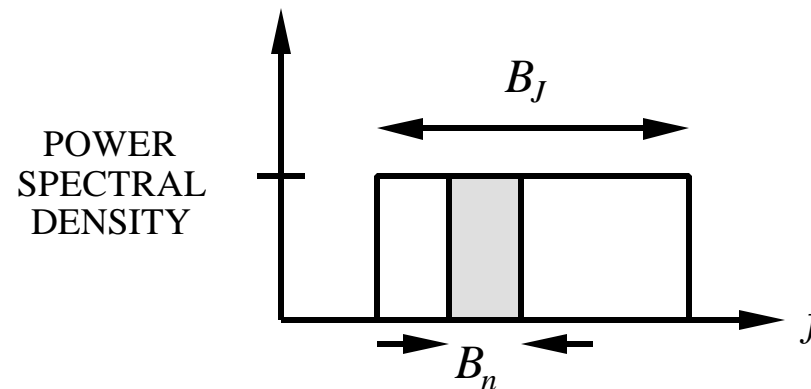
effective noise temperature of the dashed box:

$$T_e = (F_n - 1)T_o = (8.52)(290) = 2471 \text{ K}$$

Total system noise temperature:

$$T_s = T_A + T_e = 2621 \text{ K}$$

3. We calculate the equivalent noise temperature of a wideband jammer operating against a narrowband radar



# Examples (4)

---

The radar only sees a fraction of the jammer's radiated power

$$P_J \left( \frac{B_n}{B_J} \right)$$

The jammer can be modeled as a noise source at temperature  $T_J$

$$N_o \equiv P_{rJ} = k T_J B_n$$

From our earlier result the jammer power received by the radar is

$$P_{rJ} = \frac{P_J G_J G(\mathbf{q}_J) I^2}{(4\pi R_J)^2} \left( \frac{B_n}{B_J} \right)$$

which gives an equivalent jammer temperature of

$$T_J = \frac{P_{rJ}}{k B_n} = \frac{P_J G_J G(\mathbf{q}_J) I^2}{(4\pi R_J)^2 k B_J}$$

This temperature is used in the radar equation to assess the impact of jammer power on the radar's SNR.

# Examples (5)

---

4. Pulse radar with the following parameters:

$$T_{fa} = 30 \text{ days}, B_n = 1 \text{ MHz}, t = 1 \text{ } \mu\text{sec}, I = 0.1 \text{ m}, G = 30 \text{ dB} = 1000,$$

$$\mathbf{q}_{B_{el}} = 34^\circ, \mathbf{q}_{B_{az}} = 1.2^\circ, P_d = 0.95 \text{ for } \mathbf{s} = 10 \text{ m}^2 \text{ and } R = 100 \text{ mi (=161 km)}$$

$$F = 5.8 \text{ dB for the receiver}, T_A = 100 \text{ K}$$

(a) Peak power required to achieve  $P_d = 0.95$  on a single hit basis

$$P_{fa} = \frac{1}{B_n T_{fa}} = \frac{10^{-6}}{(30)(24)(3600)} = 3.86 \times 10^{-13}$$

From Fig. 2.6,  $(S/N)_1 = 16.3 \text{ dB} = 42.7$

$$P_t = \frac{(4p)^2 k(T_A + T_e) B_n (S/N)_{\min} R_{\max}^4}{G A_e \mathbf{s}}$$

$$= \frac{(4p)^2 (1.38 \times 10^{-23}) (100 + 812) (10^6) (42.7) (1.61 \times 10^5)^4}{(1000)(0.8)(10)}$$

$$P_t = 0.715 \times 10^7 \text{ W}$$



# Examples (6)

---

(b) PRF for 100 mi unambiguous range

$$f_p = \frac{c}{2R_u} = \frac{3 \times 10^8}{2(1.61 \times 10^5)} = 932 \text{ Hz}$$

(c) Number of pulses that must be integrated noncoherently for a 10 dB improvement in SNR (i.e., reduce the peak power requirement by 10 dB)

$$I_i = 10 \text{ dB} = 10$$

From Fig. 2.7(a) for,  $P_d = 0.95$  and  $n_f = 1/P_{fa} = 2.59 \times 10^{12}$  the number of pulses is

$$n_B \approx 15$$

(d) Maximum antenna scan rate if  $I_i = 10$  with a PRF of 800 Hz

$$\omega_s = \frac{\mathbf{q}_B f_p}{n_B} = \frac{(1.2)(800)}{15} = 64^\circ / \text{sec} = 10.7 \text{ rpm}$$

# Examples (7)

---

(e) Effective temperature of the receiver

$$T_e = (F - 1)T_o = (3.8 - 1)(290) = 814 \text{ K}$$

(f) If  $F$  is reduced 3 dB the increase in maximum detection range is as follows:

$$F = 2.8 \text{ dB}$$

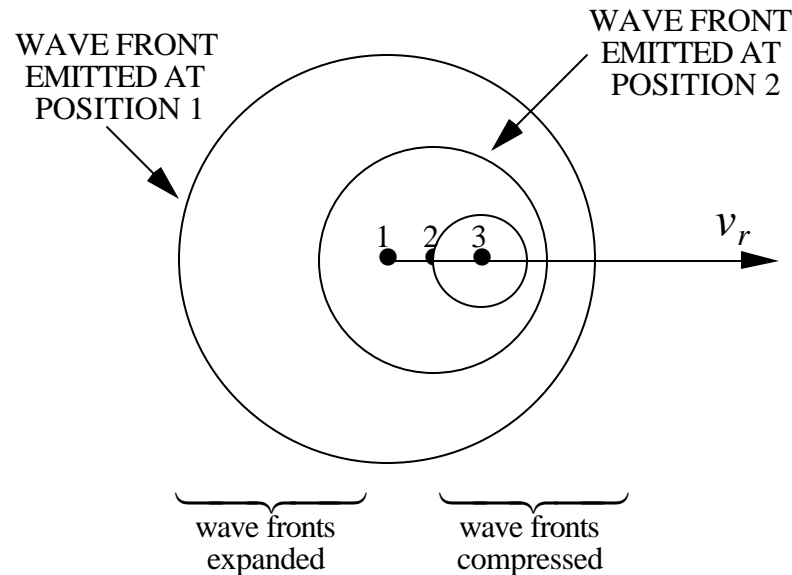
$$T_e = (0.9)(290) = 262 \text{ K}$$

$$R_{\max}^4 \propto \frac{1}{T_A + T_e}$$
$$\frac{R_{\max_2}}{R_{\max_1}} = \left( \frac{914}{362} \right)^{1/4}$$

$$R_{\max_2} = 1.26 R_{\max_1} = 126 \text{ miles}$$

# Doppler Frequency Shift (1)

Targets in motion relative to the radar cause the return signal frequency to be shifted as shown below



The time-harmonic transmitted electric field has the form  $|\vec{E}_t| \propto \cos(\omega_c t)$ . The received signal has the form  $|\vec{E}_s| \propto \cos(\omega_c t - 2kR)$ , where the factor 2 arises from the round trip path delay. Define  $\Phi(t) = -2kR$  and  $R = R_o + v_r t$  ( $v_r$  is the radial component of the relative velocity vector).

# Doppler Frequency Shift (2)

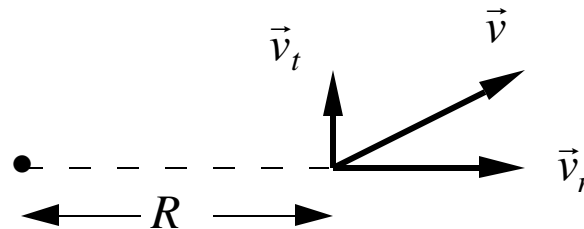
The Doppler frequency shift is given by:

$$\omega_d = \frac{d\Phi(t)}{dt} = \frac{d}{dt}(-2kR) = -2k \frac{dR}{dt} = -2k v_r$$

or in Hertz,  $f_d = -\frac{2v_r}{\lambda}$ . Rewrite the signal phase as  $\Phi(t) = -2k \left[ R_o - \left( -\frac{\omega_d}{2k} \right) t \right]$  so that

$$|\vec{E}_s| \propto \cos[(\omega_c + \omega_d)t - 2kR_o]$$

A Doppler shift only occurs when the relative velocity vector has a radial component. In general there will be both radial and tangential components to the velocity:



$$R \text{ decreasing} \Rightarrow \frac{dR}{dt} < 0 \Rightarrow f_d > 0 \text{ (closing target)}$$

$$R \text{ increasing} \Rightarrow \frac{dR}{dt} > 0 \Rightarrow f_d < 0 \text{ (receding target)}$$

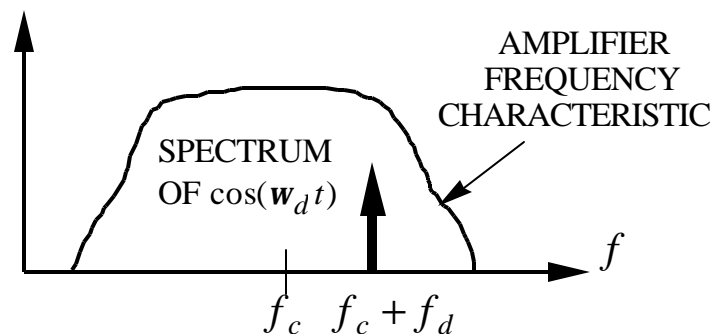
# Doppler Frequency Shift (3)

The echo returned from the target varies as  $|\vec{E}_s| \propto \cos[(\omega_c \pm \omega_d)t - 2kR_o]$ , where the + sign is used for closing targets and - for receding targets. However, mixing causes the sign to be lost. For example, mixing the return with the carrier (homodyning) gives

$$\cos(\omega_c t \pm \omega_d t) \cos(\omega_c t) = \frac{1}{2} [\cos(\pm \omega_d t) + \cos(2\omega_c t \pm \omega_d t)]$$

Although the second term in brackets contains the sign information it is too high to be of use in a narrowband radar. The sign can be recovered using I and Q channels.

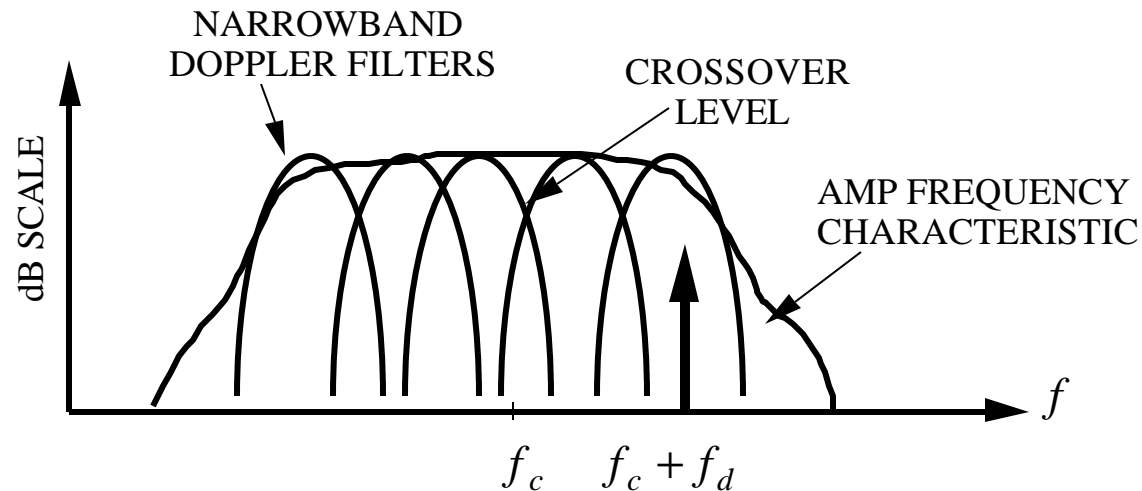
Another problem: the  $f_d$  signal is narrow and the amplifier  $B_n$  much larger so the SNR is too low.



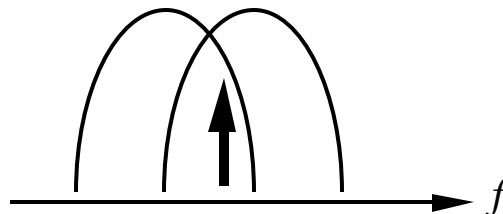
The solution is to use a collection of filters with narrower bandwidths.

# Doppler Filter Banks

The radar band is divided into narrow sub-bands. Ideally there should be no overlap in their frequency characteristics.



The noise bandwidth of the doppler filters is small compared to that of the amplifier, which improves the SNR. Velocity estimates can be made by monitoring the power out of each filter. If a signal is present in a filter, the target's velocity range is known. The energy outputs from adjacent filters can be used to interpolate velocity.



# Example

---

CW radar example:

$$f = 18 \text{ GHz } (l = 0.0167 \text{ m})$$

target speed range: mach 0.25 to mach 3.75 (mach 1 = 334.4 m/s)

resolution = 10 m/s

homodyne receiver

(a) What is the required spectral range for the filter bank?

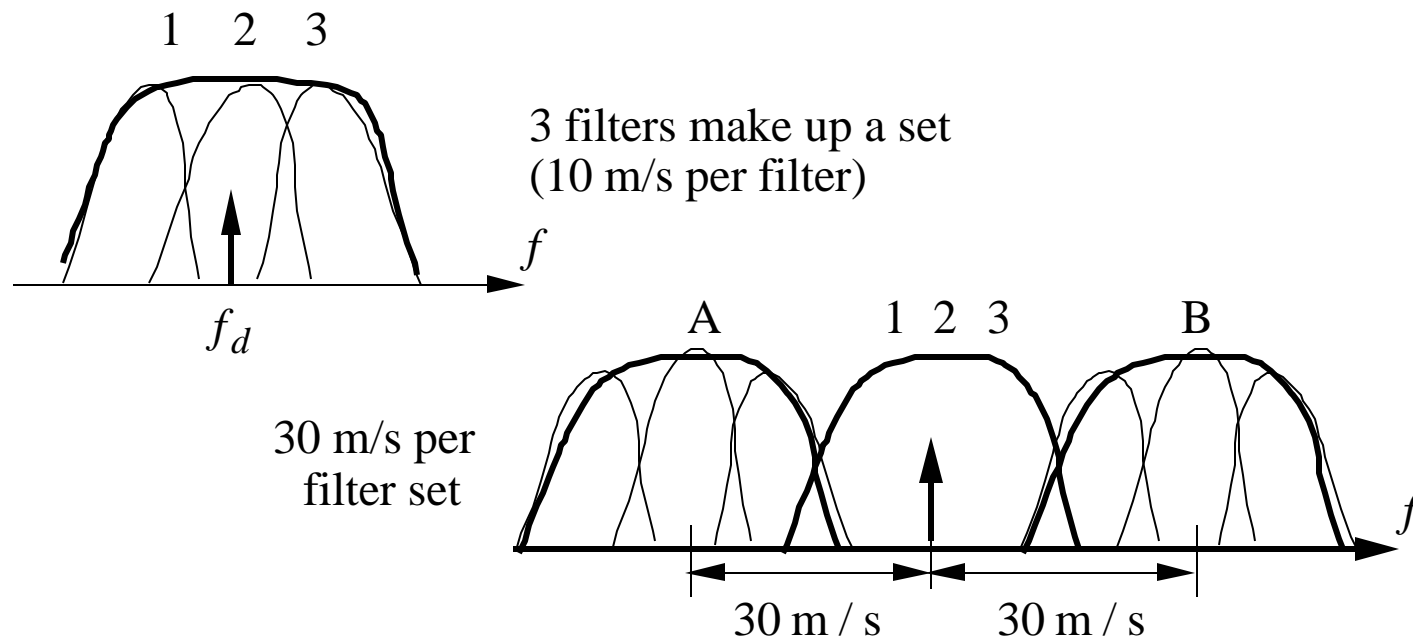
$$\left. \begin{array}{l} \text{lowest frequency : } f_{d1} = \frac{(2)(83.6)}{0.0167} = 10 \text{ kHz} \\ \text{highest frequency : } f_{d2} = \frac{(2)(1254)}{0.0167} = 150 \text{ kHz} \end{array} \right\} \Rightarrow 10 \text{ kHz} \leq f \leq 150 \text{ kHz}$$

(b) How many filters are required?

$$N_f = \frac{\Delta f_2 - \Delta f_1}{\Delta f} = \frac{v_{r2} - v_{r1}}{\Delta v} = \frac{1254 - 83.6}{10} = 117$$

# Example

- (c) When a target is located in a particular filter, the two adjacent filters are also monitored in case the velocity changes. It takes 0.5 second to shift between filter sets. How fast must a target accelerate to defeat the radar?



To defeat the radar the target's doppler must jump to A or B

$$a_r = (\pm 30 \text{ m/s}) / 0.5 \text{ s} = \pm 60 \text{ m/s}^2$$



# I and Q Representation

---

Coherent detection requires dealing with the envelope of a signal,  $g(t)$  and the phase of the sinusoidal carrier,  $\Phi(t)$ . They need not be measured directly, but can be derived using in-phase ( $I$ ) and quadrature ( $Q$ ) channels as follows. For narrowband signals we can write

$$s(t) = g(t) \cos(\omega_c t + \Phi(t))$$

or, in terms of  $I$  and  $Q$  components

$$s(t) = g_I(t) \cos(\omega_c t) - g_Q(t) \sin(\omega_c t)$$

where

$$g_I(t) = g(t) \cos(\Phi(t))$$

$$g_Q(t) = g(t) \sin(\Phi(t))$$

Define the complex envelope of the signal as

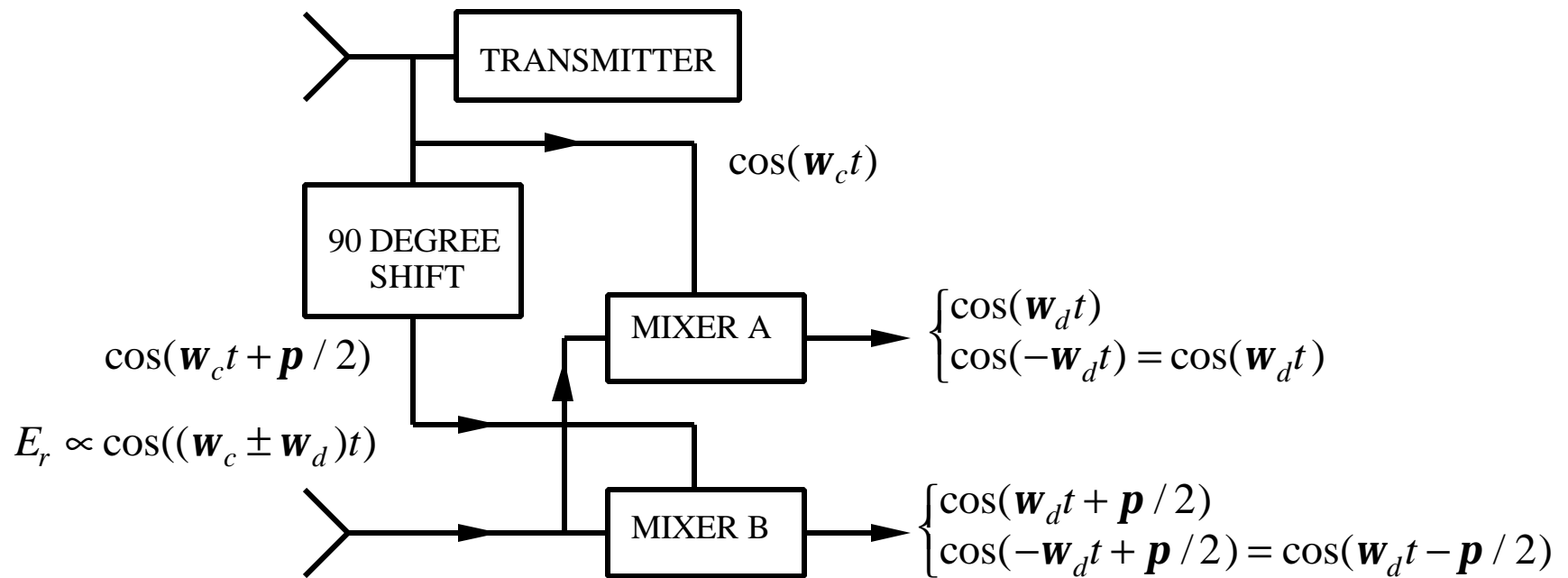
$$u(t) = g_I(t) + j g_Q(t)$$

Thus the narrowband signal can be expressed as

$$s(t) = \operatorname{Re} \left\{ u(t) e^{j\omega_c t} \right\}$$

# Doppler Frequency Shift (4)

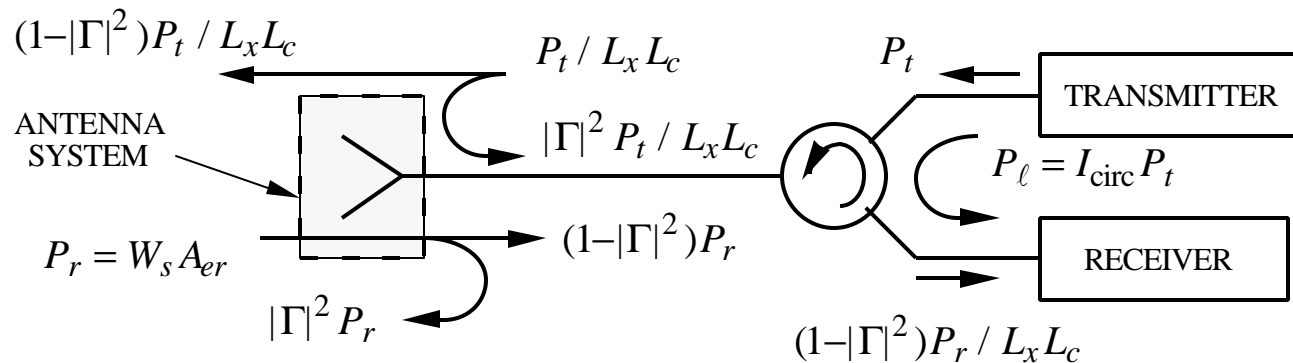
Recovering the sign of the doppler shift using *I* and *Q* channels



Positive doppler shift results in a phase lead; negative doppler shift results in a phase lag.

# CW Radar Problems (1)

## 1. Transmit/receive leakage:



$P_t$  = power out of transmitter

$P_\ell$  = power leaked directly from transmitter to receiver

$P_r$  = power scattered by target and collected by the antenna

$|\Gamma|$  = magnitude of the antenna voltage reflection coefficient (related to its VSWR)

$L_x$  = transmission line loss ( $\geq 1$ )

$L_c$  = circulator loss ( $\geq 1$ )

$I_{circ}$  = circulator isolation (fraction of incident power leaked in the reverse direction)

If higher order reflections can be ignored, then the total signal at the receiver is

$$P_{tot} = \underbrace{(1-|\Gamma|^2)P_r / L_x L_c}_{\text{TARGET RETURN}} + \underbrace{I_{circ} P_t}_{\text{LEAKAGE}} + \underbrace{|\Gamma|^2 P_t / (L_x L_c)^2}_{\text{ANTENNA MISMATCH}}$$

# CW Radar Problems (2)

---

Comments regarding leakage:

1. Circulator isolation is in the range of 30 to 100 dB. It can be increased at the expense of size, weight, volume, and insertion loss.
2. Leakage can be reduced by using two separate antennas. There is still leakage which arises from
  - near field coupling of the antennas
  - reflection from close in clutter
  - surface guided waves on platform or ground

Example: receiver MDS = -130 dBW (= -100 dBm)  
 peak transmitter power = 100 W = 20 dBW

To keep the leakage signal below the MDS requires

$$P_{\ell} = I_{\text{circ}} P_t \leq -130 \text{ dBW} \Rightarrow 20 \text{ dBW} - I_{\text{circ}}, \text{ dB} \leq -130 \text{ dBW} \Rightarrow -I_{\text{circ}}, \text{ dB} = -150 \text{ dB}$$

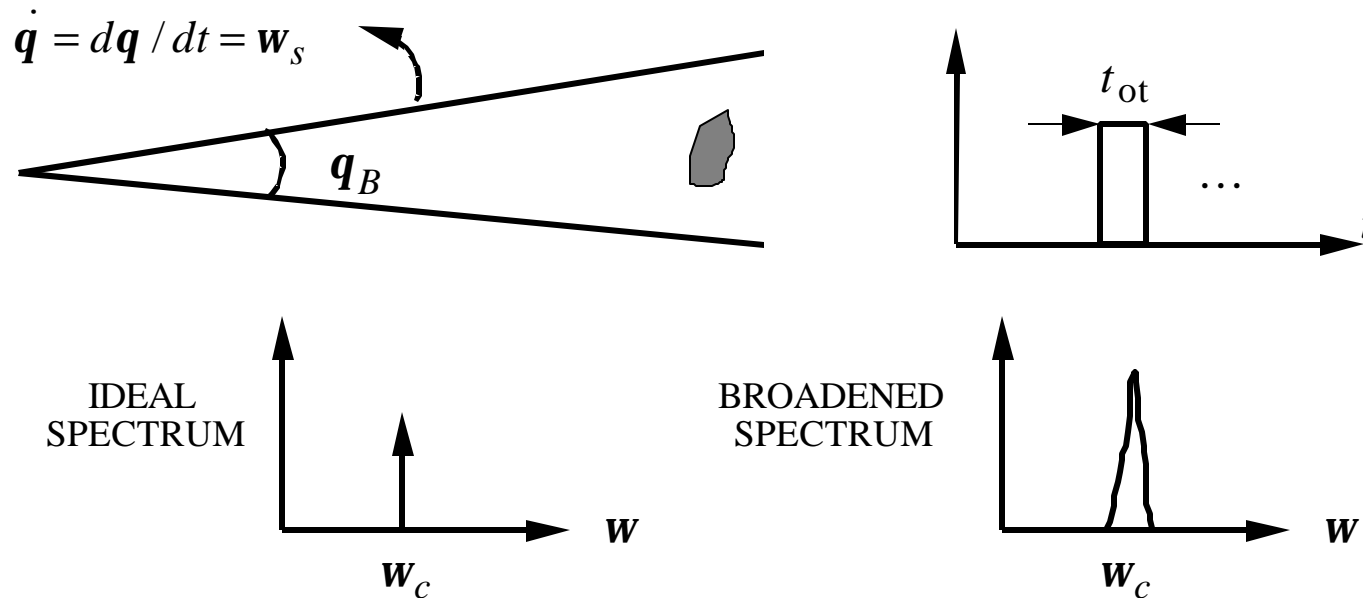
Note that circulator isolation is given in positive dB, but the negative sign is implied. Thus the required isolation is

$$I_{\text{circ}}, \text{ dB} = 150 \text{ dB}$$

# CW Radar Problems (3)

## 2. Spectrum broadening caused by:

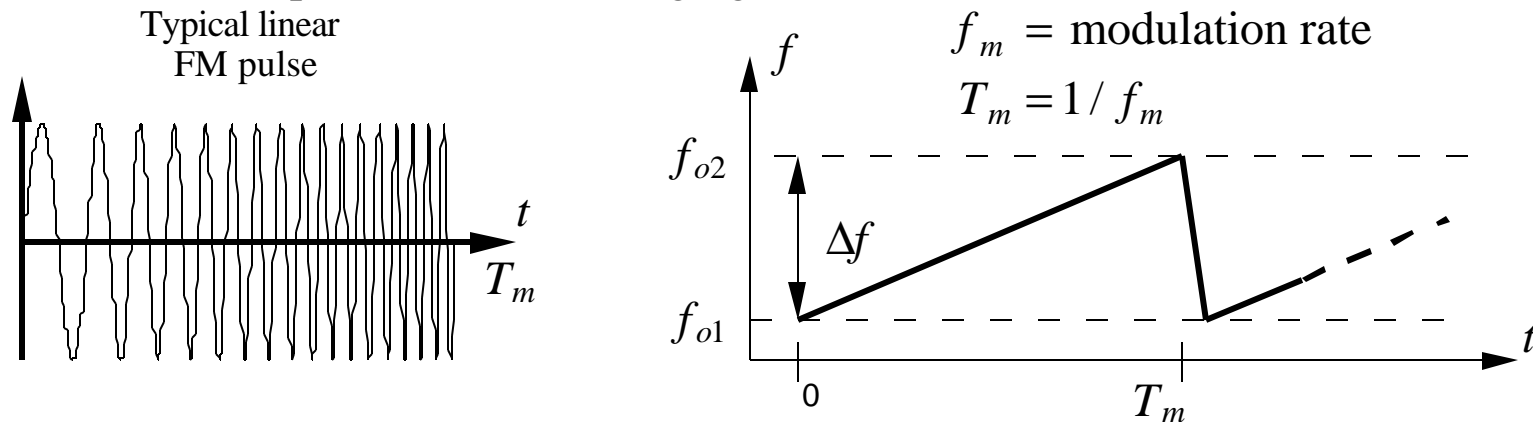
### 1. Finite duration illumination due to antenna scanning



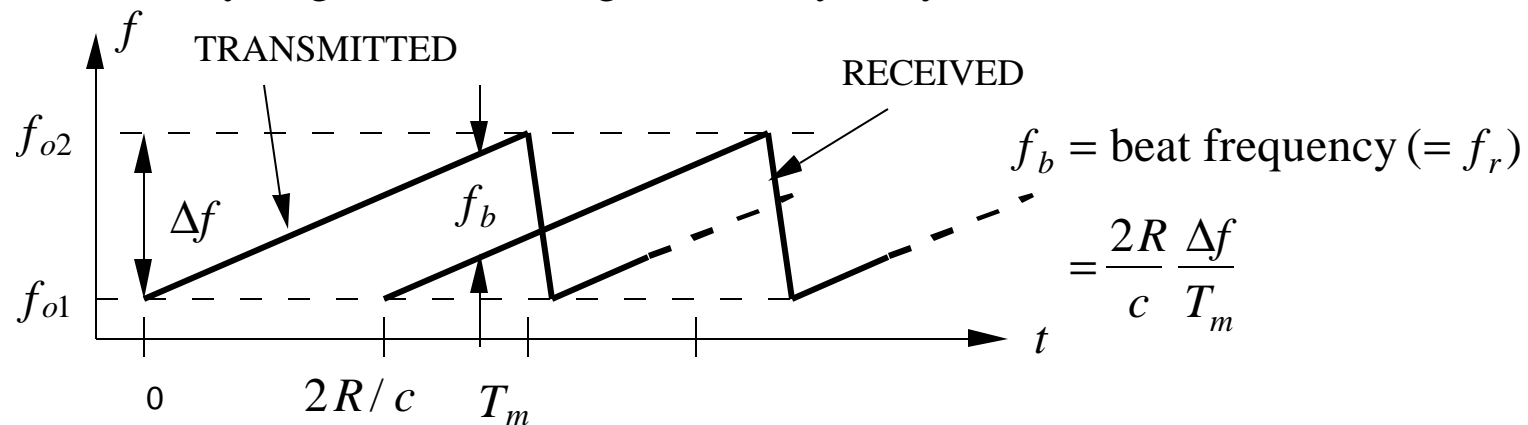
2. Modulation of the echo by target moving parts and aspect changes
3. Acceleration of the target

# Frequency Modulated CW (FMCW)

Conventional CW radars cannot measure range. To do so the transmit waveform must be "tagged." This can be done by modulating the frequency periodically with time. This technique is called FM ranging.

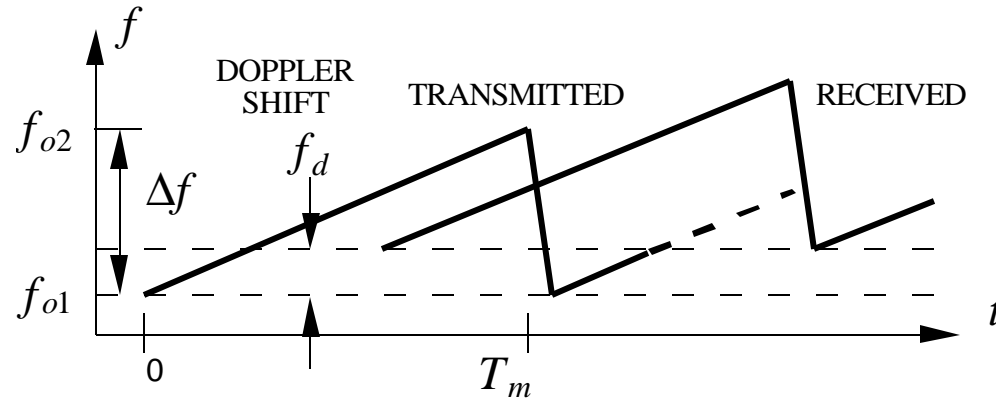


For a stationary target, the echo signal is delayed by the transit time  $2R/c$

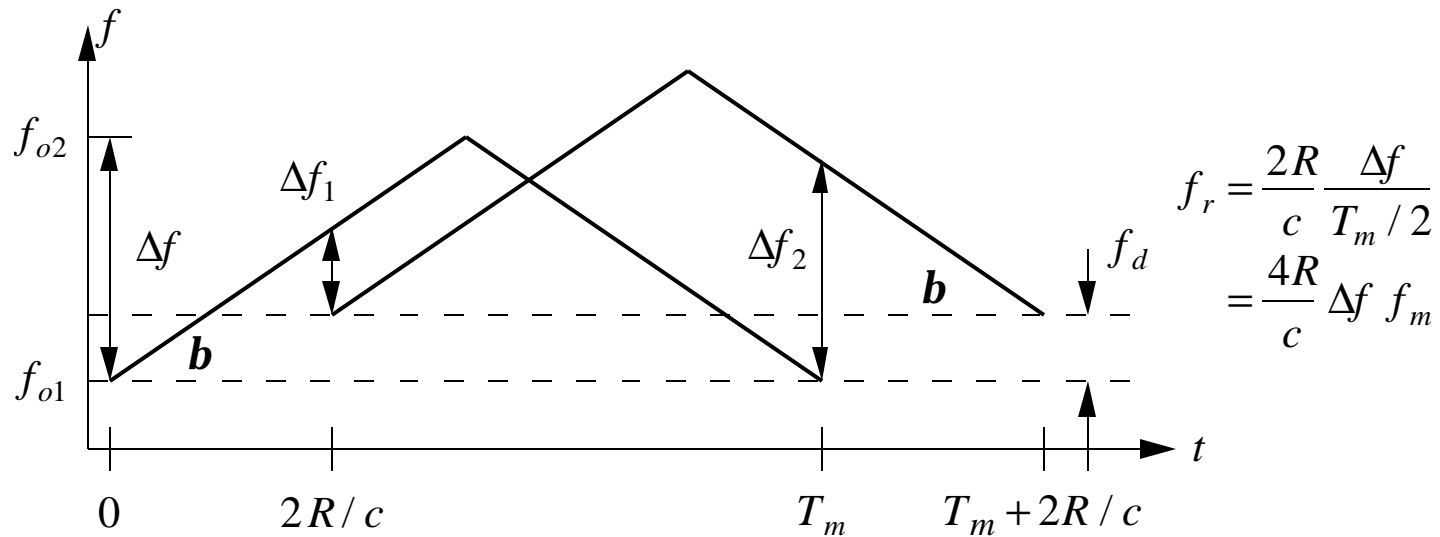


# FMCW (2)

If the target is in motion the received waveform might be doppler shifted



Use a two-slope modulation to eliminate the doppler frequency



$$f_r = \frac{2R}{c} \frac{\Delta f}{T_m/2}$$

$$= \frac{4R}{c} \Delta f f_m$$

# FMCW (3)

---

Range can be measured if  $\Delta f_1$  and  $\Delta f_2$  are known

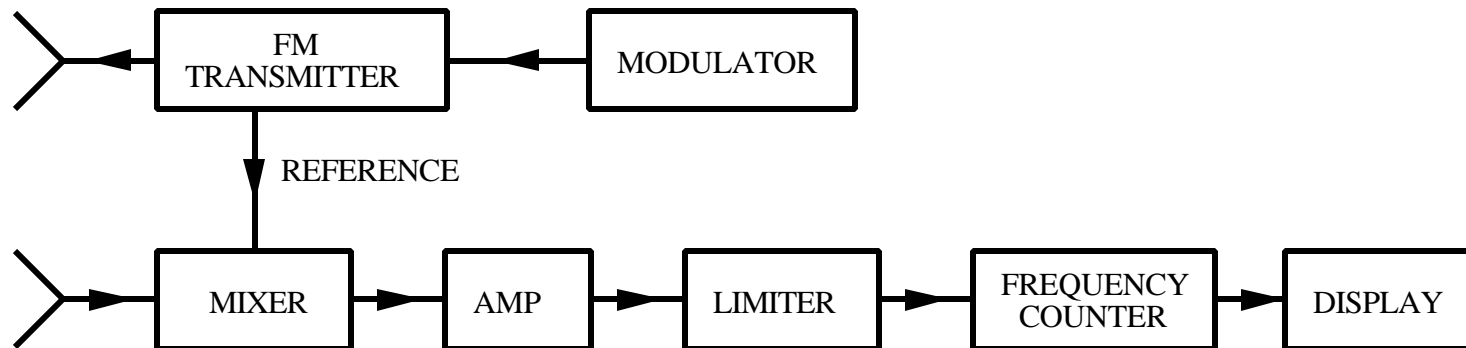
$$\tan \mathbf{b} = (\Delta f_1 + f_d)/(2R/c)$$

$$\tan \mathbf{b} = (\Delta f_2 - f_d)/(2R/c)$$

Add the two equations

$$2 \tan \mathbf{b} = (\Delta f_1 + \Delta f_2)/(2R/c) \Rightarrow R = \frac{(\Delta f_1 + \Delta f_2)c}{4 \tan \mathbf{b}}$$

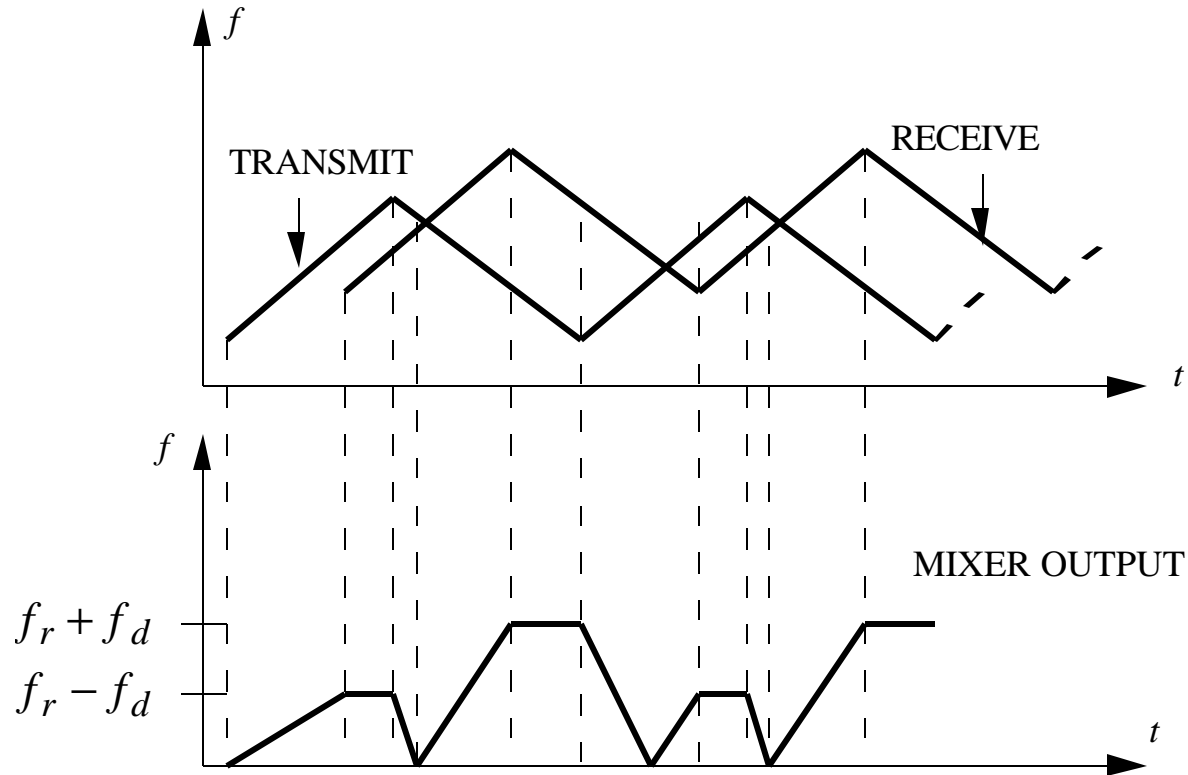
Block diagram:





# FMCW (4)

Waveform out of mixer:

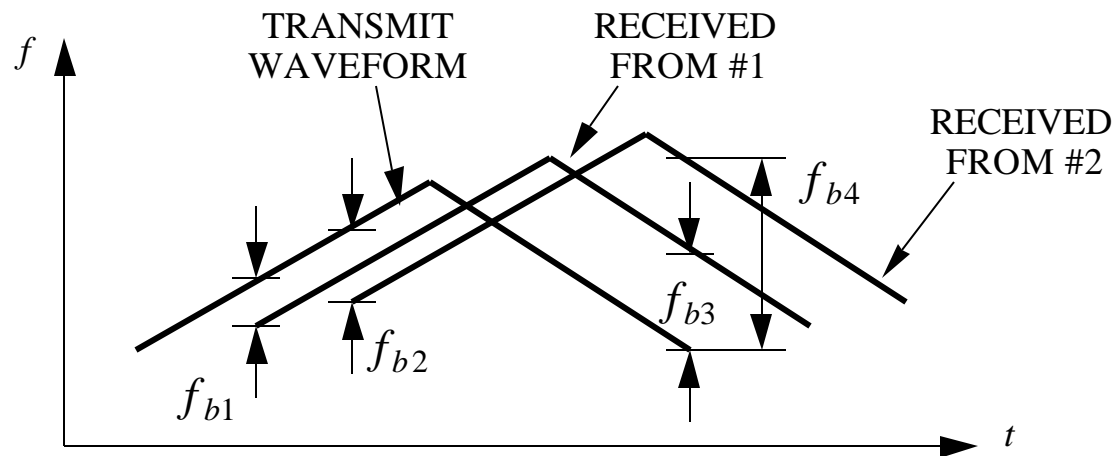


Restriction:

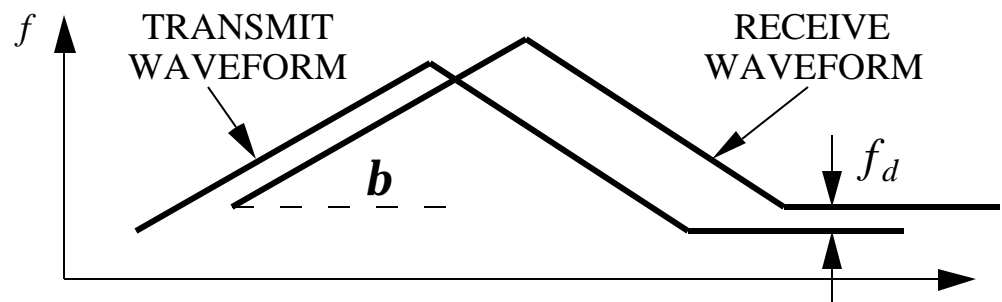
$$\frac{1}{f_m} \gg \frac{2R}{c}$$

# FMCW Complications

1. Multiple targets cause "ghosting." There are two beat frequencies at the end of each segment. The radar does not know how to pair them.

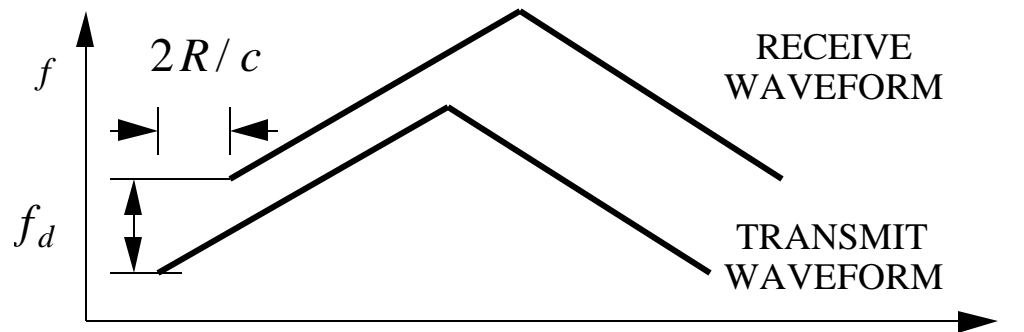


Solution: add a constant frequency segment to measure  $f_{d1}$  and  $f_{d2}$



# FMCW Complications

2. Doppler frequency greater than  $\frac{2R}{c} \tan \mathbf{b}$  (which occurs in air-to-air situations) complicates the formulas for the frequency differences.



Sinusoidal modulation can also be used. The range is determined from the average (over one cycle) beat frequency.

Example: Find the range if the low and high beat frequencies out of the mixer are  $\Delta f_1 = f_r - f_d = 4825 \text{ Hz}$  and  $\Delta f_2 = f_r + f_d = 15175 \text{ Hz}$  and the sweep rate is  $\tan \mathbf{b} = 10 \text{ Hz/msec} = 10 \times 10^6 \text{ Hz/sec}$ .

$$\text{Compute range : } R = \frac{(15175 + 4825)(3 \times 10^8)}{4(10 \times 10^6)} = 150000 \text{ m}$$

# MTI and Pulse Doppler Radar

---

The doppler frequency shift can be used with pulse waveforms to measure velocity.

The radars generally fall into one of two categories:

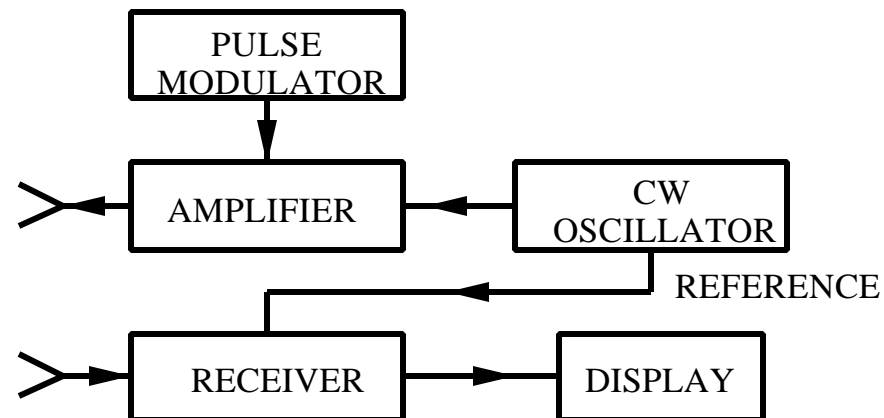
1. moving target indication (MTI)

generally uses delay line cancelers  
ambiguous velocity measurement  
unambiguous range measurement

2. pulse doppler radar

generally uses range gated doppler filters  
unambiguous velocity measurement  
ambiguous range measurement

The main feature of both is the use of a coherent reference signal.

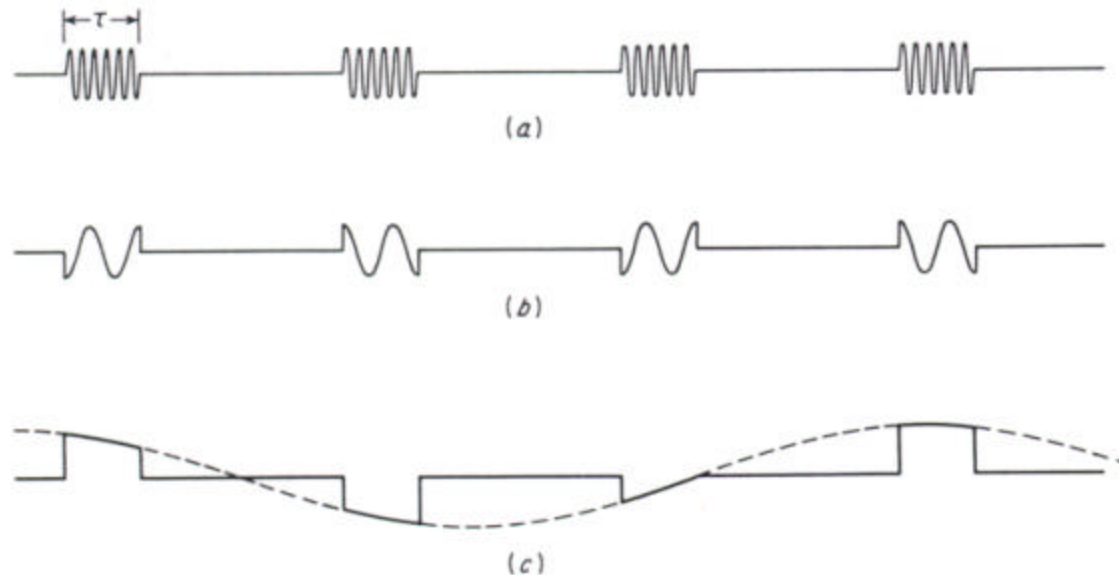


# MTI (1)

The doppler is a sinusoidal modulation of the transmitted waveform. For a pulse train:

1. large doppler shift: modulation of the waveform is rapid (e.g., a ballistic missile). Only need one or two pulses to measure doppler shift
2. small doppler shift: modulation of the waveform is slow (e.g., aircraft). Need many pulses to measure doppler shift

("Large" and "small" are by comparison to  $1/t$ .) From Fig. 3.4 in Skolnik: (a) RF echo pulse train, (b) video pulse train for  $f_d > 1/t$ , (c) for  $f_d < 1/t$ .

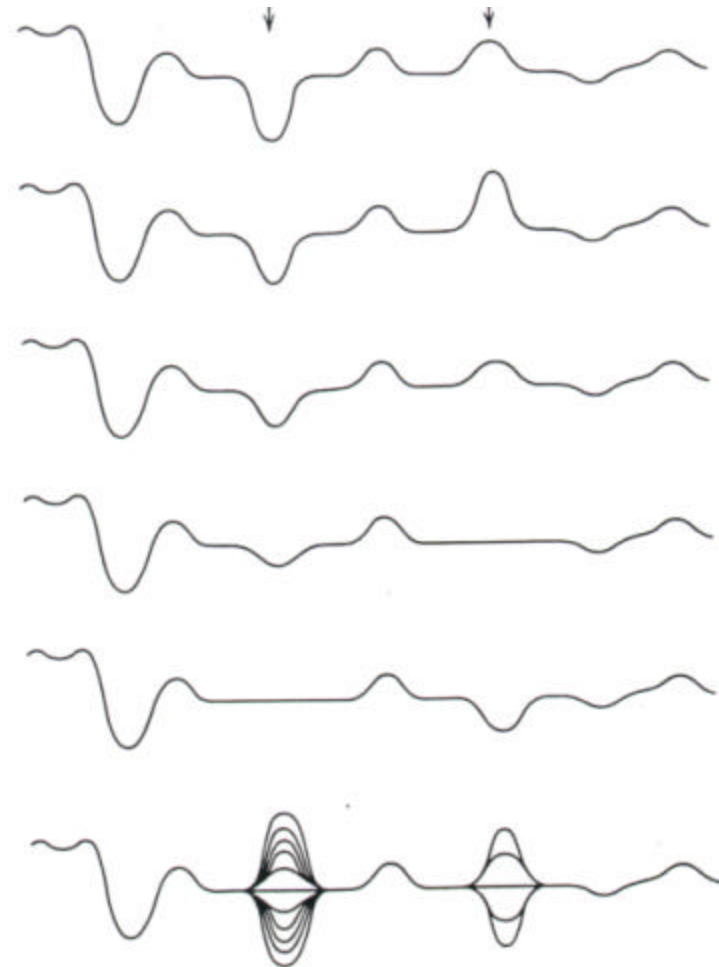


# MTI (2)

---

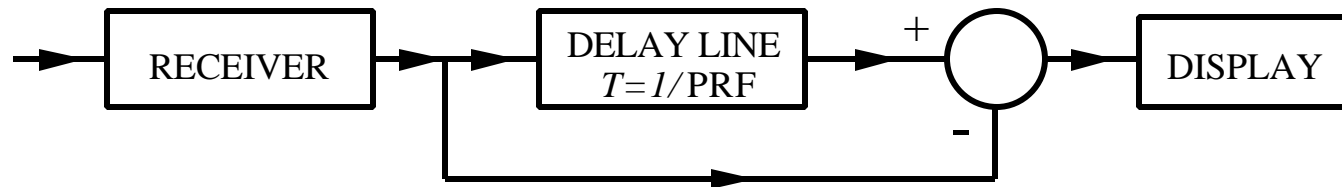
On successive "A" scope traces (amplitude vs. range), moving target returns will vary in amplitude; fixed target returns are constant.

Fig. 3.5 in Skolnik (the bottom curve is the superposition of many sweeps)



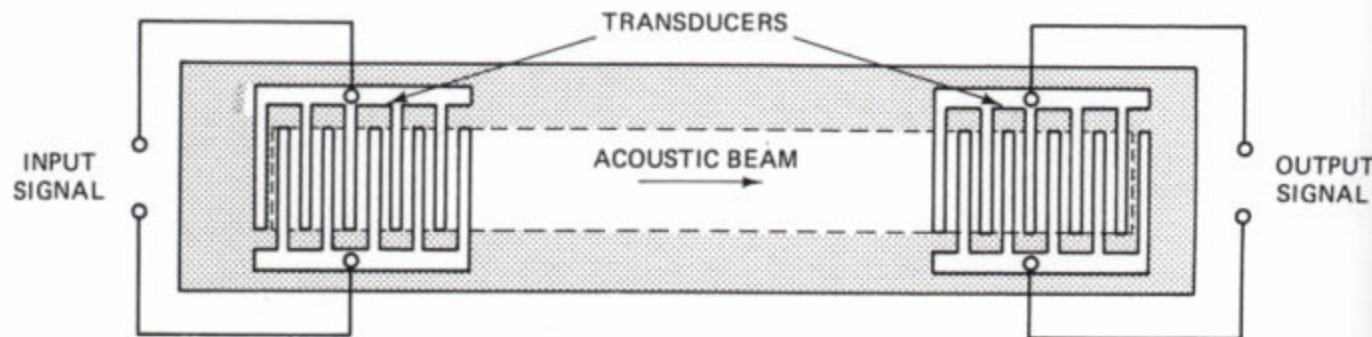
# MTI (3)

PPI displays use a delay line canceler



If two successive pulses are identical then the subtracted signal is zero; if two successive pulses are not identical then the subtraction results in a nonzero "residue."

The delay time is equal to the PRF. Typical values are several milliseconds, which requires very long line lengths for electromagnetic waves. Usually acoustic devices are used. The velocity of acoustic waves is about  $10^{-5}$  of that for electromagnetic waves.



(From *Acoustic Waves: Devices, Imaging and Analog Signal Processing*, by Kino)

# PD and MTI Problem: Eclipsing

---

To protect the receiver from transmitter leakage, the receiver is usually shut down during the transmission of a pulse. Eclipsing occurs when a target echo arrives during a transmit segment, when the radar receiver is shut down.

Points to note:

1. Targets are generally not completely eclipsed; usually some of the return gets through.
2. Partial eclipsing results in a loss of SNR because some of the target return is discarded.
3. The average eclipsing loss is given approximately by

$$L_{ec} \approx \int_0^t (t/t)^2 dt + \int_t^{t_v} dt + \int_{t_v}^{t_v+t} (t_v + t - t)^2 / t dt$$

where  $t_v$  is the video integration time. Normalization by the PRF gives

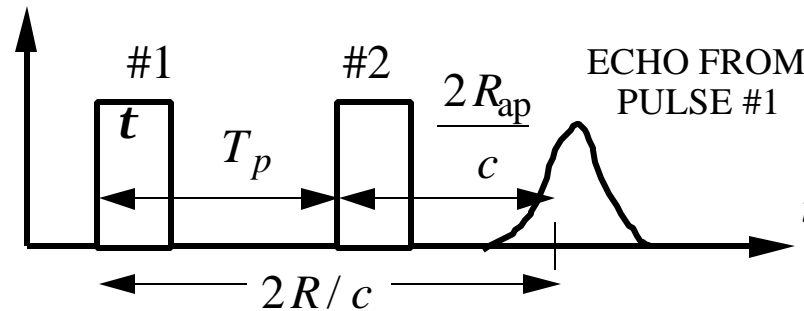
$$L_{ec} \approx \left( \underbrace{t_v \cdot \text{PRF}}_{\text{RECEIVE DUTY FACTOR}} - \underbrace{t \cdot \text{PRF}/3}_{\text{TRANSMIT DUTY FACTOR}} \right)$$

4. Eclipsing can be reduced by switching PRFs.



# PD and MTI Problem: Range Ambiguities

Maximum unambiguous range is  $R_u = cT_p / 2$ . A low PRF is desirable to maximize  $R_u$ .



Example: PRF = 800 Hz,  $T_p = 0.00125$  sec,  $R = 130$  nmi (nautical miles)

- Based on the true range

$$\frac{2R}{c} = \frac{2(130)}{\underbrace{161875}_{c \text{ IN nmi/sec}}} = 0.001606 = 1.606 \text{ ms}$$

- Based on the apparent range

$$\frac{2R_{ap}}{c} = \frac{2R}{c} - T_p = 0.001606 - 0.00125 = 0.356 \text{ ms} \Rightarrow R_{ap} = 28.8 \text{ nmi}$$

# Range Ambiguities (2)

---

The apparent range depends on the PRF but the true range does not. Therefore, changing the PRF can be used to determine whether the range is true or apparent. This is called PRF switching, pulse staggering or multiple PRFs.

Choose two PRFs:  $f_1 = N_1 f_B$  and  $f_2 = N_2 f_B$  where

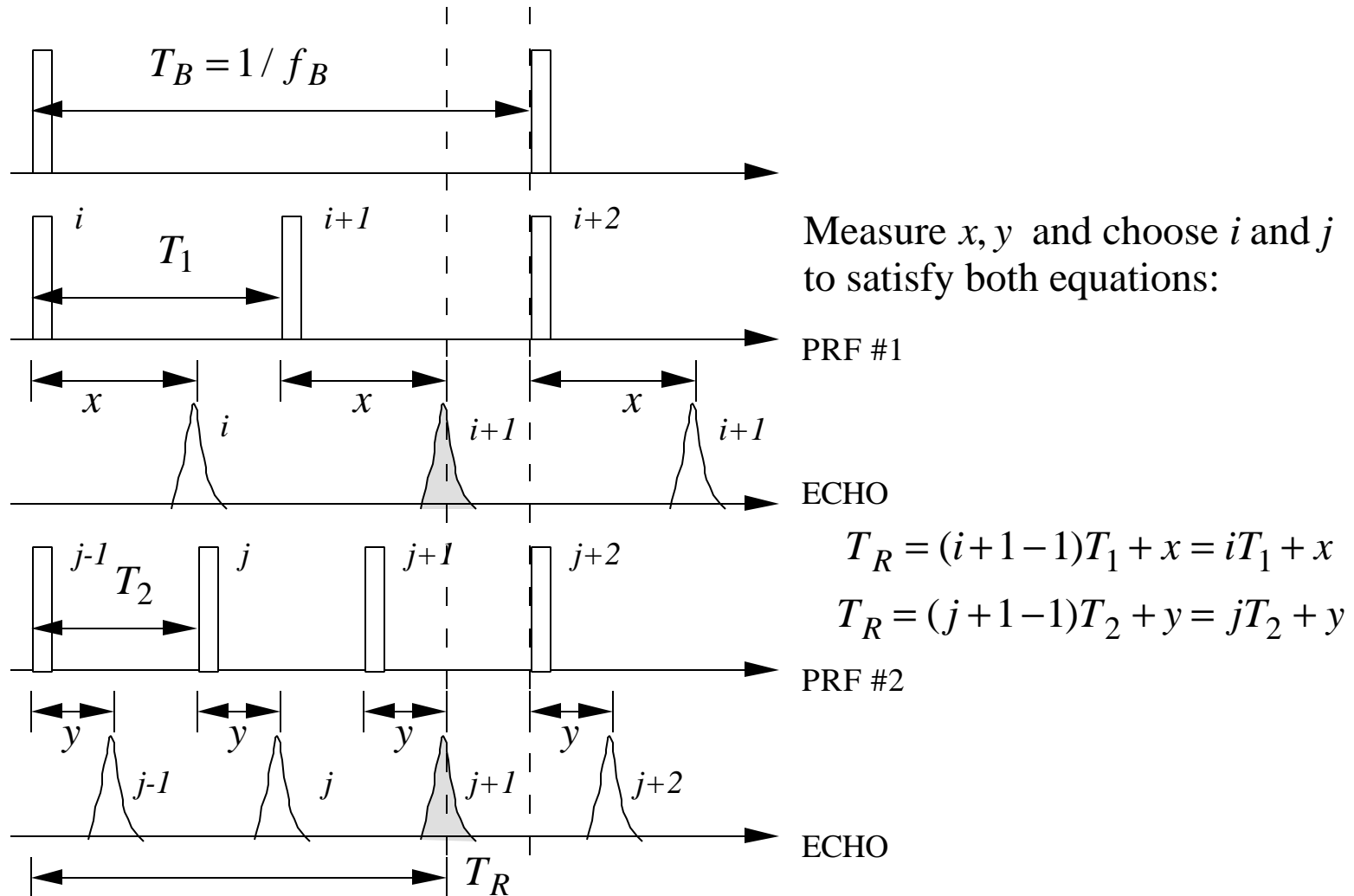
$f_B$  is the basic PRF (usually set by the unambiguous range)

$N_1, N_2$  are relatively prime integers (e.g., 11 and 13)

PRF switching method:

1. Transmit two PRFs and look for a common return which signifies a true range
2. Count the number of elapsed pulses to get the integers  $i$  and  $j$
3. Measure  $x$  and  $y$
4. Compute  $T_R$  and then  $R$

# Range Ambiguities (3)



# Example

---

We want  $R_u = 100$  nmi or  $f_B = \frac{c}{2R_u} = \frac{161875}{2(100)} = 810$  Hz

Choose  $N_1 = 79$ ,  $N_2 = 80$ :

$$f_1 = N_1 f_B = 79(810) = 63.990 \text{ kHz}$$

$$f_2 = N_2 f_B = 80(810) = 64.800 \text{ kHz}$$

Unambiguous ranges:

$$R_{u1} = c/(2f_1) = \frac{161875}{2(63.990)10^3} = 1.2648 \text{ nmi}$$

$$R_{u2} = c/(2f_2) = \frac{161875}{2(64.800)10^3} = 1.2490 \text{ nmi}$$

Assume that the target is at 53 nmi

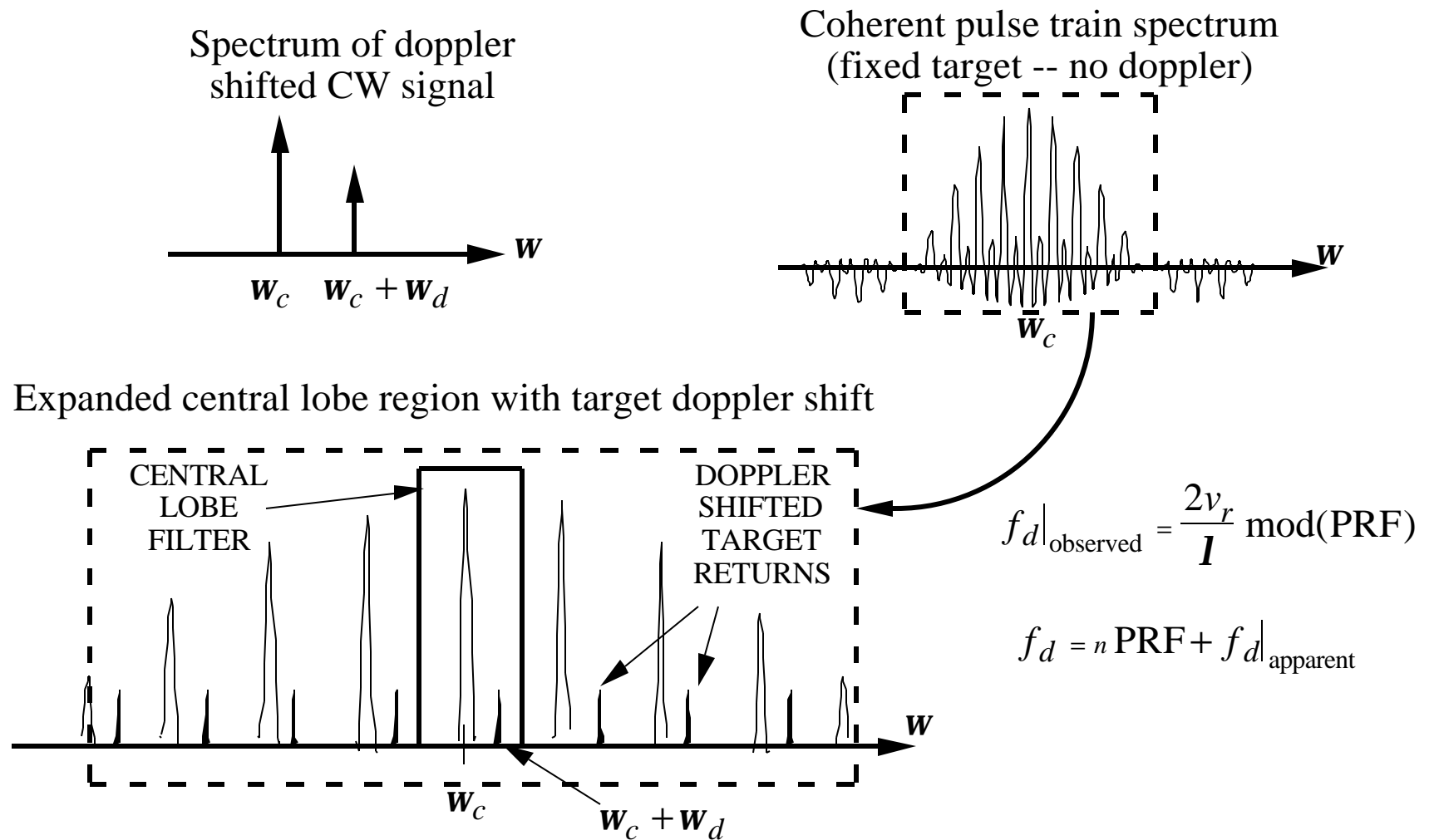
$$T_R = \frac{2(53)}{161875} = 654.8 \times 10^{-6} \text{ sec}$$

Subtract out integers

$$T_R f_1 = i + x f_1 = 41.902 \Rightarrow x = 0.902 T_1 = 14.096 \text{ nsec}$$

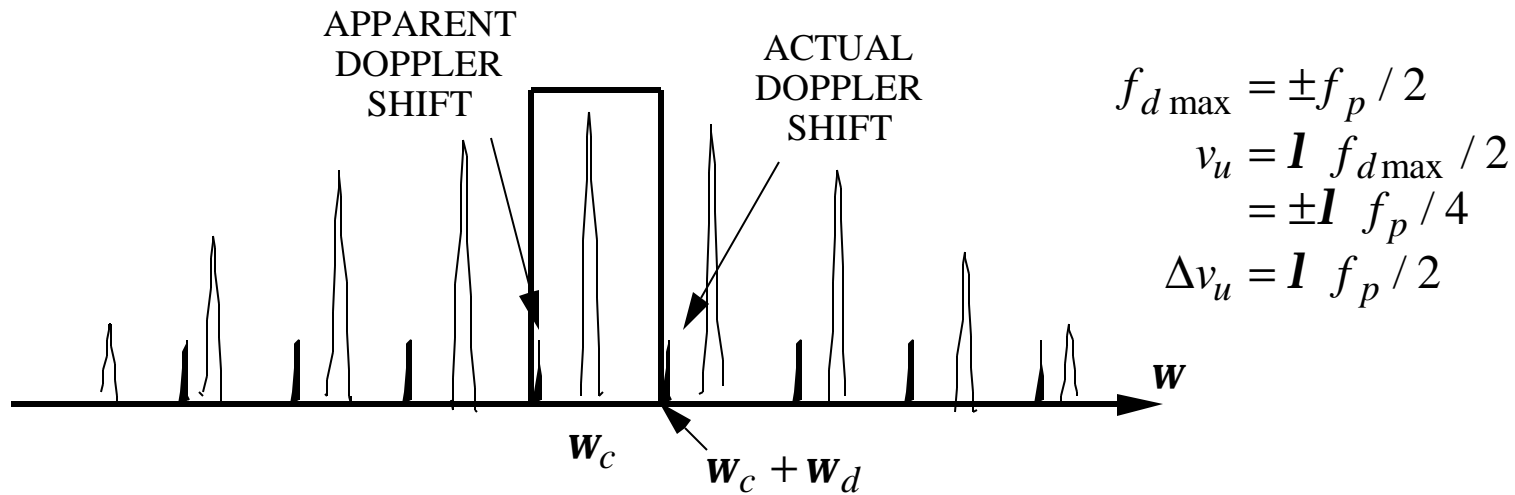
$$T_R f_2 = j + y f_2 = 42.432 \Rightarrow y = 0.432 T_2 = 6.67 \text{ msec}$$

# PD and MTI Problem: Velocity Ambiguities



# Velocity Ambiguities (2)

If  $w_d$  is increased the true target doppler shifted return moves out of the passband and a lower sideband lobe enters. Thus the doppler measurement is ambiguous.

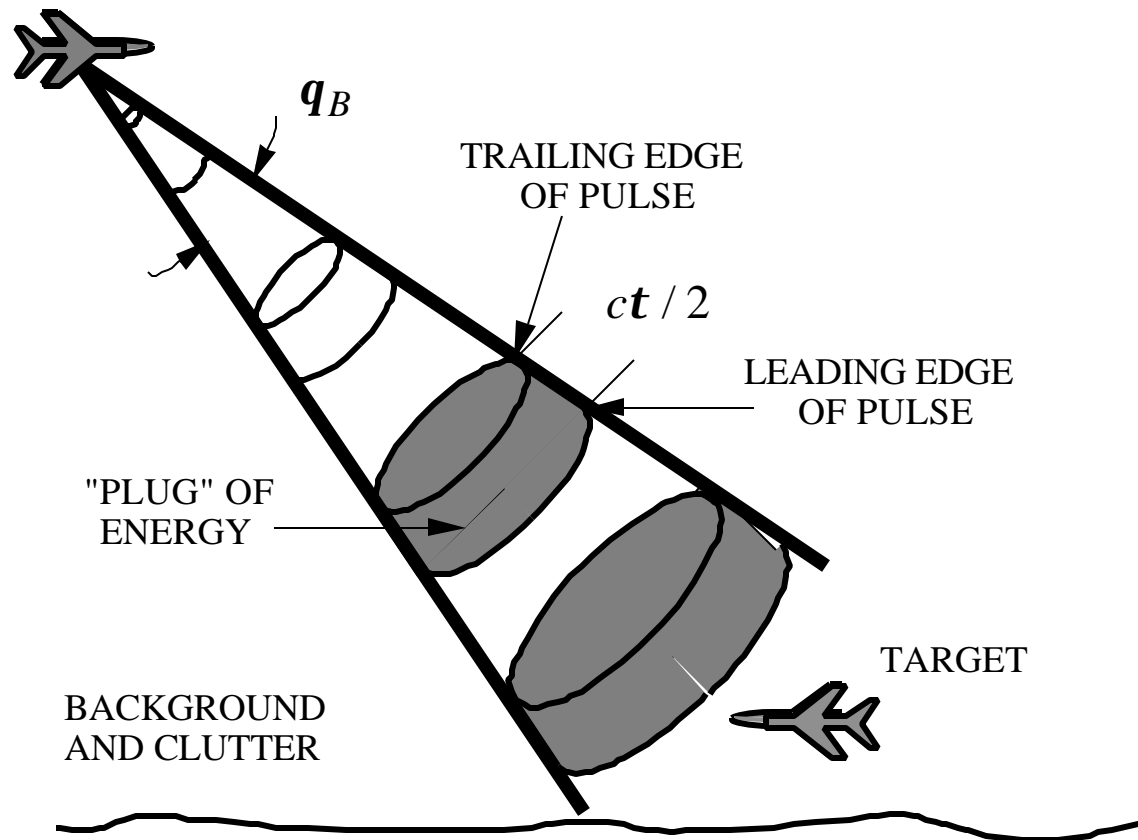


PRF determines doppler and range ambiguities:

<u>PRF</u>	<u>RANGE</u>	<u>DOPPLER</u>
High	Ambiguous	Unambiguous
Medium	Ambiguous	Ambiguous
Low	Unambiguous	Ambiguous

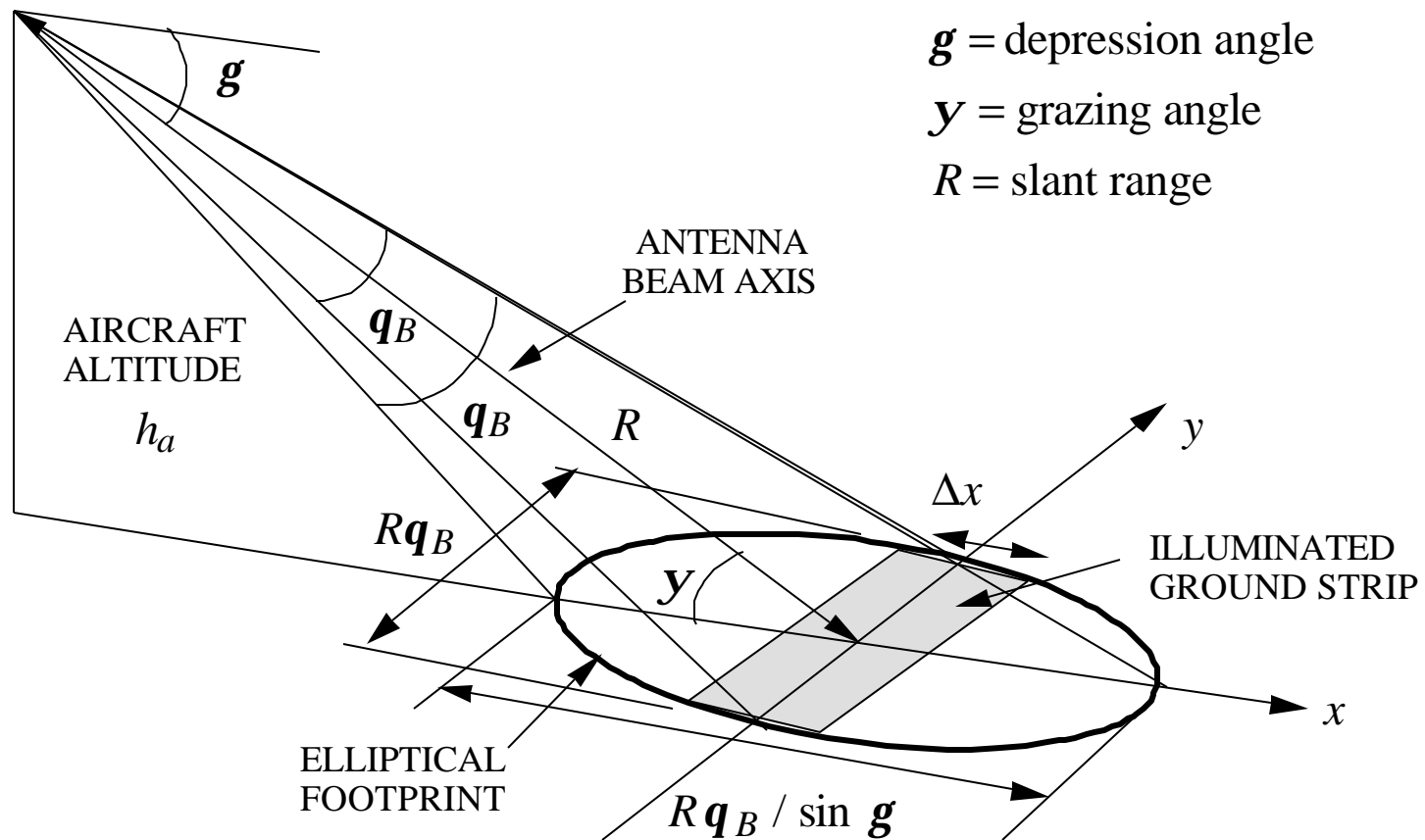
# Airborne MTI and Pulse Doppler Operation

Airborne MTI (AMTI) refers to any MTI operating on a moving platform. Motion effects include clutter spectrum frequency shift and broadening.



# Surface Clutter (1)

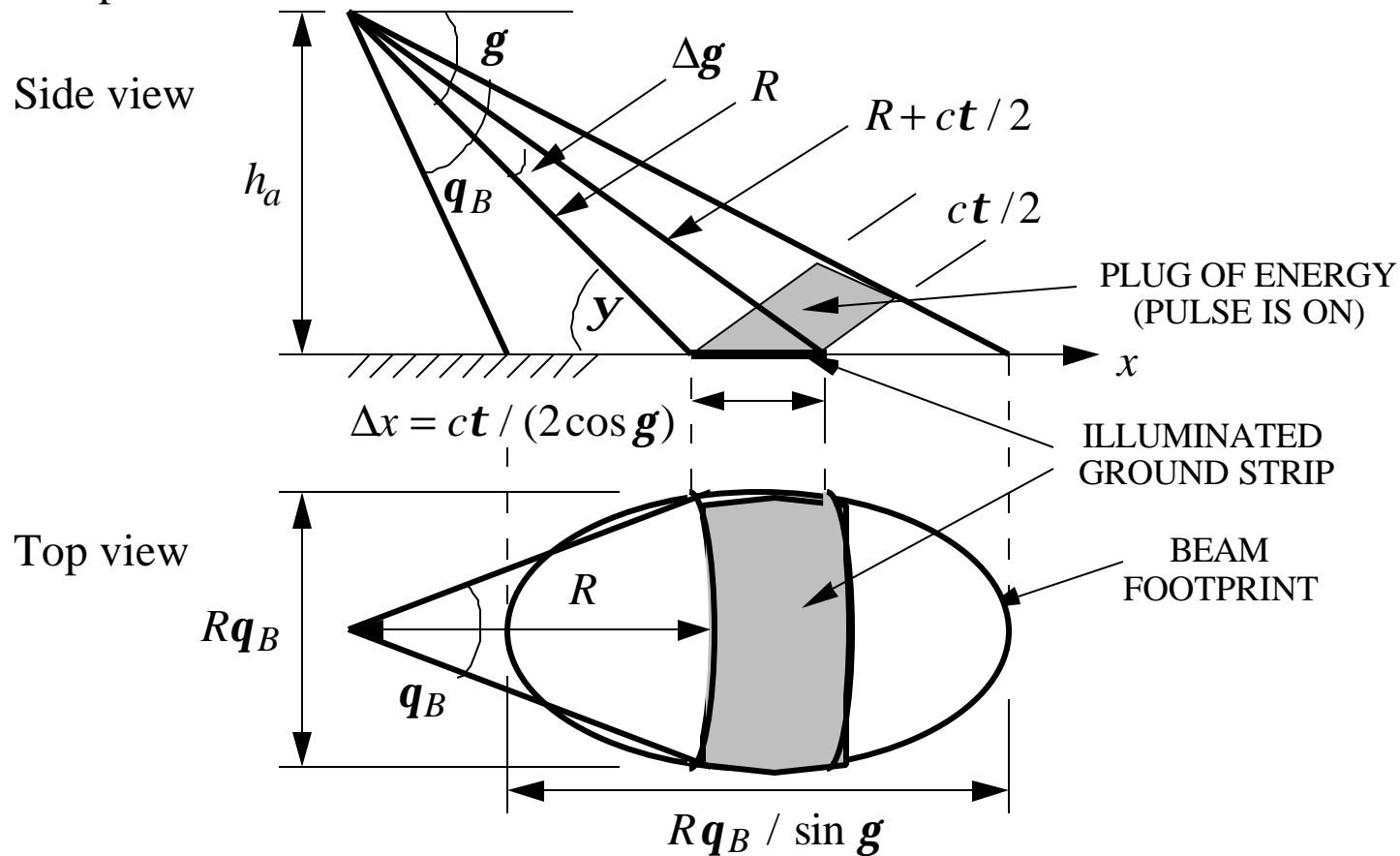
Airborne radar illuminates the ground. Simple model for the footprint dimensions:





# Surface Clutter (2)

The illumination strip is actually curved but is approximately rectangular if  $R$  is large and  $q_B$  is small. The diagram illustrates the pulse width limited case; only a portion of the footprint is illuminated.



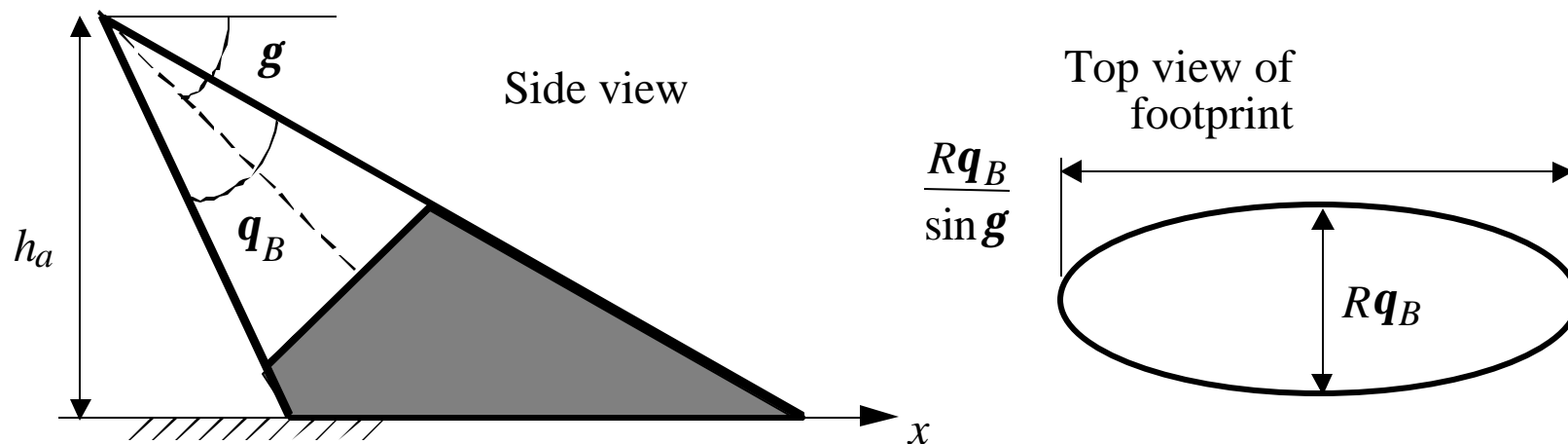
# Surface Clutter (3)

For a small depression angle the clutter area is approximately given by

$$A_c = \frac{ct Rq_B}{2 \cos g}$$

The diagram below illustrates the beamwidth limited case; the entire footprint is illuminated. The clutter area is the area of an ellipse

$$A_c = \frac{p}{4} (Rq_B)(Rq_B / \sin g) = \frac{p(Rq_B)^2}{4 \sin g}$$



# Two-Way Pattern Beamwidth

The two-way pattern refers to the product  $G_t G_r$ , and the half power points of this product define the two-way beamwidths. The previous charts have specifically dealt with monostatic radar. In a more general (bistatic) case, the clutter area is determined by the intersection of the transmit and receive footprints. The figure shows a bistatic radar with

different transmit and receive patterns. The clutter area is determined by the overlap in the two beams, or equivalently, for a monostatic radar, the two-way beamwidth.

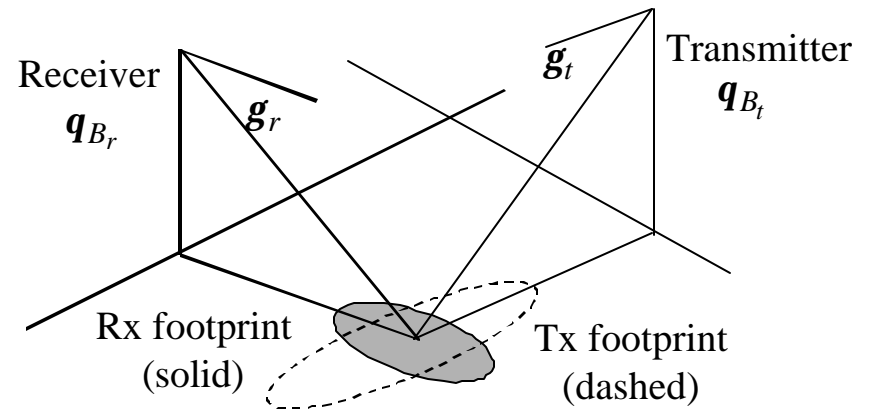
For a gaussian beam of the form

$$G(\mathbf{q}) = G_o \exp\left\{- (2.776)(\mathbf{q} / \mathbf{q}_B)^2\right\},$$

the two-way pattern is

$$G(\mathbf{q})^2 = G_o^2 \exp\left\{- (2)(2.776)(\mathbf{q} / \mathbf{q}_B)^2\right\}, \text{ and thus } \mathbf{q}_{B_{2\text{-way}}} = \frac{\mathbf{q}_{B_{1\text{-way}}}}{\sqrt{2}}. \text{ Therefore, the}$$

clutter area equations should have an additional factor of 2 in the denominator ( $\sqrt{2}$  for each plane), because  $A_c$  should be based on the two-way beamwidths. However, the area is usually greater than that found using the additional  $1/2$  because the beam edges are not sharp, so area outside of the 3 dB beamwidth contributes.



# Surface Clutter (4)

---

For extended targets we define the cross section per unit area,  $\mathbf{s}^o$ , in  $\text{m}^2/\text{m}^2$

$$\mathbf{s}^o = \underbrace{\text{Area}}_{1 \text{ m}^2} \times \underbrace{\text{Reflectivity}}_{\Gamma_g} \times \underbrace{\text{Directivity}}_{F_g}$$

This quantity is tabulated for various surfaces (for example, see Fig. 7.3 in Skolnik, reproduced on page II-63).

The radar equation for clutter return is

$$C = \frac{P_t G_t A_e \mathbf{s}^o A_c}{(4\pi)^2 R^4}$$

Neglecting noise ( $C \gg N$ ), the signal-to-clutter ratio (SCR) is

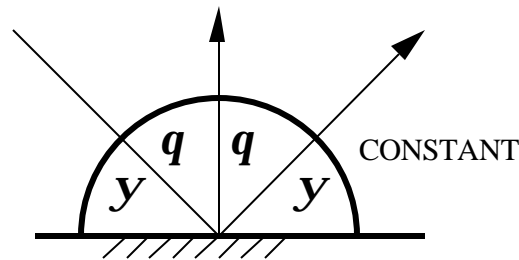
$$\text{SCR} = \frac{S}{C} = \frac{\mathbf{s}}{\mathbf{s}^o A_c}$$

where  $\mathbf{s}$  is the RCS of the target. Note: (1)  $P_t$  does not affect the SCR, and (2) a large  $t$  decreases  $N$ , but increases  $C$

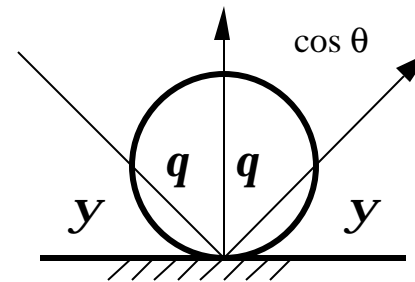
# Backscatter From Extended Surfaces

Extended surfaces: have no edges that are illuminated

ISOTROPIC (DIFFUSE) SURFACE



LAMBERTIAN SURFACE



In general:

$$G_g = \frac{2}{\int_0^{p/2} F_g(\mathbf{q}) \sin \mathbf{q} d\mathbf{q}}$$

Isotropic surface:  $F_g(\mathbf{q}) = 1 \Rightarrow G_g = \frac{2}{\int_0^{p/2} \sin \mathbf{q} d\mathbf{q}} = 2 \Rightarrow \mathbf{s}^o(\mathbf{q}) = 2\Gamma_g \cos \mathbf{q}$

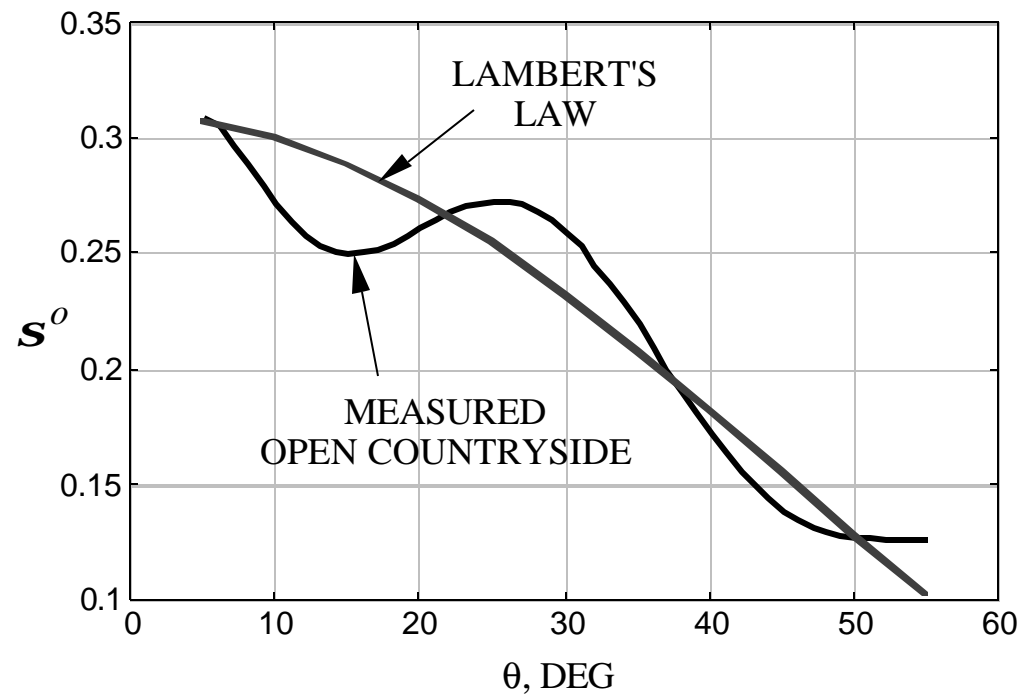
Lambertian surface:

$$F_g(\mathbf{q}) = \cos \mathbf{q} \Rightarrow G_g = \frac{2}{\int_0^{p/2} \cos \mathbf{q} \sin \mathbf{q} d\mathbf{q}} = 4 \Rightarrow \mathbf{s}^o(\mathbf{q}) = 4\Gamma_g \cos^2 \mathbf{q}$$

# Backscatter From Extended Surfaces

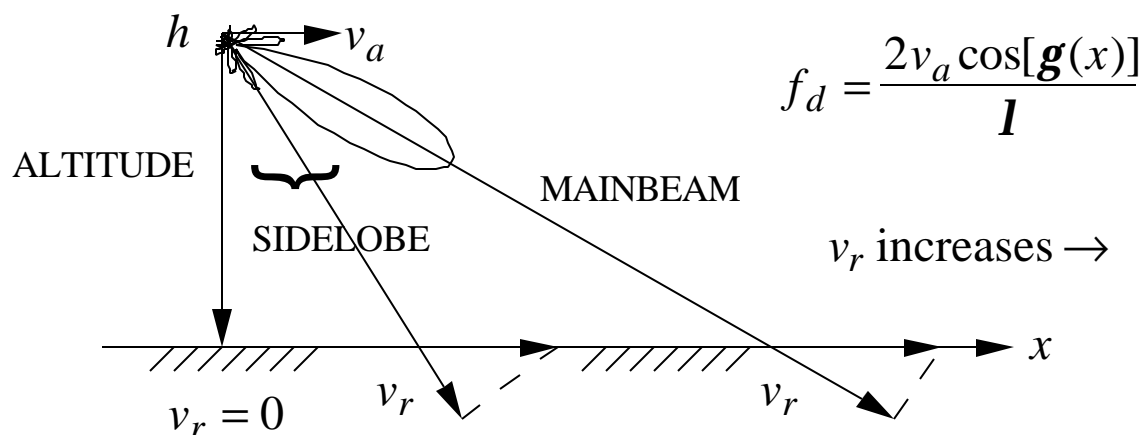
---

- HH polarization, L-band



# Clutter Spectrum (1)

Each point on the surface has a different velocity relative to the platform:



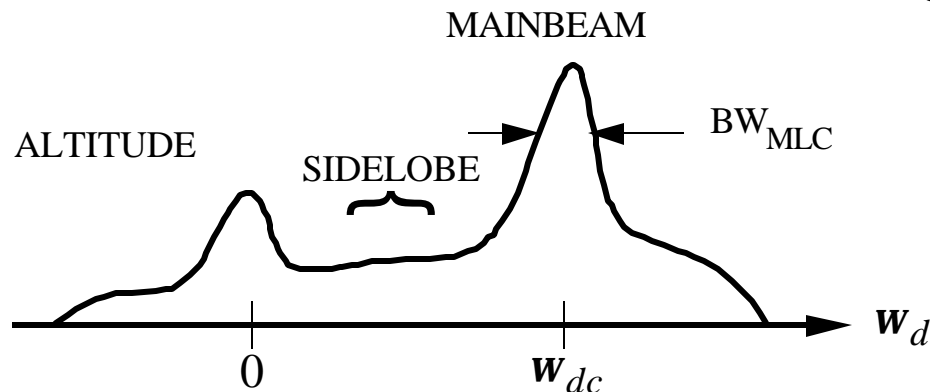
Three components of surface return:

1. mainbeam clutter: high because of high antenna gain
2. sidelobe clutter: low but covers many frequencies because of the large angular extent of the sidelobes
3. altitude return: high because of normal incidence

# Clutter Spectrum (2)

Typical clutter spectrum:

(see Fig. 3.43 in Skolnik)



Mainbeam clutter characteristics:

1. as the half-power beamwidth (HPBW) increases the spread in  $v_r$  increases and hence  $w_d$  increases
2. as  $g$  increases  $v_r$  at the center of the footprint decreases and therefore  $w_{dc}$  decreases
3. the width and center of frequencies varies as  $1/I$

$$\frac{df_d}{dg} = \frac{d}{dg} \left( \frac{2v_a}{I} \cos g \right) = -\frac{2v_a}{I} \sin g \equiv \frac{\Delta f_d}{\Delta g}$$

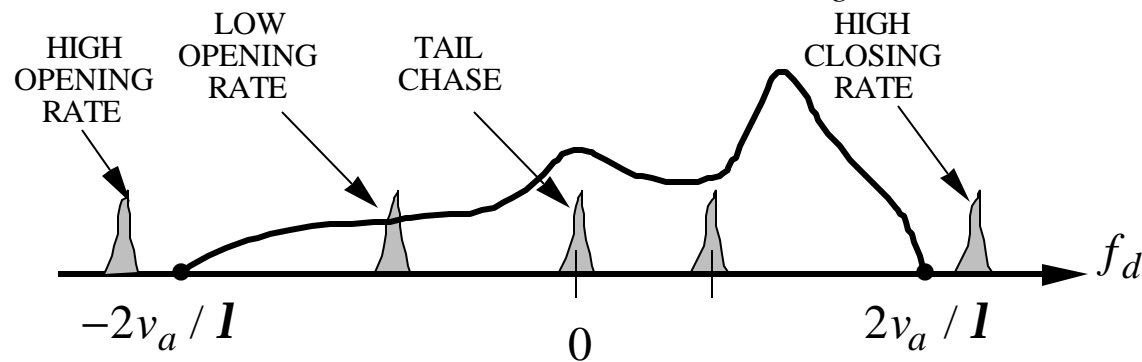




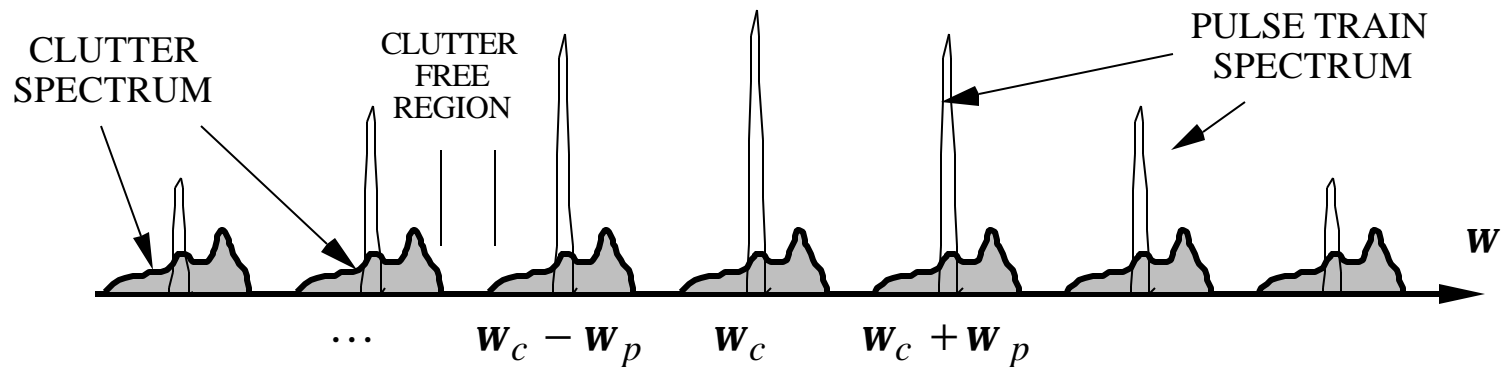
# Clutter Spectrum (4)

Altitude clutter characteristics:

1. centered at  $f_d = 0$  (unless aircraft is maneuvering)
2. slant ranges can be short at sidelobe angles but  $F_g$  can be large

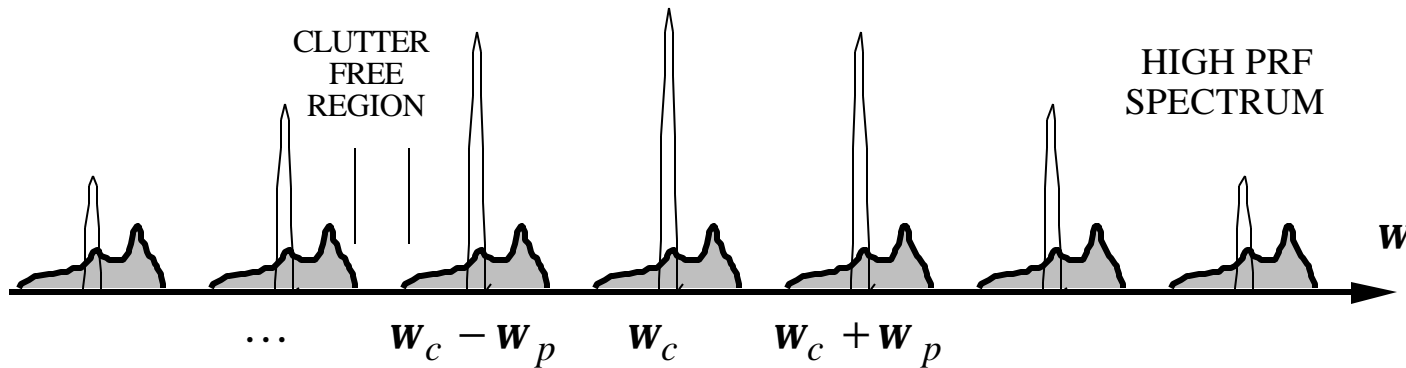


When the transmitted waveform is pulsed, the clutter spectrum repeats at multiples of the PRF ( $w_p = 2p f_p$ )

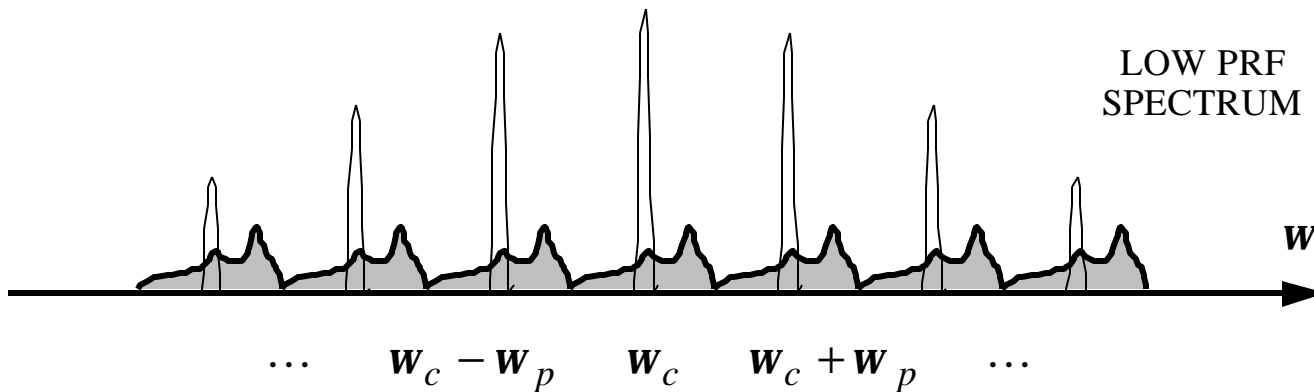


# Clutter Spectrum (5)

High PRF -- clutter-free region



Low PRF -- clutter spectra overlap; no clutter-free region



# Clutter Spectrum (6)

Example: low PRF radar with:

$$f = 9.5 \text{ GHz}, \quad v_a = 300 \text{ m/s}, \quad q_B = 2.5^\circ, \quad g = 60^\circ, \quad \text{PRF} = 2 \text{ kHz}$$

Unambiguous range and velocity:

$$R_u = \frac{c}{2f_p} = \frac{3 \times 10^8}{2(2000)} = 75 \text{ km};$$

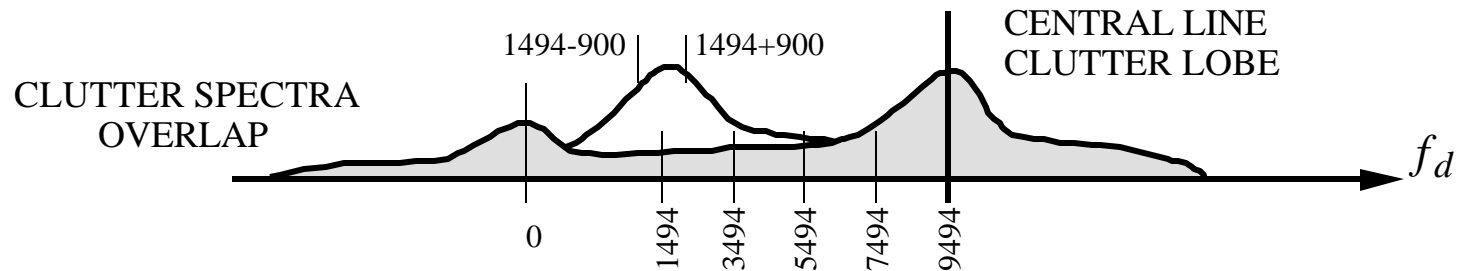
$$\Delta v_u = \frac{\pm f_{d\text{max}} I}{2} = \frac{f_p I}{2}$$

$$\text{BW}_{\text{MLC}} = \frac{2v_a}{I} \sin(60^\circ) (2.5) \underbrace{(0.0436)}_{q_B} = 1800 \text{ Hz};$$

$$= \frac{2000(0.0316)}{2} = 32 \text{ m/s}$$

$$\text{BW}_{\text{SLC}} = 2 \left( \frac{2v_a}{I} \right) = \frac{4(300)}{0.0316} \approx 38 \text{ kHz};$$

$$f_{\text{MLC}} = \frac{2v_a}{I} \cos(60^\circ) \approx 9494 \text{ Hz}$$



# Clutter Spectrum (7)

---

high PRF radar with:

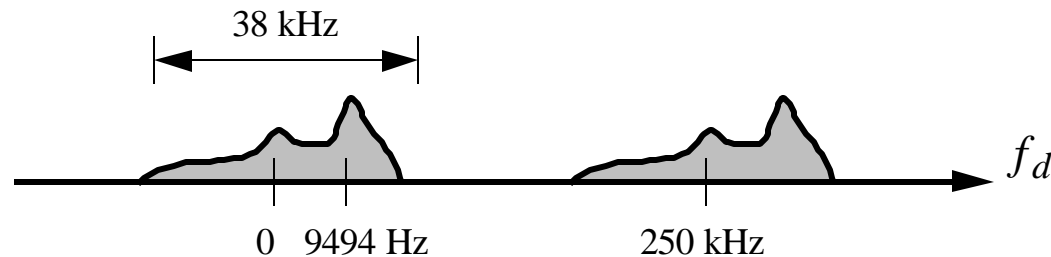
$$f = 9.5 \text{ GHz}, \quad v_a = 300 \text{ m/s}, \quad \mathbf{q}_B = 2.5^\circ, \quad \mathbf{g} = 60^\circ, \quad \text{PRF} = 250 \text{ kHz}$$

Unambiguous range and velocity:

$$R_u = \frac{c}{2f_p} = \frac{3 \times 10^8}{2(250000)} = 600 \text{ m}$$

$$\text{BW}_{\text{MLC}} = 1800 \text{ Hz}; \quad \Delta v_u = 3950 \text{ m/s}$$

$$\text{BW}_{\text{SLC}} \approx 38 \text{ kHz}; \quad f_{\text{MLC}} = 9494 \text{ Hz}$$



# Sea States\*

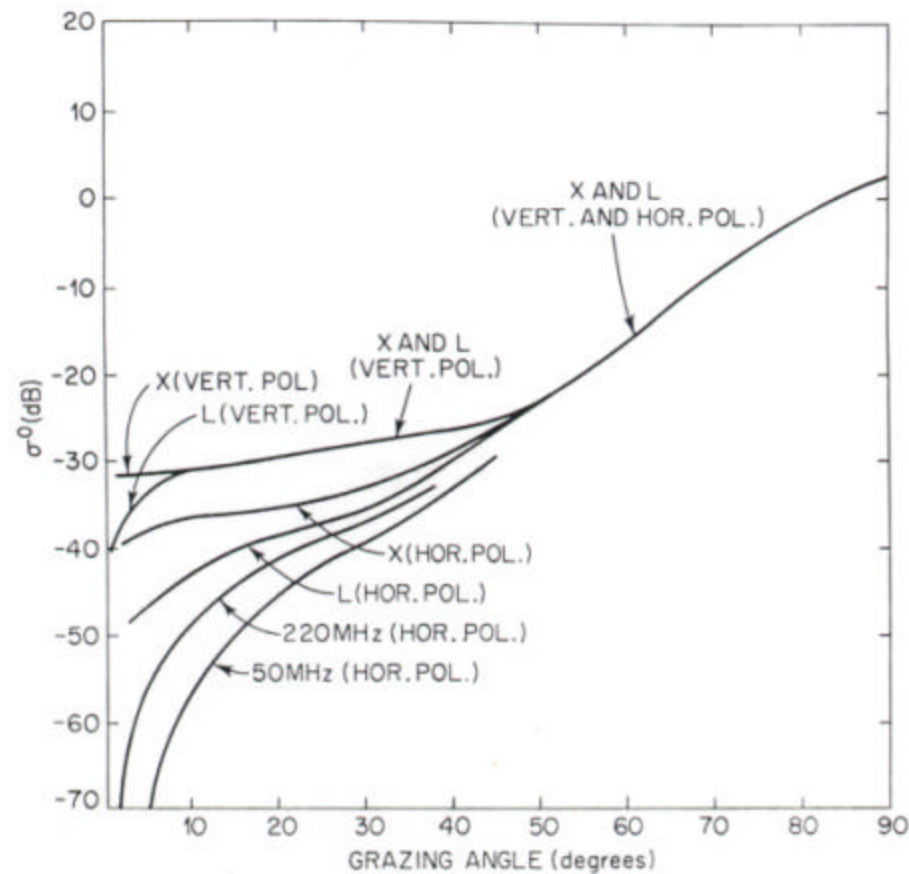
SEA STATE	WAVE HEIGHT (ft)	WAVE PERIOD (sec)	WAVE LENGTH (ft)	WAVE VELOCITY (kt)	PARTICLE VELOCITY (ft/sec)	WIND VELOCITY (kt)	REQUIRED FETCH (mi)
0 (flat)	(not a recognized sea state but often used to denote a flat sea)						
1 (smooth)	0-1	0-2	0-20	0-6	0-1.5	0-7	0-25
2 (slight)	1-3	2-3.5	20-65	6-11	1.5-2.8	7-12	25-75
3 (moderate)	3-5	3.5-4.5	65-110	11-14	2.8-3.5	12-16	75-120
4 (rough)	5-8	4.5-6	110-180	14-17	3.5-4.2	16-19	120-190
5 (very rough)	8-12	6-7	180-250	17-21	4.2-5.2	19-23	190-250
6 (high)	12-20	7-9	250-400	21-26	5.2-6.7	23-30	250-370
7 (very high)	20-40	9-12	400-750	26-35	6.7-10.5	30-45	370-600
8 (precipitous)	> 40	> 12	> 750	> 35	> 10.5	> 45	> 600

- Note:
1. Assumes deep water.
  2. Wave velocity determines clutter doppler; particle velocity determines how fast a particle moves.
  3. Data only applies to waves; swells are generated at long distances by other wind systems.
  4. Period, wavelength and wave velocity apply to swells and waves.
  5. Fetch is the distance that the wind is blowing; duration is the length of time.

\*After Edde, *Radar*, Prentice-Hall (also see Skolnik, Table 7.2)

# Sea Clutter

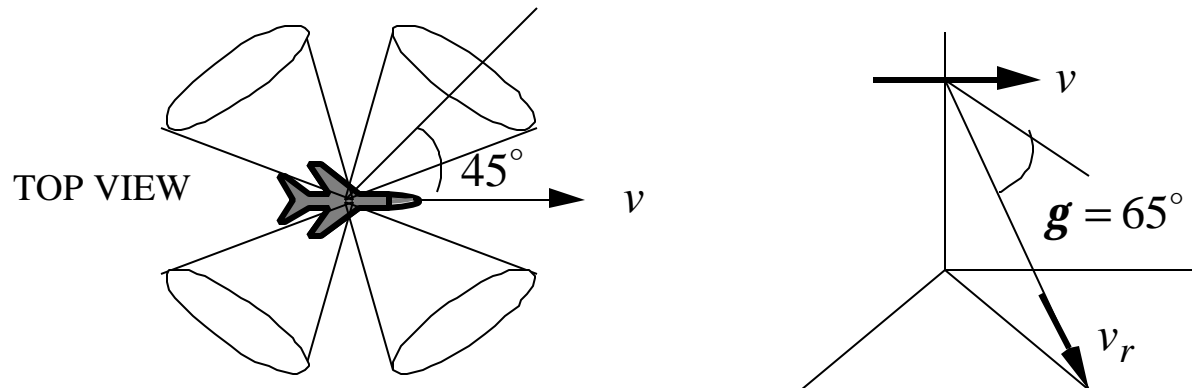
Composite of  $\sigma^0$  data for average conditions with wind speed ranging from 10 to 20 knots (Fig. 7.3, Skolnik)



# Example: AN/APS-200

The AN/APS-200 is a doppler navigation radar (see Skolnik p. 94 and *Microwaves*, October 1974). Radar parameters:

velocity range = 50 to 1000 knots; altitude = 0 to 70000 feet  
 vertical plane (elevation) beamwidth = 2.5 degrees  
 horizontal plane (azimuth) beamwidth = 5 degrees  
 $G = 30$  dB,  $P_t = 1$  W (CW),  $f = 13.3$  GHz ( $\lambda = 0.0225$  m)



The relative velocity is  $v_r = 1000 \cos(65^\circ) \cos(45^\circ) = \pm 299$  knots, or

$$f_d = \frac{2v_r}{\lambda} = \frac{1.03v_r}{\lambda} = \frac{1.03(299)}{0.0225} = 13.6 \text{ kHz}$$



# Example: AN/APS-200

---

(a) Required bandwidth:  $BW = 2(13.6) = 27.3$  kHz

(b)  $P_r$  for  $h = 40000$  feet over the ocean

For the ocean, 10 to 20 kt winds (average conditions):  $s^o = -15$  dB

$$C = P_r = \frac{P_t G_t A_{er} A_c s^o}{(4p)^2 R^4}$$

For the beamwidth limited case (CW):

$$A_c = \frac{pR^2 q_{B_{el}} q_{B_{az}}}{4 \sin g}$$

For the identical transmit and receive antennas:  $A_{er} = \frac{l^2 G}{4p} = 0.0407$  m<sup>2</sup>. Therefore

$$C = \frac{P_t G_t A_{er} s^o}{(4p)^2 R^4} \frac{pR^2 q_{B_{el}} q_{B_{az}}}{4 \sin g} = \frac{(1)(10^3)(0.0407)(0.0316)(5)(2.5) \overbrace{(0.0174)^2}^{\text{CONVERT TO RADIANS}}}{64p (13.43 \times 10^3)^2 \sin 65^\circ}$$

$$C = 1.49 \times 10^{-13} \text{ W} = -128 \text{ dBW} = -98 \text{ dBm}$$

# Example: AN/APS-200

---

(c) For the following parameters:

$$h = 40000 \text{ feet}$$

$$T_a = 300 \text{ K}$$

$$L = 5 \text{ dB}$$

$$F = 10 \text{ dB}$$

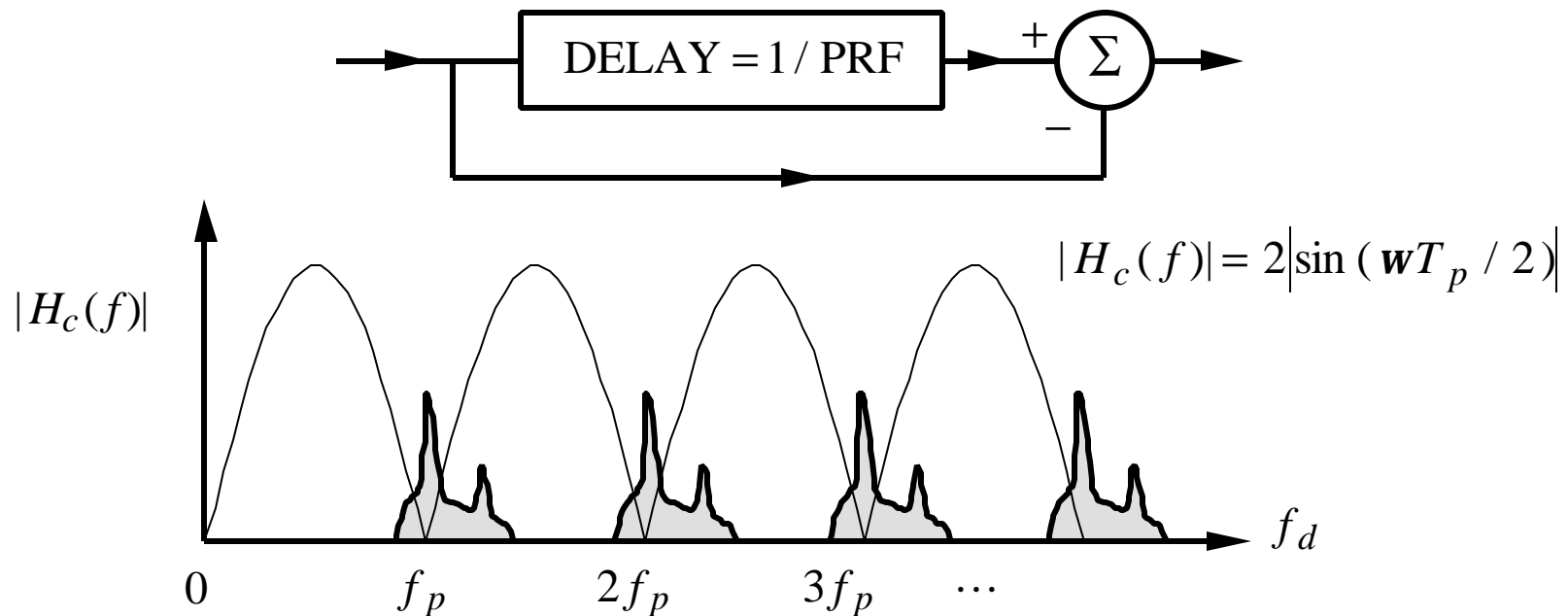
$$B_n \text{ from part (a)}$$

we can compute the clutter-to-noise ratio as follows:

$$\begin{aligned} \left(\frac{S}{N}\right)_{\text{out}} &= \frac{S_{\text{min}}}{N_{\text{out}}} = \frac{S_{\text{min}}}{kT_o \left(\frac{T_a + T_e}{T_o}\right) B_n L} \\ &= \frac{1.49 \times 10^{-13}}{kT_o \left(\frac{300 + (10 - 1)(290)}{290}\right) B_n L} \\ &= \frac{1.49 \times 10^{-13}}{1.38 \times 10^{-23} (2910)(27.3 \times 10^3)(3.16)} \\ &= 47.95 \approx 17 \text{ dB} \end{aligned}$$

# Delay Line Canceler (1)

A delay line canceler is used to eliminate clutter. (It is also known as a transversal filter, tapped delay line filter, non-recursive filter, moving average filter, and finite impulse response filter.)



It is effective if the clutter spectrum is narrow. Note that target returns with doppler frequencies in the notches are also rejected. These are blind speeds, which occur at

$$v_{bn} = n \mathbf{1} f_p / 2, \quad n = 0, \pm 1, \pm 2, \dots$$

# Delay Line Canceler (2)

Figures of merit for canceler performance:

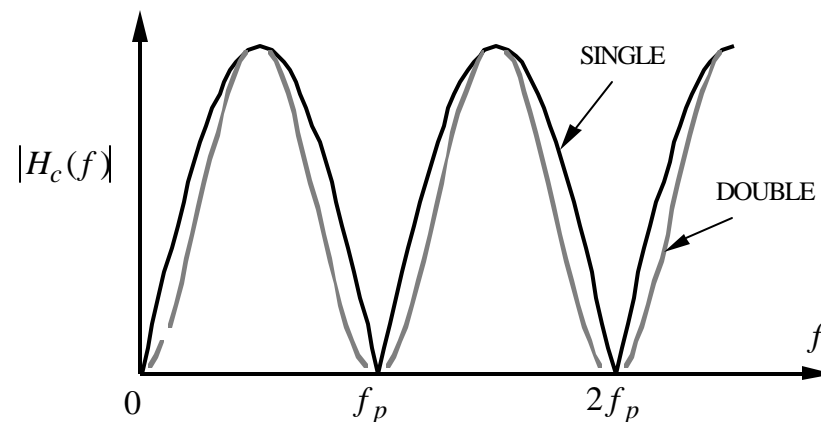
1. clutter attenuation -- where  $S_c(\omega)$  is the clutter power spectral density

$$CA = \frac{\int_{-\infty}^{\infty} S_c(\omega) d\omega}{\int_{-\infty}^{\infty} S_c(\omega) |H_c(\omega)|^2 d\omega}$$

2. clutter improvement factor -- defined in terms of SCR, the signal-to-clutter ratio

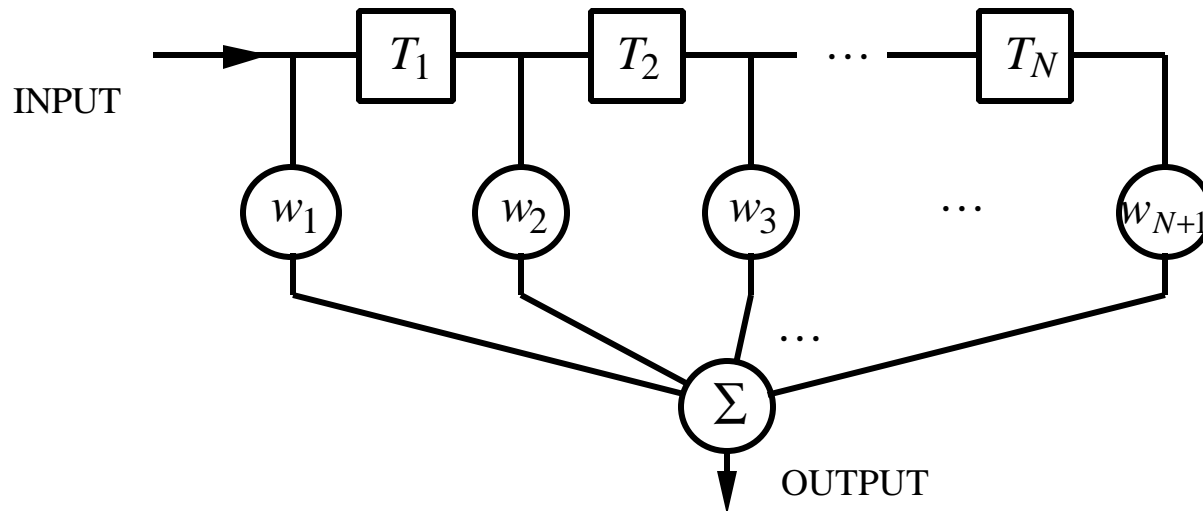
$$I_c = \frac{SCR_{out}}{SCR_{in}} = \frac{S_{out}}{S_{in}} \times CA$$

Double cancelers give a wider clutter notch



# Delay Line Canceler (3)

Multiple pulse cancelers provide the ability to control the frequency characteristic



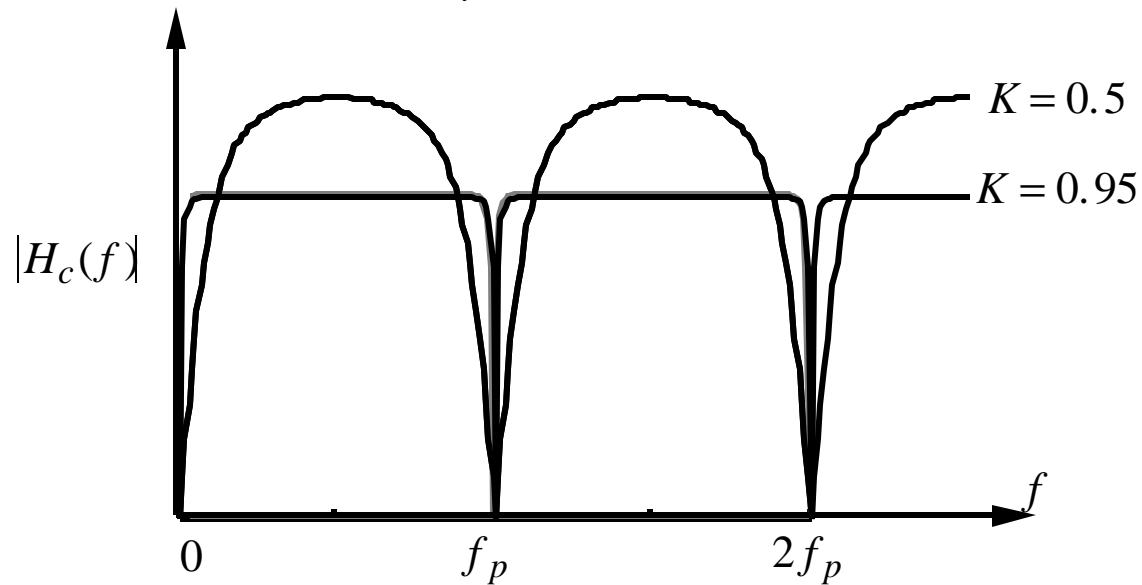
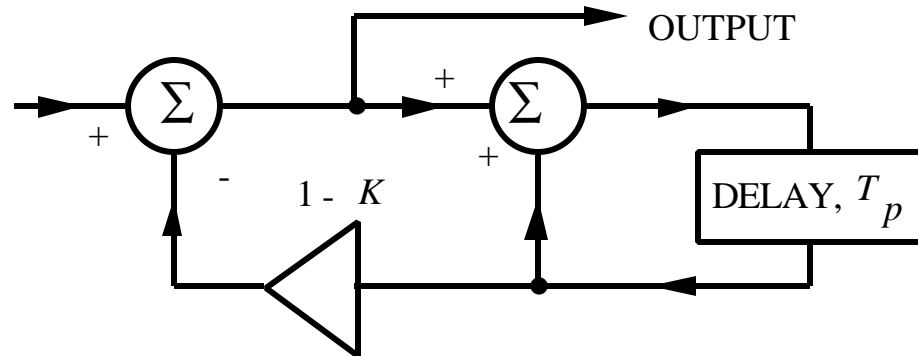
Weighting coefficients: binomial, Chebyshev, or optimum, which maximizes the clutter improvement factor,  $I_c$ . A  $N$  line canceler requires  $N + 1$  pulses, increasing the required time on target.

Delay line cancelers can be made recursive by adding a feedback loop. Frequency characteristics are of the form

$$|H_c(f)| = \frac{2|\sin(\omega T_p / 2)|}{\sqrt{1 + K^2 - 2K \cos(\omega T_p)}}$$

# Delay Line Canceler (4)

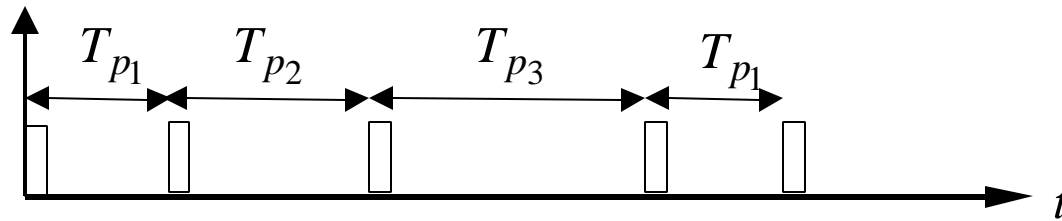
Recursive single canceler and frequency characteristics



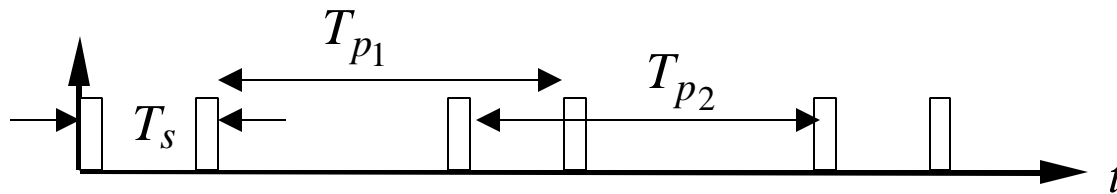
All delay lines suffer from blind speeds.

# Staggered and Multiple PRFs (1)

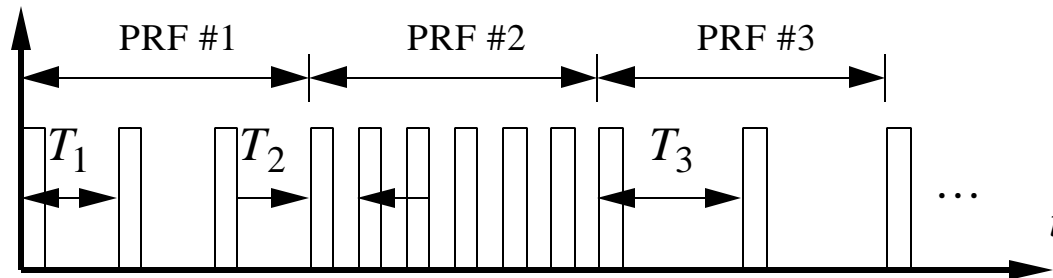
The number of blind speeds can be reduced by employing multiple PRFs. They can be used within a dwell (look) or changed from dwell to dwell.



Staggered PRFs



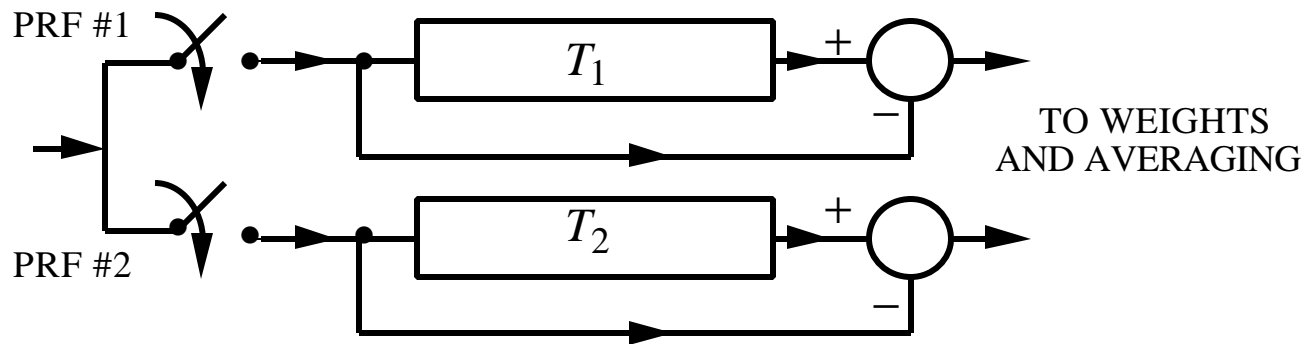
Interlaced PRFs



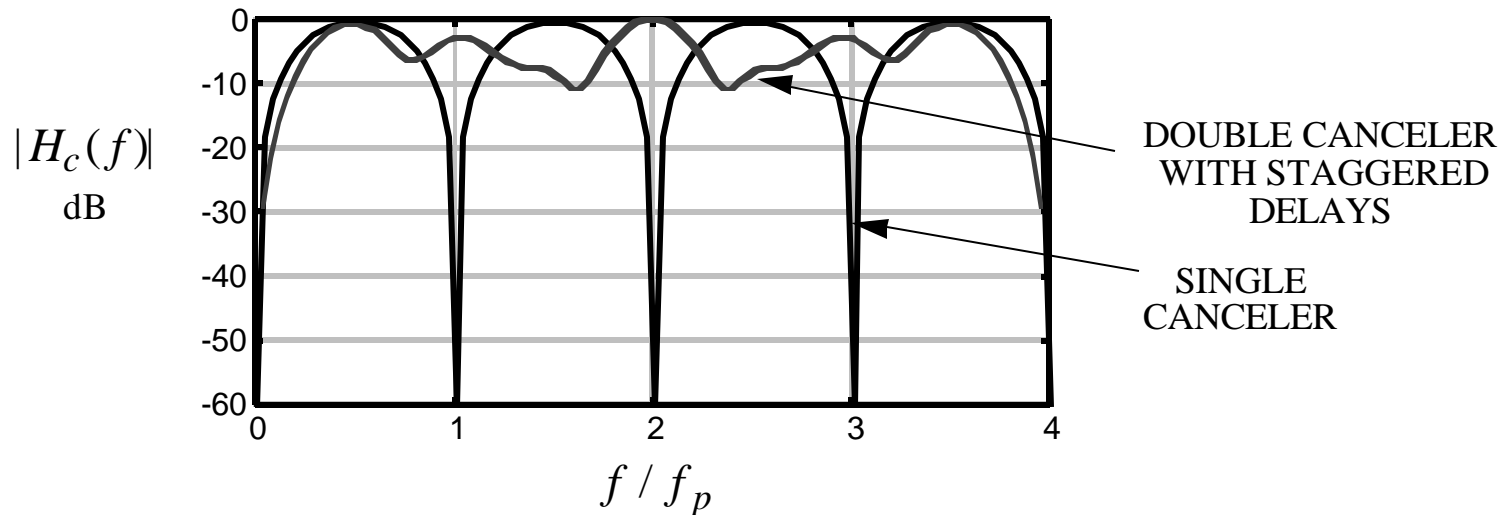
Multiple PRFs within a dwell

# Staggered and Multiple PRFs (2)

Implementation of multiple PRFs:



Frequency characteristics





## Staggered and Multiple PRFs (3)

---

Example: A MTI radar operates at 9 GHz and uses PRFs of 1 kHz and 1.25 kHz.  
What is the first blind speed?

Blind speeds for PRF #1:

$$v_n = \frac{n\lambda}{2} f_{p1}$$

and for PRF #2:

$$v_m = \frac{m\lambda}{2} f_{p2}$$

where  $m$  and  $n$  are integers. Both PRFs must have the same frequency at which the frequency characteristic is zero. Thus we require

$$\frac{n\lambda}{2} f_{p1} = \frac{m\lambda}{2} f_{p2} \Rightarrow n f_{p1} = m f_{p2} \Rightarrow \frac{m}{n} = \frac{f_{p1}}{f_{p2}} = \frac{4}{5}$$

The first blind speed ( $n = 5$ ) is

$$v_1 = \frac{5\lambda}{2} f_{p1} = \frac{5(0.033)}{2} (1000) = 83.33\text{m/s}$$

# Synchronous Detection (I and Q Channels)

Synchronous detection uses I and Q channels. The complex signal representation of  $s$

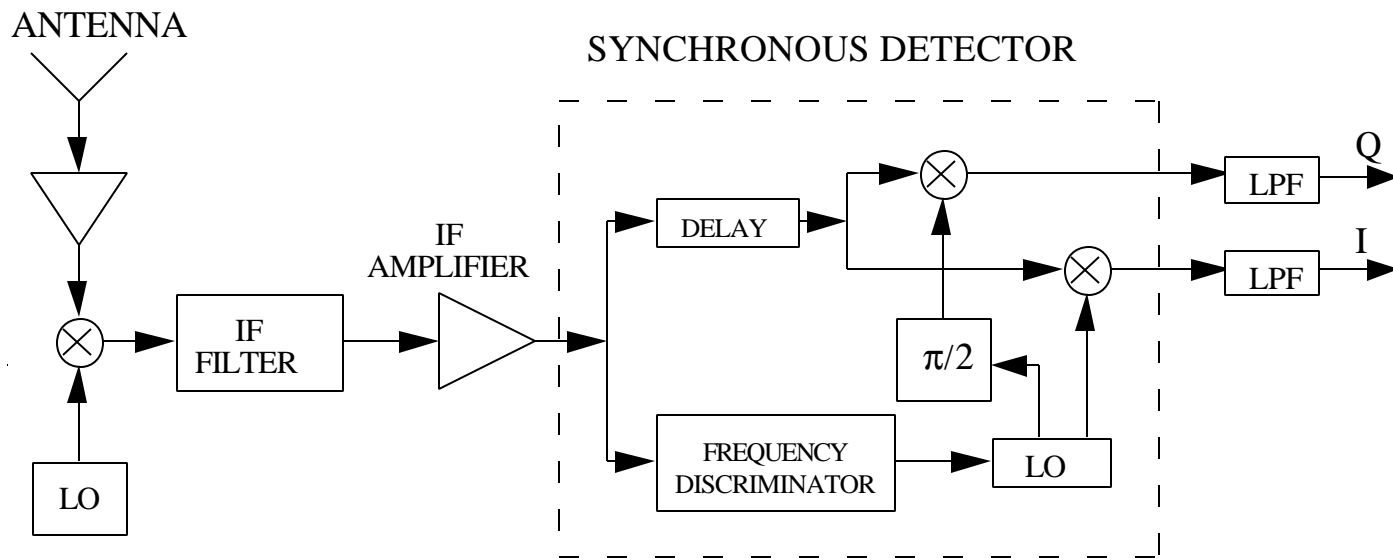
$$s = s_I - js_Q \text{ and } |s| = \sqrt{s_I^2 + s_Q^2}$$

where

$$\text{Re}\{s\} = |s| \cos \Phi_s \equiv s_I$$

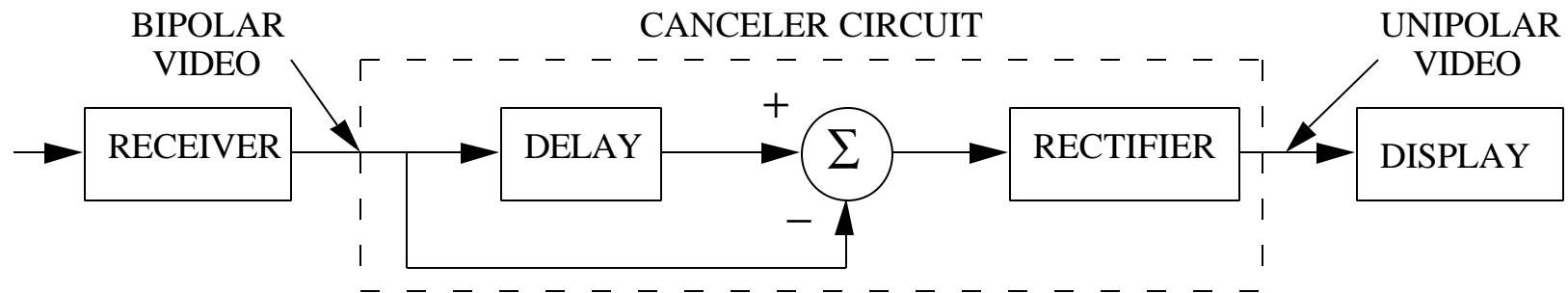
$$\text{Im}\{s\} = |s| \sin \Phi_s = |s| \cos(\Phi_s - \pi/2) \equiv s_Q$$

Hardware implementation:

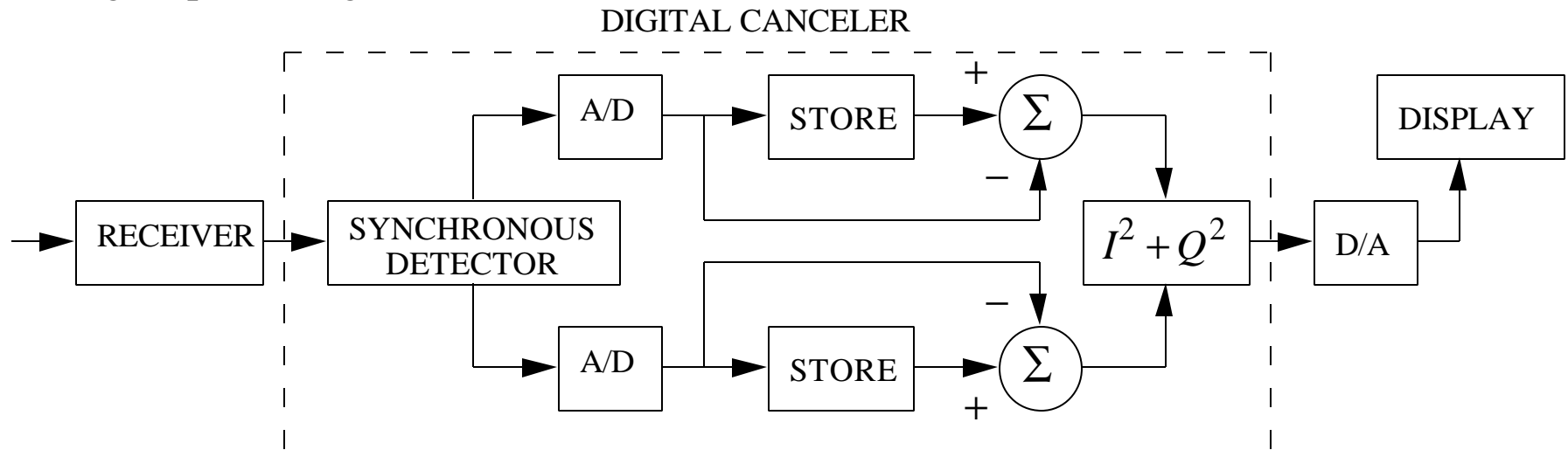


# Analog vs. Digital Processing for MTI

Analog processing:

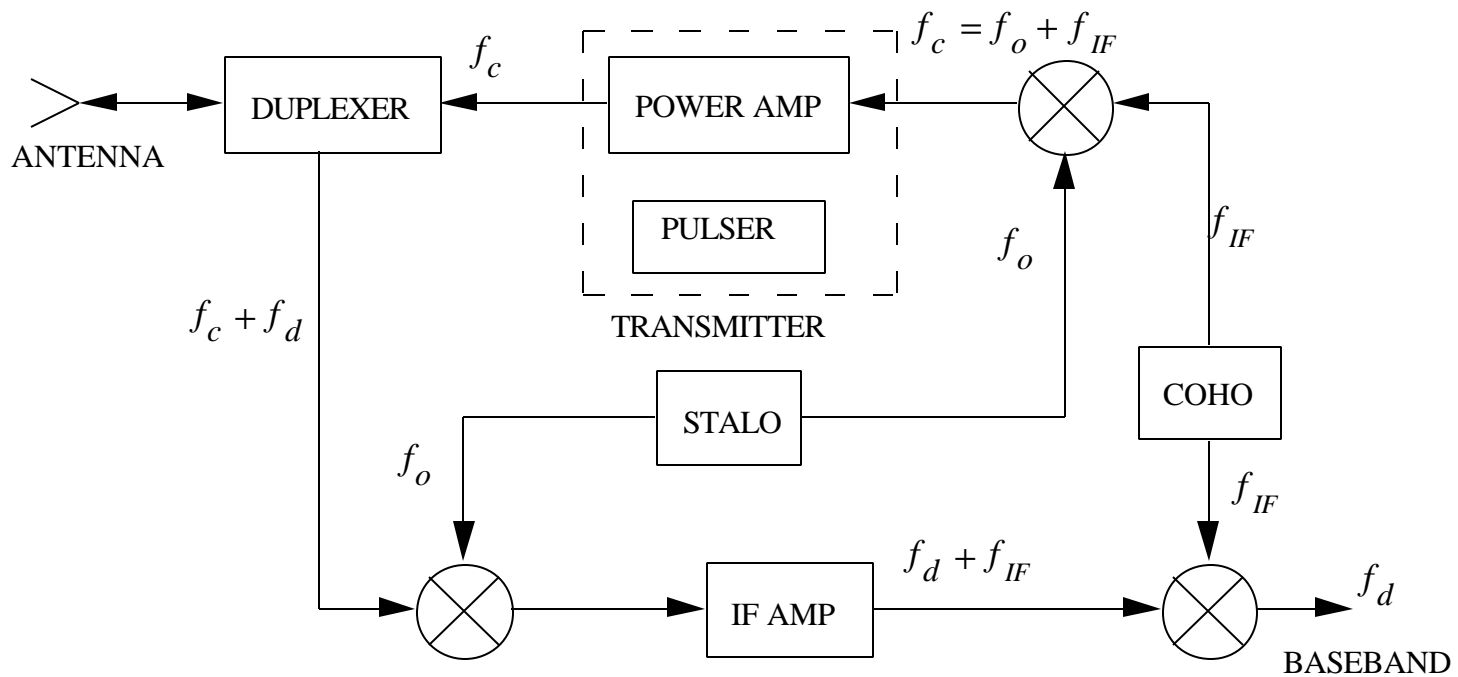


Digital processing:



# Single Channel Receiver Block Diagram

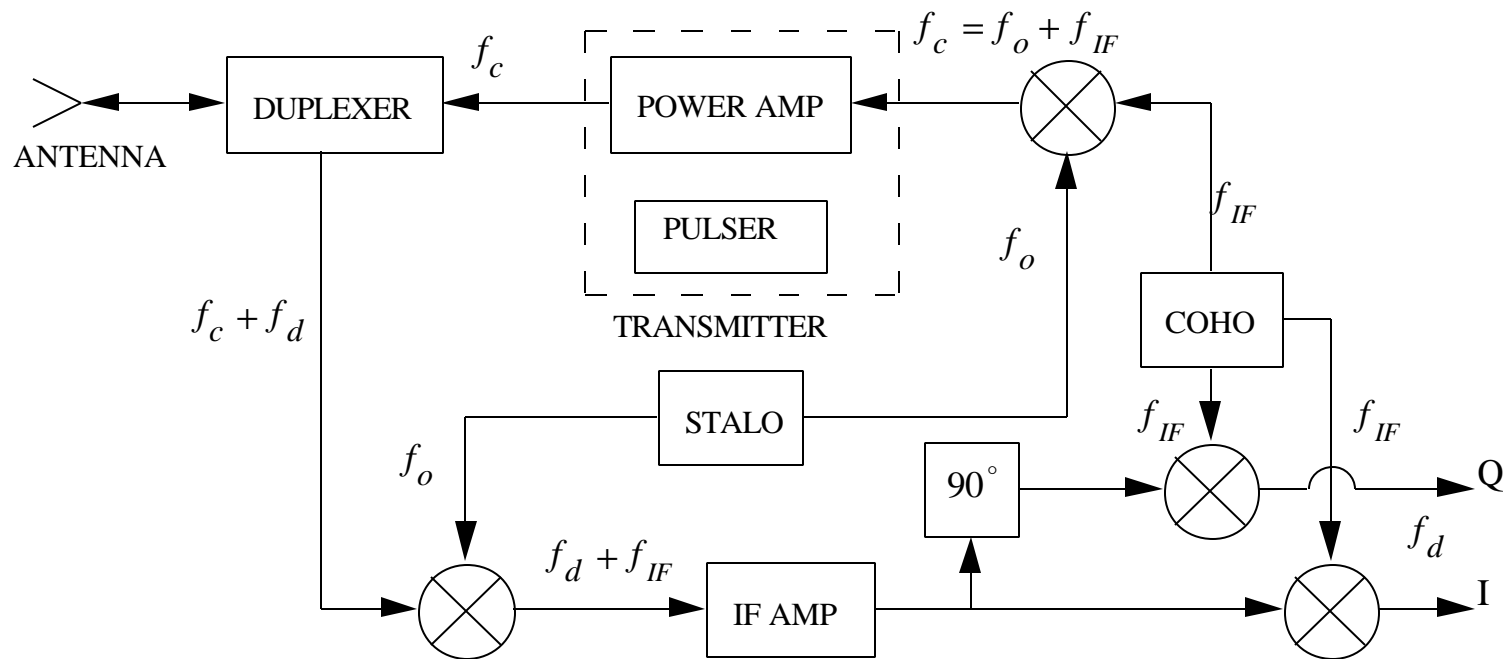
Block diagram of a single channel receiver (see Fig. 3.7 in Skolnik)



STALO = stable local oscillator  
 COHO = coherent oscillator

# Synchronous Receiver Block Diagram

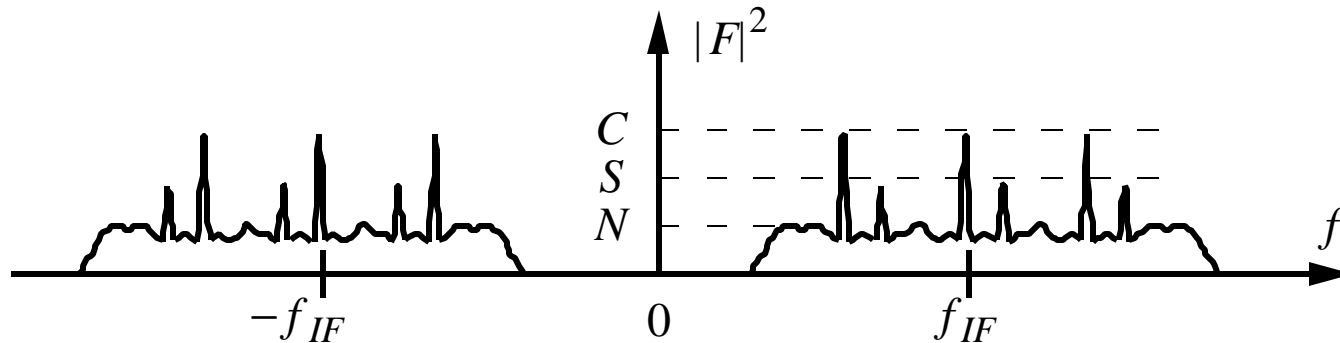
Block diagram of a synchronous receiver



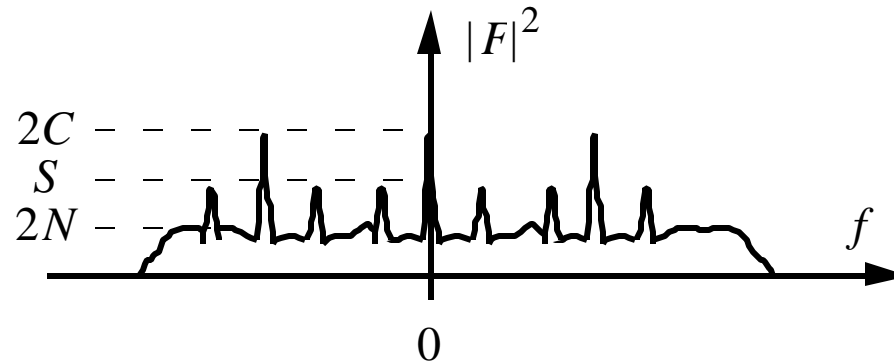
STALO = stable local oscillator  
 COHO = coherent oscillator  
 I = in phase component,  $p(t)\cos(\omega_d t)$   
 Q = quadrature component,  $p(t)\sin(\omega_d t)$

# SNR Advantage of Synchronous Detection (1)

Single channel IF spectrum: (positive and negative frequencies are mirror images)



Single channel video: (positive and negative frequencies "wrap around")

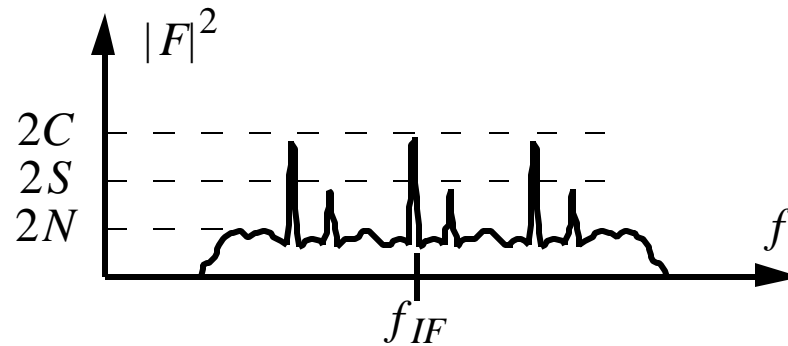


Signal-to-noise ratio:

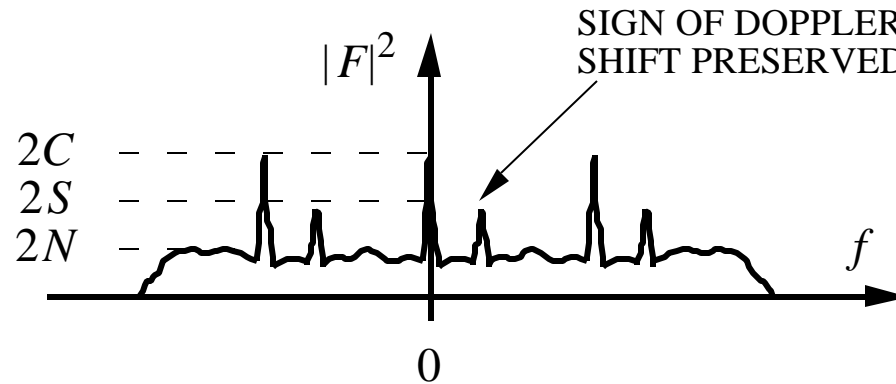
$$\text{SNR} = \frac{S}{2N}$$

# SNR Advantage of Synchronous Detection (2)

I/Q channel spectrum: (no negative frequencies due to even/odd symmetry of the real/imaginary parts)



I/Q channel baseband:



Signal-to-noise ratio:

$$\text{SNR} = \frac{2S}{2N} = \frac{S}{N}$$

# Processing of a Coherent Pulse Train (1)

Assume synchronous detection at the carrier frequency. The received signal will be of the form

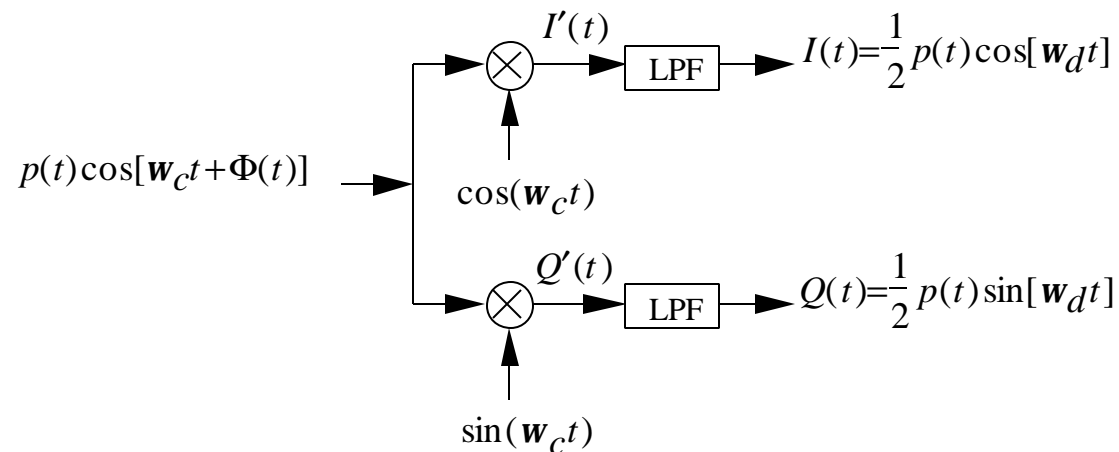
$$s(t) = p(t) \cos[\omega_c t + \Phi(t)]$$

where  $p(t)$  is the pulse train envelope and  $\Phi(t) = \omega_d t$  ( $\omega_d = 2\pi f_d$ ). Signals into the filters are

$$I'(t) = \frac{1}{2} \{p(t) \cos[2\omega_c t + \Phi(t)] + p(t) \cos[\Phi(t)]\}$$

$$Q'(t) = \frac{1}{2} \{p(t) \sin[2\omega_c t + \Phi(t)] + p(t) \sin[\Phi(t)]\}$$

Filtering removes the first terms in the brackets.





# Sampling Theorem (1)

---

Consider a waveform  $s(t) \leftrightarrow S(\mathbf{w})$  which is bandlimited ( $S(\mathbf{w}) = 0$  for  $|\mathbf{w}| \geq \mathbf{w}_o$ ). The function  $s(t)$  can be uniquely determined from the values

$$s_n = s(n\mathbf{p} / \mathbf{w}_o)$$

These are samples spaced at intervals of  $\mathbf{p} / \mathbf{w}_o = 1/(2f_o)$ , which is twice the highest frequency contained in the bandlimited signal. The waveform is reconstructed from

$$s(t) = \sum_{n=-\infty}^{\infty} s_n \text{sinc}(\mathbf{w}_o t - n\mathbf{p})$$

Real-world signals are modeled as bandlimited even though they rarely are. (They can be approximated arbitrarily closely by bandlimited functions.) Delta functions are often used as sampling functions. Multiplying a waveform by an infinite series of Dirac delta functions is an ideal sampling process

$$s(t_n) = \sum_{n=-\infty}^{\infty} s(t) \mathbf{d}(t - nT_s)$$

where  $T_s$  is the sampling interval.

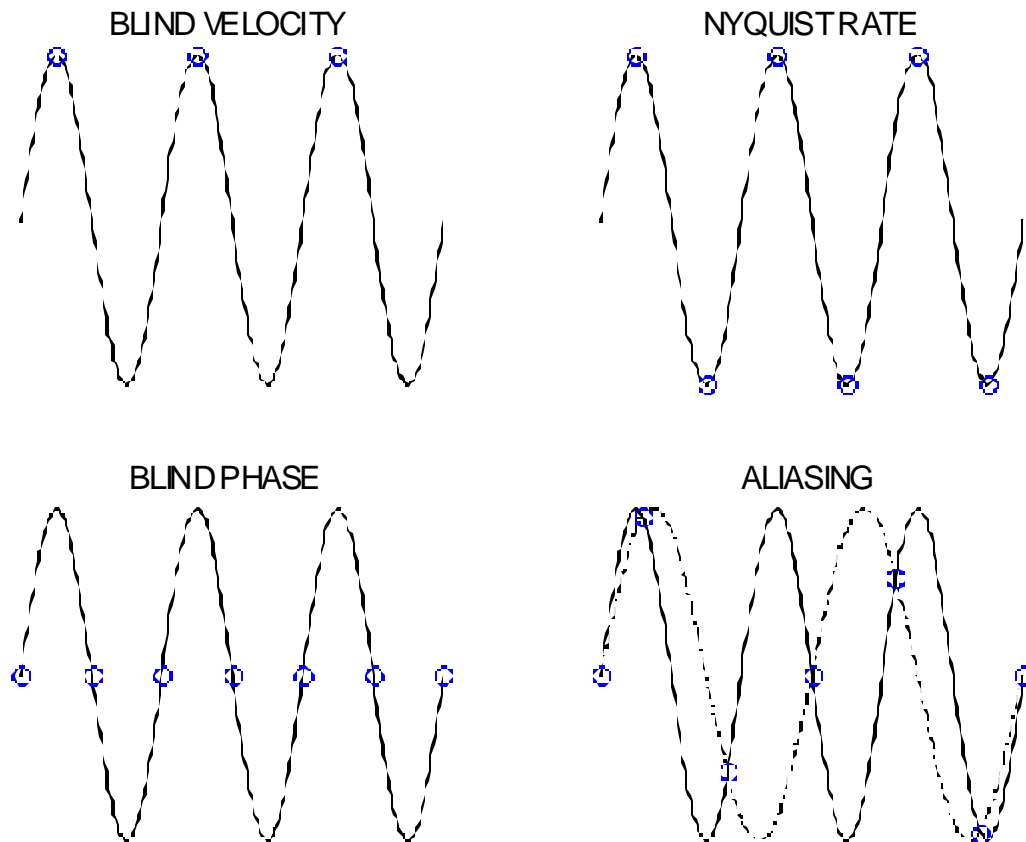
# Sampling Theorem (2)

The Nyquist sampling rate (twice the highest frequency) is the minimum sampling rate that provides unique recovery. Other values result in undersampling or oversampling.

Some specific sampling cases  
frequency  $f_o$

$$f_s = 1/T_s \begin{cases} = 2f_o, \text{ Nyquist rate} \\ > 2f_o, \text{ oversampling} \\ < 2f_o, \text{ undersampling} \end{cases}$$

(o is a sample point)



# Processing of a Coherent Pulse Train (2)

---

- Simplifications:
1. neglect noise, clutter, etc.
  2. assume that the target stays in the same range bin for all pulses in the train

The signal return from a target is reconstructed from returns with a constant delay after each pulse (i.e., same range bin)

Sample once per pulse: the sampling frequency is  $f_p$ , the sampling times  $t_1, t_2, \dots, t_N$

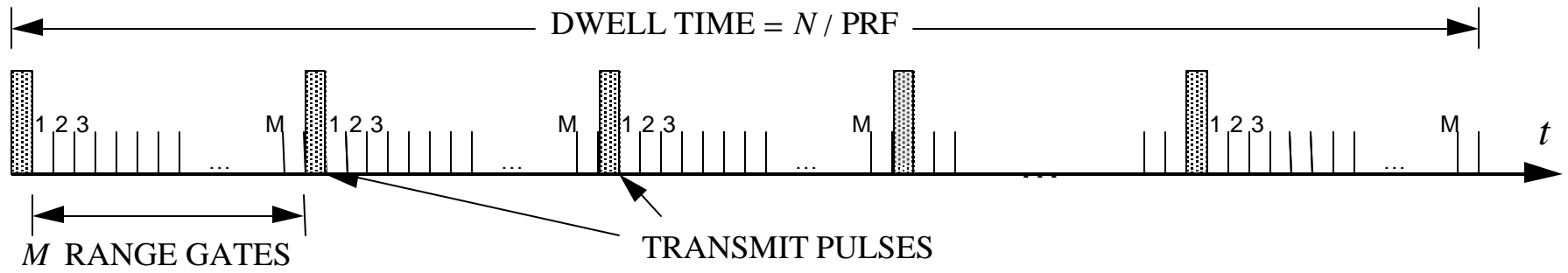
$$I(t_n) = \frac{1}{2} \{p(t_n) \cos[\mathbf{w}_d t_n]\}$$
$$Q(t_n) = \frac{1}{2} \{p(t_n) \sin[\mathbf{w}_d t_n]\}$$

This signal is equivalent to the complex form:

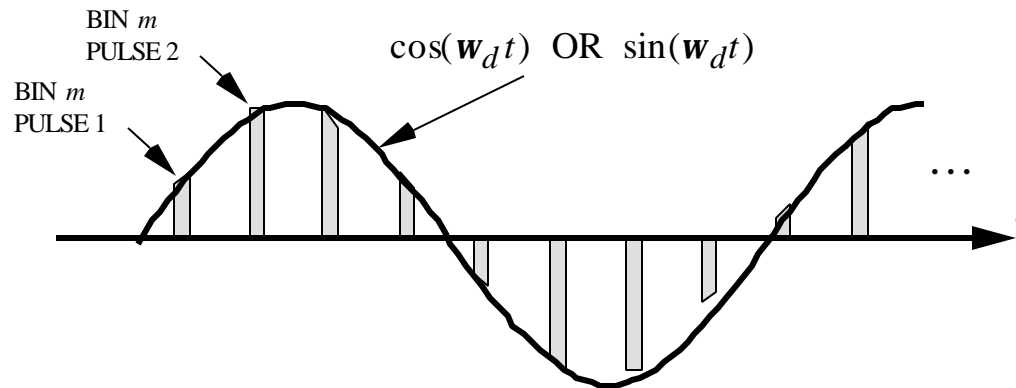
$$f(t_n) = 2\{I(t_n) + jQ(t_n)\} = p(t_n) e^{j\Phi(t_n)} = p(t_n) e^{j\mathbf{w}_d t_n}$$

# Processing of a Coherent Pulse Train (3)

Pulse train with range gates (bins):

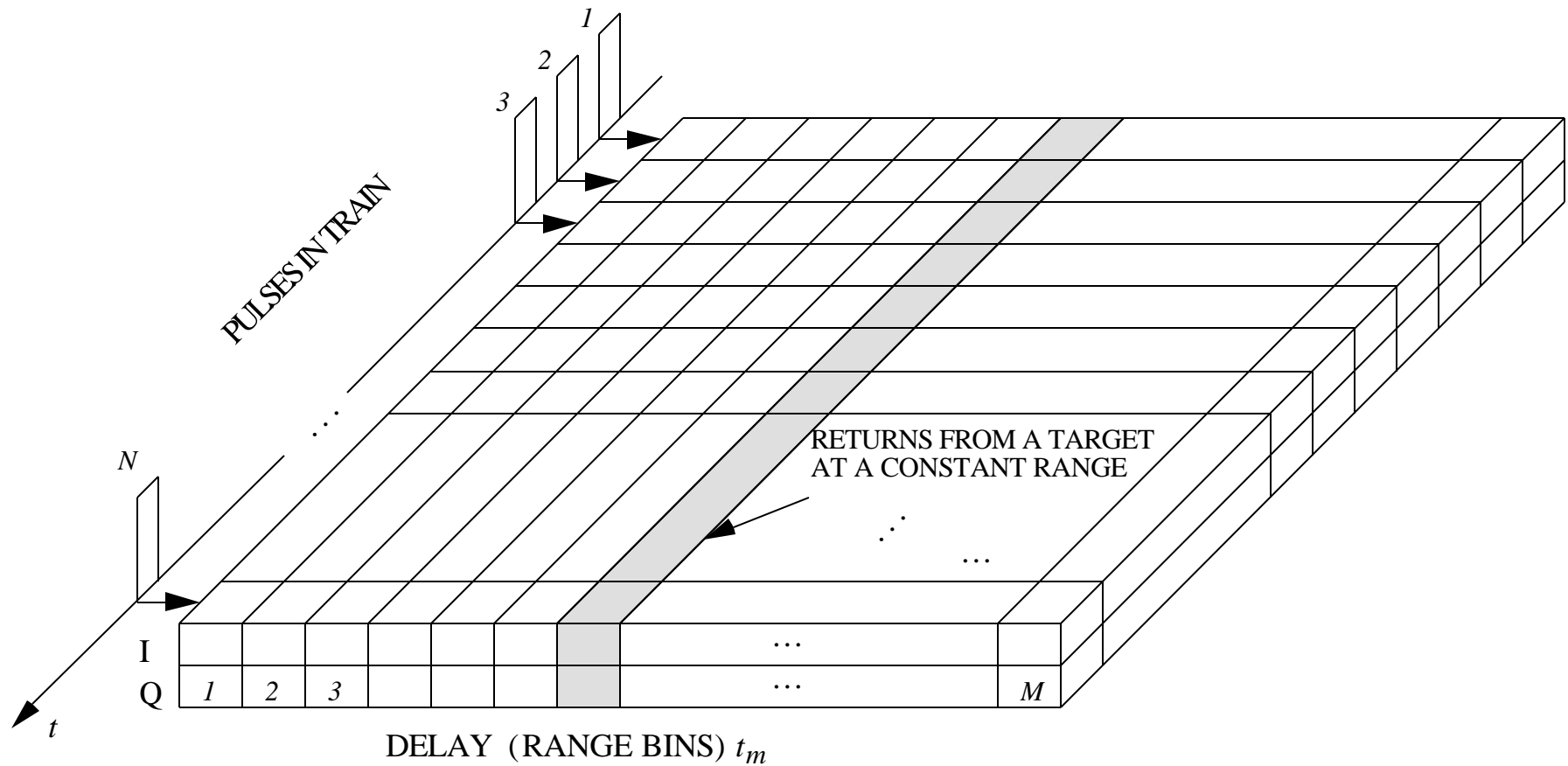


Returns for a target that remains in a single range bin (for example, bin  $m$ )



# Processing of a Coherent Pulse Train (4)

Storage of data in a two-dimensional array

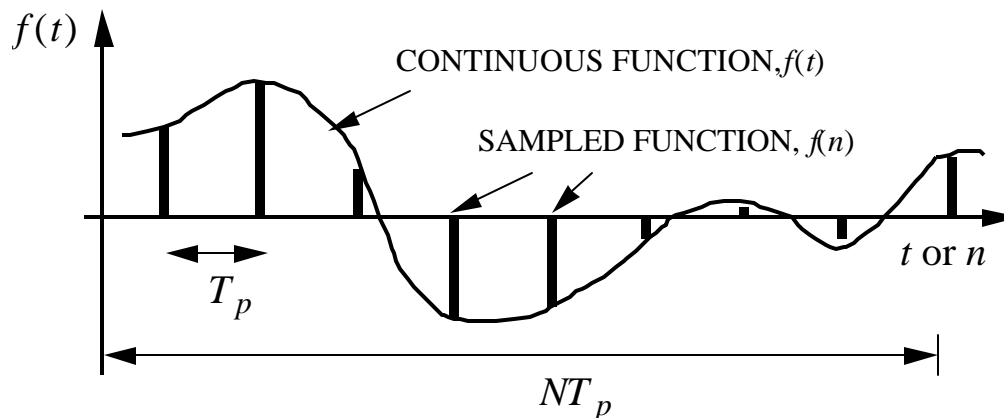


# Discrete Fourier Transform (DFT)

The discrete Fourier transform is a sampled version of the conventional Fourier transform defined by

$$F(\mathbf{w}_k) = \sum_{n=0}^{N-1} f(t_n) e^{-j\left(\frac{2\mathbf{p}}{N}\right)kn} \quad (k = 0, 1, \dots, N-1)$$

where  $\mathbf{w}_k = \frac{2\mathbf{p}}{NT_p} k$  and  $t_n = nT_p$ .  $F(k)$  and  $f(n)$  are sometimes used to denote sampled data.



Sampling rate:  $f_s = 1/T_p \equiv f_p$

Frequency resolution:  $\Delta f = 1/(NT_p)$  (signal duration is  $NT_p$ )

For unambiguous frequency measurement:  $f_s \geq 2f_{\max}$ , or  $f_{\max} \leq f_s/2$

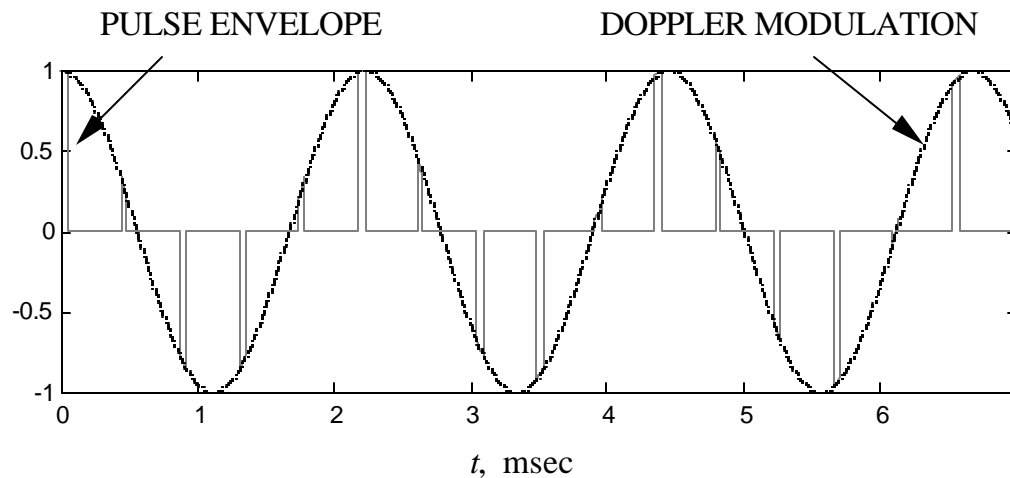
# Doppler Filtering Using the DFT (1)

---

Assume that there is a target return in a fixed range bin (e.g., #2):

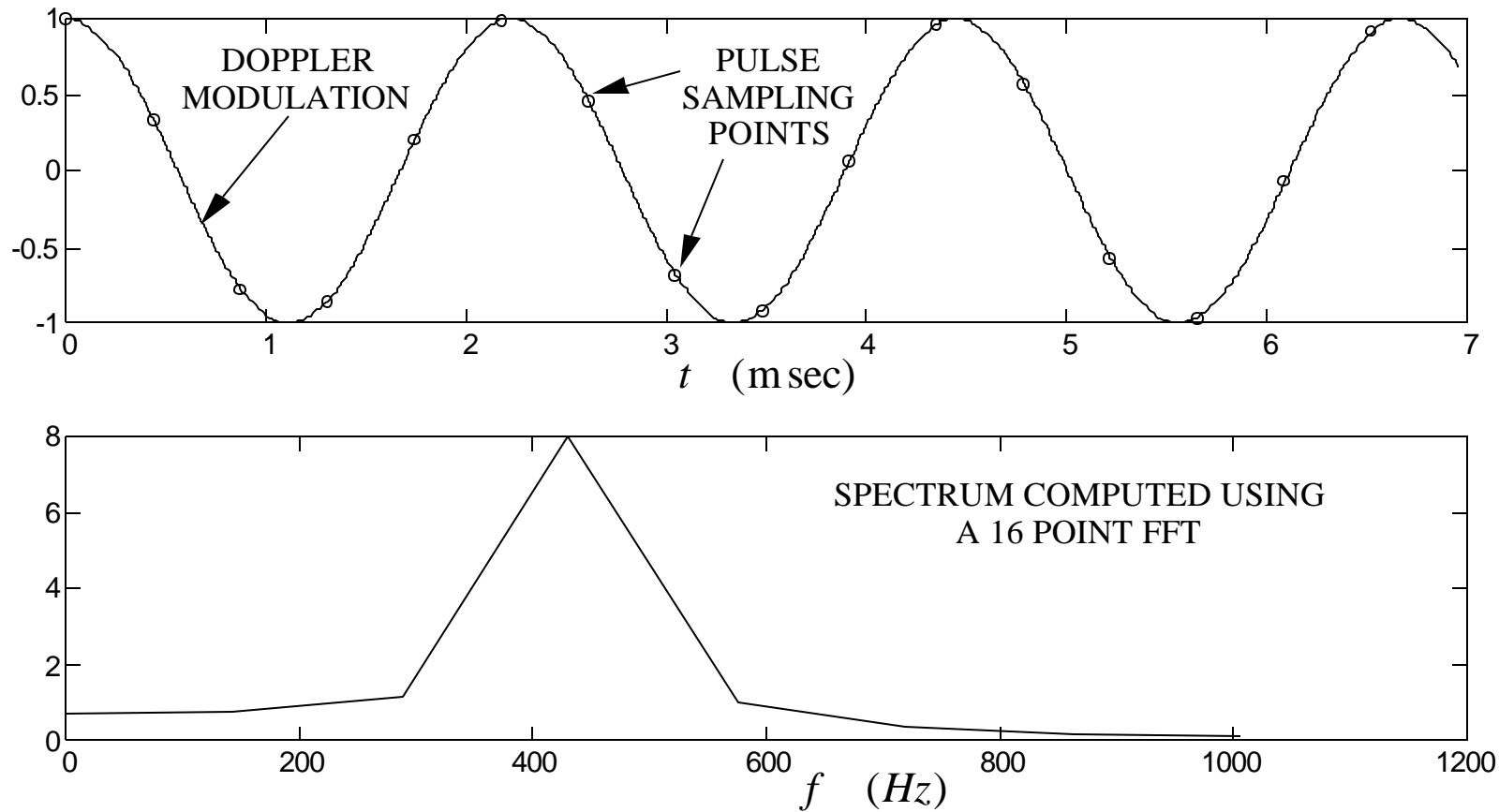
1. There are  $N$  pulses in a dwell and therefore the sinusoid is sampled  $N$  times
  - the sampling rate is the PRF
  - each range bin gets sampled  $N$  times
  - there are a total of  $N \times M$  data points per dwell
2. The data from each set of range bins is Fourier transformed. Typically the FFT is used, which requires that  $N = 2^n$ , where  $n$  is an integer.
3. The FFT returns  $N$  frequencies

Example: pulse train ( $N = 16$ ) echo return modulated by target doppler (ideal -- no dispersion or noise)



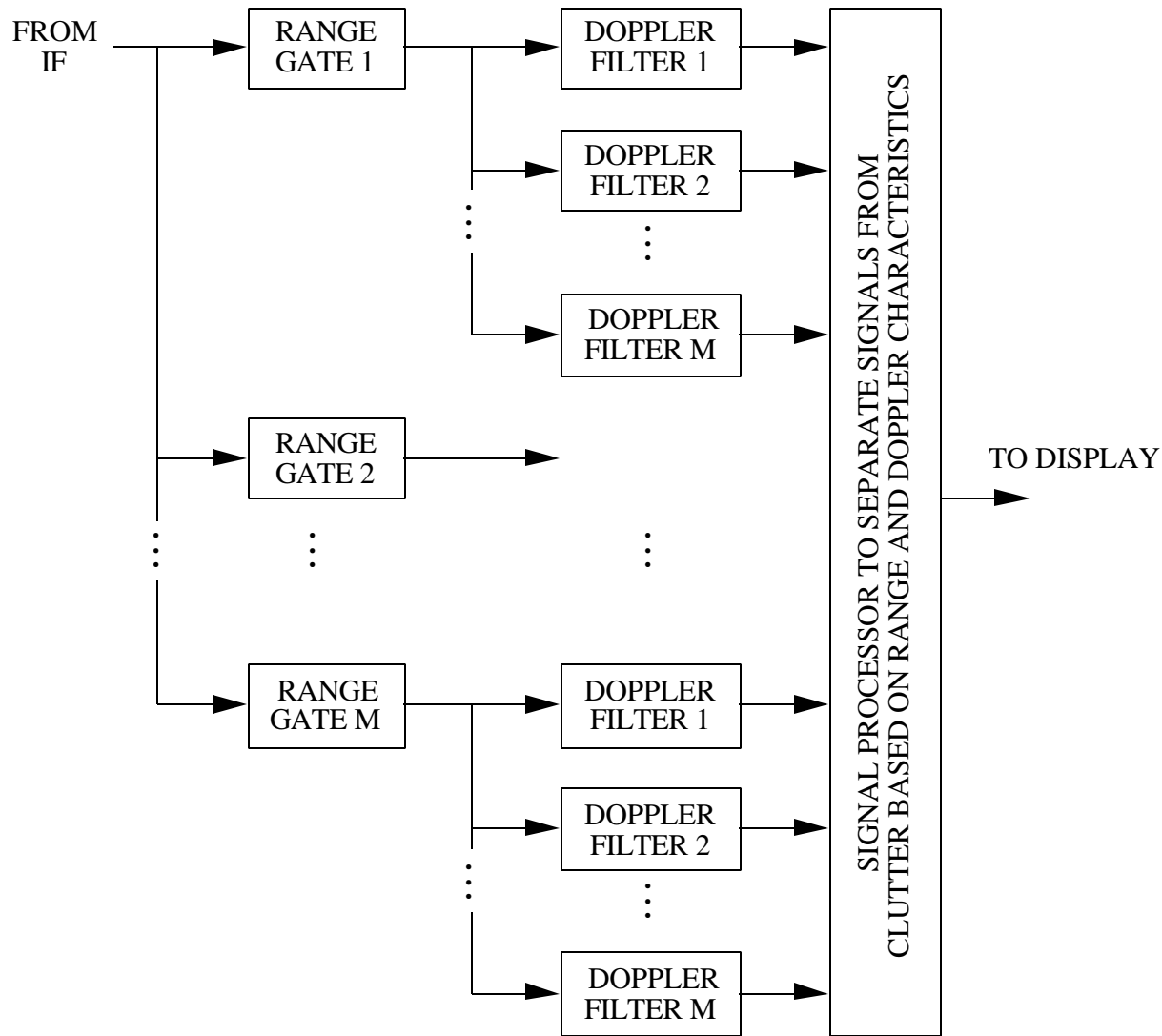
# Doppler Filtering Using the DFT (2)

Calculation parameters:  $f_d = 450$  Hz,  $t = 150$   $\mu$ sec, PRF=2300 Hz. From the parameters:  $\Delta f = 1/(NT_p) = 143.8$ Hz  $f_s = 2300$ Hz  $NT_p = 6.957$  ms



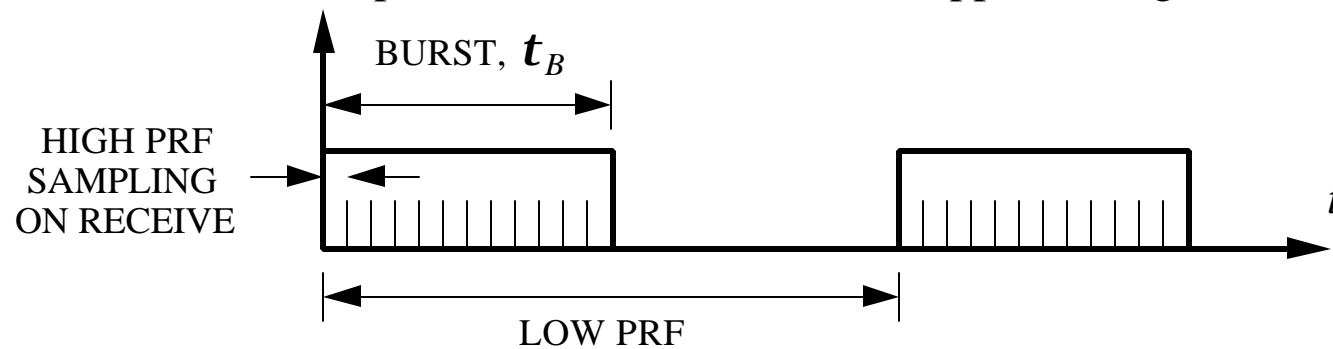


# Pulse Doppler Receiver



# Pulse Burst Mode

Pulse burst is a combination of low and high PRFs. A burst is a long pulse (of length  $t_B$ ) that is transmitted at a burst repetition frequency (BRF) which has a low PRF value. On receive, the data is sampled at a HPF rate to avoid doppler ambiguities:



Typical steps:

1. Coarse range is measured by sorting the data into blocks of length  $ct_B/2$  ("burst delay ranging").
2. Samples are sorted by doppler by taking the FFT over the dwell of samples contained in each range block. Course doppler is obtained to within  $1/t_B$ .
3. Further processing of the data can improve the doppler measurement.

Tradeoffs: short burst  $\Rightarrow$  lower competing clutter power  
 long burst  $\Rightarrow$  higher SNR and smaller doppler bin size  
 computationally demanding (i.e., computer processing and memory)

# MTI Improvement Factors

---

MTI improvement factor (clutter improvement factor):

$$I_c = \frac{\text{SCR}_{\text{out}}}{\text{SCR}_{\text{in}}} = \frac{S_{\text{out}}}{S_{\text{in}}} \times \text{CA}$$

where SCR is the signal to clutter ratio.

Subclutter visibility: ratio by which the target return may be below the coincident clutter return and still be detected (with a specified  $P_d$  and  $P_{fa}$ ).

Clutter attenuation:

$$\text{CA} = \frac{\text{clutter power into canceler or filter}}{\text{clutter power remaining after cancelation}} = \frac{\int_{-\infty}^{\infty} S_c(\mathbf{w}) d\mathbf{w}}{\int_{-\infty}^{\infty} S_c(\mathbf{w}) |H_c(\mathbf{w})|^2 d\mathbf{w}}$$

where  $S_c(\mathbf{w})$  is the clutter spectrum and  $H_c(\mathbf{w})$  the canceler/filter characteristic.

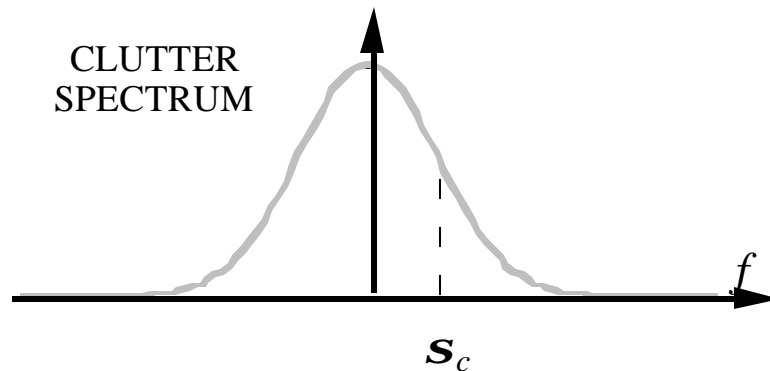
Cancellation ratio:

$$\text{CR} = \frac{\text{canceler voltage amplification}}{\text{gain of single unprocessed pulse}} \left| \begin{array}{l} \text{ANTENNA AND} \\ \text{TARGET FIXED} \end{array} \right.$$

# MTI Limitations (1)

Fluctuations in the clutter and instabilities in the radar system cause the clutter spectrum to spread. A simple model approximates the clutter spectrum as a gaussian with standard deviation  $\mathbf{s}_c$ . If the contributing random processes are independent, then the total spectrum variance is

$$\mathbf{s}_c^2 = \mathbf{s}_F^2 + \mathbf{s}_m^2 + \mathbf{s}_w^2 + \mathbf{s}_Q^2$$



1. Equipment instabilities: frequencies, pulsewidths, waveform timing, delay line response, etc. For transmitter frequency drift:

$$\mathbf{s}_F = \frac{2.67}{B_n} \left( \frac{df}{dt} \right)$$

2. Quantization errors in digital processing:  $\mathbf{s}_Q$  (rule of thumb: 6 dB per bit)

## MTI Limitations (2)

---

3. Clutter fluctuations due to wind and motion: Clutter return is a random process. Let the standard deviation of the wind velocity be  $\mathbf{s}_v$ . The corresponding standard deviation of the clutter spectrum due to wind motion is  $\mathbf{s}_w = 2\mathbf{s}_v / l$
4. Antenna scanning modulation: the antenna periodically illuminates the target and therefore the return looks like a pulse train that gets switched off and on

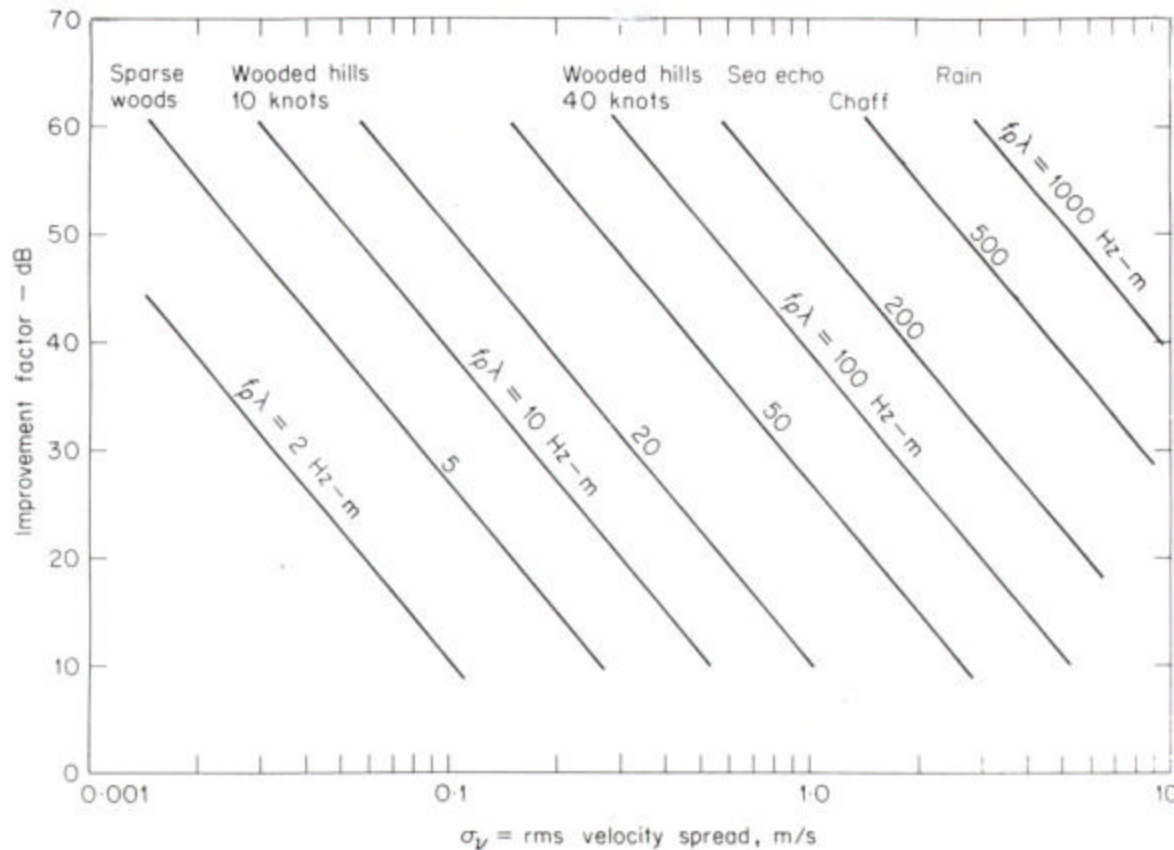
$$\mathbf{s}_m = \frac{0.265 f_p}{n_B}$$

Note that:

1. A gaussian spectrum is maintained through the frequency conversion process and synchronous detection.
2. Envelope or square law detection doubles the variance

# MTI Canceler Improvement Factors

Improvement factors for delay line cancelers (coherent, no feedback):



$$\text{Single : } I_{c1} = 2 \left( \frac{f_p}{2ps_c} \right)^2$$

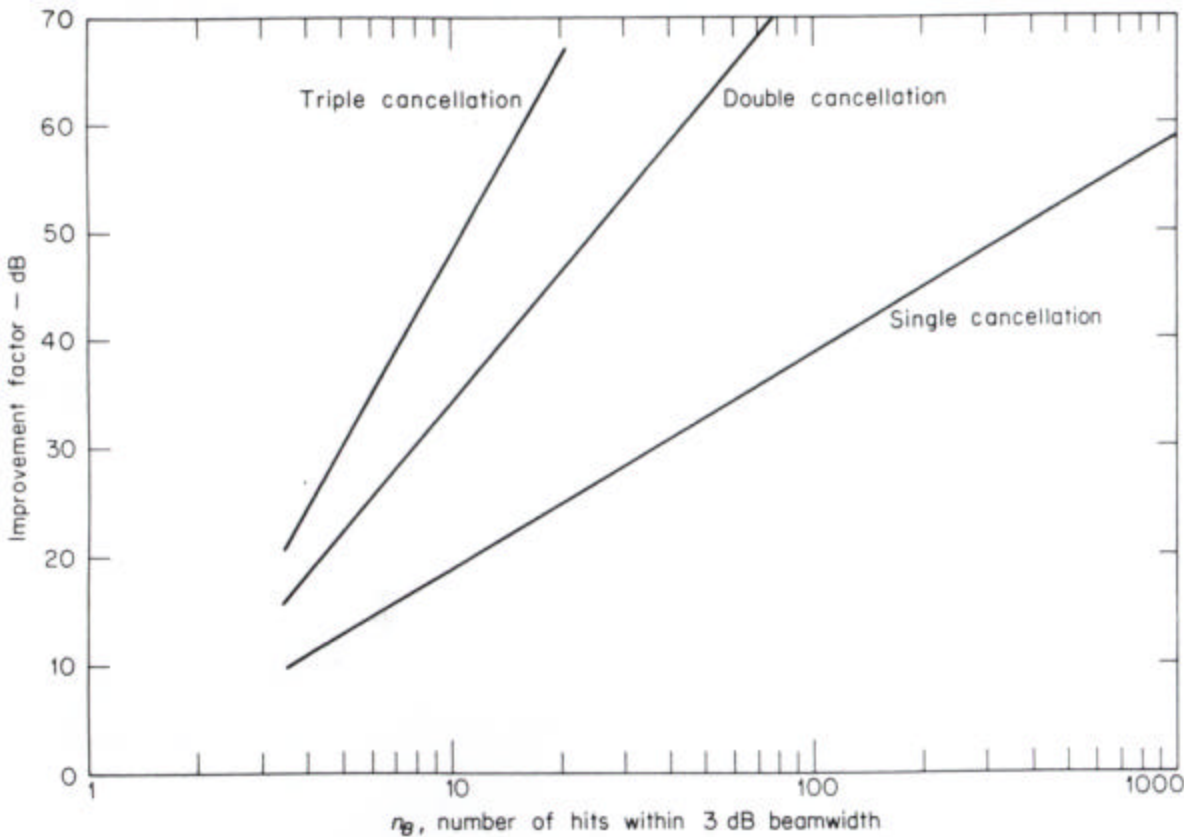
$$\text{Double : } I_{c2} = 2 \left( \frac{f_p}{2ps_c} \right)^4$$

Fig. 4.30 in Skolnik, 2<sup>nd</sup> edition

Chart for double canceler performance

# MTI Canceler Improvement Factors

Improvement factors for delay line cancelers:



$$\text{Single : } I_{s1} = \frac{n_B^2}{1.388}$$

$$\text{Double : } I_{s2} = \frac{n_B^4}{3.853}$$

Fig. 3.32 in Skolnik

Chart for limitation due to antenna scanning modulation

# Example

---

Example: A radar with  $f = 16$  GHz ( $I = 0.018$ ),  $n_B = 10$  and  $f_p = 530$  Hz using a double canceler and operating in wooded hills with 10 kt winds.

The improvement factor considering clutter motion:  $s_v = 0.04 \Rightarrow s_c = s_w = \frac{2(0.04)}{0.018}$

$$I_{c2} = 2 \left( \frac{f_p}{2ps_c} \right)^4 = 2 \left( \frac{530}{2p(4.267)} \right)^4 = 3 \times 10^6 = 54.9 \text{ dB}$$

The limitation in improvement factor due to antenna modulation if the antenna is scanning and there are  $n_B$  pulses hitting the clutter:

$$I_{s2} = \frac{n_B^4}{3.85} = 2597.4 = 34.1 \text{ dB}$$

Note that a similar result would be obtained by including the antenna modulation in the calculation of  $s_c$ :  $s_m = 0.265 f_p / n_B = 14.05 \Rightarrow s_c = \sqrt{s_w^2 + s_m^2} = 14.7$

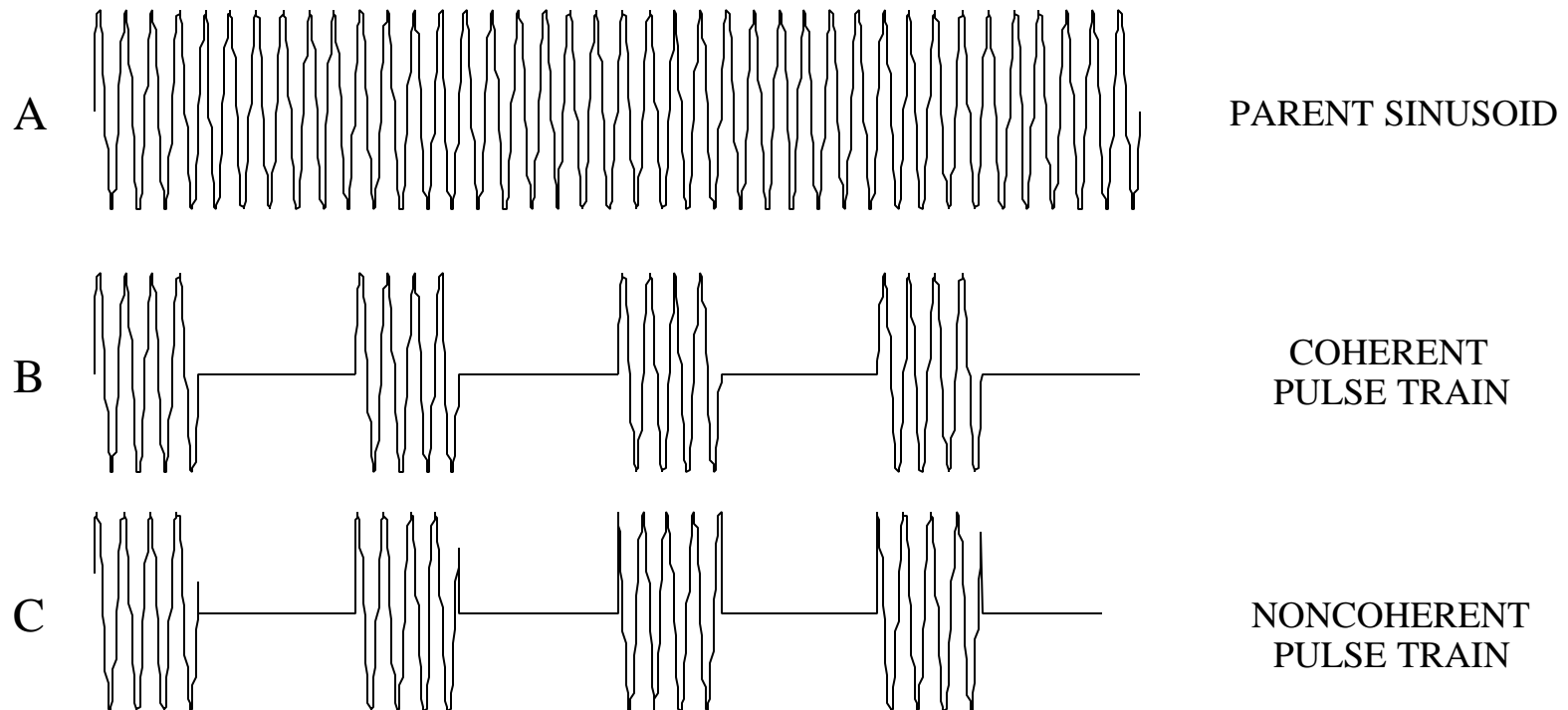
$$I_{total} = 2 \left( \frac{f_p}{2ps_c} \right)^4 = 2168 = 33.4 \text{ dB} \text{ or, alternately: } \frac{1}{I_{total}} = \frac{1}{I_{c2}} + \frac{1}{I_{s2}}$$



# Coherent and Noncoherent Pulse Trains

---

A coherent pulse train is one that is "cut" from a parent sinusoid. The waveforms A and B overlap exactly. For a noncoherent pulse train, the initial value of the carrier sinusoid for each pulse is essentially random.

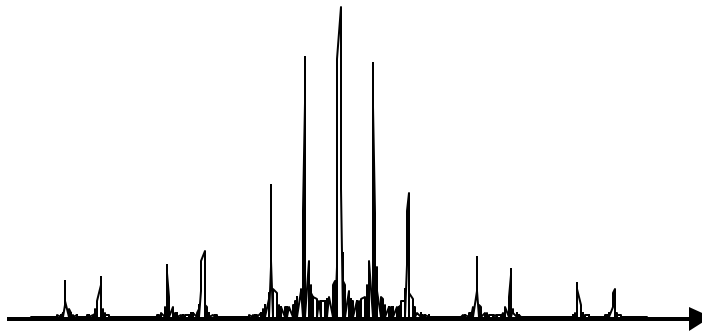


# Noncoherent Pulse Train Spectrum (1)

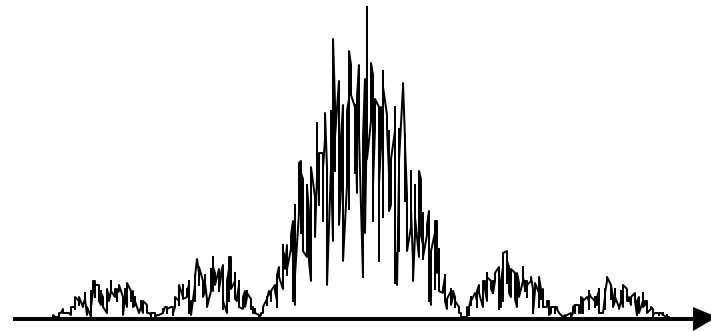
---

Random phases between pulses cause the spectrum to smear. Sharp doppler lines do not exist. However, if the target velocity is high enough and its modulation of the returned pulse is strong, the target can be detected.

SPECTRUM OF A  
COHERENT PULSE TRAIN

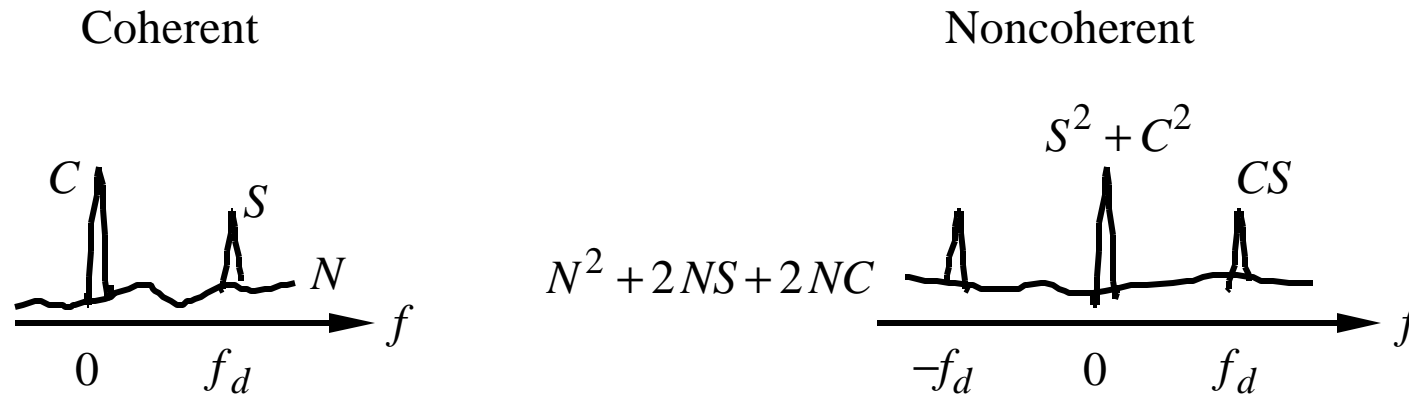


SPECTRUM OF A NON-  
COHERENT PULSE TRAIN



# Noncoherent Pulse Train Spectrum (2)

Video spectra:



The convolution of signal and clutter with noise gives the power

$$N^2 + 2NS + 2NC$$

The signal-to-noise ratio is

$$\frac{S}{N} = \frac{2SC}{N^2 + 2NS + 2NC}$$

Note that clutter must be present or the SNR is zero.

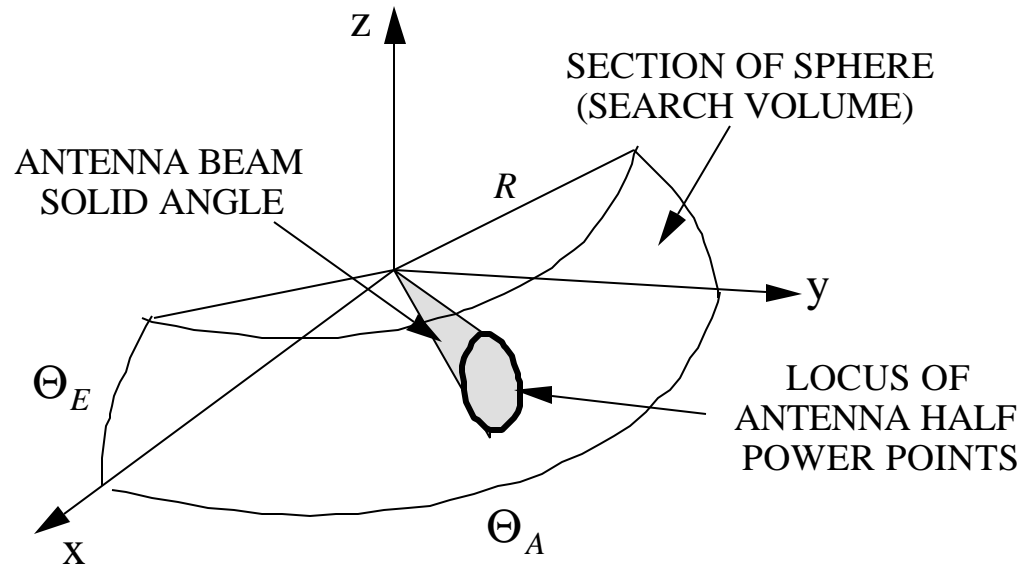
# Search Radar Equation (1)

---

Search radars are used to acquire targets and then hand them off to a tracking radar. (A multifunction radar can perform both tasks.) Search requires that the antenna cover large volumes of space (solid angles) in a short period of time. This implies:

1. fast antenna scan rate if the beam is narrow
2. large antenna beamwidth if a slow scan is used

Consider a volume search at range  $R$ :



# Search Radar Equation (2)

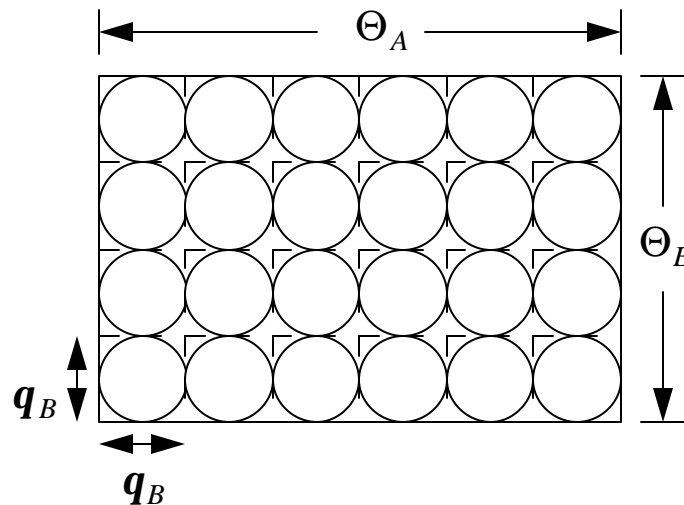
Search volume:

$$\Omega_s = \frac{A_s}{R^2} = \frac{1}{R^2} \int_{\Theta_{E1}}^{\Theta_{E2}} \int_{\Theta_{A1}}^{\Theta_{A2}} R^2 \sin \mathbf{q} d\mathbf{q} d\mathbf{f}$$

where  $(\Theta_{E2}, \Theta_{E1})$  are the elevation scan limits and  $(\Theta_{A2}, \Theta_{A1})$  are the azimuth scan limits. If the volume searched is near the horizon then  $\mathbf{q} \approx 90^\circ$  and

$$\Omega_s \approx (\Theta_{E2} - \Theta_{E1})(\Theta_{A2} - \Theta_{A1}) \equiv \Theta_E \Theta_A$$

Assume antenna beams with circular cross section. "Plan view" of the scan region:



# Search Radar Equation (3)

---

Number of beam positions required

$$N_B \approx \frac{\text{frame area}}{\text{beam area}} = \frac{\Theta_E \Theta_A}{\mathbf{q}_B^2}$$

The target can only lie in one beam. The time on target  $t_{ot}$ , or dwell time, is the time spent at each beam position

$$t_{ot} = \frac{t_f}{N_B} = \frac{t_f \mathbf{q}_B^2}{\Theta_E \Theta_A} \equiv \frac{n_B}{f_p}$$

where  $n_B$  is the number of pulses transmitted per beam position. Assuming that all pulses are integrated, the search radar equation becomes

$$\text{SNR} = \frac{P_r}{N_o} = \frac{P_t G_t A_{er} \mathbf{S} n_B}{(4\mathbf{p})^2 k T_s B_n R^4 L}$$

Now use

$$t_{ot} = t_f / N_B, B_n \mathbf{t} \approx 1, G_t = \frac{4\mathbf{p}(\mathbf{p}D^2/4)}{l^2}, \mathbf{q}_B \approx \frac{l}{D}, f_p = \frac{n_B}{t_{ot}}, \text{ and } P_t = \frac{P_{av}}{\mathbf{t} f_p}$$

# Search Radar Equation (4)

---

Search radar equation becomes

$$\text{SNR} = \frac{P_r}{N_o} = \frac{P_{\text{av}} A_{er} \mathbf{s} t_f}{16k T_s R^4 L N_B \mathbf{q}_B^2}$$

(Note: Skolnik has  $4p$  rather than 16 due to  $\mathbf{q}_B \approx 0.88\mathbf{l} / D$  vs  $\mathbf{l} / D$ ). Using  $N_B \mathbf{q}_B^2 = \Theta_E \Theta_A$  and rearranging gives the search detection range

$$R_{\text{max}} = \sqrt[4]{\frac{P_{\text{av}} A_{er} \mathbf{s} t_f}{16k T_s L \Theta_E \Theta_A \text{SNR}}}$$

Points to note:

1. independent of frequency (wavelength)
2. for given values of  $t_f / \Theta_E \Theta_A$  and  $\mathbf{s}$ , the range primarily depends on the product  $P_{\text{av}} A_{er}$
3.  $t_f / \Theta_E \Theta_A$  must be increased to increase  $R$
4. note that coherent integration of  $n_B$  pulses has been assumed

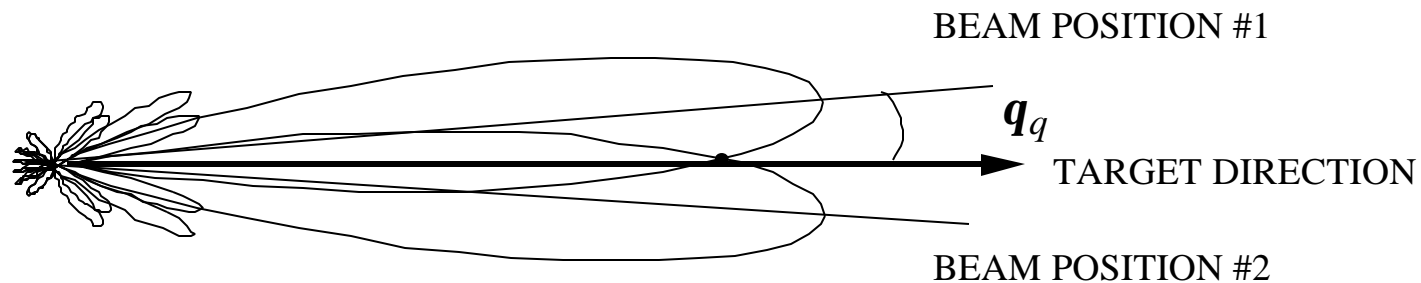
Common search patterns: raster, spiral, helical, and nodding (sinusoidal)

# Radar Tracking (1)

---

Target tracking is achieved by positioning the radar antenna boresight (direction reference with respect to the gain pattern). Several techniques can be used:

1. Sequential lobing: The beam is switched between positions #1 and #2.  $q_q$  is the squint angle. If the target return is constant and located at the bisecting angle of the two beam maxima, then the received power will be the same in both positions.



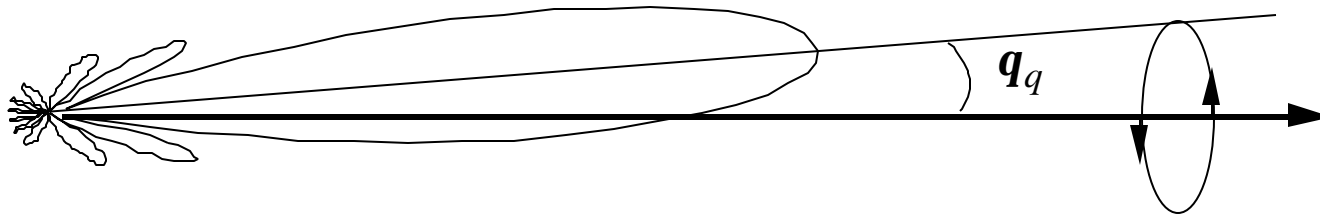
A error in the direction estimate occurs if the target RCS is not constant (which is always the case).

2. Conical scan: The antenna beam is squinted a small amount and then rotated around the reference. If the target is in the reference direction the received power is constant. If not the received power is modulated. The modulation can be used to generate an error signal to correct the antenna pointing direction.

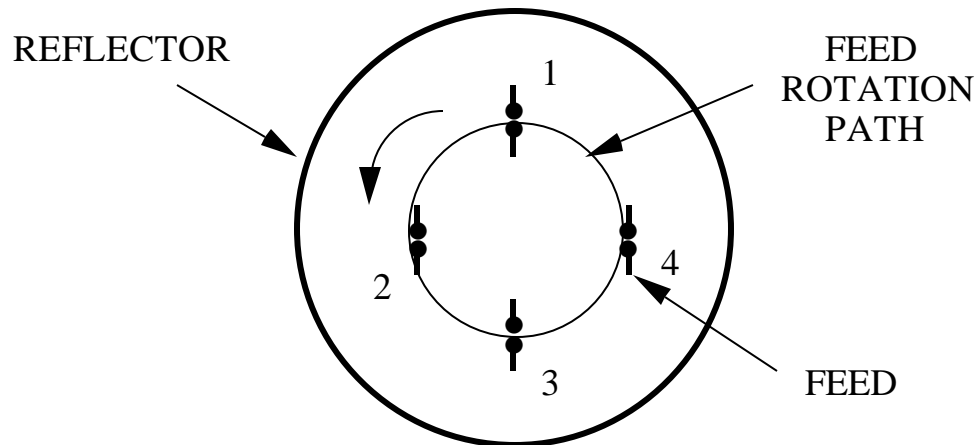


# Radar Tracking (2)

Conical scan (continued)



Note that if the antenna is physically rotated the polarization also rotates. This is undesirable. Fixed polarization is provided by a nutating feed.

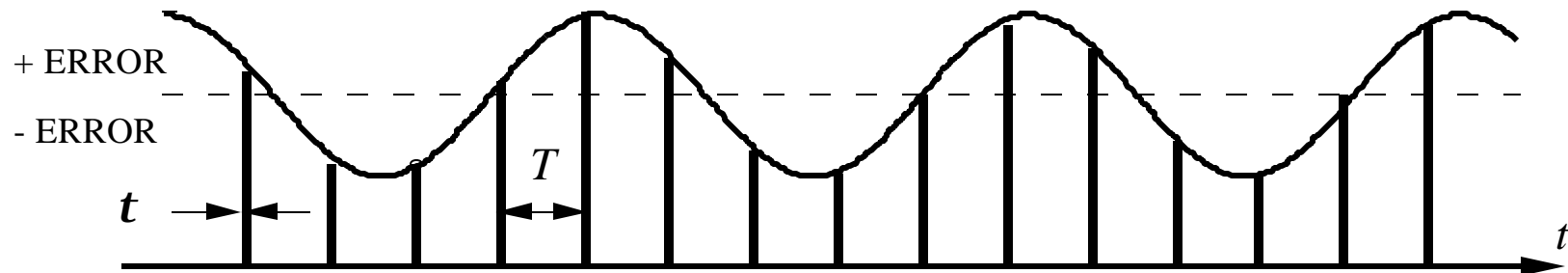


# Radar Tracking (3)

---

## Conical scan (continued)

If the target is not centered on the axis of rotation then there is a modulation of the received power



## Conical scan problems:

1. Jet turbines rotate at about the same frequency as the upper limit of antenna rotation (2400 rpm). Propellers are at the lower end of the antenna rotation limit (100 rpm).
2. Long ranges are a problem. The round trip time of transit is comparable to the antenna rotation.
3. Pulse-to-pulse RCS variations are a problem.

# Gain Control

---

The dynamic range of received signals can exceed the dynamic range of the receiver

close in targets  $\Rightarrow$  large return above receiver saturation level (any scanning modulation is lost)

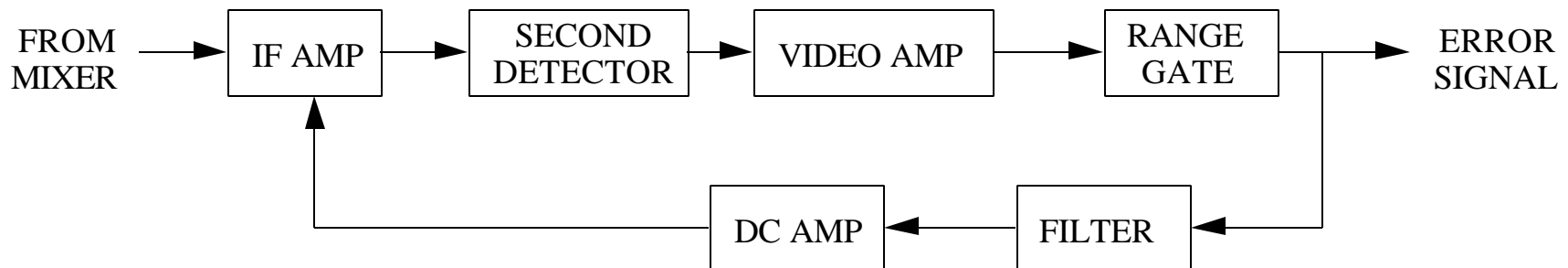
far out targets  $\Rightarrow$  small return below noise level

The dynamic range can be extended using gain controls:

Manual gain control (MGC): The operator adjusts the receiver to match the dynamic range of the display.

Automatic gain control (AGC): The signal from the target in a range gate is kept at a constant level

AGC circuit:

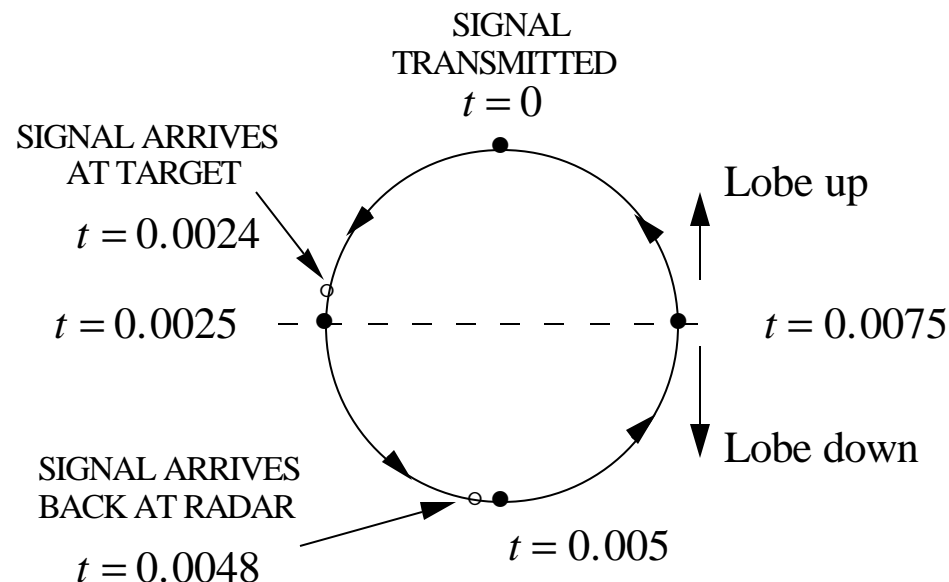


# Example

Conical scan antenna with a rotation rate of 100 Hz (0.01 sec/revolution) operates at a range of 460 miles. The one-way transit time of a pulse is

$$t = R/c = (460)(1000) / \left[ (0.62)(3 \times 10^8) \right] = 0.0024 \text{ sec}$$

The antenna rotates  $90^\circ$  in  $0.01/4 = 0.0025$  sec. The arrival time of a pulse is illustrated below:



Four pulses are generally required (top, bottom, left, and right). For the case of the target left or right, the transit time is approximately equal to half of the rotation rate, and therefore the effect of the scan is cancelled. There is no modulation of the return.

# Example

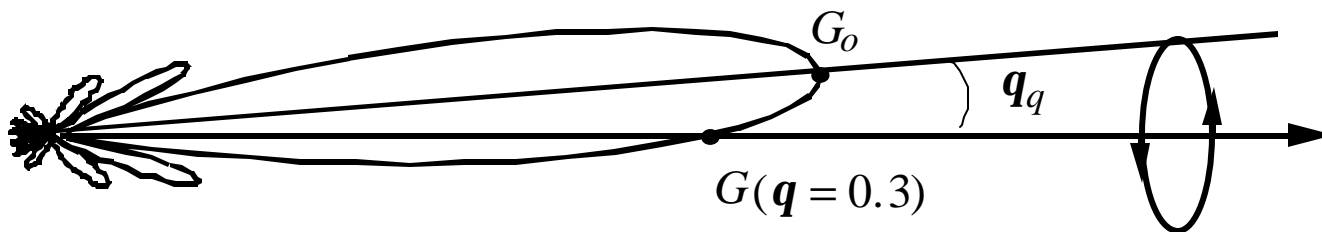
A conical scan radar has a gaussian shaped main beam gain approximated by

$$G(\mathbf{q}) = G_o e^{-K\mathbf{q}^2 / \mathbf{q}_B^2}$$

where  $\mathbf{q}_B = 1^\circ$  is the HPBW and  $K = 4 \ln(2) = 2.773$ . The crossover loss is the reduction in gain due to the fact that the target is tracked off of the beam peak. Assume that the beam is squinted at an angle  $\mathbf{q}_q = 0.3^\circ$ . The pattern level at the squint angle is

$$G(\mathbf{q}_q) = G_o \exp\left\{\left(-2.773(0.3^\circ)^2 / (1^2)\right)\right\} = 0.779G_o$$

The crossover loss is  $10 \log\left(\frac{0.779G_o}{G_o}\right) = -1.084$  dB

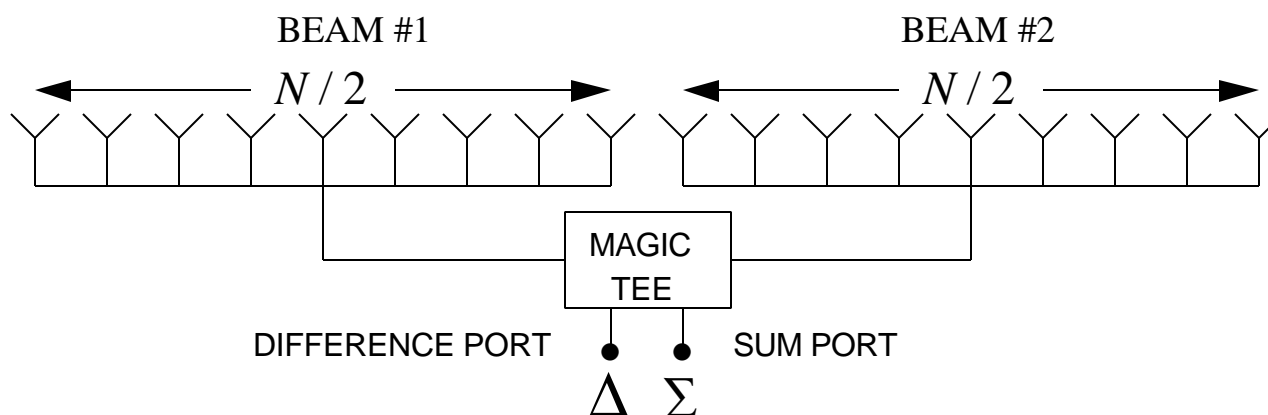


# Monopulse Tracking (1)

Pulse to pulse variations in the target RCS leads to tracking inaccuracies. We want range and angle information with a single pulse, i.e., monopulse (also called simultaneous lobing). There are two types:

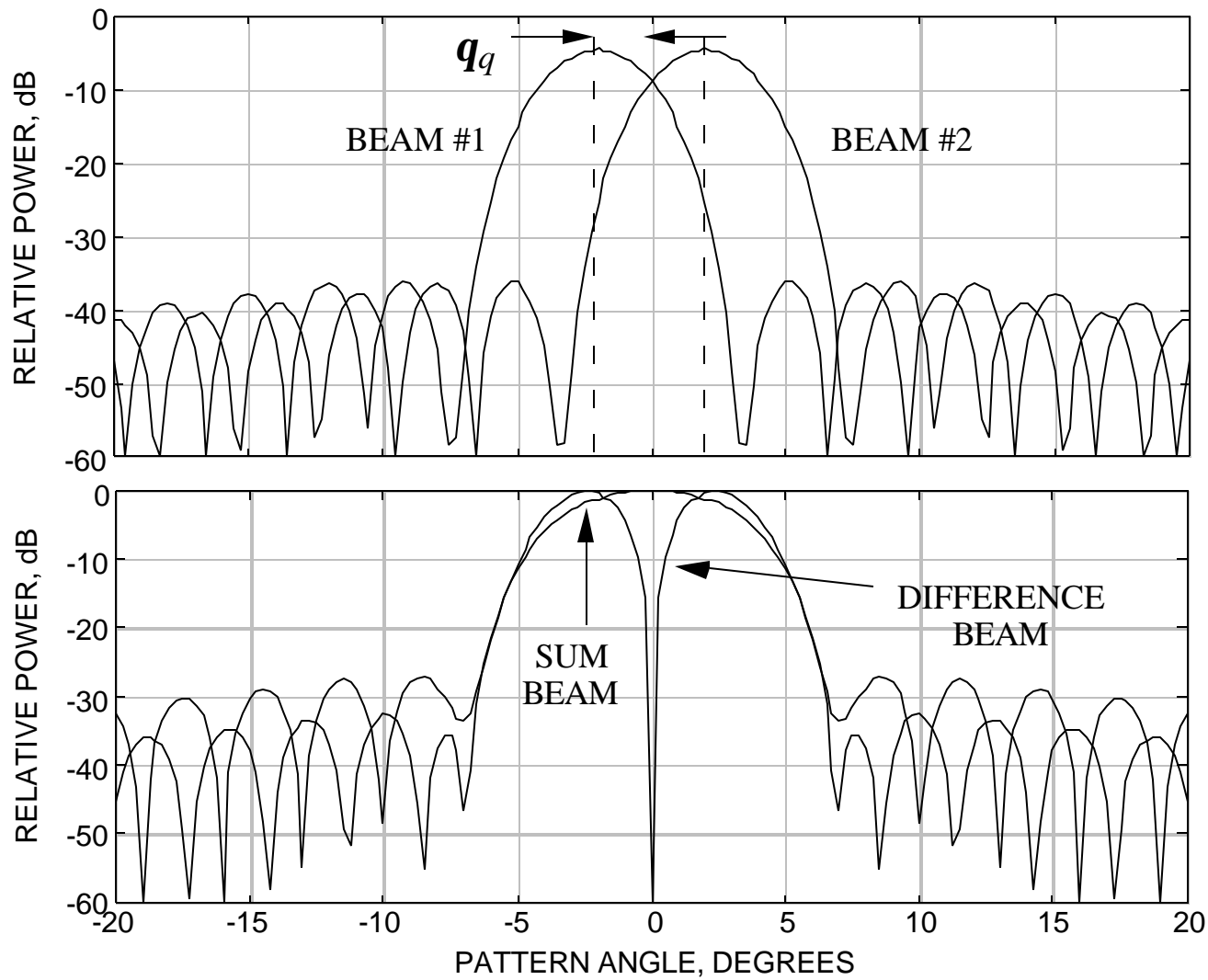
## 1. Amplitude comparison monopulse:

Two antenna beams are generated at small positive and negative squint angles. The outputs from the two beam ports are added to form a sum beam and subtracted to form a difference beam. The sum beam is used on transmit and receive; the difference beam is only used on receive.



Monopulse beamforming is implemented using a magic tee.

# Monopulse Tracking (2)



# Monopulse Tracking (3)

---

Tracking is done by processing the difference to sum voltage ratio:

$$\frac{\Delta}{\Sigma} = \frac{\text{difference voltage}}{\text{sum voltage}} = \frac{\Delta_I + j\Delta_Q}{\Sigma_I + j\Sigma_Q}$$

Now,

$$\text{Re}\{\Delta/\Sigma\} = \frac{\Delta_I\Sigma_I + \Delta_Q\Sigma_Q}{\Sigma_I^2 + \Sigma_Q^2} = \frac{|\Delta|}{|\Sigma|} \cos \mathbf{d}$$

$$\text{Im}\{\Delta/\Sigma\} = \frac{\Delta_Q\Sigma_I - \Delta_I\Sigma_Q}{\Sigma_I^2 + \Sigma_Q^2} = \frac{|\Delta|}{|\Sigma|} \sin \mathbf{d}$$

where  $\mathbf{d}$  is the relative phase between the sum and difference channels. Usually only  $\text{Re}\{\Delta/\Sigma\}$  is processed because:

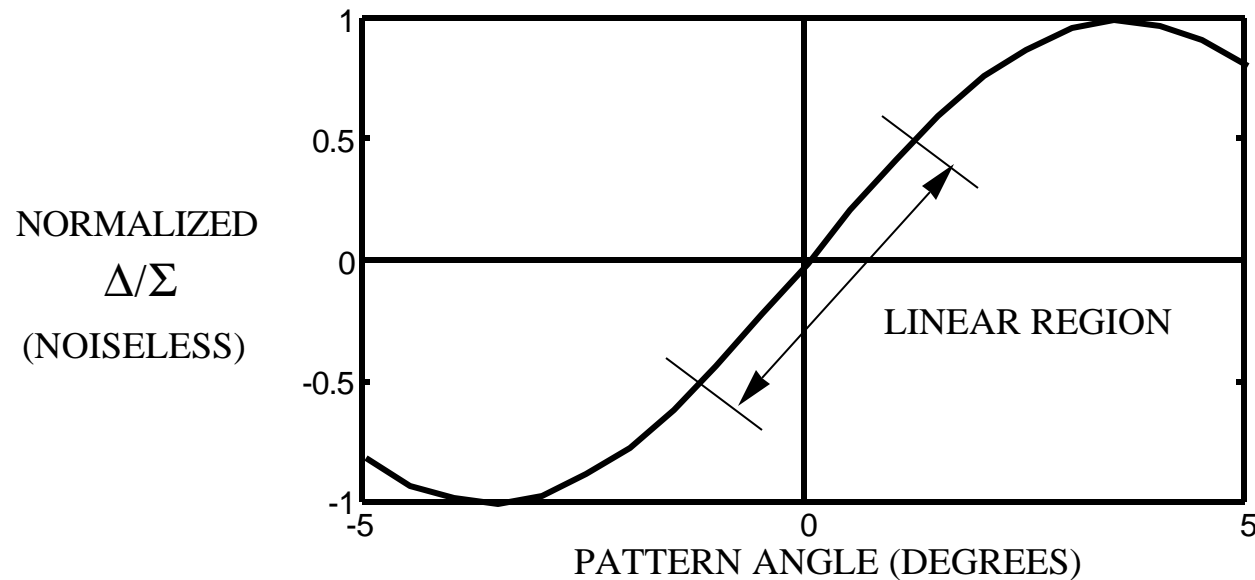
1. It has the required sign information: + ratio on positive side of null;  
- on negative side.
2. The target only contributes to  $\text{Re}\{\Delta/\Sigma\}$ ; noise, interference, etc. contribute to both terms equally.

See Fig. 5.9 in Skolnik for implementation. I and Q processing can be done after the amplifier.



# Monopulse Tracking (4)

Plot of typical  $\Delta / \Sigma$  in the vicinity of the null. (The slope depends on the antenna beamwidths and squint.)



In the linear region:

$$\Delta / \Sigma \approx Kq$$

$K$  is the monopulse slope constant. The function  $\Delta / \Sigma$  can be used to generate an error signal to place the difference beam null on the target.

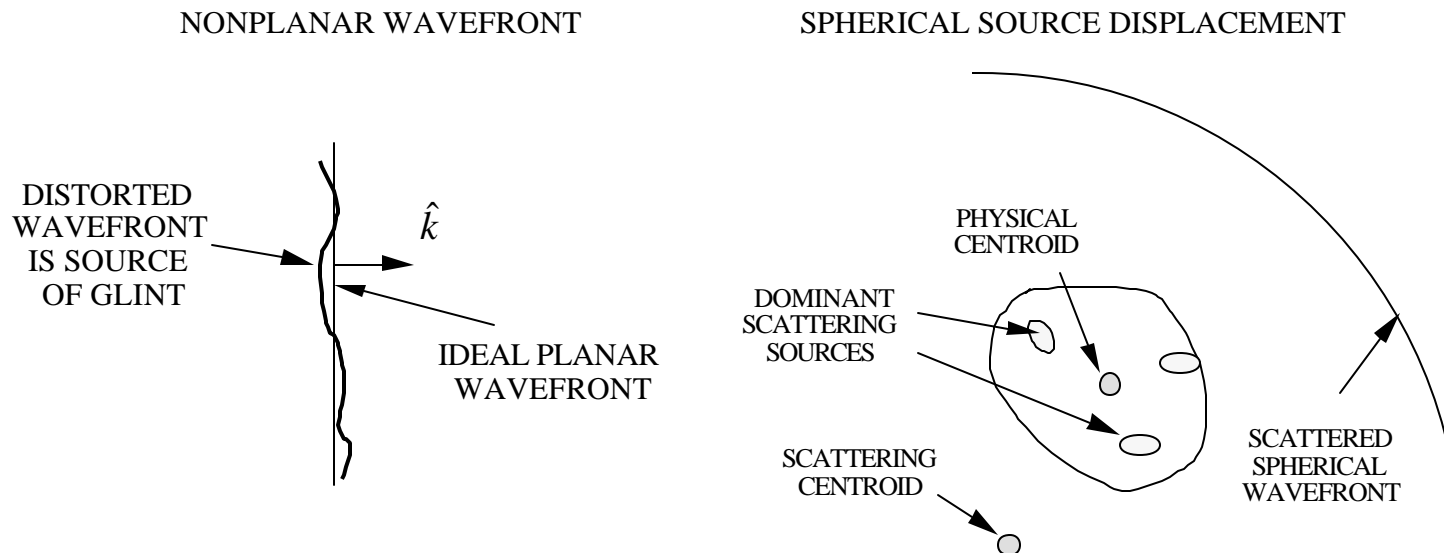
# Monopulse Tracking (5)

Sources of monopulse tracking error:

1. Antenna errors: null shift and null filling due to antenna illumination errors.
2. Thermal noise: RMS angle error for a single target, high SNR, with the target on boresight (i.e., the target would be in the null of the ideal antenna)

$$s_{q_t} = \frac{1}{K\sqrt{\text{SNR}}}$$

3. Target glint: glint refers to the distortion of the wavefront scattered from the target due to environmental and interference effects. When the wavefront is distorted, the apparent target direction can differ from the actual target direction.

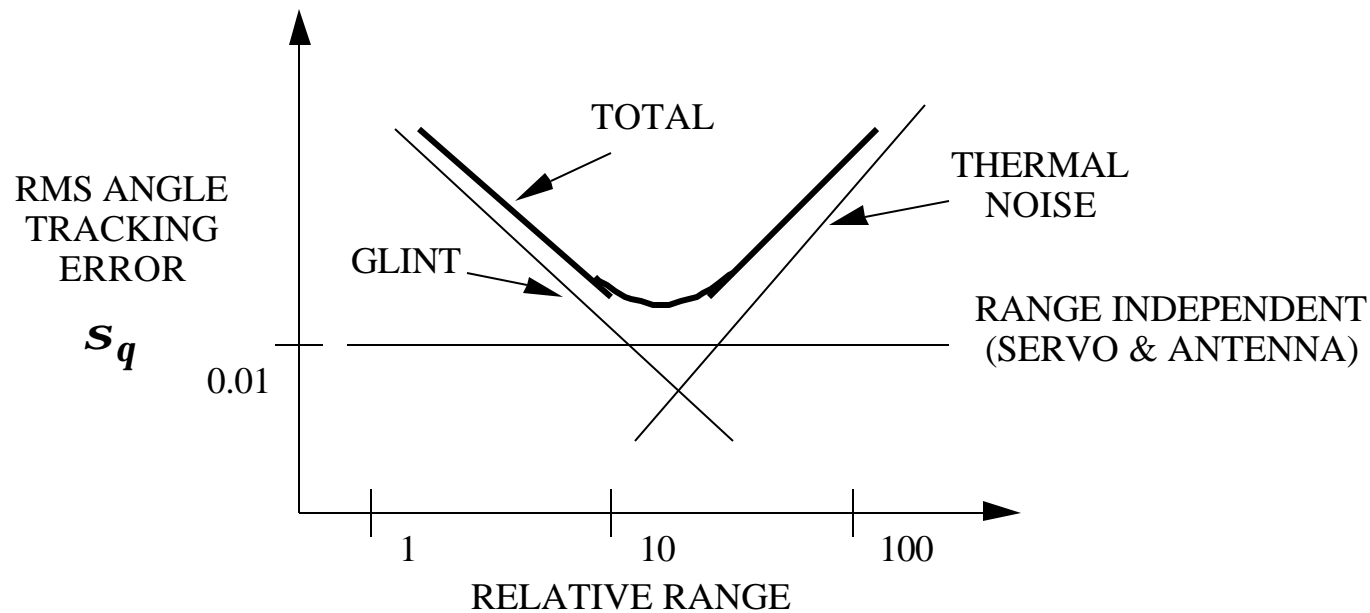


# Monopulse Tracking (6)

RMS angle error due to target glint is approximately given by the empirical formula

$$s_{q_g} \approx 0.7 \tan\left(\frac{L/2}{R}\right) \approx 0.35 \frac{L}{R}$$

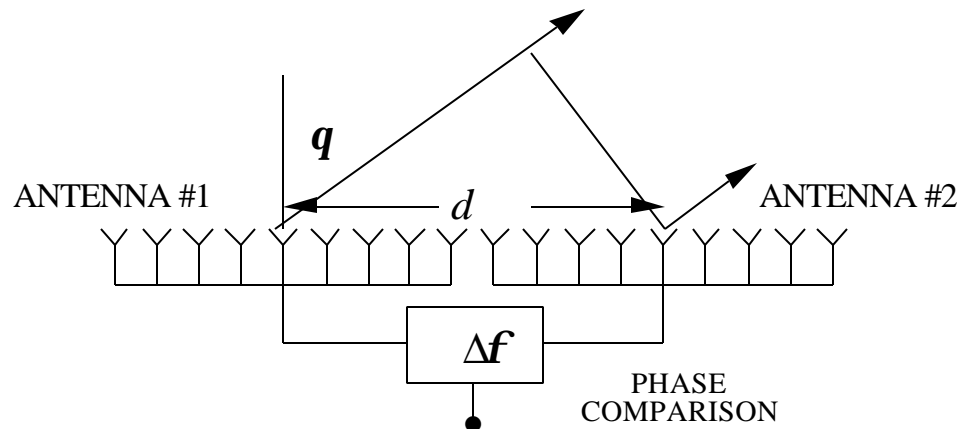
where  $L$  is the target extent (for example, the length or wingspan of an aircraft), and  $R$  is the range to the target.



# Monopulse Tracking (7)

## 1. Phase comparison monopulse (interferometer radar):

The phase difference between two widely spaced antennas is used to determine the angle of arrival of the wavefront.



For a plane wave arriving from a direction  $q$ , the phase difference between antennas #1 and #2 can be used to determine  $q$ :

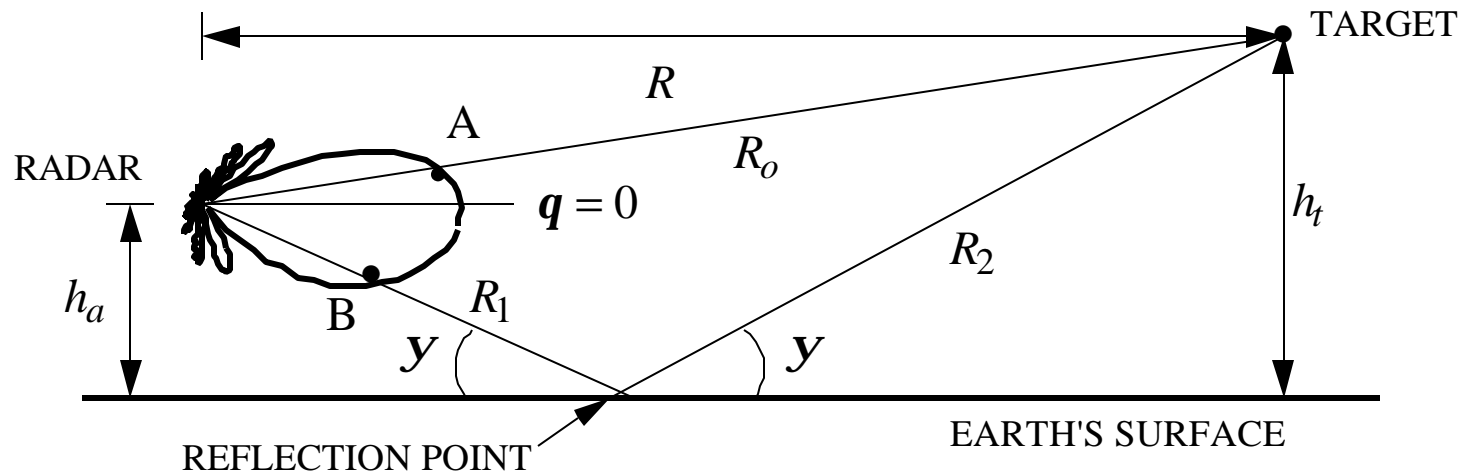
$$\Delta f = kd \sin q \approx kdq \Rightarrow q \approx \Delta f / (kd)$$

Problems:

1. ambiguities due to grating lobes because the antennas are widely spaced
2. tight phase tolerances must be maintained on the antenna
3. thermal and servo noise are sources of error

# Low Angle Tracking (1)

When a radar and target are both operating near the surface of the earth, multipath (multiple reflections) can cause extremely large angle errors. Assume a flat earth:



At low altitudes the reflection coefficient is approximately constant ( $\Gamma \approx -1$ ) and  $G_D(\mathbf{q}_A) \approx G_D(\mathbf{q}_B)$ . The difference between the direct and reflected paths is:

$$\Delta R = \underbrace{(R_1 + R_2)}_{\text{REFLECTED}} - \underbrace{R_0}_{\text{DIRECT}}$$

# Low Angle Tracking (2)

---

The total signal at the target is:

$$E_{\text{tot}} = \underbrace{E_{\text{ref}}}_{\text{REFLECTED}} + \underbrace{E_{\text{dir}}}_{\text{DIRECT}} = E(\mathbf{q}_A) + \Gamma E(\mathbf{q}_B) e^{-jk\Delta R}$$

From the low altitude approximation,  $E_{\text{dir}} = E(\mathbf{q}_A) \approx E(\mathbf{q}_B)$  so that

$$E_{\text{tot}} \approx E_{\text{dir}} + \Gamma E_{\text{dir}} e^{-jk\Delta R} = E_{\text{dir}} \underbrace{\left[ 1 + \Gamma e^{-jk\Delta R} \right]}_{\substack{\equiv F, \text{ PATH GAIN} \\ \text{FACTOR}}}$$

The path gain factor takes on the values  $0 \leq F \leq 2$ . If  $F = 0$  the direct and reflected rays cancel (destructive interference); if  $F = 2$  the two waves add (constructive interference).

An approximate expression for the path difference:

$$R_o = \sqrt{R^2 + (h_t - h_a)^2} \approx R + \frac{1}{2} \frac{(h_t - h_a)^2}{R}$$

$$R_1 + R_2 = \sqrt{R^2 + (h_t + h_a)^2} \approx R + \frac{1}{2} \frac{(h_t + h_a)^2}{R}$$

## Low Angle Tracking (3)

---

Therefore,

$$\Delta R \approx \frac{2h_a h_t}{R}$$

and

$$|F| = \left| 1 - e^{-jk2h_a h_t / R} \right| = \left| e^{jkh_a h_t / R} \left( e^{-jkh_a h_t / R} - e^{jkh_a h_t / R} \right) \right| = 2 \left| \sin(kh_a h_t / R) \right|$$

Incorporate the path gain factor into the RRE:

$$P_r \propto |F|^4 = 16 \sin^4 \left( \frac{kh_t h_a}{R} \right) \approx 16 \left( \frac{kh_t h_a}{R} \right)^4$$

The last approximation is based on

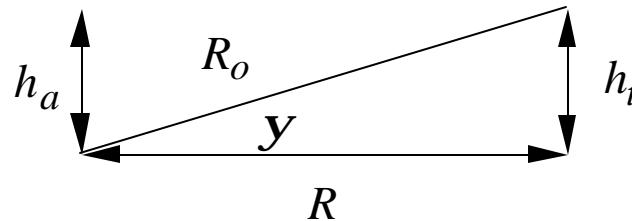
$$h_a \ll R \text{ and } h_t \ll R.$$

Finally, the RRE can be written as

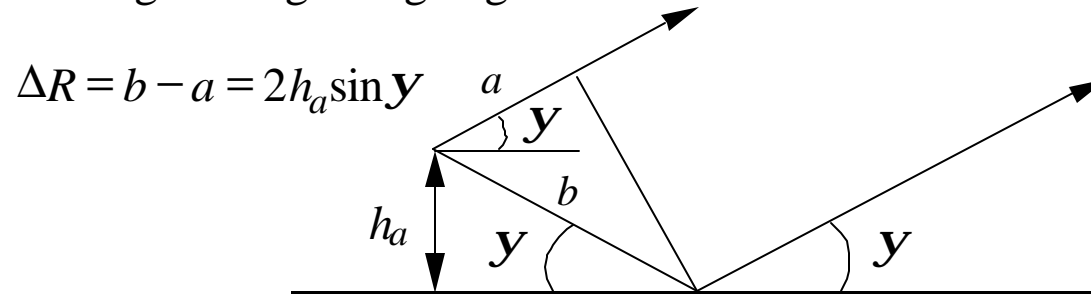
$$P_r = \frac{P_t G_t G_r I^2 \mathbf{s}}{(4\mathbf{p})^3 R^4} |F|^4 \approx \frac{4\mathbf{p} P_t G_t G_r \mathbf{s} (h_t h_a)^4}{I^2 R^8}$$

# Low Angle Tracking (4)

Two other forms of  $F$  are often used. Define  $\mathbf{y}$  as the elevation angle from the ground,  $\tan \mathbf{y} = h_t / R$ . Therefore  $|F|^4 = 16 \sin^4(kh_a \tan \mathbf{y})$



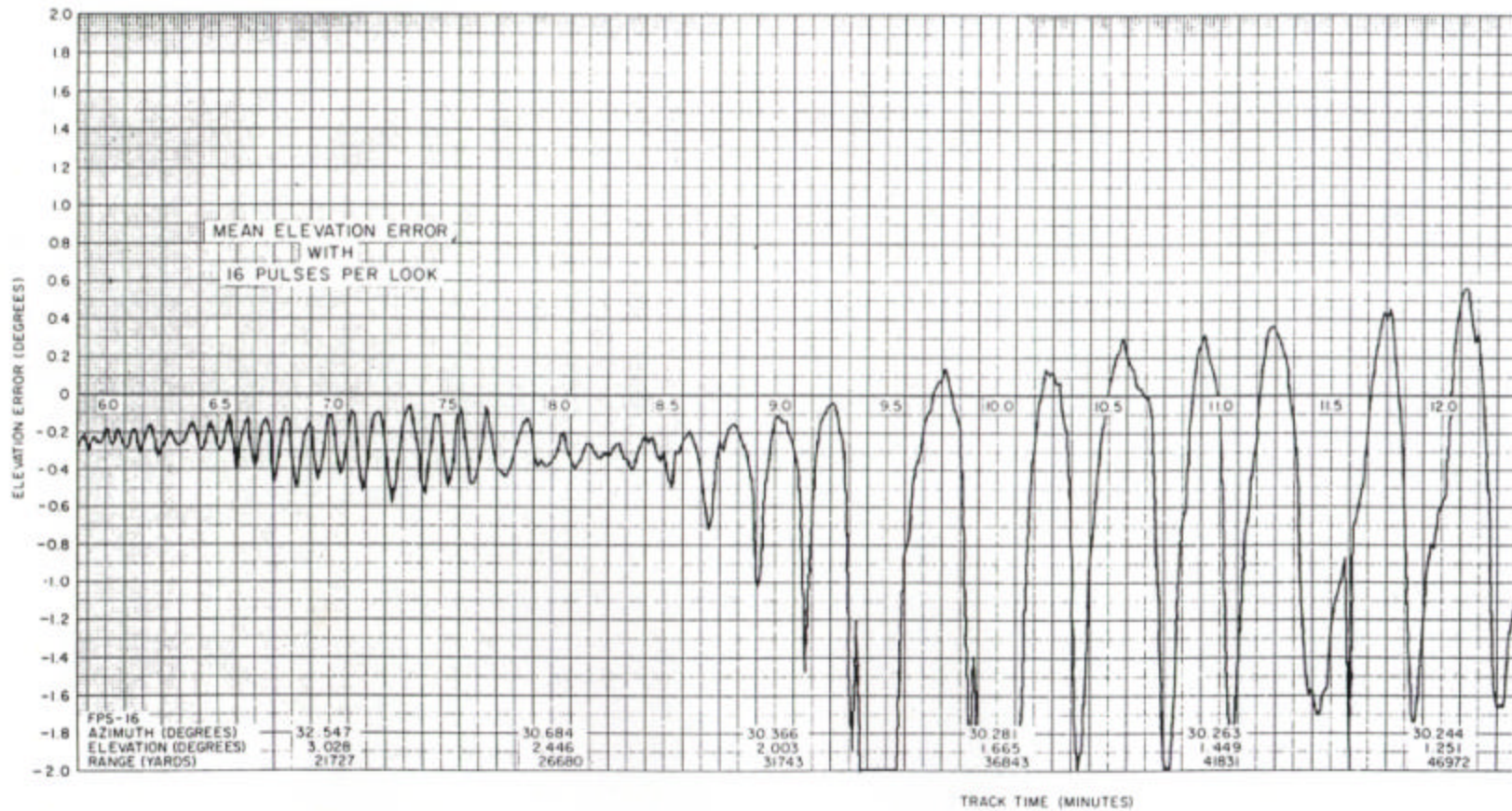
For the second form, assume the far-field parallel ray approximation is valid. Then  $\mathbf{y}$  is both the elevation angle and grazing angle.



Therefore,  $|F|^4 = 16 \sin^4 \left( \frac{2p h_a \sin \mathbf{y}}{l} \right)$  with nulls at  $\sin \mathbf{y}_n = \frac{n l}{2 h_a}, n = 0, 1, 2, \dots$



# Tracking Error Due to Multipath



(ZENITH)

(Fig. 4.18 in Skolnik)

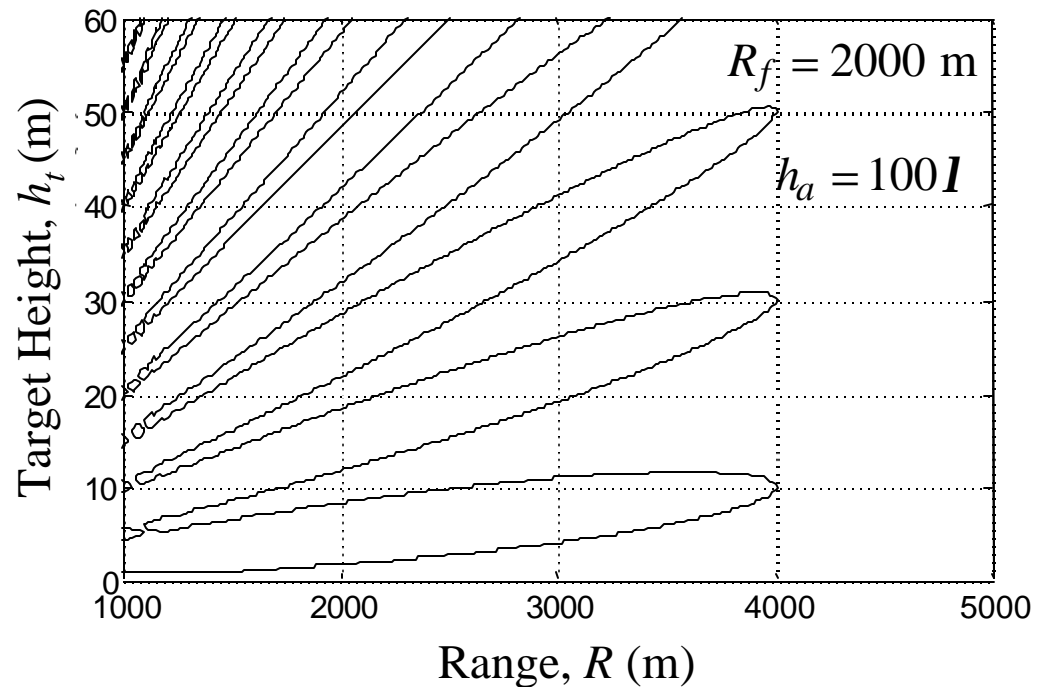
(HORIZON)

# Low Angle Tracking (5)

Methods of displaying the received power variation:

1. Coverage diagram: Contour plots of  $|F|$  in dB vs  $h_t$ ,  $R$  normalized to a reference range  $R_f$ . Contours of power equal to that of the free space reference range are plotted.

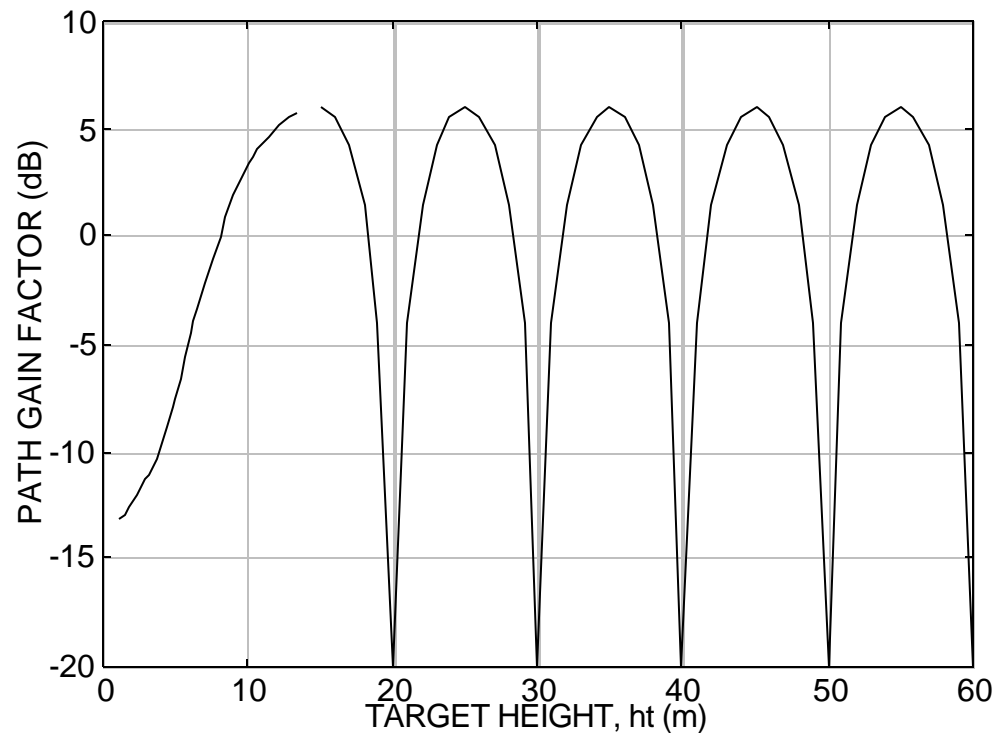
$$|F| = \left| 2 \left( \frac{R_f}{R} \right) \sin(kh_a \tan \mathbf{y}) \right|$$



# Low Angle Tracking (6)

---

2. Height-gain curves: Plots of  $|F|$  in dB vs  $h_t$  at a fixed range. The constructive and destructive interference as a function of height can be identified. At low frequencies the periodicity of the curve at low heights can be destroyed by the ground wave



# Atmospheric Refraction (1)

Refraction by the atmosphere causes waves to be bent back towards the earth's surface.

The ray trajectory is described by the equation:  $n R_e \sin \mathbf{q} = \text{CONSTANT}$

Two ways of expressing the index of refraction in the troposphere:

$$1. n = 1 + \mathbf{c}r / r_{SL} \\ + \text{HUMIDITY TERM}$$

$R_e = 6378 \text{ km} = \text{earth radius}$

$\mathbf{c} \approx 0.00029 = \text{Gladstone-Dale constant}$

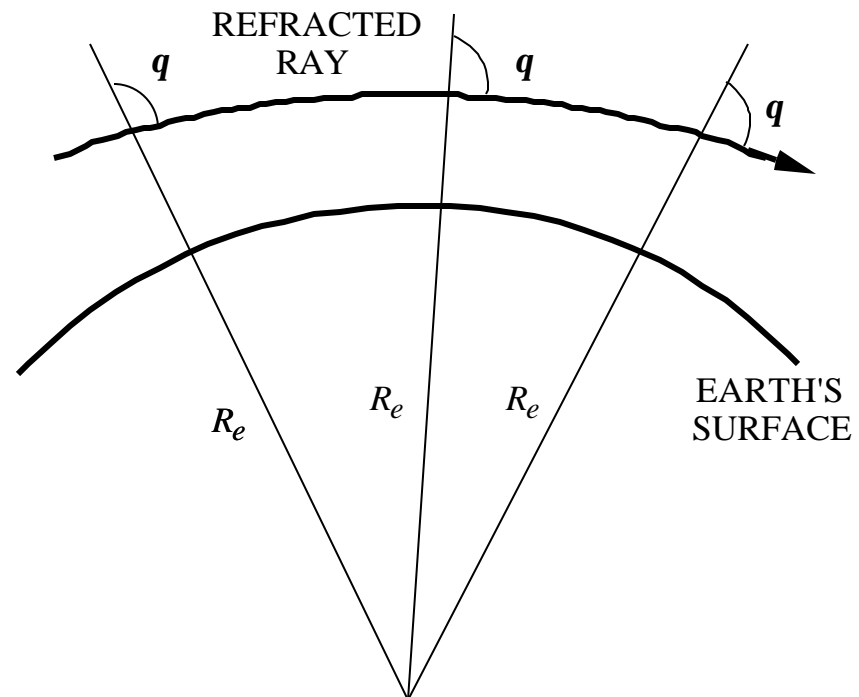
$r, r_{SL} = \text{mass densities at altitude and sea level}$

$$2. n = 77.6p/T + 7.73 \times 10^5 e/T^2$$

$p = \text{air pressure (millibars)}$

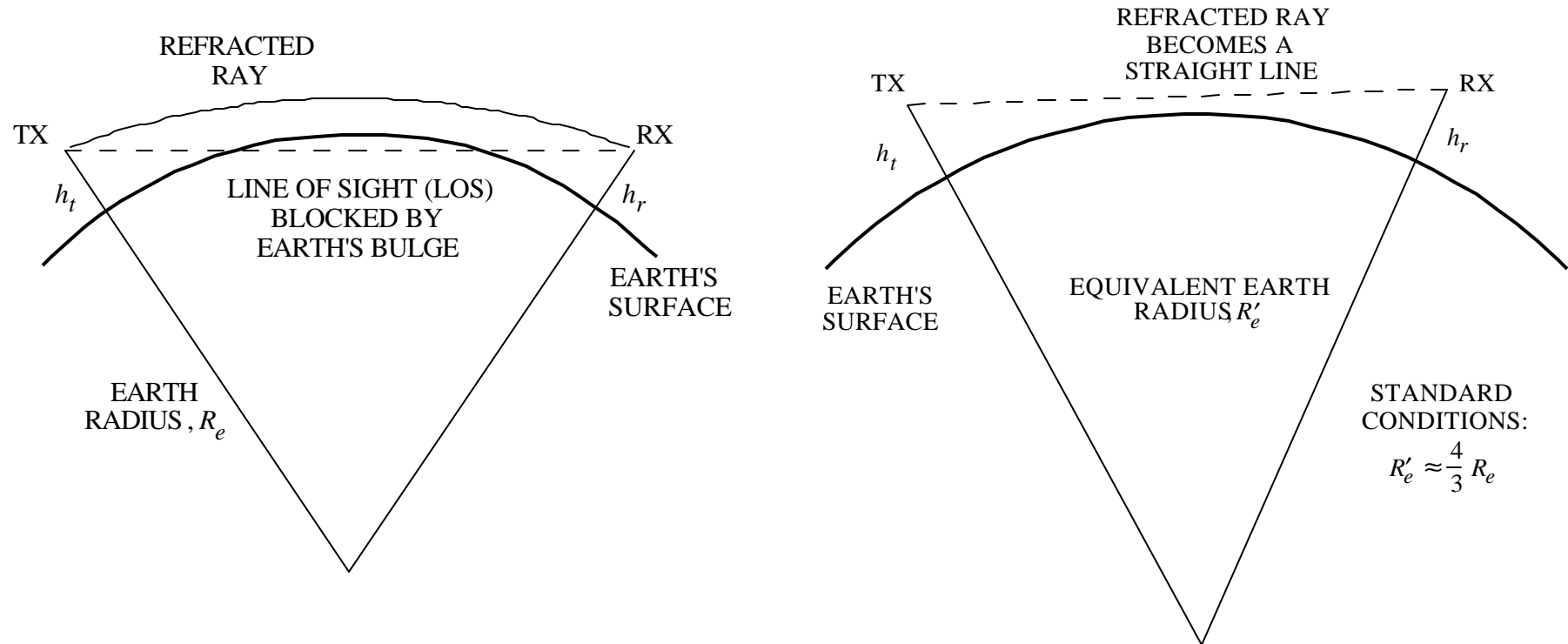
$T = \text{temperature (K)}$

$e = \text{partial pressure of water vapor (millibars)}$



# Atmospheric Refraction (2)

Refraction of a wave can provide a significant level of transmission over the horizon. A refracted ray can be represented by a straight ray if an equivalent earth radius is used.



# Atmospheric Refraction (3)

Distance from the transmit antenna to the horizon:  $R_t = \sqrt{(R'_e + h_t)^2 - (R'_e)^2}$

but  $R'_e \gg h_t$  so that

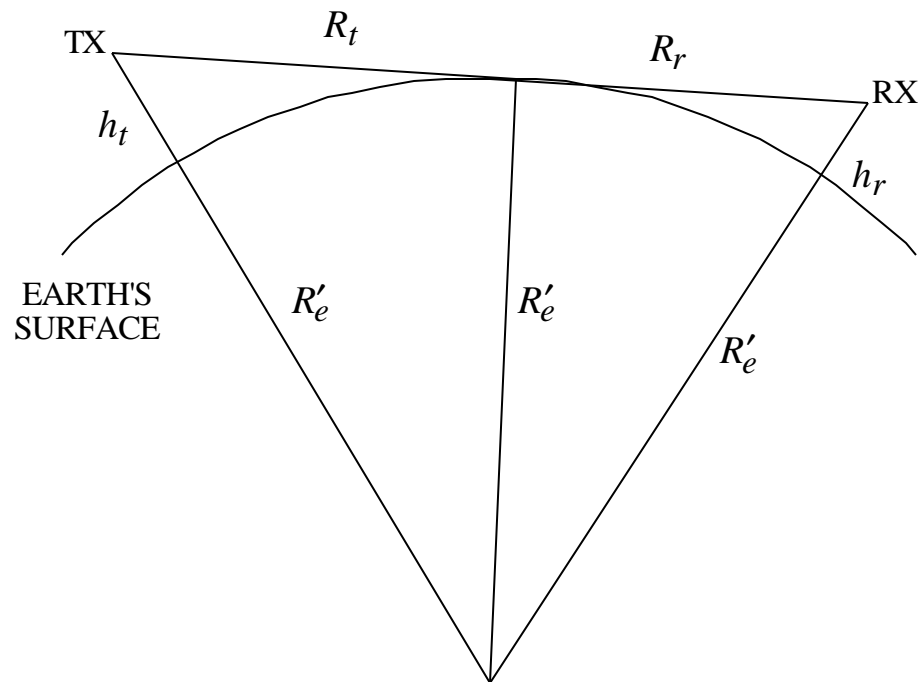
$$R_t \approx \sqrt{2R'_e h_t}$$

similarly,

$$R_r \approx \sqrt{2R'_e h_r}$$

The radar horizon is the sum

$$R_{RH} \approx \sqrt{2R'_e h_t} + \sqrt{2R'_e h_r}$$



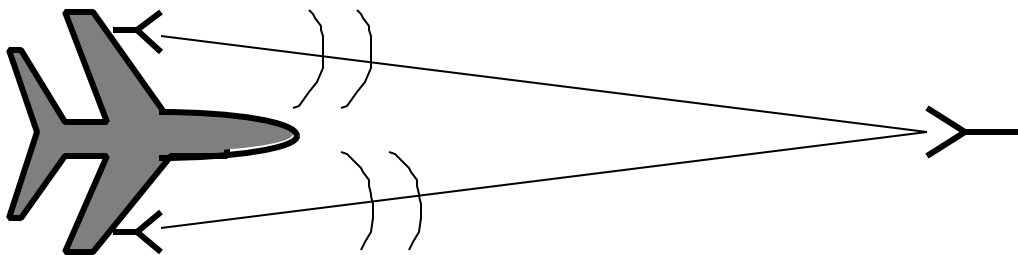
# Microwave Devices & Radar

## LECTURE NOTES VOLUME IV

by Professor David Jenn

Contributors: Professors F. Levien, G. Gill, J. Knorr and J. Lebaric

---



# Special Radar Systems and Applications

---

- Firefinder, Patriot, SPY-1, AN/APS-200, and SCR-270 radars
- Harmonic radars
- Synthetic aperture radar (SAR)
- Inverse synthetic aperture radar (ISAR)
- Stepped frequency radar
- Ultra-wideband radar (UWB)
- Radar electronic countermeasures (ECM): Crosseye; sidelobe cancelers and blanking; chaff
- HF over the horizon (OTH) radar
- Laser radar
- Ground penetrating radar (GPR)
- Doppler weather radar
- Bistatic radar



# AN/TPQ-37 Firefinder Radar

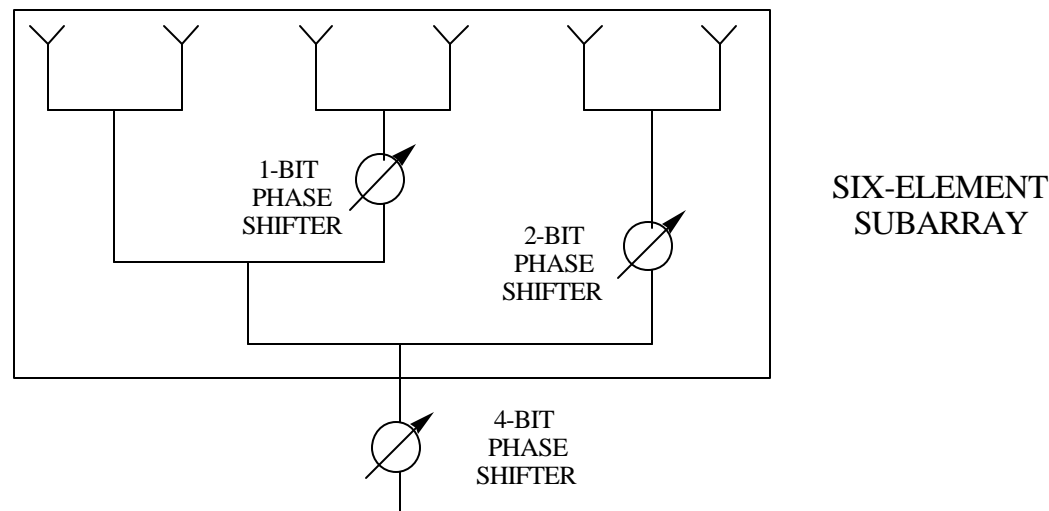
---



# Firefinder Radar Antenna (1)

Based on the concept of phase-steered subarrays: The array and subarray factors are scanned individually. The array factor has 4-bit phase shifters, whereas the subarray pattern is scanned using 2-bit phase shifters. The four possible “phase states” for the subarray are:

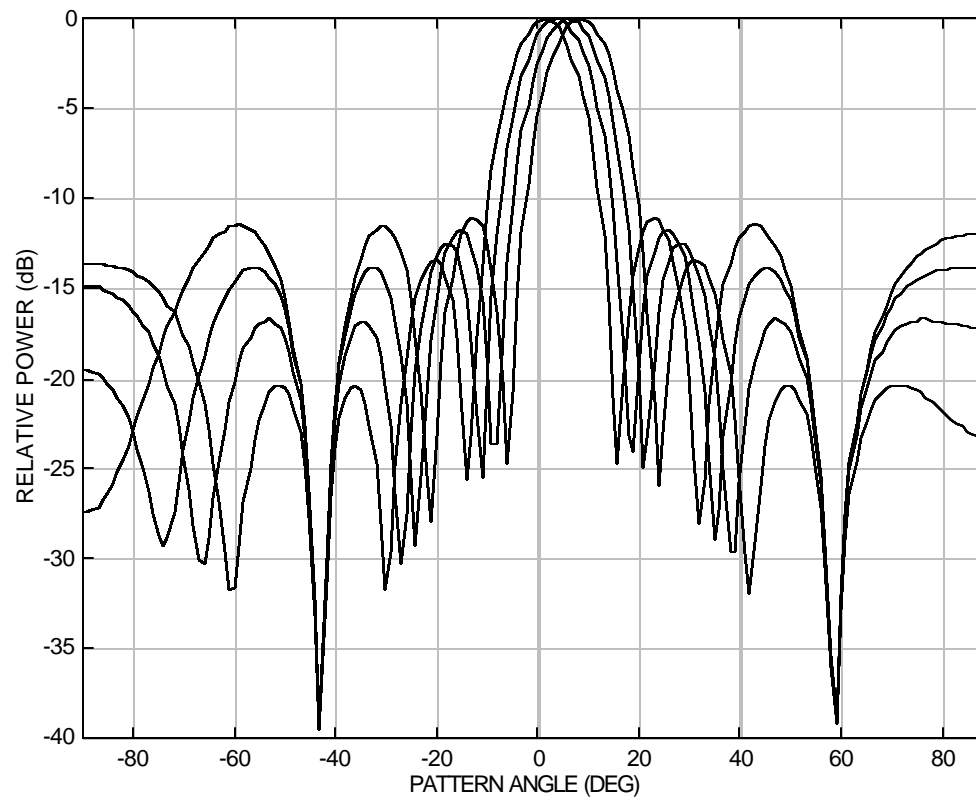
Phase State	Dipole Output Phase (Degrees)					
	1	2	3	4	5	6
1	0	-20	-19	-39	-17	-37
2	0	-20	-19	-39	-59	-79
3	0	-20	-61	-81	-101	-121
4	0	-20	-61	-81	-143	-163



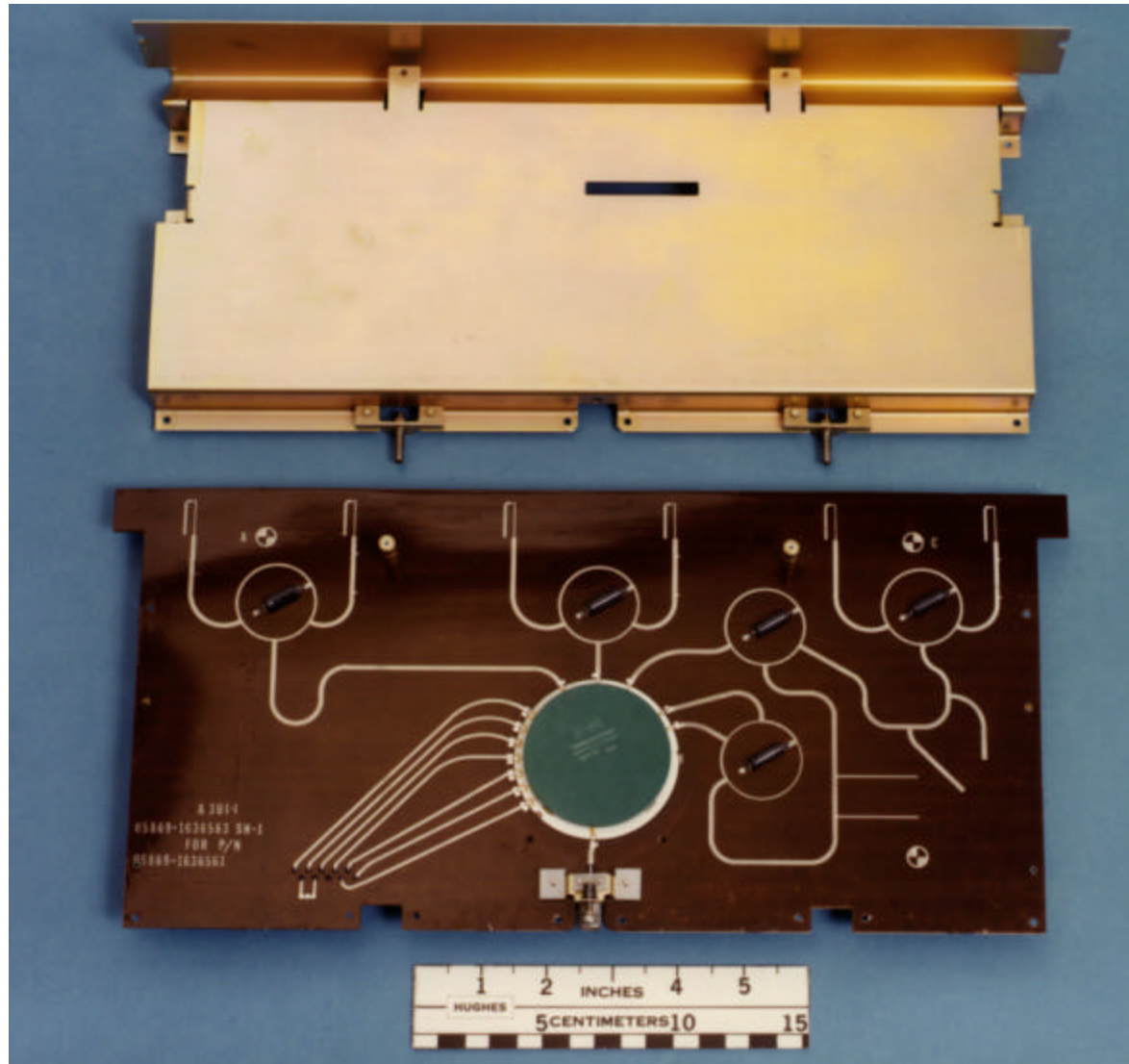
# Firefinder Radar Antenna (2)

---

Patterns of the six-element subarray (four possible phase states)



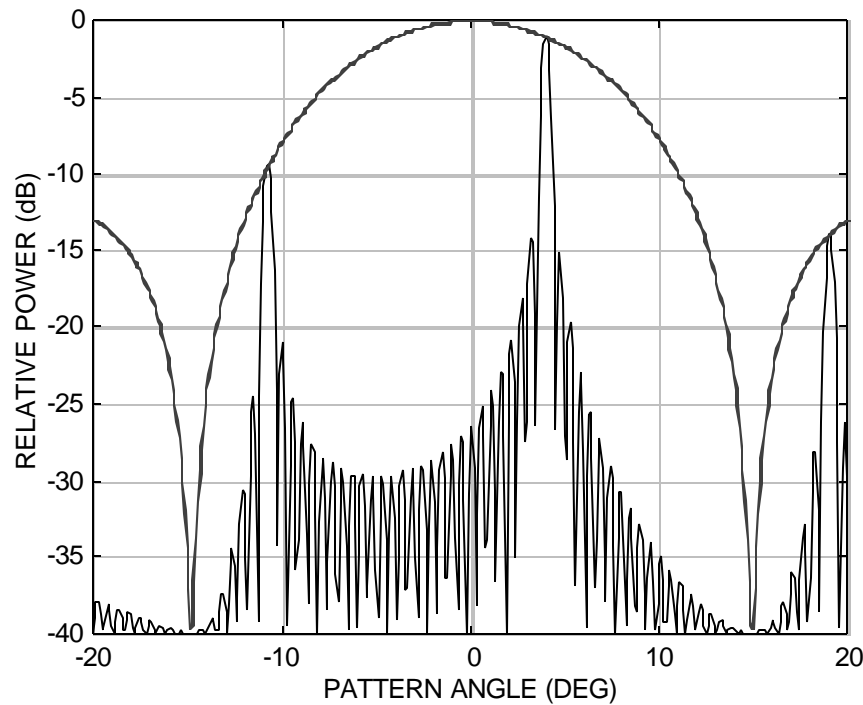
# AN/TPQ-37 Subarray



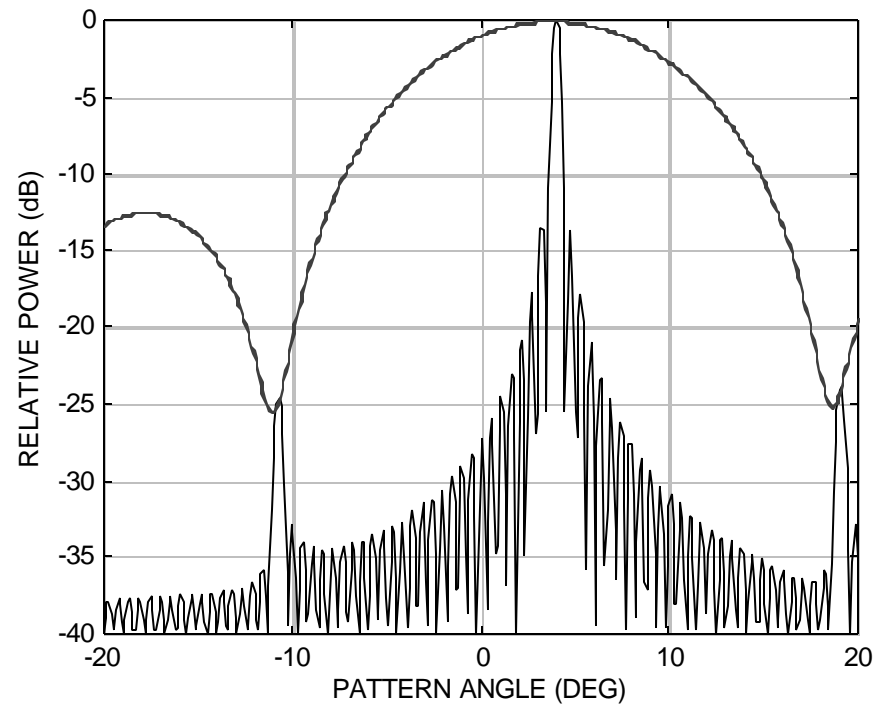
# Firefinder Radar Antenna (3)

Array patterns with and without subarray scanning ( $q_s = 4^\circ$ ). The dashed curve is the subarray pattern.

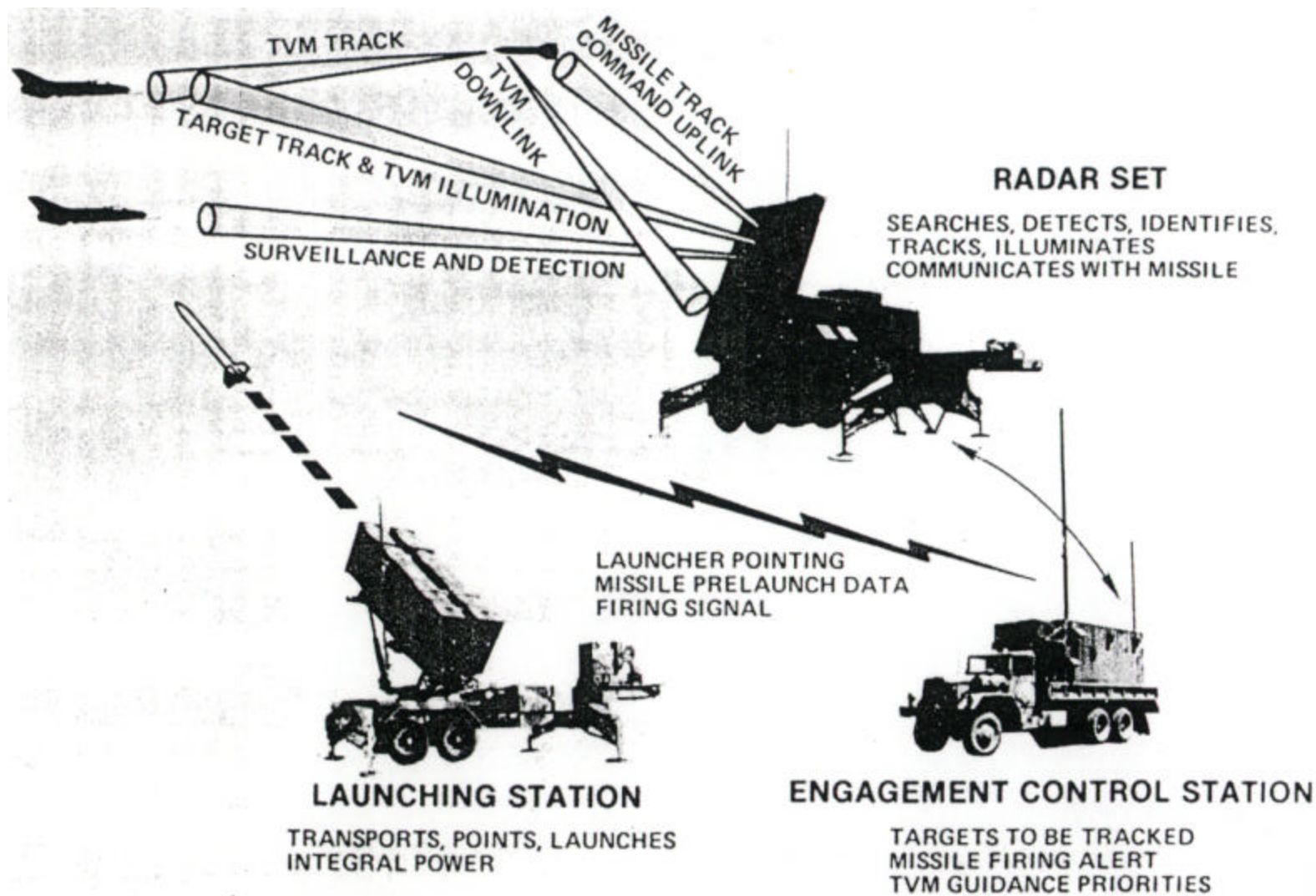
WITHOUT SUBARRAY SCANNING



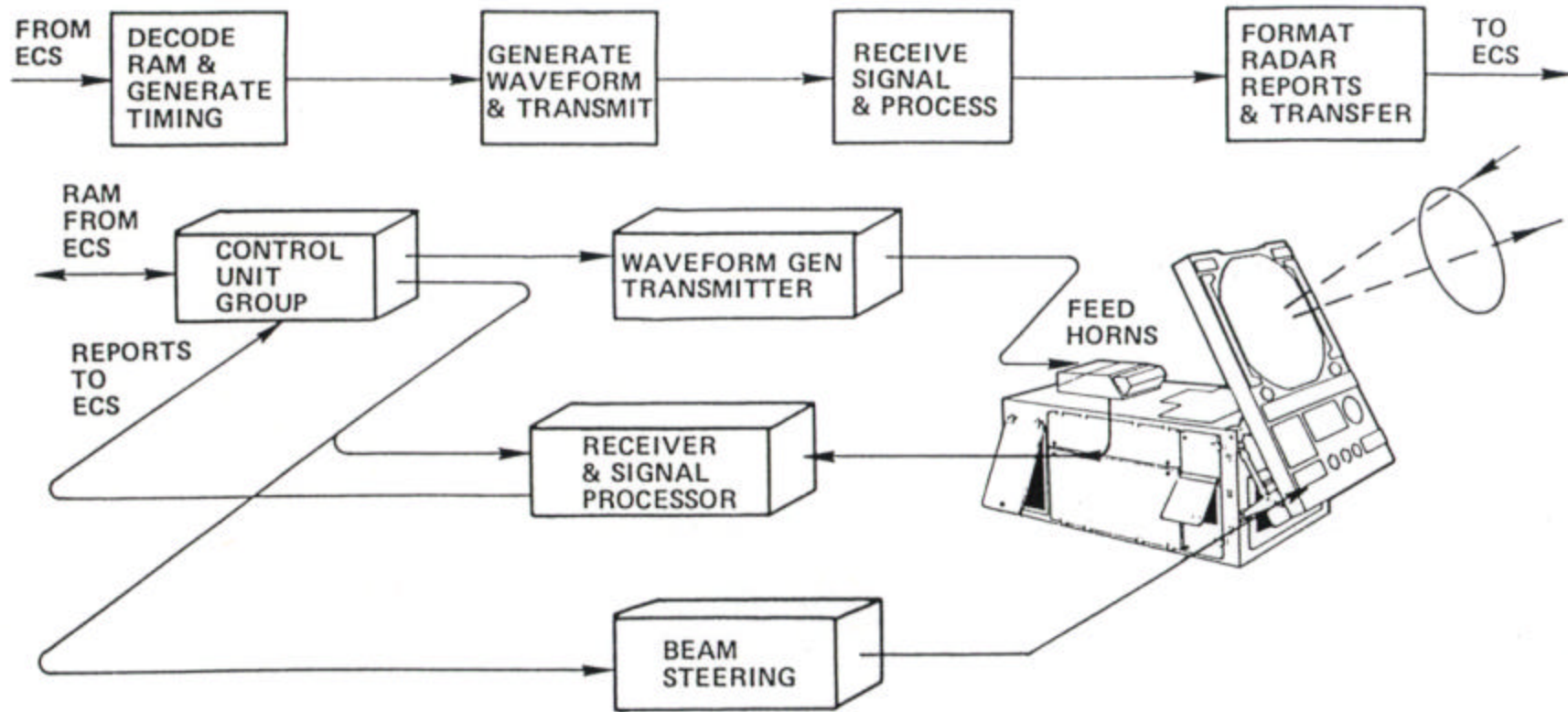
WITH SUBARRAY SCANNING



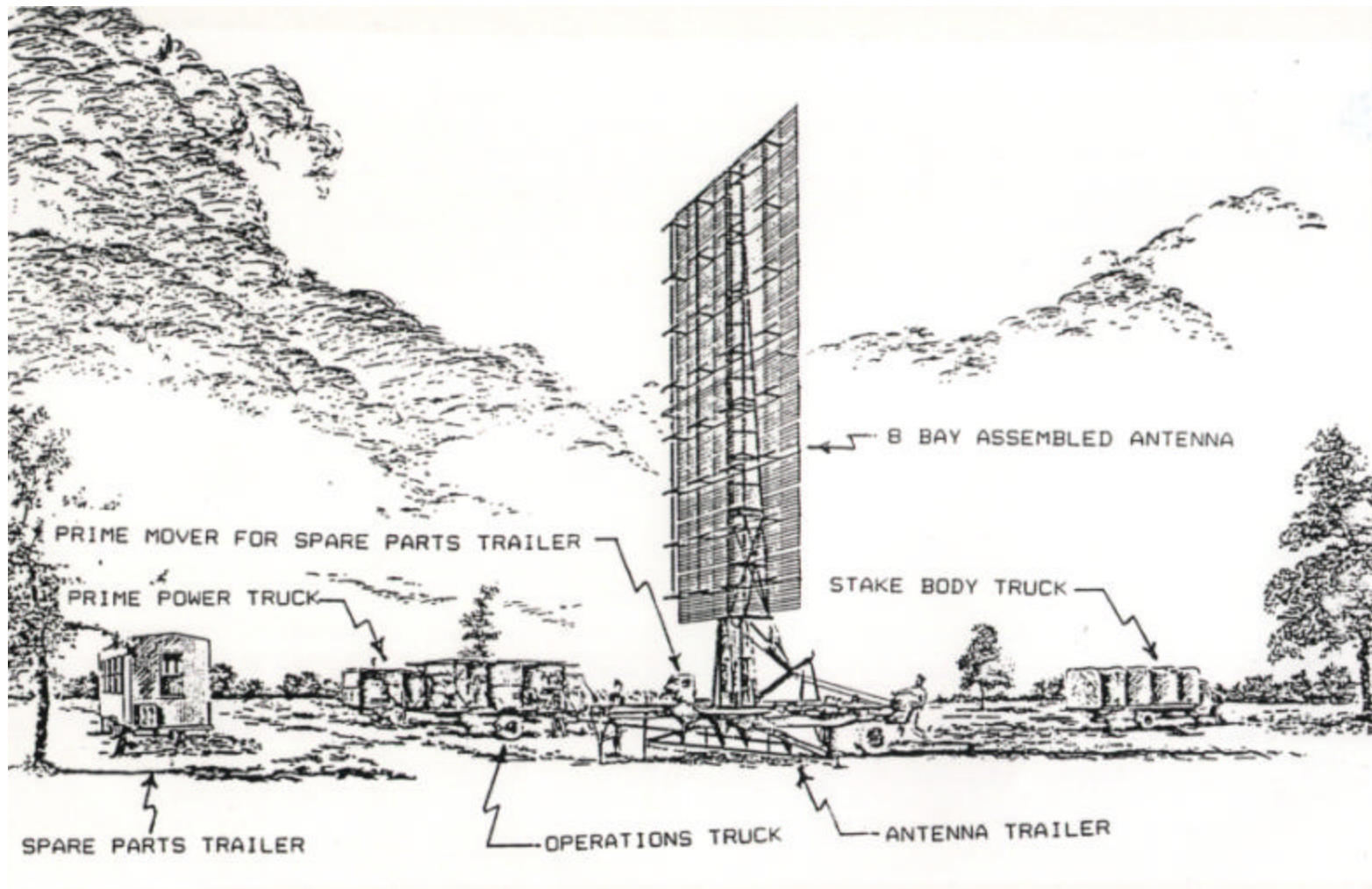
# Patriot Air Defense Radar (1)



# Patriot Air Defense Radar (2)



# SCR-270 Air Search Radar





# SCR-270-D-RADAR

---

Detected Japanese aircraft approaching Pearl Harbor.  
 Dipole array was tuned by maximizing the scattering from a metal propane storage tank.  
 Performance characteristics:

*SCR-270-D Radio Set Performance Characteristics*  
 (Source: *SCR-270-D Radio Set Technical Manual, Sep. 22, 1942*)

Maximum Detection Range . . . . .	250 miles
Maximum Detection altitude . . . . .	50,000 ft
Range Accuracy . . . . .	± 4 miles*
Azimuth Accuracy . . . . .	± 2 degrees
Operating Frequency . . . . .	104-112 MHz
Antenna . . . . .	Directive array **
Peak Power Output . . . . .	100 kw
Pulse Width . . . . .	15-40 microsecond
Pulse Repetition Rate . . . . .	621 cps
Antenna Rotation . . . . .	up to 1 rpm, max
Transmitter Tubes . . . . .	2 triodes***
Receiver . . . . .	superheterodyne
Transmit/Receive/Device . . . . .	spark gap

\* Range accuracy without calibration of range dial.  
 \*\* Consisting of dipoles, 8 high and 4 wide.  
 \*\*\* Consisting of a push-pull, self excited oscillator, using a tuned cathode circuit.

# SPY-1 Shipboard Radar

---

SPY-1 is a multifunction 3-D phased array radar with the following characteristics:

Four large (12.8 feet) antennas providing hemispherical coverage

Each array has 4480 radiating elements (140 modules)

Electronically scanned (non-rotating antennas)

Frequency is S-band (3.1 - 3.5 GHz)

Peak power 4 - 6 MW

Radar resources are adaptively allocated to counter a changing hostile environment

Primary functions:

Tracking

Fire control (missile guidance)

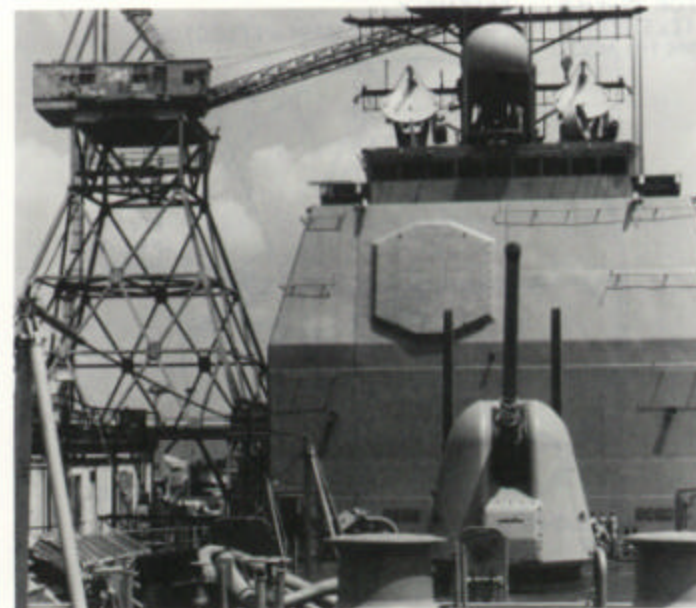
Secondary functions:

Horizon and special search

Self-test and diagnostics

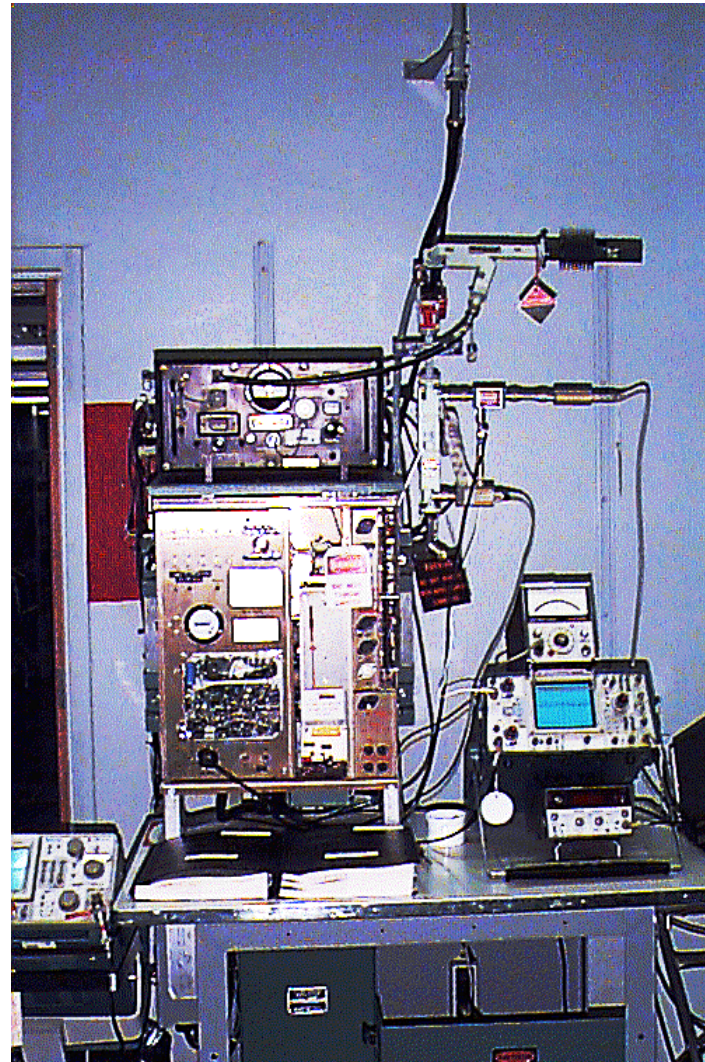
ECM operations

SPY-1 Radar Antenna



# X-Band Search Radar (AN/SPS-64)

---



# AN/SPS-64

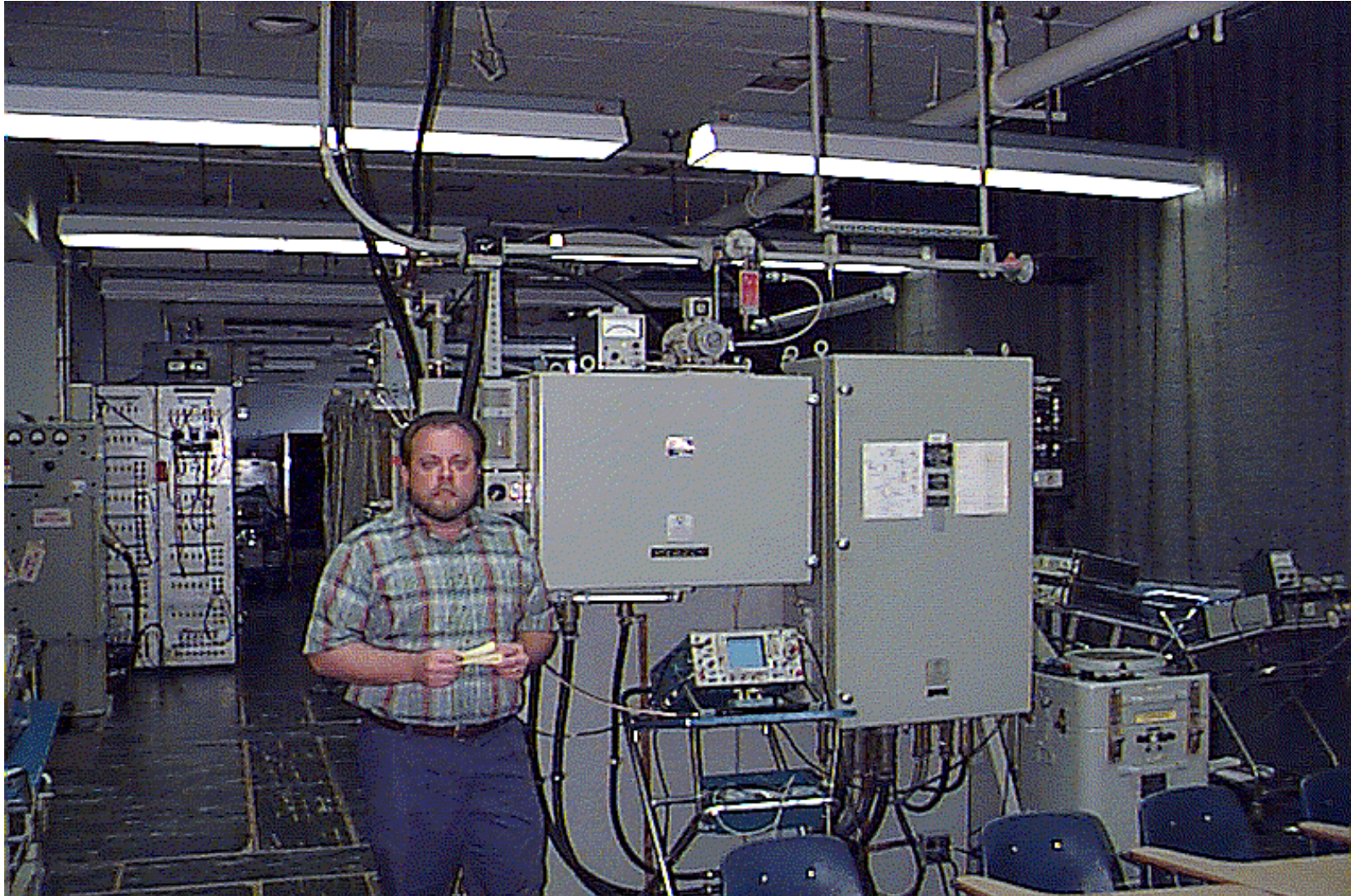
---

X-band surface search and navigation.

- Three PRFs:  
3600, 1800, 900 Hz
- Range: 64 nm
- Pulse widths:  
0.06 *ns*, 0.5 *ns*, 1.0 *ns*
- Antenna  
Parabolic reflector  
Horiz HBPW: 1.2 degrees  
Vert HPBW: 20.7 degrees  
Gain: 28.5 dB  
SLL: -29 dB  
Polarization: horizontal
- Transmitter  
Frequency: 9.375 GHz  
Peak power: 20 kW
- Receiver  
IF gain: 120 dB  
MDS: - 98 dBm  
Noise figure: 10 dB  
IF frequency: 45 MHz  
IF bandwidth: 24, 4, 1 MHz  
False alarm rate: 1 per 5 minutes

# C-Band Search Radar (AN/SPS-67)

---



# AN/SPS-67

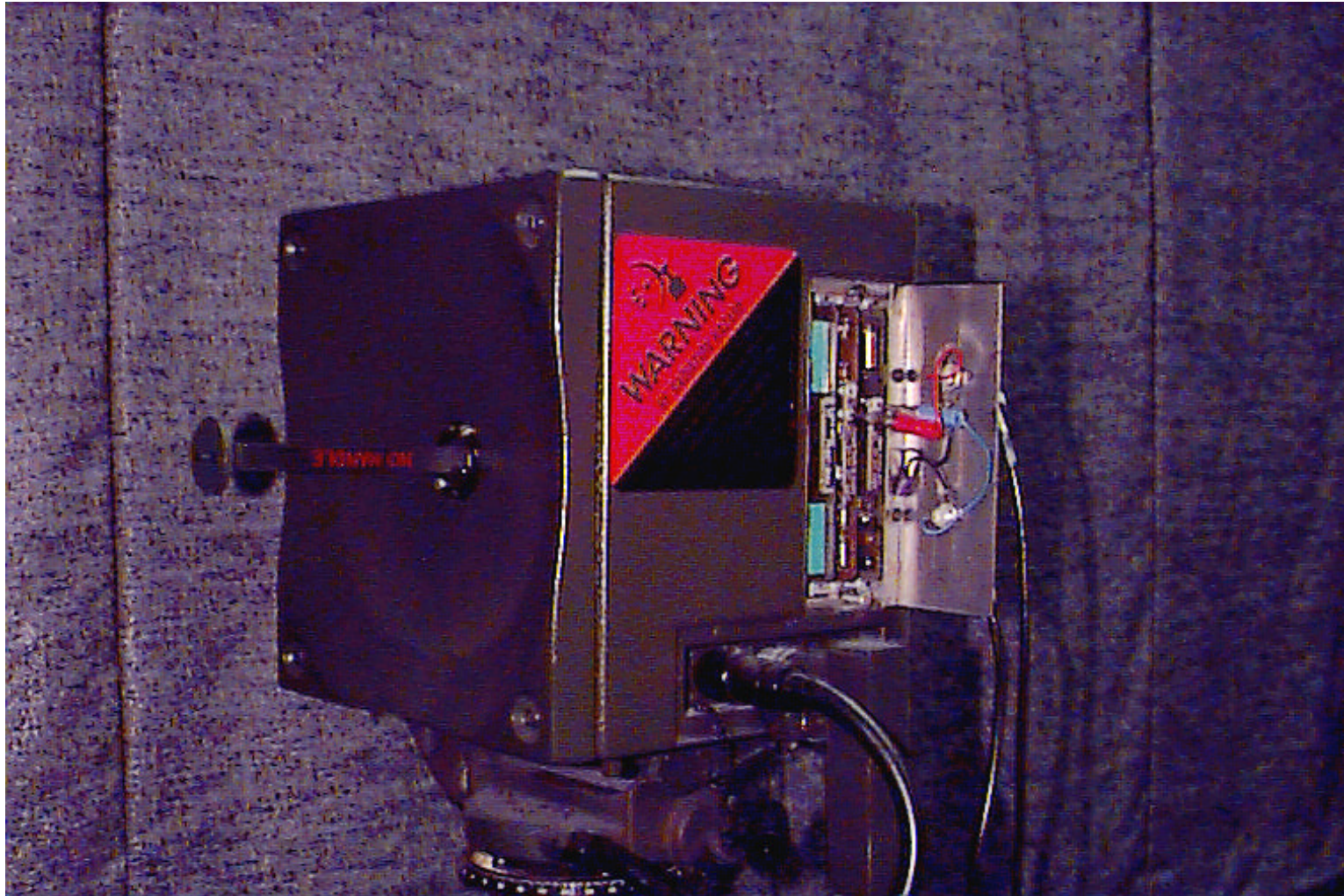
---

C-band surface search and navigation radar for detection of surface targets and low flying aircraft.

- Pulse width modes:  
1.0 *ns*, 0.25 *ns*, 0.1 *ns*
- Range in the three modes:  
300, 200, 75 yards
- Resolution in the three modes:  
200 yards, 190 ft., 75 ft.
- Transmitter  
Frequency: 9 to 9.5 GHz  
PRF: 1800 to 2200 Hz  
Pulse width: 0.22 to 0.3 *ns*
- Antenna  
Mesh reflector with dual band feed
- Transmitter frequency:  
5.45 to 5.825 GHz
- Receiver  
Noise figure: 10 dB  
MDS in the three modes:  
-102, -94, -94 dBm  
Logarithmic IF dynamic range  
90 dB or greater
- Display: PPI

# Combat Surveillance Radar (AN/PPS-6)

---



# AN/PPS-6

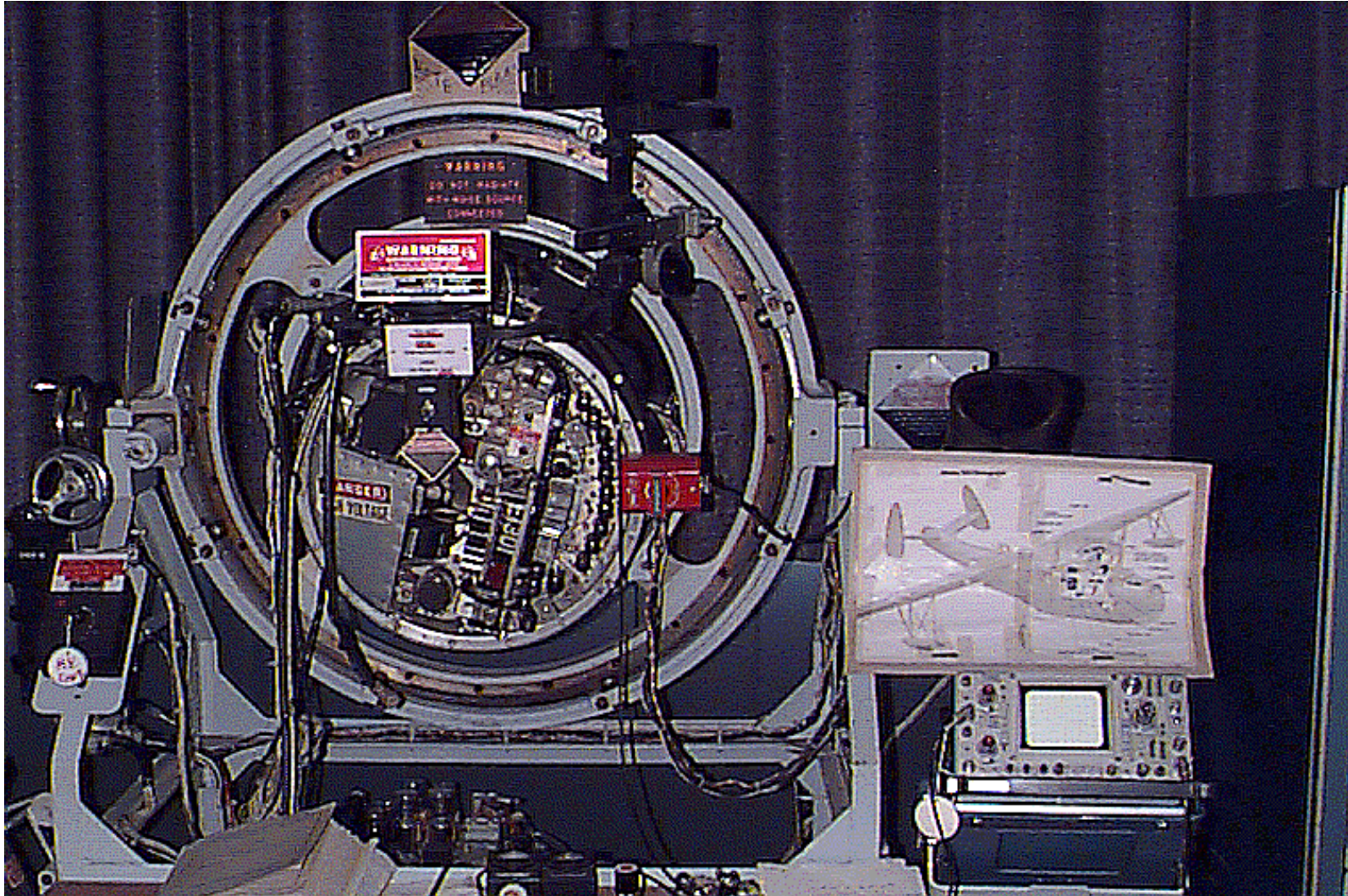
---

Noncoherent pulse-doppler radar for combat surveillance. Detects moving terrestrial targets (1 to 35 mph) under varying conditions of terrain, visibility and weather conditions

- Range
  - Personnel ( $\sigma = 0.5$  sq. m):  
50 to 1500 m
  - Vehicles ( $\sigma = 10$  sq. m):  
50 to 3000 m
  - Accuracy:  $\pm 25$  m
  - Resolution: 50 m
- Transmitter
  - Frequency: 9 to 9.5 GHz
  - PRF: 1800 to 2200 Hz
  - Pulse width: 0.22 to 0.3  $\mu$ s
- Antenna
  - Size: 12 inch reflector
  - Gain: 24.5 dB
- E-plane HPBW: 7 deg
- H-plane HPBW: 8 deg
- Receiver
  - Type: superheterodyne
  - IF frequency:  $30 \pm 2$  MHz
  - IF gain: 80 dB
  - IF bandwidth:  $6.3 \pm 0.6$  MHz
  - MDS: -95 dBm
- Display
  - Headset (audible)
  - Test meter - visual indicator
  - Elevation indicator
  - Azimuth indicator



# Early Air Surveillance Radar (AN/APS-31)



# AN/APS-31

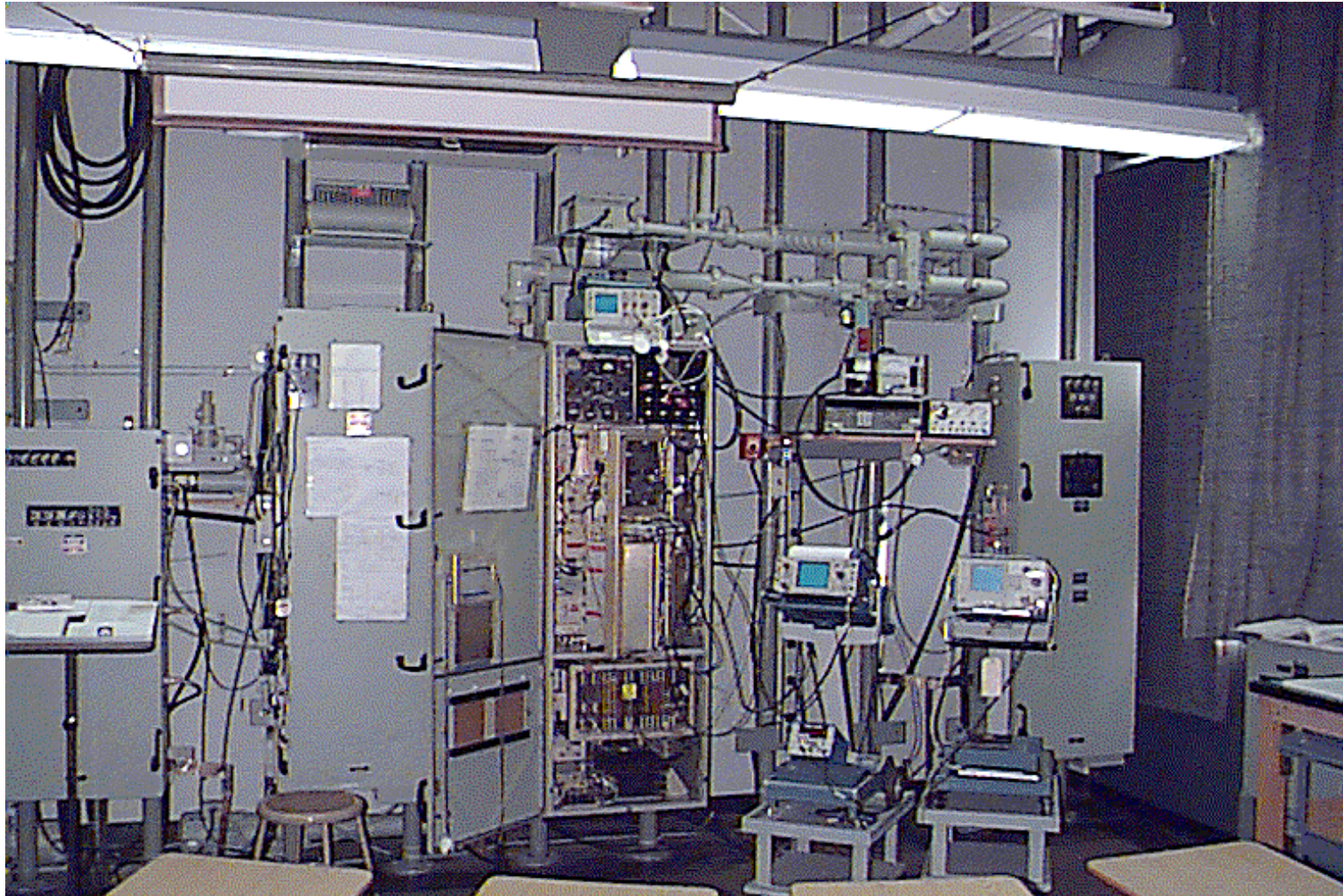
---

Early X-band surface search and navigation radar (about 1945).

- Pulse width modes:  
4.5 *ns*, 2.5 *ns*, 0.5 *ns*
- Range:  
5 to 200 nm
- PRFs in the three modes:  
200, 400, 800 Hz
- Transmitter  
Peak power: 52 kw
- Antenna  
Parabolic reflector  
HBPW: 2 degrees  
Gain: 2500
- Transmitter frequency:  
9.375 GHz
- Receiver  
IF gain: 120 dB  
MDS in the three modes:  
-102, -94, -94 dBm  
Noise figure: 5.5 dB  
IF frequency: 60 MHz

# AN/SPS-40

---



# AN/SPS-40

---

UHF long range two-dimensional surface search radar. Operates in short and long range modes.

- Range
  - Maximum: 200 nm
  - Minimum: 2 nm
- Target RCS: 1 sq. m.
- Transmitter
  - Frequency: 402.5 to 447.5 MHz
  - Pulse width: 60 *ms*
  - Peak power: 200 to 255 kw
  - Staggered PRF: 257 Hz (ave)
  - Non-staggered PRF: 300 Hz
- Antenna
  - Parabolic reflector
  - Gain: 21 dB
  - Horizontal SLL: 27 dB
  - Vertical SLL: 19 dB
  - HPBW (hor x vert): 11 by 19 degrees
- Receiver
  - 10 channels spaced 5 MHz
  - Noise figure: 4.2
  - IF frequency: 30 ± 2 MHz
  - PCR: 60:1
  - Correlation gain: 18 dB
  - MDS: -115 dBm
  - MTI improvement factor: 54 dB

# Plan Position Indicator (PPI)

---



# Radiometers (1)

---

All bodies at temperatures above absolute zero emit radiation due to thermal agitation of atoms and molecules. Radiometers are passive receiving systems that sense the emitted radiation.

A blackbody (BB) is an ideal body that absorbs all of the energy incident on it and radiates all of the energy that it absorbs. The radiation distribution as a function of wavelength (or frequency) is given by Planck's Law:

$$M_{\text{BB}}(\lambda) = \frac{2\pi h c^2}{\lambda^5 \left( e^{hc/(\lambda kT)} - 1 \right)}$$

where:  $M_{\text{BB}}(\lambda)$  = spectral excittance of the blackbody in  $\frac{\text{W}}{\text{m}^2 \cdot \text{mm}}$

$h = 6.626 \times 10^{-34}$  J · s (Planck's constant)

$k = 1.3807 \times 10^{-23}$  J/K (Boltzman's constant)

$\lambda$  = wavelength in  $\text{mm}$

T = temperature of the body in degrees Kelvin

## Radiometers (2)

---

The total radiance leaving the surface is

$$M_{\text{BB}} = \int_0^{\infty} M_{\text{BB}}(\lambda) d\lambda = \sigma T^4$$

where  $\sigma = 5.67 \times 10^{-8} \text{ W / m}^2 \cdot \text{K}^4$  (Stefan-Boltzman constant).

The wavelength (or frequency) of maximum radiation for a BB of temperature T is given by Wien's displacement law

$$\lambda_{\text{max}} T = 2897.6 \times 10^{-6} \text{ m} \cdot \text{K}$$

Only a few materials approach the characteristics of a blackbody. Most materials emit energy according to a scaled version of Planck's Law. These are called gray bodies and the scale factor is the emissivity

$$e(\lambda) = \frac{M(\lambda)}{M_{\text{BB}}(\lambda)}$$

Kirchhoff's Law states that at every wavelength the emissivity equals the absorptivity

$$e = a$$

# Radiometers (3)

---

Since conservation of energy requires that

$$\text{absorbed} + \text{reflected} + \text{transmitted} = 1$$

it follows that good reflectors are poor emitters; good absorbers are good emitters.

Blackbody and gray body radiation is diffuse, that is constant with angle. The noise power radiated by a blackbody is  $kTB$  where  $B$  is the bandwidth of the detector. The power radiated by a gray body relative to that of a blackbody is

$$e = \frac{P_{GB}}{kTB} = \frac{T_B}{T}$$

where  $T_B$  is the brightness temperature. This difference in noise powers can be measured, and the emissivities determined. Emissivity can be used to infer the material characteristics.



# Radiometers (4)

---

Applications of radiometers:

Environmental:

- Measure soil moisture
- Flood mapping
- Snow and ice cover mapping
- Ocean surface windspeed
- Atmospheric temperature and humidity profile

Military Applications:

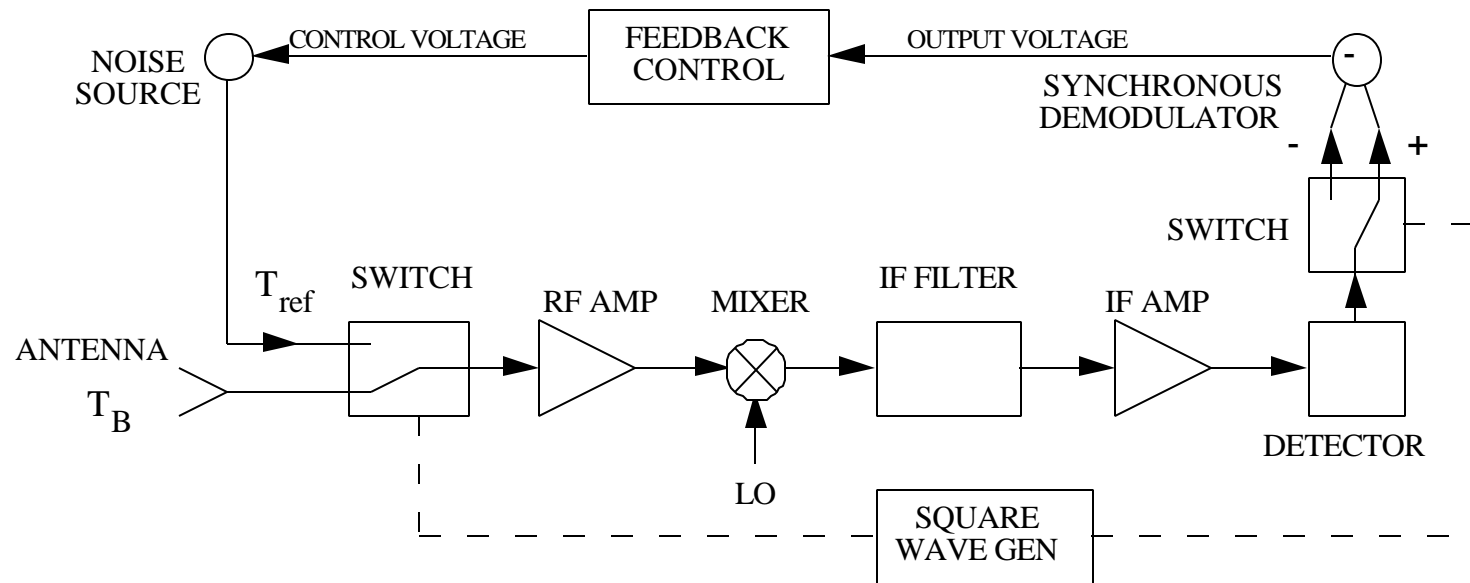
- Target detection and identification
- Surveillance
- Mapping

Astronomy:

- Planetary mapping
- Solar emissions
- Mapping galactic objects
- Cosmological background radiation

# Radiometers (5)

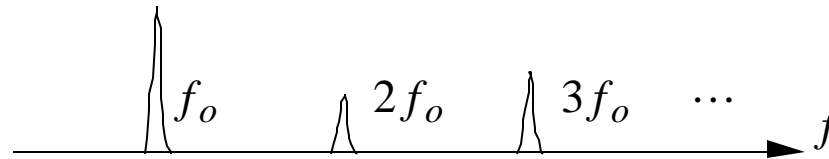
Block diagram of the Dicke radiometer:



# Harmonic Radar (1)

---

A harmonic radar transmits a frequency  $f_o$  (the fundamental) but receives a harmonic frequency ( $f_o, 2f_o, 3f_o$ , etc.). The harmonic frequencies are generated naturally by man-made objects with metal junctions. The harmonic can also be generated using a transponder circuit on the target.



## Advantages:

1. Natural clutter sources are linear. They scatter waves at the same frequency as the incident wave. Therefore a target return at a harmonic is not obscured by clutter.
2. Man-made objects generate harmonic scattered fields. Odd numbered harmonics arise from metal junctions on the target. The third harmonic is the strongest.

## Disadvantages:

1. Energy conversion from the fundamental to harmonics is very low. Higher conversion efficiencies can be obtained with cooperative targets using a nonlinear circuit device like a diode.
2. Dual frequency hardware required.
3. The received field varies as  $P_r \propto 1/R^a$  where  $a > 4$ .

# Harmonic Radar (2)

---

The harmonic radar range equation for the third harmonic is

$$P_r = \frac{(P_t G_t)^a G_r I_3^2 S_h}{(4p)^{a+2} R^{2a+2}}$$

where:

$a \approx 2.5$  is a nonlinearity parameter that determined experimentally  
(it varies slightly from target to target)

$P_t, G_t$  are transmit quantities at the fundamental frequency ( $f_o$ )

$I_3, G_r$  are receive quantities at the third harmonic frequency ( $3f_o$ )

$S_h$  is the harmonic scattering pseudo cross section

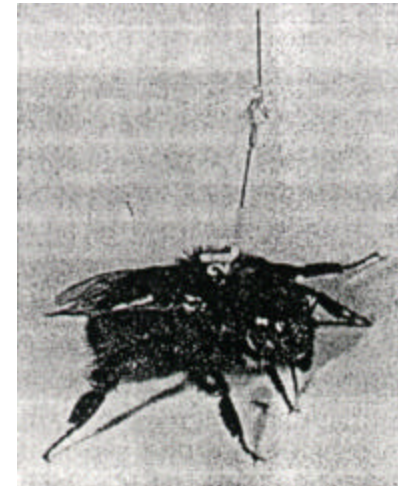
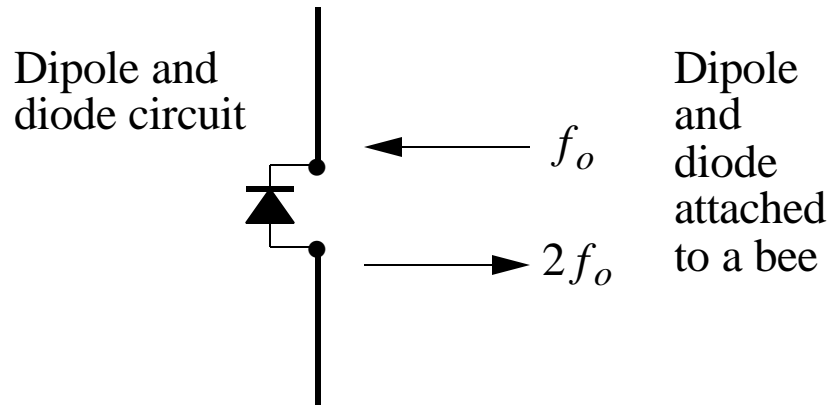
(typical values are -60 to -90 dB for  $W_i \leq 1$  W/m<sup>2</sup>)

Using  $a \approx 2.5$  the received power varies as

$$P_r \propto 1/R^7$$

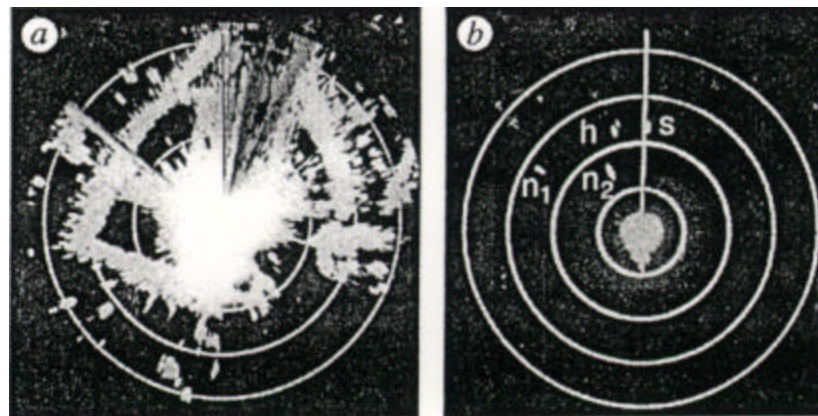
Therefore the detection ranges are very small, but foliage penetration is good for short ranges.

# Harmonic Radar Tracking of Bees



(From *Nature*, Jan. 1996, p. 30)

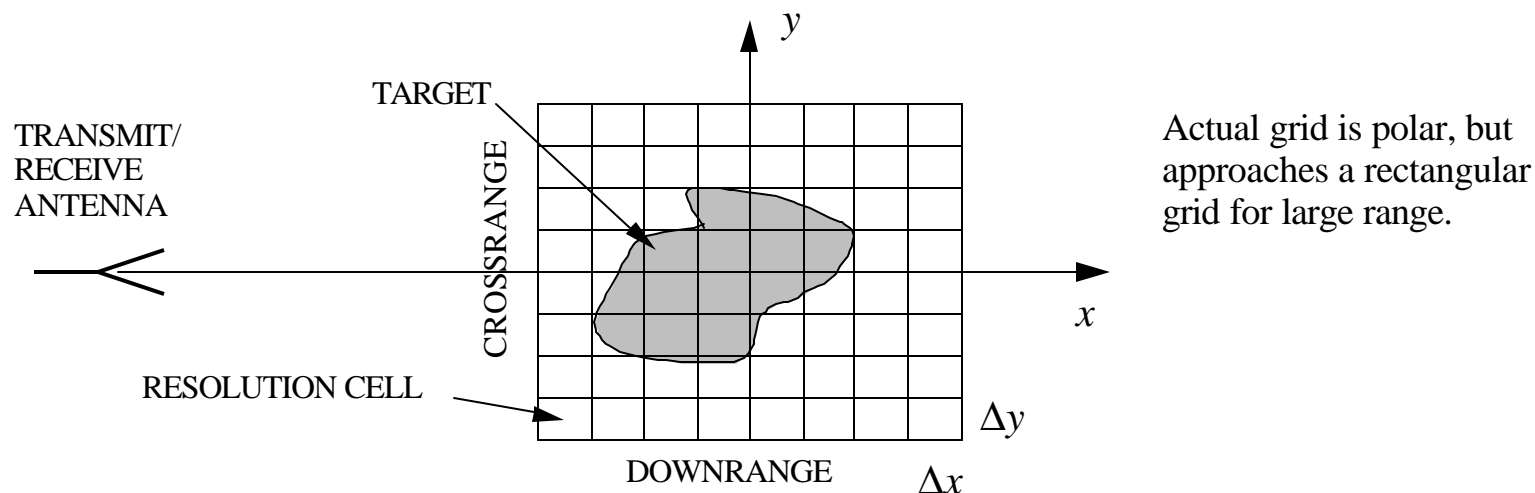
PPI traces for conventional and harmonic radars ( $l_o = 3.2$  cm)



# Synthetic Aperture Radar (SAR)

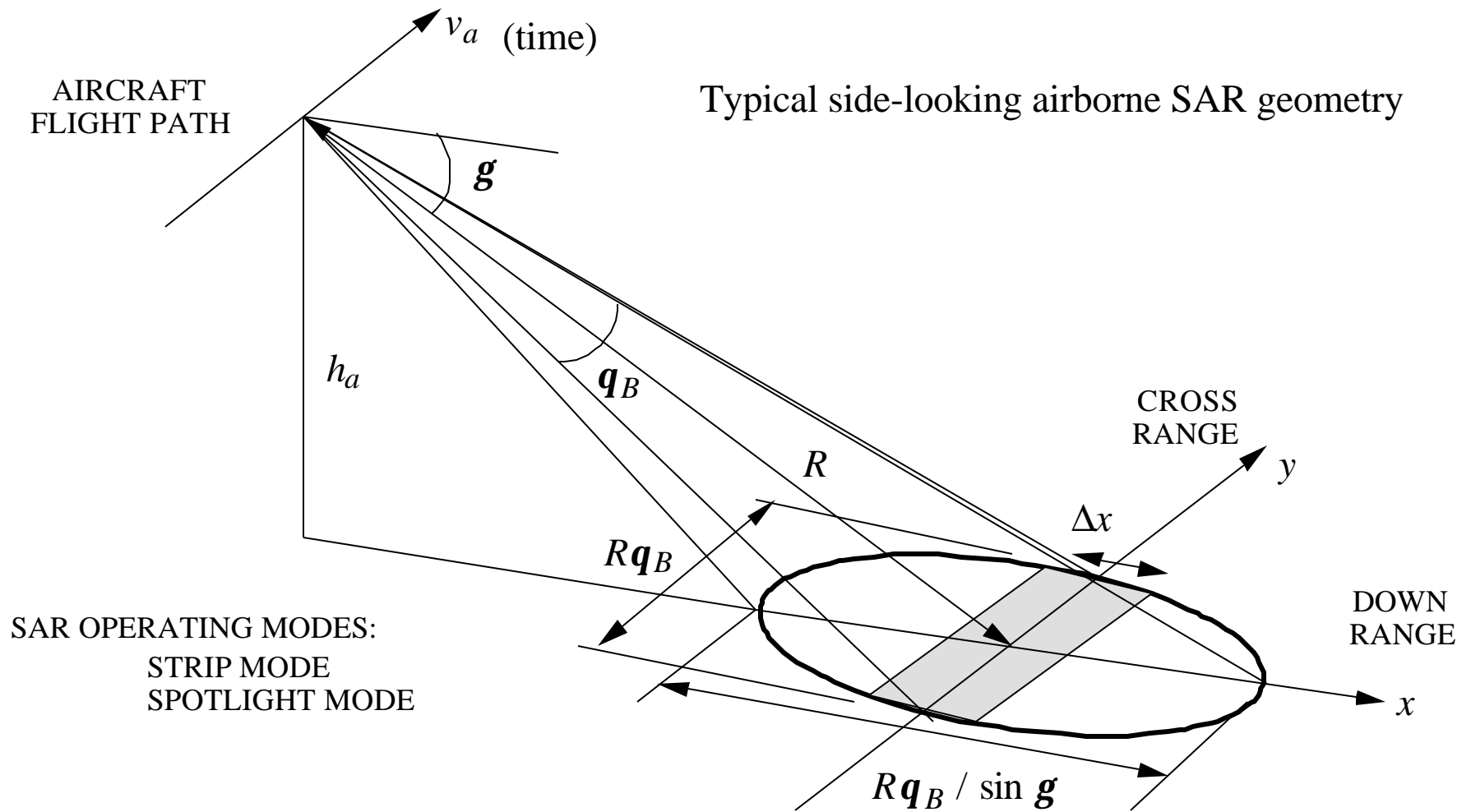
A scene (background plus targets) is imaged by plotting the received power as a function of ground coordinates. The resolution cell size is a picture element or pixel:

down range resolution ( $\Delta x$ ) is determined by the pulse width  
cross range resolution ( $\Delta y$ ) is determined by the antenna beamwidth



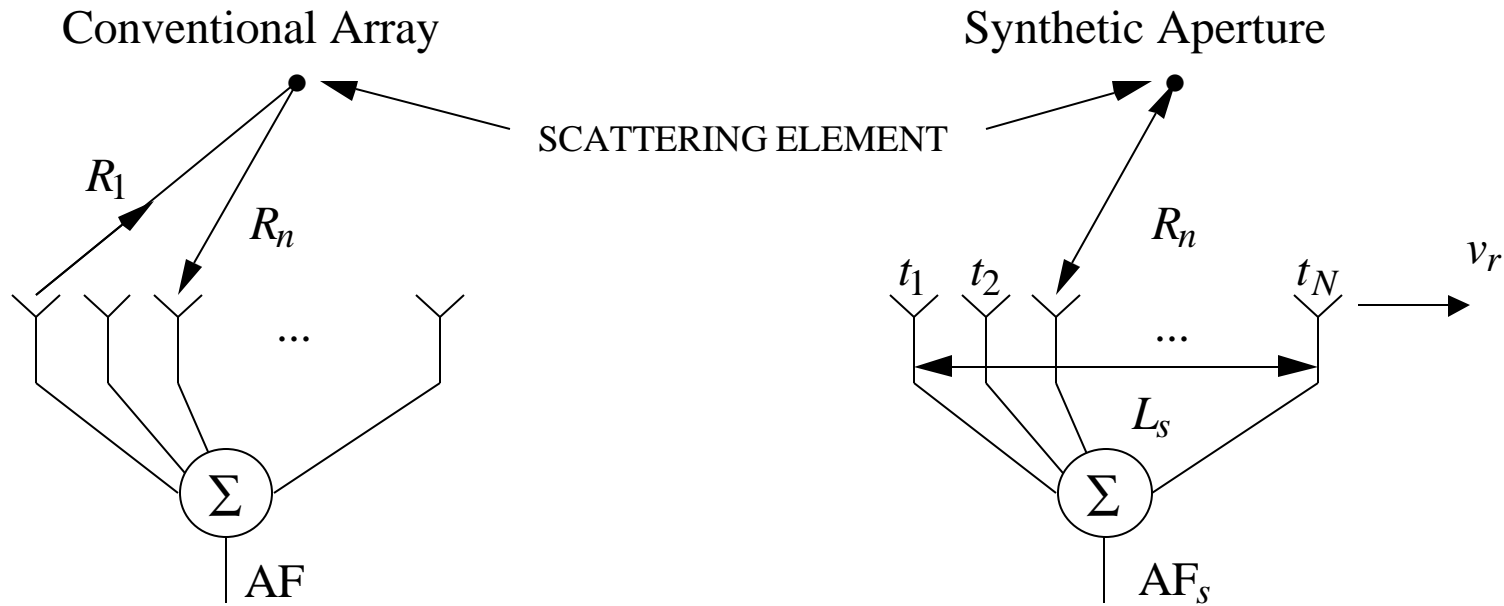
Very narrow antenna beams are required for fine cross range resolution. The resulting antenna size is very large and may not be practical. Returns from a large antenna can be synthesized using the returns from a small antenna at sequential locations along a flight path. This is the basis of synthetic aperture radar (SAR).

# SAR (2)



# SAR (3)

Comparison of array factors for conventional and synthetic apertures:



$$E_n = \sum_{m=1}^N e^{-jk(R_m + R_n)}$$

$$AF = \sum_{n=1}^N \sum_{m=1}^N e^{-jk(R_m + R_n)} = \underbrace{\left( \sum_{m=1}^N e^{-jkR_m} \right)^2}_{\text{SQUARE OF SUM}}$$

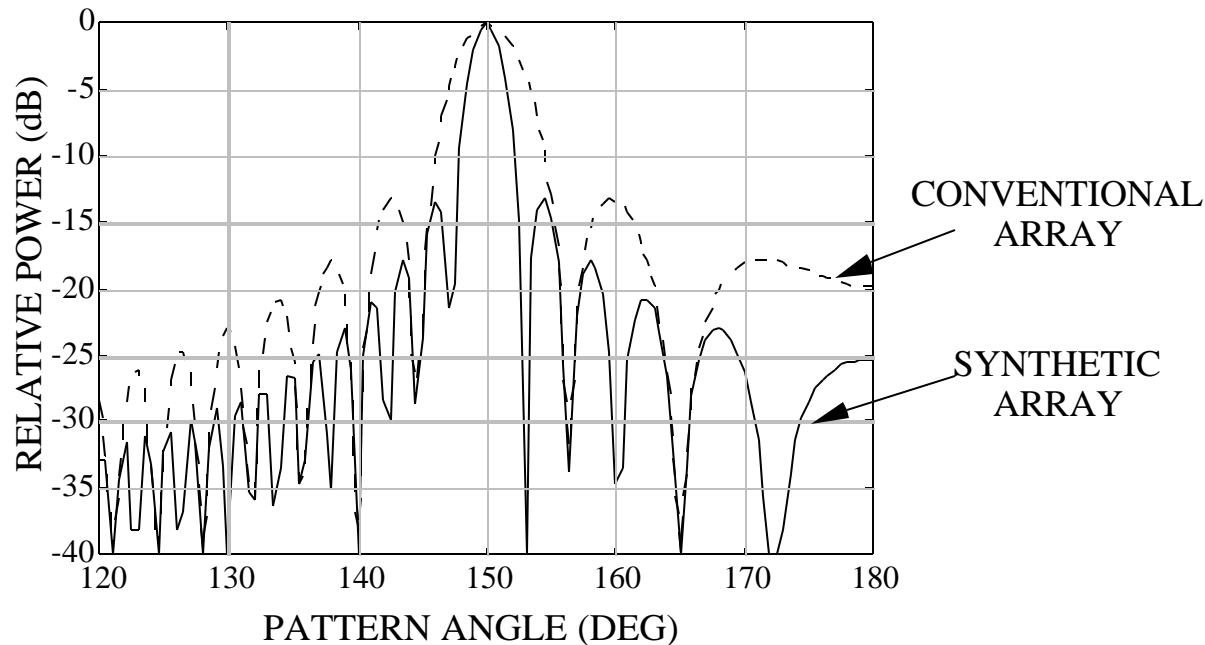
$$E_n = e^{-jk(R_n + R_n)}$$

$$AF_s = \underbrace{\sum_{m=1}^N \left( e^{-jkR_m} \right)^2}_{\text{SUM OF SQUARES}}$$



# Comparison of Array Factors

Plot of array factors for conventional and synthetic apertures of the same length:

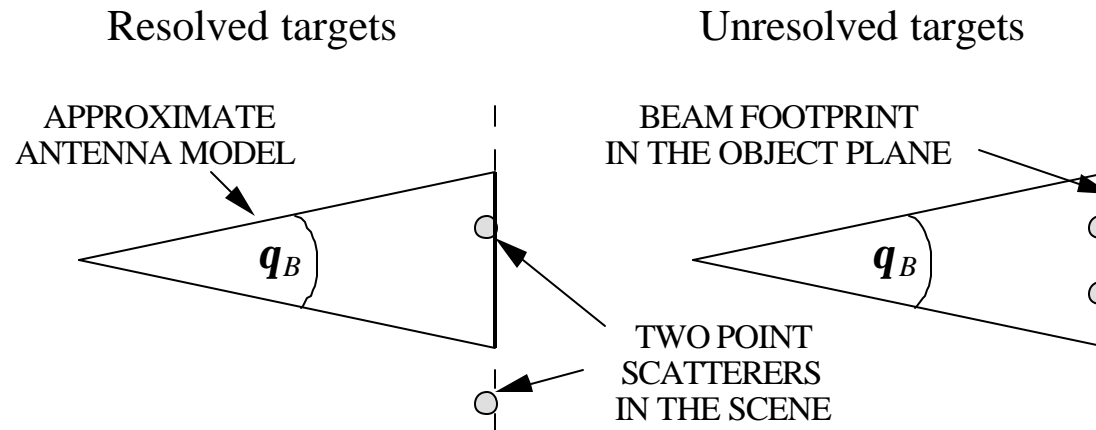


Beamwidth of the conventional array:  $q_B \approx \lambda / L$  where  $L \approx Nd$  ( $d$  is the element spacing and  $N$  the number of array elements)

Beamwidth of the synthetic array:  $q_B \approx \lambda / (2L_s)$  where  $L_s \approx t_{\text{obs}} v_a = d_{\text{obs}} N_s$  ( $t_{\text{obs}}$  is the observation time,  $N_s$  the number of samples, and  $d_{\text{obs}}$  the distance between samples)

# Image Resolution

Two closely spaced targets are resolved if two distinct scattering sources can be distinguished.



For the conventional array the cross range resolution is

$$\Delta y = Rq_B \approx Rl / L$$

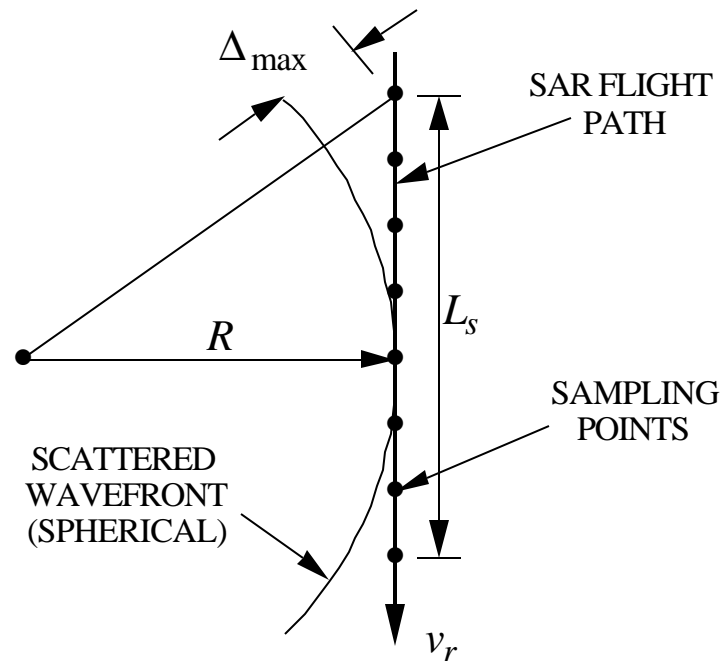
For the synthetic array the cross range resolution is

$$\Delta y = Rq_B \approx Rl / (2L_s)$$

Note that the last result, which is based on  $AF_s$ , assumes that the wave scattered from a point source in the scene is a plane wave when sampled by the SAR.

# Unfocused SAR (1)

If  $\Delta_{\max}$  is too large then  $AF_s$  becomes distorted (the beam broadens). Therefore the maximum  $L_s$  is commonly determined by the condition  $2k\Delta_{\max} \leq p/2$



$$2k\left(\sqrt{R^2 + (L_s/2)^2} - R\right) = 2kR\left\{\sqrt{1 + L_s^2/4R^2} - 1\right\} \approx 2kR\left\{\underbrace{\left[1 + L_s^2/(8R^2)\right]}_{\text{FIRST TWO TERMS OF BINOMIAL EXPANSION}} - 1\right\} \leq p/2$$

# Unfocused SAR (2)

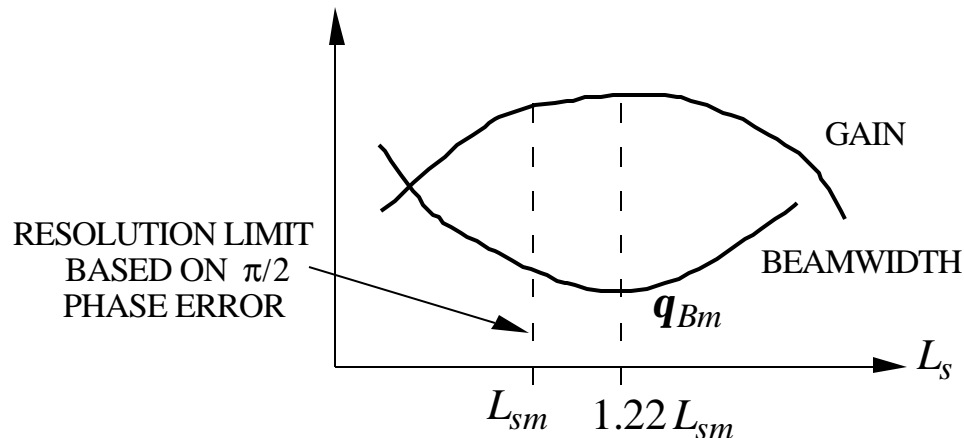
Solve for  $L_s$  and call this value  $L_{sm}$

$$L_{sm} = \sqrt{RI} \Rightarrow \mathbf{q}_{Bm} = \frac{I}{2\sqrt{RI}} = \frac{1}{2} \sqrt{\frac{I}{R}}$$

which gives a cross range resolution of

$$\Delta y_m = R\mathbf{q}_{Bm} = \frac{1}{2} \sqrt{RI}$$

This is the resolution limit for unfocused SAR (i.e., the phase error introduced by the spherical wavefront is not corrected). Note that the resolution does not depend on the actual antenna characteristics, only range and frequency. The actual optimum value is slightly different than  $L_{sm}$  depending on the antenna beamwidths and aperture distribution. A good estimate is  $1.22 L_{sm}$ .

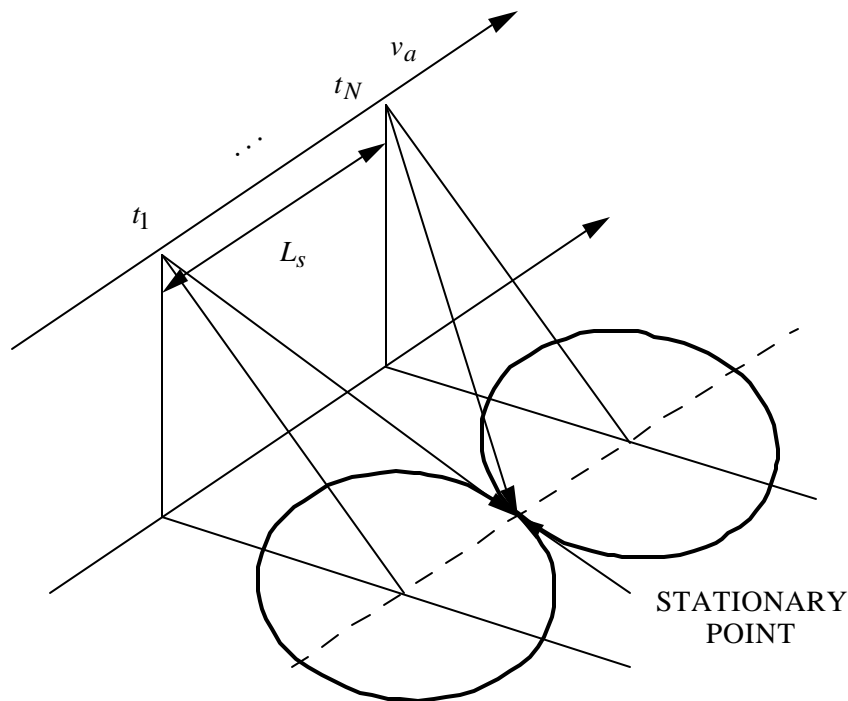


# Focused SAR

Focused SAR corrects for the path difference in the signal processing. The result is an effective beamwidth determined by the total length of the synthetic array,  $L_s = R\mathbf{I} / L$ . The corresponding resolution is

$$\Delta y = R\mathbf{q}_B = R\left(\frac{\mathbf{I}}{2L_s}\right) = \frac{L}{2}$$

which is independent of  $R$  and  $\mathbf{I}$ , and depends only on the actual size of the antenna.



The smaller the antenna used by the radar, the better the resolution because:

1. a wide beam keeps each scatterer in view longer, and
2. focusing (i.e., adding corrections) removes the range dependence.

The synthetic aperture length  $L_s$  is limited by the time that a point scatterer remains in the beam footprint.

# Example

---

SAR is used to image clutter

$$B = 20 \text{ MHz}, \quad \mathbf{q}_s = 20^\circ \quad (\mathbf{g} = 70^\circ), \quad h_a = 800 \text{ km}, \quad \mathbf{l} = 23 \text{ cm}, \quad L = 12 \text{ m}$$

The down range resolution is

$$\Delta x = \frac{ct}{2 \cos \mathbf{g}} = \frac{(3 \times 10^8) \overbrace{(1/20 \times 10^6)}^{t=1/B}}{2 \cos(70^\circ)} = 22 \text{ m}$$

The cross range resolution for a conventional antenna is

$$\Delta y = R \mathbf{q}_B = \frac{h_a}{\cos(\mathbf{q}_s)} \frac{\mathbf{l}}{L} = \frac{800 \times 10^3}{\cos(20^\circ)} \frac{0.023}{12} = 1.63 \text{ km}$$

For an unfocused SAR ( $\mathbf{p} / 2$  condition)

$$\Delta y_m = \frac{\sqrt{R\mathbf{l}}}{2} = \frac{\sqrt{(0.023)800 \times 10^3 / \cos(20^\circ)}}{2} = 70 \text{ m}$$

For a focused SAR

$$\Delta y = L/2 = 6 \text{ m}$$

# Cross Range Processing (1)

---

The cross range coordinate can be obtained in several ways. Three common approaches are:

1. Side-by-side (sequential) processing: As each new time sample is collected, the oldest time sample is discarded. A new beam footprint is generated that is slightly translated in the along-track direction. A small footprint must be generated to resolve closely spaced scatterers. A massive amount of data must be processed for each time step. Cross range resolution is limited. Early SARs used this method.

The properties of the doppler shift of a point on the ground as a function of time can be used to resolve scatterers in the cross range coordinate:

2. Chirp structure of the return: The return from a scatterer on the ground has a chirp structure. A matched filter can be designed to exploit the chirp structure and improve the resolution across the beam footprint.
3. Doppler processing of the return: The “doppler history” of individual points on the ground can be used to resolve scatterers with doppler filter banks.

# Cross Range Processing (2)

Consider an airborne SAR illuminating a stationary point target on the ground. For the geometry shown, the doppler as a function of time is given by (note:  $\mathbf{q} > 0 \rightarrow x < 0$ )

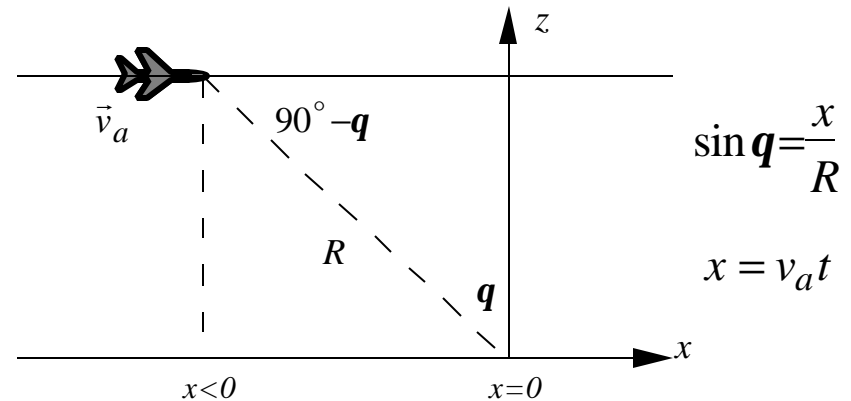
$$f_d = \frac{2v_a \sin \mathbf{q}}{\mathbf{l}} = \frac{2v_a (x / R)}{\mathbf{l}} = \frac{-2v_a^2 t}{\mathbf{l}R}$$

This is a chirp signal with  $\frac{\mathbf{m}}{2} = \frac{-4\mathbf{p}v_a^2}{\mathbf{l}R}$ . A chirp filter can be used on receive to resolve

scatterers in cross range. If the radar is in motion, then there will be a timing error (i.e., range error) in the matched filter response due to the radar's velocity. The radar motion can be compensated for by subtracting out the known doppler (using the estimated ground speed). However, if the point target is in motion, its doppler will cause the target to be displaced in the image from its actual location. In a SAR image this results in cars not on roads, ships displaced from wakes, and so forth.

$$\Delta t = \frac{\mathbf{w}_d}{\mathbf{m}/2} = \frac{\mathbf{l}R}{2v_a^2} f_d$$

Note that if motion compensation is used, then  $f_d$  will be the uncompensated doppler frequency.

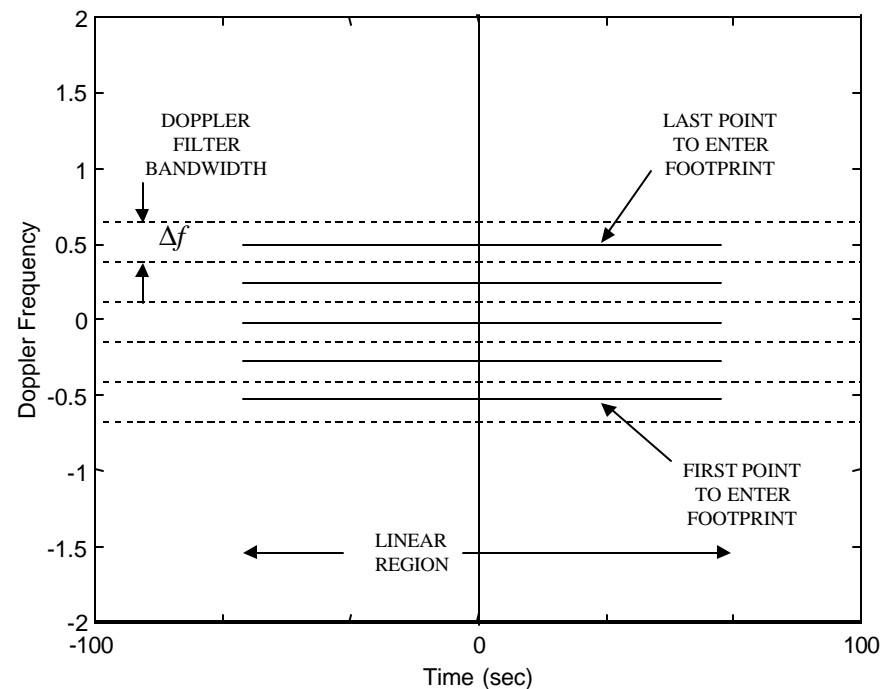
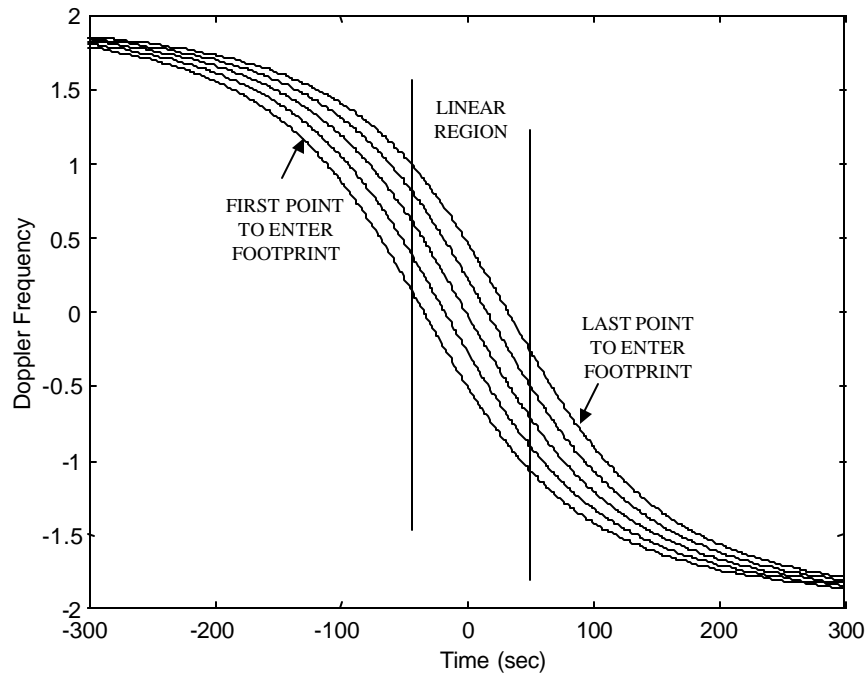




# Cross Range Processing (3)

The doppler shift of a stationary point on the ground has a unique time history as the beam footprint passes by, as shown in the example below for four scatterers. If the processing time is limited to the linear region, the curves can be “de-ramped” (slope removed) and Fourier transformed to obtain the frequency components.

$$h_a = 20 \text{ km}, \mathbf{l} = 1 \text{ m}, \mathbf{g} = 30^\circ, v_a = 300 \text{ m/s}$$

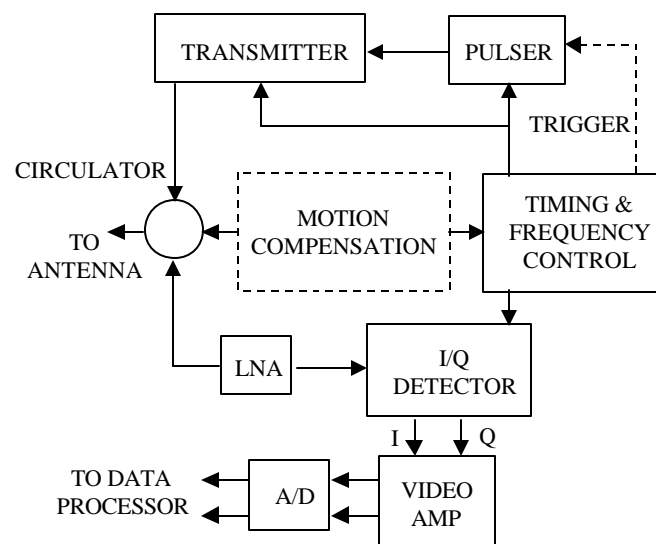
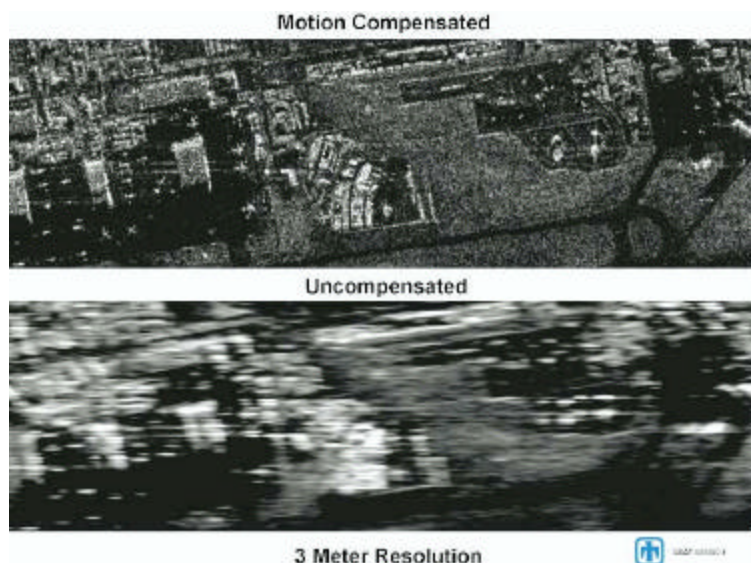


# Motion Compensation

The radar platform has motion variations that can cause blurring and displacement of objects in the image. Motion compensation involves estimating the displacement from the along track direction and deviations from a constant velocity and correcting for them in the processing.

Several levels of correction may be required:

- The antenna may have to be stabilized or re-steered
- Timing must be re-adjusted if the radar travels off of the ideal flight line by more than the range resolution
- If phase information is used in processing, then phase errors due to cross track and vertical random motion must be held to less than  $\lambda / 10$



# Radar Mapping

---

## Key features:

1. Radar provides its own illumination; operates in all conditions
2. Large area coverage in a short time
3. Surface features obtained in spite of vegetation and clouds
4. Operates at relatively low grazing angles
5. Images a plan view

## Resolution requirements:

<u>FEATURES</u>	<u>CELL SIZE</u>
Coastlines, large cities, outlines of mountains	500 feet
Major highways, variations in fields	60 – 100 feet
Road map (city streets, large buildings, airfields)	30 – 50 feet
Houses, small buildings	5 – 10 feet
Vehicles and aircraft	1 – 5 feet

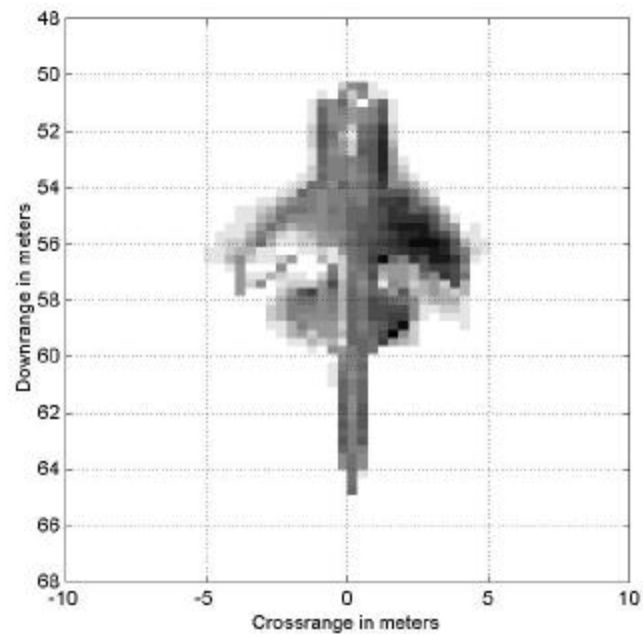
# SAR Image

Echo intensity plotted versus down range and cross range coordinates

X-29  
TARGET



STEPPED FREQUENCY IMAGE



# SAR Range Equation

---

Start with standard RRE:

$$SNR = \frac{P_t A_e^2 \mathbf{s} n_B}{4p l^2 k T_s B_n R^4}$$

Substitute the following:

$$t_{\text{obs}} = t_{\text{ot}} = \frac{n_B}{f_p} = \frac{L_s}{v_a} \Rightarrow n_B = \frac{L_s f_p}{v_a}$$

$$P_t = \frac{P_{\text{av}}}{t f_p}, \quad t B_n \approx 1 \quad \text{and} \quad \mathbf{s} = \mathbf{s}^o A_c = \mathbf{s}^o \Delta x \Delta y$$

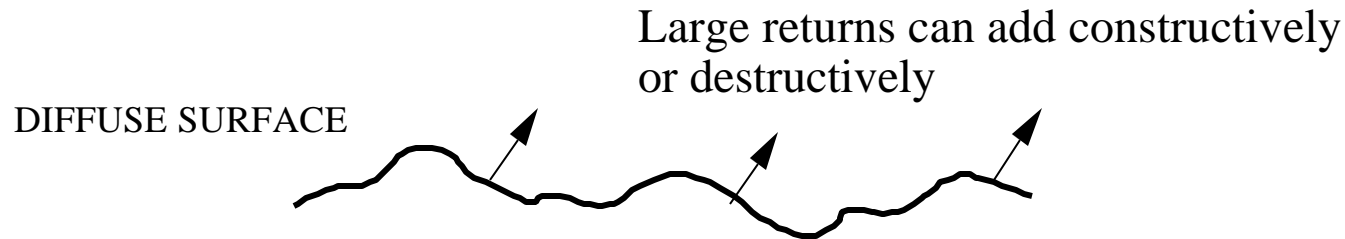
to obtain

$$SNR = \frac{P_{\text{av}} A_e^2 \mathbf{s}^o \Delta x \Delta y (L_s f_p / v_a)}{4p l^2 k T_s B_n R^4 t f_p} = \frac{P_{\text{av}} A_e^2 \mathbf{s}^o \Delta x \Delta y t_{\text{obs}}}{4p l^2 k T_s R^4}$$

For pulse width limited illumination and focused SAR,  $\Delta x = \frac{ct}{2 \cos \mathbf{g}}$  and  $\Delta y = \frac{L}{2}$

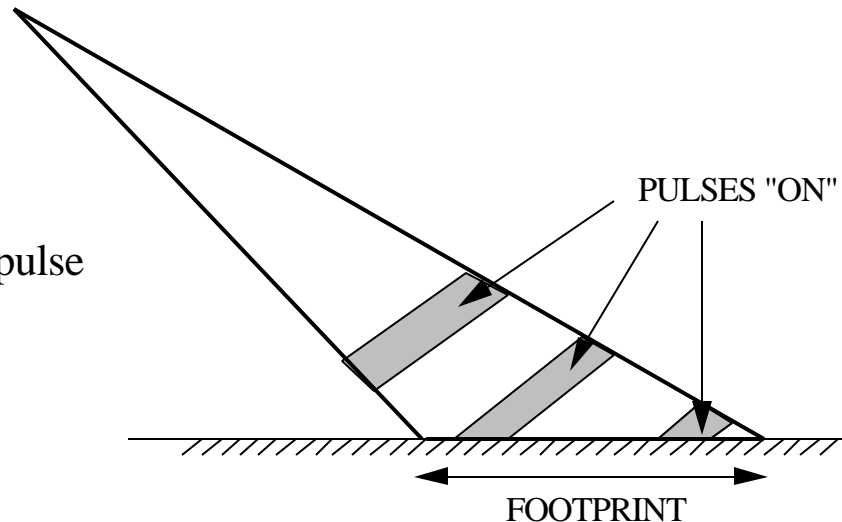
# SAR Problems (1)

1. Speckle – occurs when returns from diffuse surfaces are added coherently.



2. Motion effects – for satellite based SAR, earth's rotation can be important.
3. Range curvature – the illuminated strip can be curved rather than straight.
4. Changing atmospheric conditions – rain, moisture, dust, etc.

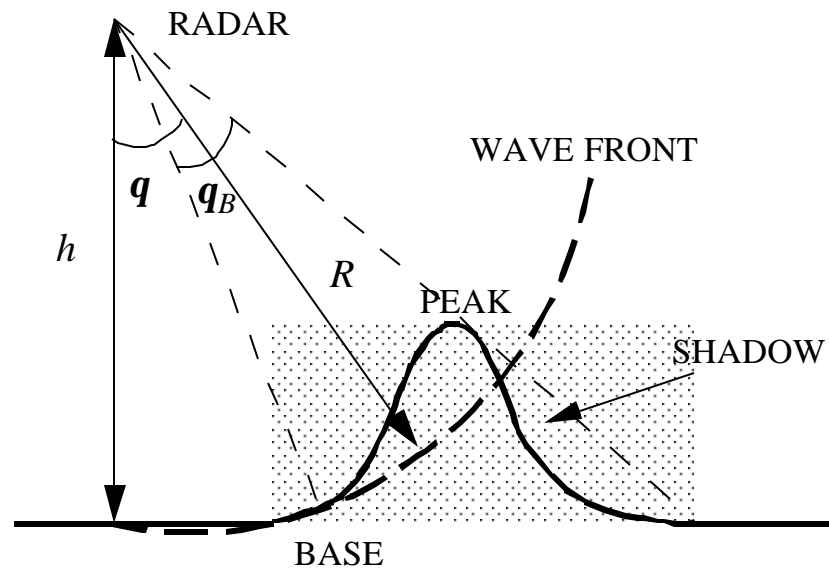
5. Ambiguities if more than one pulse in a surface swath



## SAR Problems (2)

---

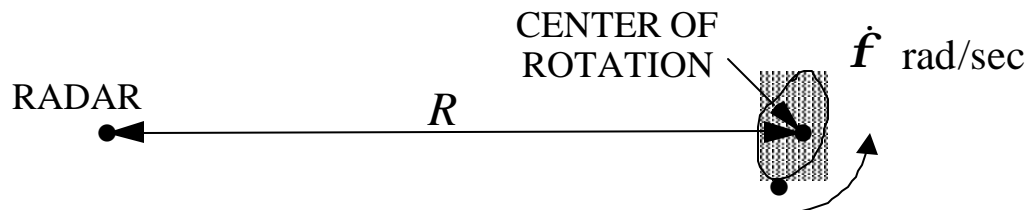
6. Layover – occurs when an object's top is in a closer range bin than the object's bottom. The object appears to be “laid over” on its side in the image.



7. Shadows – appear dark in the image due to lack of illumination of the shadowed area.
8. Multipath – can lead to multiple copies of the same object in the image, or displacement of object in the image.

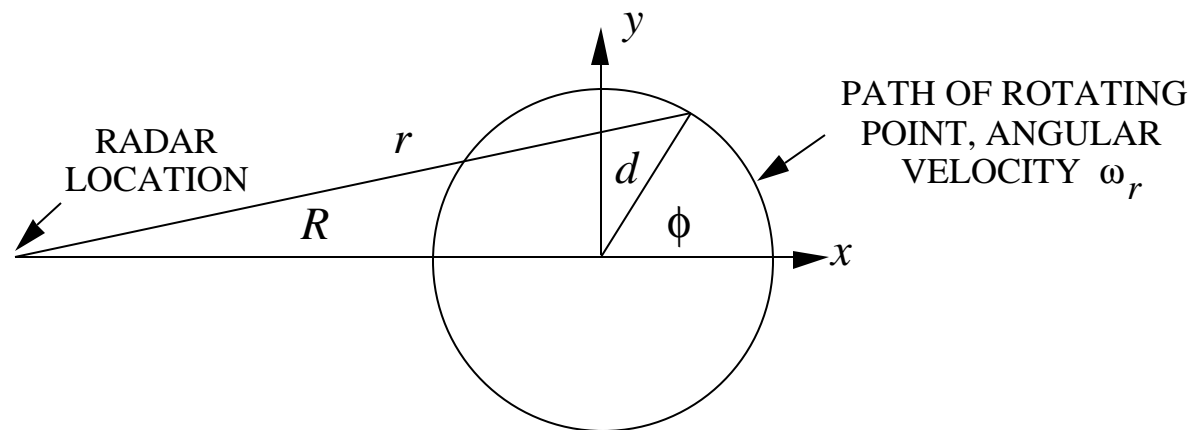
# Inverse Synthetic Aperture Radar (ISAR)

Generally, ISAR refers to the case where the cross range information is obtained from target doppler. Consider a rotating target at range  $R$ .



A typical point on the target rotates a radius  $d$  about the center of rotation. Using the law of cosines

$$r^2 = R^2 + d^2 - 2dR \cos(\mathbf{p} - \mathbf{f}) \Rightarrow_{R \gg d} r \approx R \sqrt{1 + \frac{2d \cos \mathbf{f}}{R}} \approx R + d \cos \mathbf{f}$$





# ISAR (2)

---

The scattered field from the rotating point is

$$E_s \propto e^{j\omega t} e^{-j2kr} = \underbrace{e^{j\omega t}}_{\text{CARRIER}} \cdot \underbrace{e^{-j2kR}}_{\substack{\text{DELAY} \\ \text{TO CENTER}}} \cdot \underbrace{e^{-j2kd \cos f}}_{\substack{\text{DOPPLER SHIFT} \\ \text{FROM ROTATION}}}$$

Doppler frequency

$$\omega_d = 2\dot{\mathbf{p}} f_d = \frac{d}{dt} (-2kd \cos(\dot{\mathbf{f}}t)) = \frac{2\dot{\mathbf{f}}d}{1} \sin(\dot{\mathbf{f}}t)$$

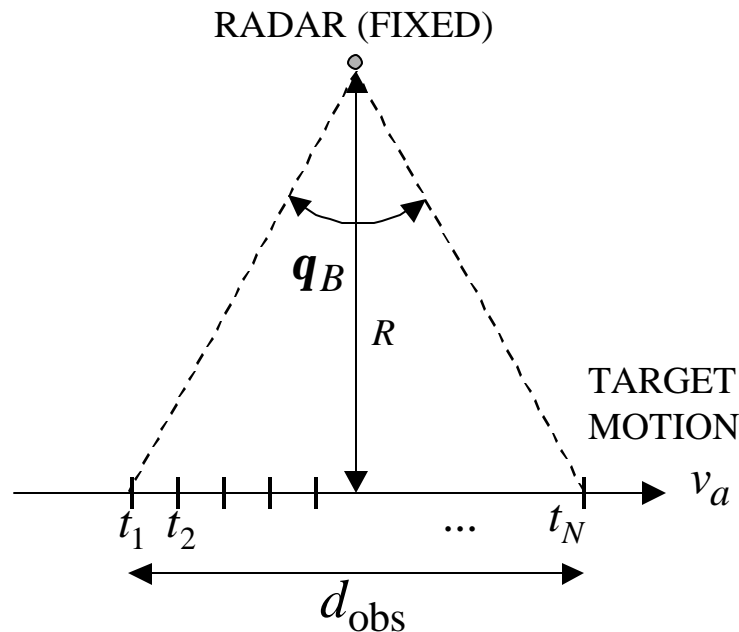
and the cross range coordinate

$$f_d = \frac{2\dot{\mathbf{f}}}{1} \underbrace{d \sin \mathbf{f}}_{=y} \Rightarrow y = \frac{1 f_d}{2\dot{\mathbf{f}}}$$

which can be found because  $\dot{\mathbf{f}}$  is known. A similar situation applies if the target is stationary and the radar circles the target.

# ISAR (3)

ISAR has been applied to targets with linear motion. The geometry is similar to that of the airborne SAR on a straight flight path, but the locations of the radar and target are reversed. Over the observation time,  $T_{\text{obs}}$ , a synthetic beam,  $\mathbf{q}_B$ , is formed. The array factor is the same as for airborne SAR.



- The cross range resolution at range  $R$  is

$$\Delta y = Rq_B$$

- The observation distance is used to determine the beamwidth (rather than the synthetic length)

$$q_B \approx \lambda / (2d_{\text{obs}})$$

- Cross range resolution can be improved by increasing the observation (integration) time

$$\Delta y = R\lambda / (2v_a T_{\text{obs}})$$

- The radar does not have control of the target's flight characteristics.

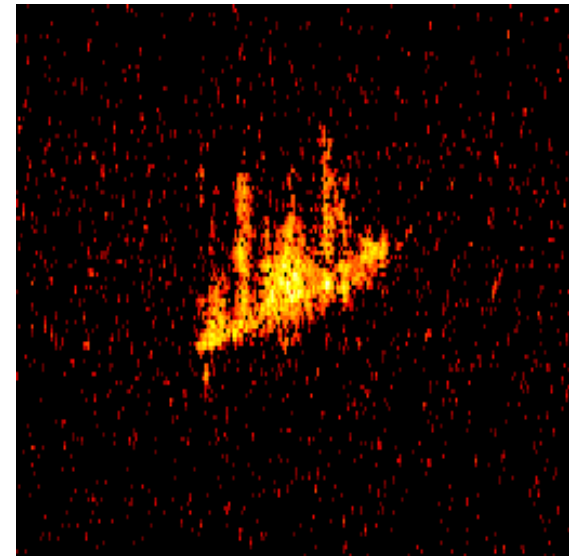
# ISAR (4)

---

USS Crocket



ISAR Image



(From NRL web site: <http://radar-www.nrl.navy.mil/Areas/ISAR/>)

# HF Radars (1)

---

- Radars that operate in the high frequency (HF) band are also called over the horizon (OTH) radars. Advantages:
  1. Long range target detection
  2. Low altitude target detection
  3. Operates in target scattering resonance region (i.e., detection of low observable targets)
  4. Low probability of intercept
- Major applications:        Protection of land mass from attack (ships and aircraft)
- Atmospheric propagation mechanisms:
  1. Sky wave: the interaction of HF waves and the Earth's ionosphere, which is the upper atmosphere (heights  $\geq 80$  km)
  2. Ground wave: over the horizon diffraction
- Comparison of operational ranges:

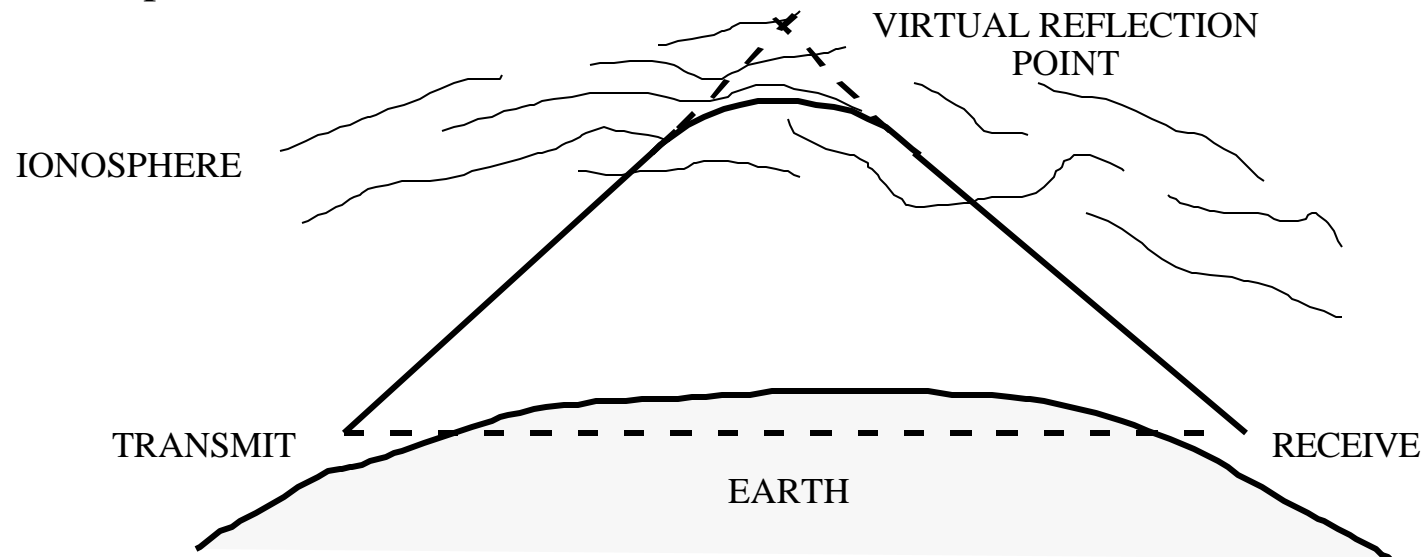
Conventional microwave:	200 km
HF ground wave:	200 to 400km
HF sky wave:	1000 to 4000 km

# HF Radars (2)

---

Atmospheric propagation issues:

1. The properties of the ionosphere are constantly changing with:  
time of day, time of year, solar activity
2. Ionospheric reflections appear to originate at multiple reflective layers at different heights. This often causes multipath fading.
3. Ionospheric reflections are strongly dependent on frequency and antenna "launch" angle. A wide range of frequencies must be used.
4. Efficient operation requires knowledge of the current state of the ionosphere.



# HF Radar (3)

---

Other HF radar issues:

External noise sources are greater than internally generated noise. They include

1. atmospheric (lightning)
2. cosmic
3. man made (radio, ignition, etc.)

The ionosphere is dispersive and hence there are limits on the information bandwidth.

Clutter is strong. Sources include the earth, auroral ionization and meteor ionization.

Ionospheric reflection allows a specific area of the earth's surface to be illuminated by only a limited band of frequencies.

Multipath fading can be severe. Ionospheric paths have high attenuation.

Conclusion: the sky wave path can be made reliable if one is willing to pay the cost.

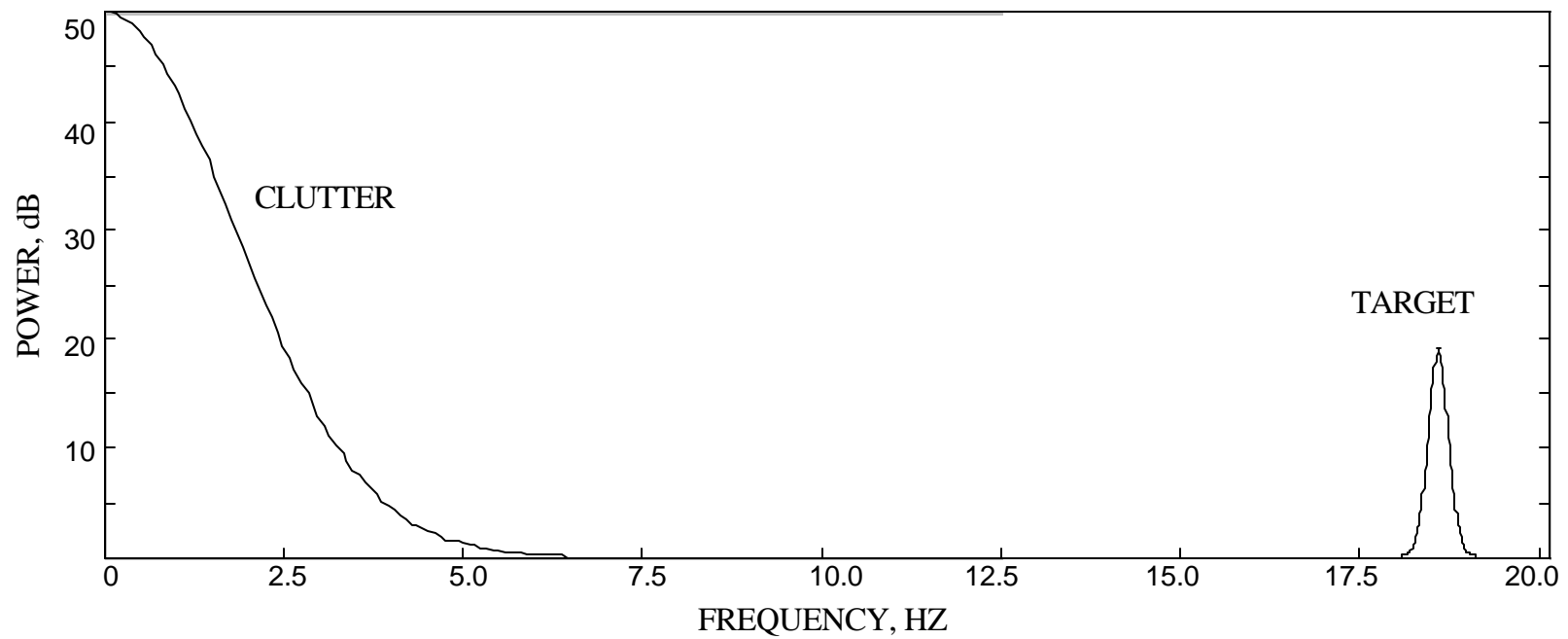
# Typical HF OTH Radar Parameters

<u>PARAMETER</u>	<u>TYPICAL VALUES</u>
range	1000 to 4000 km
range resolution	2 km to 40 km
range accuracy	2 km to 20 km
angle resolution	0.5 to several degrees (ionosphere limits angle resolution to some fraction of a degree)
angle accuracy	approximately 12 km at 1500 km
Doppler resolution	as little as 0.1 Hz (about 1.5 knots)
operating frequency	4 MHz to 40 MHz, electronically tuned
peak output power	20 kw to 1 Mw
PRF	CW to 50 Hz
pulse width	10 <i>ms</i> to 200 <i>ms</i>
antenna gains	15 dBi to 30 dBi (transmit and receive antennas are usually different and multiple beams are used on receive)
azimuth (horizontal) beamwidth	0.5 to 20 degrees (often narrow receive, wide transmit)
elevation (vertical) beamwidth	10 to 60 degrees (vertical apertures is costly)
azimuth/elevation beam steering	20 to 150 degrees/0 to 30 degrees
dwll time	ten seconds or more

# Typical HF Clutter and Target Spectrum

Example:

<i>Target Speed</i> (relative velocity)	<i>Doppler Shift (Hz)</i>	
	at 3 MHz	at 30 MHz
9 m/s (20 mph)	0.18	1.8
90 m/s (200 mph)	1.8	18



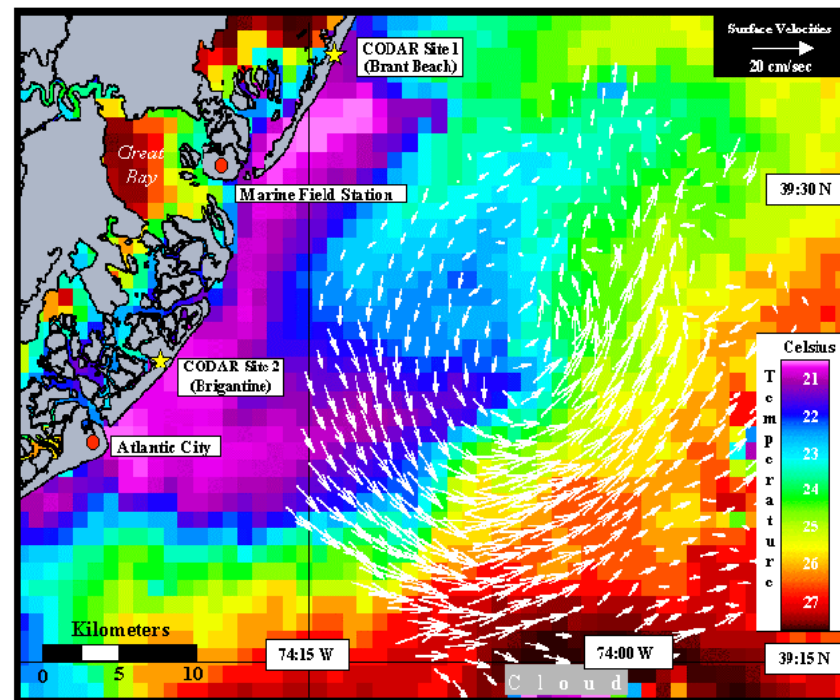


# HF Coastal Radar (CODAR)

Characteristic	Value
Operating frequency	27.65 MHz
Transmitted power	30 W
Working range (35 PSU salinity)	up to 50 km
Length of sea surface wave (Bragg)	5.42 m
Depth over which current is averaged	~0.5 m
Range resolution	0.3 km, 0.6 km, 1.2 km
Azimuthal resolution (Direction Finding)	1 degree
Azimuthal resolution (Beam Forming)	+/-3 degrees
Integration time	9 minutes, 18 minutes
Accuracy of radial component	1...2~cm/s
Accuracy of current field	1...5~cm/s



Surface current map



University of Hamburg WERA HF radar

# Relocatable Over the Horizon Radar (ROTHR)

---

- The Navy radar was originally designed for wide area ocean surveillance for fleet defense
- Since 1989 it has been used by the Coast Guard and Customs for the detection of drug running
- Operates in the 2 to 30 MHz frequency band
- Vertical and down range backscatter sounders are used to continuously monitor the ionosphere



# HF Radar Example (CONUS-B)

---

The CONUS-B radar has the following parameters:

$$P_t = 61 \text{ dBW}, G_t = 23 \text{ dB}, G_r = 28 \text{ dB}, I_i = 3 \text{ dB}$$

two-way path gain factor,  $(F_t)^2 = (F_r)^2 = 3 \text{ dB}$ , other system losses, 15 dB

noise power at the receiver,  $kT_s B_n = -164 \text{ dBW}$

(a) What frequency should the radar use to detect a target with a wingspan of 15 m and what is the target's approximate RCS?

Assume horizontal polarization and model the wing as a shorted half-wave dipole to find the first resonant frequency (see the plot in the discussion of chaff):

$$l / 2 = 15 \text{ m} \Rightarrow f = 10 \text{ MHz} \Rightarrow \sigma / l^2 \approx 0.75 \Rightarrow \sigma \approx 675 \text{ m}^2 = 28.5 \text{ dB}$$

(b) If  $SNR_{\min} = 25 \text{ dB}$ , will the target be detected at 2000 km?

Compute the SNR. It is convenient to use dB quantities in this case:

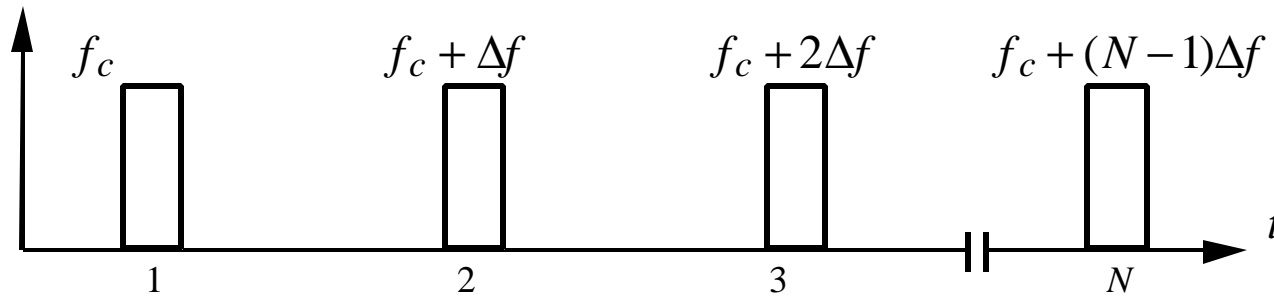
$$SNR = \underbrace{P_t G_t G_r I_i}_{115} + \underbrace{(1/4\pi)^3}_{-33} - \underbrace{kT_s B_n}_{-164} + \underbrace{(F_t F_r)^4}_{-6} + \underbrace{1/(R_t R_r)^2}_{-252} + \underbrace{\sigma}_{28.5} + \underbrace{l^2}_{29.5} - \underbrace{L}_{15} = 31 \text{ dB}$$

Since  $SNR > 25 \text{ dB}$  the target will be detected. Note that the target RCS at resonance (see UWB lectures) can be 5-10 dB higher than at other frequencies, thus operating at resonance makes detection possible.

# Stepped Frequency Radar (1)

---

In a stepped frequency radar the carrier frequency of each pulse in the train is increased



Receiver (instantaneous) bandwidth,  $B_{\text{instant}} = 1/t$ :

Controlled by the individual pulse  
 Determines the A/D sampling rate  
 $t \Delta f \leq 1$

Effective bandwidth,  $B_{\text{eff}} = N\Delta f$ :

Controlled by the frequency excursion across the burst  
 Determines the range resolution

# Stepped Frequency Radar (2)

---

Characteristics of stepped frequency radars:

1. Instantaneous bandwidth is controlled by the pulse width  $B_{\text{instant}} = 1/t$

2. Range resolution is given by

$$\Delta R = \frac{c}{2N\Delta f} = \frac{c}{2B_{\text{eff}}}$$

that is determined by the effective bandwidth,  $B_{\text{eff}} = N\Delta f$

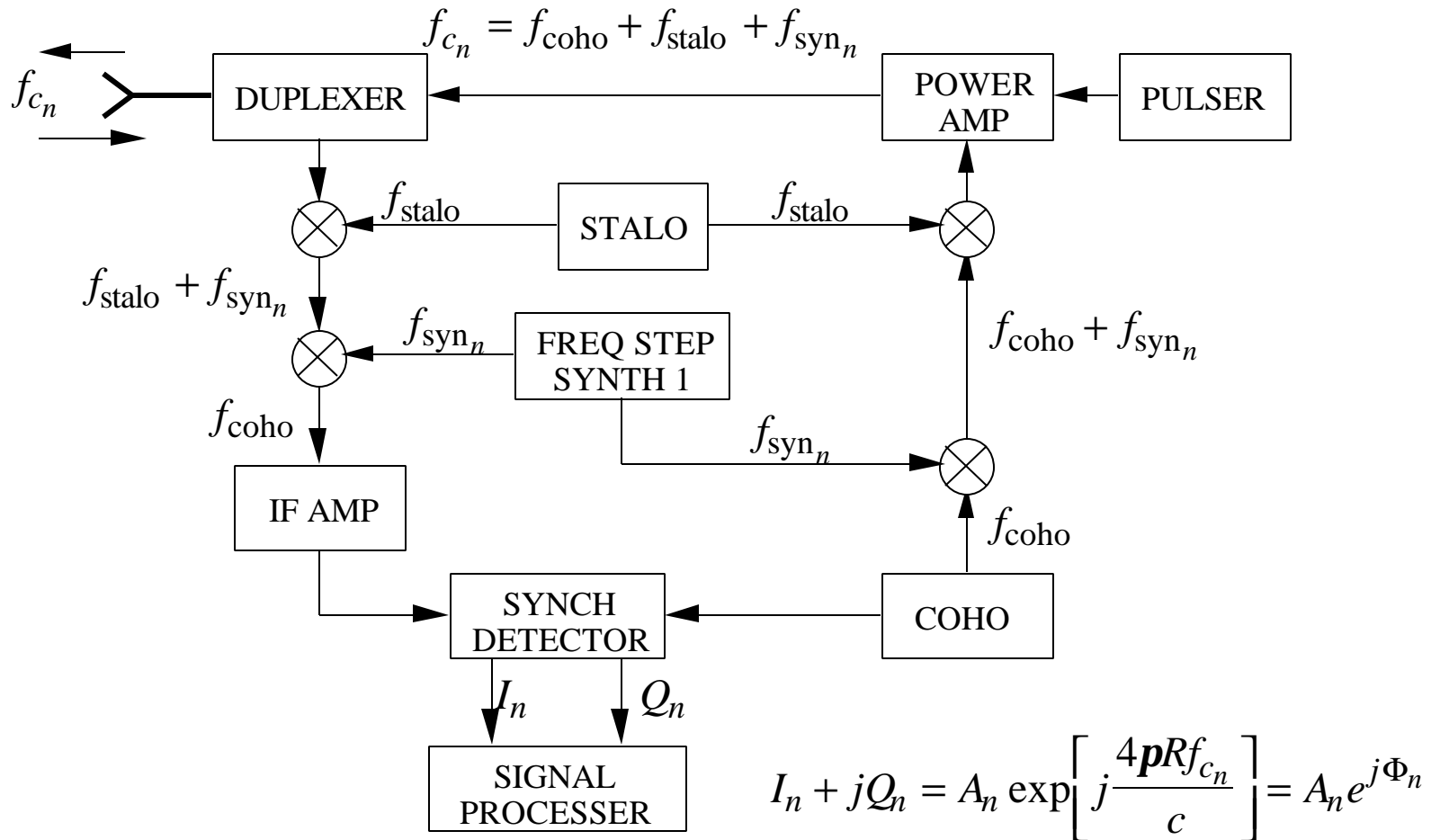
3. The effective bandwidth can be increased semi-independently of the instantaneous bandwidth (the constraint is  $t \Delta f \leq 1$ )

4. It is possible to have a large effective bandwidth (and high range resolution) with low instantaneous bandwidth

5. Low instantaneous bandwidth allows a lower A/D sampling rate than a conventional radar (high frequency A/Ds are not commercially available). Narrowband microwave hardware is simpler and less expensive.

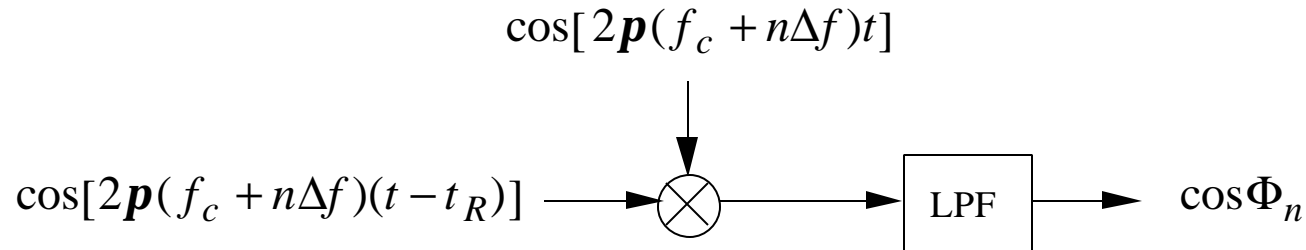
# Stepped Frequency Radar (3)

Block diagram:



# Stepped Frequency Radar (4)

Mathematical expression for phase shift:



$$\begin{aligned} \Phi_n &= 2\mathbf{p}(f_c + n\Delta f)t_R \\ &= 2\mathbf{p}(f_c + n\Delta f)\frac{2R_n}{c} \end{aligned}$$

where  $R_n = R_o + v_r nT_p$ . Therefore,

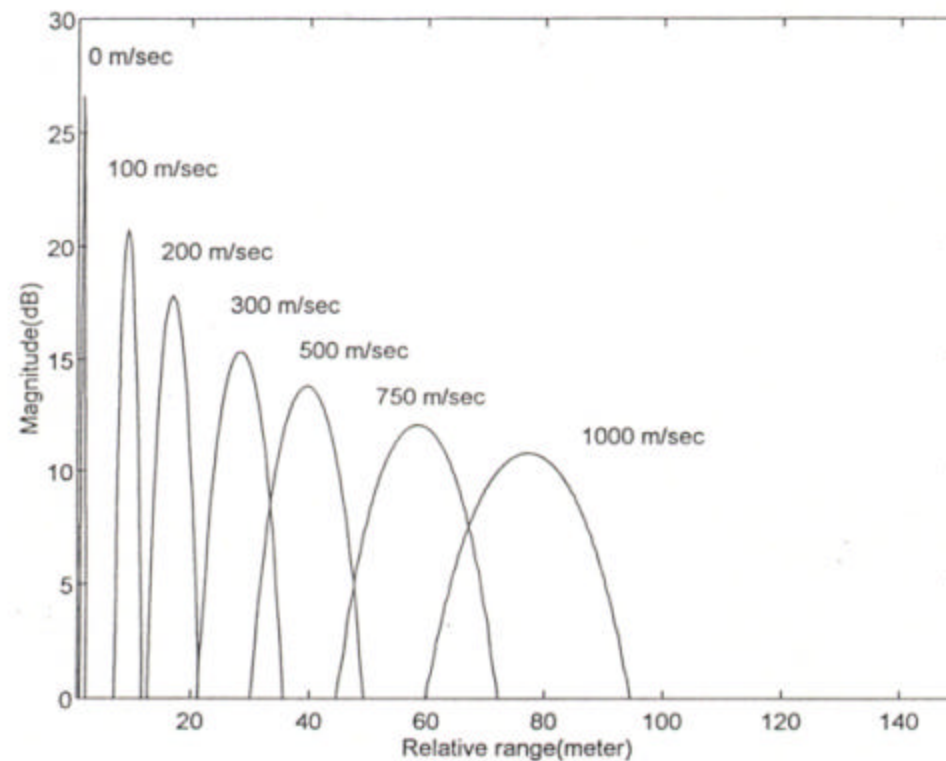
$$\begin{aligned} \Phi_n &= 2\mathbf{p}(f_c + n\Delta f)\frac{2}{c}(R_o + v_r nT_p) \\ &= \underbrace{\frac{4\mathbf{p} f_c R_o}{c}}_{\text{PHASE SHIFT DUE TO RANGE}} + 2\mathbf{p} \underbrace{\frac{\Delta f}{T_p} \frac{2R}{c}}_{\text{FREQ. SHIFT DUE TO RANGE}} T_p + 2\mathbf{p} \underbrace{\frac{2v_r f_c}{c}}_{\text{DOPPLER SHIFT}} nT_p + 2\mathbf{p} \underbrace{\frac{\Delta f}{T_p} \frac{2v_r nT_p}{c}}_{\text{DOPPLER SPREAD}} nT_p \end{aligned}$$

# Stepped Frequency Radar (5)

---

Doppler spreading, shifting and attenuation:

- Single target, different radial velocities
- Target range is unchanged
- SNR = 13 dB, PRF = 20 KHz,  $f_c = 10$  GHz,  $N = 512$ ,  $\Delta f = 1$  MHz



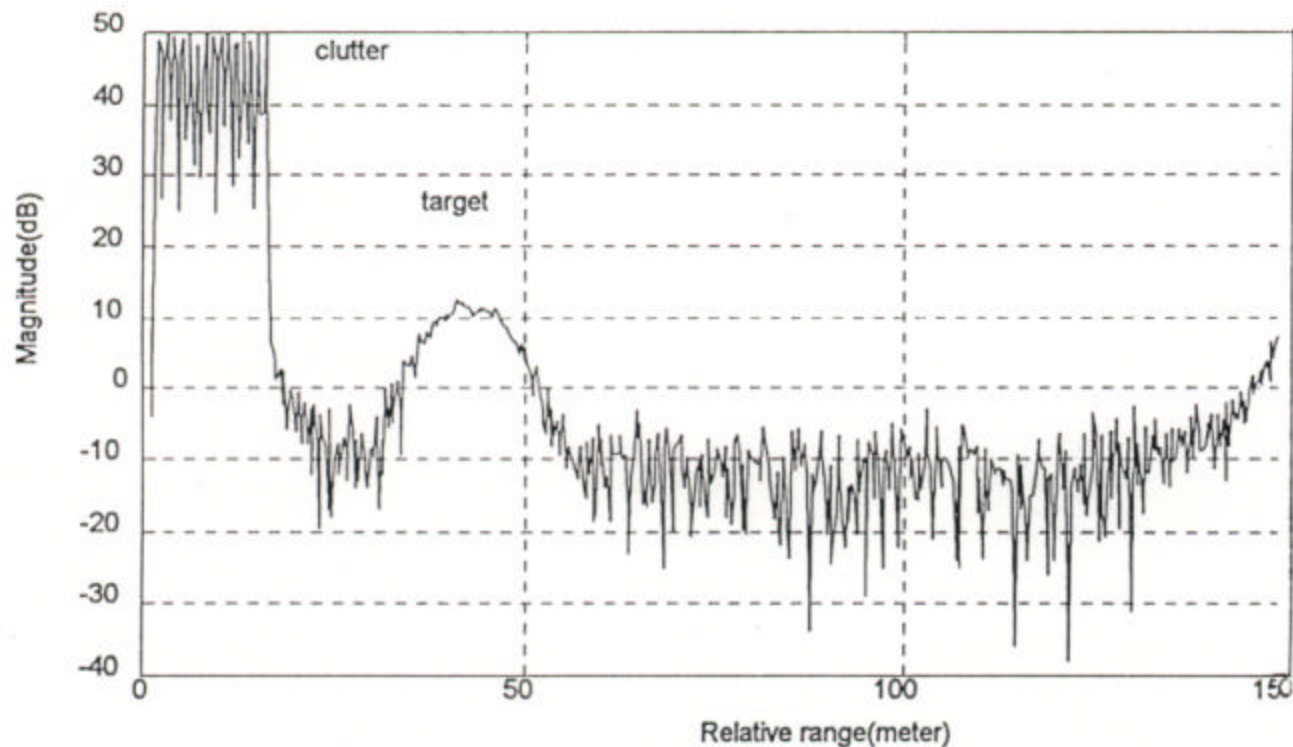


# Stepped Frequency Radar (6)

---

Doppler spreading and shifting can be used to separate targets from clutter:

- SNR = 11 dB, PRF = 20 KHz, CNR = 35 dB
- $f_c = 10$  GHz,  $N = 512$ ,  $\Delta f = 1$  MHz,  $v_r = 500$  m/s
- If an estimate of the target velocity is available, velocity compensation can be applied



# Imaging of Moving Targets

---

Objective is to find the reflectivity density function  $\mathbf{r}(x, y)$  from the frequency signature  $S(f, t)$ :

$$S(f, t) = e^{-j4\mathbf{p}fR(t)/c} \int_{-\infty}^{\infty} \int_{-\infty}^{\infty} \mathbf{r}(x, y) e^{-j4\mathbf{p}[xf_x(t) + yf_y(t)]} dx dy$$

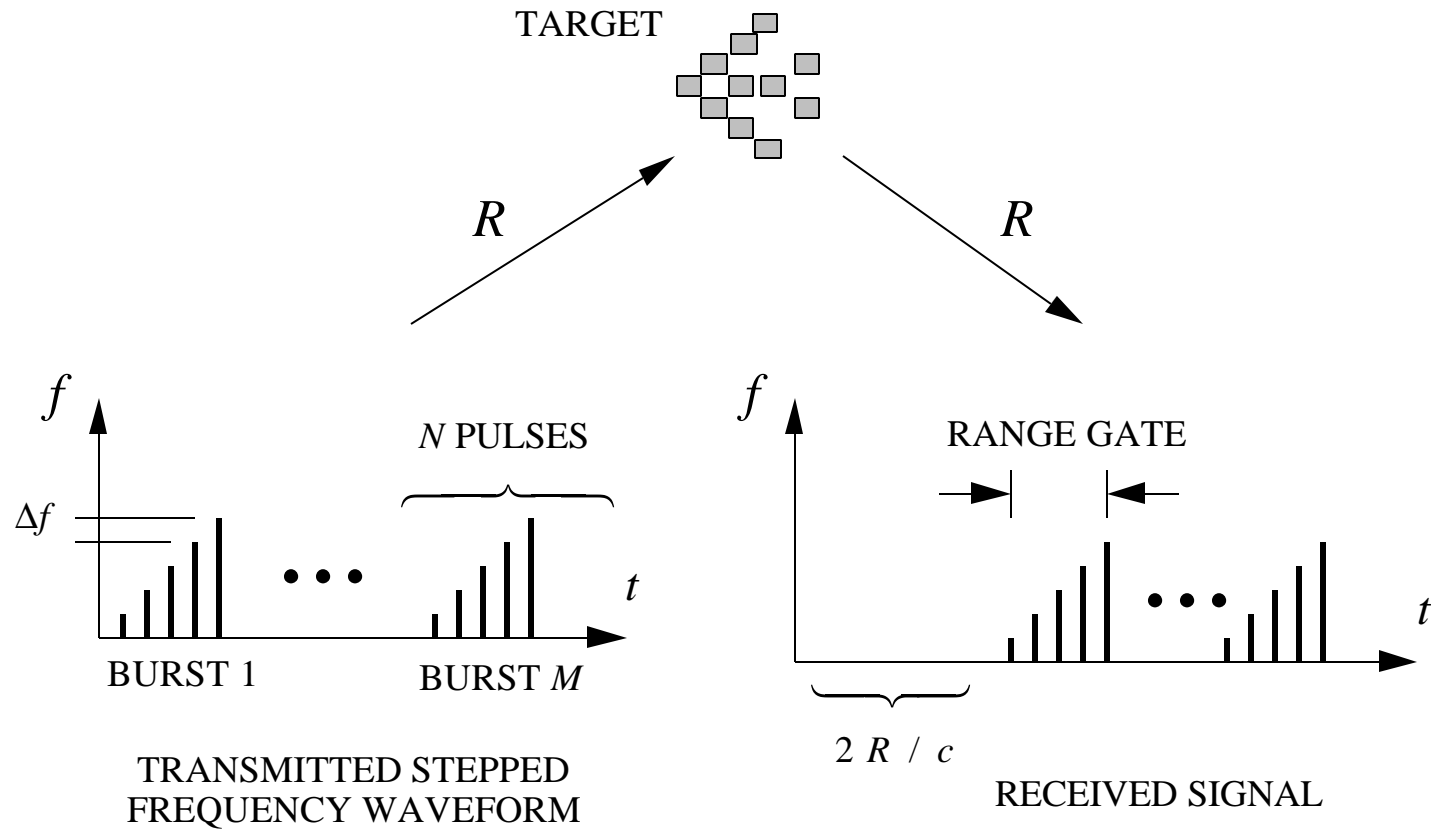
where the spatial frequencies are defined as

$$f_x(t) = \frac{2f}{c} \cos[\mathbf{f}(t)] \quad \text{and} \quad f_y(t) = \frac{2f}{c} \sin[\mathbf{f}(t)]$$

Stepped frequency imaging:

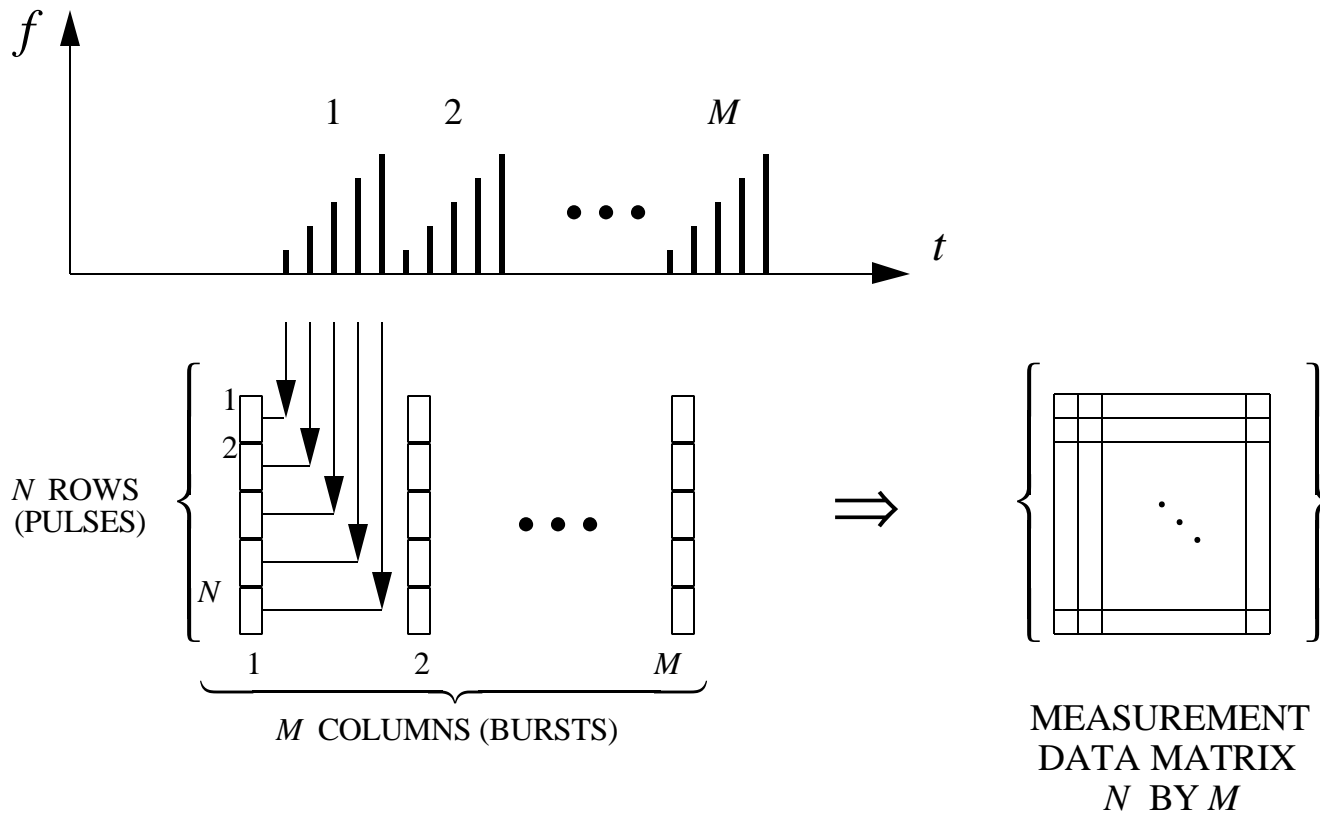
1.  $M$  bursts are transmitted, each containing  $N$  narrowband pulses
2. The center frequency  $f_n$  of each successive pulse is increased by a frequency step of  $\Delta f$
3. Total bandwidth =  $N\Delta f$
4. Cross range resolution determined by number of bursts,  $M$

# Stepped Frequency Imaging (1)



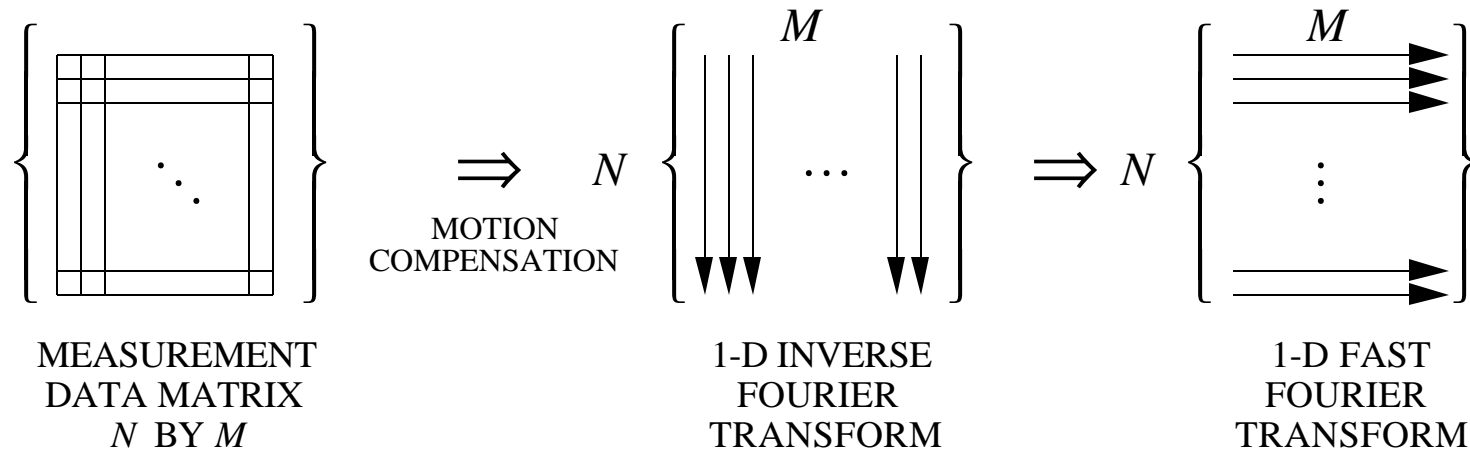
# Stepped Frequency Imaging (2)

Form a two-dimensional matrix of measurement data  $S(f_{nm}, t_{nm})$



# Stepped Frequency Imaging (3)

Time-frequency transform for Doppler processing



1. Range processing:  $N$ -point 1-D inverse Fourier transform (1-DIFT) for each of the  $M$  received frequency signatures.  $M$  range profiles result, each with  $N$  range cells.
2. Cross range (Doppler) processing: for each range cell, the  $M$  range profiles are a time history that can be I and Q sampled and fast Fourier transformed. The result is an  $M$ - point Doppler spectrum or Doppler profile.
3. Combine the  $M$  range cell data and the  $M$  Doppler data to form a two-dimensional image.

# Ultra-Wide Band Radar (1)

---

Ultra-wideband radar (UWB) refers to a class of radars with a large relative bandwidth.

They include:

1. pulse compression radar
2. stepped frequency radar
3. impulse (monocycle) radar

Impulse radars have all the advantages of conventional short pulse radars. In addition, claims have also been made in the categories of (1) improved radar performance, and (2) ability to defeat stealth. We examine the validity of the claims (ref: Proceedings of the First Los Alamos Symposium on UWB Radar, Bruce Noel, editor):

Claim: Penetrates absorbers because of molecular resonances.

Validity: True, but the effect appears to be weak.

Claim: Defeats target shaping techniques.

Validity: True at low frequencies, but above certain frequencies shaping is wideband.

Claim: Excites target "aspect-independent" resonances.

Validity: True, but weak resonances; not exploitable at present.

Claim: Defeats RCS cancelation schemes.

Validity: True, but so do conventional wideband radars.

# Ultra-Wide Band Radar (2)

---

Claim: Reduced clutter because it operates in the pulsewidth limited condition.

Validity: True, but negated by changes in clutter statistics, which vary rapidly with frequency.

Claim: Defeats multipath.

Validity: True, but multipath is often an advantage.

Claim: Overcomes the  $1/R^2$  spreading loss by "extending" the near field.

Validity: True, but not exploitable at moderate to long ranges of interest for search radars.

Claim: Low probability of intercept (LPI).

Validity: True in general, but not necessarily for long range radars.

Claim: Resistance to jamming (short pulse implies narrow range gates and therefore not susceptible to CW jamming).

Validity: True

Claim: Target identification capability.

Validity: True, but need matched filters derived from all target signature features.

# Ultra-Wide Band Radar (3)

---

Many of our assumptions used to model radar systems and components no longer are valid. For instance,

propagation characteristics,  
target RCS,  
antenna gain, and  
radar device characteristics,

are not independent of frequency because the bandwidth is so large. The frequency dependence of the system parameters must be included:

$$P_r = \frac{P_t(f)G_t(f)\sigma(f)A_{er}(f)}{(4\pi R^2)^2}$$

Important points:

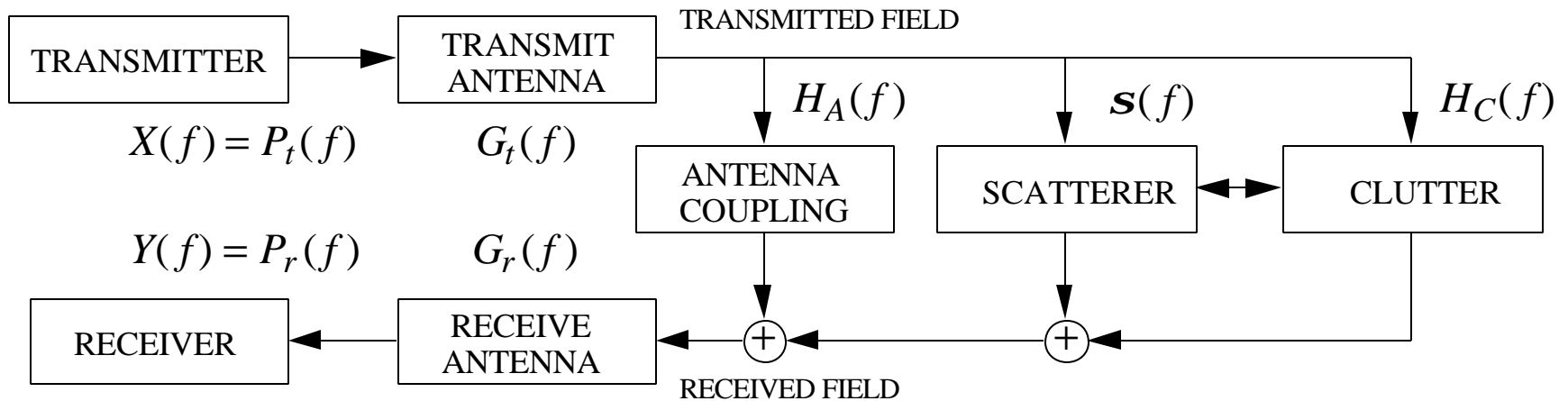
1. The waveform out of the transmitter is not necessarily the waveform that is radiated by the antenna. The antenna removes the DC and some low frequency components. The radiated signal is the time derivative of the input signal.
2. The waveform reflected by the target is not necessarily the waveform incident on the target.
3. The waveform at the receive antenna terminals is not necessarily the waveform at the antenna aperture.

To extract target information requires a substantial amount of processing.



# Ultra-Wide Band Radar (4)

Wideband model of the radar, target, and environment:



excitation waveform:	$x(t) \leftrightarrow X(f)$	transmit antenna:	$g_t(t) \leftrightarrow G_t(f)$
clutter environment:	$h_C(t) \leftrightarrow H_C(f)$	receive antenna:	$g_r(t) \leftrightarrow G_r(f)$
antenna coupling:	$h_A(t) \leftrightarrow H_A(f)$	target:	$S(t) \leftrightarrow S(f)$
noise:	$n(t) \leftrightarrow N(f)$	received signal:	$y(t) \leftrightarrow Y(f)$

The target's scattered field can be determined from  $Y(f)$  if all of the other transfer functions are known. If they are not known they must be assumed.

# Ultra-Wide Band Radar (5)

---

- In general:
1. Antenna radiation requires acceleration of charge.
  2. The radiated signal is the time derivative of the input signal.

From the definition of magnetic vector potential,  $\vec{B} = \mathbf{m}\vec{H} = \nabla \times \vec{A}$ . Take the derivative with respect to time

$$\mathbf{m} \frac{\mathcal{I}}{\mathcal{I}t} \vec{H} = \frac{\mathcal{I}}{\mathcal{I}t} (\nabla \times \vec{A}) = \nabla \times \left( \frac{\mathcal{I}}{\mathcal{I}t} \vec{A} \right)$$

Substitute this into Maxwell's first equation:

$$\nabla \times \vec{E} = -\mathbf{m} \frac{\mathcal{I}}{\mathcal{I}t} \vec{H} = -\nabla \times \left( \frac{\mathcal{I}}{\mathcal{I}t} \vec{A} \right)$$

implies

$$\vec{E} = \frac{\mathcal{I}}{\mathcal{I}t} \vec{A}$$

But the magnetic vector potential is proportional to current. As an example, for a line current

$$\vec{A}(t, R) = \frac{\mathbf{m}}{4\mathbf{p}} \int_L \frac{I(t - R/c)}{R} d\ell$$

Therefore  $\vec{E} \propto \frac{\mathcal{I}I}{\mathcal{I}t}$  and the radiated field strength depends on the acceleration of charge.

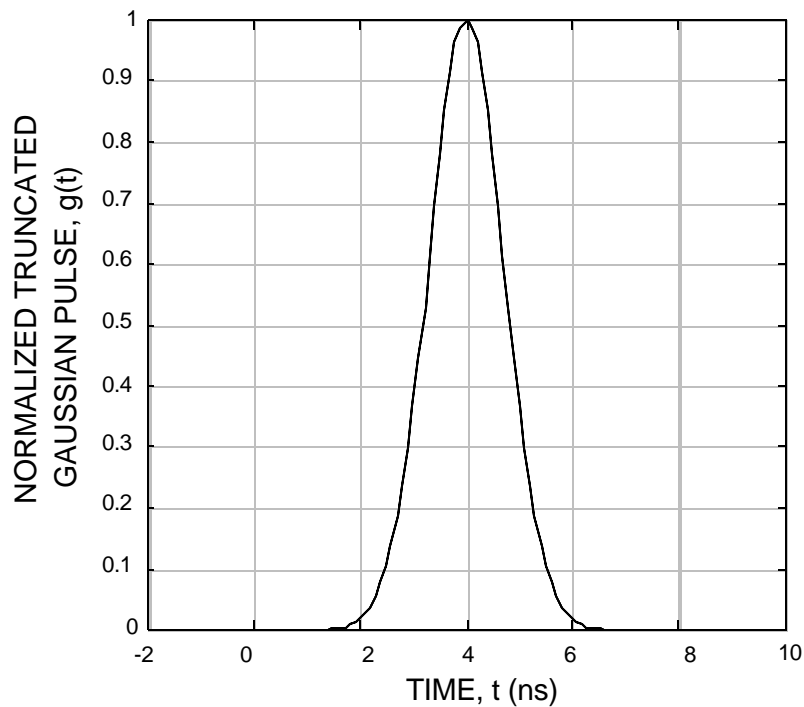
# Ultra-Wide Band Radar (6)

---

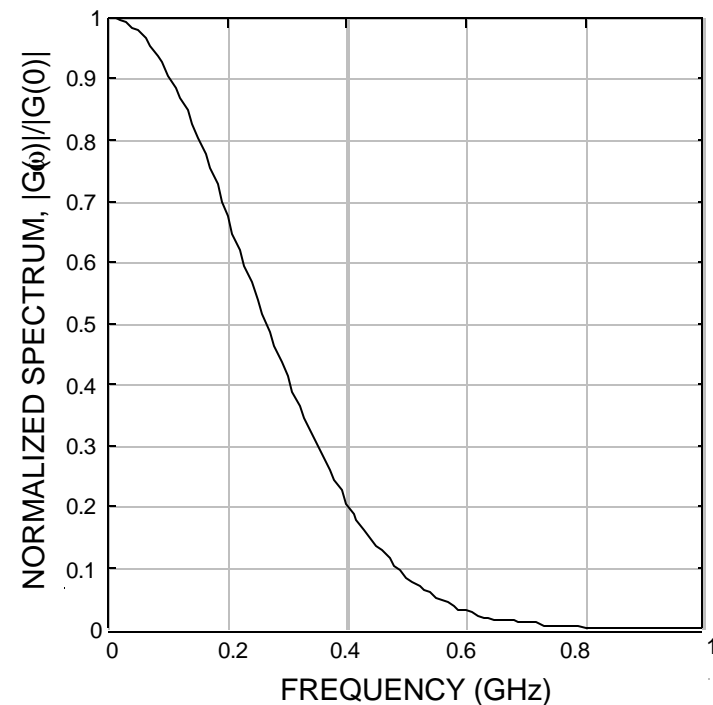
UWB waveforms: gaussian pulse

1. has the minimum time-bandwidth product of all waveforms
2. spectrum has a dc component; therefore it cannot be radiated
3. used analytically because it is mathematically convenient

Truncated gaussian pulse



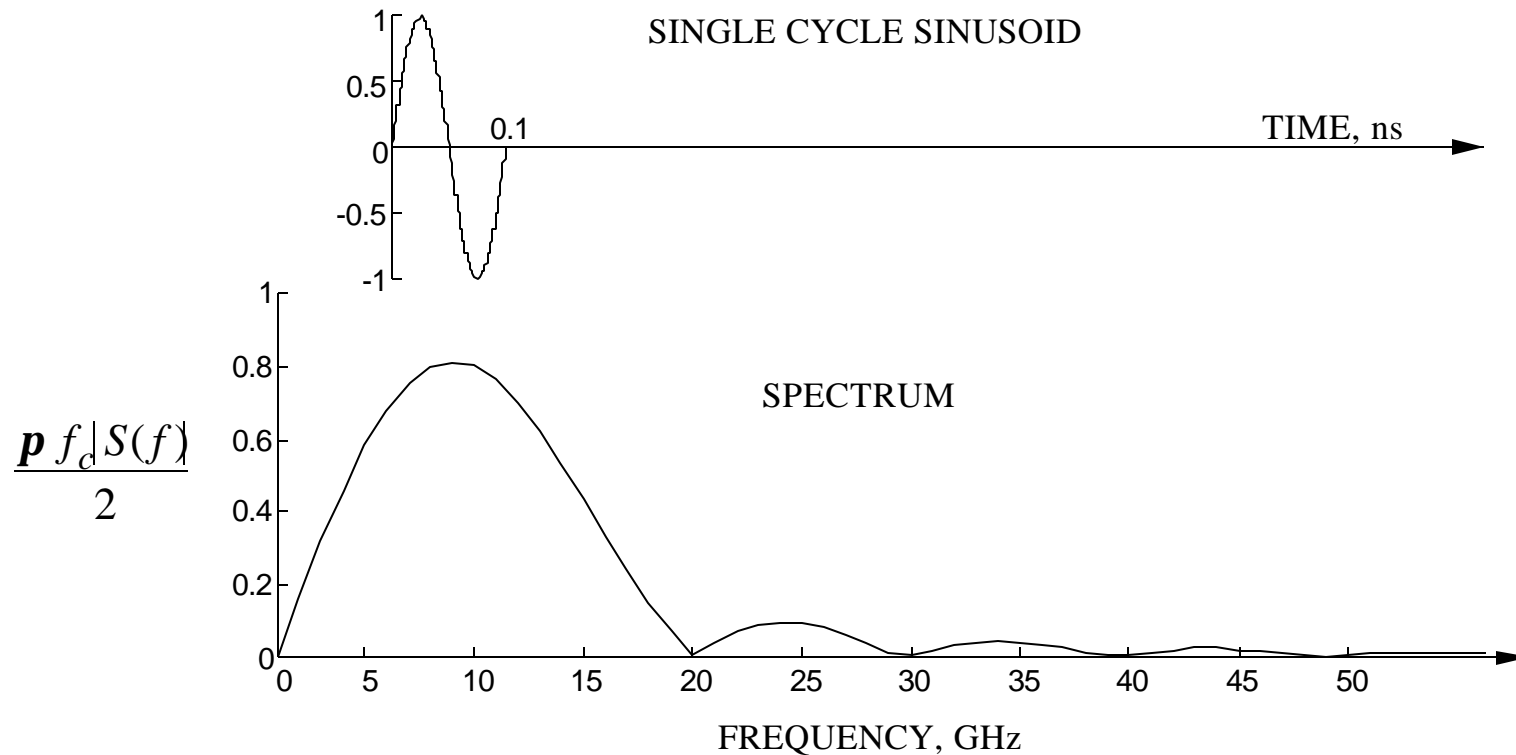
Frequency spectrum



# Ultra-Wide Band Radar (7)

UWB waveforms: single cycle sinusoid

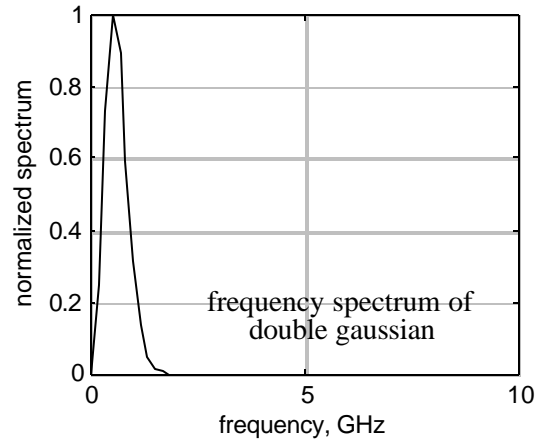
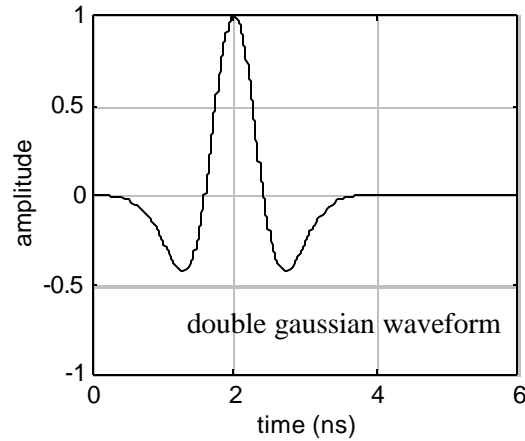
1. its frequency spectrum has no dc component and therefore it can be radiated
2. relatively convenient mathematically
3. hard to achieve with hardware



# Ultra-Wide Band Radar (8)

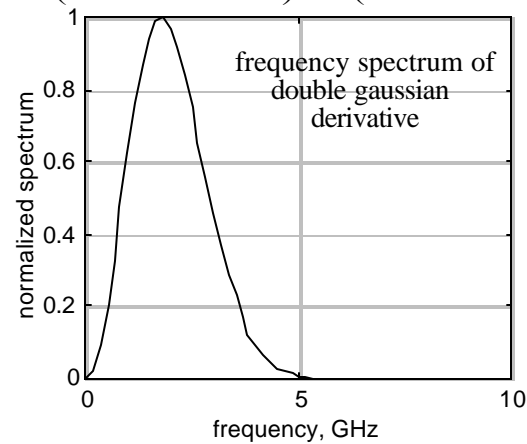
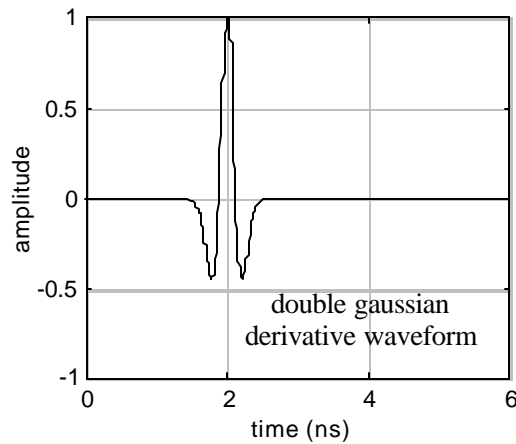
Double gaussian:

$$s(t) = A_1 e^{-a_1(t-t_o)^2} - A_2 e^{-a_2(t-t_o)^2}$$



Double gaussian derivative:

$$s(t) = \left( 1 - \frac{4p}{t_m} (t - t_o)^2 \right) \exp\left( -\frac{2p}{t_m} (t - t_o)^2 \right)$$



# RCS Considerations

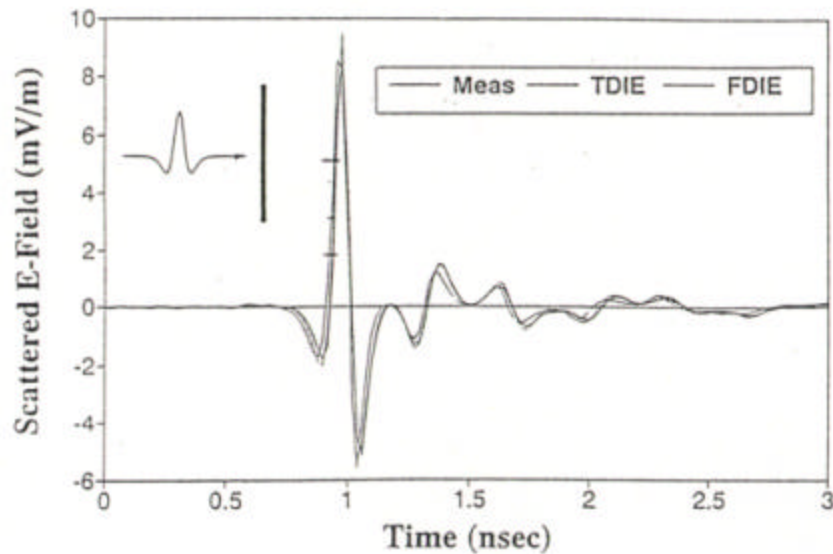
---

- Target illumination and matched filtering:
  - For very short pulses the entire target may not be illuminated simultaneously. Therefore the time response (shape) depends on angle.
  - The time response differs with each target. The basis of matched filter design no longer holds.
- Target resonances:
  - Resonances are a characteristic of conducting structures
  - Standing waves are set up on the structure when its dimension is approximately an integer multiple of a half wavelength
  - The standing waves result in enhanced RCS relative to that at non-resonant frequencies
  - In general, a target has many resonant frequencies due to its component parts (for example, aircraft: wings, fuselage, vertical tail, etc.)
  - Applications:
    1. Detection: given a specific target to be detected, use a knowledge of its resonant frequencies to take advantage of the enhanced RCS
    2. Identification (ID): when a target is detected, examine its resonant frequencies to classify it
  - Nonconducting (lossy) structures also have resonances, but the RCS enhancement is not as strong as it is for a similar conducting structure

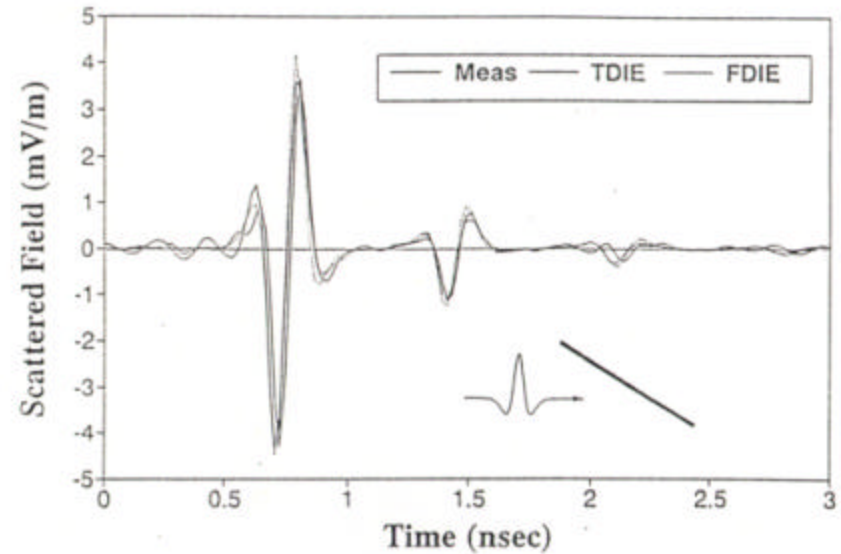
# Time Domain Scattering

- Double gaussian incident wave
- Thin wire target

Normal incidence

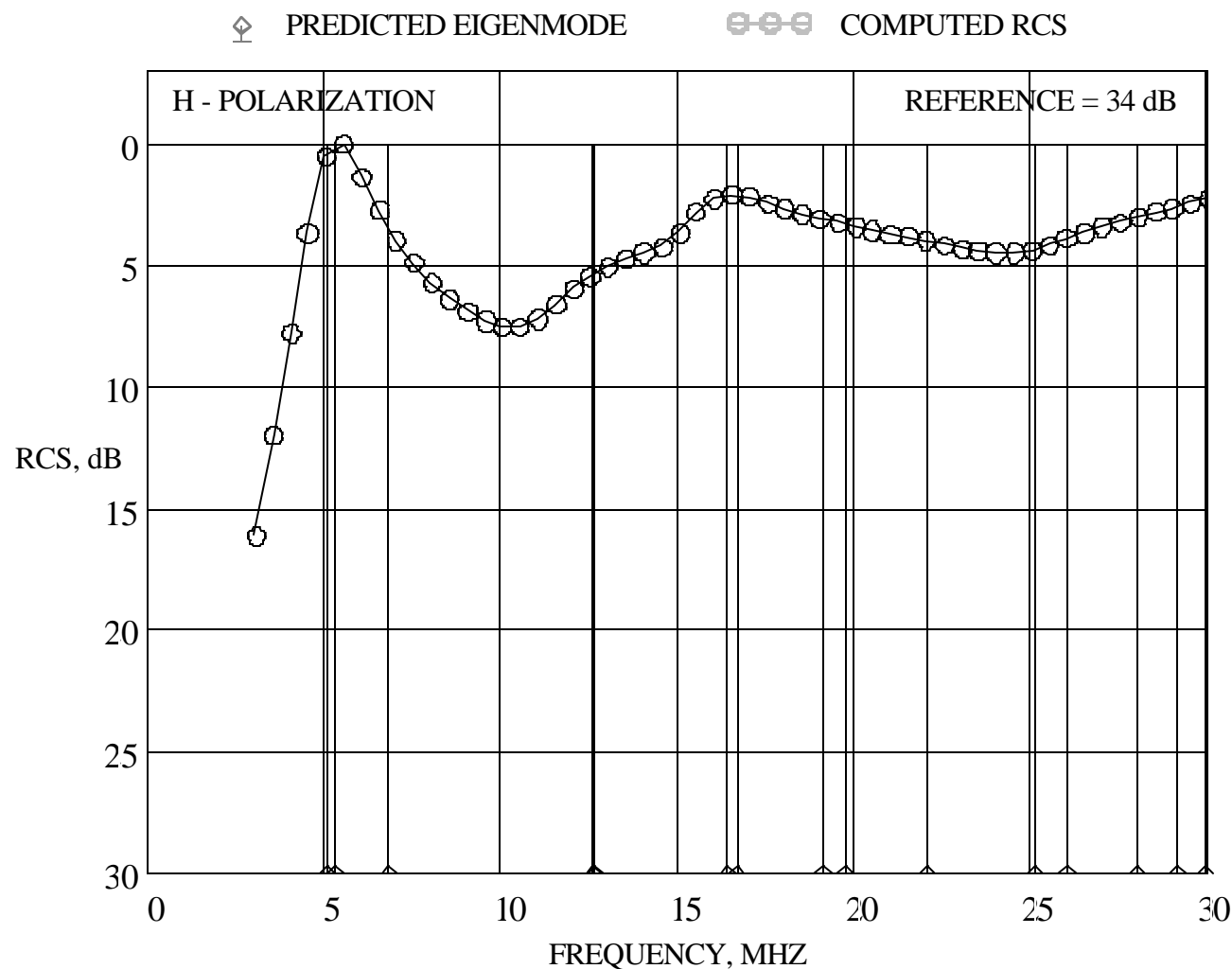


Oblique incidence (60 degrees)



(From Morgan and Walsh, IEEE AP-39, no. 8)

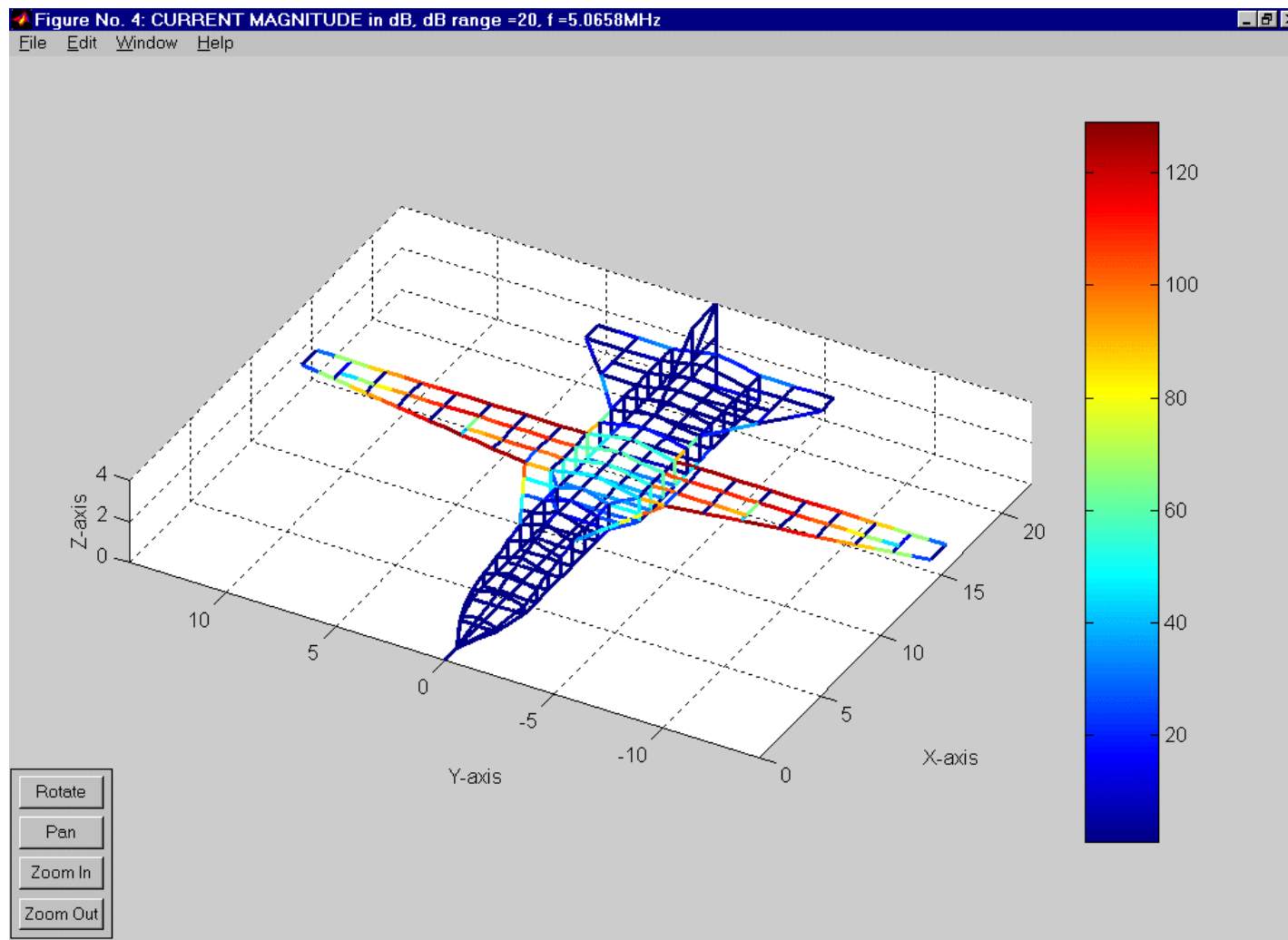
# F-111 Resonant Frequencies



(From Prof. Jovan Lebaric, Naval Postgraduate School)

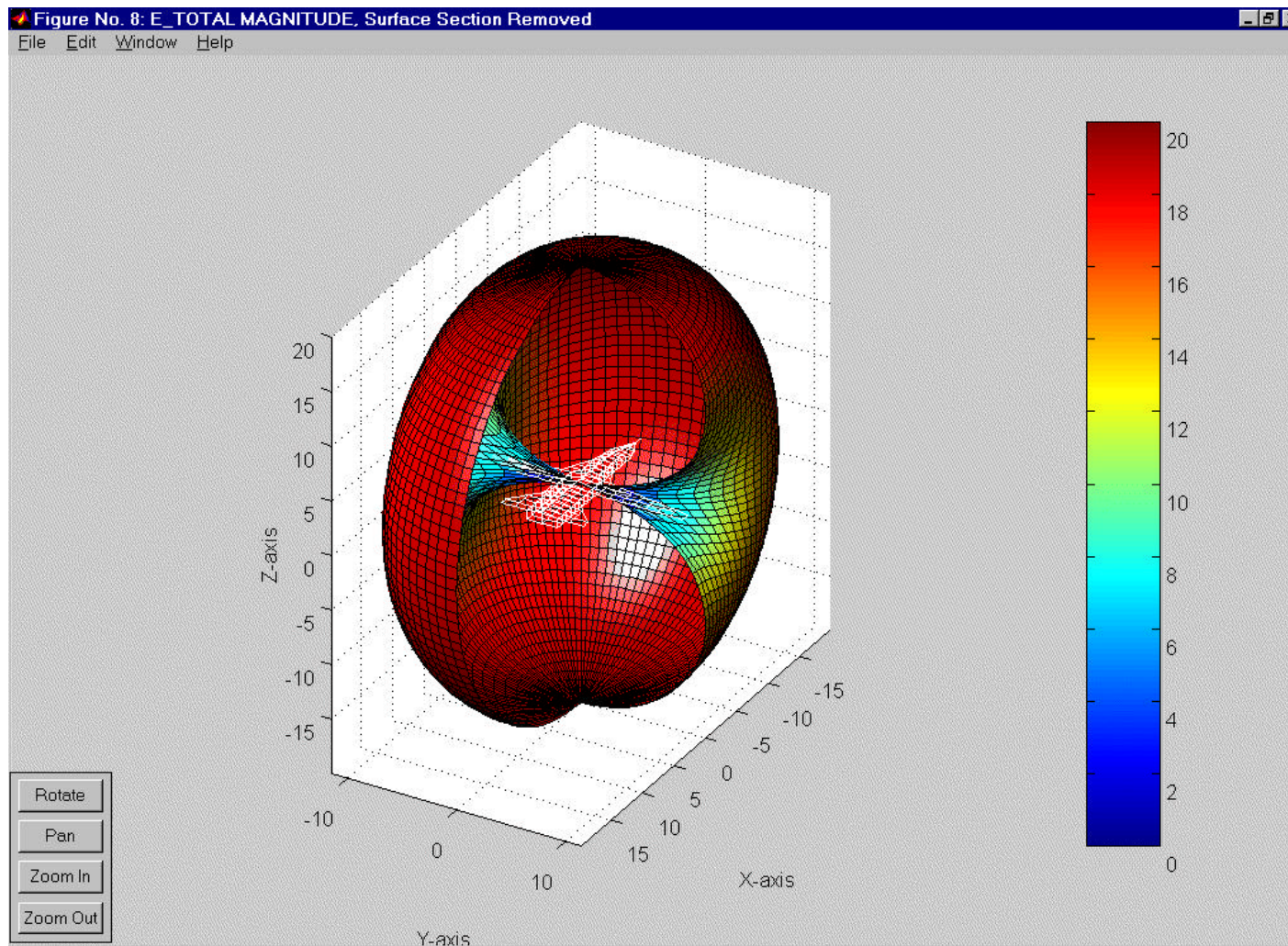


# Currents on a F-111 at its First Resonance



(From Prof. Jovan Lebaric, Naval Postgraduate School)

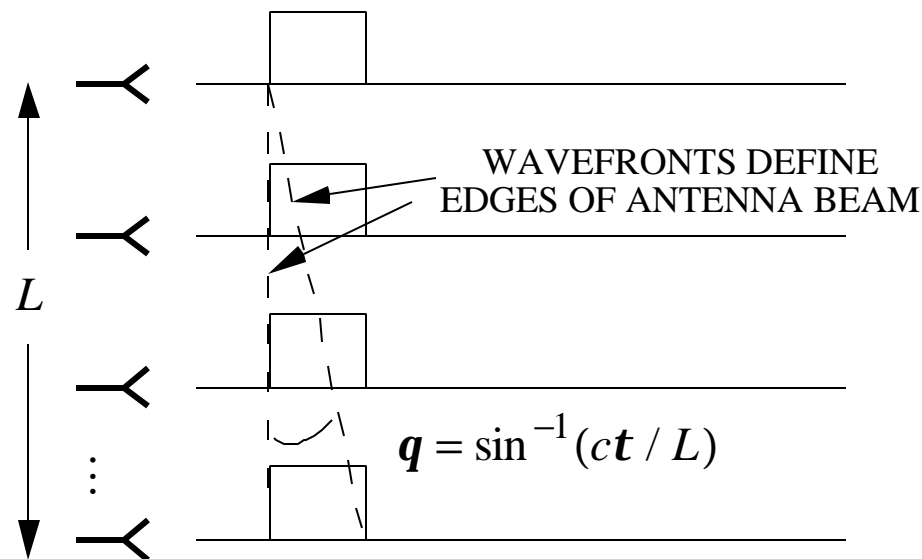
# Excitation of the First Resonance



(From Prof. Jovan Lebaric, Naval Postgraduate School)

# Antenna Considerations

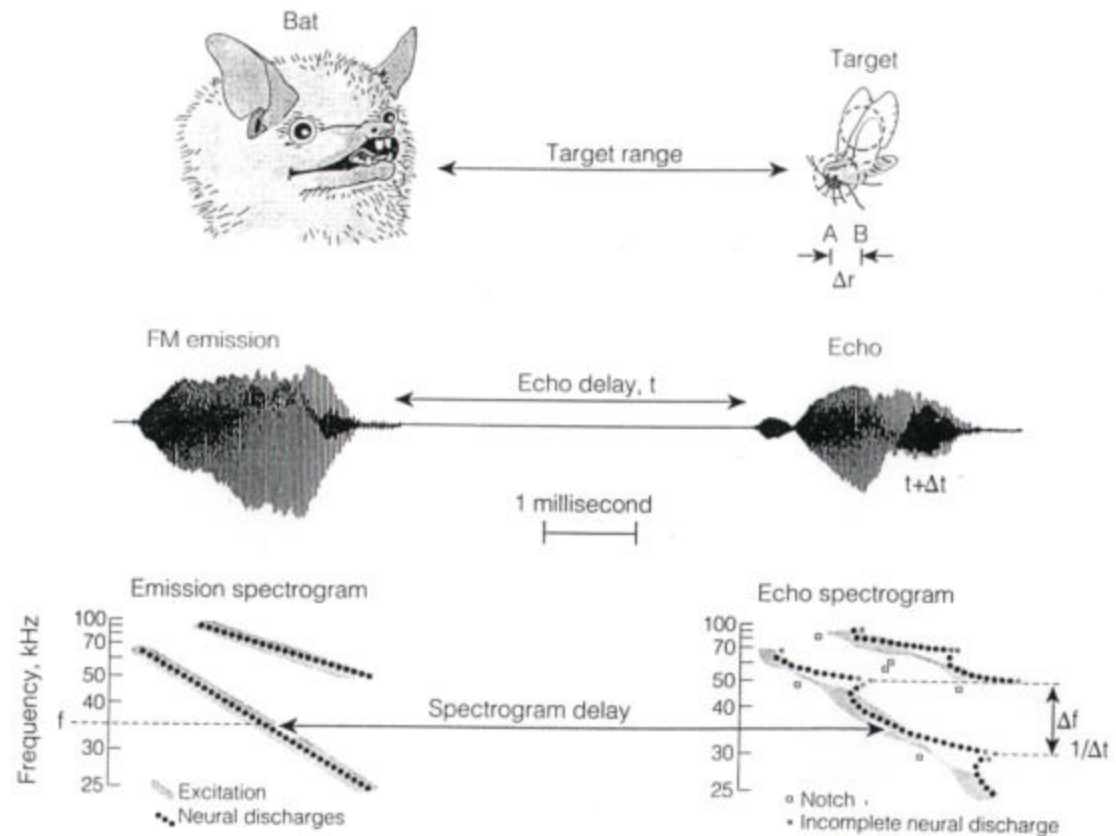
1. Referring to the UWB form of the RRE, the antenna gain aperture product  $G_t A_{er}$  should be independent of frequency. This cannot be achieved with a single antenna.
2. Low gain antennas have been used successfully. High gain antennas are not well understood.
3. Beamwidth depends on the time waveform. Example: pulse radiated from an array.



# Brown Bat Ultrasonic Radar (1)

Bats navigate and capture insects by an echo location technique that combines time and frequency domain operations. It has led to the imaging technique called spectrogram correlation and transformation (SCAT).

- Frequency range:  
15-150 kHz
- Sweeps two frequency ranges simultaneously:  
50-22 kHz  
100-44 kHz
- Linear FM waveform (chirp)
- Integration time:  
350  $\mu$ s

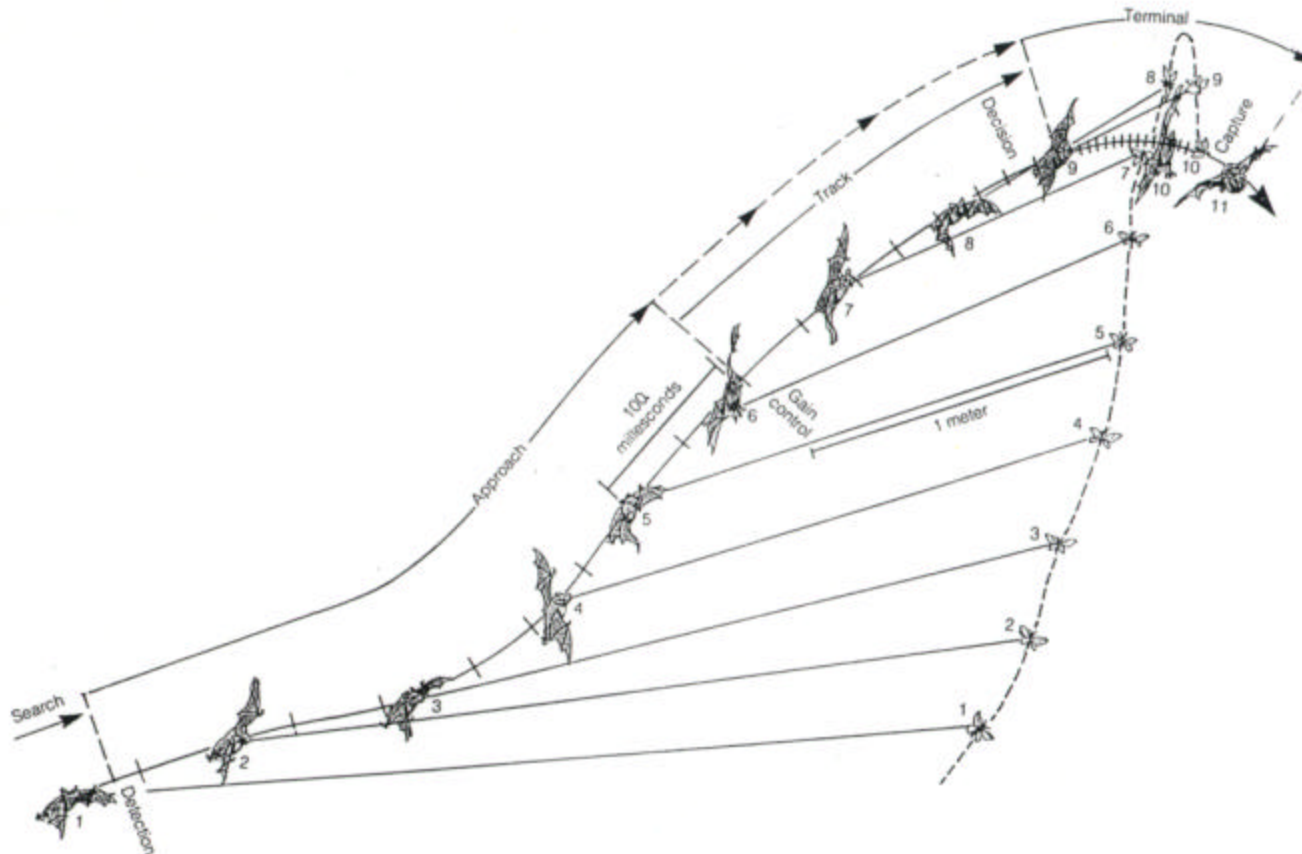


(From IEEE Spectrum, March 1992, p. 46)

# Brown Bat Ultrasonic Radar (2)

Bat pursuing prey:

- Typical target (insect) flutter rate: 10-100 Hz
- Hash marks denote positions of chirp emission



(From: *IEEE Spectrum*, March 1992, p. 46)

# Doppler Weather Radar (1)

---

The echo from weather targets (rain, snow, ice, clouds, and winds) can provide information that can be used to map precipitation and wind velocity.

Reflectivity measurements are used to estimate precipitation rates (echo power is the zeroth moment of the Doppler spectrum). Higher moments of the Doppler spectrum yield additional information:

1. Mean doppler velocity (first moment normalized to the zeroth moment)

$$\bar{v} = \frac{\int_{-\infty}^{\infty} v S(v) dv}{\int_{-\infty}^{\infty} S(v) dv}$$

gives a good approximation to the radial component of the wind.

2. Spectrum width,  $\mathbf{s}_v$  (square root of the second moment about the first moment of the normalized spectrum)

$$\mathbf{s}_v^2 = \frac{\int_{-\infty}^{\infty} (v - \bar{v})^2 S(v) dv}{\int_{-\infty}^{\infty} S(v) dv}$$

is a measure of the deviation of the velocities of particles from the average. It is an indication of turbulence and shear.

The doppler spectrum's zero and second moments can be estimated by noncoherent radars, but only coherent radars can measure the first moment.

# Doppler Weather Radar (2)

---

Radar primarily measures scattering from rain, snow and ice particles. Typical frequencies are in the L, S and C bands (1 to 8 GHz). The scattering particles are in the Rayleigh region. The RCS of an individual particle is given by

$$\mathbf{s}_i = \frac{\mathbf{p}^5}{I^4} \left| \frac{m^2 - 1}{m^2 + 2} \right|^2 D_i^6 = \frac{\mathbf{p}^5}{I^4} |K|^2 D_i^6$$

where  $m = n - jn' = \sqrt{\mathbf{e}_c}$  is the complex index of refraction ( $\mathbf{e}_c = \mathbf{e}' - j\mathbf{e}''$  is the complex dielectric constant) and  $D$  the diameter of the particle. Values of  $|K|^2$  are in the range of 0.91 to 0.93 for  $0.01 \leq I \leq 0.1$ . Define the target reflectivity  $Z$  of  $N$  particles in volume  $\Delta V$ :

$$\mathbf{s} = \sum_{i=1}^N \mathbf{s}_i \equiv \mathbf{h}(\Delta V) = \left( \frac{\mathbf{p}^5}{I^4} |K|^2 Z \right) (\Delta V) \quad \text{where} \quad Z = \frac{1}{\Delta V} \sum_{i=1}^N D_i^6$$

- Assume:
1. precipitation particles are homogeneous dielectric spheres
  2. all particles in  $\Delta V$  have the same  $|K|^2$  and  $D$
  3. the radar resolution volume  $\Delta V$  it is completely filled with particles
  4. multiple scattering is neglected

---

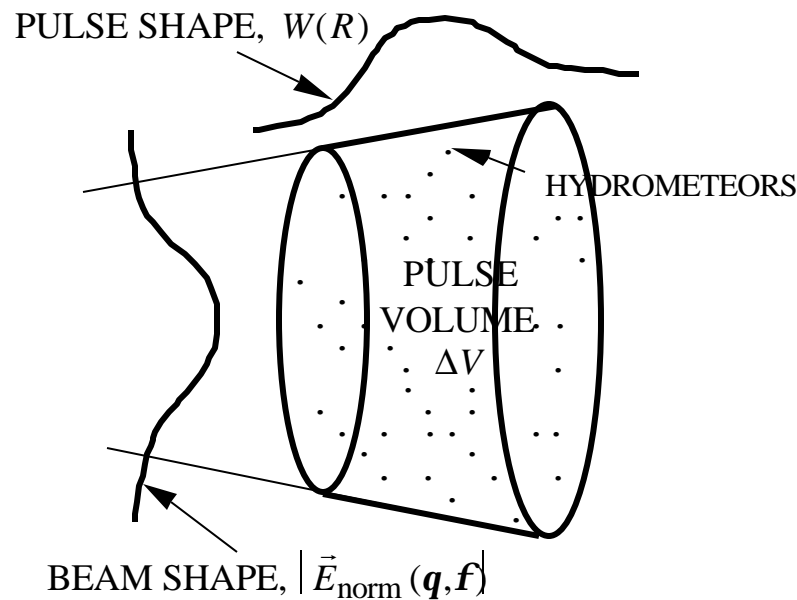
Note: Some Skolnik formulas assume a volume of  $1 \text{ m}^3$ , and therefore  $\Delta V$  (or his  $V_c$ ) does not appear explicitly in his equations.

# Doppler Weather Radar (3)

Weather radar equation for the average power received from a single particle

$$\bar{P}_r = \frac{P_t G^2 I^2 s_i}{(4\pi)^3 L_i^2 R_i^4}$$

The one-way atmospheric attenuation loss is  $1/L_i = \exp\left[-2 \int_0^{R_i} (\mathbf{a}_{\text{gas}} + \mathbf{a}_{\text{particles}}) dR\right]$



The illumination of particles within a pulse volume (resolution volume) is not uniform:

1. there are azimuth and elevation tapers due to the beam shape  $|\vec{E}_{\text{norm}}|$
2. there is a range taper due to the pulse shape and receiver frequency characteristic,  $W(R_i)$

Assume that the weight functions are a maximum at the center of the cell, range  $R_0$



# Doppler Weather Radar (4)

---

Weather radar equation becomes

$$\bar{P}_r = \frac{P_t G_o^2 I^2}{(4p)^3} \left( \sum_{i=1}^N \frac{\mathbf{s}_i |\vec{E}_{\text{norm}}|^4 W^2(R_i)}{L_i^2 R_i^4} \right)$$

Replace the summation with an integral and assume that the contributions to the integral from outside of the resolution cell are negligible

$$\bar{P}_r = \frac{P_t G_o^2 I^2 h}{(4p)^3 L_a^2 R_o^4} \underbrace{\int_0^\infty W^2(R) R_o^2 dR \int_0^p \int_0^p |\vec{E}_{\text{norm}}|^4 \sin \mathbf{q} d\mathbf{q} d\mathbf{f}}_{\Delta V}$$

where  $L_a$  is the average atmospheric loss factor at range  $R_o$ . Assume a square gaussian shaped beam of the form  $G(\mathbf{q}, \mathbf{f}) = G_o |\vec{E}_{\text{norm}}(\mathbf{q}, \mathbf{f})|^2$  where

$$|\vec{E}_{\text{norm}}(\mathbf{q}, \mathbf{f})|^2 = \exp\left\{-4\ln(2)\left(\mathbf{q}^2 / \mathbf{q}_B^2 + \mathbf{f}^2 / \mathbf{q}_B^2\right)\right\}$$

and the HPBW in both principal planes is  $\mathbf{q}_B$ . The antenna beam integral becomes

$$\int_0^p \int_0^p |\vec{E}_{\text{norm}}|^4 \sin \mathbf{q} d\mathbf{q} d\mathbf{f} = \frac{p \mathbf{q}_B^2}{8 \ln(2)}$$

# Doppler Weather Radar (5)

---

The range illumination not only depends on the pulse shape, but also the receiver frequency characteristic. In general

$$\int_0^{\infty} W^2(R_i) dR = \frac{1}{L_r} \frac{ct}{2}$$

where  $1/L_r$  is the receiver loss factor due to finite bandwidth. For a rectangular pulse and a gaussian frequency characteristic with  $B_6t \approx 1$  the loss is 2.3 dB. (In meteorological applications it is customary to use the 6 dB bandwidth of the receiver,  $B_6$ .) The radar equation becomes:

$$\bar{P}_r = \frac{P_t G_o^2 I^2 h p q_B^2}{(4p)^3 R_o^2 L_a^2 L_r 8 \ln 2} \frac{ct}{2}$$

The signal-to-noise ratio is proportional to  $\frac{ct^2}{L_r B_6 t}$ . Unlike point targets, the maximum

SNR does not necessarily occur for  $B_6t \approx 1$ . The optimum SNR consists of a matched gaussian filter and pulse that together yield the desired resolution.

---

Note: Skolnik has an additional  $p/4$  in the clutter volume for an elliptical beam cross section, as opposed to the square beam cross section that we used.

# Implementation and Interpretation of Data (1)

---

1. Spectral broadening is approximately gaussian with a variance

$$\mathbf{s}_v^2 = \mathbf{s}_s^2 + \mathbf{s}_m^2 + \mathbf{s}_d^2 + \mathbf{s}_t^2$$

where the sources are: shear,  $\mathbf{s}_s^2$   
 antenna modulation,  $\mathbf{s}_m^2$   
 different particle fall rates,  $\mathbf{s}_d^2$   
 turbulence,  $\mathbf{s}_t^2$

Large spectral widths ( $\geq 5$  m/s) are associated with turbulent gusts ( $\geq 6$  m/s).

2. Requirement for echo coherency: want large  $T_p$  for large  $R_u$  but small  $T_p$  is desired so that the returns from pulse to pulse are correlated. Typical guideline

$$\frac{l}{2T_p} \geq 2ps_v \Rightarrow \frac{cl}{4R_u} \geq 2ps_v$$

3. A single doppler radar can map the field of radial velocity. Two nearly orthogonal radars can reconstruct the two-dimensional wind field in the planes containing the radials.

# Implementation and Interpretation of Data (2)

---

4. When the assumptions about the scattering particles are not valid then an effective radar reflectivity can be used. (It is the equivalent  $Z$  for spherical water drops that would give the same echo power as the measured reflectivity.)

$$Z_e = \frac{Z I^4}{\rho^5 |K_w|^2}$$

where  $K_w$  denotes water. The units of dBZ are sometimes used

$$\text{dBZ} = 10 \log_{10} \left( \frac{Z, \text{ mm}^6 / \text{ m}^3}{1 \text{ mm}^6 / \text{ m}^3} \right)$$

Typical values:

$Z_e$	Precipitation Rate (mm/hr)	
dBZ	1	10
rain	23	39
snow	26	48

# Implementation and Interpretation of Data (3)

---

5. The echo sample voltage from  $N_s$  scatterers at time  $t_n$  is of the form

$$V(t_n) \propto \sum_{i=1}^{N_s} A_i(R_i(t_n)) \exp\{j2kR_i(t_n)\}$$

where  $A_i$  depends on  $\mathbf{s}_i$ ,  $|\vec{E}_{\text{norm}}(\mathbf{q}_i, \mathbf{f}_i)|^4$  and  $B_6 t$ . The power averaged over one cycle is

$$\bar{P}(t_n) \propto \frac{1}{2} \{VV^*\} = \frac{1}{2} \sum_{p=1}^{N_s} \sum_{q=1}^{N_s} A_p A_q^* \exp\{j2k(R_p - R_q)\}$$

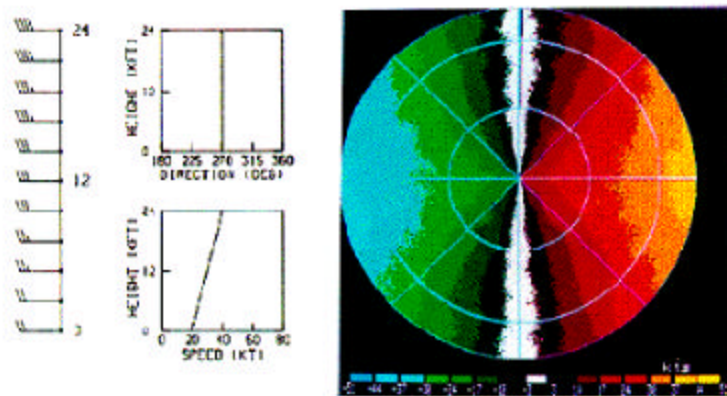
$$\bar{P}(t_n) \propto \underbrace{\frac{1}{2} \sum_{p=1}^{N_s} |A_p|^2}_{\text{INCOHERENT SCATTER}} + \underbrace{\frac{1}{2} \sum_{p=1}^{N_s} \sum_{q=1, q \neq p}^{N_s} A_p A_q^* \exp\{j2k(R_p - R_q)\}}_{\text{COHERENT SCATTER}}$$

The second term is negligible for spatially incoherent scatter, but is significant for scattering from particles that have their positions correlated. An example is Bragg scatter from spatially correlated refractivity fluctuations. Bragg scatter is usually negligible for precipitation backscatter, but not clear air echoes (Angel echoes).

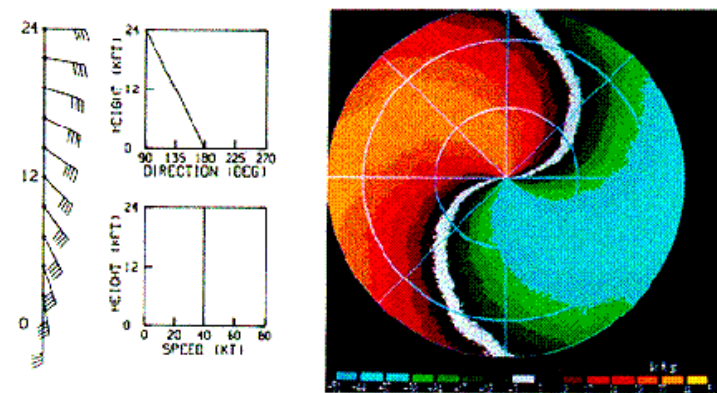
# Implementation and Interpretation of Data (4)

Sample PPI displays for wind velocity variations (from Brown & Wood)

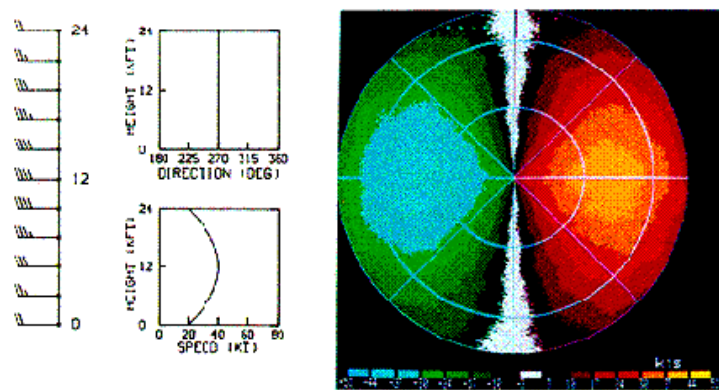
Uniform direction, linear variation with height



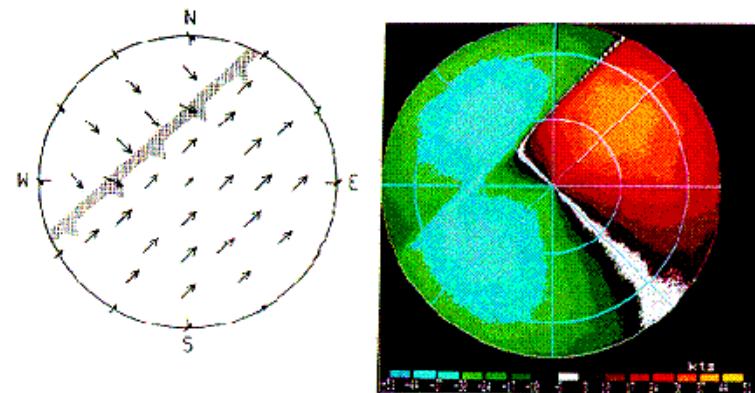
Uniform speed, linear direction change with height



Uniform direction, nonlinear variation with height



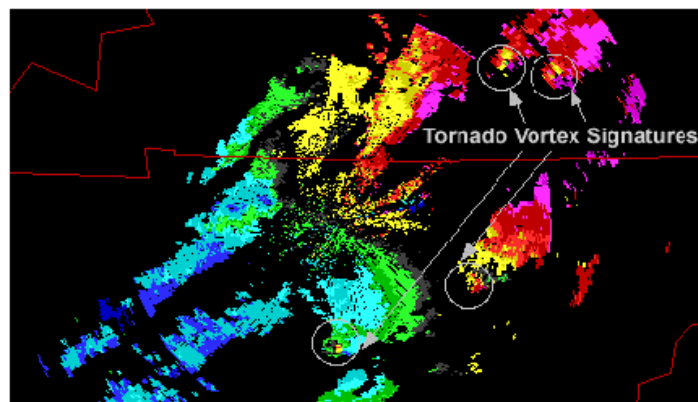
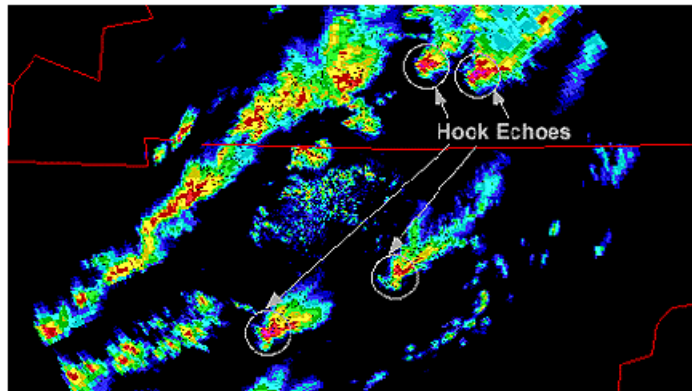
Wind shear



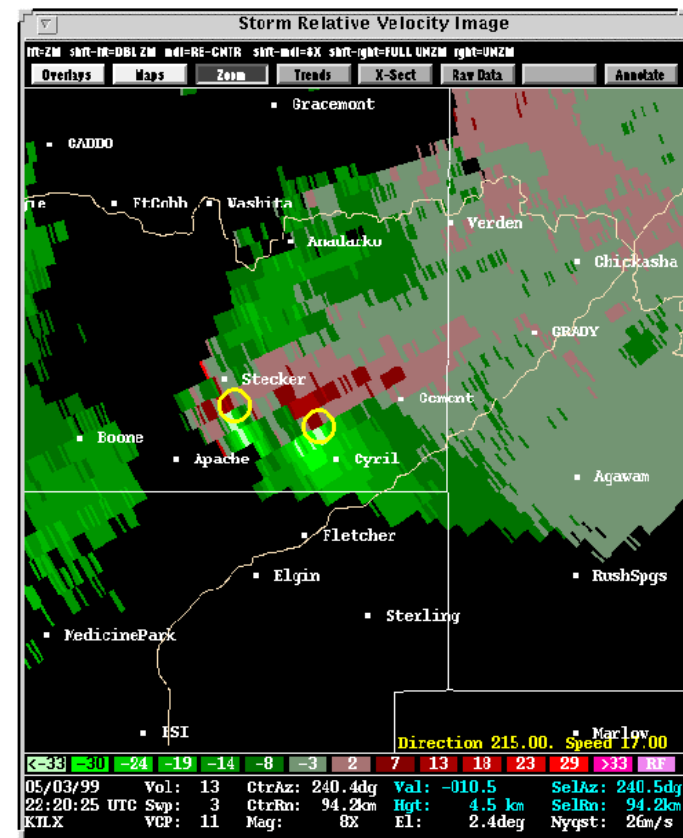
# Implementation and Interpretation of Data (5)

## Weather images (from Brown & Wood)

Tornadoes are often located at the end of hook-shaped echoes on the Southwest side of storms

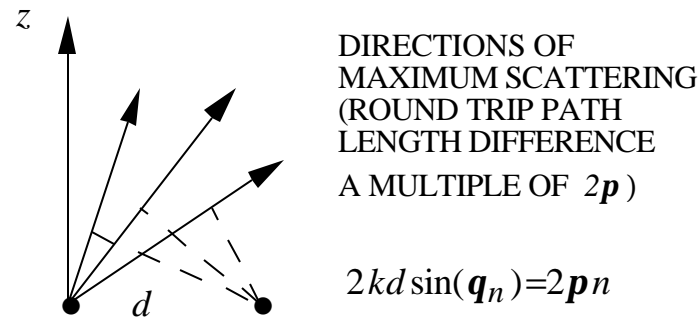


Tornado vortex signature (TVS): central pixels near the beam axis indicate exceptionally strong winds

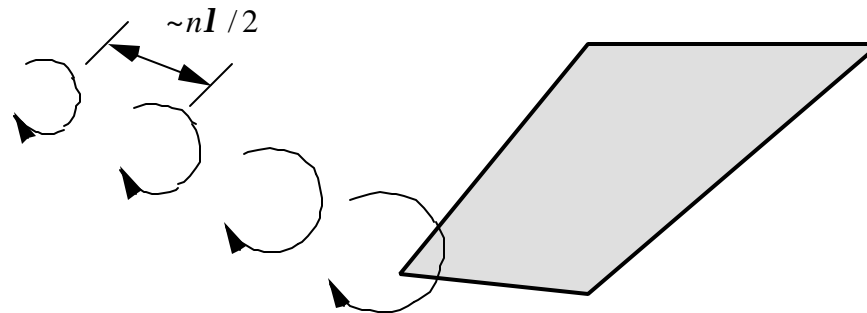


# Clear Air Echoes and Bragg Scattering

Bragg scatter occurs when the round trip path length difference between periodic scattering elements is an integer multiple of  $2p$



Periodic variations in the index of refraction occur naturally (locally periodic turbulence and waves, insect swarms, birds, etc.) Echoes from these sources are called Angel returns. Another example is wing tip vortices from an aircraft.





# Weather Radar Example

---

Radar with beamwidth of 0.02 radians tracks a 0.1 square meter target at 50 km. Find the signal to clutter ratio if  $h = 1.6 \times 10^{-8} \text{ m}^2 / \text{m}^3$  and  $t = 0.2 \text{ ns}$

Clutter return: 
$$C = \bar{P}_r = \frac{P_t G_o^2 I^2 h p q_B^2}{(4p)^3 R^2 L_a^2 L_r} \frac{ct}{8 \ln 2}$$

Target return: 
$$P_r = \frac{P_t G_o^2 I^2 s}{(4p)^3 R^4 L_a^2 L_r}$$

Assume all losses are the same for the target and clutter. Therefore, the power ratio becomes

$$SCR = \frac{P_r}{\bar{P}_r} = \frac{s_t 16 \ln 2}{q_B^2 p c t h R_o^2}$$

$$SCR = \frac{(0.1)(16) \ln 2}{p (0.02^2) (3 \times 10^8) (0.2 \times 10^{-6}) (1.6 \times 10^{-8}) 50000^2}$$

$$SCR = 0.368 = -4.3 \text{ dB}$$

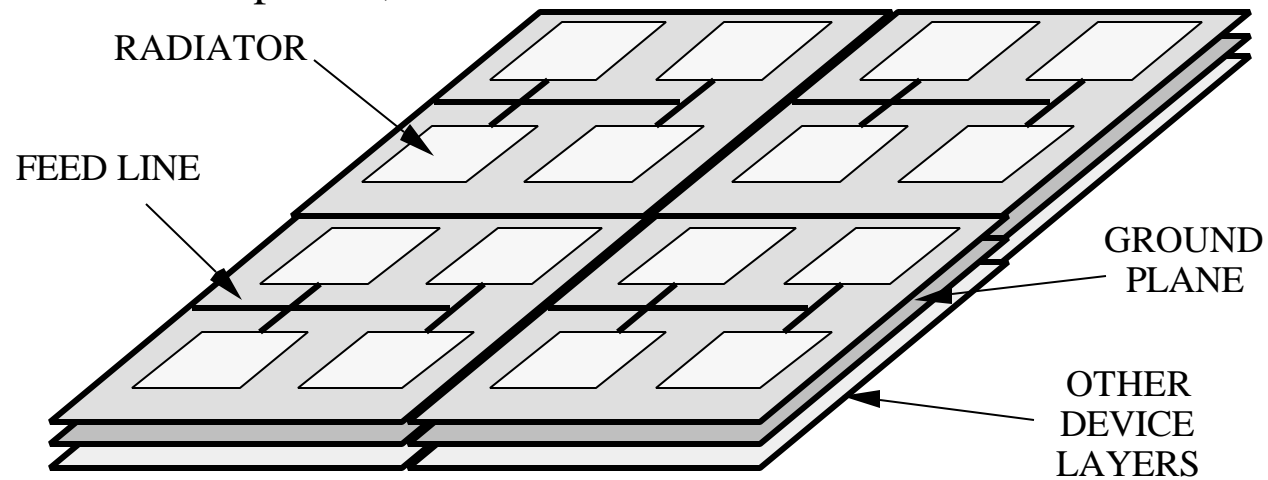
# Monolithic Microwave Integrated Circuits

---

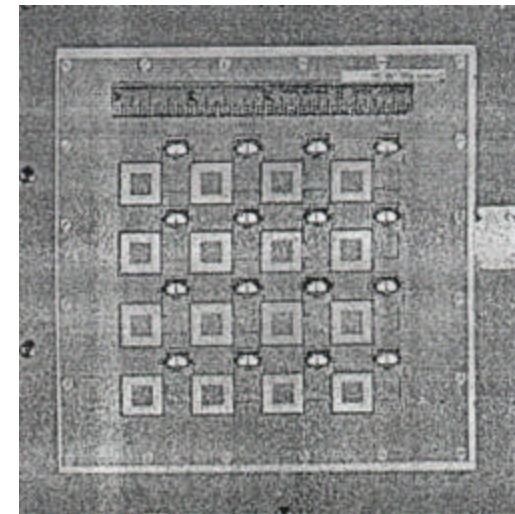
- Monolithic Microwave Integrated Circuits (MMIC): All active and passive circuit elements, components, and interconnections are formed into the bulk or onto the surface, of a semi-insulating substrate by some deposition method (epitaxy, ion implantation, sputtering, evaporation, or diffusion)
- Technology developed in late 70s and 80s is now common manufacturing technique
- Advantages:
  - ⇒ Potential low cost
  - ⇒ Improved reliability and reproducibility
  - ⇒ Compact and lightweight
  - ⇒ Broadband
  - ⇒ Design flexibility and multiple functions on a chip
- Disadvantages:
  - ⇒ Unfavorable device/chip area ratios
  - ⇒ Circuit tuning not possible
  - ⇒ Troubleshooting a problem
  - ⇒ Coupling/EMC problems
  - ⇒ Difficulty in integrating high power sources

# Tile Concept

- Low profile, conformal



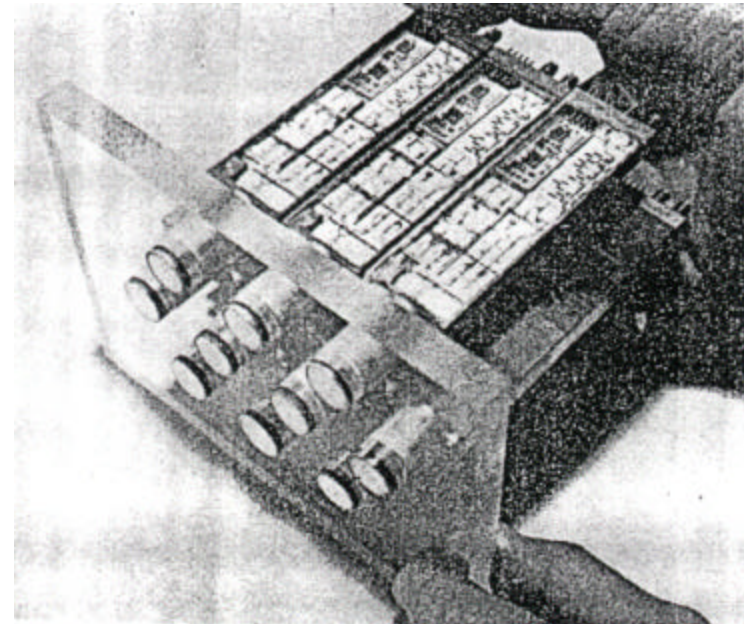
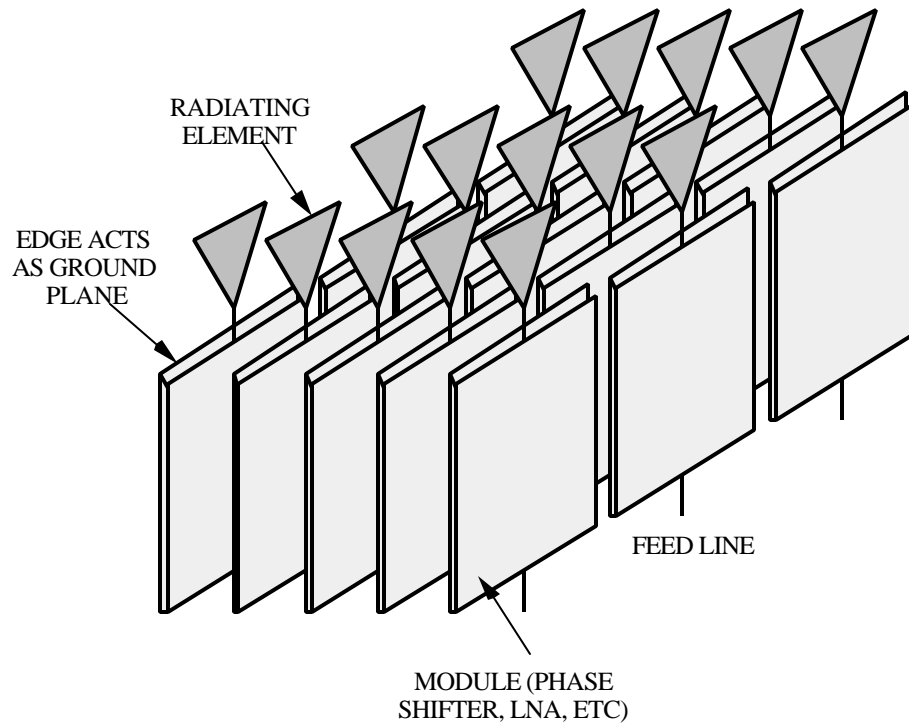
From paper by Gouker, Delisle and Duffy, IEEE Trans on MTT, vol 44, no. 11, Nov. 1996



# Module Concept

---

- Independent control of each element



From Hughes Aircraft Co.

# MMIC Single Chip Radar (1)

---

- Transmitter:

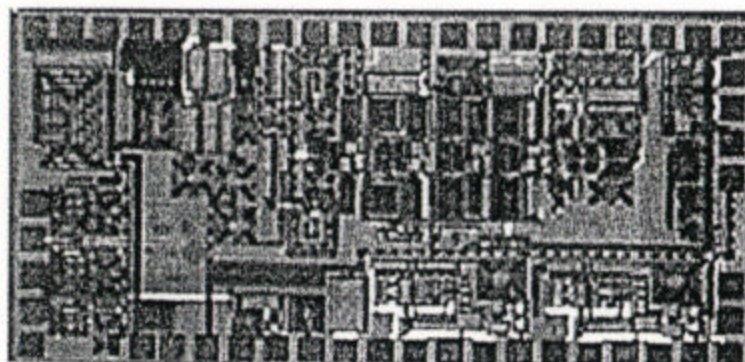
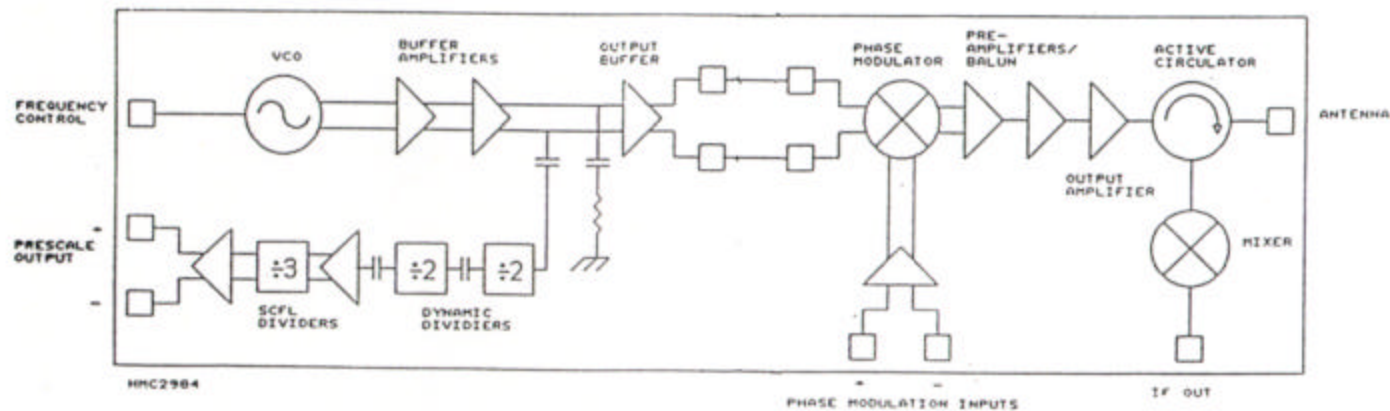
Frequency	5.136 GHz
FM mod BW	50 MHz
Output power	+17 dBm
  
- Phase modulation:

Code	BPSK
Phase Accuracy	$\pm 2^\circ$
Amp balance	$\pm 0.5$ dB
Mod rate	50 MHz
Switching speed	3 nsec
  
- Receiver:

3 dB BW	50 MHz
Noise figure	30 dB, max
  
- Power supply: 5 VDC, 400 mA
  
- Temperature range:  $-55^\circ$  to  $75^\circ$

Reference: "A MMIC Radar Chip for Use in Air-to-Air Missile Fuzing Applications," M Polman, et al, 1996 MTT International Symposium Digest, vol. 1, p. 253, 1996.

# MMIC Single Chip Radar (2)



Reference: "A MMIC Radar Chip for Use in Air-to-Air Missile Fuzing Applications," M Polman, et al, 1996 MTT International Symposium Digest, vol. 1, p. 253, 1996.

# MMIC FMCW Single Chip Radar (1)

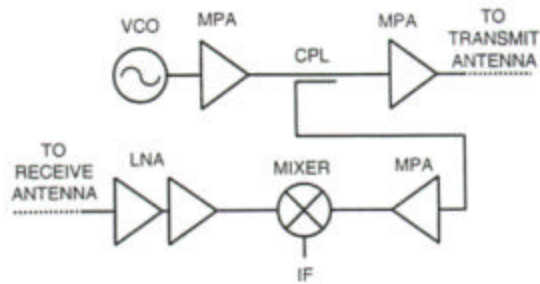
---

• Transmitter:	Frequency	94 GHz
	FM mod BW ( $\Delta f$ )	1 GHz
	Output power	5 mW
• MPA (Power amplifier):	Gain	6 dB
	1 dB compression point	7 to 8 dB
	Saturation power	12 to 13 dB
• LNA:	Gain	18 to 20 dB
	Noise figure	6 to 7 dB
• Coupler:	Coupling coefficient	10 dB
	Isolation	20 dB
	Return loss	20 dB
• Mixer:	Conversion gain	9 dB
	Noise figure	7.5 dB
	IF frequency	1.5 GHz

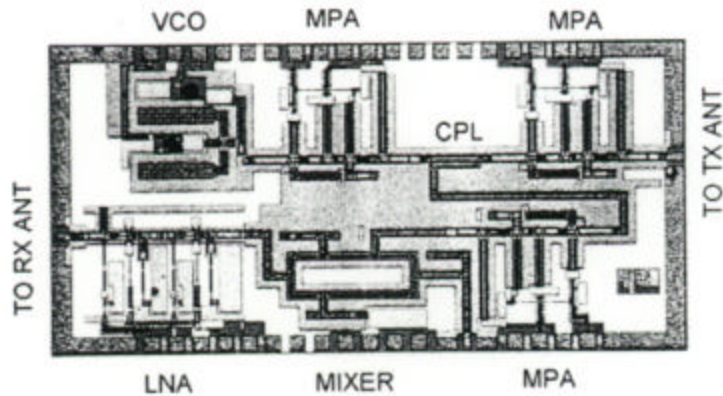
Reference: "Single Chip Coplanar 94-GHz FMCW Radar Sensors," W. Haydl, et al, IEEE Microwave and Guided Wave Letters, vol. 9, no. 2, February 1999.

# MMIC FMCW Single Chip Radar (2)

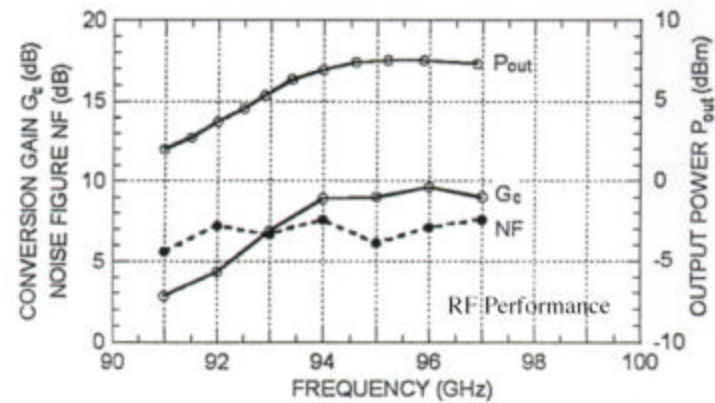
Reference: "Single Chip Coplanar 94-GHz FMCW Radar Sensors," W. Haydl, et al, IEEE Microwave and Guided Wave Letters, vol. 9, no. 2, February 1999.



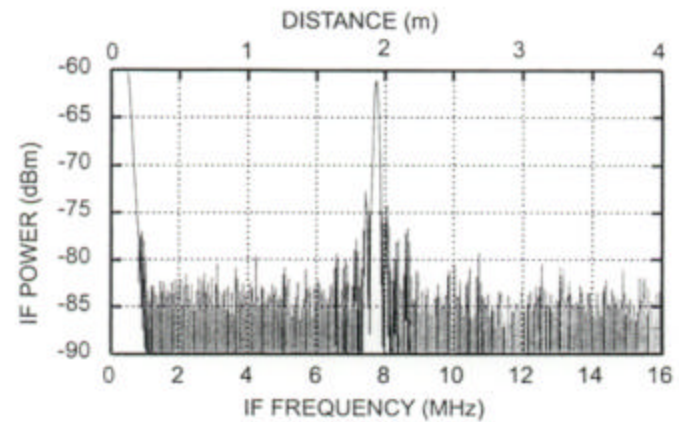
Block diagram of a 94-GHz FMCW sensor MMIC



Actual chip size is 2 by 4 square mm



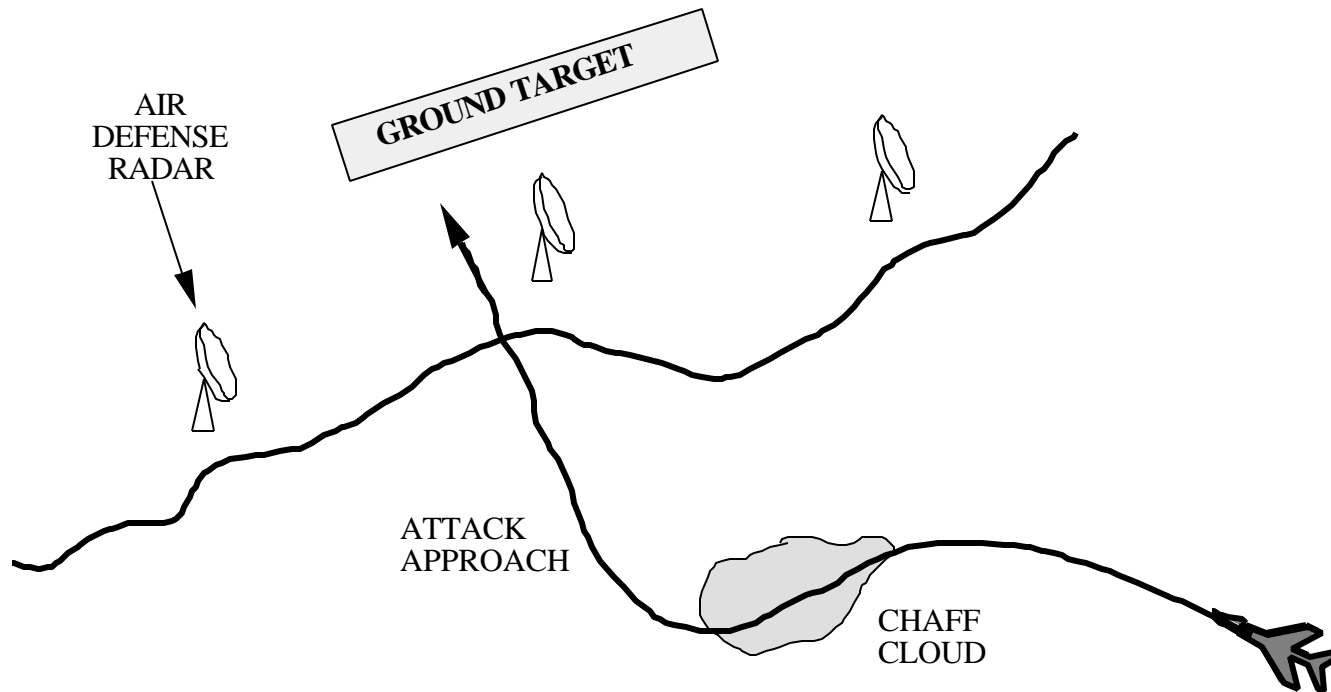
IF signal from a 1 square cm metal target at 2 m (below)





# Defeating Radar Using Chaff

---



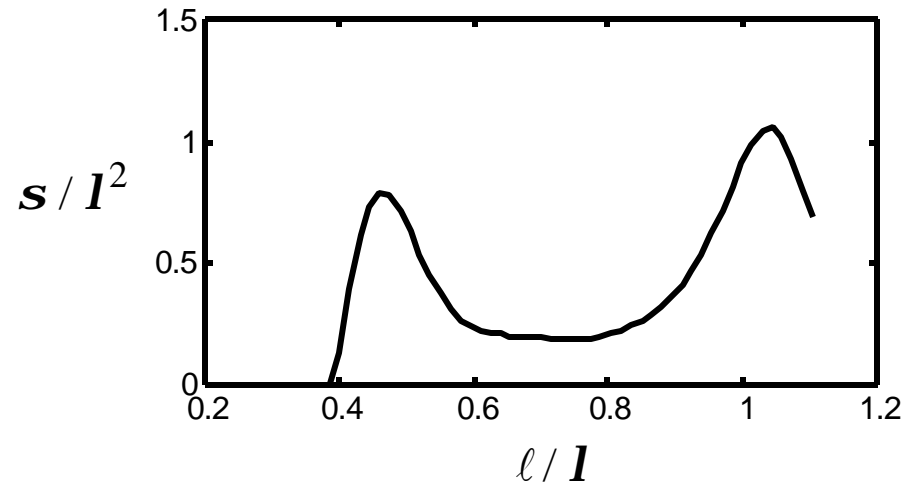
Chaff floods the radar with false targets.

The radar is aware of the intruder.

# Chaff (1)

---

Chaff is a means of clutter enhancement. Common chaff consists of thousands of thin conductive strips. For a narrowband radar the strips are usually cut to the same length; one that corresponds to a resonance. The shortest resonant length is about  $\ell = 0.45\lambda$  as shown below (the exact value depends on the dipole diameter,  $d$ ).



After the aircraft discharges the chaff, it expands to form a cloud. In the cloud, the dipoles are usually modeled as uniformly distributed (uniform density) and randomly oriented. The dipole scattering pattern, where  $\mathbf{q}$  is measured from the dipole axis, is

$$\mathbf{s}(\mathbf{q}) = \mathbf{s}_{\max} \sin^2(\mathbf{q})$$

# Chaff (2)

---

Maximum broadside backscatter for a dipole is

$$S_{\max} = \frac{p^5 \ell^6}{16l^4 (\log(2\ell/d) - 1)^2}$$

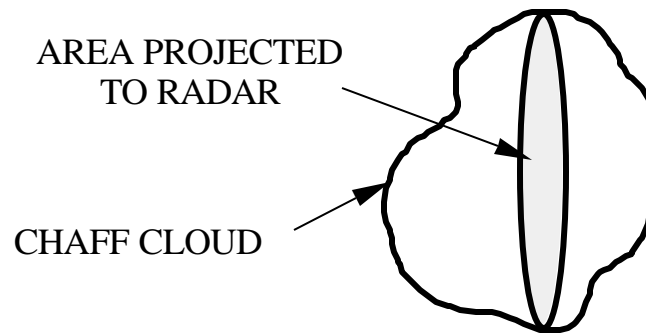
The average RCS over all angles is

$$\bar{S} = \iint \mathbf{s}(\mathbf{q}, \mathbf{f}) \sin \mathbf{q} \, d\mathbf{q} \, d\mathbf{f} = \frac{2}{3} S_{\max}$$

An approximate value good for most calculations is  $\bar{S} \approx 0.15l^2$ . For a short time after the chaff has been discharged, the RCS of the chaff cloud can be approximated by

$$S \approx A_c (1 - e^{-n\bar{S}})$$

where  $A_c$  is cross sectional area of the chaff cloud presented to the radar.



# Chaff (3)

---

The number of dipoles in the projected plane is  $n = N/A_c$ ,  $N$  being the total number of elements in the cloud. After the dipoles are widely dispersed  $n$  becomes small and

$$\bar{S}_c \approx A_c n \bar{S} = N \bar{S}$$

Example: Number of resonant dipoles required for an average cloud RCS of  $\bar{S}_c = 20$  dBsm at a frequency of 2 GHz.

The average RCS for a dipole is  $\bar{S} \approx 0.15 I^2 = 0.0034$ . Therefore the RCS of a cloud of randomly oriented dipoles (which is the case at late time) is

$$\bar{S}_c \approx N \bar{S} \Rightarrow N \approx 100 / 0.0034 = 29412$$

"Advanced" chaff designs:

1. Multiband chaff: bundles contain multiple resonant lengths
2. Absorbing chaff: resistive material absorbs rather than reflects

# Chaff and Flares

---

F-16 dispensing chaff and flares (USAF photo)



# Bistatic Radar (1)

---

Bistatic radars were among the first deployed radars. The German Klein Heidelberg radar of WW II used the British Chain Home radar as a transmitter. Receivers were located in Denmark and the Netherlands. It was capable of detecting a B-17 at 280 miles. Bistatic gave way to monostatic because of several factors:

- excessive complexity
- high costs and other solutions competing for \$
- degraded performance relative to a monostatic radar
  - reduced range and angles
  - limited engagement capability
  - degraded range and doppler resolution
- limited data and field tests
- threats insignificant
- monostatic mindset

Unique aspects and challenges of bistatic radar include:

- difficulty in measuring range
- efficient search and dealing with “pulse chasing”
- synchronization of the transmitter and receiver
- a significant advantage against stealth targets: forward scattering

# Bistatic Radar (2)

Hitchhiker radars systems do not have their own transmitters, but use “transmitters of opportunity” which include

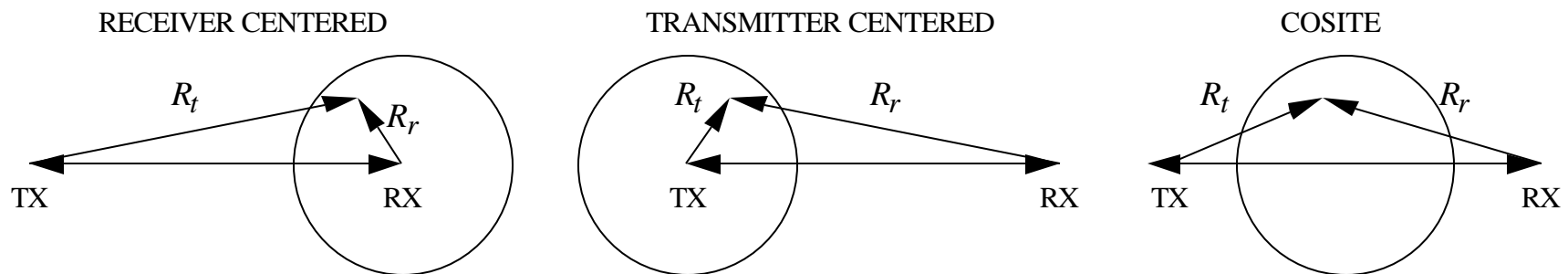
- other radars (military or civilian)
- commercial transmitters (television stations, etc.)
- may be cooperative or non-cooperative

Echoes from targets are received and processed by the hitchhiker radar

- limited ranges and engagement
- degraded performance, especially for non-cooperative transmitters

Special cases:

- $R_t \gg R_r$ : receiver centered (standoff TX with RX on penetrating aircraft)
- $R_r \gg R_t$ : transmitter centered (missile launch alert)
- cosite (trip-wire fences; satellite tracking from ground sites)



# FLIGHT-TRACKING FIRM TAKES OFF

BY MATTHEW L. WALD  
New York Times

BOHEMIA, N.Y.

**T**HE FIERY ending of TWA Flight 800 cast a harsh light into various corners of the aviation business. But some key data for investigating the disaster came from a tiny industry niche in Bohemia that the National Transportation Safety Board never knew existed.

The morning after the July 17 disaster, John R. Keller called directory assistance and asked for the New York City headquarters of the FBI. "I have a radar map of the accident," Keller told the agent who answered the phone.

Keller is executive vice president of Megadata Corp., which was able to provide air-traffic records more quickly and completely than the Federal Aviation Administration of the seconds before and after the Paris-bound Boeing 747 disappeared from radar screens.

**T**HE DATA helped investigators determine which other aircraft in the vicinity had the clearest eyewitness view of the disaster and its immediate aftermath.

Tiny Megadata's role in the investigation highlights a chink in air-to-ground communications that is not widely recognized by the public but is apparent enough to some airline and airport officials, and the company has been able to make a business of plugging the gap.

Clients include United Airlines, which uses Megadata's technology to coordinate ground crews in five cities during the last few minutes of incoming flights — a period when the FAA limits communications with planes to essential conversations with cockpit and controllers.

Other Megadata customers include airports — including San Francisco International — whose managers need to know which planes were where and

when it disputes arise over noise-abatement violations and the like.

In essence, Megadata, based in an industrial park near Long Island MacArthur Airport, produces a \$250,000 system that eavesdrops on radio transmissions between the FAA and commercial airplanes.

Using computers and software more advanced than anything available to federal air controllers, the Megadata system massages information and converts it to an instant, real-time view of all aircraft aloft and their flight paths within a 150-mile radius. The setup maintains a database of this information and is able to instantly reproduce air-traffic records that might take the FAA days or weeks to compile.

"It's a completely clandestine operation; they don't even know we're there," said George B. Litchford, an engineer who holds the system's patent.

Litchford has been licensing the technology to Megadata since 1989. Megadata is thought to be the only company in this business so far, but it is hardly a gold-mine business.

**M**EGADATA, WHOSE stock is thinly traded on the OTC Bulletin Board, has revenues of less than \$2 million a year from a range of communications products, and it lost money last year. The shares closed at 50 cents Wednesday, down 37.5 cents each, after spiking upward Tuesday on word of the company's involvement in the plane-crash investigation.

Although the National Transportation Safety Board was unaware of Megadata's existence before the crash, the FAA has known about the company but has ignored it.

Megadata's services may be useful to airlines for efficiently moving people on the ground, said Bill Jeffers, the FAA's director of air traffic. But "it doesn't have to do with the safe and efficient movement of

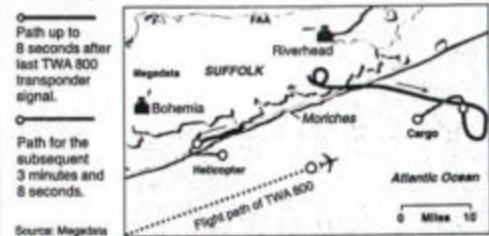
## Radar Forensics

Technology from the Megadata Corporation helps airlines fill gaps in air-to-ground communications by monitoring FAA radar and quickly reprocessing the data. Megadata's information has helped investigators determine which other aircraft were truly in a position to witness the crash of TWA Flight 800. Here is how the system works:



### What Megadata Recorded During the Crash

Megadata recorded the final path of Flight 800 and the flight paths of two military aircraft just before the disaster, and immediately afterward.



aircraft," which Jeffers said was his agency's concern.

Yet, in the case of the TWA crash, Megadata's records proved invaluable to federal officials.

After Keller's phone call, safety board investigators and FBI agents went to Megadata's office to view charts and determine what other aircraft were in position to see the final moments of Flight 800.

Eyewitness reports are considered by aviation experts to be extremely unreliable, and the Megadata information

helped establish whether the other pilots were in positions to see what they claimed to see.

Based on FAA radar scans that emanated from Riverhead, Megadata's charts indicated that two aircraft — an Army Black Hawk helicopter and an Air National Guard C-130 cargo plane — were indeed in position to have observed the fireball.

FAA radar systems of the type used in Riverhead send out pulses of energy that are reflected off metal objects in the sky, making blips on a

screen. The systems also send out electronic queries, asking the identity and altitude of planes with on-board transponders — special radios that can respond to the FAA queries by emitting electronic identification codes one one-millionth of a second later.

**S**UBTRACTING THAT microsecond and dividing by the speed of light, the FAA knows the range, or how far away the plane is. By keeping track of precisely where the circular-scan radar beam is pointed when it asks the question, the FAA knows the direction, or bearing, of the aircraft.

Megadata's system simply eavesdrops. The main components are a receive-only antenna, about 5 feet high, which can be miles from the nearest airport, and a work station to process the data.

United Airlines has become Megadata's largest client, using the systems in Chicago, Denver, San Francisco, Los Angeles and at Dulles International Airport, near Washington, D.C.

Airport managers use Megadata's information mostly to enforce noise-abatement ordinances.

"We get complaints all the time," said Ron Wilson, a representative for San Francisco International Airport, which has used the Megadata system to resolve hundreds of complaints in the past few years.

**P**EOPLE SAY: 'I saw a 747 come over my house at 500 feet. I know it was 500 feet because I could see the pilots. I could read the numbers. I could see the wheels.'

Using the Megadata work station, Wilson said, airport officials could enter the location and the time to quickly determine the facts. "We can tell them, it wasn't 500 feet — it was 3,500 feet."



# Bistatic Radar (3)

---

## “Rabbit Ear” Radar

Once upon a time people had rabbit ear antennas on their televisions. Over a relatively wide area around airports, e.g., LAX or SFO, almost every aircraft takeoff caused interference with the TV. This is the same situation as a bistatic hitchhiker radar:

- transmitter is the local TV station
- receiver is your TV set

The picture flutter and snow are due mainly to a mix of forward scattering and direct path signals

## Bistatic Alert and Cueing (BAC)

- for passive situational awareness (PSA)
- standoff aircraft such as an AWACS is used as an transmitter /illuminator
- multiple dispersed receivers are used
- important issues include bistatic clutter, ECM and cost

## Multistatic Radar

- two or more receivers with common or overlapping spatial coverage
- data is combined at a common location
- usually noncoherent (example: Space Surveillance System)
- when combined coherently, the radar net is equivalent to a large baseline array

# Bistatic Radar (4)

Bistatic radar range equation:

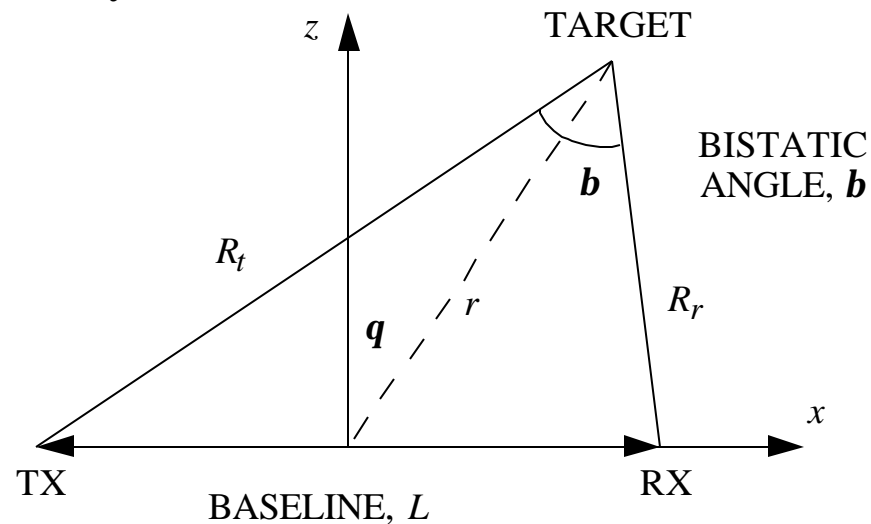
$$(R_r R_t)_{\max} = \left[ \frac{P_t G_t G_r I^2 S_B F_t^2 F_r^2 G_p}{(4\rho)^3 k T_s B_n (S/N)_{\min} L_t L_r} \right]^{\frac{1}{2}}$$

$S_B$  = bistatic RCS

$F_t, F_r$  = transmit and receive path gain factors

$L_t, L_r$  = transmit and receive losses

Radar and target geometry:



# Bistatic Radar Example

---

Example: A buoy is dropped in the center of a 1 km wide channel to detect passing ships. A 1 W transmitter on the buoy operates at 1 GHz with a 0 dBi antenna. The receiver is located on an aircraft flying directly overhead. The receiver MDS is  $-130$  dBW and the antenna on the aircraft has a 20 dBi gain.

(a) What is the maximum range of the receive aircraft if the ship RCS is 30 dB? Neglect losses and multipath.

Assume that the ship is as far from the buoy as possible and that the receive antenna beam is pointed directly at the ship

$$P_r = \frac{P_t G_t G_r I^2 s_B}{(4\pi)^3 R_r^2 R_t^2} = \frac{(1)(100)(1)(1000)(0.3^2)}{(4\pi)^3 (10^3)^2 R_r^2} = 10^{-13} \Rightarrow R_r = 6735 \text{ m}$$

(b) If the aircraft had a monostatic radar, what would be the required transmitter power?

$$P_r = \frac{P_t G^2 I^2 s}{(4\pi)^3 R^4} = 10^{-13} \Rightarrow P_t = 0.45 \text{ W}$$

The increase in transmitter antenna gain in the monostatic case more than makes up for the monostatic  $R^4$  factor.

# Bistatic Radar (5)

---

Define the bistatic radar parameter,  $K$ , and the bistatic maximum range product,  $\mathbf{k}$ :

$$(R_r R_t)_{\max}^2 = \mathbf{k}^2 = \frac{K}{(S/N)_{\min}} \quad \text{where} \quad K = \frac{P_t G_t G_r I^2 S_B F_t^2 F_r^2 G_p}{(4\mathbf{p})^3 k T_s B_n L_t L_r}$$

Constant SNR contours in polar coordinates are Ovals of Cassini

$$(R_r R_t)^2 = (r^2 + L^2/4)^2 - r^2 L^2 \cos^2 \mathbf{q}$$

$$S/N = \frac{K}{(r^2 + L^2/4)^2 - r^2 L^2 \cos^2 \mathbf{q}}$$

Operating regions:

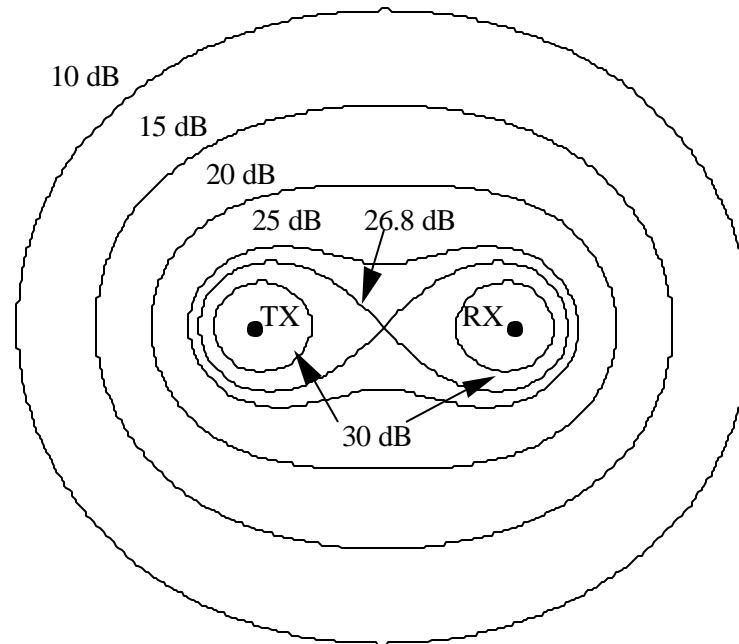
- $L > 2\sqrt{\mathbf{k}}$ , two separate ellipses enclosing the transmitter and receiver
- $L < 2\sqrt{\mathbf{k}}$ , a single continuous ellipse (semimajor axis  $b$ ; semiminor axis  $a$ )

$$a = (R_t + R_r)/2 \quad b = \sqrt{a^2 - (L/2)^2} \quad e = \frac{L}{R_t + R_r} = \frac{L}{2a}$$

- $L = 2\sqrt{\mathbf{k}}$ , lemniscate with a cusp at origin

# Bistatic Radar (6)

Example: constant SNR contours for  $K = 30L^4$  (“Ovals of Cassini”)



Special cases: receiver centered ( $L > 2\sqrt{k}$ ,  $R_t \gg R_r$ ), transmitter centered ( $L > 2\sqrt{k}$ ,  $R_r \gg R_t$ ), cosite region ( $L < 2\sqrt{k}$ ). The maximum SNR occurs at  $\mathbf{b} = 0$  and has a value  $(SNR)_{\max} = K / b^4$ . The minimum SNR occurs at the maximum bistatic angle (along the baseline perpendicular) and has the value  $(SNR)_{\min} = K(1 + \cos(2 \sin^{-1}(e)))^2 / (4b^4)$ .

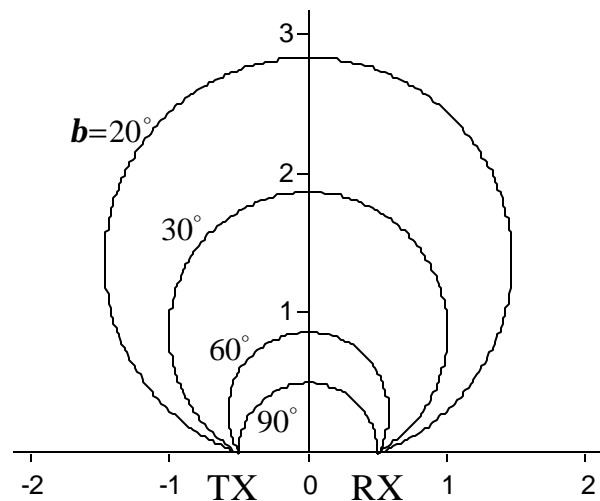
# Bistatic Radar (7)

Bistatic radar operation is often limited or constrained by the maximum or minimum bistatic angle. Contours of constant bistatic angle,  $\mathbf{b}$ , are circles of radius

$$r_{\mathbf{b}} = L / (2 \sin \mathbf{b})$$

centered on the baseline bisector at

$$d_{\mathbf{b}} = L / (2 \tan \mathbf{b})$$



The dimensions are distance normalized by baseline,  $L$

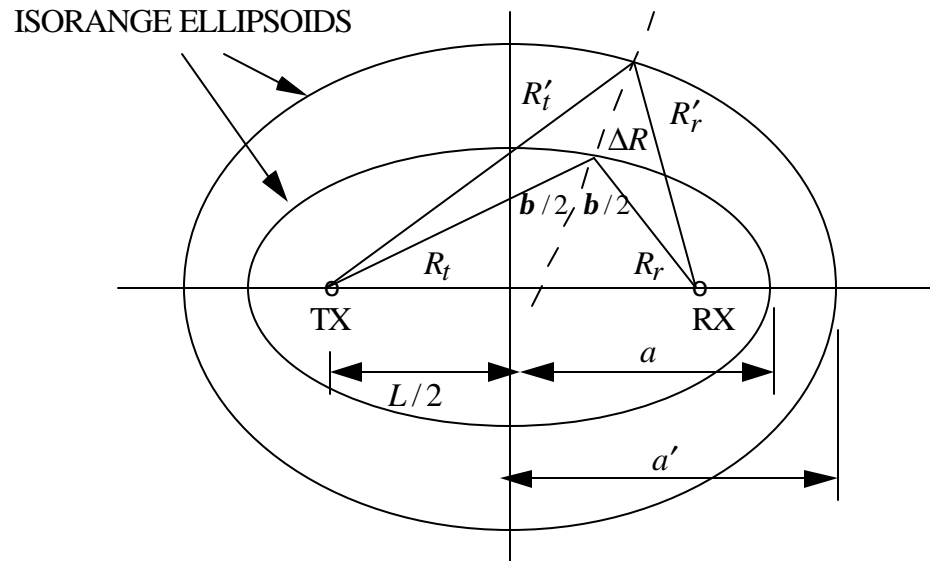
# Bistatic Radar (8)

Bistatic range cells are defined by ellipsoids  $R_t + R_r = 2a$ . The range cell size is approximately given by

$$\Delta R \approx \frac{\Delta R_{\max}}{\cos(\mathbf{b}/2)} = \frac{ct}{2 \cos(\mathbf{b}/2)}$$

The maximum error occurs along the perpendicular bisector and is given by

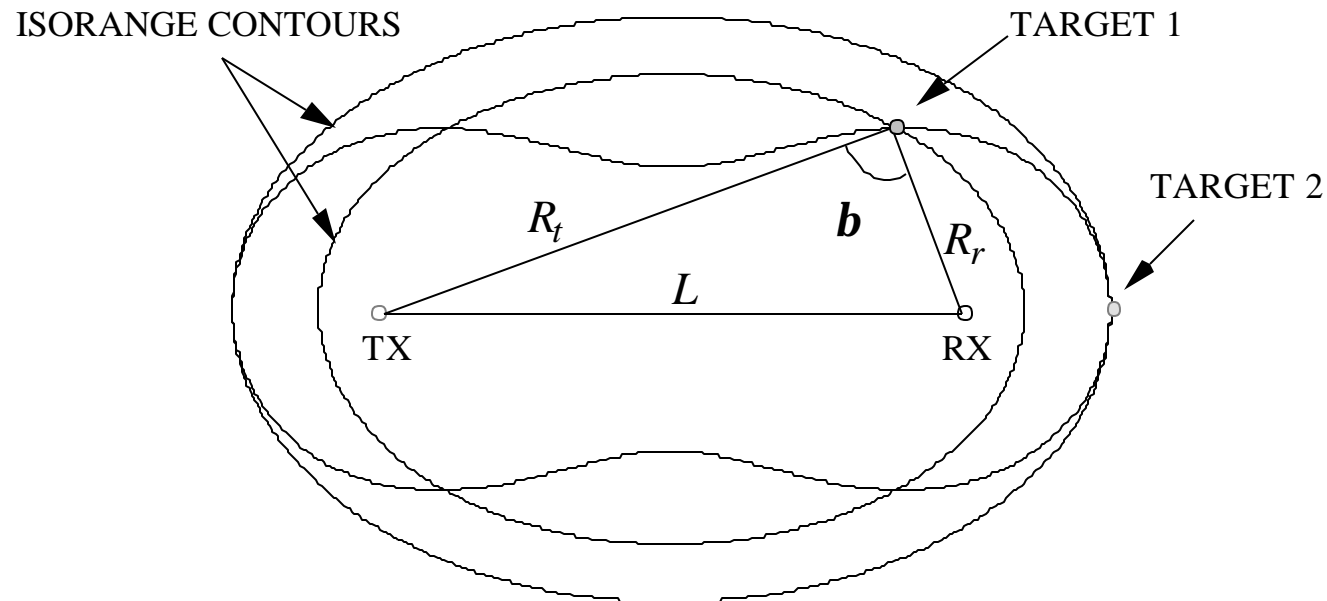
$$d_{\max} \approx \frac{a(a' - a)}{b(b' - b)} - 1 \text{ where } b = \left(a^2 - (L/2)^2\right)^{1/2} \text{ and } b' = \left((a')^2 - (L/2)^2\right)^{1/2}$$



# Bistatic Radar (9)

A family of isorange contours is associated with each Oval of Cassini (contour of constant  $(S/N)_{\min}$ ). Both equations are satisfied by the same bistatic angle,  $\mathbf{b}$ , yielding the equation

$$(R_t + R_r)_{\max} = \left[ L^2 + 2 \underbrace{(R_t R_r)_{\max}}_k (1 + \cos \mathbf{b}) \right]^{1/2}$$



The SNR is different for targets at various locations on an isorange contour.



# Bistatic Radar (10)

---

Target location can be computed if the time delay of the scattered pulse is referenced to the transmission delay directly from the transmitter

$$(R_t + R_r) = c\Delta T_L + L$$

where  $\Delta T_L$  is the time difference between reception of the echo and the direct pulse

Unambiguous range is given by  $(R_t + R_r)_u = c / f_p$  which describes an ellipse with semimajor axis of length  $c / f_p$ .

Target velocity is computed from the doppler shift, which in the bistatic case is given by

$$f_d = \frac{1}{\mathbf{I}} \left[ \frac{d}{dt} (R_t + R_r) \right] = \frac{1}{\mathbf{I}} \left[ \frac{dR_t}{dt} + \frac{dR_r}{dt} \right] = \frac{2v_t}{\mathbf{I}} \cos \mathbf{d} \cos(\mathbf{b}/2)$$

$\frac{dR_t}{dt}$  = the projection of the target velocity vector onto the transmitter-to-target LOS

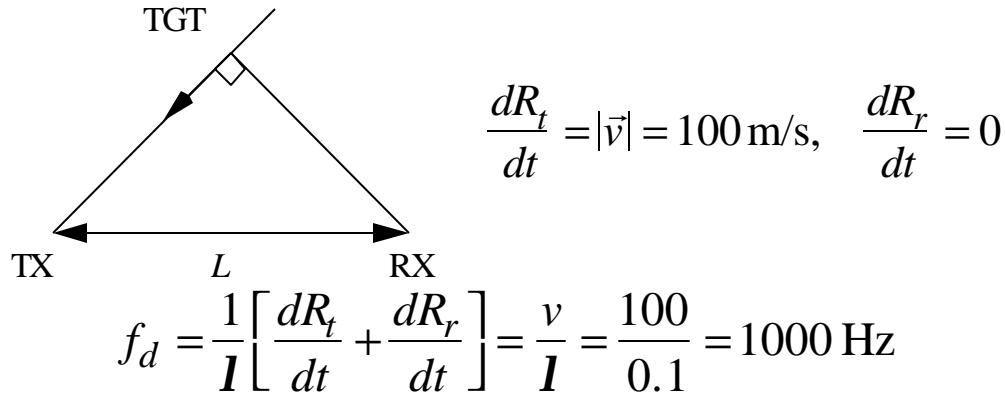
$\frac{dR_r}{dt}$  = the projection of the target velocity vector onto the receiver-to-target LOS

$v_t$  = the target velocity projected onto the bistatic plane

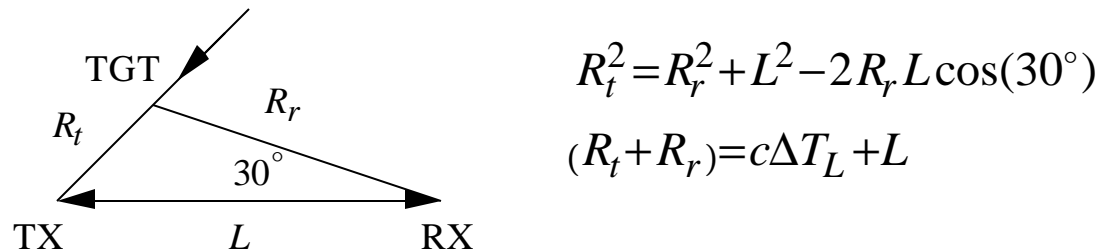
$\mathbf{d}$  = angle between target velocity vector and the bistatic angle bisector

# Bistatic Radar Example

- (a) A target is approaching the transmitter at 100 m/s. What is the doppler shift when the target location on its approach is perpendicular to the receiver line of sight?



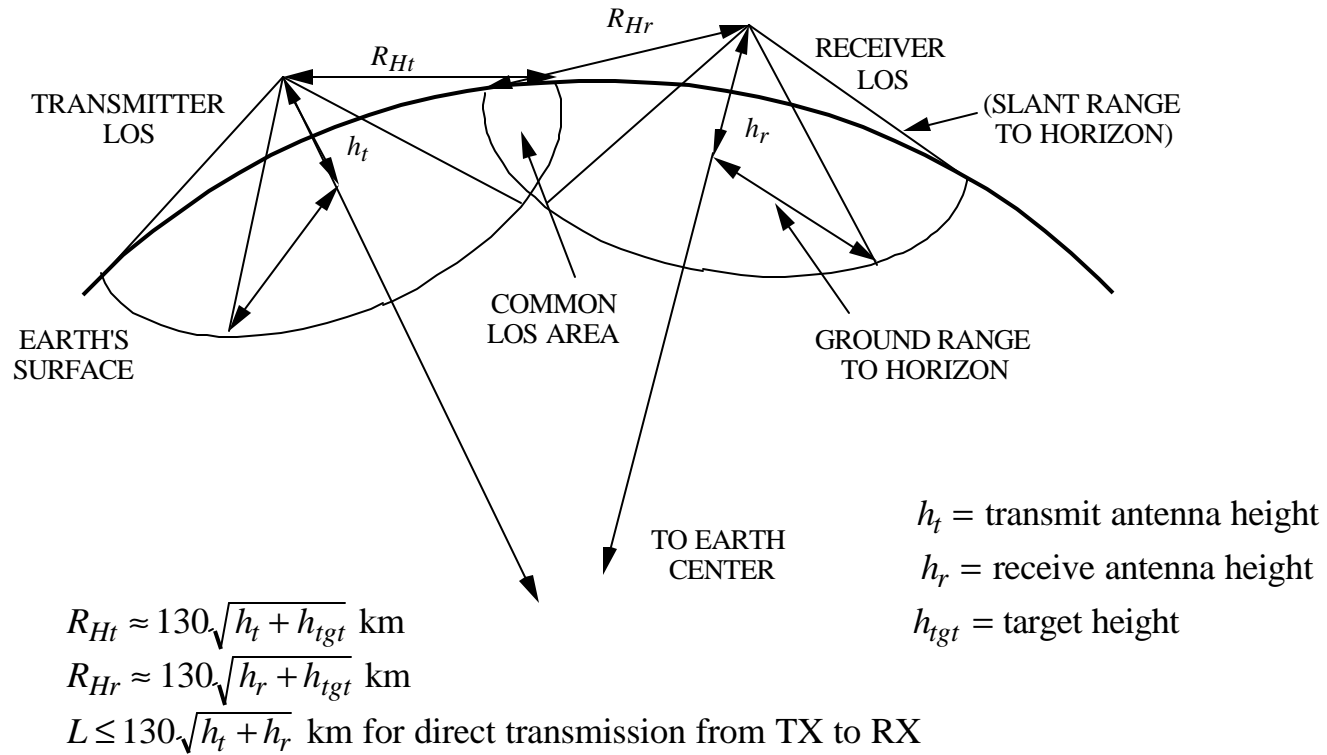
- (b) The echo from the target arrives  $\Delta T_L = 200 \text{ ns}$  after the direct transmission. The receive antenna beam is 30 degrees from the baseline. Find the target ranges to the transmitter and receiver if the baseline is 30 km.



Solve the two equations for the ranges:  $R_r = 56.23 \text{ km}$  and  $R_t = 33.76 \text{ km}$

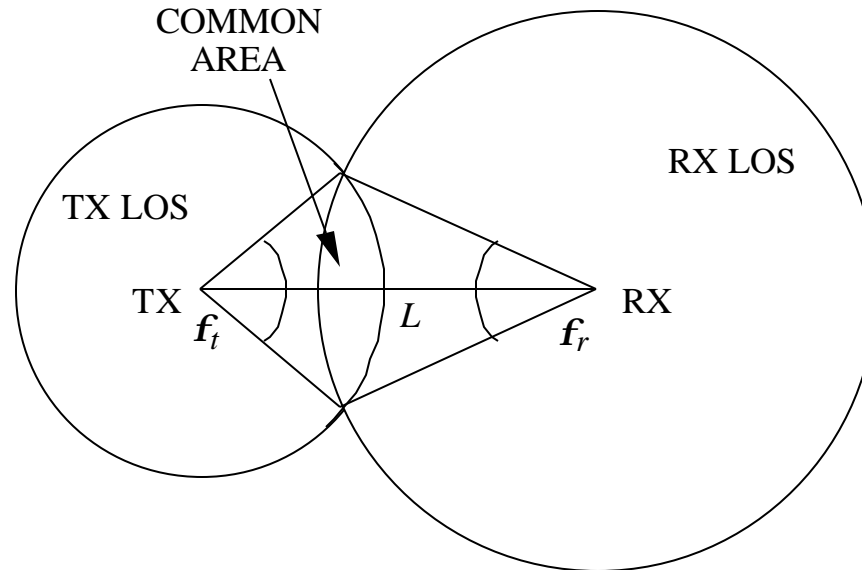
# Line-of-Sight Constrained Coverage (1)

Both the transmitter and receiver must have line of sight (LOS) to the target. Example of overlapping LOS coverage for a bistatic radar for a target height of zero:



# Line-of-Sight Constrained Coverage (2)

Top view of overlapping coverage



Common area: 
$$A_o = \frac{1}{2} [R_{Hr}^2 (f_r - \sin f_r) + R_{Ht}^2 (f_t - \sin f_t)]$$

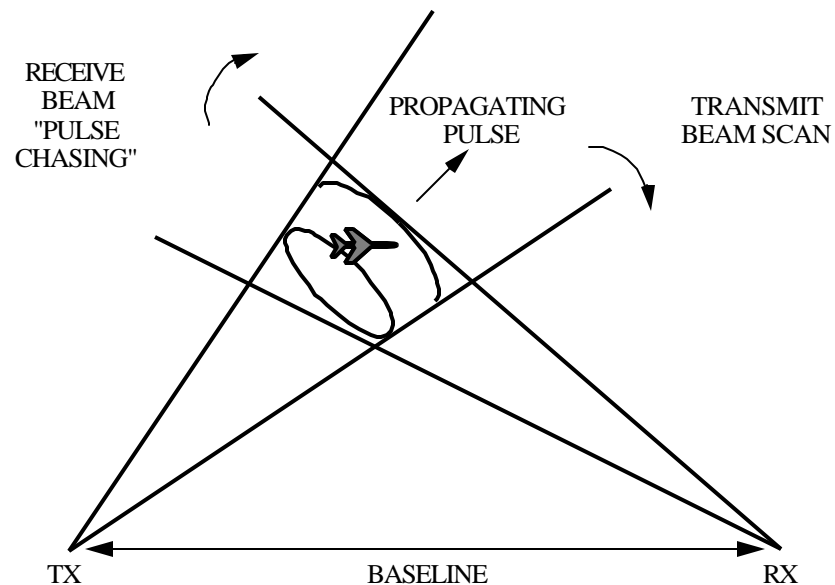
where  $f_t = 2 \cos^{-1} \left[ \frac{R_{Ht}^2 - R_{Hr}^2 + L^2}{2R_{Ht}L} \right]$  and  $f_r = 2 \cos^{-1} \left[ \frac{R_{Hr}^2 - R_{Ht}^2 + L^2}{2R_{Hr}L} \right]$ . The equation

holds for  $L + R_{Hr} \leq R_{Ht} \leq L + R_{Hr}$  or  $L + R_{Ht} \leq R_{Hr} \leq L + R_{Ht}$  (one circle does not completely overlap the other).

# Bistatic Radar (11)

Detection of a target requires that the target be in both the transmit and receive beams as the pulse illuminates the target. This is referred to as beam scan on scan, and it can be accomplished in four ways:

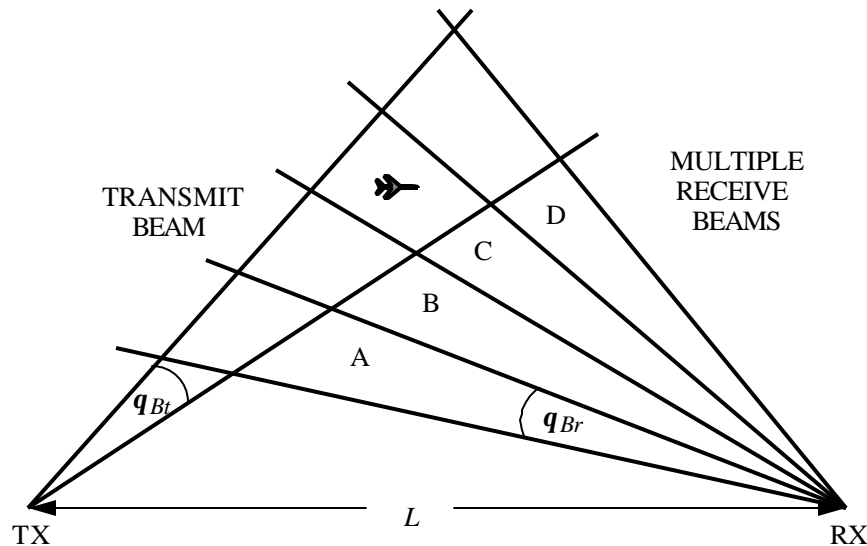
1. One high gain beam on transmit and one high gain beam on receive. This requires that the receive beam follow the pulse as it propagates through space (pulse chasing)



- Requires very fast receive beam scanning capability (implies an electronically scanned phased array)
- Time consuming for search

# Bistatic Radar (12)

2. One high gain beam on transmit and multiple high gain beams on receive.



- Complex receive array required
- Rapid search of large volumes
- Only process range cells illuminated by the transmit beam

3. Floodlight transmit ( $\Omega_{At} = \Omega_s$ ) with high gain receive beam

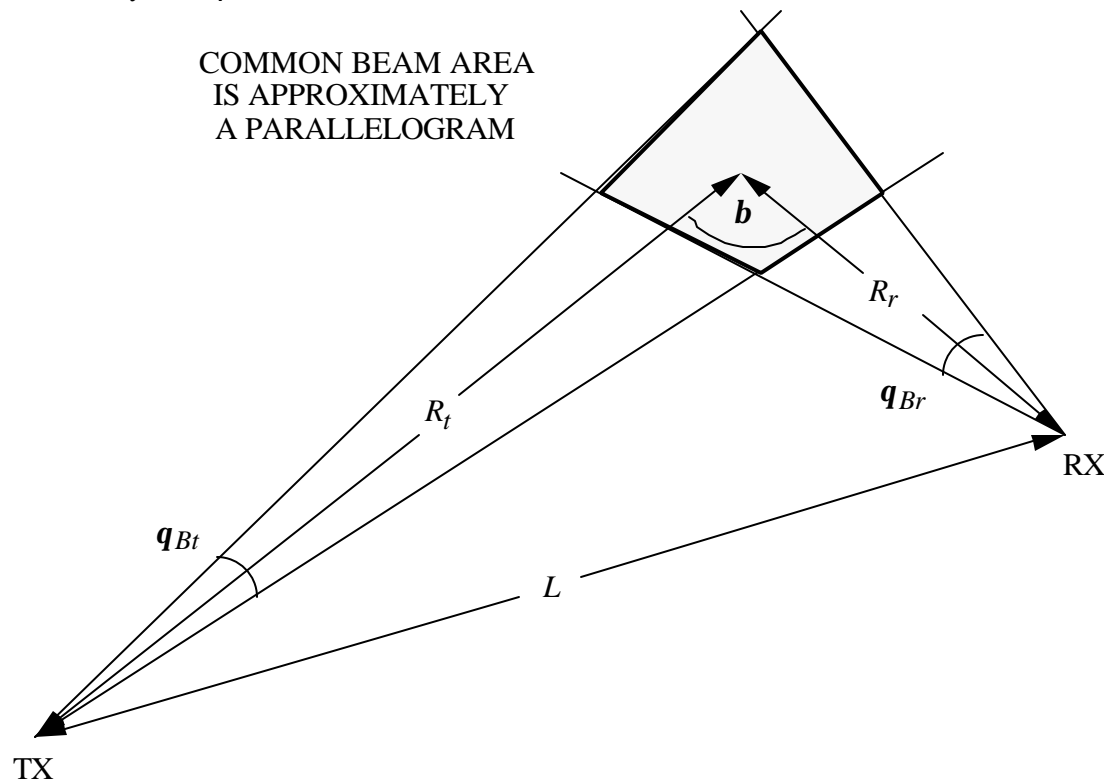
4. High gain transmit beam with floodlight receive beam ( $\Omega_{Ar} = \Omega_s$ )

The last two approaches are not normally used because

- Mainbeam clutter large
- Angle accuracy low

# Bistatic Footprint and Clutter Area (1)

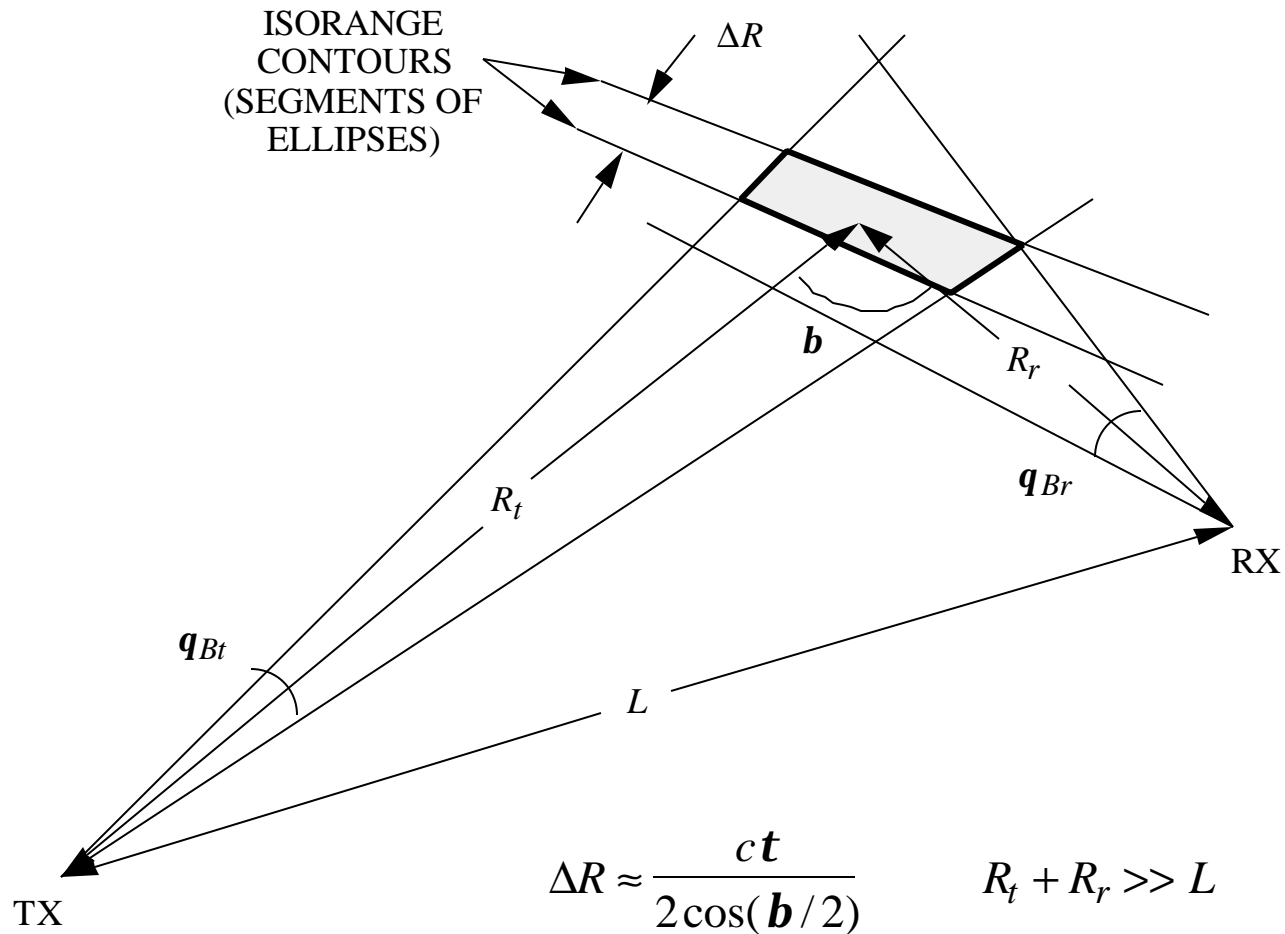
Simple antenna beam model: 1) constant gain within the HPBW, zero outside, and 2) circular arcs are approximately straight lines. Example of bistatic footprint (for small grazing angles and  $R_t + R_r \gg L$ ):



1. Beamwidth limited: (entire shaded area) 
$$A_c \approx \frac{(R_r q_{Br})(R_t q_{Bt})}{\sin b}$$

# Bistatic Footprint and Clutter Area (2)

2. Pulsewidth (range) limited:  $A_c \approx \Delta R \frac{(R_r q_{Br})}{\cos(\mathbf{b}/2)} = \frac{ctR_r q_{Br}}{2 \cos^2(\mathbf{b}/2)}$





# Bistatic Radar Cross Section (1)

---

- Bistatic RCS is characterized by large forward scatter, particularly in the optical region
- The strength of the forward scatter depends on the target size and shape, aspect angle, frequency, and polarization
- For  $\mathbf{b} \approx 180^\circ$  the radar can only detect the presence of a target between the transmitter and receiver. The range is indeterminate (due to eclipsing of the direct pulse by the scattered pulse) and the doppler is zero
- Babinet's principle can be used to compute the forward scatter

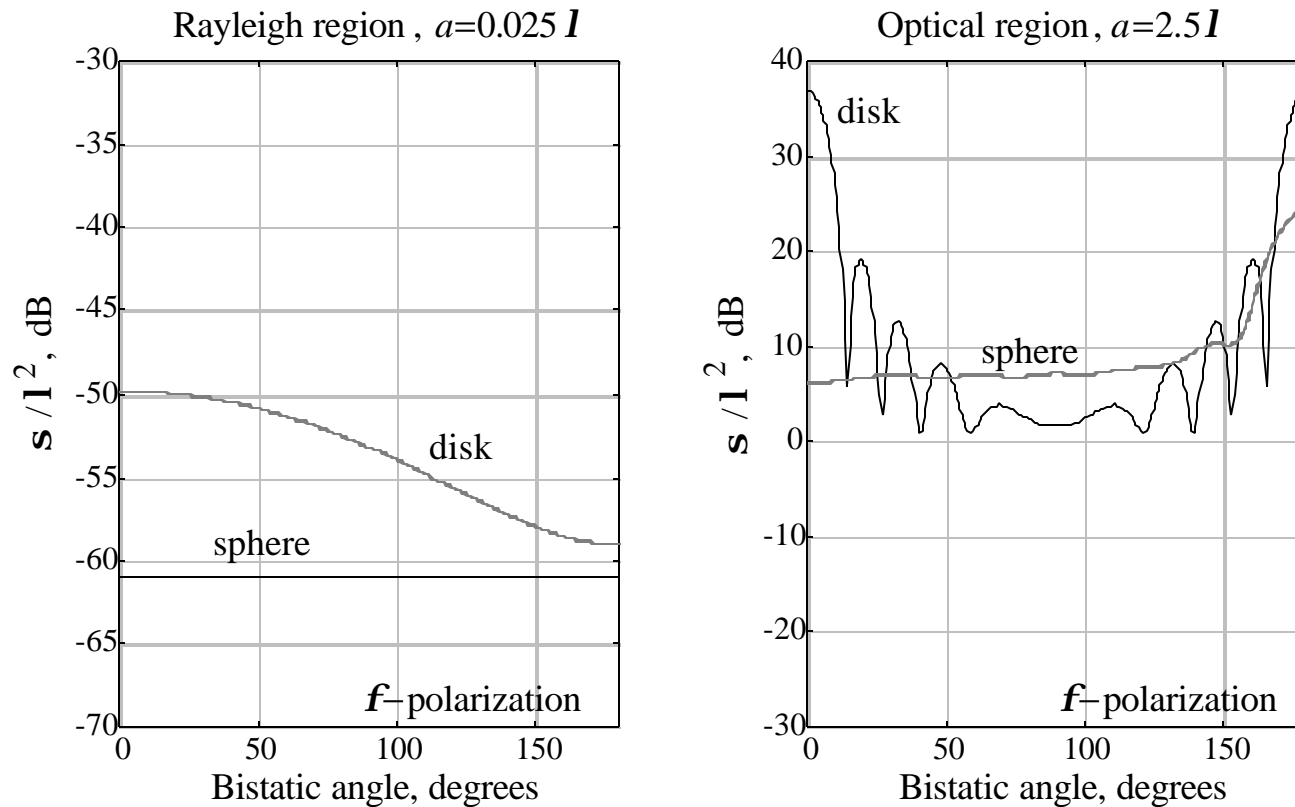
Example: A 2 m by 5 m rectangular plate at  $\mathbf{l} = 1$  m and  $\mathbf{b} \approx 180^\circ$  has a forward scatter RCS of approximately

$$\mathbf{s}_F \approx \frac{4pA^2}{\mathbf{l}^2} = 1260 \text{ m}^2$$

If the radar can detect 5 m<sup>2</sup> targets, then the detection threshold is exceeded out the fourth sidelobe of the sinc pattern (40° from the forward scatter maximum). This corresponds to a bistatic angle of  $\mathbf{b} \approx 140^\circ$ . The forward scatter HPBW is approximately  $\mathbf{l} / 2$  by  $\mathbf{l} / 5$  radians (23° by 11°).

# Bistatic Radar Cross Section (2)

Comparison of the bistatic RCS of spheres and disks of the same diameter ( $f_i = 0^\circ$ )



# Bistatic Radar Example Revisited

---

Example: Returning to the previous example regarding a buoy that is dropped in the center of the channel to detect passing ships. Compare the transmit power for the bistatic and monostatic cases if the bistatic RCS is 10 dB higher than the monostatic RCS.

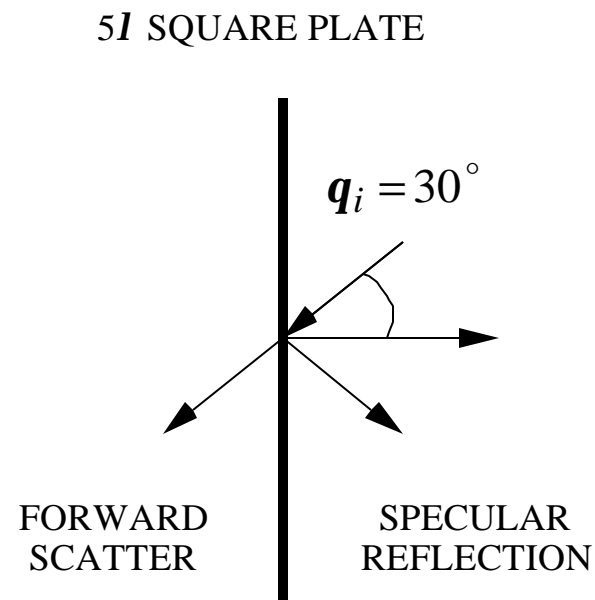
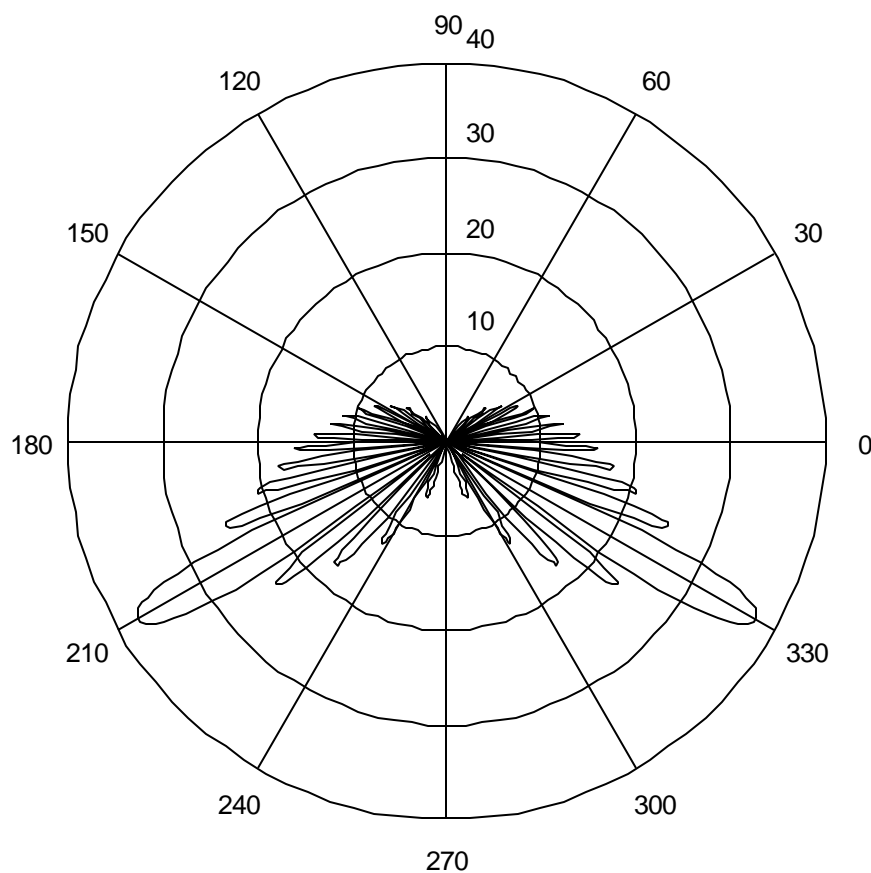
For an altitude (range) of 6735 m the monostatic radar required  $P_t = 0.45 \text{ W}$  assuming that the monostatic and bistatic cross sections are the same. If the bistatic RCS is increased by 10 dB then the buoy transmitting power can be reduced by 10 dB, or

$$P_t = 0.1 \text{ W}$$

- Comments:
1. One advantage of the bistatic radar is that the aircraft position is not given away
  2. Achieving a 10 dB RCS advantage would probably require a limited engagement geometry that puts the receiver aircraft in the target's forward scatter beam. This would be difficult to insure with a ground based transmitter and an airborne receiver.
  3. The receiver dynamic range and pulse timing may be a problem

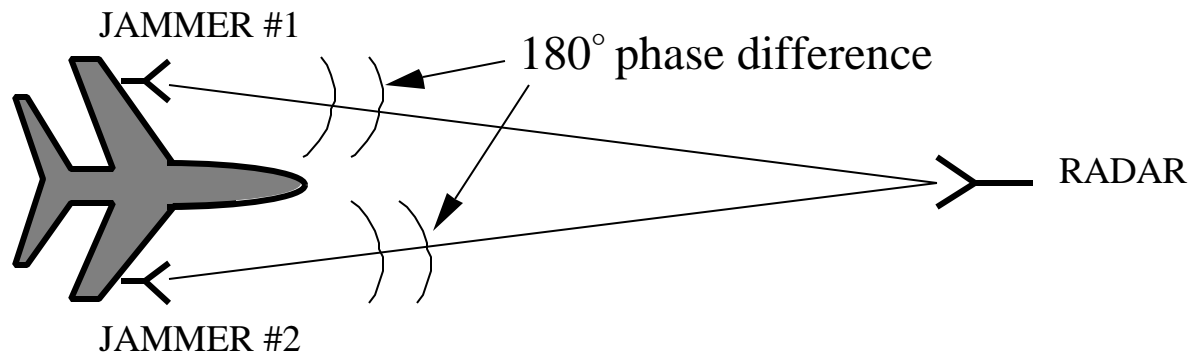
# Bistatic Radar Cross Section (3)

Bistatic RCS of a  $5\lambda$  square flat plate using the physical optics approximation



# Cross Eye Jamming (1)

The cross eye technique uses two jammers to produce a large phase error across the radar's antenna aperture:



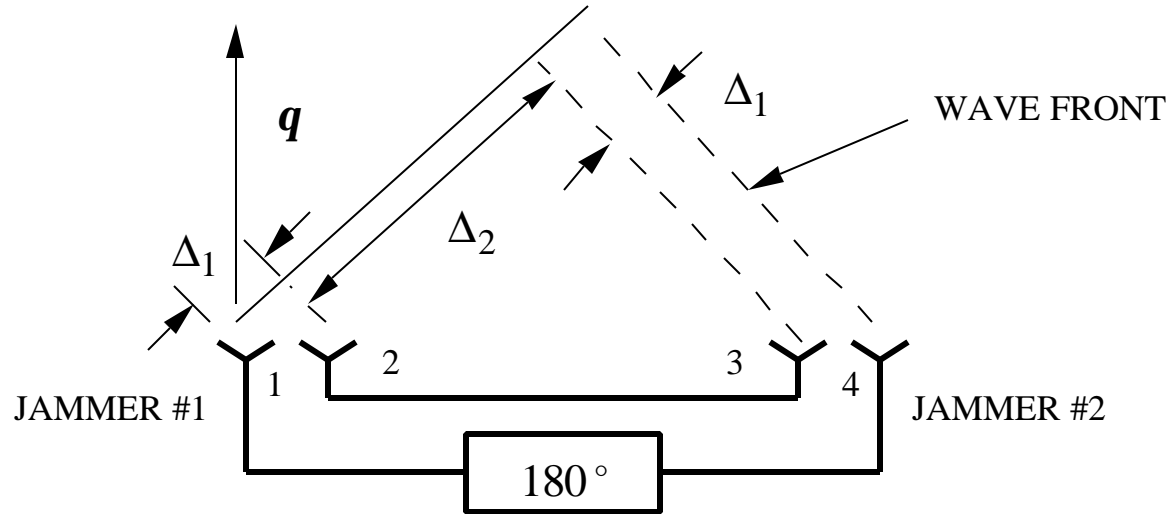
The jammers create two apparent scatterers that are out of phase with the following results:

	<u>Passive Target</u>	<u>With Cross Eye</u>
$\Sigma$ Channel	Max	Null
$\Delta$ Channel	Null	Max

Tolerances required for the microwave network: Phase:  $\sim 0.3^\circ$   
 Amplitude:  $\sim 0.05$  dB

# Cross Eye Jamming (2)

1. Radar wave arrives at an angle  $q$
2. Path difference between two adjacent elements (1-2 and 3-4) is  $\Delta_1$
3. Path difference between two inner most elements (2-3) is  $\Delta_2$
4. Line length between inner-most elements is  $L$ ; between outer most elements  $L + p$

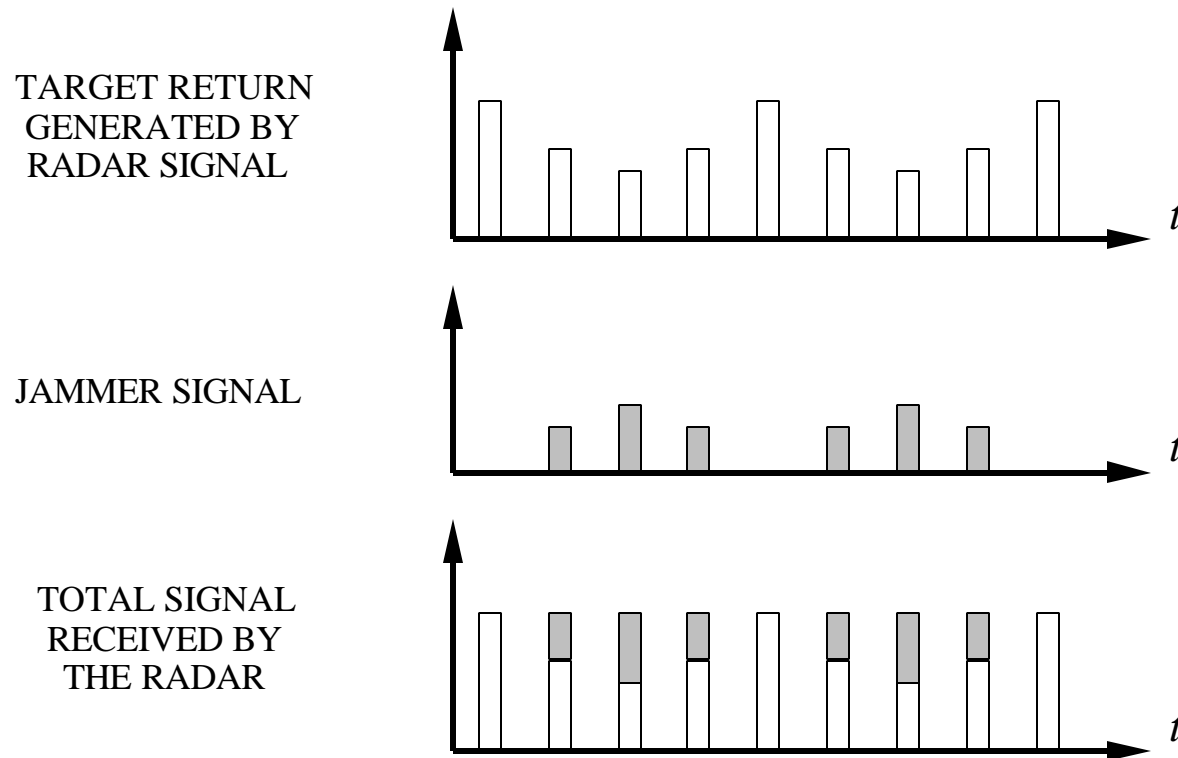


Signal path to and from radar:

$$\left. \begin{array}{l}
 \text{Outer elements : } \Phi_{14} = \underbrace{R + 2\Delta_1 + \Delta_2}_{\text{TO \#1}} + L + p + R \\
 \text{Inner elements : } \Phi_{23} = \underbrace{R + \Delta_1 + \Delta_2}_{\text{TO \#2}} + L + \underbrace{\Delta_1}_{\text{FROM \#3}} + R
 \end{array} \right\} \Rightarrow \Phi_{14} + \Phi_{23} = 0$$

# ECM for Conical Scanning

Conical scan is susceptible to ECM. A jammer can sense the radar's modulation and compensate for it. Therefore the radar believes its antenna is "on target" when in fact it is not.

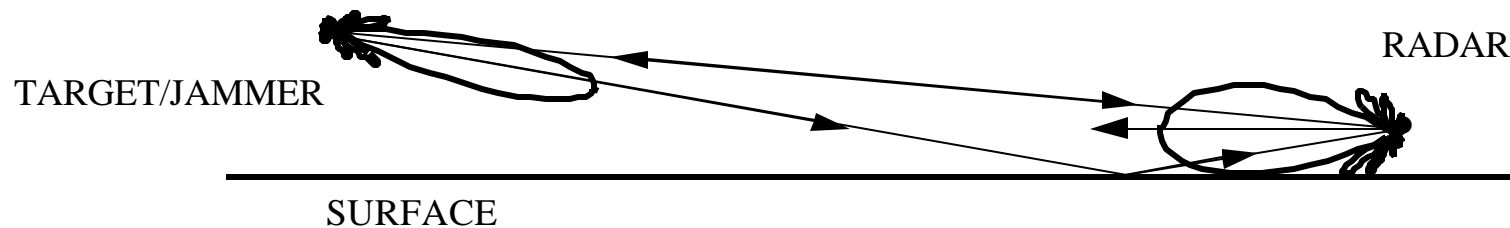


It is usually sufficient for the jammer to just change the modulation (level or period) to spoof the radar.

# Ground Bounce ECM

---

A jammer illuminates a ground spot. The radar receives a return from the target and the ground spot. The radar will track the centroid of the returns, which is an angle determined by a weighted combination of the two signals. The centroid will be in a direction closer to the strongest signal. Therefore the jammer signal must overpower the target return to defeat the radar.



Ground bounce ECM is usually only applied at low altitudes where a strong controlled reflection can be generated.

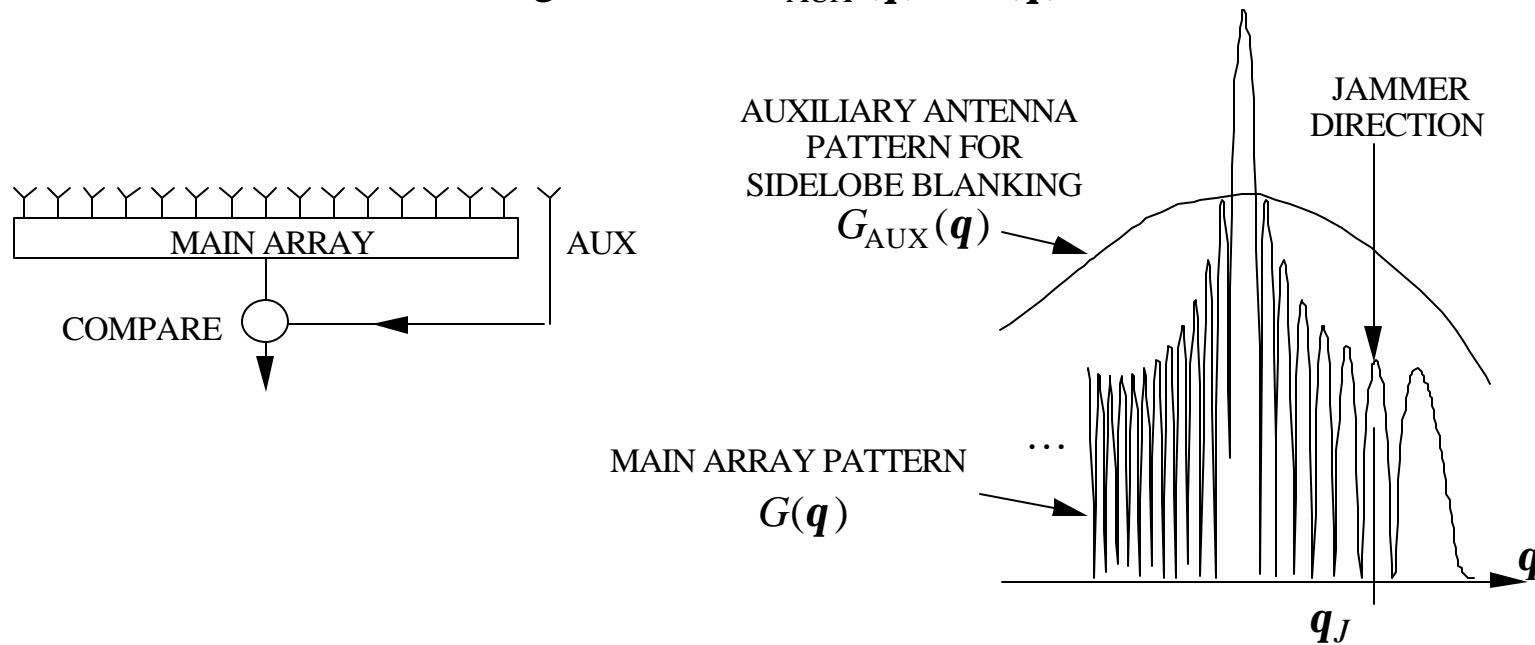


# Suppression of Sidelobe Jammers (1)

Techniques to defeat sidelobe jammers:

1. antenna sidelobe reduction
2. multi-channel receiver techniques:
  - a) sidelobe blanking: blank the main receiver channel (i.e., turn it off) if a signal arrives via a sidelobe

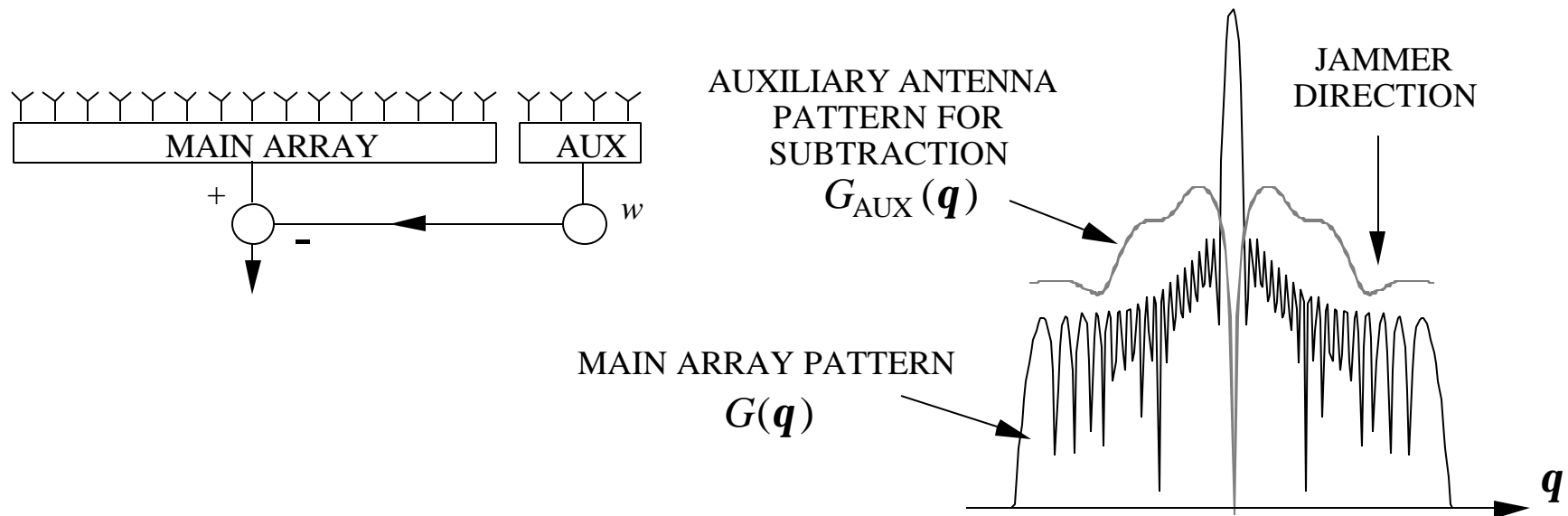
Turn off the receiver for angles where  $G_{AUX}(q) > G(q)$



# Suppression of Sidelobe Jammers (2)

- b) coherent sidelobe cancelers (CSLC): coherently subtract the signal received via the sidelobes from the main channel signal

A CSLC requires an auxiliary antenna pattern with a null colocated with the main array beam maximum.



# CSLC Equations for an Array Antenna

---

For simplicity neglect the element factor

$\mathbf{q}_J$  = jammer angle

$AF(\mathbf{q}_J)$  = main antenna array factor in the direction of the jammer

$AUX(\mathbf{q}_J)$  = auxiliary antenna pattern in the direction of the jammer

Compute the complex weight:

$$y(\mathbf{q}_J) = AF(\mathbf{q}_J) - w \cdot AUX(\mathbf{q}_J) \equiv 0$$

or, assuming that  $AUX(\mathbf{q}_J) \neq 0$ ,

$$w = \frac{AF(\mathbf{q}_J)}{AUX(\mathbf{q}_J)}$$

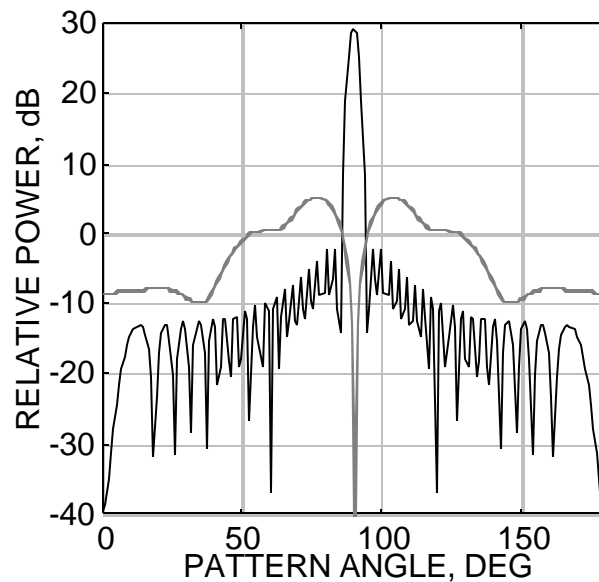
If  $AUX(\mathbf{q}_J) > AF(\mathbf{q}_J)$  then  $|w| \leq 1$ . The array response at an arbitrary angle  $\mathbf{q}$  is

$$y(\mathbf{q}) = AF(\mathbf{q}) - \frac{AF(\mathbf{q}_J)}{AUX(\mathbf{q}_J)} AUX(\mathbf{q})$$

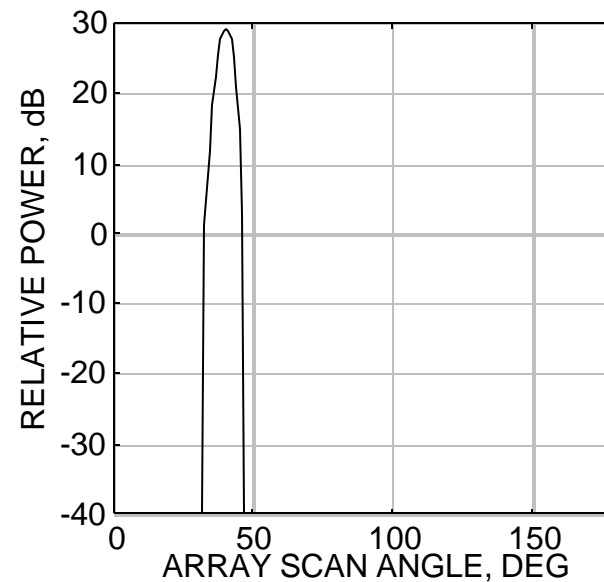
# CSLC Performance

Example of CLSC performance for a 50 element array with  $d = 0.4\lambda$ . The auxiliary array has 8 elements with "phase spoiling" to fill in the pattern nulls.

MAIN ARRAY AND AUXILIARY ANTENNA PATTERNS

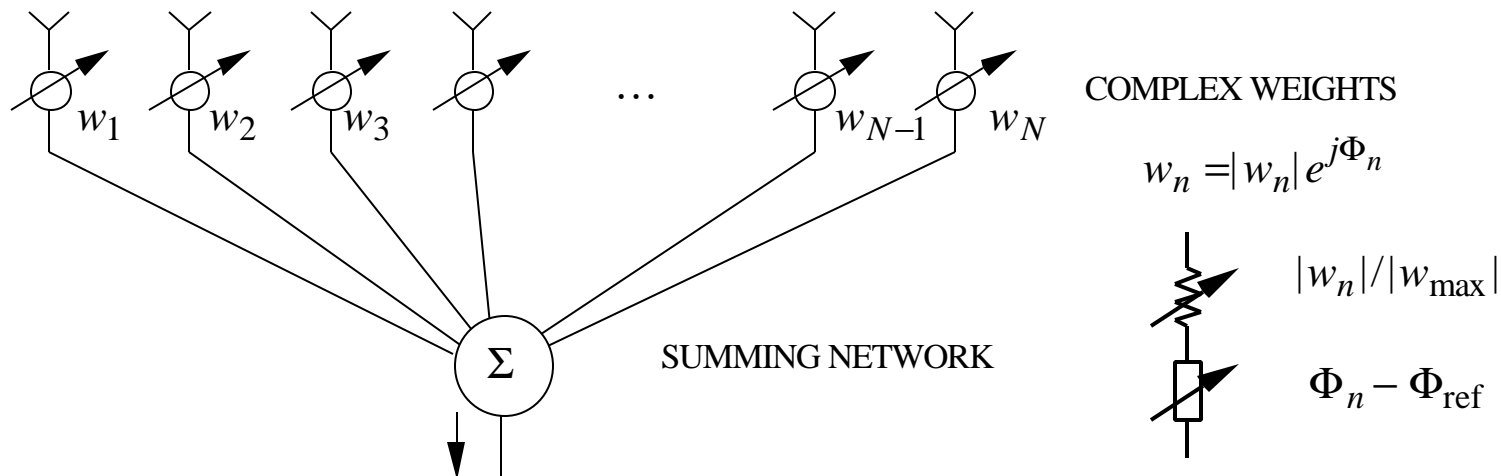


ARRAY RESPONSE FOR A JAMMER AT 40 DEGREES



# Adaptive Antennas

Adaptive antennas are capable of changing their radiation patterns to place nulls in the direction of jammers. The pattern is controlled by adjusting the relative magnitudes and phases of the signals to/from the radiating elements. Adaptive antenna model:



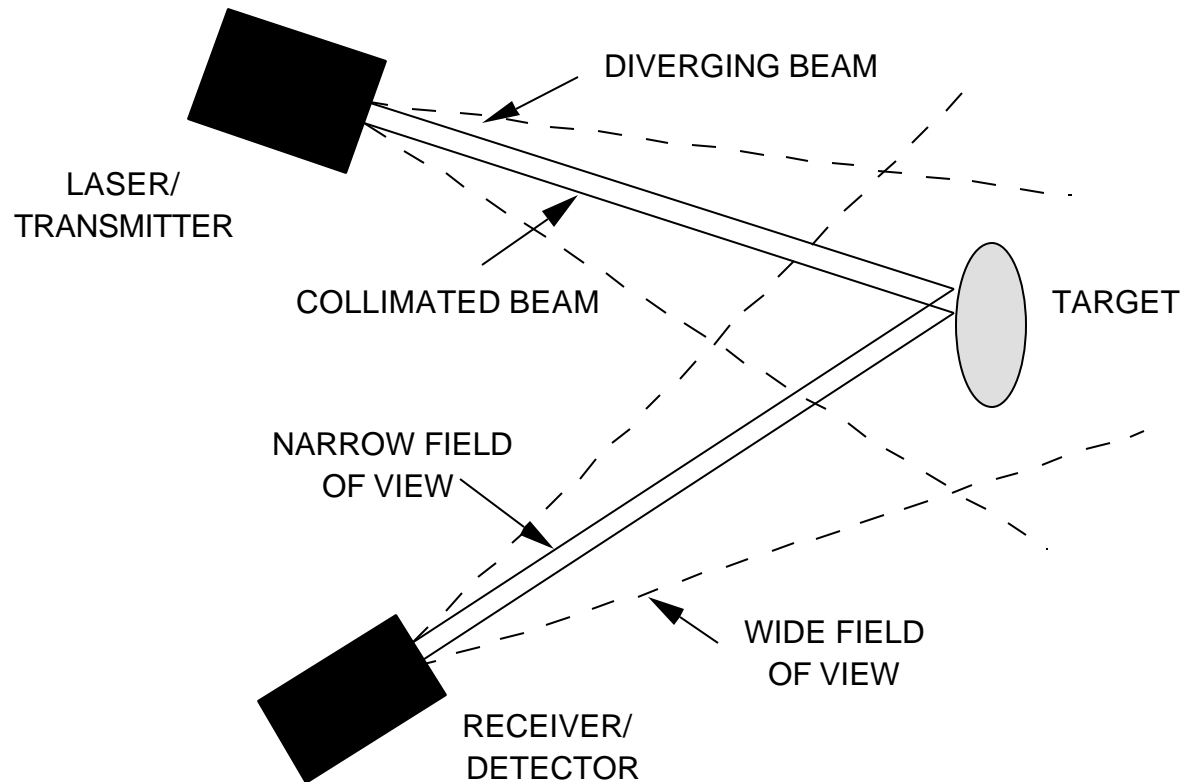
In principle, a  $N$  element array can null up to  $N - 1$  jammers, but if the number of jammers becomes a significant fraction of the total number of elements, then the pattern degrades significantly.

The performance of an adaptive array depends on the algorithm (procedure used to determine and set the weights). Under most circumstances the antenna gain is lower for an adaptive antenna than for a conventional antenna.

# Laser Radar (1)

---

Laser radar (also known as lidar and ladar) operates on the same principle as microwave radar. Typical wavelengths are 1.06 and 10.6  $\mu\text{m}$ . Atmospheric attenuation is a major concern at these frequencies. Laser radars are shorter range than microwave radar. Typical radar/target geometries:



# Laser Radar (2)

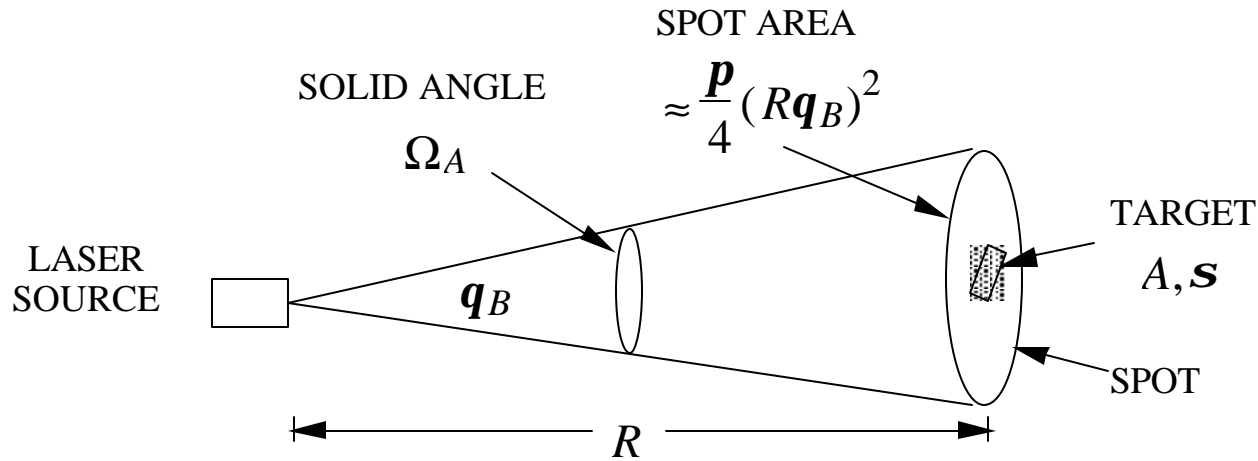
---

Advantages, disadvantages, and uses of laser radar:

- Small wavelength permits accurate range measurement
- Narrow beams and fields of view allows precise direction (pointing) information
- Narrow beams and fields of view implies poor search capability
- Laser radars are generally used in conjunction with other sensors:
  1. With infrared search and tracking (IRST) and thermal imaging systems to locate threats in volume search
  2. Used with microwave radar to improve range and angle information
- Atmospheric effects are very important:
  1. Absorption by gas molecules
  2. Scattering of light out of the laser beam by particles
  3. Path radiance (the atmosphere emits its own energy which appears as noise).
- Typical detection range of ground based system is ~ 10 km; for spaceborne systems it is thousands of km due to the absence of atmospheric losses.

# Laser Radar (3)

Consider the case where the target is completely illuminated:



The laser beam solid angle is  $\Omega_A = \frac{A_{\text{SPOT}}}{R^2} = \frac{pq_B^2}{4}$

The gain of the transmit optics is  $G_t = \frac{4p}{\Omega_A} = \frac{16p}{q_A^2}$

The target is very large in terms of wavelength. Therefore, assume that the target only scatters the laser energy back into the hemisphere containing the radar. Then the spreading factor is  $1/2pR^2$  rather than  $1/4pR^2$ .



# Laser Radar (4)

---

Target scattered power back at the receiver:

$$P_r = \frac{P_t G_t}{4pR^2} \cdot \mathbf{s} \cdot \frac{1}{2pR^2} \cdot A_{er}$$

The area of the receive optics is  $A_{er}$ . Assume that the transmit and receive optics are identical

$$A_{er} \approx A_r = A_t = p \left( \frac{D}{2} \right)^2$$

The half power beamwidth is related to the optics diameter

$$q_B = 1.02l / D \approx l / D$$

Introduce the optical efficiency  $r_o$  and atmospheric attenuation factor. The monostatic laser radar equation becomes:

$$P_r = \frac{8P_t A_r^2 \mathbf{s} r_o}{l^2 p^3 R^4} e^{-2aR}$$

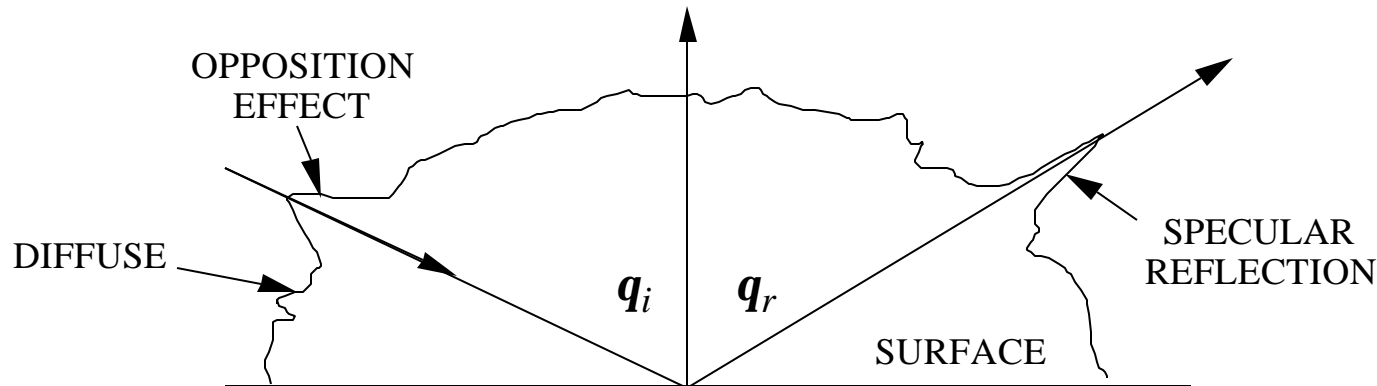
# Laser Radar (5)

Laser cross section is identical to RCS:

$$\mathbf{s} = \lim_{R \rightarrow \infty} 4p R^2 \frac{|\vec{W}_s|}{|\vec{W}_i|}$$

Important differences:

1. In practice the limiting process is rarely satisfied because  $I$  is so small.
2. The laser beam amplitude is not constant over the entire target.
3. Target surfaces are very rough in terms of wavelength. Diffuse scattering dominates.
4. Target surfaces are not perfectly diffuse nor uniform scatterers. The bidirectional reflectance distribution function (BRDF) characterizes the surface reflectivity as a function of position on the target surface, incidence direction, scattering direction, and polarization. Typical scattering pattern from a diffuse surface:

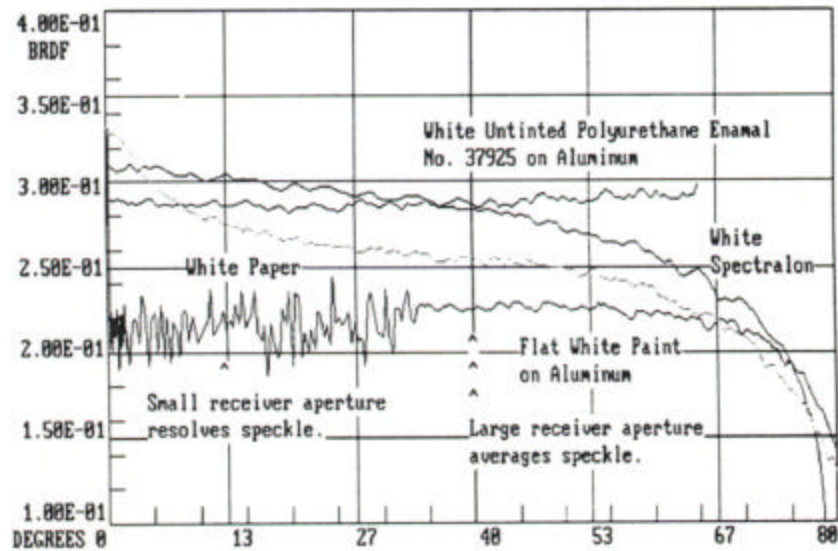


# Laser Radar (6)

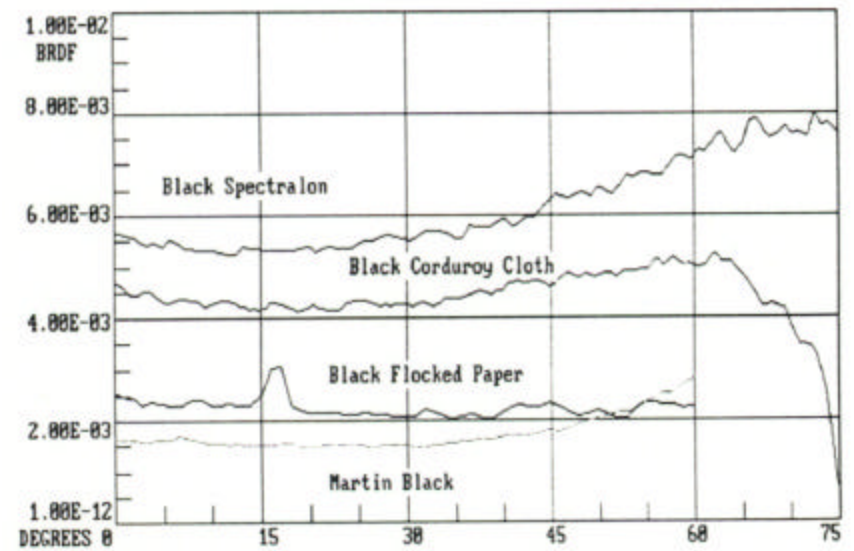
## Examples of measured BRDFs at 0.633 micrometers

(from J. Stover, *Optical Scattering*)

### White diffuse surfaces

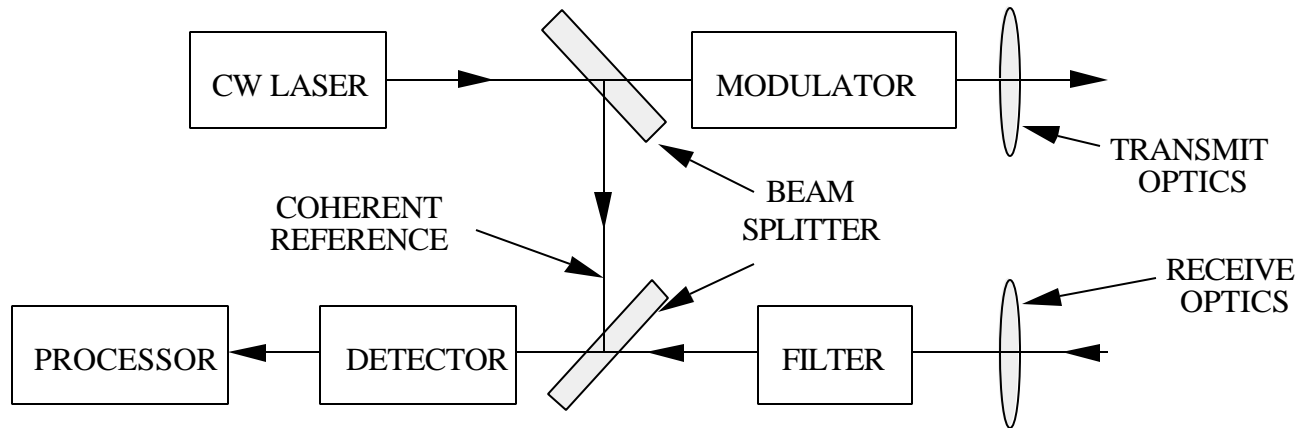


### Black diffuse surfaces

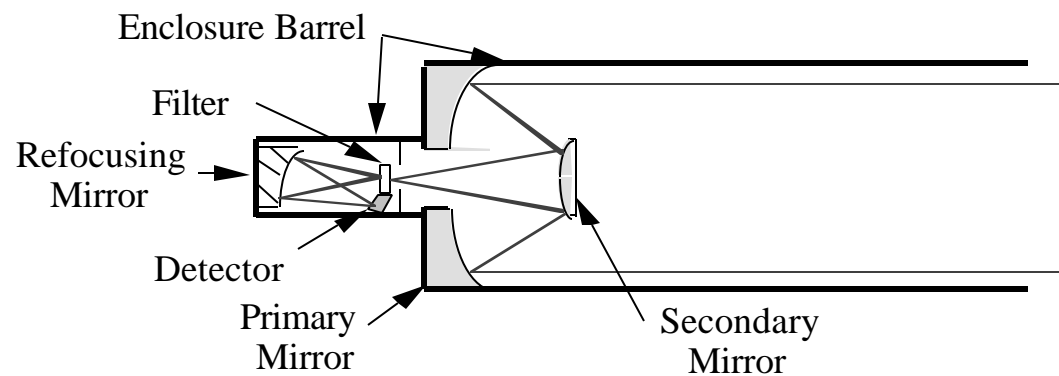


# Laser Radar (7)

System block diagram:



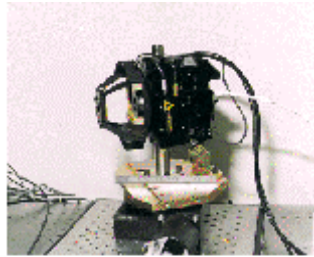
Example of receive optics (Cassegrain reflecting system):



# Laser Radar (8)

---

Laser seeker



LADAR SEEKER HEAD

Room



Laser radar image of room

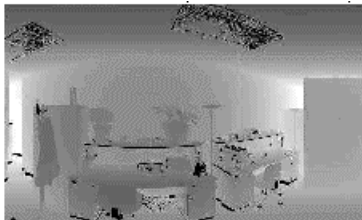
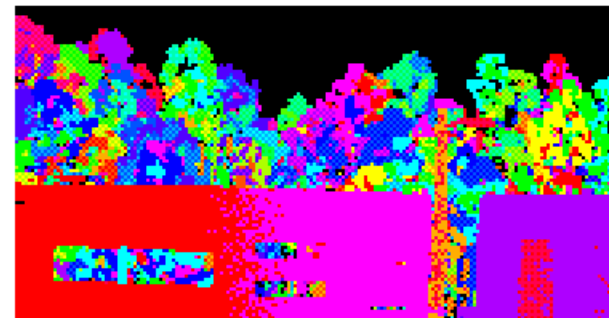


Image resolution test panel (USAF)



LARGE RESOLUTION PANELS AT SITE C-3

Image of test panel



# Ground Penetrating Radar (1)

---

Ground penetrating radar (GPR), also known as subsurface radar, refers to a wide range of EM techniques designed to locate objects or interfaces buried beneath the Earth's surface. Applications that drive the system design include:

<u>Application</u>	<u>Depth/range of interest</u>
archeology	short to medium
wall thickness and hidden objects in walls*	short
unexploded ordinance and mines	short to medium
pipes and underground structures	medium
ice thickness	long

short:  $d < 1/2$  m

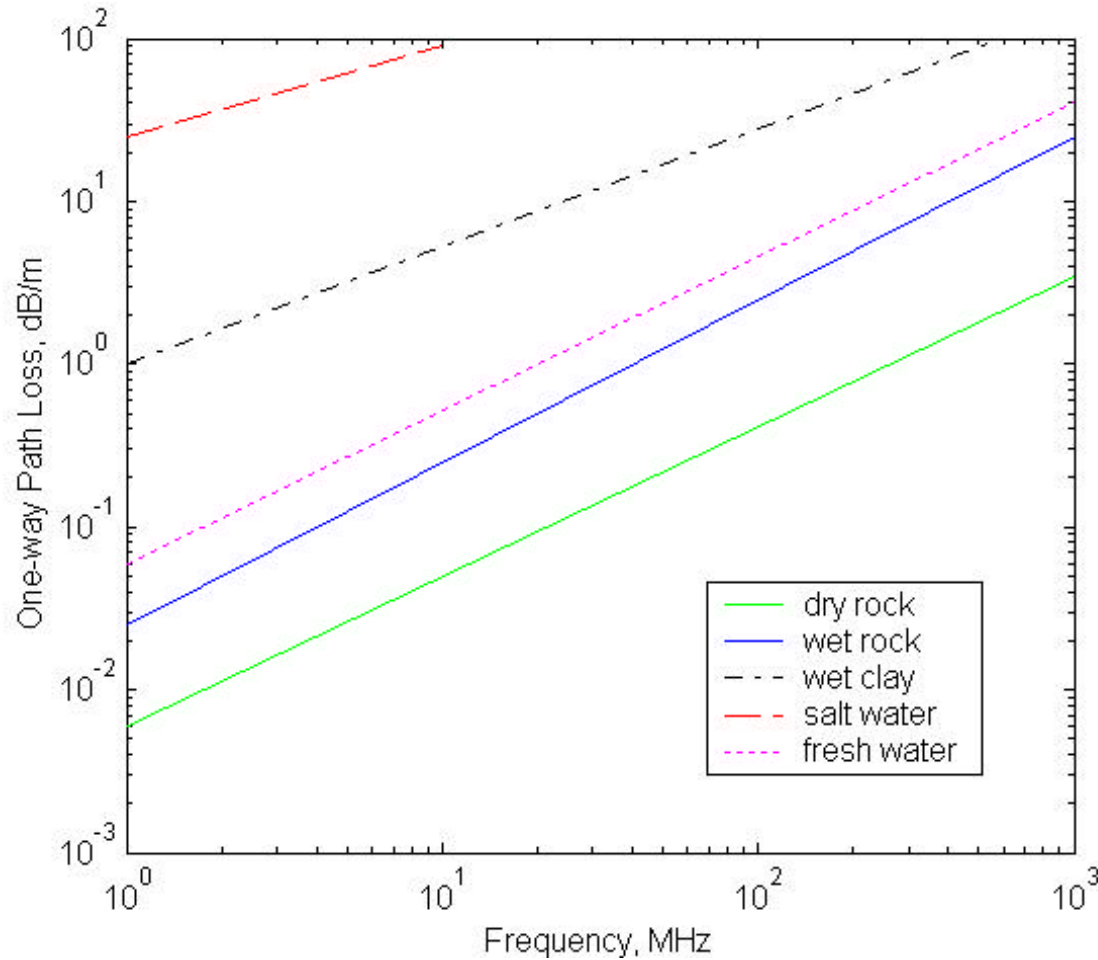
medium:  $1/2$  m  $< d < 25$  m

long:  $d > 25$  m to hundreds of meters

\*Radars for hidden object detection have requirements similar to those of ground penetrating radars.



# Ground Penetrating Radar (3)



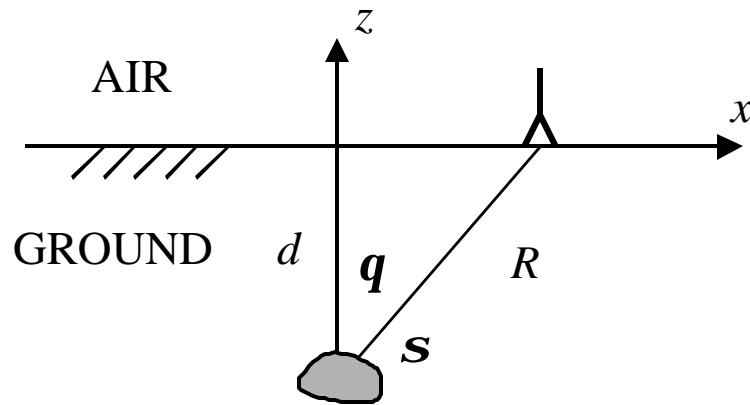
The major design consideration is the attenuation in the ground.

After figure from *Understanding Radar Systems* by Kingsley and Quegan



# Ground Penetrating Radar (4)

Horizontal resolution can be obtained in several ways. One method is based on the received power distribution as the radar moves over the target.



- The received power is

$$P_r \propto \frac{e^{-4aR}}{R^4}$$

where  $a$  is the one-way voltage attenuation constant.

- If  $d$  and  $x$  are known then  $R = \sqrt{d^2 + x^2}$  can be substituted.
- The attenuation constant is obtained from  $L$ , the “loss in dB per meter” quantity

$$L = 20 \log \left( \frac{E \text{ at 1 m depth}}{E \text{ at surface}} \right)$$

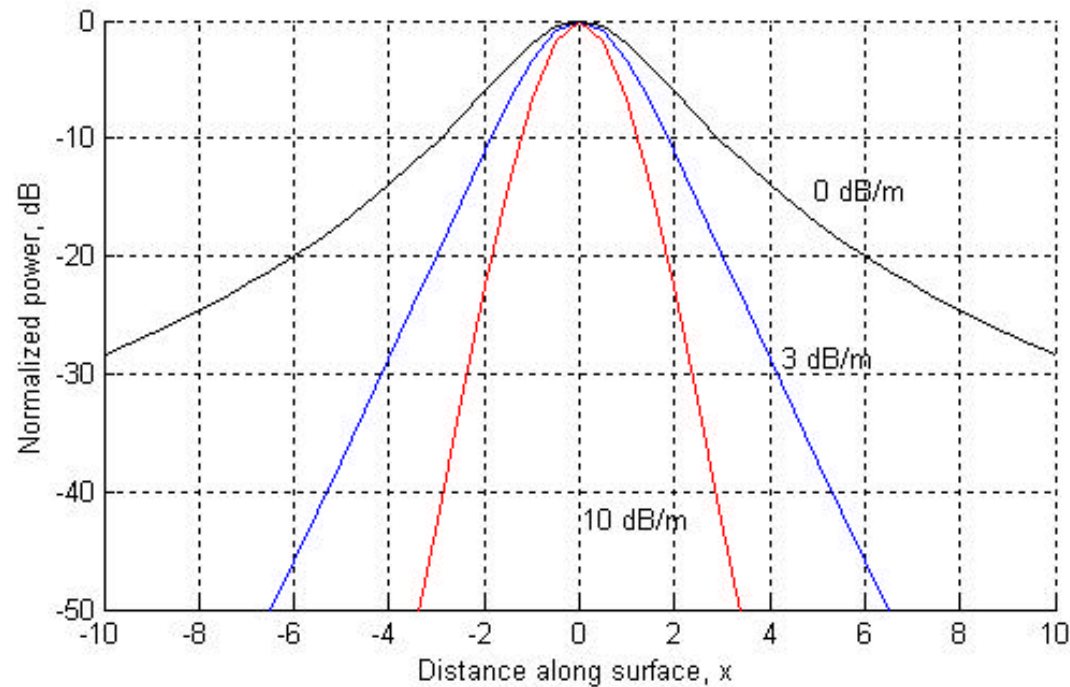
$$= 20 \log \left( e^{-a \cdot 1} \right)$$

Therefore,

$$a = -\ln \left( 10^{-L/20} \right)$$

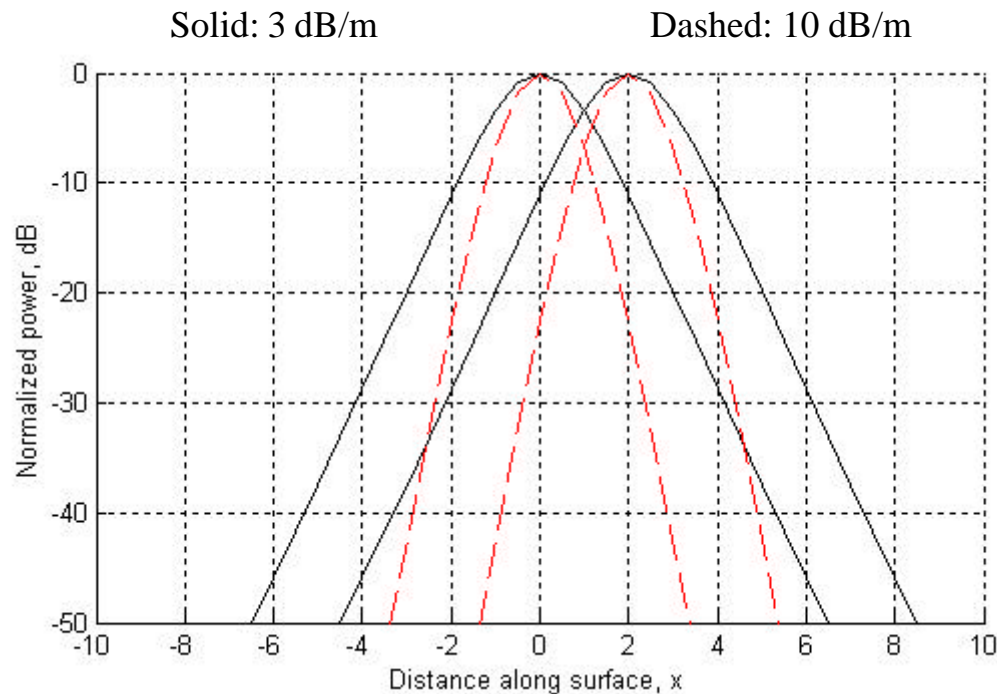
# Ground Penetrating Radar (5)

Example: Return from a target at  $x = 0$  ( $d = 2$  m) as the radar moves along the ground for several ground attenuation values.



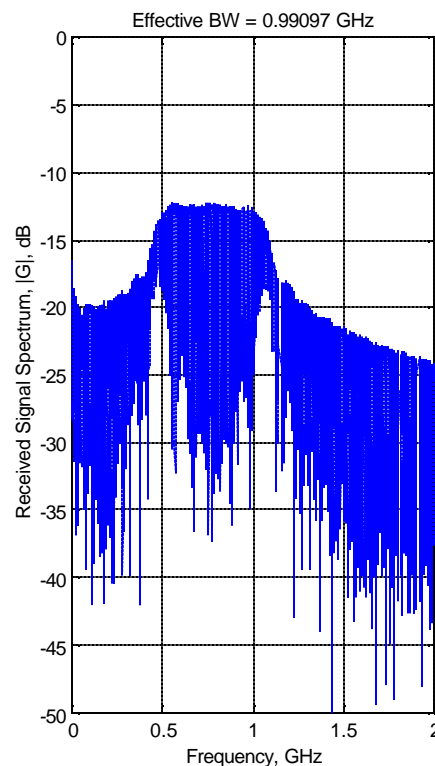
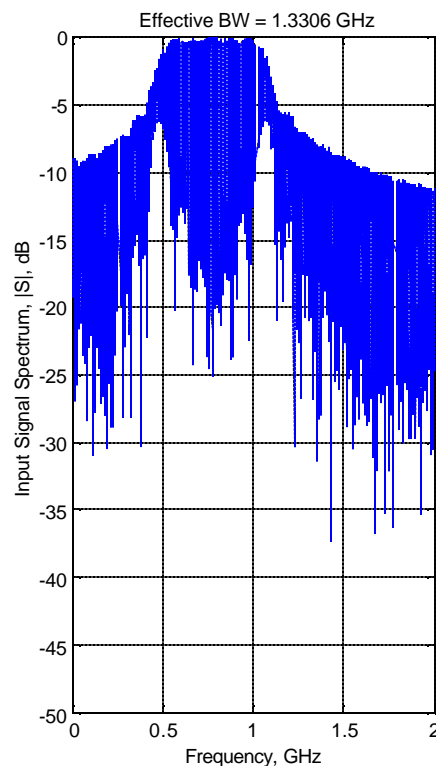
# Ground Penetrating Radar (6)

Example: Returns from two equal RCS targets at  $x = 0$  and 2 meters for various ground loss ( $d = 2$  m). Note that higher loss actually improves horizontal resolution. Increasing the loss per meter has the same effect as narrowing the antenna beamwidth.



# Ground Penetrating Radar (7)

Example: Stepped frequency waveform (12 pulses, frequency step size 50 MHz per pulse, start frequency 500 MHz, PRF 10 MHz, pulse width 0.01 microsecond)



The ground loss has reduced the effective bandwidth  $B_e$  by about 25 percent. By the uncertainty relation

$$B_e t_e \geq p$$

Since the range resolution is approximately

$$\Delta R \approx \frac{c}{2} t_e$$

the range cell has also been increased by about 25 percent due to the ground loss.

# Ground Penetrating Radar (8)

---

Cross-range can be determined in several ways:

1. narrow antenna beamwidth: Usually not practical because of the low frequencies required for ground penetration. Small “illumination spot” required for a 2D image.
2. Power distribution variation as the antenna moves over the ground, as illustrated in chart GPR (6): Performance depends on ground loss, variations in the scattering cross sections of objects, depth and separation of objects, etc. 2D transversal required for a 2D image.
3. SAR techniques: Ground loss limits the synthetic aperture length because it has the same effect as narrowing the beamwidth (i.e., cannot keep the scatterer in the antenna field of view). 2D transversal required for a 2D image.

Mobile ground penetrating radar in operation

Overall, GPR is probably the most challenging radar application.

GPR system design is specific to the particular application.

